Numerical Analysis of Algorithms for Infinitesimal Associated and Non-Associated Elasto-Plasticity

Zur Erlangung des akademisches Grades eines

DOKTORS DER NATURWISSENSCHAFTEN

von der Fakultät für Mathematik
des Karlsruher Instituts für Technologie (KIT)
genehmigte
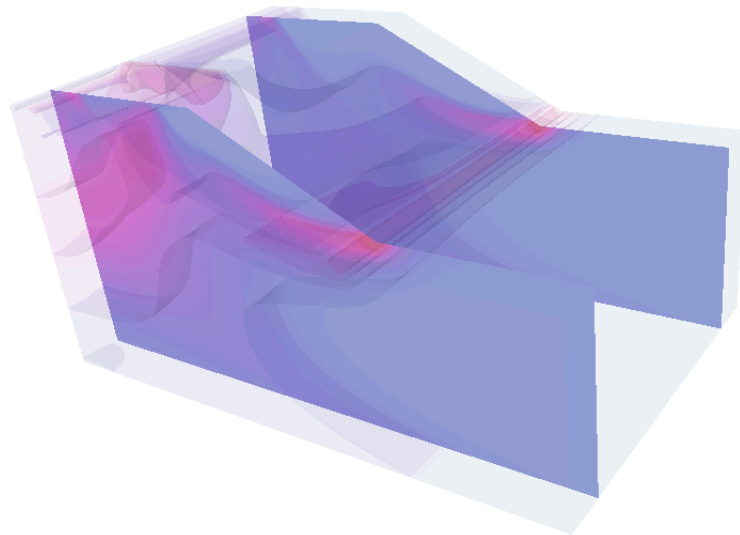
DISSERTATION

von

Dipl.-Math. techn. Martin Sauter
aus Freudenstadt

VORWORT

Die vorliegende Arbeit wurde im Rahmen meiner Tätigkeit als akademischer Angestellter in der Zeit zwischen Januar 2007 und Juni 2010 in der Arbeitsgruppe *Wissenschaftliches Rechnen* am *Institut für Angewandte und Numerische Mathematik* des *Karlsruher Instituts für Technologie* (KIT, ehem. Universität Karlsruhe) erstellt. Meine Arbeit war dabei in die Arbeitsgruppe *Effektive Löser in der Plastizität* des *Instituts für Wissenschaftliches Rechnen und Mathematische Modellbildung* (IWRMM) eingegliedert.

Mein erster Dank geht an Herrn Prof. Dr. Christian Wieners für die Aufnahme in seine Arbeitsgruppe und die damit verbundenen wissenschaftlichen Freiheiten beim Gestalten dieser Arbeit. Insbesondere danke ich für die angenehme Arbeitsatmosphäre und Betreuung während meiner Promotionszeit. Zudem wären die numerischen Untersuchungen ohne die von ihm maßgeblich entwickelte Software-Toolbox *M++* nicht in der vorliegenden Art und Weise möglich gewesen.

Für die Übernahme des Korreferats danke ich Herrn Prof. Dr. Willy Dörfler ebenso wie für die numerische Grundausbildung im Rahmen meines Studiums.

Weiter möchte ich mich bei allen Mitgliedern der Arbeitsgruppe Wissenschaftliches Rechnen für die freundliche und kooperative Arbeitsumgebung und auch die vielen anregenden (nicht-) wissenschaftlichen Diskussionen bedanken. Insbesondere waren dies Dr. Wolfgang Müller, PD Dr. Nicolas Neuß, Daniel Maurer, Tim Kreutzmann, JProf. Dr. Tobias Jahnke, Tudor Udrescu, Antje Sydow, Prof. Dr. Andreas Rieder, Prof. Dr. Rudolf Scherer, Andreas Arnold, Michael Kreim sowie Ulrike Rust und Nathalie Sonnefeld.

Schließlich möchte ich meiner Familie für die andauernde Unterstützung und die mir gebotenen Möglichkeiten danken. Zu nennen sind dabei speziell meine Eltern, Dipl.-Ing. Horst Sauter († 2009) und Margot Sauter sowie meine Schwester Dr. Linda Sauter.

Der größte Dank geht aber letztlich an meine Lebensgefährtin (oder schlicht Freundin) Ariane Braun, die das Projekt Promotion von Anfang bis Ende live (und in Farbe) verfolgt hat und dabei verständnisvoll auf das eine oder andere verzichtet hat.

CONTENTS

MOTIVATION AND A SHORT SUMMARY

Motivation

At the end of the 1990s, three books were published covering computational, mathematical and numerical questions in plasticity:

(1) *Computational inelasticity* [**SH98**] by Simo and Hughes is written from an engineering point of view in which algorithms are considered as a tool for doing mechanics. Nevertheless, it is more or less the first book covering questions of implementation.

(2) *Plasticity – Mathematical Theory and Numerical Analysis* [**HR99**] by Han and Reddy. In this book, the focus is on mathematical well-posedness of standard models for which also a numerical analysis concerning discretization errors in time and space is provided. However, solution algorithms are not a primary objective.

(3) *Materials with Memory – Initial-Boundary Value Problems for Constitutive Equations with Internal Variables* [**Alb98**] by Alber introduces a general mathematical framework for answering questions of existence and uniqueness for materials with internal variables.

Published around the same time, all three books examine different aspects of plasticity and also use a fairly different "language". While [**SH98**] mostly addresses engineering users and presents some blueprint algorithms, [**HR99**] is written for an audience in numerical mathematics with a background in partial differential equations. Finally, [**Alb98**] uses the language of functional analysis for a thorough analytical treatment. Despite the variety of covered topics, some problems remained unaddressed, and in the present work we focus on one such problem: *algorithmic plasticity*, viz. the numerical analysis of solution algorithms. This analysis quite naturally introduces a further field of mathematics into the world of plasticity, namely *optimization theory* and the related field of *complementarity problems*. Though often used for analytical considerations, this powerful framework has not been exploited in detail concerning the design and analysis of solution algorithms in plasticity.

Essentially, it turns out that the standard algorithm proposed in [**SH98**] is *Newton's method* applied to the formulation of infinitesimal plasticity as a boundary value problem for the displacement. "Essentially" means that it is a *generalized* Newton method as the considered equations are nonsmooth. Fortunately, the nonsmooth portion can be handled

1

locally (in space) by a simple case differentiation. The algorithm is then derived via linearization in the individual cases. The obtained method performs very well in practice and virtually always exhibits superlinear convergence. Based on a nonsmooth analysis framework, the good performance of the algorithm can nowadays be explained in the context of generalized Newton methods. Nevertheless, a systematic application to plasticity problems has not been performed yet, and this work can be understood as an attempt to narrow this gap. Important tools for showing superlinear convergence of generalized Newton methods in finite dimensions are *Clarke's generalized Jacobian* [**Cla83**] for Lipschitz continuous functions and *semismoothness* [**Mif77**, **QS93**]. However, these concepts often rely on *Rademacher's theorem* and therefore are mostly limited to the finite dimensional context. However, in the last decade, new concepts have been developed concerning generalizations to function space [**IK08**, **HPUU09**]. A driving force behind the development of this nonsmooth calculus was (and still is) optimization theory, as particularly optimization problems with inequality constraints naturally lead to nonsmoothness as (local) optima are characterized by nonsmooth *complementarity conditions*.

On the other hand, it is well-known that certain infinitesimal plasticity problems, known under the name of *associated plasticity*, naturally lead to *convex minimization problems* after time discretization. This problem class can always be examined in a duality framework [**ET76**] which allows the formulation of a second minimization problem, the so-called dual problem. This structure has often been exploited, either in the context of reformulating the problem, or in showing well-posedness of models, see [**Tem85**] for *perfect plasticity* and [**HR99**] for *hardening plasticity*. But as stated above, with only a few exceptions [**KLSW06**, **Wie07**], this powerful framework has not been exploited when it comes to solution algorithms. To integrate associated plasticity into a general optimization framework is another motivation for this work.

A further concern of the thesis is *non-associated* plasticity. As indicated, these problems cannot be regarded as optimization problems but only admit an interpretation as a system of partial differential equations. These models are often more appropriate for materials in which plastic deformation is related to the applied mean stress (or hydrostatic pressure). Examples are soils, rocks, concrete, and certain polymers and foams. In these materials, the yield strength strongly depends on the mean stress, e.g. a soil cannot sustain large tensile stresses but strength increases under compression, so plastic deformation (or failure) is related to the applied mean stress. Contrary, in metal plasticity it is mostly assumed that volume changes are purely elastic (*plastic incompressibility*) as plastic deformation results from crystallographic defects. Without going to much into the details, the consequence is that plasticity models in metal plasticity are typically assumed to be associated, whereas models in soil mechanics often are non-associated. For the latter, less is known as most results are limited to associated models due to their richer mathematical structure. To give an example, as known to the author, an analysis of the generalized Newton method is limited to the associated model of *von Mises*, and one goal is to extend the analysis to more general situations including non-associated plasticity.

Even though the standard algorithm performs well in practice, a further objective of this thesis is to show how new algorithms can be designed and analyzed. As far as this is possible, we try to set up the analysis in function space. However, proofs of superlinear convergence can only be given in a discrete setting as proving superlinear convergence in function space would require certain smoothing properties of the involved operators. But in contrast to certain problems in *optimal control* [**IK08**, **HPUU09**], this is not the case

in plasticity. Nevertheless, if one does not insist on superlinear convergence, it is possible to show convergence in function space as we will demonstrate.

A short summary

The thesis is divided into three main parts and an appendix. The first part addresses modeling and well-posedness of the underlying boundary value problems. The second part, which is dedicated to solution algorithms and their numerical analysis, is the main part of the thesis. Finally, we report on the numerical performance of the presented algorithms and verify theoretical results in the third part. An appendix compiles some results from nonsmooth analysis. We will shortly comment on the individual chapters and highlight some results.

Part 1 – Aspects of Mathematical Plasticity. In detail, the first part is organized as follows: in Chapter 1, we give a short introduction to modeling questions. We motivate the two basic models considered henceforth: the associated model of *von Mises* and the non-associated *Drucker-Prager* model. This chapter also introduces necessary notation concerning the problems of elasto-plasticity but does not contain new results. Similarly, the subsequent Chapter 2 mainly serves to fix notation concerning the mathematical framework. After considering the elasticity problem in a convex duality framework, we adopt this setting to introduce the model of associated perfect plasticity in a static scenario. Though it is the simplest model from a modeling point of view, the situation changes when it comes to a mathematical analysis as the problem only admits solutions in a very weak sense [**Tem85**]. Solution in standard Sobolev spaces can be obtained by considering regularized models. Two such models are presented in Chapter 3 where we introduce the viscoplastic regularization (which essentially is the *Moreau-Yosida approximation* [**DL76**]) and kinematic hardening. Though these models are well-established and have a quite different physical motivation, we are able to show some new relations between the models. Particularly, we demonstrate that viscoplasticity can be interpreted as a specific instance of kinematic hardening in the static setting. This relation will often be exploited when we analyze solution algorithms. We close the chapter with a formulation of kinematic hardening as a variational inequality. This formulation is often attributed as the "primal problem" [**HR99**]. This notion is somewhat misleading from the standpoint of optimization theory, as the "dual problem" is not linked to this problem via Lagrangian duality. Rather, this problem is a result of a reformulation by means of convex analysis. We work out this relation in detail and thereby extend results given in [**GV09**] to a broader class of problems. Especially the relation between the "primal problem" and the "actual" primal problem (being in duality with the "dual" problem) seems to be unknown in the presented generality. To summarize: many results of this chapter are known in the literature in some way or the other, but until now, these results have not been stated in a unified framework which also allows the construction and analysis of solution algorithms.

Chapter 4 then introduces the boundary value problems of non-associated plasticity. After considering a more general setting, we concentrate on the non-associated Drucker-Prager model. Despite its simplicity, analytical results for the corresponding boundary value problem are not available in the literature. We are able to give conditions which assure the existence and uniqueness of a solution in standard Sobolev spaces. Unfortunately, these conditions are very restrictive as it turns out that in contrast to associated plasticity, arbitrary small amounts of regularization are not sufficient. Again, we present

a formulation which will allow us to treat non-associated plasticity in the same framework as associated plasticity concerning the algorithmic treatment. Though extensively used in engineering, as known to the author, the present work is the first to study non-associated Drucker-Prager plasticity from a mathematical point of view.

We close the first part with Chapter 5 where we turn to quasi-static problems. Since algorithmically, time-dependent plasticity is treated incrementally via time-discretization, we only summarize existence and uniqueness results and afterwards state the time-discrete incremental problems. Overall, the incremental problems have the same structure as the static problems. The only real difference is encountered in the viscoplastic regularization where the regularization parameter α has to be replaced by $\alpha \Delta t$. As a result, we can show that incremental non-associated Drucker-Prager viscoplasticity always has a solution if the time step size Δt is sufficiently small.

Part 2 – Aspects of Algorithmic Plasticity. The second part sets the focus on solution algorithms and their analysis and can therefore be seen as the main part. In order to set up discrete algorithms, there is a need to introduce a spatial discretization. Possible finite element discretizations are presented and discussed in Chapter 6, where also a short repetition of the continuous problems is presented. Particularly, we introduce the *response function* describing the material response. Closing with some remarks on the accuracy of the finite element method, this chapter mainly serves for notational purposes. In Chapter 7 we analyze the local convergence properties of the generalized Newton method for the displacement problem. As aforementioned, superlinear convergence can only been shown in the discrete setting and relies on the semismoothness of the response function. Criteria for the semismoothness of the response function can be found in Appendix A. After stating the abstract algorithm, we give general conditions for local superlinear/quadratic convergence. In the presented framework, it is possible to examine perfect plasticity, hardening plasticity and the viscoplastic regularization for both associated and non-associated plasticity by means of the response function. Furthermore, based on the response function, the generalization to even more sophisticated models is easily accessible. For illustration, we consider the examples of von Mises and Drucker-Prager plasticity. Whereas for the former, superlinear convergence is known to hold in a discrete setting, superlinear convergence results for the model of non-associated Drucker-Prager (and smoothed Drucker-Prager) have not been reported on up to now. Altogether, the results of Chapter 7 considerably extend the known results in the literature concerning superlinear convergence in the discrete setting. Moreover, as known to the author, it is the first time that convergence properties of the algorithm are examined rigorously for non-associated models.

In Chapter 8, we have a closer look at the algorithm from a computational point of view and present a variant which is amenable to implementation. Then, we turn to globalization techniques. While this is a non-trivial task for non-associated plasticity, the associated setting permits the usage of techniques from optimization theory. To be more precise, we are able to show global convergence of a gradient-related method in function space for the regularized methods of associated plasticity. In the discrete setting and if the response function is semismooth, this result can be extended to yield a globally and locally superlinear convergent method within the context of SC^1 minimization problems. As known to the author, this is the first global convergence result in a function space setting for problems in elasto-plasticity and the interpretation as an SC^1 minimization problem in the discrete setting also seems to be unknown in the literature.

While in the above mentioned chapters, the algorithms are based on the response function (which is implicitly defined in general), the *active set* method presented in Chapter 9 avoids the explicit computation of the response function. The active set method again is a generalized Newton method, but unlike to the displacement based methods, we also take into account the stress field and the plastic multiplier. For associated von Mises plasticity, a similar method was derived in [HW09], but our approach also comprises more general non-associated models and therefore introduces a new type of algorithm. Since the regularity of the plastic multiplier still is an actual research topic, we only present the method in the discrete setting. We are able to prove locally superlinear convergence of the active set method under reasonable assumptions. In the presented form, the algorithm is limited to (non-associated) perfect plasticity but the generalization to hardening plasticity is straight forward. In the associated setting, conditions for convergence can be relaxed and we also comment on the relation with the SQP method.

Though only introduced for perfect plasticity, the *Augmented Lagrangian* methods of Chapter 10 can also be extended to hardening plasticity. However, these methods are limited to associated plasticity as they heavily rely on the convex duality framework. The whole chapter is set up in a function space setting and is built upon the framework developed in [IK00]. Based on a *generalized Moreau-Yosida approximation*, we are able to show a new approximation result for perfect plasticity. This result contains the well-known approximation result of the viscoplastic regularization as a special case. Subsequently, the Augmented Lagrangian is introduced by means of the generalized Moreau-Yosida approximation and we consider first and second order methods. For the first order method, we prove linear convergence for a fixed penalty parameter if the perfectly plastic solution has extra regularity. The second order methods are closely related to the generalized Newton method of Chapter 7 and the active set method of Chapter 9. The Augmented Lagrangian methods also admit a nice physical interpretation as they directly incorporate stresses, displacements and the (incremental) plastic strains. To the knowledge of the author, the application of Augmented Lagrangian methods to plasticity problems within a function space setting has not been considered so far.

Part 3 – Verification and Performance of Numerical Methods. The algorithms of the second part were implemented in the parallel finite element software suite M++ [Wie04, Wie10] and in the third part, we examine the numerical performance. The part is divided into two chapters. Chapter 11 exclusively considers associated perfect plasticity for which all algorithms are applicable. Application to a benchmark problem allows a comparison of the methods. As it turns out, making use of the minimization structure allows to improve the standard algorithm significantly. Particularly, the Augmented Lagrangian method and the methods based on the globalization techniques of Chapter 8 seem to be stable methods as mesh-dependent behaviour was hardly noticed. Besides [Wie07], where an SQP method has been considered, our numerical study seems to be the first systematic algorithmic study taking into account the effect of mesh-dependence. Afterwards, we close with a numerically challenging three-dimensional example which also shows the efficiency of the used software package. The chapter demonstrates that exploiting the variational structure of associated plasticity leads to more robust algorithms. This robustness is absolutely necessary if the mesh size tends to zero.

Finally, Chapter 12 considers non-associated Drucker-Prager plasticity. We begin with a parameter study of the perfectly plastic model demonstrating the mesh-dependence of the non-associated material. This is to be expected due to the ill-posedness of the model in general. We also demonstrate the superlinear convergence of the generalized

Newton method and the active set method. Eventually, we turn to a three-dimensional slope failure problem. Based on the theoretical results of the first part, as a model we choose the viscoplastic regularization. Similarly to the example of Chapter 11, we show that large scale problems can be solved efficiently within the proposed parallel programming model. As known to the author, this is the first algorithmic stability study for non-associated plasticity which also takes into account the dependence on the mesh size.

Part 4 – Appendix. Appendix A is a compilation of results from nonsmooth analysis. In detail, we introduce necessary concepts like generalized derivatives, semismoothness and also comment on generalized Newton methods. Afterwards, we pay some special attention to the projection operator as it is of fundamental importance throughout the thesis. The final section of Appendix A can then be interpreted as a blueprint approach for showing semismoothness of response functions for general plasticity models. Appendix B finally illustrates the ill-posedness of non-associated plasticity by means of a finite dimensional (counter-) example.

Part 1

Aspects of Mathematical Plasticity

CHAPTER 1

MATHEMATICAL MODELING OF PLASTIC DEFORMATION

1. Review of Continuum Mechanics and Linear Elasticity

Throughout this work, we consider a body $\Omega \subset \mathbb{R}^d$, $d \in \{2,3\}$, representing the *reference configuration* (or *undeformed configuration*) of a continuous medium filling the whole space that it occupies without leaving any void space. For brevity of notation, we restrict ourselves to $d = 3$ in this presentation but with a few modifications, everything is valid also for $d = 2$. This continuous medium or continuum is made up of *particles* and by $x = (x_1, x_2, x_3) \in \Omega$, we denote its position in the reference configuration. Ω is assumed to be open and bounded with a piecewise smooth boundary $\partial\Omega$ and the closure is denoted by $\overline{\Omega} = \Omega \cup \partial\Omega$. As we are not only interested in the stationary behavior of Ω but also in the time-dependent behavior, we consider a time interval $[0, T] \subset \mathbb{R}_+$. During that time period, we are particularly interested in the evolution of the body Ω when subjected to various forces. Throughout this work, we will work in the *geometrically linear setting* which is why we only give a short introduction into the kinematics to clarify notation. There are numerous textbooks on continuum mechanics, and we only mention [**Gur81**, **DS02**, **Lub06**].

1.1. Linearized Kinematics. The evolution of the body Ω is described by a *motion*

$$\boldsymbol{\varphi} : \Omega \times [0, T] \longrightarrow \Omega_t \subset \mathbb{R}^3 \,,$$

mapping the *reference configuration* to the *current configuration* $\Omega_t = \boldsymbol{\varphi}(\Omega, t) \subset \mathbb{R}^3$. For fixed time t we also say that $\boldsymbol{\varphi}(\cdot, t)$ is a *deformation* and we will encounter many situations in which t can simply be seen as a parameter and therefore, we will omit the explicit dependence on t when appropriate. Similarly, when considering a fixed spatial point $x \in \Omega$, we may omit this variable.

Within the geometrically linear setting, it is convenient to work with the *displacement field*

$$\boldsymbol{u} : \Omega \times [0, T] \to \mathbb{R}^3 \,, \tag{1.1}$$

and the correspondence between the motion and the displacement field is given by

$$\boldsymbol{\varphi}(x, t) = x + \boldsymbol{u}(x, t) \,.$$

1.1.1. *The Infinitesimal Strain Tensor.* Basically, we can distinguish two types of motions. The first class does not change the shape of the body but rather moves it around in the ambient space. Such deformations are called rigid body motions and correspond to translations and rotations of the reference configuration. Analogously, we speak of rigid body displacements or rigid body deformations. The second class of motions is related with changes in the internal structure of the body, so-called *straining*. A strain is a geometrical measure for the relative displacement of particles in the body, or to put it in other words, it measures how much a given deformation locally differs from a rigid body deformation. This already suggests that the strain has to be related with the spatial derivative of the motion.

Considering a fixed spatial point $x \in \Omega$ which is therefore omitted, we define two tensors, being symmetric and antisymmetric, respectively, via

$$\boldsymbol{\varepsilon} = \mathrm{sym}(D\boldsymbol{u}) = \tfrac{1}{2}\Big(D\boldsymbol{u} + D\boldsymbol{u}^T\Big) \qquad \text{and} \qquad \boldsymbol{\omega} = \mathrm{skew}(D\boldsymbol{u}) = \tfrac{1}{2}\Big(D\boldsymbol{u} - D\boldsymbol{u}^T\Big).$$

Obviously $D\boldsymbol{u} = \boldsymbol{\varepsilon} + \boldsymbol{\omega}$ and looking at the definition, we see that $\boldsymbol{\varepsilon}$ and $\boldsymbol{\omega}$ can be interpreted as functions of the displacement vector $\boldsymbol{u}$ which is why we also write $\boldsymbol{\varepsilon}(\boldsymbol{u})$ or $\boldsymbol{\omega}(\boldsymbol{u})$. At this point, we introduce the set of symmetric and skew-symmetric second order tensors

$$\begin{aligned}
\mathrm{Sym}(3) &= \{A \in \mathbb{R}^{3,3} : A = A^T\}, \\
\mathrm{Skew}(3) &= \{A \in \mathbb{R}^{3,3} : A = -A^T\},
\end{aligned} \tag{1.2}$$

and we find $\boldsymbol{\varepsilon}(\boldsymbol{u}) \in \mathrm{Sym}(3)$ and $\boldsymbol{\omega}(\boldsymbol{u}) \in \mathrm{Skew}(3)$. The tensor $\boldsymbol{\varepsilon}$ is called the *(infinitesimal) strain tensor* and $\boldsymbol{\omega}$ the *(infinitesimal) rotation tensor*. If $|D\boldsymbol{u}| \ll 1$, the infinitesimal strain tensor $\boldsymbol{\varepsilon}$ is a good approximation to the *Green-Saint-Venant strain tensor*

$$\boldsymbol{E} = \frac{1}{2}\Big(D\boldsymbol{u} + D\boldsymbol{u}^T + D\boldsymbol{u}^T D\boldsymbol{u}\Big),$$

arising in the geometrically nonlinear setting. $\boldsymbol{E}$ is one possible measure of strain in the general geometrically nonlinear setting, cf. the discussion in [Lub06, Chapter 8]. The approximation of $\boldsymbol{E}$ by $\boldsymbol{\varepsilon}$ is reasonable if the magnitude of the deformation is small w.r.t. the diameter in which the deformation is observed. As indicated above, we will always assume that this is true, i.e. we only consider the infinitesimal setting.

Introducing the set of *rigid body displacements*

$$\mathcal{R} = \big\{\boldsymbol{u} : \Omega \to \mathbb{R}^3 : \boldsymbol{u}(x) = q + Ax, \ q \in \mathbb{R}^3, \ A \in \mathrm{Skew}(3)\big\},$$

we have the following result:

$$\boldsymbol{\varepsilon}(\boldsymbol{u}) = 0 \qquad \text{if and only if} \qquad \boldsymbol{u} \in \mathcal{R}.$$

This result justifies the usage of the infinitesimal strain tensor $\boldsymbol{\varepsilon}(\boldsymbol{u})$ as a measure of strain in the geometrically linearized regime as strains are invariant under rigid body deformations/displacements.

It remains to say that the motion $\boldsymbol{\varphi}$ (and therefore also the displacement $\boldsymbol{u}$) completely describes the strain tensor $\boldsymbol{\varepsilon}(\boldsymbol{u})$. However, it can be shown that a given symmetric tensor field is a strain tensor if it satisfies six so-called *strain compatibility conditions*, cf. [DS02, Section 1.5] or [Lub06, Section 1.2.4].

Written down component-by-component, we have

$$\varepsilon(\boldsymbol{u}) = \begin{bmatrix} \partial_{x_1}\boldsymbol{u}_1 & \frac{1}{2}(\partial_{x_2}\boldsymbol{u}_1 + \partial_{x_1}\boldsymbol{u}_2) & \frac{1}{2}(\partial_{x_3}\boldsymbol{u}_1 + \partial_{x_1}\boldsymbol{u}_3) \\ \frac{1}{2}(\partial_{x_1}\boldsymbol{u}_2 + \partial_{x_2}\boldsymbol{u}_1) & \partial_{x_2}\boldsymbol{u}_2 & \frac{1}{2}(\partial_{x_3}\boldsymbol{u}_2 + \partial_{x_2}\boldsymbol{u}_3) \\ \frac{1}{2}(\partial_{x_1}\boldsymbol{u}_3 + \partial_{x_3}\boldsymbol{u}_1) & \frac{1}{2}(\partial_{x_2}\boldsymbol{u}_3 + \partial_{x_3}\boldsymbol{u}_2) & \partial_{x_3}\boldsymbol{u}_3 \end{bmatrix}.$$

The diagonal entries of ε are the *extensional strains* into the individual directions and the sum of these values represents the change in volume. Therefore also note that

$$\mathrm{tr}(\boldsymbol{\varepsilon}) = \mathrm{tr}(\boldsymbol{\varepsilon}(\boldsymbol{u})) = \sum_{i=1}^{3}(\boldsymbol{\varepsilon}(\boldsymbol{u}))_{ii} = \sum_{i=1}^{3}\partial_{x_i}\boldsymbol{u}_i = \mathrm{div}\,\boldsymbol{u}.$$

The off-diagonal entries of ε are the *shear strains* representing internal changes of angles. Every tensor field ε can be decomposed into a volumetric and a deviatoric part by setting

$$\varepsilon = \tfrac{1}{3}\mathrm{tr}(\boldsymbol{\varepsilon})\mathbf{1} + \boldsymbol{\eta},$$

with a symmetric second order tensor $\boldsymbol{\eta}$ satisfying $\mathrm{tr}(\boldsymbol{\eta}) = 0$ and $\boldsymbol{\eta}$ is called the *deviator* of ε. Defining the deviatoric subspace

$$\mathrm{Sym}_0(3) = \{A \in \mathrm{Sym}(3) : \mathrm{tr}(A) = 0\}, \tag{1.3}$$

we obtain an orthogonal decomposition $\mathrm{Sym}(3) = \mathrm{Sym}_0(3) \oplus \mathbb{R}\,\mathbf{1}$, and we also write $\mathrm{dev}(\boldsymbol{\varepsilon}) = \boldsymbol{\varepsilon} - \tfrac{1}{3}\mathrm{tr}(\boldsymbol{\varepsilon})\mathbf{1} \in \mathrm{Sym}_0(3)$. Moreover, defining the fourth order tensors $\mathbb{P}_{\mathrm{vol}} = \tfrac{1}{3}\mathbf{1}\otimes\mathbf{1}$ and $\mathbb{P}_{\mathrm{dev}} = \mathbb{I} - \mathbb{P}_{\mathrm{vol}} = \mathbb{I} - \tfrac{1}{3}\mathbf{1}\otimes\mathbf{1}$ via

$$\mathbb{P}_{\mathrm{vol}}[\boldsymbol{\varepsilon}] = \tfrac{1}{3}\mathrm{tr}(\boldsymbol{\varepsilon})\mathbf{1} \qquad \text{and} \qquad \mathbb{P}_{\mathrm{dev}}[\boldsymbol{\varepsilon}] = \boldsymbol{\varepsilon} - \tfrac{1}{3}\mathrm{tr}(\boldsymbol{\varepsilon})\mathbf{1}, \tag{1.4}$$

we obtain the corresponding orthogonal projectors, i.e.

$$\mathbb{P}_{\mathrm{vol}}^2 = \mathbb{P}_{\mathrm{vol}}, \qquad \mathbb{P}_{\mathrm{dev}}^2 = \mathbb{P}_{\mathrm{dev}}, \qquad \mathbb{P}_{\mathrm{vol}} \circ \mathbb{P}_{\mathrm{dev}} = \mathbb{P}_{\mathrm{dev}} \circ \mathbb{P}_{\mathrm{vol}} = 0.$$

1.2. Equilibrium of Forces.

1.2.1. *Forces and the Traction Vector.* We can basically distinguish two classes of forces acting on Ω_t. On the one hand, there are body forces acting on the current configuration Ω_t. The most common representative of this class of forces is gravity but there are also other examples like the electromagnetic forces. Since these forces act inside the body, they are mostly related with mass or volume.

The second class consists of contact forces which are related with surfaces rather than with volumes. Considering an infinitesimal small surface element da around x which is contained in the deformed configuration Ω_t, the corresponding force acting on da is denoted by $d\boldsymbol{f}$. If da is in the interior of Ω_t, $d\boldsymbol{f}$ is just the result of the action of the body on itself. However, if $da \subset \partial\Omega$, then the contact force $d\boldsymbol{f}$ results from some external interaction and in the simplest case, this force is known in advance. As da was assumed to be an infinitesimal small surface element, we can consider the limiting case and the resulting vector $\boldsymbol{t}(x) = \frac{d\boldsymbol{f}}{da}$ is called the *traction vector*. Of course, with an actual application in mind, the above limit has to be handled with care since it only makes sense within the continuum description.

The above definition of the traction vector strongly depends on the surface element da since a surface element around x with a different orientation would lead to a different traction vector. This gives rise to the definition of the traction vector as a function of the normal $\boldsymbol{n}(x)$ of the surface element da passing through x, i.e.

$$\boldsymbol{t} : S^2 \times \Omega_t \times [0, T] \to \mathbb{R}^3,$$

where $S^2 = \{y \in \mathbb{R}^3 : |y| = 1\}$ is the surface of the Euclidean unit sphere in $\mathbb{R}^3$. Essentially, Cauchy postulated the existence of such a vector field and physically, $\boldsymbol{t}(\boldsymbol{n}(x), x, t)$ is the force per unit area exerted on a surface element with normal $\boldsymbol{n}(x)$.

1.2.2. *Balance Equations and the Cauchy Stress Tensor.* Considering any part $\omega \subset \Omega$ of the body, we denote by $\omega_t = \boldsymbol{\varphi}(\omega, t)$ the corresponding part in the current configuration. Further, let $\rho : \Omega_t \times [0, T] \to \mathbb{R}$ be the material density and $\boldsymbol{b} : \Omega_t \times [0, T] \to \mathbb{R}^3$ the prescribed body force. Then, the balance of (linear) momentum is satisfied if for every $\omega_t \subset \Omega_t$

$$\int_{\omega_t} \rho(x, t)\, \ddot{\boldsymbol{u}}(x, t)\, dx = \int_{\omega_t} \boldsymbol{b}(x, t)\, dx + \int_{\partial \omega_t} \boldsymbol{t}(\boldsymbol{n}(x), x, t)\, da\,, \tag{1.5}$$

where $\boldsymbol{n}(x)$ is the outward normal to ω_t.

Similarly, the *balance of angular momentum* or *balance of moment of momentum* is satisfied whenever

$$\int_{\omega_t} \rho(x, t)\, (x \times \ddot{\boldsymbol{u}}(x, t))\, dx = \int_{\omega_t} \rho(x, t)(x \times \boldsymbol{b}(x, t))\, dx + \int_{\partial \omega_t} x \times \boldsymbol{t}(\boldsymbol{n}, x, t)\, da\,. \tag{1.6}$$

It remains to determine how the traction vector $\boldsymbol{t}$ depends on the normal vector $\boldsymbol{n}$ and this question was answered already in 1823 by *Cauchy's Theorem* stating that there is a symmetric tensor field $\boldsymbol{\sigma} : \Omega_t \times [0, T] \to \operatorname{Sym}(3)$, called the *Cauchy stress tensor* such that for every $(x, t) \in \Omega_t \times [0, T]$:

(1) for each $\boldsymbol{n}(x) \in S^2$: $\boldsymbol{t}(\boldsymbol{n}(x), x, t) = \boldsymbol{\sigma}(x, t)\boldsymbol{n}(x)$.
(2) $\boldsymbol{\sigma}$ satisfies the *equation of motion*

$$\rho(x, t)\ddot{\boldsymbol{u}}(x, t) - \operatorname{div}\boldsymbol{\sigma}(x, t) = \rho(x, t)\boldsymbol{b}(x, t)\,.$$

If we work in the linearized regime, we can identify Ω with Ω_t and consequently, the stress tensor $\boldsymbol{\sigma}$ is defined in the reference configuration, i.e.

$$\boldsymbol{\sigma} : \Omega \times [0, T] \to \operatorname{Sym}(3)\,. \tag{1.7}$$

Likewise, the density ρ does no longer depend on t and we can replace $\rho(x, t)$ by $\rho_0(x)$ with ρ_0 being the reference density at time $t = 0$. With this modifications, the equation of motion reduces to

$$\rho_0(x)\ddot{\boldsymbol{u}}(x, t) - \operatorname{div}\boldsymbol{\sigma}(x, t) = \boldsymbol{b}(x, t)\,, \tag{1.8}$$

where without renaming, we absorbed the density ρ_0 into $\boldsymbol{b}$. In the geometrically nonlinear setting, the Cauchy stress tensor on the current configuration can be pulled back onto the reference configuration by the first and second *Piola-Kirchhoff tensors*.

1.2.3. *Static and Quasi-Static Processes.* The above equation of motion includes the acceleration $\ddot{\boldsymbol{u}}$. In many relevant applications however, like in a slow loading process, inertial effects can be neglected due to the internal time scales of the application. So it might be reasonable to neglect the acceleration even though the problem itself is time-dependent. We group the considered problems into three classes.

(1) Static: inertial effects can be neglected and the data is not time-dependent.
(2) Quasi-static: inertial effect can be neglected but the data is not independent of time.
(3) Dynamic: inertial effects can not be neglected.

In a quasi-static setting, the equation of motion (1.8) is replaced by the *equilibrium equation*

$$-\operatorname{div}\boldsymbol{\sigma}(x, t) = \boldsymbol{b}(x, t)\,. \tag{1.9}$$

1.3. Thermodynamic Considerations. Since plasticity is best described in the framework of thermodynamics (with internal variables), we briefly introduce some basic notation. The concept of internal variables will be introduced when we turn to plasticity in the next section. A by far more elaborate exposition can be found in nearly all textbooks covering that topic, e.g. [**BdC05**]. Concerning plasticity, we refer to [**Lem00**, Chapter 2].

1.3.1. *The First and Second Law of Thermodynamics.* The first law of thermodynamics essentially states a balance of energy. Therefore, we define the *internal specific energy* by $e : \Omega \times [0,T] \to \mathbb{R}$ which may also have functional dependences w.r.t. other fields under consideration. Moreover, the heat source is defined by $s : \Omega \times [0,T] \to \mathbb{R}$ and similar to the definition of the traction vector, we can define a surface heat $g : S^2 \times \Omega \times [0,T] \to \mathbb{R}$ which gives rise to the heat flux $\boldsymbol{q} : \Omega \times [0,T] \to \mathbb{R}^3$ such that $g(\boldsymbol{n}(x), x, t) = \boldsymbol{q}(x,t) \cdot \boldsymbol{n}(x)$. Altogether, for an arbitrary part of the body $\omega \subset \Omega$, the first law is given as

$$
\frac{\partial}{\partial t} \int_\omega \rho_0(x)\big(e(x,t) + \tfrac{1}{2}|\dot{\boldsymbol{u}}(x,t)|^2\big)\, dx = \int_\omega \big(\boldsymbol{b}(x,t) \cdot \dot{\boldsymbol{u}}(x,t) + s(x,t)\big)\, dx
$$
$$
+ \int_{\partial\omega} \big(\boldsymbol{\sigma}(x,t)\boldsymbol{n}(x) + \boldsymbol{q}(x,t) \cdot \boldsymbol{n}(x)\big)\, da \,,
$$

or in words: the rate of total energy, i.e. internal energy and kinematic energy, is equal to the applied mechanical and thermal forces.

By the *mechanical work identity*

$$
\frac{\partial}{\partial t} \int_\omega \tfrac{1}{2}\rho_0(x)|\dot{\boldsymbol{u}}(x,t)|^2\, dx = - \int_\omega \boldsymbol{\sigma}(x,t) : \boldsymbol{\varepsilon}(\dot{\boldsymbol{u}}(x,t))\, dx + \int_\omega \boldsymbol{b}(x,t) \cdot \dot{\boldsymbol{u}}(x,t)\, dx
$$
$$
+ \int_{\partial\omega} \boldsymbol{\sigma}(x,t)\boldsymbol{n}(x)\, da \,,
$$

(resulting from the equation of motion (1.8) by multiplying with $\dot{\boldsymbol{u}}$, integrating over ω, applying the theorem of Gauss and using $\int_\omega \rho\ddot{\boldsymbol{u}} \cdot \dot{\boldsymbol{u}}\, dx = \frac{\partial}{\partial t}\int_\omega \tfrac{1}{2}\rho|\dot{\boldsymbol{u}}|^2\, dx$), as well as applying the theorem of Gauss applied with respect to the heat flux, we obtain the energy balance

$$
\frac{\partial}{\partial t} \int_\omega \rho_0(x)e(x,t)\, dx = \int_\omega \big(\boldsymbol{\sigma}(x,t) : \boldsymbol{\varepsilon}(\dot{\boldsymbol{u}}(x,t)) + s(x,t) - \operatorname{div}\boldsymbol{q}(x,t)\big)\, dx \,,
$$

or for short in local form

$$
\rho\dot{e} = \boldsymbol{\sigma} : \dot{\boldsymbol{\varepsilon}} + s - \operatorname{div}\boldsymbol{q} \,.
$$

The second law of thermodynamics is based on the notion of *entropy* $\eta : \Omega \times [0,T] \to \mathbb{R}$ and *absolute temperature* $\vartheta : \Omega \times [0,T] \to \mathbb{R}$, and states that

$$
\frac{\partial}{\partial t} \int_\omega \rho_0(x)\eta(x,t)\, dx \geq \int_\omega \vartheta^{-1}(x,t)\, s(x,t)\, dx + \int_{\partial\omega} \vartheta^{-1}(x,t)\boldsymbol{q}(x,t) \cdot \boldsymbol{n}(x)\, da \,,
$$

of for short in local form: $\rho_0\dot{\eta} \geq \vartheta^{-1}s - \operatorname{div}(\vartheta^{-1}\boldsymbol{q})$. The above inequality is also referred to as the *Clausius-Duhem inequality*.

Introducing the *(Helmholtz) free energy* $\mathcal{W} : \Omega \times [0,T] \to \mathbb{R}$, $\mathcal{W} = e - \eta\vartheta$, which may as well have additional functional dependencies, the energy balance and the Clausius-Duhem inequality lead to the *(local) dissipation inequality*

$$
\rho_0(\dot{\mathcal{W}} + \eta\dot{\vartheta}) - \boldsymbol{\sigma} : \dot{\boldsymbol{\varepsilon}} + \vartheta^{-1}\boldsymbol{q} \cdot \nabla\vartheta \leq 0 \,, \qquad \text{(non-isothermal)},
$$
$$
\rho_0\dot{\mathcal{W}} - \boldsymbol{\sigma} : \dot{\boldsymbol{\varepsilon}} \leq 0 \,, \qquad \text{(isothermal)}. \tag{1.10}
$$

In the following, we will always consider isothermal conditions, i.e. $\vartheta \equiv const$.

1.4. Linear Elasticity. Under isothermal conditions, concerning linear elasticity, the free energy $\mathcal{W}$ is assumed to be a quadratic function depending on the strain ε but not on time, i.e. $\mathcal{W} \equiv \mathcal{W}(\varepsilon, x)$. Substituting $\varepsilon(x,t)$ into this expression yields

$$\mathcal{W} \equiv \mathcal{W}(\varepsilon(x,t),x) = \frac{1}{2\rho_0(x)}\mathbb{C}(x)[\varepsilon(x,t)] : \varepsilon(x,t)\,,$$

with the symmetric fourth order *elasticity tensor* $\mathbb{C}(x) : \mathrm{Sym}(3) \to \mathrm{Sym}(3)$ which may depend on the spatial point x but not on time t. In the case of a homogeneous and isotropic body, we have the representation

$$\rho_0\mathcal{W} \equiv \rho_0\mathcal{W}(\varepsilon) = \tfrac{1}{2}\mathbb{C}[\varepsilon] : \varepsilon = \mu\,|\varepsilon|^2 + \tfrac{1}{2}\lambda\,\mathrm{tr}(\varepsilon)^2 = \mu|\,\mathrm{dev}(\varepsilon)|^2 + \tfrac{1}{2}\kappa\,\mathrm{tr}(\varepsilon)^2$$

with the *shear modulus* μ, the *Lamé constant* λ and the *bulk modulus* $\kappa = \lambda + \tfrac{2}{3}\mu$. This gives the representation of $\mathbb{C}$ as

$$\mathbb{C} = 2\mu\mathbb{I} + \lambda\mathbf{1}\otimes\mathbf{1} = 2\mu\mathbb{P}_{\mathrm{dev}} + 3\kappa\mathbb{P}_{\mathrm{vol}}\,, \tag{1.11a}$$

and the orthogonal decomposition (1.4) allows to easily invert $\mathbb{C}$ such that

$$\mathbb{C}^{-1} = \frac{1}{2\mu}\mathbb{P}_{\mathrm{dev}} + \frac{1}{3\kappa}\mathbb{P}_{\mathrm{vol}}\,. \tag{1.11b}$$

Taking the total differential of $\mathcal{W} \equiv \mathcal{W}(\varepsilon(x,t),x)$ w.r.t. time, we find

$$\dot{\mathcal{W}} = D_\varepsilon\mathcal{W}(\varepsilon(x,t)) : \dot{\varepsilon}(x,t)\,,$$

and substitution into the local dissipation inequality (1.10) gives

$$\Big(\rho_0(x)D_\varepsilon\mathcal{W}(\varepsilon(x,t)) - \boldsymbol{\sigma}(x,t)\Big) : \varepsilon(x,t) \leq 0\,.$$

Hence, we observe that taking

$$\boldsymbol{\sigma}(x,t) = \rho_0(x)D_\varepsilon\mathcal{W}(\varepsilon(x,t)) = \mathbb{C}[\varepsilon(x,t)] \tag{1.12}$$

automatically leads to a thermodynamic admissible *constitutive law* relating stresses and strains. In the more general geometrically nonlinear setting, whenever the stress tensor $\boldsymbol{\sigma}$ is derived as the derivative of the free energy, the constitutive (or stress-strain) law is called *hyper-elastic*. Then, the elasticity tensor is the linearization when the residual stress vanishes, cf. [**Gur81, MH94**], and linear elasticity is simply the result of linearization rather than a constitutive relation.

2. Plastic Deformation

A major difference between elasticity and plasticity is the irreversible nature of plastic deformation. Contrary to plasticity, elastic processes are reversible in the sense that after unloading, there are no remanent strains in the body. We also say that elasticity is not path-dependent, whereas plasticity is indeed path-dependent since in order to determine the actual state of the body, it is necessary to know its deformation history. An indication for reversibility in elasticity can also be seen from the local dissipation inequality (1.10), since $\boldsymbol{\sigma} = D_\varepsilon\mathcal{W}(\varepsilon)$ always gives zero dissipation.

2.1. Thermodynamic Framework for Plasticity.

2.1.1. *Admissible Stress States and the Plastic Strain Tensor.* For convenience and brevity of notation, we consider isothermal conditions and neglect the explicit dependence on x and t. Hence, the local dissipation inequality is given as $\rho_0 \dot{\mathcal{W}} - \boldsymbol{\sigma} : \dot{\boldsymbol{\varepsilon}} \leq 0$. Concerning linear elasticity, due to the linear relationship $\boldsymbol{\sigma} = \mathbb{C}[\boldsymbol{\varepsilon}(\boldsymbol{u})]$, the stress is formally unlimited. This is not a reasonable property for all materials since typically, material will fail in one or the other way if the stresses are too large. In order to describe plastic effects, we require the stress tensor to be admissible in a certain sense, and henceforth, admissibility is described by the abstract constraint $\boldsymbol{\sigma} \in K$. The set $K \subset \mathrm{Sym}(3)$ is assumed to be a convex subset of the symmetric second order tensors. The actual shape of K strongly depends on the material and also on the application. A consequence of the admissibility constraint is that Hooke's law has to be modified since $\boldsymbol{\sigma} = \mathbb{C}[\boldsymbol{\varepsilon}(\boldsymbol{u})]$ can no longer be valid in general. In order to cope with this, we impose an *additive decomposition* of the (total) strain tensor $\boldsymbol{\varepsilon}(\boldsymbol{u})$ into an elastic and a plastic part, i.e.

$$\boldsymbol{\varepsilon} = \boldsymbol{\varepsilon}(\boldsymbol{u}) = \boldsymbol{\varepsilon}_e + \boldsymbol{\varepsilon}_p \,. \tag{1.13}$$

The *elastic strain tensor* and the *plastic strain tensor* are formally given by

$$\boldsymbol{\varepsilon}_e : \Omega \times [0, T] \to \mathrm{Sym}(3) \qquad \text{and} \qquad \boldsymbol{\varepsilon}_p : \Omega \times [0, T] \to \mathrm{Sym}(3) \,. \tag{1.14}$$

The plastic strain tensor $\boldsymbol{\varepsilon}_p$ corresponds to the permanent strain after relaxation and we have $\boldsymbol{\varepsilon}_p = 0$ in elasticity due to the reversible nature of the elasticity problem. In this case, the elastic strain $\boldsymbol{\varepsilon}_e$ and the total strain $\boldsymbol{\varepsilon}(\boldsymbol{u})$ coincide and we have $\boldsymbol{\sigma} = \mathbb{C}[\boldsymbol{\varepsilon}_e]$. Using the additive decomposition (1.13) then results in

$$\boldsymbol{\sigma} = \mathbb{C}[\boldsymbol{\varepsilon}_e] = \mathbb{C}[\boldsymbol{\varepsilon}(\boldsymbol{u}) - \boldsymbol{\varepsilon}_p] \,, \tag{1.15}$$

which is the stress-strain law we will use in the context of plasticity.

2.1.2. *Internal Variables.* The above concept can be extended even further by introducing internal variables $\boldsymbol{\delta} : \Omega \times [0, T] \to \mathbb{R}^s$. These internal variables may change from application to application and often cannot be measured directly. Including internal variables, the free energy has the form $\mathcal{W} \equiv \mathcal{W}(\boldsymbol{\varepsilon}_e, \boldsymbol{\delta})$. For the total time derivative we obtain

$$\dot{\mathcal{W}} = D_{\boldsymbol{\varepsilon}_e} \mathcal{W}(\boldsymbol{\varepsilon}_e, \boldsymbol{\delta}) : \dot{\boldsymbol{\varepsilon}}_e + D_{\boldsymbol{\delta}} \mathcal{W}(\boldsymbol{\varepsilon}_e, \boldsymbol{\delta}) \cdot \dot{\boldsymbol{\delta}}$$

and substitution into the local dissipation inequality then gives

$$0 \geq \rho_0 \dot{\mathcal{W}} - \boldsymbol{\sigma} : \dot{\boldsymbol{\varepsilon}} = \left(\rho_0 D_{\boldsymbol{\varepsilon}_e} \mathcal{W}(\boldsymbol{\varepsilon}_e, \boldsymbol{\delta}) - \boldsymbol{\sigma} \right) : \dot{\boldsymbol{\varepsilon}}_e - \boldsymbol{\sigma} : \dot{\boldsymbol{\varepsilon}}_p + \rho_0 D_{\boldsymbol{\delta}} \mathcal{W}(\boldsymbol{\varepsilon}_e, \boldsymbol{\delta}) \cdot \dot{\boldsymbol{\delta}} \,.$$

Introducing the thermodynamic forces $\boldsymbol{\zeta} : \Omega \times [0, T] \to \mathbb{R}^s$, conjugate to the internal variables by setting

$$\boldsymbol{\zeta} = -\rho_0 D_{\boldsymbol{\delta}} \mathcal{W}(\boldsymbol{\varepsilon}_e, \boldsymbol{\delta}) \,,$$

and using $\boldsymbol{\sigma} = \rho_0 D_{\boldsymbol{\varepsilon}_e} \mathcal{W}(\boldsymbol{\varepsilon}_e, \boldsymbol{\delta})$, the local dissipation inequality reduces to

$$\boldsymbol{\sigma} : \dot{\boldsymbol{\varepsilon}}_p + \boldsymbol{\zeta} \cdot \dot{\boldsymbol{\delta}} \geq 0 \,.$$

2.1.3. *The Relation between $\boldsymbol{\sigma}$ and $\boldsymbol{\varepsilon}_p$.* As we have introduced the plastic strain as a further unknown, we also need a functional relationship between the stress and the plastic strain. It turns out that it is not appropriate to impose a relation between $\boldsymbol{\sigma}$ and $\boldsymbol{\varepsilon}_p$ but rather to relate the stress $\boldsymbol{\sigma}$ and the *plastic strain rate* $\dot{\boldsymbol{\varepsilon}}_p$. The same holds true for the thermodynamic forces $\boldsymbol{\zeta}$ conjugate to the internal variables $\boldsymbol{\delta}$. Before we address the question how this relationship actually looks like, we shortly consider some examples for the admissible set K.

2.2. Plastic Behavior of Metals and Geo-Materials. As outlined above, the admissible set $K \subset \mathrm{Sym}(3)$ strongly depends on the material and the application in mind. We give simple examples for plasticity of ductile metals and for plasticity observed in Geomechanics and/or granular material. We restrict ourselves to isotropic plasticity, and in this case, the convex set K can be characterized in terms of the eigenvalues of $\boldsymbol{\sigma}$.

As we only aim to give a short summary, we refer the reader to texts like [**Lem00, DS02, PZ99**] and we only give further references concerning special topics.

2.2.1. *The Principal Stress Space.* In case of isotropy, the stress tensor $\boldsymbol{\sigma}$ can be fully characterized by its eigenvalues. Since $\boldsymbol{\sigma}$ is symmetric, there are three real eigenvalues $\sigma_1 \geq \sigma_2 \geq \sigma_3$ called the *principal stresses*. Based upon the principal stresses, we define the set of *principal invariants* $\mathcal{J}_{\boldsymbol{\sigma}} = \{\iota_{\boldsymbol{\sigma}}^1, \iota_{\boldsymbol{\sigma}}^2, \iota_{\boldsymbol{\sigma}}^3\}$ via

$$\iota_{\boldsymbol{\sigma}}^1 = \mathrm{tr}(\boldsymbol{\sigma}) = \sigma_1 + \sigma_2 + \sigma_3 \,,$$
$$\iota_{\boldsymbol{\sigma}}^2 = \tfrac{1}{2}\big(\mathrm{tr}(\boldsymbol{\sigma})^2 - \mathrm{tr}(\boldsymbol{\sigma}^2)\big) = \sigma_1\sigma_2 + \sigma_2\sigma_3 + \sigma_3\sigma_1 \,,$$
$$\iota_{\boldsymbol{\sigma}}^3 = \det(\boldsymbol{\sigma}) = \sigma_1\sigma_2\sigma_3 \,,$$

which are the coefficients of the normalized characteristic polynomial $\det(\boldsymbol{\sigma} - \sigma\mathbf{1})$. Thus we see that the set of invariants $\mathcal{J}_{\boldsymbol{\sigma}}$ can be used as well for the characterization of K.

Based on the principal invariants $\mathcal{J}_{\boldsymbol{\sigma}}$ we can derive further invariants. Important examples are

$$p_{\boldsymbol{\sigma}} = \tfrac{1}{3}\iota_1(\boldsymbol{\sigma}) = \tfrac{1}{3}\mathrm{tr}(\boldsymbol{\sigma}) = \tfrac{1}{3}(\sigma_1 + \sigma_2 + \sigma_3) \,,$$
$$J_{\boldsymbol{\sigma}}^2 = \tfrac{1}{2}|\mathrm{dev}(\boldsymbol{\sigma})|^2 = \tfrac{1}{3}\iota_1(\boldsymbol{\sigma})^2 - \iota_2(\boldsymbol{\sigma}) \qquad \text{or} \qquad q_{\boldsymbol{\sigma}} = \sqrt{3\,J_{\boldsymbol{\sigma}}^2} = \sqrt{\tfrac{3}{2}}|\mathrm{dev}(\boldsymbol{\sigma})| \,.$$

Here $p_{\boldsymbol{\sigma}}$ corresponds to the *mean stress* or *hydrostatic pressure*, while $q_{\boldsymbol{\sigma}}$ is the *equivalent tensile stress*. At this point, we also make the following *sign convention*: tensile stresses and tensile strains are positive.

Coming back to the principal stress space, the corresponding eigenvectors form an orthonormal basis of $\mathbb{R}^3$ and the coordinate system with these vectors as axes form the principal stress space. In principal stress space, the (principal) diagonal corresponds to isotropic stress (compressive or tensile), i.e. $\sigma_1 = \sigma_2 = \sigma_3$ and for fixed mean stress, the surface normal to the diagonal is the *deviatoric plane*. This gives rise to a new coordinate system in principal stress space being characterized by the three invariants $(\tilde{p}_{\boldsymbol{\sigma}}, \tilde{q}_{\boldsymbol{\sigma}}, \theta_{\boldsymbol{\sigma}})$ given by

$$\tilde{p}_{\boldsymbol{\sigma}} = \tfrac{1}{\sqrt{3}}\iota_1(\boldsymbol{\sigma}) \,, \qquad \tilde{q}_{\boldsymbol{\sigma}} = \sqrt{\tfrac{2}{3}}q_{\boldsymbol{\sigma}} = |\mathrm{dev}(\boldsymbol{\sigma})| \,, \qquad \cos(3\theta_{\boldsymbol{\sigma}}) = \tfrac{3\sqrt{3}}{2}\frac{\iota_3(\mathrm{dev}(\boldsymbol{\sigma}))}{(J_{\boldsymbol{\sigma}}^2)^{3/2}} \,.$$

Here $\tilde{p}_{\boldsymbol{\sigma}}$ is the distance of the origin to the deviatoric plane, and $\tilde{q}_{\boldsymbol{\sigma}}$ and $\theta_{\boldsymbol{\sigma}}$ are polar coordinates in the deviatoric plane with the origin being the intersection of the diagonal with the deviatoric plane. To be more precise, $\tilde{q}_{\boldsymbol{\sigma}}$ is the distance of the stress state to the diagonal and $\theta_{\boldsymbol{\sigma}}$ denotes a corresponding angle, the so-called *Lode angle*. The magnitude of the Lode angle $\theta_{\boldsymbol{\sigma}} \in [0, \tfrac{1}{3}\pi]$ gives information about the magnitude of the intermediate principal stress σ_2 in comparison to the major and minor principal stresses σ_1 and σ_3.

2.2.2. *Simple Plasticity Models for Ductile Metals.* Plastic behavior in metal is mainly observed when the *shear stress* reaches a critical value, whereas isotropic stress does not result in plastic behavior. Thinking in terms of the principal stress space, this suggests that plastic behavior is independent of the actual mean stress, so K is a infinitely long prism, whose shape is determined in the deviatoric plane. Introducing $\widehat{K} \subset \mathrm{Sym}_0(3)$, we
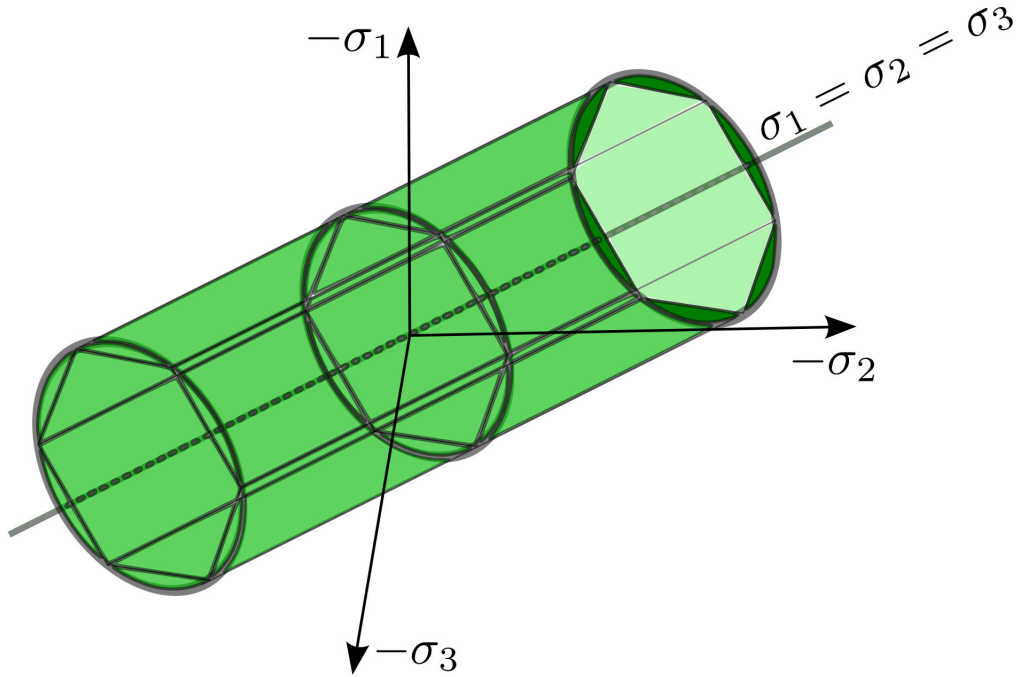
FIGURE 1.1. The admissible sets of Tresca and von Mises plasticity in principal stress space.

obtain the representation

$$K = \{\boldsymbol{\sigma} \in \mathrm{Sym}(3) : \mathrm{dev}(\boldsymbol{\sigma}) \in \widehat{K}\}. \tag{1.16}$$

Moreover, volumetric strains are typically assumed to be purely elastic, i.e. there are no volumetric plastic strains, and this leads to the notion of *incompressible plasticity*. A first example of the set K is

$$K = \{\boldsymbol{\sigma} \in \mathrm{Sym}(3) : \sigma_1 - \sigma_3 \le \sigma_T\},$$

for a given $\sigma_T > 0$ and eigenvalues $\sigma_1 \ge \sigma_2 \ge \sigma_3$. This model was proposed by *Tresca* in 1864 and in the deviatoric plane, the surface of $\widehat{K}$ is a regular hexagon.

A similar model that is only limiting the admissible shear stress was given by *von Mises*. The model is obtained by

$$K = \{\boldsymbol{\sigma} \in \mathrm{Sym}(3) : q_{\boldsymbol{\sigma}} \le \sigma_Y\},$$

with $\sigma_Y > 0$ being the yield stress. In this case, $\widehat{K}$ is just the scaled unit sphere in $\mathrm{Sym}_0(3)$ and thus in the deviatoric plane, the yield surface is a circle. The model is also attributed as J^2-plasticity since it only depends on the second invariant of the stress deviator. In Figure 1.1, the admissible sets are shown in principal stress space for both von Mises and Tresca plasticity.

2.2.3. *Simple Plasticity Models for Cohesive, Frictional Materials.* Whereas in simple plasticity models for metals, plastic behavior is generally not dependent on the mean stress, the situation changes when we consider cohesive, frictional materials like soil. We have to mention that for saturated soil, the *effective stress* concept comes into play accounting for the contribution of the pore water pressure as well. However, we will not go into details but refer to [**Ehl02, dB00, Cou04**] where these concepts are presented elaborately.

The first plasticity model for a soil was proposed by *Coulomb* in 1773. He wrote a failure criterion for a soil as $\tau = c - p \tan \phi$ where τ and p are the shear and normal (effective)
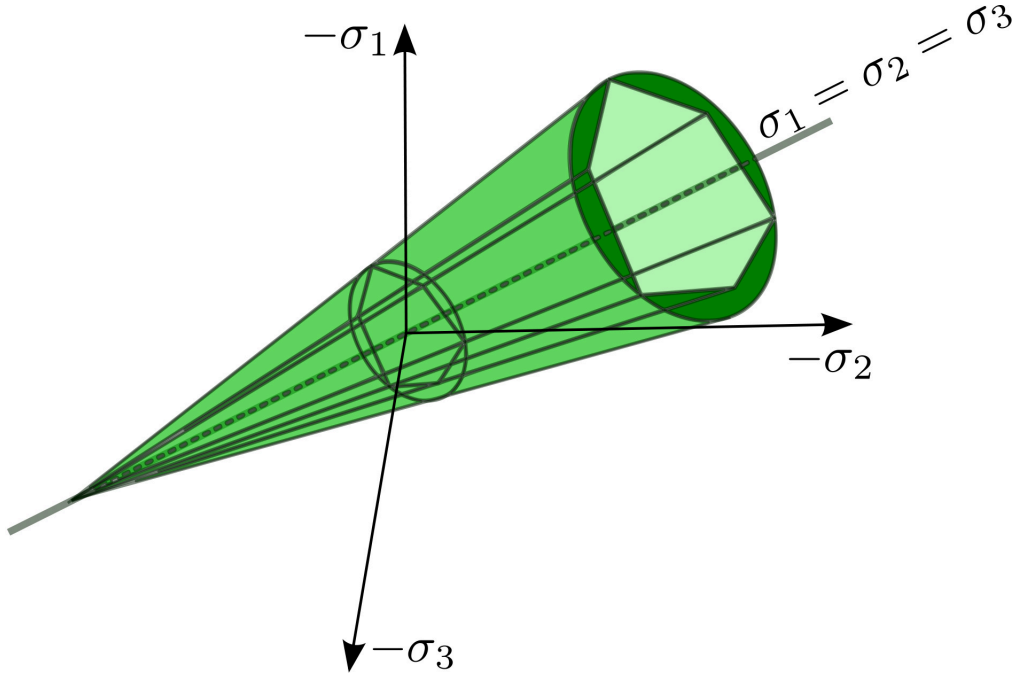
FIGURE 1.2. The admissible sets of Mohr-Coulomb and Drucker-Prager plasticity in principal stress space.

stress on the failure plane. The materials constants c and ϕ are related with the cohesion and the friction angle. This failure criterion defines the admissible set in the sense of *Mohr-Coulomb* as

$$K = \{\boldsymbol{\sigma} \in \mathrm{Sym}(3) : \sigma_1(1 - \sin\phi) - \sigma_3(1 + \sin\phi) \leq 2c\cos\phi\},$$

where again $\sigma_1 \geq \sigma_2 \geq \sigma_3$ are the eigenvalues of $\boldsymbol{\sigma}$. We see that the admissible set only relies on the major and the minor principal stress and the boundary of K in the deviatoric plane is again a hexagon. But due to the occurrence of the friction angle, the hexagon is not regular. As K depends on the mean stress, K is a hexagonal cone with vertex $\sqrt{3}c\cot\phi\,\mathbf{1}$. Note that if $\phi = 0$, K becomes the admissible set of Tresca with $\sigma_T = 2c$ and K is no longer a cone but has infinite length.

Analogously to the pair of Tresca and von Mises, we obtain the admissible set of *Drucker-Prager* by setting

$$K = \{\boldsymbol{\sigma} \in \mathrm{Sym}(3) : q_{\boldsymbol{\sigma}} - k_0(c - \tan\phi\, p_{\boldsymbol{\sigma}}) \leq 0\}$$

where again c and ϕ are related with the cohesion and the friction angle, respectively. Furthermore, k_0 is a material constant. In principal stress space, K is a circular cone and if $\phi = 0$, K becomes the infinitely long cylinder of von Mises with $\sigma_Y = k_0\, c$. The parameter k_0 can be used to adjust the radius of the yield surface in the deviatoric plane w.r.t. the Mohr-Coulomb hexagon, e.g. for $k_0 = \frac{3\sqrt{2}}{\sqrt{9 + 12\tan^2\phi}}$, the Drucker-Prager cone is the inner tangential cone to the Mohr-Coulomb pyramid, see [**BCDS01**].

In both models, large tensile stresses lead to failure, and for vanishing cohesion $c = 0$, we find $0 \in \partial K$, i.e. the body Ω cannot sustain any tensile stresses. The shape of the admissible sets is shown in Figure 1.2. In that figure, k_0 is chosen such that in the deviatoric plane, the Mohr-Coulomb hexagon is inscribed in the Drucker-Prager circle.

2.2.4. *Hardening Rules.* The most prominent internal variables are related with hardening laws altering the shape of the admissible set. We distinguish between *isotropic* and *kinematic hardening*. Whereas isotropic hardening changes the diameter of the admissible set isotropically, kinematic hardening rather translates the admissible set in $\mathrm{Sym}(3)$. The isotropic expansion (or shrinking) of the admissible set can be characterized by a single scalar hardening parameter $\delta : \Omega \times [0,T] \to \mathbb{R}$ and corresponding force $\zeta : \Omega \times [0,T] \to \mathbb{R}$. It turns out that the plastic strain itself is a suitable internal variable to describe kinematic hardening and the corresponding force is the *back-stress* $\boldsymbol{\zeta} : \Omega \times [0,T] \to \mathrm{Sym}(3)$.

2.3. Yield and Plastic Flow - Associated and Non-Associated Flow Rules. In the beginning of the section we introduced the plastic strain tensor $\boldsymbol{\varepsilon}_p$ and mentioned that it remains to give a relationship between the plastic strain rate $\dot{\boldsymbol{\varepsilon}}_p$ and the stress tensor $\boldsymbol{\sigma}$. In the preceding subsection, we introduced the concept of admissible stress states and it is reasonable to impose that plastic flow can only occur if the stress tensor tends to leave the admissible set, i.e. if the stress tensor reaches the boundary ∂K of the admissible set K, the so called *yield surface*. Thus, a first requirement is that $\dot{\boldsymbol{\varepsilon}}_p = 0$ whenever $\boldsymbol{\sigma} \in \mathrm{int}\,K$. The interior of the admissible set is also called the *elastic domain*.

Formally, by a *flow rule*, we mean the functional relationship

$$\dot{\boldsymbol{\varepsilon}}_p \in G(\boldsymbol{\sigma})\,,$$

where $G : \mathrm{Sym}(3) \rightrightarrows \mathrm{Sym}(3)$ is a set-valued multi-function satisfying $G(\boldsymbol{\sigma}) = \{0\}$ whenever $\boldsymbol{\sigma} \in \mathrm{int}\,K$. To be thermodynamically admissible, the *plastic work* has to be non-negative, i.e.

$$\boldsymbol{\sigma} : \dot{\boldsymbol{\varepsilon}}_p \geq 0 \qquad \text{for all } \boldsymbol{\sigma} \in \mathrm{dom}(G) \text{ and for all } \dot{\boldsymbol{\varepsilon}}_p \in G(\boldsymbol{\sigma})\,.$$

Under an additional assumption, G takes a specific form which also guarantees the compliance with the second law of thermodynamics. This assumption is the maximum plastic work inequality, cf. [**Lem00**], leading to the *associated flow rule* or *normality law*. Particularly, we seek $\boldsymbol{\sigma} \in K$ such that

$$\boldsymbol{\sigma} : \dot{\boldsymbol{\varepsilon}}_p = \max!$$

which is equivalent to minimizing $-\boldsymbol{\sigma} : \dot{\boldsymbol{\varepsilon}}_p$ over K. Obviously, if $\dot{\boldsymbol{\varepsilon}}_p = 0$, then the problem can be trivially solved by choosing an arbitrary admissible stress state $\boldsymbol{\sigma} \in K$. We will derive two equivalent formulations which will be linked together afterwards.

2.3.1. *Normality Law I.* By introducing the convex indicator function

$$\chi_K : \mathrm{Sym}(3) \to \overline{\mathbb{R}}\,, \qquad \chi_K(\boldsymbol{\sigma}) = \begin{cases} 0 & ,\ \boldsymbol{\sigma} \in K\,, \\ \infty & ,\ \boldsymbol{\sigma} \notin K\,, \end{cases}$$

we can rewrite the minimization problem as: find $\boldsymbol{\sigma} \in \mathrm{Sym}(3)$ such that

$$-\boldsymbol{\sigma} : \dot{\boldsymbol{\varepsilon}}_p + \chi_K(\boldsymbol{\sigma}) = \min!$$

Since this is an unconstrained convex minimization problem, a necessary and sufficient condition for a minimum (if it exists) is

$$0 \in -\dot{\boldsymbol{\varepsilon}}_p + \partial\chi_K(\boldsymbol{\sigma})\,.$$

Here, $\partial\chi_K$ is the convex subdifferential of the indicator function χ_K (we also refer to Figure 1.3 for the convex subdifferential of a convex function):

$$\partial\chi_K(\boldsymbol{\sigma}) = \{\boldsymbol{\tau} \in \mathrm{Sym}(3) : \chi_K(\boldsymbol{\eta}) \geq \chi_K(\boldsymbol{\sigma}) + \boldsymbol{\tau} : (\boldsymbol{\eta} - \boldsymbol{\sigma}) \quad \text{for all } \boldsymbol{\eta} \in \mathrm{Sym}(3)\}\,.$$

This gives a characterization of the flow rule as

$$\dot{\varepsilon}_p : (\boldsymbol{\eta} - \boldsymbol{\sigma}) \leq 0 \quad \text{for all } \boldsymbol{\eta} \in K \,,$$

and by definition, this is equivalent to

$$\dot{\varepsilon}_p \in N_K(\boldsymbol{\sigma}) = \{\boldsymbol{\tau} \in \mathrm{Sym}(3) : \boldsymbol{\tau} : (\boldsymbol{\eta} - \boldsymbol{\sigma}) \leq 0 \text{ for all } \boldsymbol{\eta} \in K\}. \tag{1.17}$$

Thus, under the requirement of maximal plastic work, the multi-function G does not have to be specified separately but coincides with the normal cone N_K at $\boldsymbol{\sigma} \in K$. If $G \equiv N_K$, we call the flow rule *associated*. However, it is still not possible to evaluate G at a stress state $\boldsymbol{\sigma}$. Whenever $0 \in K$, we also find that the associated flow rule assures thermodynamic admissibility as $\boldsymbol{\sigma} : \dot{\varepsilon}_p \geq 0 : \dot{\varepsilon}_p = 0$.

2.3.2. *Normality Law II.* To facilitate the computation of $\dot{\varepsilon}_p$, the above concept is not very useful. However, in typical applications, the admissible set K can be characterized by $p \in \mathbb{N}$ convex *yield functions* $f_i : \mathrm{Sym}(3) \to \mathbb{R}$, $i = 1, \ldots, p$, such that

$$K = \{\boldsymbol{\sigma} \in \mathrm{Sym}(d) : f(\boldsymbol{\sigma}) \leq 0 \text{ (component-wise)}\} \,,$$

where $f : \mathrm{Sym}(3) \to \mathbb{R}^p$, $f = (f_1, \ldots, f_p)$.

A more amenable concept for the computation of $\dot{\varepsilon}_p$ is therefore to use the characterization of K by means of the yield function f and to write the minimization problem as

$$-\boldsymbol{\sigma} : \dot{\varepsilon}_p = \min! \quad \text{subject to} \quad f(\boldsymbol{\sigma}) \leq 0 \,.$$

The corresponding *Lagrange functional* or *Lagrangian* $L : \mathrm{Sym}(3) \times \mathbb{R}^p \to \mathbb{R}$ is given by

$$L(\boldsymbol{\sigma}, \lambda) = -\boldsymbol{\sigma} : \dot{\varepsilon}_p + \lambda^T f(\boldsymbol{\sigma}) = -\boldsymbol{\sigma} : \dot{\varepsilon}_p + \sum_{i=1}^{p} \lambda_i \, f_i(\boldsymbol{\sigma}) \,.$$

We assume that the set K has non-vanishing interior or equivalently, we demand the existence of some $\boldsymbol{\sigma}_0 \in K$ such that $f(\boldsymbol{\sigma}_0) < 0$. This condition is also referred to as the *strong Slater condition* and under this condition, the necessary and sufficient conditions for a minimum (if it exists) are the *Karush-Kuhn-Tucker (KKT) conditions*

$$0 \in -\dot{\varepsilon}_p + \sum_{i=1}^{p} \lambda_i \, \partial f_i(\boldsymbol{\sigma}) \,,$$

$$\lambda_i \geq 0 \,, \qquad f_i(\boldsymbol{\sigma}) \leq 0 \,, \qquad \lambda_i f_i(\boldsymbol{\sigma}) = 0 \qquad \text{for all } i = 1, \ldots, p \,.$$

The strong Slater condition can be weakened in the sense that the KKT-conditions are sufficient and necessary if only the *weak Slater condition* is satisfied, i.e. there is some $\boldsymbol{\sigma}_0 \in K$ such that $f_i(\boldsymbol{\sigma}_0) < 0$ for all *active indices* $i \in I(\boldsymbol{\sigma}) = \{j \in \{1, \ldots, p\} : f_i(\boldsymbol{\sigma}) = 0\}$. Note that the strong (and therefore also the weak) Slater condition is always fulfilled as long as the elastic domain in nonempty.
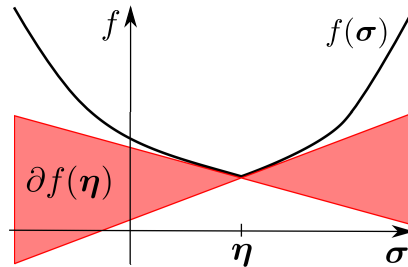
FIGURE 1.3. Convex subdifferential.

Proposition 1.1. *If the weak Slater condition is fulfilled, the normal cone $N_K(\boldsymbol{\sigma})$ has the representation*

$$N_K(\boldsymbol{\sigma}) = \left\{ \boldsymbol{\tau} \in \mathrm{Sym}(3) : \boldsymbol{\tau} = \sum_{i \in I(\boldsymbol{\sigma})} \lambda_i \, \boldsymbol{s}_i \,, \ \boldsymbol{s}_i \in \partial f_i(\boldsymbol{\sigma}) \,, \ \lambda_i \geq 0 \,, \ for \ i \in I(\boldsymbol{\sigma}) \right\}.$$

PROOF. We refer to [**HUL93a**, Chapter VII], and particularly Proposition VII.2.2.1. □

A similar equivalence also holds in locally convex, linear topological spaces [**IT79**, Chapter 4]. Using the complementarity we obtain the representation

$$N_K(\boldsymbol{\sigma}) = \left\{ \boldsymbol{\tau} \in \mathrm{Sym}(3) : \boldsymbol{\tau} = \sum_{i=1}^{p} \lambda_i \, \boldsymbol{s}_i \,, \ \boldsymbol{s}_i \in \partial f_i(\boldsymbol{\sigma}) \,, \ \lambda_i \geq 0 \,, \ f_i(\boldsymbol{\sigma}) \leq 0 \,, \right.$$

$$\left. \lambda_i \, f_i(\boldsymbol{\sigma}) = 0 \ \text{ for } \ i = 1, \ldots, p \right\}.$$

If additionally f is smooth at $\boldsymbol{\sigma}$, i.e. $\partial f_i(\boldsymbol{\sigma}) = \{Df_i(\boldsymbol{\sigma})\}$, we obtain $\dot{\boldsymbol{\varepsilon}}_p = \sum_{i=1}^{p} \lambda_i \, Df_i(\boldsymbol{\sigma})$, cf. [**SH98**, Chapter 5] or [**SKG88**].

2.3.3. *Non-Associated Flow Rule.* Even though the associated flow rule has a nice variational structure, there are situations in which the associated flow rule is not appropriate. However, then the multi-function G has to be specified explicitly. Plastic flow is then typically determined by requiring

$$\dot{\boldsymbol{\varepsilon}}_p = \sum_{i=1}^{p} \lambda_i \boldsymbol{r}_i(\boldsymbol{\sigma}) \,,$$

$$\lambda \geq 0 \,, \qquad f(\boldsymbol{\sigma}) \leq 0 \,, \qquad \lambda^T f(\boldsymbol{\sigma}) = 0 \,,$$

with the plastic flow directions $\boldsymbol{r}_i : \mathrm{Sym}(3) \to \mathrm{Sym}(3)$, $i = 1, \ldots, p$. In most cases, $\boldsymbol{r}_i$ is defined as the convex sub-differential of a *plastic potential* $g_i : \mathrm{Sym}(3) \to \mathbb{R}^p$, viz. $\boldsymbol{r}_i = \partial g_i$ and then we obtain the representation

$$\dot{\boldsymbol{\varepsilon}}_p = \sum_{i=1}^{p} \lambda_i \, \boldsymbol{s}_i \,, \quad \boldsymbol{s}_i \in \partial g_i(\boldsymbol{\sigma}) \,.$$

With this, we then find G to take the form

$$G(\boldsymbol{\sigma}) = \left\{ \boldsymbol{\tau} \in \mathrm{Sym}(3) : \boldsymbol{\tau} = \sum_{i=1}^{p} \lambda_i \, \boldsymbol{s}_i \,, \ \boldsymbol{s}_i \in \partial g_i(\boldsymbol{\sigma}) \,, \ \lambda_i \geq 0 \,, \ f_i(\boldsymbol{\sigma}) \leq 0 \,, \right.$$

$$\left. \lambda_i \, f_i(\boldsymbol{\sigma}) = 0 \ \text{ for } \ i = 1, \ldots, p \right\}.$$

Obviously, the associated flow rule is recovered if $g = f$.

2.4. Hardening. As mentioned earlier, internal variables $\boldsymbol{\delta}$ (with dual forces $\boldsymbol{\zeta}$) may change the set of admissible stress states. Looking at the local dissipation inequality, we see that similarly to the relation connecting the current stress state and the plastic strain rate via $\dot{\boldsymbol{\varepsilon}}_p \in G(\boldsymbol{\sigma})$, we need to relate ζ and $\dot{\boldsymbol{\delta}}$. We will discuss isotropic and kinematic hardening separately but also the combination of both is possible. Throughout, we will assume that the free energy $\mathcal{W}(\boldsymbol{\varepsilon}_e, \boldsymbol{\delta})$ can be split up additively into

$$\mathcal{W}(\boldsymbol{\varepsilon}_e, \boldsymbol{\delta}) = \mathcal{W}_e(\boldsymbol{\varepsilon}_e) + \mathcal{W}_p(\boldsymbol{\delta}) \,.$$

The set of admissible stress states is then generalized to

$$\widetilde{K} = \{(\boldsymbol{\sigma}, \boldsymbol{\zeta}) \in \mathrm{Sym}(3) \times \mathbb{R}^s : \widetilde{f}(\boldsymbol{\sigma}, \boldsymbol{\zeta}) \leq 0\} \,,$$

with a suitable yield function $\widetilde{f} : \mathrm{Sym}(3) \times \mathbb{R}^s \to \mathbb{R}^p$. However, for the ease of notation, we only consider the case of a single yield function, i.e. $\widetilde{f} : \mathrm{Sym}(3) \times \mathbb{R}^s \to \mathbb{R}$.

2.4.1. *Isotropic Hardening.* As outlined earlier, the notion of isotropic hardening is related to an isotropic expansion of the yield surface resulting in increased strength of the body under consideration as the set of admissible stress states becomes larger. Isotropic hardening is described by the scalar internal variable $\delta : \Omega \times [0, T] \to \mathbb{R}$ and the corresponding force $\zeta : \Omega \times [0, T] \to \mathbb{R}$. In this case, $\mathcal{W}_p(\delta)$ is a scalar potential and the conjugate force ζ is given by

$$\zeta = -\rho_0 D_\delta \mathcal{W}(\varepsilon_e, \delta) = -\rho_0 \mathcal{W}_p'(\delta) \,.$$

We consider the special case of isotropic hardening where the generalized yield function $\widetilde{f}$ reads as

$$\widetilde{f}(\boldsymbol{\sigma}, \zeta) = f(\boldsymbol{\sigma}) + h(\zeta) \,,$$

where f is the yield function of the previous subsection and $h : \mathbb{R} \to \mathbb{R}$ is a monotone increasing function satisfying $h(0) = 0$. Often, $h(\zeta) \equiv \zeta$ which we will use in the following. Generalizing the maximum plastic work inequality, i.e. $(\boldsymbol{\sigma}, \zeta)$ maximizes the local dissipation $\boldsymbol{\sigma} : \dot{\varepsilon}_p + \zeta \dot{\delta}$ over $\widetilde{K}$, we obtain the generalized normality condition $\left[\begin{smallmatrix} \dot{\varepsilon}_p \\ \dot{\delta} \end{smallmatrix}\right] \in N_{\widetilde{K}}(\boldsymbol{\sigma}, \zeta)$. Using the yield function, we obtain

$$\dot{\boldsymbol{\varepsilon}}_p = \lambda \boldsymbol{s} \,, \quad \boldsymbol{s} \in \partial f(\boldsymbol{\sigma}) \qquad \text{and} \qquad \dot{\delta} = \lambda \,.$$

We close by considering two examples of how $\mathcal{W}_p(\delta)$ may actually look like. The first example corresponds to linear isotropic hardening in which case $\rho_0 \mathcal{W}_p(\delta) = \frac{1}{2} h_0 \delta^2$ with $h_0 > 0$ and therefore $\zeta = -h_0 \delta$ or alternatively $\delta = -h_0^{-1} \zeta$. However, more complicated possibilities exist. A more general (convex) energy is given by

$$\rho_0 \mathcal{W}_p(\delta) = \tfrac{1}{2} h_0 \delta^2 + (\overline{h} - \underline{h})\big(\delta + \tfrac{1}{\beta} \exp(-\beta \delta)\big) - h_1 \delta$$

with $\overline{h} \geq \underline{h} \geq 0$ and $\beta, h_1, h_0 > 0$. This energy is often used with $h_0 = 0$, leading to isotropic hardening in the sense of *Voce*, cf. [SH98].

2.4.2. *Kinematic Hardening.* Whereas isotropic hardening expands the yield surface, kinematic hardening changes the center of the admissible set in $\mathrm{Sym}(3)$. This type of hardening is more appropriate for materials exhibiting the so-called *Bauschinger effect*. Consequently, an internal variable capable of doing this must be a second order tensor $\boldsymbol{\delta} \in \mathrm{Sym}(3)$. Once more, the corresponding force is denoted by $\boldsymbol{\zeta} = -\rho_0 D_{\boldsymbol{\delta}} \mathcal{W}_p(\boldsymbol{\delta})$. If the admissible set K is characterized as $K = \{\boldsymbol{\sigma} \in \mathrm{Sym}(3) : f(\boldsymbol{\sigma}) \leq 0\}$, we can shift the admissible set by setting $\widetilde{K} = \{(\boldsymbol{\sigma}, \boldsymbol{\zeta}) : f(\boldsymbol{\sigma} + \boldsymbol{\zeta}) \leq 0\}$. The force $\boldsymbol{\zeta}$ is called the *back-stress* and $\boldsymbol{\alpha} = \boldsymbol{\sigma} + \boldsymbol{\zeta}$ the *relative stress*. Note that in the literature, the back-stress often has a different sign if the conjugate force is introduced without the minus sign.

Using the maximum plastic work inequality again leads to a minimization problem.

$$\text{Minimize} \quad -\boldsymbol{\sigma} : \dot{\boldsymbol{\varepsilon}}_p - \boldsymbol{\zeta} : \dot{\boldsymbol{\delta}} \qquad \text{subject to } f(\boldsymbol{\sigma} + \boldsymbol{\zeta}) \leq 0 \,.$$

Again assuming $p = 1$, the Lagrangian is $L((\boldsymbol{\sigma}, \boldsymbol{\zeta}), \lambda) = -\boldsymbol{\sigma} : \dot{\boldsymbol{\varepsilon}}_p - \boldsymbol{\zeta} : \dot{\boldsymbol{\delta}} + \lambda f(\boldsymbol{\sigma} + \boldsymbol{\zeta})$ and the optimality conditions are

$$0 \in \partial_{\boldsymbol{\sigma}} L((\boldsymbol{\sigma}, \boldsymbol{\zeta}), \lambda) = -\dot{\boldsymbol{\varepsilon}}_p + \lambda \partial f(\boldsymbol{\sigma} + \boldsymbol{\zeta}) \,,$$
$$0 \in \partial_{\boldsymbol{\zeta}} L((\boldsymbol{\sigma}, \boldsymbol{\zeta}), \lambda) = -\dot{\boldsymbol{\delta}} + \lambda \partial f(\boldsymbol{\sigma} + \boldsymbol{\zeta}) \,,$$
$$\lambda \geq 0 \,, \qquad f(\boldsymbol{\sigma} + \boldsymbol{\zeta}) \leq 0 \,, \qquad \lambda f(\boldsymbol{\sigma} + \boldsymbol{\zeta}) = 0 \,.$$

The first two inclusions allow to identify $\varepsilon_p \equiv \boldsymbol{\delta}$, i.e. the plastic strain itself serves as an internal variable. As indicated in [**Lem00**, Section 5.4], it is difficult to justify a nonlinear relationship between $\boldsymbol{\zeta}$ and $\boldsymbol{\delta}$, and we therefore only consider linear kinematic hardening, i.e. there is a hardening modulus $\mathbb{H} : \mathrm{Sym}(3) \to \mathrm{Sym}(3)$ such that $\rho_0 \mathcal{W}_p(\boldsymbol{\delta}) = \frac{1}{2}\boldsymbol{\delta} : \mathbb{H}[\boldsymbol{\delta}]$. The conjugate force then is $\boldsymbol{\zeta} = -\rho_0 D_{\boldsymbol{\sigma}} \mathcal{W}_p(\boldsymbol{\delta}) = -\mathbb{H}[\boldsymbol{\delta}]$ and eventually, the free energy can be written as

$$\rho_0 \mathcal{W} \equiv \frac{1}{2}\boldsymbol{\varepsilon}_e : \mathbb{C}[\boldsymbol{\varepsilon}_e] + \frac{1}{2}\boldsymbol{\varepsilon}_p : \mathbb{H}[\boldsymbol{\varepsilon}_p] = \frac{1}{2}(\boldsymbol{\varepsilon} - \boldsymbol{\varepsilon}_p) : \mathbb{C}[\boldsymbol{\varepsilon} - \boldsymbol{\varepsilon}_p] + \frac{1}{2}\boldsymbol{\varepsilon}_p : \mathbb{H}[\boldsymbol{\varepsilon}_p] \,.$$

2.5. Particular Flow Rules. In this section we will specify the flow rule for a set of model problems. Particularly, we address the models of von Mises and Drucker-Prager, as well as a slight modification of the latter.

2.5.1. *Von Mises Plasticity.* To describe the admissible set by means of a yield function, we define

$$f : \mathrm{Sym}(3) \to \mathbb{R}\,, \qquad\qquad\qquad f(\boldsymbol{\sigma}) = |\mathrm{dev}(\boldsymbol{\sigma})| - K_0 \,. \qquad\qquad (1.18)$$

with $K_0 = \sqrt{\frac{2}{3}}\sigma_Y$. In light of the characterization given before, we have

$$K = \{\boldsymbol{\sigma} \in \mathrm{Sym}(3) : f(\boldsymbol{\sigma}) \le 0\}\,.$$

Plasticity in ductile metals is mainly due to dislocations causing slip processes. Indeed, these processes may change the shape of the body, but typically the volume of the body remains unchanged and it is therefore assumed that plastic strains are incompressible, i.e. $\mathrm{tr}(\dot{\boldsymbol{\varepsilon}}_p) = 0$. Since K is a cylinder with infinite length aligned with the isotropic stress axis, we have $\mathrm{tr}(\dot{\boldsymbol{\varepsilon}}_p) = 0$ for all $\dot{\boldsymbol{\varepsilon}}_p \in N_K(\boldsymbol{\sigma})$. Since the yield criterion defines a circle in the deviatoric plane, its is also convenient to use associativity with respect to the deviatoric portion of the stress space.

2.5.2. *Drucker-Prager Plasticity.* Whereas in metal plasticity, the associated flow rule is commonly adopted, for frictional materials the situation is different, particularly because in contrast to metal plasticity, plastic flow is not incompressible. Concerning the examples of Mohr-Coulomb and Drucker-Prager, which both describe a cone in principal stress space, we see that the normality condition naturally implies $\mathrm{tr}(\dot{\boldsymbol{\varepsilon}}_p) \ne 0$. We focus on the Drucker-Prager model which is suited for cohesive and frictional materials like soil. Soil is assumed to consists of particles (e.g. sand, clay) and for a moment, we assume that the particles are densely packed. Following Coulomb, the strength of the soil is due to cohesion and friction. Strengthening effects resulting from friction are two-fold: first, strength increases due to grinding of particles over each other, and secondly, strength is increased by *interlocking* of particles which prevents relative movement of the particles.

Thus, if plastic flow is going to happen as a result of shearing, the particles will have to move relative to each other and this naturally causes an increase of volume to overcome interlocking; so-called *dilation* or *dilatancy*. Another description of dilation is that close to the shear band, the displacement is not only tangentially to the shear band, but also has an (upward) normal component and this gives rise to the definition of the *angle of dilatancy* $\psi \ge 0$ describing the ratio between normal and tangential displacement components. $\psi = 0$ corresponds to no dilation, i.e. there is no normal displacement w.r.t. the shear band and consequently, this implies plastic incompressibility. Typically, the angle of friction ϕ serves as an upper bound, i.e. $\psi \le \phi$.
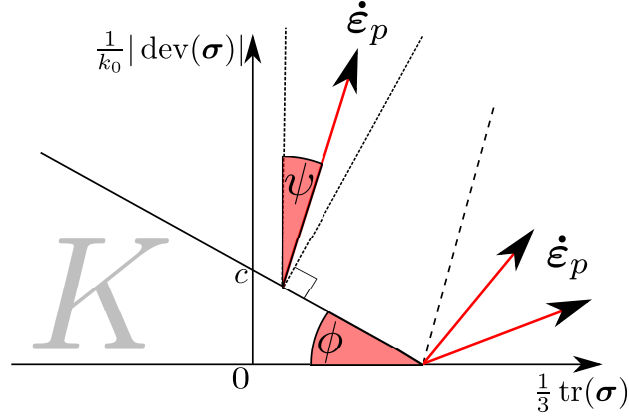
FIGURE 1.4. The Drucker-Prager flow rule.

Rescaling k_0 by $\sqrt{\frac{2}{3}}$, the yield function of the Drucker-Prager model is given by

$$f(\boldsymbol{\sigma}) = |\operatorname{dev}(\boldsymbol{\sigma})| + k_0(p_{\boldsymbol{\sigma}} \tan \phi - c)$$

with the convex sub-differential

$$\partial f(\boldsymbol{\sigma}) = \begin{cases} \left\{ \frac{\operatorname{dev}(\boldsymbol{\sigma})}{|\operatorname{dev}(\boldsymbol{\sigma})|} + \frac{k_0}{3} \tan \phi \, \mathbf{1} \right\} & , \operatorname{dev}(\boldsymbol{\sigma}) \neq 0 \,, \\ \left\{ \operatorname{dev}(\boldsymbol{\eta}) + \frac{k_0}{3} \tan \phi \, \mathbf{1} : |\operatorname{dev}(\boldsymbol{\eta})| \leq 1 \right\} & , \operatorname{dev}(\boldsymbol{\sigma}) = 0 \,. \end{cases}$$

For all $\boldsymbol{s} \in \partial f(\boldsymbol{\sigma})$, we therefore obtain $\operatorname{tr}(\boldsymbol{s}) = k_0 \tan \phi > 0$. However, it is observed that using the normality condition overestimates the effects due to dilation. This is when the non-associated flow rule, and particularly the angle of dilatancy comes into play.

We introduce the plastic potential $g : \operatorname{Sym}(3) \to \mathbb{R}$,

$$g(\boldsymbol{\sigma}) = |\operatorname{dev}(\boldsymbol{\sigma})| + k_0(p_{\boldsymbol{\sigma}} \tan \psi - c) + \tilde{c} \,,$$

where $\tilde{c}$ is a constant only depending on the material parameters and which can essentially be omitted since we are only interested in elements of the sub-gradient of g. For modeling aspects including $\tilde{c}$, we refer to [**PZ99**, Chapter VII] or [**HFdS03**].

The significant difference between f and g is the replacement of the friction angle ϕ in the yield function by the angle of dilatancy ψ in the plastic potential, giving the sub-gradient of g as

$$\partial g(\boldsymbol{\sigma}) = \begin{cases} \left\{ \frac{\operatorname{dev}(\boldsymbol{\sigma})}{|\operatorname{dev}(\boldsymbol{\sigma})|} + \frac{k_0}{3} \tan \psi \, \mathbf{1} \right\} & , \operatorname{dev}(\boldsymbol{\sigma}) \neq 0 \,, \\ \left\{ \operatorname{dev}(\boldsymbol{\eta}) + \frac{k_0}{3} \tan \psi \, \mathbf{1} : |\operatorname{dev}(\boldsymbol{\eta})| \leq 1 \right\} & , \operatorname{dev}(\boldsymbol{\sigma}) = 0 \,. \end{cases}$$

Due to $\psi \leq \phi$, for a given stress state $\boldsymbol{\sigma}$, we infer $\operatorname{tr}(\boldsymbol{s}_g) = k_0 \tan \psi \leq k_0 \tan \phi = \operatorname{tr}(\boldsymbol{s}_f)$ for all $\boldsymbol{s}_g \in \partial g(\boldsymbol{\sigma})$ and $\boldsymbol{s}_f \in \partial f(\boldsymbol{\sigma})$. Thus, we see that the angle of dilatancy allows to control the plastic volume change. We define $\mathbb{T} : \operatorname{Sym}(3) \to \operatorname{Sym}(3)$ by

$$\mathbb{T}[\boldsymbol{\varepsilon}] = \mathbb{P}_{\operatorname{dev}}[\boldsymbol{\varepsilon}] + \frac{\tan \psi}{\tan \phi} \mathbb{P}_{\operatorname{vol}}[\boldsymbol{\varepsilon}] = \operatorname{dev}(\boldsymbol{\varepsilon}) + \frac{\tan \psi}{\tan \phi} \frac{\operatorname{tr}(\boldsymbol{\varepsilon})}{3} \mathbf{1} \,, \tag{1.19}$$

and note that $\mathbb{T}$ is well-defined if $\tan \phi \neq 0$, which is no limitation as in this case, we reobtain the von Mises yield criteria. Obviously, we have $\partial g(\boldsymbol{\sigma}) = \mathbb{T}[\partial f(\boldsymbol{\sigma})]$ and considering the non-associated flow rule $\dot{\boldsymbol{\varepsilon}}_p = \lambda \boldsymbol{s} \,, \boldsymbol{s} \in \partial g(\boldsymbol{\sigma})$, we find

$$\dot{\boldsymbol{\varepsilon}}_p = \lambda \, \mathbb{T}[\boldsymbol{s}] \,, \qquad \boldsymbol{s} \in \partial f(\boldsymbol{\sigma})$$

Note that whenever $\tan\psi \neq 0$, $\mathbb{T}$ is invertible and we can write

$$\mathbb{T}^{-1}[\dot{\boldsymbol{\varepsilon}}_p] = \lambda\,\boldsymbol{s}\,, \qquad \boldsymbol{s} \in \partial f(\boldsymbol{\sigma})\,.$$

If $\psi = 0$, this is not possible, but we obtain $\dot{\boldsymbol{\varepsilon}}_p = \lambda\,\mathrm{dev}(\boldsymbol{s})$, with $\boldsymbol{s} \in \partial f(\boldsymbol{\sigma})$.

Figure 1.4 illustrates the flow rule of non-associated Drucker-Prager plasticity in terms of the stress deviator and the mean stress. The angle of dilatancy is constrained by $0 \leq \psi \leq \phi$ and this corresponds to the dashed lines. If the stress state is the apex of the cone, the flow direction is not uniquely defined.

2.5.3. *Smoothed Drucker-Prager Plasticity.* The fact that the apex of the Drucker-Prager cone is a singular point on the yield surface, and thereby prevents the definition of a unique flow direction, is often considered as a handicap. An approach to bypass this drawback is to introduce a smoothing parameter $0 < \theta < c\,k_0$ leading to the smoothed yield function

$$f_\theta(\boldsymbol{\sigma}) = \sqrt{|\mathrm{dev}(\boldsymbol{\sigma})|^2 + \theta^2} + k_0(p_{\boldsymbol{\sigma}}\tan\phi - c)\,,$$

cf. [**KLSW06**, **ML99**]. Again, by replacing the angle of friction by the angle of dilatancy, we obtain the plastic potential

$$g_\theta(\boldsymbol{\sigma}) = \sqrt{|\mathrm{dev}(\boldsymbol{\sigma})|^2 + \theta^2} + k_0(p_{\boldsymbol{\sigma}}\tan\psi - c) + \tilde{c}\,.$$

The derivatives of f_θ and g_θ are given by

$$Df_\theta(\boldsymbol{\sigma}) = \frac{\mathrm{dev}(\boldsymbol{\sigma})}{\sqrt{|\mathrm{dev}(\boldsymbol{\sigma})|^2 + \theta^2}} + \frac{k_0}{3}\tan\phi\,\mathbf{1}\,,$$

$$Dg_\theta(\boldsymbol{\sigma}) = \frac{\mathrm{dev}(\boldsymbol{\sigma})}{\sqrt{|\mathrm{dev}(\boldsymbol{\sigma})|^2 + \theta^2}} + \frac{k_0}{3}\tan\psi\,\mathbf{1}\,,$$

respectively, and again we have $\mathbb{T}[Df_\theta(\boldsymbol{\sigma})] = Dg_\theta(\boldsymbol{\sigma})$. Moreover, we find $D^2 f_\theta(\boldsymbol{\sigma}) = D^2 g_\theta(\boldsymbol{\sigma})$ for all $\boldsymbol{\sigma} \in \mathrm{Sym}(3)$.

The difference between Drucker-Prager plasticity and smoothed Drucker-Prager plasticity is shown in Figure 1.5. The figure also illustrates why it is meaningful to require $\theta < c\,k_0$ since otherwise, the stress free state $\boldsymbol{\sigma} = 0$ is not contained in the elastic domain.
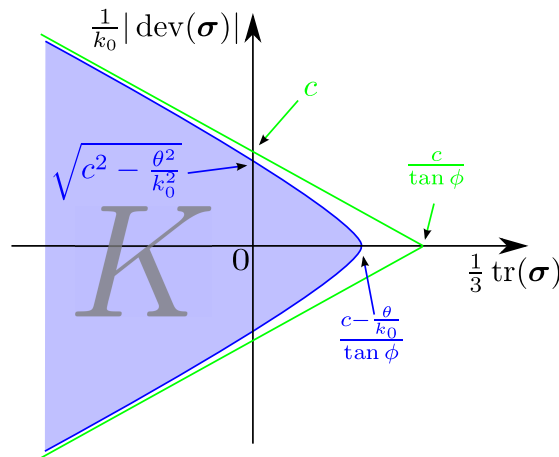
FIGURE 1.5. Comparison of Drucker-Prager and smoothed Drucker-Prager plasticity. The admissible set of smoothed Drucker-Prager plasticity is shaded blue, and the green lines denote the Drucker-Prager yield surface. For illustration, the $|\mathrm{dev}(\boldsymbol{\sigma})|$-half-space is reflected at the mean stress axis.

CHAPTER 2

ASSOCIATED STATIC PERFECT PLASTICITY

In the previous chapter we gave a brief review of the governing equations in solid mechanics under isothermal conditions and particularly considered the case of infinitesimal elasticity and plasticity. The constitutive relations were derived point-wise for a fixed spatial point $x \in \Omega$ in the reference configuration but the corresponding initial boundary value problems were not given up to now. This is the aim of this chapter where we start with the problem of linear elasticity which will be presented in a convex duality framework. This duality framework will then be extended to associated perfect plasticity. From a mathematical point of view, the problems are posed in suitable Banach and/or Hilbert spaces making it necessary to introduce some notation first. Though static perfect plasticity might not be meaningful from a physical/mechanical standpoint, it is very well suited for an exposition from a mathematical point of view since it highlights most analytical difficulties accompanying plasticity problems.

The material in this chapter is not new and mainly serves to introduce notation and to give some insight into the problems. Concerning references, we particularly mention [**Tem85**] and [**ABM06**], whereas the standard work concerning convex duality is [**ET76**].

1. Notation

We shortly remind that $\Omega \subset \mathbb{R}^d$ (with $d \in \mathbb{N}$) is open and bounded and we assume that the boundary $\partial\Omega$ is disjointly decomposed into $\partial\Omega = \Gamma_D \cup \Gamma_T$. For simplicity, we also assume $\mathrm{meas}_{d-1}(\Gamma_D) > 0$, where meas_{d-1} is the $(d-1)$-dimensional Hausdorff measure, cf. [**Alt06**]. Γ_D corresponds to the part of the boundary where the displacement is prescribed whereas on Γ_T, a traction force is prescribed. Tacitly, we will also assume some regularity of the boundary, but all results are valid in the case of a Lipschitz boundary, i.e. for each $x \in \partial\Omega$ there is a neighborhood $\mathcal{U}(x) \subset \mathbb{R}^d$ such that $\partial\Omega \cap \mathcal{U}(x)$ is the graph of a Lipschitz function with respect to a suitable local coordinate system around x. Moreover, Ω is required to be simple connected. More background information about these assumptions can be found in [**GR86**, Chapter 1] or in [**IS93**, Chapter 2].

1.1. Abstract Function Spaces. In the following, let $S \subset \mathbb{R}^d$ and let Y denote any Banach space (i.e. a complete and normed space) with norm $|\cdot|_Y$.

1.1.1. *Continuous Spaces.* The space of k-times continuous differentiable functions is denoted as

$$C^k(S, Y) = \Big\{ z : S \to Y : \|z\|_{C^k(S,Y)} := \sum_{|\alpha| \le k} \sup_{x \in S} |\partial^\alpha z(x)|_Y < \infty \Big\},$$

where $\alpha \in \mathbb{N}_0^d$ is a multi-index. With the given norms, the spaces $C^k(S, Y)$ are Banach spaces if Y is a Banach space. For $m \in (0, 1]$, we also use the notation $C^{k,m}(S, Y)$ to denote the Hölder-continuous spaces, and particularly $C^{k,1}$ corresponds to the k-times Lipschitz-differentiable functions.

1.1.2. *Lebesgue Spaces.* For $1 \le p < \infty$, we define the Lebesgue spaces

$$L^p(S, Y) = \Big\{ z : S \to Y : \|z\|_{L^p(S,Y)} := \Big(\int_\Omega |z(x)|_Y^p \, dx \Big)^{1/p} < \infty \Big\},$$

$$L^\infty(S, Y) = \Big\{ z : S \to Y : \|z\|_{L^\infty(S,Y)} := \operatorname*{ess\,sup}_{x \in S} |z(x)|_Y \Big\}.$$

Note that $L^2(S, Y)$ is a Hilbert space if Y is a Hilbert space and that all L^p-spaces are Banach spaces as long as Y is a Banach space.

1.1.3. *Sobolev Spaces.* Based on the concept of weak differentiability, we introduce the Sobolev spaces of integer order as

$$W^{k,p}(S, Y) = \Big\{ z : S \to Y : \|z\|_{W^{k,p}(S,Y)} := \Big(\sum_{|\alpha| \le k} \|\partial^\alpha z\|_{L^p(S,Y)}^p \Big)^{1/p} < \infty \Big\},$$

where again, $\alpha \in \mathbb{N}_0^d$ is a multi-index. Particularly, all weak derivatives up to order k are contained in $L^p(S, Y)$. Whenever Y is a Hilbert space and $p = 2$, we use the shorthand notation $H^k(S, Y) = W^{k,2}(S, Y)$ to emphasize the Hilbert space structure. Again, all $W^{k,p}$-spaces are Banach spaces if Y is a Banach space. On $W^{k,p}(S, Y)$, we also define a semi-norm by

$$|z|_{W^{k,p}(S,Y)} := \Big(\sum_{|\alpha| = k} \|\partial^\alpha z\|_{L^p(S,Y)}^p \Big)^{1/p}.$$

For Sobolev spaces, there exist a variety of embedding theorems, see [**Rou05**, Chapter 1] or [**IS93**, Chaper 2]. We quote only the simplest version stating that if $S \subset \mathbb{R}^d$ and $kp > d$, then $W^{k,p}(S, Y) \subset C(S, Y)$. Contrary, one can show that if $d > 1$, functions in the Hilbert space $H^1(S, Y)$ are not continuous in general. This also raises the question of how to give a meaning to the evaluation of functions at a subset of measure zero, particularly on the boundary of S. This problem is resolved by the trace theorem stating that there exists a continuous linear operator $\gamma_T : W^{1,p}(S, Y) \to W^{1-1/p,p}(\partial S, Y)$. Here, the fractional Sobolev space $W^{1-1/p,p}$ occurs and for details we refer to [**Ada75**]. We just quote that in the case $d \in \{2, 3\}$, by a suitable embedding theorem, we find that γ_T, when considered as a function from $H^1(S, Y) \to H^{1/2}(\partial S, Y) \subset L^2(\partial S, Y)$, is continuous.

1.2. Function Spaces in Continuum Mechanics of Solid Deformation. Henceforth, we will frequently use the spaces $L^2(\Omega, \operatorname{Sym}(d))$ and $H^1(\Omega, \mathbb{R}^d)$ and therefore, we use the abbreviations

$$\boldsymbol{P} = L^2(\Omega, \operatorname{Sym}(d)) \qquad \text{and} \qquad \boldsymbol{V} = H^1(\Omega, \mathbb{R}^d). \tag{2.1}$$

We equip these spaces with the natural duality pairings, inner products and norms. Particularly, we use the Euclidean norm in $\mathbb{R}^d$ and the Frobenius norm on $\mathrm{Sym}(d)$, which both can be derived from inner products on the spaces $\mathbb{R}^d$ and $\mathrm{Sym}(d)$ and therefore make $\boldsymbol{P}$ and $\boldsymbol{V}$ Hilbert spaces. Particularly, we will often use the identification of $\boldsymbol{P}$ with its dual by means of the *Riesz representation theorem*. However, it will often be convenient to define other inner products and norms on $\boldsymbol{P}$, as well as on (subsets of) $\boldsymbol{V}$ as we will just see.

1.2.1. *Displacement Spaces.* The choice of a suitable space for the displacements is clear in the context of linear elasticity as we will shortly see, but not so obvious in infinitesimal perfect plasticity. Remembering that we assumed $\mathrm{meas}_{d-1}(\Gamma_D) > 0$, it is possible to prescribe a boundary condition

$$\boldsymbol{u}_D \in H^{1/2}(\Gamma_D, \mathbb{R}^d) \,,$$

on Γ_D. Then, we define the affine subspace

$$\boldsymbol{X}(\boldsymbol{u}_D) = \{\boldsymbol{u} \in \boldsymbol{V} : \gamma_T(\boldsymbol{u}) = \boldsymbol{u}_D\} \,,$$

and if $\boldsymbol{u}_D = 0$, we simply write $\boldsymbol{X} \equiv \boldsymbol{X}(0)$. If $\mathrm{meas}_{d-1}(\Gamma_D) > 0$, by the *Poincaré-Friedrich's inequality*, there exists a constant $C_P > 0$ such that

$$\|\boldsymbol{u}\|_{L^2(\Omega,\mathbb{R}^d)} \le C_P|\boldsymbol{u}|_{\boldsymbol{V}} \,, \qquad \boldsymbol{u} \in \boldsymbol{X} \,.$$

This yields $\|\boldsymbol{u}\|_{\boldsymbol{V}} \le (C_P + 1)|\boldsymbol{u}|_{\boldsymbol{V}}$ for all $\boldsymbol{u} \in \boldsymbol{X}$ and accordingly, $|\cdot|_{\boldsymbol{V}}$ is a norm on $\boldsymbol{X}$. The symmetrized gradient operator can be considered as an operator

$$\boldsymbol{\varepsilon} : \boldsymbol{V} \to \boldsymbol{P} \,, \qquad\qquad \boldsymbol{\varepsilon}(\boldsymbol{u})(x) = \tfrac{1}{2}\Big(D\boldsymbol{u}(x) + D\boldsymbol{u}(x)^T\Big) \,, \tag{2.2}$$

and *Korn's inequality* states that there is a constant $C_K > 0$ such that

$$\|\boldsymbol{u}\|_{\boldsymbol{V}}^2 \, dx \le C_K\Big(\|\boldsymbol{u}\|_{L^2(\Omega,\mathbb{R}^d)}^2 + \|\boldsymbol{\varepsilon}(\boldsymbol{u})\|_{\boldsymbol{P}}^2\Big) \,, \qquad \boldsymbol{u} \in \boldsymbol{X} \,.$$

The Poincaré-Friedrich's and Korn's inequality are proved in several textbooks, we refer to [**DL76**] or [**GR86**]. Another interesting proof of Korn's inequality can be found in [**CC04**], making use of the strain compatibility relations as mentioned in section 1.1.1. With these two inequalities, it is then possible to show that there is a constant $C > 0$ such that

$$\frac{1}{C}\|\boldsymbol{u}\|_{\boldsymbol{V}} \le \|\boldsymbol{\varepsilon}(\boldsymbol{u})\|_{\boldsymbol{P}} \le \|\boldsymbol{u}\|_{\boldsymbol{V}} \,, \qquad \boldsymbol{u} \in \boldsymbol{X} \,,$$

showing a norm equivalence. We define the bilinear form $c : \boldsymbol{V} \times \boldsymbol{V} \to \mathbb{R}$,

$$c(\boldsymbol{u}, \boldsymbol{v}) = \int_\Omega \boldsymbol{\varepsilon}(\boldsymbol{u}(x)) : \mathbb{C}[\boldsymbol{\varepsilon}(\boldsymbol{v}(x))] \, dx \,, \tag{2.3}$$

and on $\boldsymbol{X}$, $c(\cdot,\cdot)$ is an inner product as the definiteness follows from the above norm equivalence on $\boldsymbol{X}$ and the fact that $\mathbb{C} \in L(\mathrm{Sym}(d), \mathrm{Sym}(d))$ is positive definite on $\mathrm{Sym}(d)$, see (1.11). Based on this inner product we also define the energy norm $\|\boldsymbol{u}\| = \sqrt{c(\boldsymbol{u},\boldsymbol{u})}$ in $\boldsymbol{X}$. This bilinear form also defines an operator $C : \boldsymbol{X} \to \boldsymbol{X}^*$ by

$$\langle C\boldsymbol{u}, \boldsymbol{w}\rangle_{\boldsymbol{X}^* \times \boldsymbol{X}} = c(\boldsymbol{u}, \boldsymbol{w}) \,. \tag{2.4}$$

1.2.2. *Stress Spaces.* The stress tensor is a symmetric second order tensor, and a natural canditate for $\boldsymbol{\sigma}$ is the space $\boldsymbol{P}$. However, as we indicated before, it may be convenient to use other inner products and norm on $\boldsymbol{P}$. Due to the finite-dimensionality of $\mathrm{Sym}(d)$, we can choose any norm in $\mathrm{Sym}(d)$ without changing $\boldsymbol{P}$ topologically. In order to obtain a Hilbert space, we require that the norm in $\mathrm{Sym}(d)$ is deduced from an inner product. Apart form the usual Frobenius inner product, we will often use the energy product $\boldsymbol{\sigma} : \mathbb{C}^{-1}[\boldsymbol{\eta}]$ on $\mathrm{Sym}(d)$. Based on this inner product, we define

$$a(\boldsymbol{\sigma}, \boldsymbol{\eta}) = \int_{\Omega} \boldsymbol{\sigma}(x) : \mathbb{C}^{-1}[\boldsymbol{\eta}(x)] \, dx, \qquad\qquad \|\boldsymbol{\sigma}\|_{\Sigma} = \sqrt{a(\boldsymbol{\sigma}, \boldsymbol{\sigma})}. \qquad (2.5)$$

As previously, this bilinear form also gives rise to the definition of an operator

$$A : \boldsymbol{P} \to \boldsymbol{P}^*, \qquad\qquad \langle A\boldsymbol{\sigma}, \boldsymbol{\eta} \rangle_{P^* \times P} = a(\boldsymbol{\sigma}, \boldsymbol{\eta}), \qquad (2.6)$$

and A is the Riesz mapping with respect to the inner product $a(\cdot, \cdot)$. Obviously the norms $\|\boldsymbol{\sigma}\|_P$ and $\|\boldsymbol{\sigma}\|_{\Sigma}$ are equivalent due the properties of the elasticity tensor and the inverse operator $A^{-1} : \boldsymbol{P}^* \to \boldsymbol{P}$ exists and pointwise corresponds to the elasticity tensor $\mathbb{C}$.

Throughout the rest of the work, we will frequently employ orthogonal projections onto convex subsets of Hilbert spaces. At this point, we introduce the projection onto a convex set $\boldsymbol{K} \subset \boldsymbol{P}$ w.r.t. the inner product $a(\cdot, \cdot)$ as

$$P_{\boldsymbol{K}} : \boldsymbol{P} \to \boldsymbol{K} \subset \boldsymbol{P}. \qquad (2.7)$$

For given $\boldsymbol{\eta} \in \boldsymbol{P}$, the projection $P_{\boldsymbol{K}}(\boldsymbol{\eta})$ is characterized by the variational inequality

$$a\big(\boldsymbol{\eta} - P_{\boldsymbol{K}}(\boldsymbol{\eta}), \boldsymbol{\tau} - P_{\boldsymbol{K}}(\boldsymbol{\eta})\big) \le 0, \qquad \boldsymbol{\tau} \in \boldsymbol{K}.$$

If $\boldsymbol{K} = \{\boldsymbol{\sigma} \in \boldsymbol{P} : \boldsymbol{\sigma}(x) \in K \text{ a.e.}\}$ for some convex set $K \subset \mathrm{Sym}(d)$, the projection $P_{\boldsymbol{K}}$ locally a.e. coincides with the projection of $\boldsymbol{\sigma}(x)$ onto K w.r.t. the inner product induced by the inverse elasticity tensor $\mathbb{C}^{-1}$. We will also encounter situations in which the projection is w.r.t. a different metric.

As we have already seen in the equation of motion (1.8), or in the equilibrium equation (1.9), respectively, it may be convenient to be capable of taking the divergence of the stress tensor. This gives raise to the introduction of

$$H(\mathrm{div}, \Omega, \mathrm{Sym}(d)) = \{\boldsymbol{\sigma} \in \boldsymbol{P} : \mathrm{div}\,\boldsymbol{\sigma} \in L^2(\Omega, \mathbb{R}^d)\},$$

where the divergence operator is defined to act row-wise on second order tensors. Using

$$(\boldsymbol{\sigma}, \boldsymbol{\eta})_{H(\mathrm{div}, \Omega, \mathrm{Sym}(d))} = (\boldsymbol{\sigma}, \boldsymbol{\eta})_P + (\mathrm{div}\,\boldsymbol{\sigma}, \mathrm{div}\,\boldsymbol{\eta})_{L^2(\Omega, \mathbb{R}^d)}$$

and $\|\boldsymbol{\sigma}\|_{H(\mathrm{div}, \Omega, \mathrm{Sym}(d))} = \sqrt{(\boldsymbol{\sigma}, \boldsymbol{\eta})_{H(\mathrm{div}, \Omega, \mathrm{Sym}(d))}}$ makes $H(\mathrm{div}, \Omega, \mathrm{Sym}(d))$ a Hilbert space. But as $H^1(\Omega, \mathrm{Sym}(d)) \subsetneq H(\mathrm{div}, \Omega, \mathrm{Sym}(d))$, the trace operator γ_T cannot be used in general. Nevertheless, a trace operator can be defined as it turns out that there is a continuous linear operator $\gamma_N : H(\mathrm{div}, \Omega, \mathrm{Sym}(d)) \to H^{-1/2}(\partial\Omega, \mathbb{R}^d)$ such that with $H_{\partial\Omega} = H^{1/2}(\partial\Omega, \mathbb{R}^d)$ we find *Green's formula*, cf. [GR86, Section I.2],

$$\langle \gamma_N(\boldsymbol{\sigma}), \gamma_T(\boldsymbol{u}) \rangle_{H^*_{\partial\Omega} \times H_{\partial\Omega}} = (\boldsymbol{\sigma}, \boldsymbol{\varepsilon}(\boldsymbol{u}))_P + (\mathrm{div}\,\boldsymbol{\sigma}, \boldsymbol{u})_{L^2(\Omega, \mathbb{R}^d)} \qquad (2.8)$$

for all $\boldsymbol{\sigma} \in H(\mathrm{div}, \Omega, \mathrm{Sym}(d))$ and $\boldsymbol{u} \in \boldsymbol{V}$ and we will also write

$$\langle \gamma_N(\boldsymbol{\sigma}), \gamma_T(\boldsymbol{u}) \rangle_{H^*_{\partial\Omega} \times H_{\partial\Omega}} = \int_{\partial\Omega} \big(\boldsymbol{\sigma}(x)\boldsymbol{n}(x)\big) \cdot \boldsymbol{u}(x) \, da.$$

Essentially, this allows to prescribe the normal component on the boundary, and in the same spirit as for the displacement space, for a given $\boldsymbol{t}_N \in H^{-1/2}(\Gamma_T, \mathbb{R}^d)$, we define

$$\boldsymbol{\Sigma}_{\mathrm{div}}(\boldsymbol{t}_N) = \{\boldsymbol{\sigma} \in H(\mathrm{div}, \Omega, \mathrm{Sym}(d)) : \gamma_N(\boldsymbol{\sigma}) = \boldsymbol{t}_N\}.$$

In the homogeneous case, we also write $\Sigma_{\text{div}} \equiv \Sigma_{\text{div}}(0)$.

1.2.3. *Strain Spaces.* In plasticity, as well as in other applications dealing with minimization problems in function spaces, one is often confronted with measure valued functions. It will turn out that in perfect plasticity, certain quantities can only be defined as measures. Therefore, by $M_1(\Omega, \mathbb{R}) = C(\Omega, \mathbb{R})^*$, we denote the space of bounded measures and we set

$$\boldsymbol{M}_{\text{Sym}}(\Omega) = \{\boldsymbol{\tau} : \Omega \to \text{Sym}(d) : (\boldsymbol{\tau})_{ij} = (\boldsymbol{\tau})_{ji} \in M_1(\Omega, \mathbb{R}),\ i, j = 1, \dots, d\}\,.$$

In perfect plasticity, the space $\boldsymbol{X}$ as defined previously is generally no longer reasonable concerning the displacements as $\boldsymbol{\varepsilon}(\boldsymbol{u}) \in \boldsymbol{P}$ cannot no longer be guaranteed. For the correct treatment of the displacement field, we introduce the space of bounded deformations

$$BD(\Omega) = \{\boldsymbol{u} \in L^1(\Omega, \mathbb{R}^d) : \boldsymbol{\varepsilon}(\boldsymbol{u}) \in \boldsymbol{M}_{\text{Sym}}(\Omega)\}\,,$$

and on $BD(\Omega)$ a norm is defined by

$$\|\boldsymbol{u}\|_{BD(\Omega)} = \|\boldsymbol{u}\|_{L^1(\Omega, \mathbb{R})} + \sum_{i,j=1}^{d} \|(\boldsymbol{\varepsilon}(\boldsymbol{u}))_{ij}\|_{M_1(\Omega, \mathbb{R})}\,.$$

Even in $BD(\Omega)$, a suitable trace operator $\gamma_B : BD(\Omega) \to L^1(\partial\Omega, \mathbb{R}^{d-1})$, $d \in \{2, 3\}$ can be defined and $BD(\Omega)$ is continuously embedded into $L^p(\Omega, \mathbb{R}^d)$ for all $1 \le p \le \frac{d}{d-1}$. The space of bounded deformations has been discussed by various authors at the end of the 1970s, cf. [**Suq78a, Suq78b, Suq79, TS80**] or the monograph [**Tem85**]. Details can also be found in the textbooks [**FS00, IS93, ABM06**].

2. Linear Elasticity – a Duality Framework

After having introduced the necessary functional analytic background, we shortly consider the linear elasticity problem. This problem serves as a model problem and we set up the problem in a duality framework being extendable to infinitesimal plasticity.

We shortly repeat the governing equations and we focus on the static setting. Again, we assume that Ω is open, bounded and simple connected with Lipschitz boundary $\partial\Omega$ which is disjointly decomposed into a part $\Gamma_D \subset \partial\Omega$ where the displacement $\boldsymbol{u}_D$ is prescribed, and a part $\Gamma_T \subset \partial\Omega$ where the traction $\boldsymbol{t}_N$ is prescribed. Moreover, in Ω, we require that the stress tensor is in equilibrium (1.9), and that stresses and strains are related by Hooke's law (1.12). This results in the following system:

$$\begin{aligned}
-\operatorname{div}(\boldsymbol{\sigma}(x)) &= \boldsymbol{b}(x)\,, & x &\in \Omega\,, & \text{(2.9a)} \\
\boldsymbol{\sigma}(x) &= \mathbb{C}[\boldsymbol{\varepsilon}(\boldsymbol{u}(x))]\,, & x &\in \Omega\,, & \text{(2.9b)} \\
\boldsymbol{u}(x) &= \boldsymbol{u}_D(x)\,, & x &\in \Gamma_D\,, & \text{(2.9c)} \\
\boldsymbol{\sigma}(x)\boldsymbol{n}(x) &= \boldsymbol{t}_N(x)\,, & x &\in \Gamma_T\,. & \text{(2.9d)}
\end{aligned}$$

2.1. The Displacement Problem. The displacement (or also primal) problem is obtained by formally eliminating the stress tensor by means of Hooke's law (2.9b) and to impose the traction boundary condition only weakly. In order to obtain the weak formulation, we multiply with test functions $\boldsymbol{w} \in \boldsymbol{X}$ and integrate over Ω to arrive at

$$-\int_\Omega \operatorname{div}\big(\boldsymbol{\sigma}(x)\big) \cdot \boldsymbol{w}(x)\,dx = \int_\Omega \boldsymbol{b}(x) \cdot \boldsymbol{w}(x)\,dx\,, \qquad \boldsymbol{w} \in \boldsymbol{X}\,.$$

Application of Green's formula (2.8) then gives

$$\int_\Omega \boldsymbol{\sigma}(x) : \boldsymbol{\varepsilon}(\boldsymbol{w}(x))\, dx = \ell(\boldsymbol{w})\,, \qquad \boldsymbol{w} \in \boldsymbol{X}\,,$$

with the load functional

$$\ell(\boldsymbol{w}) = \int_\Omega \boldsymbol{b}(x) \cdot \boldsymbol{w}(x)\, dx + \int_{\Gamma_T} \boldsymbol{t}_N(x) \cdot \boldsymbol{w}(x)\, da\,. \tag{2.10}$$

Substitution of Hooke's law (2.9b) leads to the variational problem of finding $\boldsymbol{u} \in \boldsymbol{X}(\boldsymbol{u}_D)$ such that

$$c(\boldsymbol{u}, \boldsymbol{w}) = \ell(\boldsymbol{w})\,, \qquad \boldsymbol{w} \in \boldsymbol{X}\,. \tag{2.11}$$

It is well known that (2.11) is the optimality condition (or *Euler condition*) of a minimization problem.

$$\text{Minimize} \quad \mathcal{E}_{\text{el}}(\boldsymbol{u}) := \tfrac{1}{2}c(\boldsymbol{u},\boldsymbol{u}) - \ell(\boldsymbol{u}) \qquad \text{subject to} \quad \boldsymbol{u} \in \boldsymbol{X}(\boldsymbol{u}_D)\,. \tag{2.12}$$

The existence of a unique minimizer can either be obtained by the *direct method in the calculus of variations*, cf. [**Dac89**, **Giu03**], or by applying the *Lax-Milgram lemma* to the optimality conditions (2.11), cf. [**AH05**, Chapter 8].

We shortly remark that $\boldsymbol{v} \mapsto \tfrac{1}{2}c(\boldsymbol{v},\boldsymbol{v})$ is just the integrated free energy $\mathcal{W}_e$ introduced in the previous chapter. Therefore, using the same notation, we introduce the elastic free energy

$$\mathcal{W}_e : \boldsymbol{P} \to \mathbb{R}\,, \qquad\qquad \mathcal{W}_e(\boldsymbol{\varepsilon}_e) = \tfrac{1}{2}\int_\Omega \boldsymbol{\varepsilon}_e(x) : \mathbb{C}[\boldsymbol{\varepsilon}_e(x)]\, dx\,, \tag{2.13}$$

which is equal to the total free energy in the context of elasticity and obviously, we have $\mathcal{W}_e(\boldsymbol{\varepsilon}(\boldsymbol{v})) = \tfrac{1}{2}c(\boldsymbol{v},\boldsymbol{v}) = \tfrac{1}{2}\|\!|\boldsymbol{v}|\!\|^2$. Moreover, (2.11) can also be written as the abstract operator equation

$$C\boldsymbol{u} = \ell \qquad \text{in } \boldsymbol{X}^*\,,$$

with C as in (2.4). Since C is uniformly monotone, existence of a unique solution can also be obtained in the framework of monotone operators, and particularly by means of the *Browder-Minty theorem*, cf. [**Sho97**, Section II.2]. The Browder-Minty theorem is standard in the context of monotone operators and can be found in many textbooks, see [**Zei90**, **Růž04**, **Eva08**].

2.2. Mixed Problems. Based on (2.9) we can also derive different formulations of the elasticity problem, leading to the mixed formulations involving the stress tensor as well as the displacement field as unknowns. As we will see, there is more than one way to formulate these mixed methods. However, it turns out that they also describe a minimization problem.

2.2.1. *Mixed Problem I.* Contrary to the formulation of the displacement problem, we do not substitute Hooke's law into the equilibrium equation. Instead, we multiply the equilibrium equation (2.9a) by $\boldsymbol{w} \in \boldsymbol{X}$, integrate over Ω and use Green's formula (2.8). Furthermore, we apply $\mathbb{C}^{-1}$ to the constitutive relation (2.9b), multiply with $\boldsymbol{\eta} \in \boldsymbol{P}$ and integrate over Ω. Together, we obtain

$$\int_\Omega \mathbb{C}^{-1}[\boldsymbol{\sigma}(x)] : \boldsymbol{\eta}(x)\, dx - \int_\Omega \boldsymbol{\varepsilon}(\boldsymbol{u}(x)) : \boldsymbol{\eta}(x)\, dx = 0\,, \qquad \boldsymbol{\eta} \in \boldsymbol{P}\,,$$

$$\int_\Omega \boldsymbol{\sigma}(x) : \boldsymbol{\varepsilon}(\boldsymbol{w}(x))\, dx = \ell(\boldsymbol{w})\,, \qquad \boldsymbol{w} \in \boldsymbol{X}\,. \tag{2.14}$$

We define an operator $B : \boldsymbol{P} \to \boldsymbol{V}^*$ and its dual $B^* : \boldsymbol{V} \to \boldsymbol{P}^*$ as well as a bilinear form $b : \boldsymbol{P} \times \boldsymbol{V} \to \mathbb{R}$ as

$$\langle B\boldsymbol{\eta}, \boldsymbol{w} \rangle_{\boldsymbol{V}^* \times \boldsymbol{V}} = \langle B^* \boldsymbol{w}, \boldsymbol{\eta} \rangle_{\boldsymbol{P}^* \times \boldsymbol{P}} = b(\boldsymbol{\eta}, \boldsymbol{w}) = - \int_\Omega \boldsymbol{\eta}(x) : \boldsymbol{\varepsilon}(\boldsymbol{w}(x)) \, dx \tag{2.15}$$

When appropriate, we will also consider B as an operator from $\boldsymbol{P}$ to $\boldsymbol{X}^*$ and B^* as an operator from $\boldsymbol{X}$ to $\boldsymbol{P}^*$. By the above definition, B^* can be identified with $-\boldsymbol{\varepsilon}$ when $\boldsymbol{P}$ is identified with $\boldsymbol{P}^*$. Likewise, B can be considered as the divergence operator as by Green's formula (2.8) we find (note that $\boldsymbol{X}$ and Σ_{div} we have homogeneous boundary conditions)

$$\langle B\boldsymbol{\eta}, \boldsymbol{w} \rangle_{\boldsymbol{V}^* \times \boldsymbol{V}} = -(\boldsymbol{\eta}, \boldsymbol{\varepsilon}(\boldsymbol{w}))_{\boldsymbol{P}} = (\text{div}(\boldsymbol{\eta}), \boldsymbol{w})_{L^2(\Omega, \mathbb{R}^d)} \,, \qquad \boldsymbol{w} \in \boldsymbol{X}, \ \boldsymbol{\eta} \in \Sigma_{\text{div}} \,.$$

Using the bilinear forms $a(\cdot, \cdot)$ and $b(\cdot, \cdot)$ as defined in (2.5) and (2.15), we obtain the weak formulation: find $(\boldsymbol{\sigma}, \boldsymbol{u}) \in \boldsymbol{P} \times \boldsymbol{X}(\boldsymbol{u}_D)$ such that

$$\begin{array}{llllll} a(\boldsymbol{\sigma}, \boldsymbol{\eta}) & + & b(\boldsymbol{\eta}, \boldsymbol{u}) & = & 0 \,, & \boldsymbol{\eta} \in \boldsymbol{P} \,, \\ b(\boldsymbol{\sigma}, \boldsymbol{w}) & & & = & -\ell(\boldsymbol{w}) \,, & \boldsymbol{w} \in \boldsymbol{X} \,. \end{array} \tag{2.16}$$

Likewise, this can be expressed as an operator equation

$$\begin{array}{llllll} A\boldsymbol{\sigma} & + & B^* \boldsymbol{u} & = & 0 \,, & \text{in } \boldsymbol{P}^* \,, \\ B\boldsymbol{\sigma} & & & = & -\ell \,, & \text{in } \boldsymbol{X}^* \,. \end{array} \tag{2.17}$$

This has the structure of a saddle point problem and existence and uniqueness relies on an *inf-sup condition*, cf. [**BF91**, **Bre74**, **Ern04**], which can easily be verified as $a(\cdot, \cdot)$ is elliptic on $\boldsymbol{P}$ and

$$\sup_{\boldsymbol{\eta} \in \boldsymbol{P}} \frac{b(\boldsymbol{\eta}, \boldsymbol{w})}{\|\boldsymbol{\eta}\|_\Sigma} = \sup_{\boldsymbol{\eta} \in \boldsymbol{P}} \frac{- \int_\Omega \boldsymbol{\eta}(x) : \boldsymbol{\varepsilon}(\boldsymbol{w}(x)) \, dx}{\|\boldsymbol{\eta}\|_\Sigma} \overset{\boldsymbol{\eta} = -\mathbb{C}[\boldsymbol{\varepsilon}(\boldsymbol{w})]}{\geq} \|\boldsymbol{w}\| \,.$$

Here, we used that $\|\mathbb{C}[\boldsymbol{\varepsilon}(\boldsymbol{w})]\|_\Sigma^2 = \int_\Omega \mathbb{C}[\boldsymbol{\varepsilon}(\boldsymbol{w}(x))] : \boldsymbol{\varepsilon}(\boldsymbol{w}(x)) \, dx = \|\boldsymbol{w}\|^2$.

2.2.2. *Mixed Problem II.* The above mixed formulation is not the only possible. Rather than using Green's formula in the equilibrium equation, we can also use it in Hooke's law. Then, the traction boundary condition becomes the essential boundary condition. After applying $\mathbb{C}^{-1}$ to the constitutive relation (2.9b), we multiply with $\boldsymbol{\eta} \in \Sigma_{\text{div}}$ and apply Green's formula (2.8). Similarly, we multiply the equilibrium equation with $\boldsymbol{v} \in L^2(\Omega, \mathbb{R}^d)$ to obtain

$$\begin{aligned} \int_\Omega \mathbb{C}^{-1}[\boldsymbol{\sigma}(x)] : \boldsymbol{\eta}(x) \, dx + \int_\Omega \boldsymbol{u}(x) \cdot \text{div}(\boldsymbol{\eta}(x)) \, dx &= h(\boldsymbol{\eta}) \,, & \boldsymbol{\eta} \in \Sigma_{\text{div}} \,, \\ \int_\Omega \boldsymbol{v}(x) \cdot \text{div}(\boldsymbol{\sigma}(x)) \, dx &= - \int_\Omega \boldsymbol{b}(x) \cdot \boldsymbol{v}(x) \,, & \boldsymbol{v} \in L^2(\Omega, \mathbb{R}^3) \,, \end{aligned} \tag{2.18}$$

with $h \in \Sigma_{\text{div}}^*$ given by

$$h(\boldsymbol{\eta}) = \int_{\Gamma_D} \big(\boldsymbol{\eta}(x) \boldsymbol{n}(x) \big) \cdot \boldsymbol{u}_D(x) \, da \,. \tag{2.19}$$

This problem can be solved via the same inf-sup-framework but using different spaces, i.e. the product space $\Sigma_{\text{div}}(\boldsymbol{t}_N) \times L^2(\Omega, \mathbb{R}^3)$. For a proof of the inf-sup-condition in this setting, we refer to [**Bra07**, **BF91**].

Similarly to the displacement problem, the mixed formulations correspond to the optimality system of a minimization problem.

$$
\begin{aligned}
\text{Minimize} \quad & \tfrac{1}{2}a(\boldsymbol{\sigma}, \boldsymbol{\sigma}) - h(\boldsymbol{\sigma}) \\
\text{subject to} \quad & \boldsymbol{\sigma} \in \Sigma_{\mathrm{div}}(\boldsymbol{t}_N), \quad -\operatorname{div}(\boldsymbol{\sigma}(x)) = \boldsymbol{b}(x) \ \text{ in } \ \Omega.
\end{aligned}
\tag{2.20}
$$

The mixed formulation is also attributed as the *Hellinger-Reissner principle*. The link between the two minimization problems will be established in the next subsection.

2.3. Convex Duality. We see that the two mixed formulations lead to different function space settings and they also differ concerning the treatment of boundary values. Whereas in the first formulation (2.14), the Dirichlet boundary condition is essential and already incorporated in the formulation of the space $\boldsymbol{X}(\boldsymbol{u}_D)$, the traction boundary condition is only imposed weakly. Contrary, in (2.18), the Dirichlet condition is only imposed weakly via the functional h whereas the Neumann condition is essential. We will now introduce a duality framework linking the two minimization problems (2.12) and (2.20). For the derivation, we will distinguish $\boldsymbol{P}$ from its dual $\boldsymbol{P}^*$. Following the framework of [**ET76**, Chapter III] (see also [**ABM06**, Chapter 9]), and as illustrated in [**Tem85**, Section I.2], based on the primal problem (2.12), we introduce a perturbed problem leading to a dual problem which we will identify with problem (2.20). In the derivation, we will use the symmetrized gradient operator $\boldsymbol{\varepsilon}(\cdot)$ as an operator $\boldsymbol{\varepsilon} : \boldsymbol{V} \to \boldsymbol{P}$ and the free elastic energy (2.13). Moreover, defining the functional $F \in \boldsymbol{V}^*$ by setting

$$
F(\boldsymbol{u}) = \begin{cases} -\ell(\boldsymbol{u}) & , \ \boldsymbol{u} \in \boldsymbol{X}(\boldsymbol{u}_D), \\ \infty & , \ \text{else}, \end{cases}
\tag{2.21}
$$

the primal problem (2.12) can be recast as

$$
\text{Minimize} \quad \mathcal{W}_e(\boldsymbol{\varepsilon}(\boldsymbol{u})) + F(\boldsymbol{u}), \qquad \boldsymbol{u} \in \boldsymbol{V}.
$$

Note that this time, the minimization is over all of $\boldsymbol{V} = H^1(\Omega, \mathbb{R}^d)$ rather than over the affine space $\boldsymbol{X}(\boldsymbol{u}_D)$. We introduce the perturbation

$$
\Psi : \boldsymbol{P} \times \boldsymbol{V} \to \overline{\mathbb{R}}, \qquad\qquad \Psi(\boldsymbol{\tau}, \boldsymbol{u}) = \mathcal{W}_e(\boldsymbol{\varepsilon}(\boldsymbol{u}) + \boldsymbol{\tau}) + F(\boldsymbol{u}),
$$

and if $\boldsymbol{\tau} \in \boldsymbol{P}$ is fixed, the corresponding perturbed problem is

$$
\text{Minimize} \quad \Psi(\boldsymbol{\tau}, \boldsymbol{u}), \qquad \boldsymbol{u} \in \boldsymbol{V}.
\tag{2.22}
$$

The primal problem is recovered by $\mathcal{E}_{\mathrm{el}}(\boldsymbol{u}) = \Psi(0, \boldsymbol{u})$. Based on the perturbed problem we now define the dual problem with respect to the primal problem (2.12) as

$$
\text{Minimize} \quad \Psi^*(\boldsymbol{\sigma}^*, 0) \qquad \boldsymbol{\sigma}^* \in \boldsymbol{P}^*,
\tag{2.23}
$$

where the *Legendre-Fenchel conjugate function* $\Psi^* : (\boldsymbol{P} \times \boldsymbol{V})^* \to \overline{\mathbb{R}}$ is given by

$$
\Psi^*(\boldsymbol{\sigma}^*, \boldsymbol{u}^*) = \sup_{(\boldsymbol{\sigma}, \boldsymbol{u}) \in \boldsymbol{P} \times \boldsymbol{V}} \left\{ \left\langle (\boldsymbol{\sigma}^*, \boldsymbol{u}^*), (\boldsymbol{\sigma}, \boldsymbol{u}) \right\rangle_{(\boldsymbol{P} \times \boldsymbol{V})^* \times (\boldsymbol{P} \times \boldsymbol{V})} - \Psi(\boldsymbol{\sigma}, \boldsymbol{u}) \right\}.
$$

To Ψ, we can associate a *Lagrange function* or *Lagrangian* $L : \boldsymbol{P}^* \times \boldsymbol{V} \to \overline{\mathbb{R}}$ via

$$
L(\boldsymbol{\sigma}^*, \boldsymbol{u}) = \sup_{\boldsymbol{\sigma} \in \boldsymbol{P}} \left\{ \langle \boldsymbol{\sigma}^*, \boldsymbol{\sigma} \rangle_{\boldsymbol{P}^* \times \boldsymbol{P}} - \Psi(\boldsymbol{\sigma}, \boldsymbol{u}) \right\},
$$

and an easy computation shows

$$
L(\boldsymbol{\sigma}^*, \boldsymbol{u}) = \mathcal{W}_e^*(\boldsymbol{\sigma}^*) - \langle \boldsymbol{\sigma}^*, \boldsymbol{\varepsilon}(\boldsymbol{u}) \rangle_{\boldsymbol{P}^* \times \boldsymbol{P}} - F(\boldsymbol{u}).
\tag{2.24}
$$

Here, the conjugate energy $\mathcal{W}_e^*$ is just the Legendre-Fenchel conjugate function of the free energy $\mathcal{W}_e$, and it is easy to see that

$$\mathcal{W}_e^*(\boldsymbol{\sigma}^*) = \sup_{\boldsymbol{\varepsilon} \in \boldsymbol{P}} \left\{ \langle \boldsymbol{\sigma}^*, \boldsymbol{\varepsilon} \rangle_{\boldsymbol{P}^* \times \boldsymbol{P}} - \mathcal{W}_e(\boldsymbol{\varepsilon}) \right\} = \frac{1}{2} \int_\Omega \boldsymbol{\sigma}^*(x) : \mathbb{C}^{-1}[\boldsymbol{\sigma}^*(x)] \, dx = \frac{1}{2} a(\boldsymbol{\sigma}^*, \boldsymbol{\sigma}^*) \,,$$

where the last two representations require the identification $\boldsymbol{P} \cong \boldsymbol{P}^*$. It remains to specify the goal functional of the dual problem (2.23). Reconsidering $\boldsymbol{\varepsilon} : \boldsymbol{V} \to \boldsymbol{P}$, for the corresponding dual operator we have $\boldsymbol{\varepsilon}^* : \boldsymbol{P}^* \to \boldsymbol{V}^*$, and then

$$\begin{aligned}
\Psi^*(\boldsymbol{\sigma}^*, 0) &= \sup_{(\boldsymbol{\sigma}, \boldsymbol{u}) \in \boldsymbol{P} \times \boldsymbol{V}} \left\{ \langle \boldsymbol{\sigma}^*, \boldsymbol{\sigma} \rangle_{\boldsymbol{P}^* \times \boldsymbol{P}} - \Psi(\boldsymbol{\sigma}, \boldsymbol{u}) \right\} \\
&= \sup_{\boldsymbol{u} \in \boldsymbol{V}} \sup_{\boldsymbol{\sigma} \in \boldsymbol{P}} \left\{ \langle \boldsymbol{\sigma}^*, \boldsymbol{\sigma} \rangle_{\boldsymbol{P}^* \times \boldsymbol{P}} - \Psi(\boldsymbol{\sigma}, \boldsymbol{u}) \right\} = \sup_{\boldsymbol{u} \in \boldsymbol{V}} L(\boldsymbol{\sigma}^*, \boldsymbol{u}) \\
&= \mathcal{W}_e^*(\boldsymbol{\sigma}^*) + \sup_{\boldsymbol{u} \in \boldsymbol{V}} \left\{ \langle -\boldsymbol{\sigma}^*, \boldsymbol{\varepsilon}(\boldsymbol{u}) \rangle_{\boldsymbol{P}^* \times \boldsymbol{P}} - F(\boldsymbol{u}) \right\} \\
&= \mathcal{W}_e^*(\boldsymbol{\sigma}^*) + \sup_{\boldsymbol{u} \in \boldsymbol{V}} \left\{ \langle -\boldsymbol{\varepsilon}^*(\boldsymbol{\sigma}^*), \boldsymbol{u} \rangle_{\boldsymbol{V}^* \times \boldsymbol{V}} - F(\boldsymbol{u}) \right\} \\
&= \mathcal{W}_e^*(\boldsymbol{\sigma}^*) + F^*(-\boldsymbol{\varepsilon}^*(\boldsymbol{\sigma}^*)) \,.
\end{aligned}$$

As a result of [Tem85, Lemma I.2.2], we have

$$F^*(-\boldsymbol{\varepsilon}^*(\boldsymbol{\sigma}^*)) = \begin{cases} -\int_{\Gamma_T} \boldsymbol{\sigma}^*(x)\boldsymbol{n}(x) \cdot \boldsymbol{u}_D(x) \, da & , \text{if} \begin{cases} -\operatorname{div}(\boldsymbol{\sigma}^*(x)) = \boldsymbol{b}(x) \text{ in } \Omega \,, \\ \boldsymbol{\sigma}^*(x)\boldsymbol{n}(x) = \boldsymbol{t}_N(x) \text{ on } \Gamma_T \,, \end{cases} \\ +\infty & , \text{else} \,. \end{cases}$$

Defining the *statically admissible set*

$$\boldsymbol{S}(\boldsymbol{b}, \boldsymbol{t}_N) = \{ \boldsymbol{\sigma} \in \Sigma_{\operatorname{div}}(\boldsymbol{t}_N) : -\operatorname{div}(\boldsymbol{\sigma}(x)) = \boldsymbol{b}(x) \text{ in } \Omega \} \,, \tag{2.25}$$

and identifying $\boldsymbol{P}$ and $\boldsymbol{P}^*$, the dual problem (2.23) finally takes the form

$$\text{Minimize} \quad \tfrac{1}{2} a(\boldsymbol{\sigma}, \boldsymbol{\sigma}) - h(\boldsymbol{\sigma}) \qquad \text{subject to} \quad \boldsymbol{\sigma} \in \boldsymbol{S}(\boldsymbol{b}, \boldsymbol{t}_N) \,. \tag{2.26}$$

which is just problem (2.20), with h as defined in (2.19).

Using the operator notation, the Lagrangian (2.24) can be rephrased as

$$L(\boldsymbol{\sigma}, \boldsymbol{u}) = \tfrac{1}{2} \langle A\boldsymbol{\sigma}, \boldsymbol{\sigma} \rangle_{\boldsymbol{P}^* \times \boldsymbol{P}} + \langle B^* \boldsymbol{u}, \boldsymbol{\sigma} \rangle_{\boldsymbol{P}^* \times \boldsymbol{P}} - \langle F, \boldsymbol{u} \rangle_{\boldsymbol{V}^* \times \boldsymbol{V}} \,, \tag{2.27}$$

and restricting the Lagrangian to $\boldsymbol{P} \times \boldsymbol{X}(\boldsymbol{u}_D)$, we arrive at

$$\begin{aligned}
L(\boldsymbol{\sigma}, \boldsymbol{u}) &= \tfrac{1}{2} a(\boldsymbol{\sigma}, \boldsymbol{\sigma}) - \int_\Omega \boldsymbol{\sigma}(x) : \boldsymbol{\varepsilon}(\boldsymbol{u}(x)) \, dx + \ell(\boldsymbol{u}) \\
&= \tfrac{1}{2} a(\boldsymbol{\sigma}, \boldsymbol{\sigma}) + \int_\Omega \boldsymbol{u}(x) \cdot \big(\operatorname{div}(\boldsymbol{\sigma}(x)) + \boldsymbol{b}(x) \big) \, dx \\
&\quad + \int_{\Gamma_T} \boldsymbol{u}(x) \cdot \big(\boldsymbol{t}_N(x) - \boldsymbol{\sigma}(x)\boldsymbol{n}(x) \big) \, da - \int_{\Gamma_D} \boldsymbol{\sigma}(x)\boldsymbol{n}(x) \cdot \boldsymbol{u}_D(x) \, da \,.
\end{aligned}$$

We see that depending on whether we seek stationary points of the Lagrangian based on the representation in the first or the second line, we arrive at the two different mixed formulations (2.14) and (2.18) presented in the previous subsection.

The solutions of the primal and the dual problem define a *saddle point* of the Lagrange functional L, i.e. if $\boldsymbol{u} \in \boldsymbol{X}(\boldsymbol{u}_D)$ solves (2.12) and $\boldsymbol{\sigma} \in \boldsymbol{S}(\boldsymbol{b}, \boldsymbol{t}_N)$ solves (2.26), then

$$L(\boldsymbol{\sigma}, \boldsymbol{v}) \leq L(\boldsymbol{\sigma}, \boldsymbol{u}) \leq L(\boldsymbol{\eta}, \boldsymbol{u}) \,, \qquad \text{for all } \boldsymbol{\eta} \in \Sigma, \ \boldsymbol{v} \in \boldsymbol{X}(\boldsymbol{u}_D) \,.$$

In terms of the Lagrangian, the primal and dual problem can be recast as

$$\text{Minimize} \quad \sup_{\boldsymbol{\sigma} \in \boldsymbol{P}} \{-L(\boldsymbol{\sigma}, \boldsymbol{u})\} , \qquad \boldsymbol{u} \in \boldsymbol{X}(\boldsymbol{u}_D) .$$

$$\text{Minimize} \quad \sup_{\boldsymbol{u} \in \boldsymbol{X}(\boldsymbol{u}_D)} \{L(\boldsymbol{\sigma}, \boldsymbol{u})\} , \qquad \boldsymbol{\sigma} \in \boldsymbol{P} .$$

The optimality system for the two minimization problems is then equivalent to finding a saddle point of the Lagrangian, i.e.

$$0 \in \langle \partial_{\boldsymbol{\sigma}} L(\boldsymbol{\sigma}, \boldsymbol{u}), \boldsymbol{\eta} \rangle_{\boldsymbol{P}^* \times \boldsymbol{P}} = a(\boldsymbol{\sigma}, \boldsymbol{\eta}) - \int_\Omega \boldsymbol{\eta}(x) : \boldsymbol{\varepsilon}(\boldsymbol{u}(x)) \, dx , \qquad \boldsymbol{\eta} \in \boldsymbol{P} ,$$

$$0 \in \langle \partial_{\boldsymbol{u}} L(\boldsymbol{\sigma}, \boldsymbol{u}), \boldsymbol{v} \rangle_{\boldsymbol{X}^* \times \boldsymbol{X}} = - \int_\Omega \boldsymbol{\sigma}(x) : \boldsymbol{\varepsilon}(\boldsymbol{v}(x)) \, dx + \ell(\boldsymbol{v}) , \qquad \boldsymbol{v} \in \boldsymbol{X} .$$

Since all derivatives exist, the inclusions can be replaced by equalities and we see that the first equation is the constitutive equation in weak form, whereas the second equation is the equilibrium equation in weak form and we recover the formulation (2.16).

3. Associated Perfect Plasticity

As we have outlined in the previous chapter, the major difference between elastic and plastic behavior is the path dependent behavior of plasticity due to the irreversibility of plastic deformation. Essentially, this property disallows to consider the static case and demands to consider the full history of the deformation. Nevertheless, we start by considering the static case. This is reasonable from an algorithmic as well as analytic point of view, since time discretization is essential in both fields.

3.1. Associated Static Perfect Plasticity. We begin by recapitulating the governing equations of static perfect plasticity, a model often called *Hencky model* when combined with the flow rule of von Mises.

$$-\operatorname{div}(\boldsymbol{\sigma}(x)) = \boldsymbol{b}(x) , \qquad\qquad x \in \Omega , \qquad\qquad \text{(2.28a)}$$

$$\boldsymbol{\sigma}(x) = \mathbb{C}[\boldsymbol{\varepsilon}(\boldsymbol{u}(x)) - \boldsymbol{\varepsilon}_p(x)] , \qquad\qquad x \in \Omega , \qquad\qquad \text{(2.28b)}$$

$$\boldsymbol{\sigma}(x) \in K , \qquad\qquad x \in \Omega , \qquad\qquad \text{(2.28c)}$$

$$\boldsymbol{\varepsilon}_p(x) \in N_K(\boldsymbol{\sigma}(x)) \qquad\qquad x \in \Omega , \qquad\qquad \text{(2.28d)}$$

$$\boldsymbol{u}(x) = \boldsymbol{u}_D , \qquad\qquad x \in \Gamma_D , \qquad\qquad \text{(2.28e)}$$

$$\boldsymbol{\sigma}(x)\boldsymbol{n}(x) = \boldsymbol{t}_N(x) , \qquad\qquad x \in \Gamma_T . \qquad\qquad \text{(2.28f)}$$

In the static setting, the flow rule (1.17) is replaced by (2.28d) and for the definition of the normal cone N_K, we also refer to (1.17). Contrary to linear elasticity, the choice of spaces is not obvious because of the presence of the two inclusions (2.28c) and (2.28d), rendering the problem of perfect plasticity significantly harder than the problem of linear elasticity. Indeed, results have only been obtained for the case of associated plasticity and even in this case, most results rely on a particular shape of K given by the yield criteria of von Mises. We will not derive a complete duality framework for plasticity since this is far beyond the scope of this work, but we will only provide a basic exposition suitable for our purposes. An extensive study based on the von Mises yield condition including regularity results can be found in [FS00] or [BF02]. Major progress was already made around 1980, in the already mentioned papers [Suq78a, Suq78b, Suq79, TS80] leading to the monograph [Tem85].

3.2. The Dual Problem in Associated Static Perfect Plasticity. In associated plasticity, the flow rule is derived from a variational principle as we have seen in the introductory chapter. This allows to treat associated plasticity in the same duality framework as presented above. But contrary to the previous section, we will not give a full derivation, but we will rather state the dual minimization problem directly and show that the governing equations are satisfied. For this derivation, we proceed formally, assuming $\boldsymbol{u} \in \boldsymbol{X}(\boldsymbol{u}_D)$ which however is not reasonable as we will see later.

In the last chapter, our approach to plasticity was to confine the stress tensor to the set of admissible stress states via the inclusion (2.28c). This is a pointwise constraint and defining

$$\boldsymbol{K} = \{\boldsymbol{\eta} \in \boldsymbol{P} : \boldsymbol{\eta}(x) \in K \text{ a.e. in } \Omega\}, \qquad \chi_{\boldsymbol{K}}(\boldsymbol{\sigma}) = \begin{cases} 0 & , \boldsymbol{\sigma} \in \boldsymbol{K}, \\ \infty & , \boldsymbol{\sigma} \notin \boldsymbol{K}, \end{cases} \qquad (2.29)$$

admissibility can be reformulated as $\boldsymbol{\sigma} \in \boldsymbol{K}$. Here, $\chi_{\boldsymbol{K}}$ is the (convex) indicator function of the set $\boldsymbol{K}$. To incorporate this constraint into the duality framework of the previous chapter, we simply modify the Lagrangian (2.27) by adding $\chi_{\boldsymbol{K}}(\boldsymbol{\sigma})$, i.e.

$$L(\boldsymbol{\sigma}, \boldsymbol{u}) = \tfrac{1}{2} a(\boldsymbol{\sigma}, \boldsymbol{\sigma}) + \chi_{\boldsymbol{K}}(\boldsymbol{\sigma}) - \int_{\Omega} \boldsymbol{\sigma}(x) : \boldsymbol{\varepsilon}(\boldsymbol{u}(x)) \, dx + \ell(\boldsymbol{u}), \qquad (2.30)$$

where we already considered the restriction to $\boldsymbol{P} \times \boldsymbol{X}(\boldsymbol{u}_D)$. Formally the Lagrangian is defined on $\boldsymbol{P} \times \boldsymbol{V}$ as

$$L(\boldsymbol{\sigma}, \boldsymbol{u}) = \tfrac{1}{2} \langle A\boldsymbol{\sigma}, \boldsymbol{\sigma} \rangle_{\boldsymbol{P}^* \times \boldsymbol{P}} + \chi_{\boldsymbol{K}}(\boldsymbol{\sigma}) + \langle B^*\boldsymbol{u}, \boldsymbol{\sigma} \rangle_{\boldsymbol{P}^* \times \boldsymbol{P}} - \langle F, \boldsymbol{u} \rangle_{\boldsymbol{V}^* \times \boldsymbol{V}},$$

with F as defined in (2.21). Sticking to the terminology previously introduced, the dual problem is given as:

$$\text{Minimize} \quad \sup_{\boldsymbol{u} \in \boldsymbol{X}(\boldsymbol{u}_D)} \{L(\boldsymbol{\sigma}, \boldsymbol{u})\}, \qquad \boldsymbol{\sigma} \in \boldsymbol{P}.$$

and thus:

$$\text{Minimize} \quad \tfrac{1}{2} a(\boldsymbol{\sigma}, \boldsymbol{\sigma}) + \chi_{\boldsymbol{K}}(\boldsymbol{\sigma}) - h(\boldsymbol{\sigma}) \qquad \text{subject to} \quad \boldsymbol{\sigma} \in \boldsymbol{S}(\boldsymbol{b}, \boldsymbol{t}_N). \qquad (2.31)$$

It is well-known, cf. [Tem85, Section II.8] or [FS00, Section 1.3], that this problem admits a unique solution under the following *safe-load condition*:

Assumption 2.1. *There exist $\widehat{\boldsymbol{\sigma}} \in \boldsymbol{P}$ and $\varepsilon > 0$ such that for all $\boldsymbol{\xi} \in \mathrm{Sym}(d)$ with $|\boldsymbol{\xi}| \leq \varepsilon$:*

$$\widehat{\boldsymbol{\sigma}} \in \boldsymbol{S}(\boldsymbol{b}, \boldsymbol{t}_N) \qquad and \qquad \widehat{\boldsymbol{\sigma}}(x) + \boldsymbol{\xi} \in K \quad a.e. \text{ in } \Omega. \qquad (2.32)$$

The safe-load condition can be interpreted as a uniform Slater condition.

Before we consider the optimality conditions, we note that formally, the convex subdifferential of the indicator function $\chi_{\boldsymbol{K}}$ is a multi-valued map

$$\partial \chi_{\boldsymbol{K}} : \boldsymbol{P} \rightrightarrows \boldsymbol{P}^*, \qquad \partial \chi_{\boldsymbol{K}}(\boldsymbol{\sigma}) = \{\boldsymbol{\varepsilon} \in \boldsymbol{P}^* : \chi_{\boldsymbol{K}}(\boldsymbol{\eta}) \geq \chi_{\boldsymbol{K}}(\boldsymbol{\sigma}) + \langle \boldsymbol{\varepsilon}, \boldsymbol{\eta} - \boldsymbol{\sigma} \rangle_{\boldsymbol{P}^* \times \boldsymbol{P}}\},$$

which coincides with the normal cone $N_{\boldsymbol{K}}$ of $\boldsymbol{K}$, also reconsider Subsection 1.2.3. The optimality conditions are given as

$$0 \in \partial_{\boldsymbol{\sigma}} L(\boldsymbol{\sigma}, \boldsymbol{u}) = A\boldsymbol{\sigma} + \partial \chi_{\boldsymbol{K}}(\boldsymbol{\sigma}) + B^*\boldsymbol{u}, \qquad \qquad \text{in } \boldsymbol{P}^*, \qquad (2.33a)$$

$$0 \in \partial_{\boldsymbol{u}} L(\boldsymbol{\sigma}, \boldsymbol{u}) = B\boldsymbol{\sigma} - F, \qquad \qquad \text{in } \boldsymbol{V}^*. \qquad (2.33b)$$

The only difference to the optimality conditions of linear elasticity (2.17) is the presence of the subdifferential of the indicator function. The second inclusion can be transformed

into an equation in $\boldsymbol{X}^*$, i.e. $B\boldsymbol{\sigma} = -\ell$ in $\boldsymbol{X}^*$. However, the first line is indeed an inclusion, and after the usual identification $\boldsymbol{P} \cong \boldsymbol{P}^*$, we explicitly obtain

$$\chi_{\boldsymbol{K}}(\boldsymbol{\eta}) \geq \chi_{\boldsymbol{K}}(\boldsymbol{\sigma}) + \int_\Omega \big(- \mathbb{C}^{-1}[\boldsymbol{\sigma}(x)] + \boldsymbol{\varepsilon}(\boldsymbol{u}(x))\big) : \big(\boldsymbol{\eta}(x) - \boldsymbol{\sigma}(x)\big)\, dx\,, \qquad \boldsymbol{\eta} \in \boldsymbol{P}\,.$$

Reconsidering (2.28b), and testing with $\boldsymbol{\eta} \in \boldsymbol{K}$, we arrive at

$$\int_\Omega \boldsymbol{\varepsilon}_p(x) : \big(\boldsymbol{\eta}(x) - \boldsymbol{\sigma}(x)\big)\, dx \leq 0\,, \qquad \boldsymbol{\eta} \in \boldsymbol{K}\,.$$

Looking back at Section 1.2.3, this is just the associated flow rule in integrated form. We conclude that if we define the dual problem of associated perfect plasticity in the above way, we automatically fulfill the governing equations (2.28) in weak form.

We also remark that the dual problem (2.31) has a representation as the variational inequality

$$a(\boldsymbol{\sigma}, \boldsymbol{\eta} - \boldsymbol{\sigma}) \geq h(\boldsymbol{\eta} - \boldsymbol{\sigma})\,, \qquad \boldsymbol{\eta} \in \boldsymbol{S}(\boldsymbol{b}, \boldsymbol{t}_N) \cap \boldsymbol{K}\,. \tag{2.34}$$

This formulation is particularly useful in the (time-dependent) quasi-static scenario as we will see later.

3.3. The Primal Problem in Associated Static Perfect Plasticity. Based on Lagrangian duality, we now consider the primal problem

$$\text{Minimize} \quad \sup_{\boldsymbol{\sigma} \in \boldsymbol{P}}\{-L(\boldsymbol{\sigma}, \boldsymbol{u})\}\,, \qquad \boldsymbol{u} \in \boldsymbol{X}(\boldsymbol{u}_D)\,,$$

and again, we proceed formally in order to derive the primal minimization problem. We find

$$
\begin{aligned}
\sup_{\boldsymbol{\sigma} \in \boldsymbol{P}}\{-L(\boldsymbol{\sigma}, \boldsymbol{u})\} &= \sup_{\boldsymbol{\sigma} \in \boldsymbol{P}}\Big\{ -\tfrac{1}{2}a(\boldsymbol{\sigma}, \boldsymbol{\sigma}) - \chi_{\boldsymbol{K}}(\boldsymbol{\sigma}) + \int_\Omega \boldsymbol{\sigma}(x) : \boldsymbol{\varepsilon}(\boldsymbol{u}(x))\, dx - \ell(\boldsymbol{u}) \Big\} \\
&= \sup_{\boldsymbol{\sigma} \in \boldsymbol{P}}\Big\{ -\tfrac{1}{2}a\big(\boldsymbol{\sigma} - \mathbb{C}[\boldsymbol{\varepsilon}(\boldsymbol{u})], \boldsymbol{\sigma} - \mathbb{C}[\boldsymbol{\varepsilon}(\boldsymbol{u})]\big) + \tfrac{1}{2}a\big(\mathbb{C}[\boldsymbol{\varepsilon}(\boldsymbol{u})], \mathbb{C}[\boldsymbol{\varepsilon}(\boldsymbol{u})]\big) - \chi_{\boldsymbol{K}}(\boldsymbol{\sigma}) - \ell(\boldsymbol{u}) \Big\} \\
&= \sup_{\boldsymbol{\sigma} \in \boldsymbol{P}}\Big\{ -\tfrac{1}{2}\|\boldsymbol{\sigma} - \mathbb{C}[\boldsymbol{\varepsilon}(\boldsymbol{u})]\|_\Sigma^2 - \chi_{\boldsymbol{K}}(\boldsymbol{\sigma}) \Big\} + \tfrac{1}{2}\|\mathbb{C}[\boldsymbol{\varepsilon}(\boldsymbol{u})]\|_\Sigma^2 - \ell(\boldsymbol{u}) \\
&= \sup_{\boldsymbol{\sigma} \in \boldsymbol{K}}\Big\{ -\tfrac{1}{2}\|\boldsymbol{\sigma} - \mathbb{C}[\boldsymbol{\varepsilon}(\boldsymbol{u})]\|_\Sigma^2 \Big\} + \tfrac{1}{2}\|\mathbb{C}[\boldsymbol{\varepsilon}(\boldsymbol{u})]\|_\Sigma^2 - \ell(\boldsymbol{u}) \\
&= -\tfrac{1}{2}\|P_{\boldsymbol{K}}\big(\mathbb{C}[\boldsymbol{\varepsilon}(\boldsymbol{u})]\big) - \mathbb{C}[\boldsymbol{\varepsilon}(\boldsymbol{u})]\|_\Sigma^2 + \tfrac{1}{2}\|\mathbb{C}[\boldsymbol{\varepsilon}(\boldsymbol{u})]\|_\Sigma^2 - \ell(\boldsymbol{u})\,,
\end{aligned}
$$

where in the last line, the projection $P_{\boldsymbol{K}} : \boldsymbol{P} \to \boldsymbol{K}$ is w.r.t. the inner product $a(\cdot, \cdot)$ in $\boldsymbol{P}$ and therefore differs from the Euclidean projection in general, cf. (2.7).

We introduce the functional

$$\Upsilon : \boldsymbol{P} \to \mathbb{R}\,, \qquad\qquad \Upsilon(\boldsymbol{\eta}) = \tfrac{1}{2}\|\boldsymbol{\eta}\|_\Sigma^2 - \tfrac{1}{2}\|P_{\boldsymbol{K}}(\boldsymbol{\eta}) - \boldsymbol{\eta}\|_\Sigma^2\,, \tag{2.35}$$

and it is well-known that Υ is differentiable and convex, cf. [Zar71] or [HR99, Chapter 8], with the Fréchet derivative

$$\langle D\Upsilon(\boldsymbol{\sigma}), \boldsymbol{\eta}\rangle_{\boldsymbol{P}^* \times \boldsymbol{P}} = a(P_{\boldsymbol{K}}(\boldsymbol{\sigma}), \boldsymbol{\eta})\,.$$

The convexity easily follows from the monotonicity of the projection mapping w.r.t. to the associated metric, i.e. $a(P_{\boldsymbol{K}}(\boldsymbol{\sigma}) - P_{\boldsymbol{K}}(\boldsymbol{\eta}), \boldsymbol{\sigma} - \boldsymbol{\eta}) \geq 0$ for all $\boldsymbol{\sigma}, \boldsymbol{\eta} \in \boldsymbol{P}$. However, it must be noted that Υ is not uniformly convex. This is easy to see by considering two elements $\boldsymbol{\sigma}, \boldsymbol{\eta} \in \boldsymbol{P}$, $\boldsymbol{\sigma} \neq \boldsymbol{\eta}$ such that $P_{\boldsymbol{K}}(\boldsymbol{\sigma}) = P_{\boldsymbol{K}}(\boldsymbol{\sigma})$.

Introducing the primal functional $\mathcal{E}_{\mathrm{pl}} : \boldsymbol{X} \to \mathbb{R}$,

$$\begin{aligned} \mathcal{E}_{\mathrm{pl}}(\boldsymbol{u}) &= \tfrac{1}{2}\|\mathbb{C}[\boldsymbol{\varepsilon}(\boldsymbol{u})]\|_{\Sigma}^2 - \tfrac{1}{2}\|P_{\boldsymbol{K}}\big(\mathbb{C}[\boldsymbol{\varepsilon}(\boldsymbol{u})]\big) - \mathbb{C}[\boldsymbol{\varepsilon}(\boldsymbol{u})]\|_{\Sigma}^2 - \ell(\boldsymbol{u}) \\ &= \Upsilon\big(\mathbb{C}[\boldsymbol{\varepsilon}(\boldsymbol{u})]\big) - \ell(\boldsymbol{u}) \,, \end{aligned} \tag{2.36}$$

we obtain the primal problem:

$$\text{Minimize} \quad \mathcal{E}_{\mathrm{pl}}(\boldsymbol{u}) \,, \qquad \boldsymbol{u} \in \boldsymbol{X}(\boldsymbol{u}_D) \,, \tag{2.37}$$

We remark that setting $\boldsymbol{K} = \boldsymbol{P}$ returns the primal problem in elasticity since then $\Upsilon(\boldsymbol{\eta}) = \tfrac{1}{2}a(\boldsymbol{\eta}, \boldsymbol{\eta})$ and $\tfrac{1}{2}a(\mathbb{C}[\boldsymbol{\varepsilon}(\boldsymbol{u})], \mathbb{C}[\boldsymbol{\varepsilon}(\boldsymbol{u})]) = \tfrac{1}{2}c(\boldsymbol{u}, \boldsymbol{u})$. Since the composition of a convex function and a linear transformation is again convex, the convexity of Υ also shows the convexity of the primal functional $\mathcal{E}_{\mathrm{pl}}$. By the chain rule we find the necessary and sufficient optimality condition for a minimum $\boldsymbol{u} \in \boldsymbol{X}(\boldsymbol{u}_D)$ of the primal problem to be

$$a(P_{\boldsymbol{K}}(\mathbb{C}[\boldsymbol{\varepsilon}(\boldsymbol{u})]), \mathbb{C}[\boldsymbol{\varepsilon}(\boldsymbol{w})]) = \ell(\boldsymbol{w}) \,, \qquad \boldsymbol{w} \in \boldsymbol{X} \,.$$

Written out explicitly, this is

$$\int_{\Omega} P_K(\mathbb{C}[\boldsymbol{\varepsilon}(\boldsymbol{u}(x))]) : \boldsymbol{\varepsilon}(\boldsymbol{w}(x)) \, dx = \ell(\boldsymbol{w}) \,, \qquad \boldsymbol{w} \in \boldsymbol{X} \,. \tag{2.38}$$

We emphasize that just as in the elasticity problem, the primal problem is unconstrained whereas the dual problem is a constrained minimization problem. But contrary to the elastic case, this time the primal functional exhibits some unpleasant features as we will see.

3.4. Linear or Anisotropic Linear Growth of the Primal Problem. Besides the favorable properties of being differentiable and convex, the major drawback is that generally Υ only has linear or anisotropic linear growth (linear growth into certain directions). To explain this notion, we shortly consider the case of incompressible plasticity, cf. Subsection 1.2.2, in which the admissible set is given by $K = \mathbb{R}\mathbf{1} \oplus \widehat{K}$ with $\widehat{K} \subset \mathrm{Sym}_0(d)$ which we assume to be bounded in $\mathrm{Sym}_0(d)$. This assumption is typically fulfilled, e.g. for ductile metals (von Mises and Tresca plasticity).

Provided $\mathbb{C}^{-1} = \tfrac{1}{2\mu}\mathbb{P}_{\mathrm{dev}} + \tfrac{1}{d\kappa}\mathbb{P}_{\mathrm{vol}}$, the projection onto K can be computed independently on the volumetric and deviatoric subspace and on the volumetric subspace, the projection is the identity. On the deviatoric subspace $\mathrm{Sym}_0(d)$, the projection $\widehat{P}_{\widehat{K}}$ is the Euclidean projection (up to scaling by $\tfrac{1}{2\mu}$), and pointwise a.e. we find

$$P_{\boldsymbol{K}}(\boldsymbol{\sigma})(x) = \widehat{P}_{\widehat{K}}(\mathbb{P}_{\mathrm{dev}}[\boldsymbol{\sigma}(x)]) + \mathbb{P}_{\mathrm{vol}}[\boldsymbol{\sigma}(x)] \,.$$

This leads to

$$\Upsilon(\boldsymbol{\eta}) = \tfrac{1}{2}\|\boldsymbol{\eta}\|_{\Sigma}^2 - \tfrac{1}{2}\|P_{\boldsymbol{K}}(\mathbb{P}_{\mathrm{dev}}[\boldsymbol{\eta}]) - \mathbb{P}_{\mathrm{dev}}[\boldsymbol{\eta}]\|_{\Sigma}^2 \,, \tag{2.39}$$

and as a result, Υ has quadratic growth with respect to the subset $\mathbb{P}_{\mathrm{vol}}[\boldsymbol{P}]$ but only linear growth otherwise. To understand this, we fix $\boldsymbol{\eta} \in \boldsymbol{P}$ by requiring $\boldsymbol{\eta}(x) \in \mathrm{Sym}_0(d)$ a.e. in Ω and $\|\boldsymbol{\eta}\|_{\Sigma} = 1$. Moreover, since $\widehat{K}$ is bounded, for sufficiently large $t > 0$, there is a unique $\widehat{\boldsymbol{\eta}} \in \boldsymbol{K}$ such that $P_{\boldsymbol{K}}(t\boldsymbol{\eta}) = \widehat{\boldsymbol{\eta}}$. Substituted into Υ, we then find

$$\frac{\Upsilon(t\boldsymbol{\eta})}{t} = \frac{1}{t}a(P_{\boldsymbol{K}}(t\boldsymbol{\eta}), t\boldsymbol{\eta}) - \frac{1}{2t}a(P_{\boldsymbol{K}}(t\boldsymbol{\eta}), P_{\boldsymbol{K}}(t\boldsymbol{\eta})) \quad \stackrel{t\to\infty}{\longrightarrow} \quad a(\widehat{\boldsymbol{\eta}}, \boldsymbol{\eta}) = const \,,$$

showing the linear growth of Υ into the direction of $\boldsymbol{\eta}$.

3.5. Ill-Posedness in Sobolev Spaces and Relaxation. Concerning the von Mises yield function, the following results can be found in [**Tem85**, Chapter 2] and [**FS00**, Chapter 1]. For a more general exposition to problems with linear growth, we refer to [**ABM06**, Section 11.3]. Since Υ only has linear growth, the same holds for the primal functional $\mathcal{E}_{\mathrm{pl}}$ since it is a composition of Υ and a linear operator. Hence, we cannot expect to find a minimizer in $\boldsymbol{X}(\boldsymbol{u}_D)$ and a more natural space would be $W^{1,1}(\Omega, \mathbb{R}^d)$. However, due to the non-reflexivity of this space, the direct method in the calculus of variations [**Giu03**, **Dac89**] fails in this case as the primal functional is not lower semicontinuous w.r.t. the weak topology of $W^{1,1}(\Omega, \mathbb{R}^d)$. An explicit example for the non-existence of a solution in case of the von Mises flow rule is given in [**FS00**, Section 1.1]. To circumvent this difficulty, one considers the *lower semicontinuous envelope* of the primal functional and its domain which essentially is the space in which the primal problem admits a solution. This relaxation naturally leads to the space of bounded deformations $BD(\Omega)$ as introduced in the opening section of this chapter. This space allows discontinuities of the displacement field within the body Ω as well as on the boundary. This also imposes the necessity to relax the boundary condition in a suitable way. We remark that the relaxation procedure is just one special case of Γ-*convergence*, cf. [**Mas93**, Chapter 4]. Moreover, choosing the right topology right from the beginning re-enables the use of the direct method, cf. [**MDM06**, Section 3].

3.6. Monotonicity Properties. We close the chapter by briefly commenting on monotonicity properties of the associated perfectly plastic problem. Therefore, we rewrite the problem as a nonlinear operator equation. At this point, we use a more abstract notation as we distinguish $\boldsymbol{P}$ and its dual space $\boldsymbol{P}^*$.

Again we proceed formally and define the mapping

$$T : \boldsymbol{X} \to \boldsymbol{X}^*, \qquad\qquad T = -B \circ P_{\boldsymbol{K}} \circ A^{-1} \circ (-B^*). \qquad (2.40)$$

Less abstract, this corresponds to $T(\boldsymbol{u}) = -\operatorname{div}\big(P_{\boldsymbol{K}}\big(\mathbb{C}[\varepsilon(\boldsymbol{u})]\big)\big)$ and therefore, the optimality condition of the primal problem (2.38) can be reformulated as the nonlinear operator equation

$$T(\boldsymbol{u}) = \ell \qquad \text{in } \boldsymbol{X}^*.$$

Contrary to elasticity, T is not strongly monotone but only a monotone operator. The monotonicity again follows from the monotonicity of the projection $P_{\boldsymbol{K}}$ with respect to the metric induced by $a(\cdot, \cdot)$ as

$$
\begin{aligned}
&\langle T(\boldsymbol{u}) - T(\boldsymbol{v}), \boldsymbol{u} - \boldsymbol{v}\rangle_{\boldsymbol{X}^* \times \boldsymbol{X}} \\
&= \langle -B^*(\boldsymbol{u} - \boldsymbol{v}), P_{\boldsymbol{K}}\big(A^{-1}(-B^*(\boldsymbol{u}))\big) - P_{\boldsymbol{K}}\big(A^{-1}(-B^*(\boldsymbol{v}))\big)\rangle_{\boldsymbol{P}^* \times \boldsymbol{P}} \\
&= \langle AA^{-1}B^*(\boldsymbol{u} - \boldsymbol{v}), P_{\boldsymbol{K}}\big(-A^{-1}B^*(\boldsymbol{u})\big) - P_{\boldsymbol{K}}\big(-A^{-1}B^*(\boldsymbol{v})\big)\rangle_{\boldsymbol{P}^* \times \boldsymbol{P}} \\
&= a\Big(P_{\boldsymbol{K}}\big(-A^{-1}B^*(\boldsymbol{u})\big) - P_{\boldsymbol{K}}\big(-A^{-1}B^*(\boldsymbol{v})\big), -A^{-1}B^*\boldsymbol{u} - (-A^{-1}B^*\boldsymbol{v})\Big) \geq 0.
\end{aligned}
$$

Despite the monotonicity of T, the theory of monotone operators [**Rou05**, **Růž04**] cannot work here, as $\boldsymbol{u} \to \langle T(\boldsymbol{u}), \boldsymbol{u}\rangle_{\boldsymbol{X}^* \times \boldsymbol{X}}$ only has (anisotropic) linear growth. In the next chapter, we will consider regularization schemes for which the corresponding operators are strongly monotone.

CHAPTER 3

REGULARIZATION AND EXTENDED MODELS IN ASSOCIATED PLASTICITY

In the previous chapter, we shortly outlined the ill-posedness of the problem of perfect plasticity in Sobolev spaces. The aim of this chapter is to give a short overview how it is possible to regularize the model such that solutions in Sobolev spaces can be recovered. We will present two such regularizations which are physically motivated. The first is the viscoplastic regularization whereas the second is kinematic hardening plasticity. It will turn out that both methods have a very similar structure in the static case even though the derivation differs considerably.

1. Viscoplasticity

Physically, the viscoplastic regularization is obtained by introducing a viscosity into the model. Mathematically, we relax the requirement $\boldsymbol{\sigma}(x) \in K$ and allow stress states lying outside the admissible set. There are many ways how to define a viscoplastic flow rule, but we focus on the regularization by means of the *Moreau-Yosida approximation* of the indicator function χ_K, or the Yosida-approximation of the multi-valued operator $\partial \chi_K$, respectively. For the von Mises model, this regularization has been extensively discussed in [**DL76**] where also questions of well-posedness were addressed.

1.1. Moreau-Yosida Approximation.
We shortly present the Moreau-Yosida approximation in the Hilbert space setting, but note that it is possible to transfer this approximation to a more general Banach space setting, cf. [**PR01**]. Though the Moreau-Yosida approximation can be applied to arbitrary convex functionals, we will only consider the application to the convex indicator function $\chi_K : \boldsymbol{P} \to \overline{\mathbb{R}}$, or to the operator $\partial \chi_K : \boldsymbol{P} \rightrightarrows \boldsymbol{P}^*$, respectively. It is known that $\partial \chi_K$ is a *maximal monotone operator* since it is the subdifferential of a closed convex mapping and for $\alpha > 0$ we define the Moreau-Yosida approximation

$$\chi_K^\alpha(\boldsymbol{\sigma}) = \inf_{\boldsymbol{\eta} \in \boldsymbol{P}} \left\{ \tfrac{\alpha}{2} \|\boldsymbol{\sigma} - \boldsymbol{\eta}\|_\Sigma^2 + \chi_K(\boldsymbol{\eta}) \right\}.$$

Concerning the Moreau-Yosida approximation, we have the following result:

Proposition 3.1. *The Moreau-Yosida approximation χ_K^α of the indicator function χ_K is given as $\chi_K^\alpha(\boldsymbol{\sigma}) = \frac{\alpha}{2}\|\boldsymbol{\sigma} - P_K(\boldsymbol{\sigma})\|_\Sigma^2$. Moreover, χ_K^α is convex and Fréchet differentiable with Lipschitz continuous derivative and we have*

$$\langle D\chi_K^\alpha(\boldsymbol{\sigma}), \boldsymbol{\eta}\rangle_{P^* \times P} = \alpha\, \langle A(\boldsymbol{\sigma} - P_K(\boldsymbol{\sigma})), \boldsymbol{\eta}\rangle_{P^* \times P}, = \alpha\, a(\boldsymbol{\sigma} - P_K(\boldsymbol{\sigma}), \boldsymbol{\eta}), \tag{3.1a}$$

$$\left\|A^{-1}\big(D\chi_K^\alpha(\boldsymbol{\sigma}) - D\chi_K^\alpha(\boldsymbol{\eta})\big)\right\|_\Sigma \le \alpha\, \|\boldsymbol{\sigma} - \boldsymbol{\eta}\|_\Sigma. \tag{3.1b}$$

PROOF. Obviously

$$\chi_K^\alpha(\boldsymbol{\sigma}) = \inf_{\boldsymbol{\eta} \in P} \left\{\frac{\alpha}{2}\|\boldsymbol{\sigma} - \boldsymbol{\eta}\|_\Sigma^2 + \chi_K(\boldsymbol{\eta})\right\} = \inf_{\boldsymbol{\eta} \in K}\left\{\frac{\alpha}{2}\|\boldsymbol{\sigma} - \boldsymbol{\eta}\|_\Sigma^2\right\} = \frac{\alpha}{2}\|\boldsymbol{\sigma} - P_K(\boldsymbol{\sigma})\|_\Sigma^2,$$

by the definition of the projection $P_K : P \to K$, see (2.7), and the characterization of the derivative follows as in the previous chapter, see (2.35).

We now consider the Lipschitz continuity of the derivative. Let $\boldsymbol{\sigma}, \boldsymbol{\eta} \in P$ be arbitrary. Then, the orthogonal projections onto K w.r.t. the inner product $a(\cdot, \cdot)$ are characterized by $a(\boldsymbol{\sigma} - P_K(\boldsymbol{\sigma}), \boldsymbol{\tau} - P_K(\boldsymbol{\sigma})) \le 0$ for all $\boldsymbol{\tau} \in K$ and similarly for $\boldsymbol{\eta}$. Testing with $\boldsymbol{\tau} = P_K(\boldsymbol{\eta})$ and $\boldsymbol{\tau} = P_K(\boldsymbol{\sigma})$ then leads to

$$a\big(\boldsymbol{\sigma} - P_K(\boldsymbol{\sigma}) - (\boldsymbol{\eta} - P_K(\boldsymbol{\eta})), P_K(\boldsymbol{\eta}) - P_K(\boldsymbol{\sigma})\big) \le 0.$$

Rearranging this inequality also shows the non-expansiveness of P_K w.r.t. the norm $\|\cdot\|_\Sigma$. From the representation of the derivative, we obtain

$$\frac{1}{\alpha}\left\|A^{-1}\big(D\chi_K^\alpha(\boldsymbol{\sigma}) - D\chi_K^\alpha(\boldsymbol{\eta})\big)\right\|_\Sigma^2$$

$$= \alpha\, a\big(\boldsymbol{\sigma} - P_K(\boldsymbol{\sigma}) - (\boldsymbol{\eta} - P_K(\boldsymbol{\eta})), \boldsymbol{\sigma} - P_K(\boldsymbol{\sigma}) - (\boldsymbol{\eta} - P_K(\boldsymbol{\eta}))\big)$$

$$\le \alpha\, a\big(\boldsymbol{\sigma} - P_K(\boldsymbol{\sigma}) - (\boldsymbol{\eta} - P_K(\boldsymbol{\eta})), \boldsymbol{\sigma} - \boldsymbol{\eta}\big)$$

$$= a\big(A^{-1}\big(D\chi_K^\alpha(\boldsymbol{\sigma}) - D\chi_K^\alpha(\boldsymbol{\eta})\big), \boldsymbol{\sigma} - \boldsymbol{\eta}\big),$$

from which (3.1b) follows by the Cauchy-Schwarz inequality. □

For a proof in a more general setting, see [Sho97, Section 4.1] or [AF90, Section 3.5]. For $\alpha \to \infty$, it follows $\chi_K^\alpha(\boldsymbol{\eta}) \to \chi_K(\boldsymbol{\eta})$ for all $\boldsymbol{\eta} \in P$. We also remark that we used the norm $\|\cdot\|_\Sigma$ in the definition of the Moreau-Yosida approximation rather than the natural norm in P. The reason will become clear in the next subsection.

1.2. Viscoplastic Regularization. In perfect plastic, the flow rule is given pointwise as $\boldsymbol{\varepsilon}_p(x) \in \partial\chi_K(\boldsymbol{\sigma}(x))$ as we have seen before. We relax this condition by imposing

$$\boldsymbol{\varepsilon}_p(x) = D\chi_K^\alpha(\boldsymbol{\sigma}(x)) = \alpha\, \mathbb{C}^{-1}[\boldsymbol{\sigma}(x) - P_K(\boldsymbol{\sigma}(x))],$$

where $D\chi_K^\alpha$ is the Yosida approximation of $\partial\chi_K : \mathrm{Sym}(d) \rightrightarrows \mathrm{Sym}(d)$ w.r.t. the inner product induced by $\mathbb{C}^{-1}$. Obviously, this is the pointwise a.e. interpretation of the result of the previous subsection. This allows to eliminate the plastic strain $\boldsymbol{\varepsilon}_p$ in the constitutive relation (2.28b) and we have

$$\boldsymbol{\sigma}(x) = \mathbb{C}\big[\boldsymbol{\varepsilon}(\boldsymbol{u}(x)) - \alpha\, D\chi_K(\boldsymbol{\sigma}(x))\big] = \mathbb{C}\big[\boldsymbol{\varepsilon}(\boldsymbol{u}(x)) - \alpha\, \mathbb{C}^{-1}[\boldsymbol{\sigma}(x) - P_K(\boldsymbol{\sigma}(x))]\big]$$

$$= \mathbb{C}[\boldsymbol{\varepsilon}(\boldsymbol{u}(x))] - \alpha\big(\boldsymbol{\sigma}(x) - P_K(\boldsymbol{\sigma}(x))\big)$$

almost everywhere in Ω, or simply

$$\boldsymbol{\sigma} = \mathbb{C}[\boldsymbol{\varepsilon}(\boldsymbol{u})] - \alpha\big(\boldsymbol{\sigma} - P_K(\boldsymbol{\sigma})\big). \tag{3.2}$$

The following lemma will be important also in the algorithmic treatment later on which is why we state it in a more abstract way.

Lemma 3.2. *Let H be a Hilbert space with inner product $(\cdot,\cdot)_H$ and let $L \subset H$ be a closed convex set. Let $P_L : H \to L$ denote the orthogonal projection onto L with respect to the inner product $(\cdot,\cdot)_H$ and let $x,y \in H$ satisfy $x = y - \alpha(x - P_L(x))$ for all $\alpha > 0$. Then $P_L(x) = P_L(y)$.*

PROOF. We note that we have $y = (1+\alpha)x - \alpha P_L(x)$. With respect to the inner product $(\cdot,\cdot)_H$, the projection $P_L(y)$ onto L is characterized by

$$\big(y - P_L(y), z - P_L(y)\big)_H \le 0, \qquad z \in L.$$

Now let $z \in L$ be arbitrary and consider

$$\begin{aligned}
\big(y - P_L(x), z - P_L(x)\big)_H &= \big((1+\alpha)x - \alpha P_L(x) - P_L(x), z - P_L(x)\big)_H \\
&= (1+\alpha)\big(x - P_L(x), z - P_L(x)\big)_H \le 0,
\end{aligned}$$

where in the last step, we used the characterization of the projection. Together this gives $(y - P_L(x), z - P_L(x))_H \le 0$ for all $z \in L$ and consequently we have $P_L(y) = P_L(x)$. $\qquad\square$

Applying the Lemma to our current setting with $H = \boldsymbol{P}$, $(\cdot,\cdot)_H = a(\cdot,\cdot)$, $x = \boldsymbol{\sigma}$ and $y = \mathbb{C}[\boldsymbol{\varepsilon}(\boldsymbol{u})]$, we directly obtain

$$P_{\boldsymbol{K}}(\mathbb{C}[\boldsymbol{\varepsilon}(\boldsymbol{u})]) = P_{\boldsymbol{K}}(\boldsymbol{\sigma}).$$

Note that this does not hold if the Moreau-Yosida approximation is introduced with a different norm than $\|\cdot\|_{\boldsymbol{\Sigma}}$. Rearranging (3.2) and using the last equality then leads to

$$\boldsymbol{\sigma} = \tfrac{1}{1+\alpha}\big(\mathbb{C}[\boldsymbol{\varepsilon}(\boldsymbol{u})] + \alpha P_{\boldsymbol{K}}(\mathbb{C}[\boldsymbol{\varepsilon}(\boldsymbol{u})])\big) = \tfrac{1}{1+\alpha}\mathbb{C}[\boldsymbol{\varepsilon}(\boldsymbol{u})] + \big(1 - \tfrac{1}{1+\alpha}\big)P_{\boldsymbol{K}}(\mathbb{C}[\boldsymbol{\varepsilon}(\boldsymbol{u})]). \tag{3.3}$$

Thus, the stress is found to be a convex combination of the limiting constitutive models of elasticity ($\alpha \to 0$) and perfect plasticity ($\alpha \to \infty$). Later, we will see that such a relation also holds in the quasi-static case. A similar interpretation was given in [**IS93**, Section 3.3].

1.3. Duality. Formally replacing the indicator function by the Moreau-Yosida approximation in the Lagrangian (2.30) of the perfect plasticity problem leads to

$$L(\boldsymbol{\sigma}, \boldsymbol{u}) = \tfrac{1}{2}a(\boldsymbol{\sigma}, \boldsymbol{\sigma}) + \chi_{\boldsymbol{K}}^{\alpha}(\boldsymbol{\sigma}) - \int_{\Omega} \boldsymbol{\sigma}(x) : \boldsymbol{\varepsilon}(\boldsymbol{u}(x))\, dx + \ell(\boldsymbol{u}).$$

The dual problem is then given as

$$\text{Minimize} \quad \tfrac{1}{2}a(\boldsymbol{\sigma}, \boldsymbol{\sigma}) + \chi_{\boldsymbol{K}}^{\alpha}(\boldsymbol{\sigma}) - h(\boldsymbol{\sigma}) \qquad \text{subject to} \quad \boldsymbol{\sigma} \in \boldsymbol{S}(\boldsymbol{b}, \boldsymbol{t}_N). \tag{3.4}$$

In order to define the primal problem, we again consider

$$\sup_{\boldsymbol{\sigma} \in \boldsymbol{P}}\{-L(\boldsymbol{\sigma}, \boldsymbol{u})\} = \sup_{\boldsymbol{\sigma} \in \boldsymbol{P}} \Big\{ -\tfrac{1}{2}a(\boldsymbol{\sigma}, \boldsymbol{\sigma}) - \chi_{\boldsymbol{K}}^{\alpha}(\boldsymbol{\sigma}) + \int_{\Omega} \boldsymbol{\sigma}(x) : \boldsymbol{\varepsilon}(\boldsymbol{u}(x))\, dx - \ell(\boldsymbol{u}) \Big\}.$$

Now, the function on the right is uniformly concave and differentiable and to find the supremum, we need to find a stationary point of the Lagrangian, i.e. find $\boldsymbol{\sigma} \in \boldsymbol{P}$ such that

$$0 = \langle D_{\boldsymbol{\sigma}} L(\boldsymbol{\sigma}, \boldsymbol{u}), \boldsymbol{\eta}\rangle_{\boldsymbol{P}^* \times \boldsymbol{P}} = a(\boldsymbol{\sigma}, \boldsymbol{\eta}) + \alpha\, a(\boldsymbol{\sigma} - P_{\boldsymbol{K}}(\boldsymbol{\sigma}), \boldsymbol{\eta}) - \int_{\Omega} \boldsymbol{\eta}(x) : \boldsymbol{\varepsilon}(\boldsymbol{u}(x))\, dx.$$

Pointwise a.e., this is

$$\mathbb{C}^{-1}[\boldsymbol{\sigma}(x)] + \alpha\, \mathbb{C}^{-1}[\boldsymbol{\sigma} - P_K(\boldsymbol{\sigma}(x))] - \boldsymbol{\varepsilon}(\boldsymbol{u}(x)) = 0,$$

and by applying Lemma 3.2, we find (3.2) once more. Hence, the primal problem is

$$\text{Minimize}\quad -L\Big(\tfrac{1}{1+\alpha}\mathbb{C}[\varepsilon(\boldsymbol{u})] + \big(1 - \tfrac{1}{1+\alpha}\big)P_{\boldsymbol{K}}(\mathbb{C}[\varepsilon(\boldsymbol{u})])\,,\,\boldsymbol{u}\Big)\,,\qquad \boldsymbol{u}\in\boldsymbol{X}(\boldsymbol{u}_D)\,.$$

So far, we again proceeded formally, but this time, it is possible to show the existence and uniqueness of a unique solution $\boldsymbol{u}\in\boldsymbol{X}(\boldsymbol{u}_D)$, i.e. the solution is contained in H^1. In order to prove this, we show the quadratic growth of the primal functional for a fixed regularization parameter α.

Theorem 3.3. *For fixed $\alpha \in [0,\infty)$, the primal functional $\mathcal{E}_{\mathrm{vp},\alpha}:\boldsymbol{X}(\boldsymbol{u}_D)\to\mathbb{R}$,*

$$\mathcal{E}_{\mathrm{vp},\alpha}(\boldsymbol{u}) = -L\Big(\tfrac{1}{1+\alpha}\mathbb{C}[\varepsilon(\boldsymbol{u})] + \big(1 - \tfrac{1}{1+\alpha}\big)P_{\boldsymbol{K}}(\mathbb{C}[\varepsilon(\boldsymbol{u})])\,,\,\boldsymbol{u}\Big)\,,$$

takes the form

$$\mathcal{E}_{\mathrm{vp},\alpha}(\boldsymbol{u}) = \tfrac{\alpha}{1+\alpha}\,\Upsilon(\mathbb{C}[\varepsilon(\boldsymbol{u})]) + (1 - \tfrac{\alpha}{1+\alpha})\mathcal{W}_e(\varepsilon(\boldsymbol{u})) - \ell(\boldsymbol{u})\,,$$

and is uniformly convex with modulus $\tfrac{1}{1+\alpha}$ w.r.t. the energy norm $\|\cdot\|$. Furthermore, the necessary and sufficient condition for a minimum is

$$\int_\Omega \tfrac{1}{1+\alpha}\mathbb{C}[\varepsilon(\boldsymbol{u}(x))] : \varepsilon(\boldsymbol{w}(x)) + \tfrac{\alpha}{1+\alpha}P_K(\mathbb{C}[\varepsilon(\boldsymbol{u}(x))]) : \varepsilon(\boldsymbol{w}(x))\,dx = \ell(\boldsymbol{w})\,, \qquad (3.5)$$

for all $\boldsymbol{w}\in\boldsymbol{X}$.

PROOF. We introduce $\lambda = \tfrac{1}{1+\alpha}$ and note that $(1-\lambda)^2 + \alpha\lambda^2 = \tfrac{\alpha}{1+\alpha}$. By Lemma 3.2, we have $P_{\boldsymbol{K}}(\mathbb{C}[\varepsilon(\boldsymbol{u})]) = P_{\boldsymbol{K}}(\boldsymbol{\sigma})$. With $\boldsymbol{\sigma} = \lambda\mathbb{C}[\varepsilon(\boldsymbol{u})] + (1-\lambda)P_{\boldsymbol{K}}(\mathbb{C}[\varepsilon(\boldsymbol{u})])$, the primal functional is given as

$$
\begin{aligned}
-L(\boldsymbol{\sigma},\boldsymbol{u}) &= -\tfrac{1}{2}a(\boldsymbol{\sigma},\boldsymbol{\sigma}) - \tfrac{\alpha}{2}\|\boldsymbol{\sigma} - P_{\boldsymbol{K}}(\boldsymbol{\sigma})\|_{\boldsymbol{\Sigma}}^2 + \int_\Omega \boldsymbol{\sigma}(x):\varepsilon(\boldsymbol{u}(x))\,dx - \ell(\boldsymbol{u}) \\
&= -\tfrac{1}{2}\|\boldsymbol{\sigma} - \mathbb{C}[\varepsilon(\boldsymbol{u})]\|_{\boldsymbol{\Sigma}}^2 + \tfrac{1}{2}\|\mathbb{C}[\varepsilon(\boldsymbol{u})]\|_{\boldsymbol{\Sigma}}^2 - \tfrac{\alpha}{2}\|\boldsymbol{\sigma} - P_{\boldsymbol{K}}(\mathbb{C}[\varepsilon(\boldsymbol{u})])\|_{\boldsymbol{\Sigma}}^2 - \ell(\boldsymbol{u}) \\
&= -\tfrac{1}{2}\|\lambda\mathbb{C}[\varepsilon(\boldsymbol{u})] + (1-\lambda)P_{\boldsymbol{K}}(\mathbb{C}[\varepsilon(\boldsymbol{u})]) - \mathbb{C}[\varepsilon(\boldsymbol{u})]\|_{\boldsymbol{\Sigma}}^2 \\
&\quad -\tfrac{\alpha}{2}\|\lambda\mathbb{C}[\varepsilon(\boldsymbol{u})] + (1-\lambda)P_{\boldsymbol{K}}(\mathbb{C}[\varepsilon(\boldsymbol{u})]) - P_{\boldsymbol{K}}(\mathbb{C}[\varepsilon(\boldsymbol{u})])\|_{\boldsymbol{\Sigma}}^2 + \tfrac{1}{2}\|\mathbb{C}[\varepsilon(\boldsymbol{u})]\|_{\boldsymbol{\Sigma}}^2 - \ell(\boldsymbol{u}) \\
&= -\tfrac{(1-\lambda)^2}{2}\big\|P_{\boldsymbol{K}}(\mathbb{C}[\varepsilon(\boldsymbol{u})]) - \mathbb{C}[\varepsilon(\boldsymbol{u})]\big\|_{\boldsymbol{\Sigma}}^2 - \tfrac{\alpha\lambda^2}{2}\big\|P_{\boldsymbol{K}}(\mathbb{C}[\varepsilon(\boldsymbol{u})]) - \mathbb{C}[\varepsilon(\boldsymbol{u})]\big\|_{\boldsymbol{\Sigma}}^2 \\
&\quad + \tfrac{1}{2}\|\mathbb{C}[\varepsilon(\boldsymbol{u})]\|_{\boldsymbol{\Sigma}}^2 - \ell(\boldsymbol{u}) \\
&= -\tfrac{1}{2}\tfrac{\alpha}{1+\alpha}\big\|P_{\boldsymbol{K}}(\mathbb{C}[\varepsilon(\boldsymbol{u})]) - \mathbb{C}[\varepsilon(\boldsymbol{u})]\big\|_{\boldsymbol{\Sigma}}^2 + \tfrac{1}{2}\|\mathbb{C}[\varepsilon(\boldsymbol{u})]\|_{\boldsymbol{\Sigma}}^2 - \ell(\boldsymbol{u}) \\
&= \tfrac{1}{2}\tfrac{\alpha}{1+\alpha}\Big(\|\mathbb{C}[\varepsilon(\boldsymbol{u})]\|_{\boldsymbol{\Sigma}}^2 - \big\|P_{\boldsymbol{K}}(\mathbb{C}[\varepsilon(\boldsymbol{u})]) - \mathbb{C}[\varepsilon(\boldsymbol{u})]\big\|_{\boldsymbol{\Sigma}}^2\Big) \\
&\quad + \tfrac{1}{2}\big(1 - \tfrac{\alpha}{1+\alpha}\big)\|\mathbb{C}[\varepsilon(\boldsymbol{u})]\|_{\boldsymbol{\Sigma}}^2 - \ell(\boldsymbol{u}) \\
&= \tfrac{\alpha}{1+\alpha}\Upsilon(\mathbb{C}[\varepsilon(\boldsymbol{u})]) + \tfrac{1}{2}\tfrac{1}{1+\alpha}\|\mathbb{C}[\varepsilon(\boldsymbol{u})]\|_{\boldsymbol{\Sigma}}^2 - \ell(\boldsymbol{u})\,.
\end{aligned}
$$

The identity $\|\mathbb{C}[\varepsilon(\boldsymbol{u})]\|_{\boldsymbol{\Sigma}}^2 = \|\boldsymbol{u}\|^2 = 2\mathcal{W}_e(\varepsilon(\boldsymbol{u}))$ then gives the claimed representation of the primal functional. According to the last chapter, Υ is convex and differentiable, and consequently, $D\Upsilon$ is monotone. We now show the uniform convexity of $\mathcal{E}_{\mathrm{vp},\alpha}$ by showing

the strong monotonicity of $D\mathcal{E}_{\mathrm{vp},\alpha}$.

$$\langle D\mathcal{E}_{\mathrm{vp},\alpha}(\boldsymbol{u}) - D\mathcal{E}_{\mathrm{vp},\alpha}(\boldsymbol{v}), \boldsymbol{u} - \boldsymbol{v}\rangle_{\boldsymbol{X}^* \times \boldsymbol{X}}$$

$$= (1 - \lambda)\, a\Big(P_{\boldsymbol{K}}(\mathbb{C}[\boldsymbol{\varepsilon}(\boldsymbol{u})]) - P_{\boldsymbol{K}}(\mathbb{C}[\boldsymbol{\varepsilon}(\boldsymbol{v})]), \boldsymbol{u} - \boldsymbol{v}\Big) + \lambda\, c\big(\boldsymbol{u} - \boldsymbol{v}, \boldsymbol{u} - \boldsymbol{v}\big)$$

$$\geq \lambda \|\boldsymbol{u} - \boldsymbol{v}\|^2 = \tfrac{1}{1+\alpha}\|\boldsymbol{u} - \boldsymbol{v}\|^2\,.$$

The optimality condition follows from (3.3). $\qquad\qquad\qquad\qquad\qquad\qquad\qquad\qquad\square$

The direct method in the calculus of variations [**Giu03**, **Dac89**] then directly gives:

Corollary 3.4. *For $\alpha \in [0, \infty)$, the primal problem*

$$\textit{Minimize} \qquad \mathcal{E}_{\mathrm{vp},\alpha}(\boldsymbol{u}) \qquad \textit{subject to} \quad \boldsymbol{u} \in \boldsymbol{X}(\boldsymbol{u}_D) \tag{3.6}$$

admits a unique solution $\boldsymbol{u} \in \boldsymbol{X}(\boldsymbol{u}_D)$.

PROOF. For $\alpha \in [0, \infty)$, the functional $\mathcal{E}_{\mathrm{vp},\alpha}$ is convex and has quadratic growth. Thus, $\mathcal{E}_{\mathrm{vp},\alpha}$ is weakly lower semicontinuous on $H^1(\Omega, \mathbb{R}^d)$. Since $\boldsymbol{X}(\boldsymbol{u}_D)$ is a closed (affine) subspace, it follows that the primal minimization problem has a unique minimizer. $\qquad\square$

Of course, the uniform convexity modulus $\tfrac{1}{1+\alpha}$ vanishes as $\alpha \to \infty$ since in this case, the problem degenerates into the problem of perfect plasticity which has no solution in $\boldsymbol{X}(\boldsymbol{u}_D)$. As briefly mentioned earlier, the derivative of the Moreau-Yosida regularization of $\chi_{\boldsymbol{K}}$ is just the Yosida-regularization of the multivalued operator $\partial\chi_{\boldsymbol{K}}$. In the language of operator equations, Theorem 3.3 states that the operator equation

$$\Big(\tfrac{\alpha}{1+\alpha}T + \big(1 - \tfrac{\alpha}{1+\alpha}\big)C\Big)(\boldsymbol{u}) = \ell \qquad \text{in } \boldsymbol{X}^*,$$

with T being the operator of perfect plasticity as defined in (2.40), has a unique solution. The optimality conditions for the dual and primal problem once more define a saddle point of the Lagrangian, which is characterized by

$$\begin{array}{rcll} A\big((1+\alpha)\boldsymbol{\sigma} - \alpha P_{\boldsymbol{K}}(\boldsymbol{\sigma})\big) & + \quad B^*\boldsymbol{u} & = & 0, \qquad \text{in } \boldsymbol{P}^*, \\ B\boldsymbol{\sigma} & & = & -\ell, \qquad \text{in } \boldsymbol{X}^*. \end{array}$$

1.4. Approximation of Perfect Plasticity. We introduced the viscoplastic flow rule as an approximation of the perfectly plastic flow rule and we briefly state an approximation result showing that the dual solution of the perfectly plastic problem can indeed be obtained by letting $\alpha \to \infty$ when considering the viscoplastic regularization. At this point we only state the result and defer the proof to Section 10.2 where we will proof a more general result. Similar approximation results can be found in [**Joh76**, **HR99**, **Tem85**].

Theorem 3.5. *If the safe load condition holds, i.e. Assumption 2.1, then the solution $\boldsymbol{\sigma}_\alpha$ of the regularized problem (3.4) converges strongly to the solution of the perfect plasticity problem (2.31) as $\alpha \to \infty$.*

2. Kinematic Hardening

As we have seen in the opening chapter, cf. Subsection 1.2.4, concerning hardening plasticity, the free energy has to be augmented by a term including hardening parameters and we showed that for linear kinematic hardening, the internal variable can be identified with the plastic strain. This gave the decomposition

$$\mathcal{W} \equiv \mathcal{W}(\varepsilon_e, \varepsilon_p) = \mathcal{W}_e(\varepsilon_e) + \mathcal{W}_p(\varepsilon_p) = \tfrac{1}{2}\varepsilon_e : \mathbb{C}[\varepsilon_e] + \tfrac{1}{2}\varepsilon_p : \mathbb{H}[\varepsilon_p] \,.$$

In the following, we assume $\mathbb{H} \in L(\mathrm{Sym}(d), \mathrm{Sym}(d))$ to be symmetric and positive definite on $\mathrm{Sym}(d)$. This is a too strong requirement in incompressible plasticity, and we refer to subsection 3.2.4 concerning this topic, where it will be shown that this seemingly too strong assumption is not a restriction at all.

The dual (or complementary) energy to $\mathcal{W}$ is given by

$$\mathcal{W}^*(\boldsymbol{\sigma}, \boldsymbol{\zeta}) = \sup_{(\varepsilon_e, \varepsilon_p) \in \boldsymbol{P} \times \boldsymbol{P}} \left\{ \langle \boldsymbol{\sigma}, \varepsilon_e \rangle_{\boldsymbol{P}^* \times \boldsymbol{P}} + \langle \boldsymbol{\zeta}, \varepsilon_p \rangle_{\boldsymbol{P}^* \times \boldsymbol{P}} - \mathcal{W}(\varepsilon_e, \varepsilon_p) \right\}$$

$$= \tfrac{1}{2} \int_\Omega \boldsymbol{\sigma}(x) : \mathbb{C}^{-1}[\boldsymbol{\sigma}(x)] \, dx + \tfrac{1}{2} \int_\Omega \boldsymbol{\zeta}(x) : \mathbb{H}^{-1}[\boldsymbol{\zeta}(x)] \, dx$$

$$= \tfrac{1}{2} a(\boldsymbol{\sigma}, \boldsymbol{\sigma}) + \tfrac{1}{2} d(\boldsymbol{\zeta}, \boldsymbol{\zeta})$$

with $a(\cdot, \cdot)$ as defined in (2.5) and

$$d : \boldsymbol{P} \times \boldsymbol{P} \to \mathbb{R}\,, \qquad\qquad d(\boldsymbol{\zeta}, \boldsymbol{\eta}) = \int_\Omega \boldsymbol{\zeta}(x) : \mathbb{H}^{-1}[\boldsymbol{\eta}(x)] \, dx \,.$$

2.1. Problem Setting and the Dual Problem.
Again, we repeat the governing equations

$$-\mathrm{div}(\boldsymbol{\sigma}(x)) = \boldsymbol{b}(x, t)\,, \qquad\qquad\qquad x \in \Omega\,, \qquad\qquad (3.7\mathrm{a})$$

$$\boldsymbol{\sigma}(x) = \mathbb{C}[\varepsilon(\boldsymbol{u}(x)) - \varepsilon_p(x)]\,, \qquad\qquad x \in \Omega\,, \qquad\qquad (3.7\mathrm{b})$$

$$\boldsymbol{\sigma}(x) + \boldsymbol{\zeta}(x) \in K\,, \qquad\qquad\qquad x \in \Omega\,, \qquad\qquad (3.7\mathrm{c})$$

$$\varepsilon_p(x) \in N_K(\boldsymbol{\sigma}(x) + \boldsymbol{\zeta}(x)) \qquad\qquad x \in \Omega\,, \qquad\qquad (3.7\mathrm{d})$$

$$\boldsymbol{\zeta}(x) = -\mathbb{H}[\varepsilon_p(x)] \qquad\qquad\qquad x \in \Omega\,, \qquad\qquad (3.7\mathrm{e})$$

$$\boldsymbol{u}(x) = \boldsymbol{u}_D(x)\,, \qquad\qquad\qquad\qquad x \in \Gamma_D\,, \qquad\qquad (3.7\mathrm{f})$$

$$\boldsymbol{\sigma}(x)\boldsymbol{n}(x) = \boldsymbol{t}_N(x)\,, \qquad\qquad\qquad x \in \Gamma_T\,. \qquad\qquad (3.7\mathrm{g})$$

Though the dual force $\boldsymbol{\zeta}$ can essentially be eliminated by (3.7e), we formally continue to include $\boldsymbol{\zeta}$ in our formulation to clearly distinguish "dual" and "primal" quantities. From time to time, it will also be convenient to use the *relative stress* $\boldsymbol{\alpha} = \boldsymbol{\sigma} + \boldsymbol{\zeta}$. We introduce the Lagrangian $L : (\boldsymbol{P} \times \boldsymbol{P}) \times \boldsymbol{X}(\boldsymbol{u}_D) \to \overline{\mathbb{R}}$ as

$$L((\boldsymbol{\sigma}, \boldsymbol{\zeta}), \boldsymbol{u}) = \tfrac{1}{2} a(\boldsymbol{\sigma}, \boldsymbol{\sigma}) + \tfrac{1}{2} d(\boldsymbol{\zeta}, \boldsymbol{\zeta}) + \chi_{\boldsymbol{K}}(\boldsymbol{\sigma} + \boldsymbol{\zeta}) - \int_\Omega \boldsymbol{\sigma}(x) : \varepsilon(\boldsymbol{u}(x)) \, dx + \ell(\boldsymbol{u}) \,.$$

and formulate the dual problem.

$$\text{Minimize} \quad \sup_{\boldsymbol{u} \in \boldsymbol{X}(\boldsymbol{u}_D)} \{ L((\boldsymbol{\sigma}, \boldsymbol{\zeta}), \boldsymbol{u}) \}\,, \quad (\boldsymbol{\sigma}, \boldsymbol{\zeta}) \in \boldsymbol{P} \times \boldsymbol{P}\,.$$

Similarly to the previous chapter, this gives

$$\text{Minimize} \quad \tfrac{1}{2} a(\boldsymbol{\sigma}, \boldsymbol{\sigma}) + \tfrac{1}{2} d(\boldsymbol{\zeta}, \boldsymbol{\zeta}) + \chi_{\boldsymbol{K}}(\boldsymbol{\sigma} + \boldsymbol{\zeta}) - h(\boldsymbol{\sigma})$$

$$\text{subject to} \quad \boldsymbol{\sigma} \in \boldsymbol{S}(\boldsymbol{b}, \boldsymbol{t}_N)\,, \quad \boldsymbol{\zeta} \in \boldsymbol{P} \,.$$

Note that this problem always has a unique solution, since $S(\boldsymbol{b}, \boldsymbol{t}_N)$ is closed and non-empty and $\boldsymbol{\zeta}$ can always be chosen such that $\boldsymbol{\sigma} + \boldsymbol{\zeta} \in \boldsymbol{K}$. Additionally, the objective function is uniformly convex. Hence, no safe-load condition is necessary.

2.2. The Primal Problem. Once more, we consider the primal problem.

$$\text{Minimize} \quad \sup_{(\boldsymbol{\sigma}, \boldsymbol{\zeta}) \in P \times P} \{-L((\boldsymbol{\sigma}, \boldsymbol{\zeta}), \boldsymbol{u})\}, \qquad \boldsymbol{u} \in \boldsymbol{X}(\boldsymbol{u}_D).$$

We will shortly see that this problem is again well posed in the (affine) Sobolev space $\boldsymbol{X}(\boldsymbol{u}_D)$. Before stating this result, we need to introduce some notation. We define the fourth order tensors

$$\mathbb{N} : \operatorname{Sym}(d) \to \operatorname{Sym}(d), \qquad\qquad \mathbb{N} = \mathbb{C} + \mathbb{H},$$

$$\mathbb{D} : \operatorname{Sym}(d) \to \operatorname{Sym}(d), \qquad\qquad \mathbb{D}^{-1} = \mathbb{C}^{-1} + \mathbb{H}^{-1},$$

both being positive definite on the symmetric second order tensors and we infer

$$\mathbb{N}^{-1} : \operatorname{Sym}(d) \to \operatorname{Sym}(d), \qquad\qquad \mathbb{N}^{-1} = \mathbb{H}^{-1} - \mathbb{H}^{-1} \circ \mathbb{D} \circ \mathbb{H}^{-1}.$$

Introducing the inner product and norm

$$n(\boldsymbol{\sigma}, \boldsymbol{\eta}) = \int_\Omega \boldsymbol{\sigma}(x) : \mathbb{N}^{-1}[\boldsymbol{\eta}(x)] \, dx, \qquad\qquad \|\boldsymbol{\sigma}\|_N = \sqrt{n(\boldsymbol{\sigma}, \boldsymbol{\sigma})},$$

we define the projection onto $\boldsymbol{K}$ w.r.t. this metric by $P_{\boldsymbol{K}}^N : \boldsymbol{P} \to \boldsymbol{K}$. Accordingly, we define $\Upsilon^N : \boldsymbol{P} \to \mathbb{R}$,

$$\Upsilon^N(\boldsymbol{\eta}) = \tfrac{1}{2}\|\boldsymbol{\eta}\|_N^2 - \tfrac{1}{2}\|P_{\boldsymbol{K}}^N(\boldsymbol{\eta}) - \boldsymbol{\eta}\|_N^2.$$

Theorem 3.6. *Assume that $\mathbb{H}$ is positive definite on the symmetric second order tensors. Then, the primal functional*

$$\mathcal{E}_{\mathrm{hd}} : \boldsymbol{X}(\boldsymbol{u}_D) \to \mathbb{R}, \qquad \mathcal{E}_{\mathrm{hd}}(\boldsymbol{u}) = \sup_{(\boldsymbol{\sigma}, \boldsymbol{\zeta}) \in P \times P} \{-L((\boldsymbol{\sigma}, \boldsymbol{\zeta}), \boldsymbol{u})\},$$

is given as

$$\mathcal{E}_{\mathrm{hd}}(\boldsymbol{u}) = \Upsilon^N(\mathbb{C}[\boldsymbol{\varepsilon}(\boldsymbol{u})]) + \tfrac{1}{2} \int_\Omega \boldsymbol{\varepsilon}(\boldsymbol{u}(x)) : \mathbb{D}[\boldsymbol{\varepsilon}(\boldsymbol{u}(x))] \, dx - \ell(\boldsymbol{u}), \qquad (3.8)$$

and is uniformly convex w.r.t. the energy norm $\|\cdot\|$.

PROOF. For ease of notation, we omit the dependence on x and also omit the composition operator $\circ$. Using $\boldsymbol{\alpha} = \boldsymbol{\sigma} + \boldsymbol{\zeta}$, we consider

$$\mathcal{E}_{\mathrm{hd}}(\boldsymbol{u}) = \sup_{(\boldsymbol{\sigma}, \boldsymbol{\zeta}) \in P \times P} \{-L((\boldsymbol{\sigma}, \boldsymbol{\zeta}), \boldsymbol{u})\}$$

$$= \sup_{(\boldsymbol{\sigma}, \boldsymbol{\zeta}) \in P \times P} \left\{ -\tfrac{1}{2}a(\boldsymbol{\sigma}, \boldsymbol{\sigma}) - \tfrac{1}{2}d(\boldsymbol{\zeta}, \boldsymbol{\zeta}) - \chi_K(\boldsymbol{\sigma} + \boldsymbol{\zeta}) + \int_\Omega \boldsymbol{\sigma} : \boldsymbol{\varepsilon}(\boldsymbol{u}) \, dx - \ell(\boldsymbol{u}) \right\}$$

$$= \sup_{\boldsymbol{\alpha} \in P} \left\{ \sup_{\boldsymbol{\sigma} \in P} \left\{ -\tfrac{1}{2}a(\boldsymbol{\sigma} - \mathbb{C}[\boldsymbol{\varepsilon}(\boldsymbol{u})], \boldsymbol{\sigma} - \mathbb{C}[\boldsymbol{\varepsilon}(\boldsymbol{u})]) - \tfrac{1}{2}d(\boldsymbol{\alpha} - \boldsymbol{\sigma}, \boldsymbol{\alpha} - \boldsymbol{\sigma}) \right\} - \chi_K(\boldsymbol{\alpha}) \right\}$$

$$\quad + \tfrac{1}{2}c(\boldsymbol{u}, \boldsymbol{u}) - \ell(\boldsymbol{u}).$$

Defining $\mathbb{L} : \operatorname{Sym}(d) \to \operatorname{Sym}(d)$, $\mathbb{L} = \mathbb{D}\mathbb{H}^{-1}$, we also find $\mathbb{L} = \mathbb{C}\mathbb{N}^{-1}$ and we first consider the unconstrained inner problem which is uniformly concave. The supremum

$$\sup_{\boldsymbol{\sigma} \in P} \left\{ -\tfrac{1}{2}a(\boldsymbol{\sigma} - \mathbb{C}[\boldsymbol{\varepsilon}(\boldsymbol{u})], \boldsymbol{\sigma} - \mathbb{C}[\boldsymbol{\varepsilon}(\boldsymbol{u})]) - \tfrac{1}{2}d(\boldsymbol{\alpha} - \boldsymbol{\sigma}, \boldsymbol{\alpha} - \boldsymbol{\sigma}) \right\}$$

is attained at

$$\boldsymbol{\sigma} = \mathbb{D}\big[\boldsymbol{\varepsilon}(\boldsymbol{u}) + \mathbb{H}^{-1}[\boldsymbol{\alpha}]\big] = \mathbb{D}[\boldsymbol{\varepsilon}(\boldsymbol{u})] + \mathbb{L}[\boldsymbol{\alpha}]\,.$$

Thus, $\boldsymbol{\alpha} - \boldsymbol{\sigma} = (\mathbb{I} - \mathbb{L})[\boldsymbol{\alpha}] - \mathbb{D}[\boldsymbol{\varepsilon}(\boldsymbol{u})]$ and substitution into the formula for $\mathcal{E}_{\mathrm{hd}}$ then yields

$$\sup_{(\boldsymbol{\sigma},\boldsymbol{\zeta}) \in \boldsymbol{P} \times \boldsymbol{P}} \{-L((\boldsymbol{\sigma}, \boldsymbol{\zeta}, \boldsymbol{u})\}$$

$$= \sup_{\boldsymbol{\alpha} \in \boldsymbol{P}} \Big\{ -\tfrac{1}{2} \int_{\Omega} \big(\mathbb{L}[\boldsymbol{\alpha}] + (\mathbb{D} - \mathbb{C})[\boldsymbol{\varepsilon}(\boldsymbol{u})]\big) : \mathbb{C}^{-1}\big[\mathbb{L}[\boldsymbol{\alpha}] + (\mathbb{D} - \mathbb{C})[\boldsymbol{\varepsilon}(\boldsymbol{u})]\big]\, dx$$

$$- \tfrac{1}{2} \int_{\Omega} \big((\mathbb{I} - \mathbb{L})[\boldsymbol{\alpha}] - \mathbb{D}[\boldsymbol{\varepsilon}(\boldsymbol{u})]\big) : \mathbb{H}^{-1}\big[(\mathbb{I} - \mathbb{L})[\boldsymbol{\alpha}] - \mathbb{D}[\boldsymbol{\varepsilon}(\boldsymbol{u})]\big]\, dx$$

$$- \chi_{\boldsymbol{K}}(\boldsymbol{\alpha})\Big\} + \tfrac{1}{2}c(\boldsymbol{u}, \boldsymbol{u}) - \ell(\boldsymbol{u})$$

$$= \sup_{\boldsymbol{\alpha} \in \boldsymbol{P}} \Big\{ -\tfrac{1}{2} \int_{\Omega} \boldsymbol{\alpha} : \big(\mathbb{L}\mathbb{C}^{-1}\mathbb{L} + (\mathbb{I} - \mathbb{L})\mathbb{H}^{-1}(\mathbb{I} - \mathbb{L})\big)[\boldsymbol{\alpha}]\, dx$$

$$+ \int_{\Omega} \boldsymbol{\alpha} : \big((\mathbb{I} - \mathbb{L})\mathbb{H}^{-1}\mathbb{D} - \mathbb{L}\mathbb{C}^{-1}(\mathbb{D} - \mathbb{C})\big)[\boldsymbol{\varepsilon}(\boldsymbol{u})]\, dx$$

$$- \tfrac{1}{2} \int_{\Omega} \boldsymbol{\varepsilon}(\boldsymbol{u}) : \big((\mathbb{D} - \mathbb{C})\mathbb{C}^{-1}(\mathbb{D} - \mathbb{C}) + \mathbb{D}\mathbb{H}^{-1}\mathbb{D}\big)[\boldsymbol{\varepsilon}(\boldsymbol{u})]\, dx$$

$$- \chi_{\boldsymbol{K}}(\boldsymbol{\alpha})\Big\} + \tfrac{1}{2}c(\boldsymbol{u}, \boldsymbol{u}) - \ell(\boldsymbol{u})\,.$$

We find the following relations by algebraic transformations:

$$\mathbb{L}\mathbb{C}^{-1}\mathbb{L} + (\mathbb{I} - \mathbb{L})\mathbb{H}^{-1}(\mathbb{I} - \mathbb{L}) = \mathbb{H}^{-1} - \mathbb{H}^{-1}\mathbb{D}\mathbb{H}^{-1}$$

$$(\mathbb{I} - \mathbb{L})\mathbb{H}^{-1}\mathbb{D} - \mathbb{L}\mathbb{C}^{-1}(\mathbb{D} - \mathbb{C}) = \mathbb{L}$$

$$(\mathbb{D} - \mathbb{C})\mathbb{C}^{-1}(\mathbb{D} - \mathbb{C}) + \mathbb{D}\mathbb{H}^{-1}\mathbb{D} = \mathbb{C} - \mathbb{D}$$

and by further transformations, we find $\mathbb{L} = \mathbb{N}^{-1}\mathbb{C}$ and $\mathbb{C} - \mathbb{D} = \mathbb{C}\mathbb{N}^{-1}\mathbb{C}$. This yields

$$\mathcal{E}_{\mathrm{hd}}(\boldsymbol{u}) = \sup_{(\boldsymbol{\sigma},\boldsymbol{\zeta}) \in \boldsymbol{P} \times \boldsymbol{P}} \{-L((\boldsymbol{\sigma}, \boldsymbol{\zeta}, \boldsymbol{u})\}$$

$$= \sup_{\boldsymbol{\alpha} \in \boldsymbol{P}} \Big\{ -\tfrac{1}{2} \int_{\Omega} \boldsymbol{\alpha} : \mathbb{N}^{-1}[\boldsymbol{\alpha}] - 2\boldsymbol{\alpha} : \mathbb{N}^{-1}\big[\mathbb{C}[\boldsymbol{\varepsilon}(\boldsymbol{u})]\big] + \mathbb{C}[\boldsymbol{\varepsilon}(\boldsymbol{u})] : \mathbb{N}^{-1}\big[\mathbb{C}[\boldsymbol{\varepsilon}(\boldsymbol{u})]\big]\, dx$$

$$- \chi_{\boldsymbol{K}}(\boldsymbol{\alpha})\Big\} + \tfrac{1}{2}c(\boldsymbol{u}, \boldsymbol{u}) - \ell(\boldsymbol{u})$$

$$= \sup_{\boldsymbol{\alpha} \in \boldsymbol{P}} \Big\{ -\tfrac{1}{2}\|\boldsymbol{\alpha} - \mathbb{C}[\boldsymbol{\varepsilon}(\boldsymbol{u})]\|_N^2 - \chi_{\boldsymbol{K}}(\boldsymbol{\alpha})\Big\} + \tfrac{1}{2}c(\boldsymbol{u}, \boldsymbol{u}) - \ell(\boldsymbol{u})$$

$$= -\tfrac{1}{2}\|P_{\boldsymbol{K}}^N(\mathbb{C}[\boldsymbol{\varepsilon}(\boldsymbol{u})]) - \mathbb{C}[\boldsymbol{\varepsilon}(\boldsymbol{u})]\|_N^2 + \tfrac{1}{2}c(\boldsymbol{u}, \boldsymbol{u}) - \ell(\boldsymbol{u})\,.$$

Remembering $\mathbb{D} = \mathbb{C} - \mathbb{C}\mathbb{N}^{-1}\mathbb{C}$, we observe

$$c(\boldsymbol{u}, \boldsymbol{u}) = \tfrac{1}{2} \int_{\Omega} \boldsymbol{\varepsilon}(\boldsymbol{u}) : \big(\mathbb{C} - \mathbb{C}\mathbb{N}^{-1}\mathbb{C} + \mathbb{C}\mathbb{N}^{-1}\mathbb{C}\big)[\boldsymbol{\varepsilon}(\boldsymbol{u})]\, dx$$

$$= \tfrac{1}{2}\|\mathbb{C}[\boldsymbol{\varepsilon}(\boldsymbol{u})]\|_N^2 + \tfrac{1}{2} \int_{\Omega} \boldsymbol{\varepsilon}(\boldsymbol{u}) : \mathbb{D}[\boldsymbol{\varepsilon}(\boldsymbol{u})]\, dx\,,$$

and this finally gives the claimed representation

$$\mathcal{E}_{\mathrm{hd}}(\boldsymbol{u}) = \Upsilon^N(\mathbb{C}[\varepsilon(\boldsymbol{u})]) + \tfrac{1}{2} \int_{\Omega} \boldsymbol{\varepsilon}(\boldsymbol{u}) : \mathbb{D}[\varepsilon(\boldsymbol{u})]\, dx - \ell(\boldsymbol{u})\,.$$

Uniform convexity follows from showing the strong monotonicity of the gradient $D\mathcal{E}_{\text{hd}}$. The derivative is characterized by

$$\langle D\mathcal{E}_{\text{hd}}(\boldsymbol{u}), \boldsymbol{w}\rangle_{\boldsymbol{X}^* \times \boldsymbol{X}} = n\big(P_{\boldsymbol{K}}^N(\mathbb{C}[\boldsymbol{\varepsilon}(\boldsymbol{u})]), \mathbb{C}[\boldsymbol{\varepsilon}(\boldsymbol{w})]\big) + \int_\Omega \boldsymbol{\varepsilon}(\boldsymbol{u}) : \mathbb{D}[\boldsymbol{\varepsilon}(\boldsymbol{w})]\, dx - \ell(\boldsymbol{w})$$

$$= \int_\Omega \Big((\mathbb{C} \circ \mathbb{N}^{-1})\big[P_{\boldsymbol{K}}^N\big(\mathbb{C}[\boldsymbol{\varepsilon}(\boldsymbol{u})]\big)\big] + \mathbb{D}[\boldsymbol{\varepsilon}(\boldsymbol{u})]\Big) : \boldsymbol{\varepsilon}(\boldsymbol{w})\, dx - \ell(\boldsymbol{w})\,,$$

$$(3.9)$$

and the strong monotonicity then follows from the monotonicity of the projection.

$$\langle D\mathcal{E}_{\text{hd}}(\boldsymbol{u}) - D\mathcal{E}_{\text{hd}}(\boldsymbol{w}), \boldsymbol{u} - \boldsymbol{w}\rangle_{\boldsymbol{X}^* \times \boldsymbol{X}}$$

$$= n\Big(P_{\boldsymbol{K}}^N(\mathbb{C}[\boldsymbol{\varepsilon}(\boldsymbol{u})]) - P_{\boldsymbol{K}}^N(\mathbb{C}[\boldsymbol{\varepsilon}(\boldsymbol{w})]), \mathbb{C}[\boldsymbol{\varepsilon}(\boldsymbol{u})] - \mathbb{C}[\boldsymbol{\varepsilon}(\boldsymbol{u})]\Big)$$

$$+ \int_\Omega \boldsymbol{\varepsilon}(\boldsymbol{u} - \boldsymbol{w}) : \mathbb{D}[\boldsymbol{\varepsilon}(\boldsymbol{u} - \boldsymbol{w})]\, dx \geq \int_\Omega \boldsymbol{\varepsilon}(\boldsymbol{u} - \boldsymbol{w}) : \mathbb{D}[\boldsymbol{\varepsilon}(\boldsymbol{u} - \boldsymbol{w})]\, dx$$

$$\geq \frac{1}{|\mathbb{D}^{-1}|}\|\boldsymbol{\varepsilon}(\boldsymbol{u} - \boldsymbol{v})\|_{\boldsymbol{P}}^2 \geq \frac{1}{|\mathbb{D}^{-1}|\,|\mathbb{C}|}\|\boldsymbol{u} - \boldsymbol{v}\|^2\,.$$

Provided $\mathbb{H}$ is positive definite, we infer that $\mathbb{D} = \mathbb{C} - \mathbb{C}\mathbb{N}^{-1}\mathbb{C}$ is positive definite and this completes the proof. $\square$

Note that during the derivation, we found

$$\boldsymbol{\alpha} = P_{\boldsymbol{K}}^N(\mathbb{C}[\boldsymbol{\varepsilon}(\boldsymbol{u})])\,,$$

$$\boldsymbol{\sigma} = (\mathbb{D} \circ \mathbb{C}^{-1})\big[\mathbb{C}[\boldsymbol{\varepsilon}(\boldsymbol{u})]\big] + (\mathbb{C} \circ \mathbb{N}^{-1})\big[P_{\boldsymbol{K}}^N(\mathbb{C}[\boldsymbol{\varepsilon}(\boldsymbol{u})])\big]\,,$$

$$\boldsymbol{\zeta} = -(\mathbb{D} \circ \mathbb{C}^{-1})\big[\mathbb{C}[\boldsymbol{\varepsilon}(\boldsymbol{u})]\big] + (\mathbb{I} - \mathbb{C} \circ \mathbb{N}^{-1})\big[P_{\boldsymbol{K}}^N(\mathbb{C}[\boldsymbol{\varepsilon}(\boldsymbol{u})])\big]\,,$$

which gives rise to the definition of a response function

$$R_{\text{hd}} : \boldsymbol{P} \to (\boldsymbol{P} \times \boldsymbol{P})\,, \quad R_{\text{hd}}(\boldsymbol{\eta}) = \begin{bmatrix} (\mathbb{D} \circ \mathbb{C}^{-1})[\boldsymbol{\eta}] + (\mathbb{C} \circ \mathbb{N}^{-1})[P_{\boldsymbol{K}}^N(\boldsymbol{\eta})] \\ -(\mathbb{D} \circ \mathbb{C}^{-1})[\boldsymbol{\eta}] + (\mathbb{I} - \mathbb{C} \circ \mathbb{N}^{-1})[P_{\boldsymbol{K}}^N(\boldsymbol{\eta})] \end{bmatrix}\,, \quad (3.10)$$

from which we conclude

$$\begin{bmatrix} \boldsymbol{\sigma} \\ \boldsymbol{\zeta} \end{bmatrix} = R_{\text{hd}}(\mathbb{C}[\boldsymbol{\varepsilon}(\boldsymbol{u})])\,.$$

Similarly to the former section, we obtain an existence and uniqueness results.

Corollary 3.7. *If $\mathbb{H}$ is symmetric positive definite on the second order tensors, the primal problem admits a unique solution $\boldsymbol{u} \in \boldsymbol{X}(\boldsymbol{u}_D)$.*

PROOF. Once more, this is a consequence of the direct method in the calculus of variations, cf. the previous section. $\square$

Of course, this does not hold in the case $|\mathbb{H}| \to 0$ which would recover the problem of perfect plasticity. This can also be seen by observing the loss of strong monotonicity in the operator equation $D\mathcal{E}_{\text{hd}}(\boldsymbol{u}) = 0$ if $|\mathbb{H}| \to 0$.

2.3. The Relation with the Viscoplastic Regularization. The following observation seems to be fairly unknown in the literature and will simplify many proofs in this work. The surprising result is that a particular choice of the hardening modulus leads to the same primal problem as the viscoplastic regularization. This is why we will often be able to identify viscoplasticity with kinematic hardening plasticity from a mathematical point of view.

Lemma 3.8. *If $\mathbb{H} = H_0\,\mathbb{C}$ with the dimensionless scaling factor $H_0 > 0$, then the primal functional of associated hardening plasticity $\mathcal{E}_{\mathrm{hd}}$ coincides with the primal functional $\mathcal{E}_{\mathrm{vp},\alpha}$ of the viscoplastic regularization with $\alpha = H_0^{-1}$.*

PROOF. For the proof, we introduce $h = H_0^{-1}$ and thus $\frac{1}{1+h} = \frac{H_0}{1+H_0}$. We note that $\mathbb{N} = \mathbb{C} + \mathbb{H} = \mathbb{C} + \frac{1}{h}\mathbb{C}$ and hence $\mathbb{N}^{-1} = \frac{h}{1+h}\mathbb{C}^{-1}$ by definition and likewise, we have $\mathbb{D} = \frac{1}{1+h}\mathbb{C}$. Consequently, up to scaling by a constant factor, the inner products $a(\cdot,\cdot)$ and $n(\cdot,\cdot)$ coincide and consequently $P_K = P_K^N$. The corresponding norms scale with $\|\boldsymbol{\eta}\|_N^2 = \frac{h}{1+h}\|\boldsymbol{\eta}\|_\Sigma^2$ and we have $\Upsilon^N(\boldsymbol{\eta}) = \frac{h}{1+h}\Upsilon(\boldsymbol{\eta})$. Hence,

$$\mathcal{E}_{\mathrm{hd}}(\boldsymbol{u}) = \Upsilon^N(\mathbb{C}[\boldsymbol{\varepsilon}(\boldsymbol{u})]) + \frac{1}{2}\int_\Omega \boldsymbol{\varepsilon}(\boldsymbol{u}) : \mathbb{D}[\boldsymbol{\varepsilon}(\boldsymbol{u})]\, dx - \ell(\boldsymbol{u})$$

$$= \frac{h}{1+h}\Upsilon(\mathbb{C}[\boldsymbol{\varepsilon}(\boldsymbol{u})]) + \frac{1}{2}\frac{1}{1+h}\int_\Omega \boldsymbol{\varepsilon}(\boldsymbol{u}) : \mathbb{C}[\boldsymbol{\varepsilon}(\boldsymbol{u})]\, dx - \ell(\boldsymbol{u})$$

$$= \frac{H_0^{-1}}{1+H_0^{-1}}\Upsilon(\mathbb{C}[\boldsymbol{\varepsilon}(\boldsymbol{u})]) + \frac{1}{1+H_0^{-1}}\frac{1}{2}c(\boldsymbol{u},\boldsymbol{u}) - \ell(\boldsymbol{u}) = \mathcal{E}_{\mathrm{vp},H_0^{-1}}(\boldsymbol{u})\,,$$

giving the conclusion. $\qquad\square$

Corollary 3.9. *If $\mathbb{H} = H_0\,\mathbb{C}$ with $H_0 > 0$, the primal function is uniformly convex with modulus $\frac{H_0}{1+H_0}$ in the energy norm, i.e.*

$$\langle D\mathcal{E}_{\mathrm{hd}}(\boldsymbol{u}) - D\mathcal{E}_{\mathrm{hd}}(\boldsymbol{w}), \boldsymbol{u} - \boldsymbol{w}\rangle_{X^*\times X} \geq \frac{H_0}{1+H_0}\|\boldsymbol{u} - \boldsymbol{w}\|\,. \tag{3.11}$$

PROOF. This can either be observed directly by reconsidering the proof of Theorem 3.6, or we can use Theorem 3.3 via the above Lemma 3.8. $\qquad\square$

We will later see that in incremental (time-discrete) plasticity, the situation changes, since then, α will be replaced by $\alpha\Delta t$, thus depending on the time step size Δt, whereas in the hardening case, this will not be the case. Nevertheless, if only one time step is considered, incremental viscoplasticity will correspond to incremental hardening plasticity via the relation $\alpha\Delta t = H_0^{-1}$ with the hardening modulus $\mathbb{H} = H_0\,\mathbb{C}$.

2.4. Incompressible Plasticity. As indicated in the beginning of the section, in incompressible plasticity, it is sufficient that $\mathbb{H}$ is positive definite on the deviatoric subspace $\mathrm{Sym}_0(d)$ as defined in (1.3). If moreover, we assume isotropic elasticity (1.11), then we can assume $\mathbb{H}$ to be of the form $\mathbb{H} = H_0\,2\mu\,\mathbb{P}_{\mathrm{dev}}$ with the dimensionless quantity $H_0 > 0$. Thus, $\mathbb{P}_{\mathrm{dev}} \circ \mathbb{H} = H_0\,\mathbb{P}_{\mathrm{dev}} \circ \mathbb{C}$ and as in the previous subsection, on the deviatoric subspace, the hardening modulus is a multiple on the elasticity tensor. Since K takes the form (1.16), we find Υ to be of the form (2.39). Then, with the same computation as in Lemma 3.8, it is easy to show that also in this case, $\mathcal{E}_{\mathrm{hd}}$ has the representation as given in

Lemma 3.8, i.e.

$$\mathcal{E}_{\mathrm{hd}}(\boldsymbol{u}) = \frac{H_0^{-1}}{1+H_0^{-1}} \Upsilon(\mathbb{C}[\boldsymbol{\varepsilon}(\boldsymbol{u})]) + \frac{1}{1+H_0^{-1}} \frac{1}{2} c(\boldsymbol{u}, \boldsymbol{u}) - \ell(\boldsymbol{u})$$

$$= \frac{1}{1+H_0} \Upsilon(\mathbb{C}[\boldsymbol{\varepsilon}(\boldsymbol{u})]) + \frac{H_0}{1+H_0} \frac{1}{2} c(\boldsymbol{u}, \boldsymbol{u}) - \ell(\boldsymbol{u}) \,.$$

Proposition 3.10. *If we consider incompressible plasticity, then Theorem 3.6, Corollary 3.7, Lemma 3.8 and Corollary 3.9 remain true if* $\mathbb{H} = H_0 \, 2\mu \, \mathbb{P}_{\mathrm{dev}}$, *i.e. the hardening modulus is only definite on the deviatoric subspace* $\mathrm{Sym}_0(d)$.

As a result of this proposition, we will restrict ourselves to the case that $\mathbb{H}$ is definite on $\mathrm{Sym}(d)$. Concerning incompressible von Mises plasticity, a similar observation was made in [**Wie08**].

3. A (Primal) Variational Inequality Formulation

So far the notion primal problem always corresponded to a problem in duality with a dual problem by means of a Lagrangian. However, in the literature the notion primal problem is also used for a related problem which is based on a reformulation of the flow rule. As a result, the variables under consideration are the displacement $\boldsymbol{u}$ and the plastic strain $\boldsymbol{\varepsilon}_p$. The advantage of this formulation (which results in a variational inequality) is that it admits a time-dependent analogue in the quasi-static setting and we already refer to Chapter 5. For elaborate surveys, we refer to [**HR95, HR99**] and we will shortly derive this problem in the case of associated hardening. Afterwards, we will work out the connection between the primal minimization problem of the last section and the extended primal problem which we will derive next.

3.1. Derivation. Starting with the governing equations (3.7), we will use the relative stress $\boldsymbol{\alpha} = \boldsymbol{\sigma} + \boldsymbol{\zeta}$. The key point is to reformulate the flow rule $\boldsymbol{\varepsilon}_p(x) \in \partial\chi_K(\boldsymbol{\alpha}(x))$ as $\boldsymbol{\alpha}(x) \in \partial\chi_K^*(\boldsymbol{\varepsilon}_p(x))$ by the rules of convex analysis, see [**ET76, IT79, HUL93b, RW98**]. Here, χ_K^* is the *support function* of K, being defined as the Fenchel-conjugate function of the indicator function.

$$\chi_K^*(\boldsymbol{\tau}) = \sup_{\boldsymbol{\eta} \in \mathrm{Sym}(d)} \{\boldsymbol{\eta} : \boldsymbol{\tau} - \chi_K(\boldsymbol{\tau})\} = \sup_{\boldsymbol{\eta} \in K} \{\boldsymbol{\eta} : \boldsymbol{\tau}\} \,.$$

The physical interpretation of χ_K^* is that of dissipation and we remark that support functions are linearly homogeneous, i.e. $\chi_K^*(t\,\boldsymbol{\tau}) = t\,\chi_K^*(\boldsymbol{\tau})$ for all $t \geq 0$.

The inclusion $\boldsymbol{\alpha}(x) \in \partial\chi_K^*(\boldsymbol{\varepsilon}_p(x))$ can be written as $\chi_K^*(\boldsymbol{\tau}) \geq \chi_K^*(\boldsymbol{\varepsilon}_p(x)) + \boldsymbol{\alpha}(x) : (\boldsymbol{\tau} - \boldsymbol{\varepsilon}_p(x))$ for all $\boldsymbol{\tau} \in \mathrm{Sym}(d)$ and after integration over Ω, we arrive at

$$\chi_{\boldsymbol{K}}^*(\boldsymbol{\tau}) \geq \chi_{\boldsymbol{K}}^*(\boldsymbol{\varepsilon}_p) + \int_\Omega (\boldsymbol{\sigma}(x) + \boldsymbol{\zeta}(x)) : (\boldsymbol{\tau}(x) - \boldsymbol{\varepsilon}_p(x)) \, dx \,, \qquad \boldsymbol{\tau} \in \boldsymbol{P} \,,$$

with $\chi_{\boldsymbol{K}}^*(\boldsymbol{\tau}) = \sup_{\boldsymbol{\eta} \in \boldsymbol{P}} \{\langle \boldsymbol{\eta}, \boldsymbol{\tau} \rangle_{P^* \times P} - \chi_{\boldsymbol{K}}(\boldsymbol{\eta})\} = \sup_{\boldsymbol{\eta} \in \boldsymbol{K}} \{\langle \boldsymbol{\eta}, \boldsymbol{\tau} \rangle_{P^* \times P}\}$. From the weak form of the equilibrium constraint, we find $-\int_\Omega \boldsymbol{\sigma}(x) : \boldsymbol{\varepsilon}(\boldsymbol{w}(x) - \boldsymbol{u}(x)) \, dx + \ell(\boldsymbol{w} - \boldsymbol{u}) = 0$, and adding this to the above inequality leads to

$$\chi_{\boldsymbol{K}}^*(\boldsymbol{\tau}) \geq \chi_{\boldsymbol{K}}^*(\boldsymbol{\varepsilon}_p) + \int_\Omega \boldsymbol{\sigma}(x) : \big(\boldsymbol{\tau}(x) - \boldsymbol{\varepsilon}_p(x) - \boldsymbol{\varepsilon}(\boldsymbol{w}(x)) + \boldsymbol{\varepsilon}(\boldsymbol{u}(x))\big) \, dx$$

$$+ \int_\Omega \boldsymbol{\zeta}(x) : (\boldsymbol{\tau}(x) - \boldsymbol{\varepsilon}_p(x)) \, dx + \ell(\boldsymbol{w} - \boldsymbol{u}) \,, \qquad (\boldsymbol{\tau}, \boldsymbol{w}) \in \boldsymbol{P} \times \boldsymbol{X} \,.$$

Using the constitutive equations (3.7b), (3.7e), we arrive at

$$\int_\Omega (\boldsymbol{\varepsilon}(\boldsymbol{u}(x)) - \boldsymbol{\varepsilon}_p(x)) : \mathbb{C}\big[\boldsymbol{\varepsilon}(\boldsymbol{w}(x)) - \boldsymbol{\varepsilon}(\boldsymbol{u}(x)) - (\boldsymbol{\tau}(x) - \boldsymbol{\varepsilon}_p(x))\big]$$

$$+ \int_\Omega \boldsymbol{\varepsilon}_p(x) : \mathbb{H}[\boldsymbol{\tau}(x) - \boldsymbol{\varepsilon}_p(x)]\, dx + \chi_{\boldsymbol{K}}^*(\boldsymbol{\tau}) - \chi_{\boldsymbol{K}}^*(\boldsymbol{\varepsilon}_p) \geq \ell(\boldsymbol{w} - \boldsymbol{u})\,,$$

for all $(\boldsymbol{\tau}, \boldsymbol{w}) \in \boldsymbol{P} \times \boldsymbol{X}$. With the bilinear form $q : (\boldsymbol{V} \times \boldsymbol{P}) \times (\boldsymbol{V} \times \boldsymbol{P}) \to \mathbb{R}$,

$$q((\boldsymbol{u}, \boldsymbol{\varepsilon}_p), (\boldsymbol{w}, \boldsymbol{\tau}))$$

$$= \int_\Omega (\boldsymbol{\varepsilon}(\boldsymbol{u}(x)) - \boldsymbol{\varepsilon}_p(x)) : \mathbb{C}\big[\boldsymbol{\varepsilon}(\boldsymbol{w}(x)) - \boldsymbol{\tau}(x)\big] + \int_\Omega \boldsymbol{\varepsilon}_p(x) : \mathbb{H}[\boldsymbol{\tau}(x)]\, dx\,, \qquad (3.12)$$

the problem takes the form

$$q\big((\boldsymbol{u}, \boldsymbol{\varepsilon}_p), (\boldsymbol{w}, \boldsymbol{\tau}) - (\boldsymbol{u}, \boldsymbol{\varepsilon}_p)\big) + \chi_{\boldsymbol{K}}^*(\boldsymbol{\tau}) - \chi_{\boldsymbol{K}}^*(\boldsymbol{\varepsilon}_p) \geq \ell(\boldsymbol{w} - \boldsymbol{u})\,, \qquad (\boldsymbol{\tau}, \boldsymbol{w}) \in \boldsymbol{P} \times \boldsymbol{X}\,. \tag{3.13}$$

This is a *variational inequality* of the second kind, cf. [**Glo84**, **AH05**]. Moreover, as q is symmetric, the variational inequality is equivalent to the minimization problem

$$\begin{aligned} &\text{Minimize} \quad \tfrac{1}{2}q\big((\boldsymbol{u}, \boldsymbol{\varepsilon}_p), (\boldsymbol{u}, \boldsymbol{\varepsilon}_p)\big) + \chi_{\boldsymbol{K}}^*(\boldsymbol{\varepsilon}_p) - \ell(\boldsymbol{u})\,, \\ &\text{subject to} \quad (\boldsymbol{u}, \boldsymbol{\varepsilon}_p) \in \boldsymbol{X}(\boldsymbol{u}_D) \times \boldsymbol{P}\,. \end{aligned} \tag{3.14}$$

Note that this minimization problem corresponds to the minimization of the total energy which is composed of the free energy $\tfrac{1}{2}q\big((\boldsymbol{u}, \boldsymbol{\varepsilon}_p), (\boldsymbol{u}, \boldsymbol{\varepsilon}_p)\big)$, the dissipation $\chi_{\boldsymbol{K}}^*(\boldsymbol{\varepsilon}_p)$ and the exterior forces which are represented by the load functional. Concerning existence and uniqueness of solutions, we have the following result.

Proposition 3.11. *If $\mathbb{H}$ is positive definite on the symmetric second order tensors, the variational inequality* (3.13) *admits a unique solution* $(\boldsymbol{u}, \boldsymbol{\varepsilon}_p) \in \boldsymbol{X}(\boldsymbol{u}_D) \times \boldsymbol{P}$.

PROOF. It suffices to show that $q(\cdot, \cdot)$ is bounded and elliptic on $\boldsymbol{X} \times \boldsymbol{P}$. For this, we refer to [**HR99**, Section 7.3] where this is proven in a more general setting also including the possibility of isotropic hardening. Then, a standard existence and uniqueness proof for variational inequalities of the second kind yields the claimed assertion. This proof is standard and can be found in many textbooks, cf. [**HR99**, Theorem 6.6], [**Glo84**, Theorem I.4.1] or [**Rou05**, Section 5] for a proof in a slightly different setting. $\square$

Remark 3.12. *For incompressible plasticity, it is sufficient that $\mathbb{H}$ is positive definite on the deviatoric subspace, cf. the discussion in Subsection* 3.2.4.

3.2. Partial Minimization. We will now show that by partial minimization of (3.14) w.r.t. $\boldsymbol{\varepsilon}_p$, we arrive at the primal problem of the previous section. For this, we have a closer look at the bilinear form $q(\cdot, \cdot)$ and note that

$$q((\boldsymbol{u}, \boldsymbol{\varepsilon}_p), (\boldsymbol{u}, \boldsymbol{\varepsilon}_p)) = c(\boldsymbol{u}, \boldsymbol{u}) + \int_\Omega \boldsymbol{\varepsilon}_p(x) : \mathbb{N}[\boldsymbol{\varepsilon}_p(x)]\, dx - 2 \int_\Omega \boldsymbol{\varepsilon}(\boldsymbol{u}(x)) : \mathbb{C}[\boldsymbol{\varepsilon}_p(x)]\, dx\,.$$

Lemma 3.13. *Let $\tilde{\mathcal{E}}_{\text{hd}} : \boldsymbol{X}(\boldsymbol{u}_D) \to \mathbb{R}$ be defined as*

$$\tilde{\mathcal{E}}_{\text{hd}}(\boldsymbol{u}) = \inf_{\boldsymbol{\varepsilon}_p \in \boldsymbol{P}} \big\{\tfrac{1}{2}q\big((\boldsymbol{u}, \boldsymbol{\varepsilon}_p), (\boldsymbol{u}, \boldsymbol{\varepsilon}_p)\big) + \chi_{\boldsymbol{K}}^*(\boldsymbol{\varepsilon}_p)\big\} - \ell(\boldsymbol{u})\,.$$

Then $\tilde{\mathcal{E}}_{\text{hd}} = \mathcal{E}_{\text{hd}}$ with $\mathcal{E}_{\text{hd}}$ as given in Theorem 3.6.

PROOF. Once more, we omit the dependence on x. Using the structure of $q(\cdot, \cdot)$, we arrive at

$$\tilde{\mathcal{E}}_{\text{hd}}(\boldsymbol{u}) = \inf_{\varepsilon_p \in \boldsymbol{P}} \left\{ \frac{1}{2} \int_\Omega \varepsilon_p : \mathbb{N}[\varepsilon_p] \, dx - \int_\Omega \boldsymbol{\varepsilon}(\boldsymbol{u}) : \mathbb{C}[\varepsilon_p] \, dx + \chi_{\boldsymbol{K}}^*(\varepsilon_p) \right\} + \frac{1}{2} c(\boldsymbol{u}, \boldsymbol{u}) - \ell(\boldsymbol{u}) \,.$$

and defining $I : \boldsymbol{P} \to \overline{\mathbb{R}}$ via

$$I(\varepsilon_p) = \frac{1}{2} \int_\Omega \varepsilon_p : \mathbb{N}[\varepsilon_p] \, dx - \int_\Omega \boldsymbol{\varepsilon}(\boldsymbol{u}) : \mathbb{C}[\varepsilon_p] \, dx + \chi_{\boldsymbol{K}}^*(\varepsilon_p) \,,$$

we consider the minimization problem $I(\varepsilon_p) = \min!$ I is convex and has at least quadratic growth since we assumed that $\mathbb{N}$ is positive definite and $\chi_{\boldsymbol{K}}^*$ is the support function of $\boldsymbol{K}$. The necessary and sufficient condition for a minimum is $0 \in \partial I(\varepsilon_p)$, viz.

$$-\mathbb{N}[\varepsilon_p] + \mathbb{C}[\boldsymbol{\varepsilon}(\boldsymbol{u})] \in \partial \chi_{\boldsymbol{K}}^*(\varepsilon_p) \,,$$

and since $\chi_{\boldsymbol{K}}^*$ is a closed convex functional and $(\chi_{\boldsymbol{K}}^*)^* = \chi_{\boldsymbol{K}}$, this is equivalent to

$$\varepsilon_p \in \partial \chi_{\boldsymbol{K}} \big(- \mathbb{N}[\varepsilon_p] + \mathbb{C}[\boldsymbol{\varepsilon}(\boldsymbol{u})] \big) \,.$$

This can be rewritten as

$$\int_\Omega \varepsilon_p : \big(\boldsymbol{\tau} - \big(- \mathbb{N}[\varepsilon_p] + \mathbb{C}[\boldsymbol{\varepsilon}(\boldsymbol{u})] \big) \big) \, dx \leq 0 \,, \qquad \boldsymbol{\tau} \in \boldsymbol{K} \,. \tag{3.15}$$

By the flow rule (3.7d), we also find $\varepsilon_p \in \partial \chi_{\boldsymbol{K}}(\boldsymbol{\alpha})$ and the previous section already suggests $\boldsymbol{\alpha} = P_{\boldsymbol{K}}^N(\mathbb{C}[\boldsymbol{\varepsilon}(\boldsymbol{u})])$. In view of this, we will show that

$$\varepsilon_p = \mathbb{N}^{-1} \big[\mathbb{C}[\boldsymbol{\varepsilon}(\boldsymbol{u})] - P_{\boldsymbol{K}}^N(\mathbb{C}[\boldsymbol{\varepsilon}(\boldsymbol{u})]) \big] \,,$$

indeed satisfies the flow rule and therefore is the minimizer of $I(\varepsilon_p)$. Therefore, we substitute the above expression into (3.15) and then for all $\boldsymbol{\tau} \in \boldsymbol{K}$, we have

$$\int_\Omega \varepsilon_p : \big(\boldsymbol{\tau} - \big(- \mathbb{N}[\varepsilon_p] + \mathbb{C}[\boldsymbol{\varepsilon}(\boldsymbol{u})] \big) \big) \, dx$$

$$= \int_\Omega \mathbb{N}^{-1} \big[\mathbb{C}[\boldsymbol{\varepsilon}(\boldsymbol{u})] - P_{\boldsymbol{K}}^N(\mathbb{C}[\boldsymbol{\varepsilon}(\boldsymbol{u})]) \big] : \big(\boldsymbol{\tau} - P_{\boldsymbol{K}}^N(\mathbb{C}[\boldsymbol{\varepsilon}(\boldsymbol{u})]) \big) \, dx$$

$$= n \big(\mathbb{C}[\boldsymbol{\varepsilon}(\boldsymbol{u})] - P_{\boldsymbol{K}}^N(\mathbb{C}[\boldsymbol{\varepsilon}(\boldsymbol{u})]), \boldsymbol{\tau} - P_{\boldsymbol{K}}^N(\mathbb{C}[\boldsymbol{\varepsilon}(\boldsymbol{u})]) \leq 0$$

since $P_{\boldsymbol{K}}^N$ is the projection with respect to $n(\cdot, \cdot)$. Hence, we are able to conclude that $\varepsilon_p = \mathbb{N}^{-1} \big[\mathbb{C}[\boldsymbol{\varepsilon}(\boldsymbol{u})] - P_{\boldsymbol{K}}^N(\mathbb{C}[\boldsymbol{\varepsilon}(\boldsymbol{u})]) \big]$ is the minimizer of $I(\cdot)$. It remains to show $\tilde{\mathcal{E}}_{\text{hd}} = \mathcal{E}_{\text{hd}}$.

$$\tilde{\mathcal{E}}_{\text{hd}}(\boldsymbol{u}) = I \big(\mathbb{N}^{-1} \big[\mathbb{C}[\boldsymbol{\varepsilon}(\boldsymbol{u})] - P_{\boldsymbol{K}}^N(\mathbb{C}[\boldsymbol{\varepsilon}(\boldsymbol{u})]) \big] \big) + \frac{1}{2} c(\boldsymbol{u}, \boldsymbol{u}) - \ell(\boldsymbol{u})$$

$$= \frac{1}{2} \| \mathbb{C}[\boldsymbol{\varepsilon}(\boldsymbol{u})] - P_{\boldsymbol{K}}^N(\mathbb{C}[\boldsymbol{\varepsilon}(\boldsymbol{u})]) \|_N^2 - \int_\Omega \mathbb{C}[\boldsymbol{\varepsilon}(\boldsymbol{u})] : \mathbb{N}^{-1} \big[\mathbb{C}[\boldsymbol{\varepsilon}(\boldsymbol{u})] - P_{\boldsymbol{K}}^N(\mathbb{C}[\boldsymbol{\varepsilon}(\boldsymbol{u})]) \big] \, dx$$

$$+ \chi_{\boldsymbol{K}}^* \big(\mathbb{N}^{-1} \big[\mathbb{C}[\boldsymbol{\varepsilon}(\boldsymbol{u})] - P_{\boldsymbol{K}}^N(\mathbb{C}[\boldsymbol{\varepsilon}(\boldsymbol{u})]) \big] \big) + \frac{1}{2} c(\boldsymbol{u}, \boldsymbol{u}) - \ell(\boldsymbol{u})$$

$$= -\frac{1}{2} \| \mathbb{C}[\boldsymbol{\varepsilon}(\boldsymbol{u})] \|_N^2 + \frac{1}{2} \| P_{\boldsymbol{K}}^N \mathbb{C}[\boldsymbol{\varepsilon}(\boldsymbol{u})] \|_N^2$$

$$+ \chi_{\boldsymbol{K}}^* \big(\mathbb{N}^{-1} \big[\mathbb{C}[\boldsymbol{\varepsilon}(\boldsymbol{u})] - P_{\boldsymbol{K}}^N(\mathbb{C}[\boldsymbol{\varepsilon}(\boldsymbol{u})]) \big] \big) + \frac{1}{2} c(\boldsymbol{u}, \boldsymbol{u}) - \ell(\boldsymbol{u}) \,.$$

Since $\frac{1}{2} c(\boldsymbol{u}, \boldsymbol{u}) - \frac{1}{2} \| \mathbb{C}[\boldsymbol{\varepsilon}(\boldsymbol{u})] \|_N^2 = \frac{1}{2} \int_\Omega \mathbb{C}[\boldsymbol{\varepsilon}(\boldsymbol{u})] : \mathbb{D}\big[\mathbb{C}[\boldsymbol{\varepsilon}(\boldsymbol{u})] \big] \, dx$ it remains to show

$$\frac{1}{2} \| P_{\boldsymbol{K}}^N(\mathbb{C}[\boldsymbol{\varepsilon}(\boldsymbol{u})]) \| + \chi_{\boldsymbol{K}}^* \big(\mathbb{N}^{-1} \big[\mathbb{C}[\boldsymbol{\varepsilon}(\boldsymbol{u})] - P_{\boldsymbol{K}}^N(\mathbb{C}[\boldsymbol{\varepsilon}(\boldsymbol{u})]) \big] \big) = \Upsilon^N(\mathbb{C}[\boldsymbol{\varepsilon}(\boldsymbol{u})]) \,.$$

To show this, we consider the definition of the support function $\chi_{\boldsymbol{K}}^*$

$$\chi_{\boldsymbol{K}}^* \big(\mathbb{N}^{-1} \big[\mathbb{C}[\boldsymbol{\varepsilon}(\boldsymbol{u})] - P_{\boldsymbol{K}}^N(\mathbb{C}[\boldsymbol{\varepsilon}(\boldsymbol{u})]) \big] \big) = \sup_{\boldsymbol{\eta} \in \boldsymbol{K}} \left\{ n \big(\boldsymbol{\eta}, \mathbb{C}[\boldsymbol{\varepsilon}(\boldsymbol{u})] - P_{\boldsymbol{K}}^N(\mathbb{C}[\boldsymbol{\varepsilon}(\boldsymbol{u})]) \big) \right\}$$

The maximum is attained at $\boldsymbol{\eta} = P_{\boldsymbol{K}}^N(\mathbb{C}[\boldsymbol{\varepsilon}(\boldsymbol{u})])$ due to the characterization of the flow rule which is just the optimality condition of this optimization problem. Hence,

$$
\begin{aligned}
\chi_{\boldsymbol{K}}^*\big(\mathbb{N}^{-1}\big[\mathbb{C}[\boldsymbol{\varepsilon}(\boldsymbol{u})] - P_{\boldsymbol{K}}^N(\mathbb{C}[\boldsymbol{\varepsilon}(\boldsymbol{u})])\big]\big) &= n\big(P_{\boldsymbol{K}}^N(\mathbb{C}[\boldsymbol{\varepsilon}(\boldsymbol{u})], \mathbb{C}[\boldsymbol{\varepsilon}(\boldsymbol{u})] - P_{\boldsymbol{K}}^N(\mathbb{C}[\boldsymbol{\varepsilon}(\boldsymbol{u})])\big) \\
&= -\tfrac{1}{2}\|P_{\boldsymbol{K}}^N(\mathbb{C}[\boldsymbol{\varepsilon}(\boldsymbol{u})])\|_N^2 + \Upsilon^N(\mathbb{C}[\boldsymbol{\varepsilon}(\boldsymbol{u})])\,,
\end{aligned}
$$

which assures $\tilde{\mathcal{E}}_{\text{hd}} = \mathcal{E}_{\text{hd}}$. $\qquad\qquad\qquad\qquad\qquad\qquad\qquad\qquad\qquad\qquad\qquad\square$

The extended primal problem therefore admits the interpretation of an augmented problem whose formulation is based on the governing equations rather than a direct derivation from an extremum principle. The corresponding variational inequality (3.13) is equivalent to a minimization problem as long as $q(\cdot, \cdot)$ is symmetric. In the next section, we will see that in certain cases, the non-associated flow rule also transfers the problem into a variational inequality. However, the corresponding bilinear form will no longer be symmetric reflecting the lack of an underlying minimization problem.

CHAPTER 4

NON-ASSOCIATED PLASTICITY – DRUCKER-PRAGER PLASTICITY

In Section 2.3, we simply added the constraint $\boldsymbol{\sigma} \in \boldsymbol{K}$ to the dual problem of elasticity and afterwards showed that this procedure automatically implies the associated flow rule. This is coherent with Subsection 1.2.3, where the associated flow rule was introduced by means of a variational principle, viz. the maximum plastic work inequality. In the non-associated setting, no such variational principle exists and therefore the boundary value problem cannot be derived by a pair of minimization problems in duality as in Section 2.3. But even worse, the occuring boundary value problem may no longer be elliptic, cf. [VP96], and may suffer from instabilities. In the case of Drucker-Prager plasticity, we will show that the introduction of the non-associated flow rule may lead to the loss of monotonicity in the underlying boundary value problem and we also refer to Appendix B for an elementary (counter-) example showing the ill-posedness of the model. From a mechanical point of view, the loss of monotonicity can cause softening behaviour as it was observed in [BCDS01] for a special loading regime. As a consequence, the amount of regularization which is necessary to obtain solutions strongly depends on the magnitude of non-associativity as we will show below.

After introducing a general setting and stating some abstract results, we focus on non-associated Drucker-Prager plasticity as introduced in Section 1.2. Afterwards, we briefly come back to the general setting.

1. The Response Function

1.1. Perfect Plasticity. In Subsection 1.2.3 (and again adopting the static scenario), we introduced the general non-associated flow rule as $\boldsymbol{\varepsilon}_p(x) \in G(\boldsymbol{\sigma}(x))$ with $G : \mathrm{Sym}(d) \rightrightarrows \mathrm{Sym}(d)$. Transferring this into the function space setting, we request $\boldsymbol{\varepsilon}_p \in \boldsymbol{G}(\boldsymbol{\sigma})$ with $\boldsymbol{G} : \boldsymbol{P} \rightrightarrows \boldsymbol{P}^*$ being the multi-function defined via the inclusion $\boldsymbol{\varepsilon}_p(x) \in G(\boldsymbol{\sigma}(x))$ in the a.e. sense. In addition to the flow rule, we must also ensure admissibility $\boldsymbol{\sigma} \in \boldsymbol{K}$. Again, we will proceed formally, assuming that all operations are well defined in the Hilbert

space setting. We shortly repeat the governing equations of non-associated plasticity:

$$-\operatorname{div}(\boldsymbol{\sigma}(x)) = \boldsymbol{b}(x,t)\,, \qquad\qquad x \in \Omega\,, \qquad (4.1a)$$

$$\boldsymbol{\sigma}(x) = \mathbb{C}[\boldsymbol{\varepsilon}(\boldsymbol{u}(x)) - \boldsymbol{\varepsilon}_p(x)]\,, \qquad\qquad x \in \Omega\,, \qquad (4.1b)$$

$$\boldsymbol{\sigma}(x) \in K\,, \qquad\qquad x \in \Omega\,, \qquad (4.1c)$$

$$\boldsymbol{\varepsilon}_p(x) \in G(\boldsymbol{\sigma}(x)) \qquad\qquad x \in \Omega\,, \qquad (4.1d)$$

$$\boldsymbol{u}(x) = \boldsymbol{u}_D\,, \qquad\qquad x \in \Gamma_D\,, \qquad (4.1e)$$

$$\boldsymbol{\sigma}(x)\boldsymbol{n}(x) = \boldsymbol{t}_N(x)\,, \qquad\qquad x \in \Gamma_T\,. \qquad (4.1f)$$

In the associated case, it was possible to handle the two inclusions $\boldsymbol{\sigma} \in \boldsymbol{K}$ and $\boldsymbol{\varepsilon}_p \in \boldsymbol{G}(\boldsymbol{\sigma})$ simultaneously due to the special structure $\boldsymbol{G} = \partial\chi_{\boldsymbol{K}}$ which automatically guaranteed admissibility and the flow rule. Since the latter was a result of the first, this naturally cannot be true in non-associated case.

Substituting (4.1b) into (4.1d), we seek $\boldsymbol{\sigma} \in \boldsymbol{P}$ and $\boldsymbol{u} \in \boldsymbol{X}(\boldsymbol{u}_D)$ satisfying

$$0 \in \mathbb{C}^{-1}[\boldsymbol{\sigma}(x)] - \boldsymbol{\varepsilon}(\boldsymbol{u}(x)) + G(\boldsymbol{\sigma}(x))\,, \qquad \text{a.e. in } \Omega\,, \qquad (4.2a)$$

$$\boldsymbol{\sigma}(x) \in K\,, \qquad \text{a.e. in } \Omega\,, \qquad (4.2b)$$

$$\int_\Omega \boldsymbol{\sigma}(x) : \boldsymbol{\varepsilon}(\boldsymbol{w}(x))\,dx = \ell(\boldsymbol{w})\,, \qquad \boldsymbol{w} \in \boldsymbol{X}\,, \qquad (4.2c)$$

with the equilibrium condition (4.1a) in weak form. These three conditions replace the optimality conditions (2.33) of associated plasticity. Adopting the ideas of the associated case, we define a response function

$$R_{\boldsymbol{K}} : \boldsymbol{P} \to \boldsymbol{K} \subset \boldsymbol{P} \qquad\qquad (4.3)$$

and its pointwise counterpart $R_K : \operatorname{Sym}(d) \to K$, such that $\boldsymbol{\sigma} = R_{\boldsymbol{K}}(\mathbb{C}[\boldsymbol{\varepsilon}(\boldsymbol{u})])$ satisfies (4.2a) and (4.2b). Afterwards, substitution into the weak equilibrium condition results in the problem of finding $\boldsymbol{u} \in \boldsymbol{X}(\boldsymbol{u}_D)$ such that

$$\int_\Omega R_K\big(\mathbb{C}[\boldsymbol{\varepsilon}(\boldsymbol{u}(x))]\big) : \boldsymbol{\varepsilon}(\boldsymbol{w}(x))\,dx = \ell(\boldsymbol{w})\,, \qquad \boldsymbol{w} \in \boldsymbol{X}\,. \qquad (4.4)$$

In the associated case, the response function $R_{\boldsymbol{K}}$ was simply the projection operator $P_{\boldsymbol{K}}$, cf. (2.38), and by duality, this condition was the Euler condition of the primal minimization problem. However, this no longer holds here, but (4.4) is the weak formulation of the boundary value problem

$$-\operatorname{div}\Big(R_K\big(\mathbb{C}[\boldsymbol{\varepsilon}(\boldsymbol{u}(x))]\big)\Big) = \boldsymbol{b}(x)\,, \qquad x \in \Omega\,,$$

with boundary values (4.1e) and (4.1f). Defining the operator

$$S : \boldsymbol{X} \to \boldsymbol{X}^*\,, \qquad\qquad S = -B \circ R_{\boldsymbol{K}} \circ A^{-1} \circ (-B^*) \qquad (4.5)$$

the operator equation

$$S(\boldsymbol{u}) = \ell \qquad \text{in } \boldsymbol{X}^*\,,$$

is just the reformulation of (4.4). Whereas in the case of associated plasticity, the operator T as defined in (2.40) was monotone, the operator S may no longer be monotone in the non-associated case, essentially meaning that the boundary value problem is no longer elliptic, cf. [Eva08, Section 9.1]. We will make this more precise for non-associated Drucker-Prager plasticity in the next section.

1.2. Kinematic Hardening Plasticity. Concerning kinematic hardening, the governing equations (4.1) are supplemented by the relation $\varepsilon_p(x) = -\mathbb{H}^{-1}[\zeta(x)]$ a.e. in Ω and the admissibility (4.1c) and flow rule (4.1d) are replaced by

$$\boldsymbol{\sigma}(x) + \boldsymbol{\zeta}(x) \in K\,, \qquad\qquad\qquad x \in \Omega\,,$$

$$\boldsymbol{\varepsilon}_p(x) \in G\big(\boldsymbol{\sigma}(x) + \boldsymbol{\zeta}(x)\big)\,, \qquad\qquad x \in \Omega\,.$$

Using $\boldsymbol{\varepsilon}_p(x) = -\mathbb{H}^{-1}[\boldsymbol{\zeta}(x)]$ and writing $\boldsymbol{\eta} = \mathbb{C}[\varepsilon(\boldsymbol{u})]$ leads to the system

$$0 = \mathbb{C}^{-1}[\boldsymbol{\sigma}(x)] - \mathbb{C}^{-1}[\boldsymbol{\eta}(x)] - \mathbb{H}^{-1}[\boldsymbol{\zeta}(x)]\,, \qquad \text{a.e. in } \Omega\,, \tag{4.6a}$$

$$0 \in \mathbb{H}^{-1}[\boldsymbol{\zeta}(x)] + G\big(\boldsymbol{\sigma}(x) + \boldsymbol{\zeta}(x)\big)\,, \qquad \text{a.e. in } \Omega\,, \tag{4.6b}$$

$$\boldsymbol{\sigma}(x) + \boldsymbol{\zeta}(x) \in K\,, \qquad \text{a.e. in } \Omega\,, \tag{4.6c}$$

$$\int_\Omega \boldsymbol{\sigma} : \varepsilon(\boldsymbol{v})\, dx = \ell(\boldsymbol{v})\,, \qquad \boldsymbol{v} \in \boldsymbol{X}\,. \tag{4.6d}$$

This time, we use (4.6a)-(4.6c) to implicitly define the response function

$$R_{\mathrm{hd}} : \boldsymbol{P} \to (\boldsymbol{P} \times \boldsymbol{P})\,, \qquad\qquad \begin{bmatrix} \boldsymbol{\sigma} \\ \boldsymbol{\zeta} \end{bmatrix} = R_{\mathrm{hd}}(\boldsymbol{\eta})\,,$$

such that $(\boldsymbol{\sigma}, \boldsymbol{\zeta}, \boldsymbol{\eta})$ satisfies (4.6a)-(4.6c). Afterwards, the first component of R_{hd} is substituted into the weak equilibrium equation (4.6d). In the associated case, this coincides with the response function (3.10).

1.3. A General Existence Result. We shortly indicate under which assumptions on the response function, we obtain a unique solution in $\boldsymbol{X}(\boldsymbol{u}_D)$.

Theorem 4.1. *Suppose that $\beta > 0$ exists such that the response function $R : \mathrm{Sym}(d) \to \mathrm{Sym}(d)$ satisfies*

$$\big(R(\boldsymbol{\sigma}) - R(\boldsymbol{\eta})\big) : \mathbb{C}^{-1}[\boldsymbol{\sigma} - \boldsymbol{\eta}] \geq \tfrac{\beta}{2}(\boldsymbol{\sigma} - \boldsymbol{\eta}) : \mathbb{C}^{-1}[\boldsymbol{\sigma} - \boldsymbol{\eta}]$$

for all $\boldsymbol{\sigma}, \boldsymbol{\eta} \in \mathrm{Sym}(d)$. Then, the variational problem of finding $\boldsymbol{u} \in \boldsymbol{X}(\boldsymbol{u}_D)$ such that

$$\int_\Omega R(\mathbb{C}[\varepsilon(\boldsymbol{u}(x))]) : \varepsilon(\boldsymbol{w}(x))\, dx = \ell(\boldsymbol{w})\,, \qquad \boldsymbol{w} \in \boldsymbol{X}\,,$$

has a unique solution.

PROOF. We introduce the mapping $F : \boldsymbol{X} \to \boldsymbol{X}^*$, by setting

$$\langle F(\boldsymbol{u}), \boldsymbol{w} \rangle_{\boldsymbol{X}^* \times \boldsymbol{X}} = \int_\Omega R(\mathbb{C}[\varepsilon(\boldsymbol{u}(x))]) : \varepsilon(\boldsymbol{w}(x))\, dx - \ell(\boldsymbol{w})\,, \tag{4.7}$$

and show the strong monotonicity of F. Therefore consider

$$\langle F(\boldsymbol{u}) - F(\boldsymbol{w}), \boldsymbol{u} - \boldsymbol{w} \rangle_{\boldsymbol{X}^* \times \boldsymbol{X}}$$

$$= \int_\Omega \Big(R(\mathbb{C}[\varepsilon(\boldsymbol{u}(x))]) - R(\mathbb{C}[\varepsilon(\boldsymbol{w}(x))]) \Big) : \big(\varepsilon(\boldsymbol{u}(x)) - \varepsilon(\boldsymbol{w}(x))\big)\, dx$$

$$= \int_\Omega \Big(R(\mathbb{C}[\varepsilon(\boldsymbol{u}(x))]) - R(\mathbb{C}[\varepsilon(\boldsymbol{w}(x))]) \Big) : \mathbb{C}^{-1}\big[\mathbb{C}[\varepsilon(\boldsymbol{u}(x))] - \mathbb{C}[\varepsilon(\boldsymbol{w}(x))]\big]\, dx$$

$$\geq \tfrac{\beta}{2} \int_\Omega \mathbb{C}\big[\varepsilon(\boldsymbol{u}(x)) - \varepsilon(\boldsymbol{w}(x))\big] : \big(\varepsilon(\boldsymbol{u}(x)) - \varepsilon(\boldsymbol{w}(x))\big)\, dx = \tfrac{\beta}{2} \|\boldsymbol{u} - \boldsymbol{w}\|^2\,.$$

The proof then follows from a fixed-point argument. This will later be shown in Theorem 8.1. Alternatively, the monotonicity can again be exploited. □

Remark 4.2. *It is easy to verify that the response function for associated hardening plasticity, i.e.*
$R(\boldsymbol{\eta}) = \mathbb{D} \circ \mathbb{C}^{-1}[\boldsymbol{\eta}] + \mathbb{C} \circ \mathbb{N}^{-1}[P_K^F(\boldsymbol{\eta})]$, *satisfies the above condition if the hardening modulus* $\mathbb{H}$
is positive definite, cf. Theorem 3.6. Likewise the viscoplastic regularization of associated perfect
plasticity satisfies this properties as $R(\boldsymbol{\eta}) = \frac{1}{1+\alpha}\boldsymbol{\eta} + \frac{\alpha}{1+\alpha}P_K(\boldsymbol{\eta})$, *cf. (3.3). For associated perfect*
plasticity however, we only have $\beta = 0$.

2. Drucker-Prager Plasticity

We now consider the special case of non-associated Drucker-Prager plasticity. After having a look at the response function in this specific case, we once more consider the viscoplastic flow rule and kinematic hardening. As we will demonstrate, in both cases the necessary amount of regularization cannot be arbitrarily small but depends on the magnitude of non-associativity. Just as in Section 3.3, it is possible to derive a formulation as a variational inequality.

In this section, we exclusively consider the non-associated flow rule

$$\boldsymbol{\varepsilon}_p(x) \in \mathbb{T}\big[\partial\chi_K(\boldsymbol{\sigma}(x))\big]\,,$$

introduced in Section 1.2.5, and we will show that it is possible to regain some variational principles. Particularly, the response function is locally characterized as the solution of a minimization problem.

2.1. The Response Function.
For simplicity, we will always assume that $\mathbb{T}$ is invertible on $\mathrm{Sym}(d)$. This corresponds to a strictly positive angle of dilatancy $\psi > 0$. With some modifications, also the case $\psi = 0$ can be handled, but we do not go into details here.

2.1.1. *Perfect Plasticity.* Using $G = \mathbb{T}[\partial\chi_K]$, the response function is characterized by the two inclusions

$$
\begin{aligned}
&0 \in \mathbb{T}^{-1} \circ \mathbb{C}^{-1}[\boldsymbol{\sigma}(x)] - \mathbb{T}^{-1}[\boldsymbol{\varepsilon}(\boldsymbol{u}(x))] + \partial\chi_K(\boldsymbol{\sigma}(x))\,, \qquad \text{a.e. in } \Omega\,, \\
&\boldsymbol{\sigma}(x) \in K\,, \qquad \text{a.e. in } \Omega\,,
\end{aligned}
\tag{4.8}
$$

After integration, multiplication by $\boldsymbol{\eta} \in \boldsymbol{P}$ and integration, we arrive at

$$0 \in \int_\Omega \boldsymbol{\tau}(x) : (\mathbb{C} \circ \mathbb{T})^{-1}[\boldsymbol{\sigma}(x)]\,dx - \int_\Omega \boldsymbol{\tau}(x) : (\mathbb{C} \circ \mathbb{T})^{-1}\big[\mathbb{C}[\boldsymbol{\varepsilon}(\boldsymbol{u}(x))]\big]\,dx + \partial\chi_{\boldsymbol{K}}(\boldsymbol{\sigma})\,.$$

We define $\mathbb{F} = \mathbb{C} \circ \mathbb{T}$ and assume that $\mathbb{F}$ is symmetric which is justified in an isotropic medium, i.e. if $\mathbb{C} = 2\mu\mathbb{P}_{\mathrm{dev}} + 3\kappa\mathbb{P}_{\mathrm{vol}}$. Then, $\mathbb{F}$ gives rise to the inner product $f : \boldsymbol{P} \times \boldsymbol{P} \to \mathbb{R}$ and norm $\|\cdot\|_F$ via

$$f(\boldsymbol{\sigma}, \boldsymbol{\eta}) = \int_\Omega \boldsymbol{\sigma}(x) : \mathbb{F}^{-1}[\boldsymbol{\eta}(x)]\,dx\,, \qquad\qquad \|\boldsymbol{\sigma}\|_F = \sqrt{f(\boldsymbol{\sigma}, \boldsymbol{\sigma})}\,.$$

Then, the inclusions (4.8) are equivalent to the optimality conditions of the minimization problem:

$$\text{Minimize} \quad \tfrac{1}{2}\|\boldsymbol{\sigma} - \mathbb{C}[\boldsymbol{\varepsilon}(\boldsymbol{u})]\|_F^2 + \chi_{\boldsymbol{K}}(\boldsymbol{\sigma})\,, \qquad \boldsymbol{\sigma} \in \boldsymbol{P}\,,$$

and again, the solution is a projection which we denote $P_{\boldsymbol{K}}^F : \boldsymbol{P} \to \boldsymbol{K}$. Thus, $R_K = P_{\boldsymbol{K}}^F$ and we have $\boldsymbol{\sigma} = P_{\boldsymbol{K}}^F(\mathbb{C}[\boldsymbol{\varepsilon}(\boldsymbol{u})])$.

We define operators

$$\tilde{B}^* : \boldsymbol{V} \to \boldsymbol{P}^* , \qquad \langle \tilde{B}^* u, \boldsymbol{\sigma} \rangle_{\boldsymbol{P}^* \times \boldsymbol{P}} = - \int_\Omega \boldsymbol{\sigma}(x) : \mathbb{T}^{-1}[\boldsymbol{\varepsilon}(\boldsymbol{u}(x))] \, dx ,$$

$$F : \boldsymbol{P} \to \boldsymbol{P}^* , \qquad \langle F\boldsymbol{\sigma}, \boldsymbol{\eta} \rangle_{\boldsymbol{P}^* \times \boldsymbol{P}} = f(\boldsymbol{\sigma}, \boldsymbol{\eta}) ,$$

the latter being the Riesz operator with respect to the inner product $f(\cdot, \cdot)$. Together, the replacement of the optimality conditions (2.33) of associated plasticity is then given by the inclusions

$$0 \in F\boldsymbol{\sigma} + \partial\chi_{\boldsymbol{K}}(\boldsymbol{\sigma}) + \tilde{B}^* u , \qquad\qquad \text{in } \boldsymbol{P}^* , \tag{4.9a}$$

$$0 = B\boldsymbol{\sigma} - \ell , \qquad\qquad \text{in } \boldsymbol{X}^* , \tag{4.9b}$$

We note that whenever $\tilde{B}^* \neq B^*$, these two inclusions cannot define a saddle point of a Lagrangian underlining the non-existence of a duality framework in the non-associated setting. The associated flow rule is recovered for $\mathbb{T} = \mathbb{I}$, since then obviously $\tilde{B}^* = B^*$ and $F = A$.

2.1.2. *Hardening Plasticity.* The response function is determined by (4.6a)-(4.6c) and in the given context, these relations are

$$0 = \mathbb{C}^{-1}[\boldsymbol{\sigma}(x)] - \mathbb{C}^{-1}[\boldsymbol{\eta}(x)] - \mathbb{H}^{-1}[\boldsymbol{\zeta}(x)] , \qquad \text{a.e. in } \Omega , \tag{4.10}$$

$$0 \in (\mathbb{T}^{-1} \circ \mathbb{H}^{-1})[\boldsymbol{\zeta}(x)] + \partial\chi_K\big(\boldsymbol{\sigma}(x) + \boldsymbol{\zeta}(x)\big) , \qquad \text{a.e. in } \Omega , \tag{4.11}$$

$$\boldsymbol{\sigma}(x) + \boldsymbol{\zeta}(x) \in K , \qquad \text{a.e. in } \Omega . \tag{4.12}$$

We rewrite this in terms of $\boldsymbol{\sigma}$ and $\boldsymbol{\alpha} = \boldsymbol{\sigma} + \boldsymbol{\zeta}$. Substitution into the first equation gives

$$0 = (\mathbb{C}^{-1} + \mathbb{H}^{-1})[\boldsymbol{\sigma}] - \mathbb{C}^{-1}[\boldsymbol{\eta}] - \mathbb{H}^{-1}[\boldsymbol{\alpha}] ,$$

and thus

$$\boldsymbol{\sigma} = \mathbb{D}\big[\mathbb{C}^{-1}[\boldsymbol{\eta}] + \mathbb{H}^{-1}[\boldsymbol{\alpha}]\big] .$$

Substituting this into the inclusion and making use of the tensors $\mathbb{N}$ and $\mathbb{D}$ as defined in Section 3.2.2, we arrive at

$$0 \in (\mathbb{T}^{-1} \circ \mathbb{N}^{-1})[\boldsymbol{\alpha} - \boldsymbol{\eta}] + \partial\chi_K(\boldsymbol{\alpha}) , \qquad \text{a.e. in } \Omega ,$$

$$\boldsymbol{\alpha} \in \boldsymbol{K} .$$

Assuming $\mathbb{M} = \mathbb{N} \circ \mathbb{T}$ to be symmetric, we obtain $\boldsymbol{\alpha}$ as the projection of $\boldsymbol{\eta}$ in the metric defined by $\mathbb{M}^{-1}$, i.e. $\boldsymbol{\alpha} = P_K^M(\boldsymbol{\eta})$. Using $\boldsymbol{\eta} = \mathbb{C}[\boldsymbol{\varepsilon}(\boldsymbol{u})]$, we find that

$$\boldsymbol{\sigma} = \mathbb{D}[\boldsymbol{\varepsilon}(\boldsymbol{u})] + (\mathbb{D} \circ \mathbb{H}^{-1})\big[P_K^M(\mathbb{C}[\boldsymbol{\varepsilon}(\boldsymbol{u})])\big] .$$

2.2. Monotonicity Properties. We have seen that the response function is again a projection, i.e. $R_K = P_K^F$. Projections onto convex sets are monotone operators w.r.t. the metric in which they are defined. But the key difference to associated plasticity is that the metric in which the projection P_K^F is defined (the metric induced by $f(\cdot, \cdot)$) and the metric in which the boundary value problem is posed (the metric induced by $a(\cdot, \cdot)$) do no longer coincide. As a consequence, the operator (4.5) in the corresponding boundary value problem is no longer monotone in general. However, it is possible to give a lower bound for the lack of monotonicity as we have the following result.

Lemma 4.3. *With* $\mathbb{T} = \mathbb{P}_{\text{dev}} + M \, \mathbb{P}_{\text{vol}}$, $0 < M \leq 1$, *the operator* S *as defined in* (4.5) *satisfies*

$$\langle S(\boldsymbol{u}) - S(\boldsymbol{v}), \boldsymbol{u} - \boldsymbol{v} \rangle_{\boldsymbol{X}^* \times \boldsymbol{X}} \geq -\tfrac{1-M}{M} \|\boldsymbol{u} - \boldsymbol{v}\|_{\boldsymbol{X}}^2$$

for all $\boldsymbol{u}, \boldsymbol{v} \in \boldsymbol{X}$.

PROOF. We use the orthogonal decomposition of $\operatorname{Sym}(d) = \operatorname{Sym}_0(d) \oplus \mathbb{R}\,\mathbf{1}$ and

   (a) the monotonicity of P_K^F with respect to $f(\cdot, \cdot)$,
   (b) the Cauchy-Schwarz inequality,
   (c) the non-expansiveness of P_K^F w.r.t. the norm $\|\cdot\|_F$,
   (d) $\|\boldsymbol{\eta}\|_{\Sigma}^2 \geq M\|\boldsymbol{\eta}\|_F^2$ for all $\boldsymbol{\eta} \in \boldsymbol{P}$,
   (e) $\|\mathbb{C}[\boldsymbol{\varepsilon}(\boldsymbol{u})]\|_{\Sigma}^2 = \|\boldsymbol{u}\|^2$.

Then, we have

$$
\begin{aligned}
&\langle S(\boldsymbol{u}) - S(\boldsymbol{v}), \boldsymbol{u} - \boldsymbol{v} \rangle_{\boldsymbol{X}^* \times \boldsymbol{X}} \\
&= \int_{\Omega} \Big(P_K^F(\mathbb{C}[\boldsymbol{\varepsilon}(\boldsymbol{u}(x))]) - P_K^F(\mathbb{C}[\boldsymbol{\varepsilon}(\boldsymbol{v}(x))]) \Big) : \big(\boldsymbol{\varepsilon}(\boldsymbol{u}(x) - \boldsymbol{\varepsilon}(\boldsymbol{v}(x))) \big) \, dx \\
&= a\Big(P_K^F(\mathbb{C}[\boldsymbol{\varepsilon}(\boldsymbol{u})]) - P_K^F(\mathbb{C}[\boldsymbol{\varepsilon}(\boldsymbol{v})]), \mathbb{C}[\boldsymbol{\varepsilon}(\boldsymbol{u})] - \mathbb{C}[\boldsymbol{\varepsilon}(\boldsymbol{v})] \Big) \\
&= f\Big(P_K^F(\mathbb{C}[\boldsymbol{\varepsilon}(\boldsymbol{u})]) - P_K^F(\mathbb{C}[\boldsymbol{\varepsilon}(\boldsymbol{v})]), \mathbb{C}[\boldsymbol{\varepsilon}(\boldsymbol{u})] - \mathbb{C}[\boldsymbol{\varepsilon}(\boldsymbol{v})] \Big) \\
&\quad - (1 - M) f\Big(\mathbb{P}_{\text{vol}}\big[P_K^F(\mathbb{C}[\boldsymbol{\varepsilon}(\boldsymbol{u})]) - P_K^F(\mathbb{C}[\boldsymbol{\varepsilon}(\boldsymbol{v})]) \big], \mathbb{P}_{\text{vol}}\big[\mathbb{C}[\boldsymbol{\varepsilon}(\boldsymbol{u})] - \mathbb{C}[\boldsymbol{\varepsilon}(\boldsymbol{v})] \big] \Big) \\
&\overset{(a)}{\geq} -(1 - M) f\Big(\mathbb{P}_{\text{vol}}\big[P_K^F(\mathbb{C}[\boldsymbol{\varepsilon}(\boldsymbol{u})]) - P_K^F(\mathbb{C}[\boldsymbol{\varepsilon}(\boldsymbol{v})]) \big], \mathbb{P}_{\text{vol}}\big[\mathbb{C}[\boldsymbol{\varepsilon}(\boldsymbol{u})] - \mathbb{C}[\boldsymbol{\varepsilon}(\boldsymbol{v})] \big] \Big) \\
&\overset{(b)}{\geq} -(1 - M) \big\| \mathbb{P}_{\text{vol}}\big[P_K^F(\mathbb{C}[\boldsymbol{\varepsilon}(\boldsymbol{u})]) - P_K^F(\mathbb{C}[\boldsymbol{\varepsilon}(\boldsymbol{v})]) \big] \big\|_F \big\| \mathbb{P}_{\text{vol}}\big[\mathbb{C}[\boldsymbol{\varepsilon}(\boldsymbol{u})] - \mathbb{C}[\boldsymbol{\varepsilon}(\boldsymbol{v})] \big] \big\|_F \\
&\geq -(1 - M) \big\| P_K^F(\mathbb{C}[\boldsymbol{\varepsilon}(\boldsymbol{u})]) - P_K^F(\mathbb{C}[\boldsymbol{\varepsilon}(\boldsymbol{v})]) \big\|_F \big\| \mathbb{C}[\boldsymbol{\varepsilon}(\boldsymbol{u})] - \mathbb{C}[\boldsymbol{\varepsilon}(\boldsymbol{v})] \big\|_F \\
&\overset{(c)}{\geq} -(1 - M) \big\| \mathbb{C}[\boldsymbol{\varepsilon}(\boldsymbol{u})] - \mathbb{C}[\boldsymbol{\varepsilon}(\boldsymbol{v})] \big\|_F^2 \\
&\overset{(d)}{\geq} -\tfrac{1-M}{M} \big\| \mathbb{C}[\boldsymbol{\varepsilon}(\boldsymbol{u})] - \mathbb{C}[\boldsymbol{\varepsilon}(\boldsymbol{v})] \big\|_{\Sigma}^2 \overset{(e)}{=} -\tfrac{1-M}{M} \| \boldsymbol{u} - \boldsymbol{v} \|^2 \,,
\end{aligned}
$$

quantifying the lack of monotonicity. $\qquad\qquad\qquad\qquad\qquad\qquad\qquad\qquad\square$

We once more remark that we proceeded formally, since even in the associated case the space $\boldsymbol{X}$ is far to restrictive in order to obtain a solution. Moreover, in the associated setting when $\mathbb{T} = \mathbb{I}$, we reobtain monotonicity as $M = 1$.

2.3. Viscoplastic Regularization. As before, we drop the condition $\boldsymbol{\sigma}(x) \in K$ and use the Yosida approximation of $\partial \chi_K = N_K$. However, the Yosida approximation as introduced earlier will have to be slightly modified as we will shortly indicate: introducing the viscoplastic flow rule as $\varepsilon_p(x) = \mathbb{T}\big[D\chi_K^\alpha(\boldsymbol{\sigma}(x)) \big]$, by (4.1b) we find

$$
\mathbb{C}^{-1}[\boldsymbol{\sigma}(x)] = \boldsymbol{\varepsilon}(\boldsymbol{u}(x)) - \mathbb{T}[D\chi_K(\boldsymbol{\sigma}(x))] \,.
$$

Inserting the formula for the derivative as found in Proposition 3.1, we find

$$
\boldsymbol{\sigma}(x) = \mathbb{C}[\boldsymbol{\varepsilon}(\boldsymbol{u}(x))] - \alpha(\mathbb{C} \circ \mathbb{T} \circ \mathbb{C}^{-1})[\boldsymbol{\sigma}(x) - P_K(\boldsymbol{\sigma}(x))] \,.
$$

Unfortunately, it is now not possible to apply Lemma 3.2 due to the presence of $\mathbb{T}$ which is distorting the underlying metric. To circumvent this difficulty, we redefine the Moreau-Yosida approximation by means of the inner product $f(\cdot, \cdot)$ and the projection P_K^F. Based on this inner product, we define

$$
\widehat{\chi}_K^\alpha(\boldsymbol{\sigma}) = \inf_{\boldsymbol{\eta} \in \boldsymbol{P}} \{ \chi_K(\boldsymbol{\sigma}) + \tfrac{\alpha}{2} \|\boldsymbol{\sigma} - \boldsymbol{\eta}\|_F^2 \} = \tfrac{\alpha}{2} \|\boldsymbol{\sigma} - P_K^F(\boldsymbol{\sigma})\|_F^2 \,.
$$

The derivative $D\widehat{\chi}_K^\alpha$ is now characterized by

$$\langle D\widehat{\chi}_K^\alpha(\boldsymbol{\sigma}), \boldsymbol{\eta}\rangle_{P^* \times P} = \alpha\, f\big(\boldsymbol{\sigma} - P_K^F(\boldsymbol{\sigma}), \boldsymbol{\eta}\big) = \alpha\, \Big(\mathbb{F}^{-1}[\boldsymbol{\sigma} - P_K^F(\boldsymbol{\sigma})], \boldsymbol{\eta}\Big)_P,$$

cf. Lemma 3.1. This time, we make the ansatz $\boldsymbol{\varepsilon}_p(x) = \mathbb{T}\big[D\widehat{\chi}_K^\alpha(\boldsymbol{\sigma}(x))\big]$ to obtain

$$\begin{aligned}
\boldsymbol{\sigma} &= \mathbb{C}[\boldsymbol{\varepsilon}(\boldsymbol{u})] - \mathbb{C}[\boldsymbol{\varepsilon}_p] = \mathbb{C}[\boldsymbol{\varepsilon}(\boldsymbol{u})] - (\mathbb{C} \circ \mathbb{T})[D\widehat{\chi}_K^\alpha(\boldsymbol{\sigma})] \\
&= \mathbb{C}[\boldsymbol{\varepsilon}(\boldsymbol{u})] - \alpha\big(\mathbb{F} \circ \mathbb{F}^{-1}\big)[\boldsymbol{\sigma} - P_K^F(\boldsymbol{\sigma})] = \mathbb{C}[\boldsymbol{\varepsilon}(\boldsymbol{u})] - \alpha\big(\boldsymbol{\sigma} - P_K^F(\boldsymbol{\sigma})\big).
\end{aligned}$$

Now, we are in the position to apply Lemma 3.2, and we conclude $P_K^F(\boldsymbol{\sigma}) = P_K^F(\mathbb{C}[\boldsymbol{\varepsilon}(\boldsymbol{u})])$. Thus,

$$\boldsymbol{\sigma} = \tfrac{1}{1+\alpha}\big(\mathbb{C}[\boldsymbol{\varepsilon}(\boldsymbol{u})] + \alpha P_K^F(\mathbb{C}[\boldsymbol{\varepsilon}(\boldsymbol{u})])\big) = \tfrac{1}{1+\alpha}\mathbb{C}[\boldsymbol{\varepsilon}(\boldsymbol{u})] + \big(1 - \tfrac{1}{1+\alpha}\big)P_K^F(\mathbb{C}[\boldsymbol{\varepsilon}(\boldsymbol{u})]),\tag{4.13}$$

which is exactly equation (3.3) with P_K replaced by P_K^F.

We conclude that for a given displacement field, the response function of the viscoplastic regularization of non-associated Drucker-Prager can again be interpreted as a convex combination of linear elasticity and the perfect plasticity. After substitution of the response function into the weak form of the equilibrium constraint we arrive at

$$\frac{1}{1+\alpha}\int_\Omega \mathbb{C}[\boldsymbol{\varepsilon}(\boldsymbol{u}(x))] : \boldsymbol{\varepsilon}(\boldsymbol{w}(x))\, dx + \frac{\alpha}{1+\alpha}\int_\Omega P_K^F(\mathbb{C}[\boldsymbol{\varepsilon}(\boldsymbol{u}(x))]) : \boldsymbol{\varepsilon}(\boldsymbol{w}(x))\, dx = \ell(\boldsymbol{w}),\tag{4.14}$$

for all $\boldsymbol{w} \in \boldsymbol{X}$.

Due to the lack of monotonicity of the operator S, the regularization parameter α cannot become arbitrarily large in order to obtain a solution of (4.14). However, we have the following result.

Lemma 4.4. *If* $(1 - M)\alpha < M$*, equation* (4.14) *has a unique solution in* $\boldsymbol{X}$*.*

PROOF. Writing $\lambda = \tfrac{1}{1+\alpha}$, we define the operator

$$S^\lambda : \boldsymbol{X} \to \boldsymbol{X}^*, \qquad\qquad\qquad S^\lambda = \lambda C + (1 - \lambda)S.$$

If $\alpha < \tfrac{M}{1-M}$, then $\delta := \lambda - (1 - \lambda)\tfrac{1-M}{M} > 0$ and by Lemma 4.3 we have

$$\begin{aligned}
&\langle S^\lambda(\boldsymbol{u}) - S^\lambda(\boldsymbol{v}), \boldsymbol{u} - \boldsymbol{v}\rangle_{\boldsymbol{X}^* \times \boldsymbol{X}} \\
&\geq \lambda\|\boldsymbol{u} - \boldsymbol{v}\|^2 - (1 - \lambda)\tfrac{1-M}{M}\|\boldsymbol{u} - \boldsymbol{v}\|^2 = \big(\lambda - (1 - \lambda)\tfrac{1-M}{M}\big)\|\boldsymbol{u} - \boldsymbol{v}\|^2 \\
&= \delta\|\boldsymbol{u} - \boldsymbol{v}\|^2.
\end{aligned}$$

Thus, S^λ is strongly monotone and then, by the Browder-Minty theorem, cf. [Sho97, Section II.2] or [Rou05, Theorem 2.18], the operator S^λ is surjective and the equation $S^\lambda(\boldsymbol{u}) = \ell$ has a unique solution. $\square$

We see that in order to be well-posed, the non-associativity demands for a certain amount of regularization and we cannot pass to the limit $\alpha \to \infty$. The situation will be different when we consider the incremental problem since then, α is replaced by $\alpha\Delta t$ and for sufficiently small time steps, monotonicity can be regained.

2.4. Non-Associated Drucker-Prager Plasticity with Kinematic Hardening. Since the viscoplastic regularization cannot assure well-posedness in X for arbitrary regularization parameters, we turn to the case of kinematic hardening. Unfortunately, we obtain the same result as in the viscoplastic case. This appears correct, as in the static case, the viscoplastic regularization as introduced is a special case of the linear kinematic hardening. Nevertheless, we get more precise results concerning the magnitude of regularization necessary to recover well-posedness in Hilbert spaces. We adopt the derivation of Section 3.2 and 3.3, with the subtle but significant difference that this time, the flow rule is given as $\varepsilon_p(x) \in \mathbb{T}\big[\partial\chi_K(\boldsymbol{\sigma}(x) + \boldsymbol{\zeta}(x))\big]$. Assuming regularity of $\mathbb{T}$, after using the subdifferential calculus and integration over Ω, the flow rule can be rewritten as

$$\chi_{\boldsymbol{K}}^*(\mathbb{T}^{-1}[\boldsymbol{\tau}]) \geq \chi_{\boldsymbol{K}}^*(\mathbb{T}^{-1}[\boldsymbol{\varepsilon}_p]) + \int_\Omega \big(\boldsymbol{\sigma}(x) + \boldsymbol{\zeta}(x)\big) : \mathbb{T}^{-1}\big[\boldsymbol{\tau}(x) - \boldsymbol{\varepsilon}_p(x)\big]\, dx\,.$$

Adding the equilibrium constraint in weak form, we arrive at

$$\int_\Omega \boldsymbol{\sigma}(x) : \big(\boldsymbol{\varepsilon}(\boldsymbol{w}(x)) - \boldsymbol{\varepsilon}(\boldsymbol{u}(x)) - \mathbb{T}^{-1}[\boldsymbol{\tau}(x) - \boldsymbol{\varepsilon}_p(x)]\big)\, dx$$

$$- \int_\Omega \boldsymbol{\zeta}(x) : \mathbb{T}^{-1}[\boldsymbol{\tau}(x) - \boldsymbol{\varepsilon}_p(x)]\, dx + \chi_{\boldsymbol{K}}^*(\mathbb{T}^{-1}[\boldsymbol{\tau}]) - \chi_{\boldsymbol{K}}^*(\mathbb{T}^{-1}[\boldsymbol{\varepsilon}_p]) \geq \ell(\boldsymbol{w} - \boldsymbol{u})\,.$$

Defining the bilinear form $\widehat{q} : (\boldsymbol{X} \times \boldsymbol{P}) \times (\boldsymbol{X} \times \boldsymbol{P}) \to \mathbb{R}$ via

$$\widehat{q}\big((\boldsymbol{u}, \boldsymbol{\varepsilon}_p), (\boldsymbol{w}, \boldsymbol{\tau})\big) = \int_\Omega \big(\boldsymbol{\varepsilon}(\boldsymbol{u}(x)) - \boldsymbol{\varepsilon}_p(x)\big) : \mathbb{C}\big[\boldsymbol{\varepsilon}(\boldsymbol{w}(x)) - \mathbb{T}^{-1}[\boldsymbol{\tau}(x)]\big]\, dx$$

$$+ \int_\Omega \boldsymbol{\varepsilon}_p(x) : \mathbb{H}\big[\mathbb{T}^{-1}[\boldsymbol{\tau}(x)]\big]\, dx\,,$$

and substituting (4.1b) and $\boldsymbol{\zeta}(x) = -\mathbb{H}[\boldsymbol{\varepsilon}_p(x)]$ into the variational inequality gives

$$\widehat{q}\big((\boldsymbol{u}, \boldsymbol{\varepsilon}_p), (\boldsymbol{w} - \boldsymbol{u}, \boldsymbol{\tau} - \boldsymbol{\varepsilon}_p)\big) + \chi_{\boldsymbol{K}}^*(\mathbb{T}^{-1}[\boldsymbol{\tau}]) - \chi_{\boldsymbol{K}}^*(\mathbb{T}^{-1}[\boldsymbol{\varepsilon}_p]) \geq \ell(\boldsymbol{w} - \boldsymbol{u})\,. \tag{4.15}$$

Obviously, $\widehat{q}(\cdot, \cdot)$ is not symmetric and contrary to the associated setting, cf. (3.14), no minimization problem can be attributed to this variational inequality. But even worse, the bilinear form $\widehat{q}$ is only positive definite if sufficient hardening is present as we will demonstrate.

Lemma 4.5. *Assuming the special structures* $\mathbb{C} = 2\mu\mathbb{P}_{\text{dev}} + 3\kappa\mathbb{P}_{\text{vol}}$, $\mathbb{H} = h_d\mathbb{P}_{\text{dev}} + h_v\mathbb{P}_{\text{vol}}$, *and* $\mathbb{T} = \mathbb{P}_{\text{dev}} + M\mathbb{P}_{\text{vol}}$ *with* $0 < M \leq 1$, *the (non-symmetric) bilinear form* $\widehat{q}(\cdot, \cdot)$ *is coercive on* $\boldsymbol{X} \times \boldsymbol{P}$ *if* $h_d > 0$ *and* $h_v > \kappa\frac{(M-1)^2}{4M}$.

PROOF. By a slight abuse of notation, we interpret the bilinear form $\widehat{q}$ as a bilinear form on $(\text{Sym}(d))^2 \times (\text{Sym}(d))^2$, i.e.

$$\widehat{q}\big((\boldsymbol{\varepsilon}, \boldsymbol{\varepsilon}_p), (\boldsymbol{\tau}, \boldsymbol{\eta})\big) = (\boldsymbol{\varepsilon} - \boldsymbol{\varepsilon}_p) : \mathbb{C}\big[\boldsymbol{\tau} - \mathbb{T}^{-1}[\boldsymbol{\eta}]\big] + \boldsymbol{\varepsilon}_p : \mathbb{H}\big[\mathbb{T}^{-1}[\boldsymbol{\eta}]\big]$$

and we need to verify the definiteness on $(\text{Sym}(d))^2$. By the orthogonal decomposition into the deviatoric and volumetric part by means of the orthogonal projectors $\mathbb{P}_{\text{dev}}$ and $\mathbb{P}_{\text{vol}}$, this reads as

$$\widehat{q}\big((\boldsymbol{\tau}, \boldsymbol{\varepsilon}_p), (\boldsymbol{\tau}, \boldsymbol{\varepsilon}_p)\big) = 2\mu|\text{dev}(\boldsymbol{\tau}) - \text{dev}(\boldsymbol{\varepsilon}_p)|^2 + h_d|\text{dev}(\boldsymbol{\varepsilon}_p)|^2$$

$$+ \kappa\big(\text{tr}(\boldsymbol{\tau}) - \text{tr}(\boldsymbol{\varepsilon}_p)\big)\big(\text{tr}(\boldsymbol{\tau}) - \tfrac{1}{M}\text{tr}(\boldsymbol{\varepsilon}_p)\big) + \tfrac{h_v}{M}\big(\text{tr}(\boldsymbol{\varepsilon}_p)\big)^2$$

It is well known that the first line is definite on the deviatoric subspace whenever $h_d > 0$ and it remains to consider the second line where for simplicity, we set $a = \text{tr}(\boldsymbol{\tau})$ and we assume $a \neq 0$ (otherwise, the definiteness is trivial). Since this is a scalar quantity, we can

write $\mathrm{tr}(\boldsymbol{\varepsilon}_p) = \delta\, a$ with $\delta \in \mathbb{R}$ and once more, we exclude the trivial case $\delta = 0$. Then we have

$$\kappa\big(\mathrm{tr}(\boldsymbol{\tau}) - \mathrm{tr}(\boldsymbol{\varepsilon}_p)\big)\big(\mathrm{tr}(\boldsymbol{\tau}) - \tfrac{1}{M}\mathrm{tr}(\boldsymbol{\varepsilon}_p)\big) + \tfrac{h_v}{M}\big(\mathrm{tr}(\boldsymbol{\varepsilon}_p)\big)^2$$
$$= \Big(\kappa(1-\delta)(1-\tfrac{\delta}{M}) + h_v\tfrac{\delta^2}{M}\Big)a^2$$

Hence, definiteness holds if $h_v > -\tfrac{M}{\delta^2}\kappa(1-\delta)(1-\tfrac{\delta}{M}) =: s(\delta)$. It can easily be shown that the maximum of $s(\delta)$ is attained at $\delta^* = \tfrac{2M}{M+1}$ and thus we require $h_v > s(\delta^*) = \kappa\tfrac{(M-1)^2}{4M}$ for $0 < M \le 1$. □

In the limit case $M = 1$ corresponding to the associated flow rule, once more we obtain the requirement $h_v > 0$, but for non-associated flow we have $M < 1$. Then, the necessary magnitude of h_v to show definiteness strongly depends on the non-associativity represented by the value of M. Thus, we conclude that contrary to the associated case where any positive definite hardening modulus $\mathbb{H}$ assured the definiteness of the bilinear form $q(\cdot,\cdot)$, a similar result does not hold in the non-associated case. Particularly, we see that kinematic hardening has no regularized effect in general but we only have the following.

Theorem 4.6. *Let the hardening modulus be of the form $\mathbb{H} = h_d\mathbb{P}_{\mathrm{dev}} + h_v\mathbb{P}_{\mathrm{vol}}$ with $h_d > 0$ and $h_v > \kappa\tfrac{(M-1)^2}{4M}$. Then, the variational inequality (4.15) has a unique solution.*

PROOF. By Lemma 4.5, the bilinear form $\widehat{q}$ is coercive on $\boldsymbol{X} \times \boldsymbol{P}$. Moreover, since $\chi_{\boldsymbol{K}}^*$ is a convex lower semicontinous and proper functional, so is $\chi_{\boldsymbol{K}}^* \circ \mathbb{T}^{-1}$ due to the linearity of $\mathbb{T}^{-1}$, and the existence and uniqueness is a standard result, cf. [**HR99**, Theorem 6.6] or [**Glo84**]. □

3. The General Case Revisited

Though the above approach may not always be possible for arbitrary flow rules, the result can be transferred to arbitrary flow rules when considering the viscoplastic regularization as a type of homotopy. Looking back at (4.13), or (3.3) in the associated setting, in static plasticity we can interpret the viscoplastic regularization as a convex combination of elasticity and perfect plasticity in which the viscosity (indirectly) is the parameter in the convex combination. Hence, for arbitrary flow rules, we postulate the viscoplastic regularization to be defined via the response function

$$R(\boldsymbol{\eta}) = \tfrac{1}{1+\alpha}\boldsymbol{\eta} + \tfrac{\alpha}{1+\alpha}R_K(\boldsymbol{\eta})\,, \tag{4.16}$$

with R_K being the response function of perfectly plasticity as defined in (4.3). This results in the variational problem of finding $\boldsymbol{u} \in \boldsymbol{X}(\boldsymbol{u}_D)$ such that

$$\tfrac{1}{1+\alpha}\int_\Omega \mathbb{C}[\boldsymbol{\varepsilon}(\boldsymbol{u}(x))] : \boldsymbol{\varepsilon}(\boldsymbol{w}(x))\,dx + \tfrac{\alpha}{1+\alpha}\int_\Omega R_K(\mathbb{C}[\boldsymbol{\varepsilon}(\boldsymbol{u}(x))]) : \boldsymbol{\varepsilon}(\boldsymbol{w}(x))\,dx = \ell(\boldsymbol{w})\,, \tag{4.17}$$

for all $\boldsymbol{w} \in \boldsymbol{X}$. Under certain assumptions on R_K, we can apply Theorem 4.1.

Corollary 4.7. *Assume that the response function $R_K : \mathrm{Sym}(d) \to K \subset \mathrm{Sym}(d)$ of perfect plasticity satisfies*

$$\big(R_K(\boldsymbol{\sigma}) - R_K(\boldsymbol{\eta})\big) : \mathbb{C}^{-1}[\boldsymbol{\sigma} - \boldsymbol{\eta}] \ge -L(\boldsymbol{\sigma} - \boldsymbol{\eta}) : \mathbb{C}^{-1}[\boldsymbol{\sigma} - \boldsymbol{\eta}]\,,$$

for some $L \in \mathbb{R}$ and all $\boldsymbol{\sigma}, \boldsymbol{\eta} \in \mathrm{Sym}(d)$. Then, the regularized problem (4.17) has a unique solution if $\alpha L < 1$.

PROOF. The response function (4.16) satisfies

$$\big(R(\boldsymbol{\sigma}) - R(\boldsymbol{\eta})\big) : \mathbb{C}^{-1}[\boldsymbol{\sigma} - \boldsymbol{\eta}] \geq \big(\tfrac{1}{1+\alpha} - \tfrac{\alpha L}{1+\alpha}\big)(\boldsymbol{\sigma} - \boldsymbol{\eta}) : \mathbb{C}^{-1}[\boldsymbol{\sigma} - \boldsymbol{\eta}]$$

and if $\alpha L < 1$, we have existence and uniqueness according to Theorem 4.1. $\square$

CHAPTER 5

A REVIEW OF QUASI-STATIC AND INCREMENTAL PLASTICITY

As we have indicated before, static plasticity is not reasonable from a physical point of view since the irreversibility of plastic deformation is not reflected. Therefore, this chapters is dedicated to the time-dependent problems. Nevertheless, the static scenario will naturally reappear when we turn to incremental plasticity. These problems are considered in Section 5.4 where we introduce a time discretization.

Whereas in perfect plasticity and also hardening plasticity, the introduction of time can be considered as artificial in the sense that time is only incorporated to represent the path-dependency of plastic evolution, the situation changes in viscoplasticity where time has a physical meaning. In the former case, one speaks of *rate-independent plasticity* and in the latter of *rate-dependence* since time is attributed a physical interpretation. In rate-independence processes, it is irrelevant how fast a load is applied and the system has no inherent dynamics. Thus, this concept can only be applied if the underlying physical problem admits this simplification. For a mathematical precise definition of rate-independence, we refer to [Mie05, Section 1] and we will shortly strife this framework when considering the primal problem. In rate-dependent plasticity on the other side, the dynamics of the system depend on the time in which the load is applied. We also remind that the notion quasi-static only reflects the fact that inertial forces are neglected.

We briefly remark on the notation used in this chapter: let

$$\vartheta : \Omega \times [0, T] \to \mathbb{R}^s \,,$$

be any field under consideration (with suitable $s \in \mathbb{N}$), and let V be a function space w.r.t. the spatial variable $x \in \Omega$, e.g. for $\vartheta = \boldsymbol{u}$ we formally set $s = d$ and $V = \boldsymbol{X}$. Then, for fixed $t \in [0, T]$, we will interpret $\vartheta(t) \equiv \vartheta(\cdot, t)$ as an element of V. As in Chapter 1, time derivatives are indicated by a superimposed dot.

1. Associated Quasi-Static Perfect Plasticity

We begin by recapitulizing the governing equations of perfect plasticity in the absence of hardening:

$$-\operatorname{div}(\boldsymbol{\sigma}(x,t)) = \boldsymbol{b}(x,t)\,, \qquad\qquad x \in \Omega\,, t \in (0,T)\,, \qquad (5.1\text{a})$$

$$\boldsymbol{\sigma}(x,t) = \mathbb{C}[\boldsymbol{\varepsilon}(\boldsymbol{u}(x,t)) - \boldsymbol{\varepsilon}_p(x,t)]\,, \qquad x \in \Omega\,, t \in (0,T)\,, \qquad (5.1\text{b})$$

$$\boldsymbol{\sigma}(x,t) \in K\,, \qquad\qquad x \in \Omega\,, t \in (0,T)\,, \qquad (5.1\text{c})$$

$$\dot{\boldsymbol{\varepsilon}}_p(x,t) \in \partial\chi_K(\boldsymbol{\sigma}(x,t)) \qquad\qquad x \in \Omega\,, t \in (0,T)\,, \qquad (5.1\text{d})$$

$$\boldsymbol{u}(x,t) = \boldsymbol{u}_D(x,t)\,, \qquad\qquad x \in \Gamma_D\,, t \in (0,T)\,, \qquad (5.1\text{e})$$

$$\boldsymbol{\sigma}(x,t)\boldsymbol{n}(x,t) = \boldsymbol{t}_N(x,t)\,, \qquad\qquad x \in \Gamma_T\,, t \in (0,T)\,, \qquad (5.1\text{f})$$

$$\boldsymbol{\sigma}(x,0) = \boldsymbol{\sigma}^0(x)\,, \qquad\qquad x \in \Omega\,, \qquad (5.1\text{g})$$

$$\boldsymbol{u}(x,0) = \boldsymbol{u}^0(x)\,, \qquad\qquad x \in \Omega\,. \qquad (5.1\text{h})$$

We remark that two initial conditions are necessary since otherwise it is not be possible to determine the state of the body. Even though the incorporation of time does not allow to consider two convex minimization problems in duality, it is possible to formulate a primal and dual problem in the sense of time-dependent variational inequalities. For a short mathematical survey on quasi-static perfect plasticity, we also refer to [ER04].

1.1. The Dual Problem of Associated Quasi-Static Plasticity. Taking the time derivative in the constitutive relation (5.1b) and inverting the elasticity tensor, we obtain the relation $-\mathbb{C}^{-1}[\dot{\boldsymbol{\sigma}}(x,t)] + \boldsymbol{\varepsilon}(\dot{\boldsymbol{u}}(x,t)) = \dot{\boldsymbol{\varepsilon}}_p(x,t)$. Inserting into the flow rule (5.1d) leads to

$$-\mathbb{C}^{-1}[\dot{\boldsymbol{\sigma}}(x,t)] + \boldsymbol{\varepsilon}(\dot{\boldsymbol{u}}(x,t)) \in \partial\chi_K(\boldsymbol{\sigma}(x,t))\,,$$

and after integration over Ω, we obtain

$$\int_\Omega \left(\mathbb{C}^{-1}[\dot{\boldsymbol{\sigma}}(x,t)] - \boldsymbol{\varepsilon}(\dot{\boldsymbol{u}}(x,t))\right) : \left(\boldsymbol{\eta}(x) - \boldsymbol{\sigma}(x,t)\right) dx \geq 0\,, \qquad \boldsymbol{\eta} \in \boldsymbol{K}\,.$$

Defining the load functionals $\ell(t) = \ell(t,\cdot)$ and $h(t) = h(t,\cdot)$ via

$$\ell(t,\boldsymbol{w}) = \int_\Omega \boldsymbol{b}(x,t) \cdot \boldsymbol{w}(x)\,dx + \int_{\Gamma_T} \boldsymbol{t}_N(x,t) \cdot \boldsymbol{w}(x)\,da\,, \qquad (5.2)$$

$$h(t,\boldsymbol{\eta}) = \int_{\Gamma_D} \left(\boldsymbol{\eta}(x)\boldsymbol{n}(x)\right) \cdot \boldsymbol{u}_D(x,t)\,da\,, \qquad (5.3)$$

and using the equilibrium constraint in weak form, we arrive at

$$a\big(\dot{\boldsymbol{\sigma}}(t),\boldsymbol{\eta} - \boldsymbol{\sigma}(t)\big) + b\big(\boldsymbol{\eta} - \boldsymbol{\sigma}(t),\dot{\boldsymbol{u}}(t)\big)\,dx \geq 0\,, \qquad \boldsymbol{\eta} \in \boldsymbol{K}\,, \qquad (5.4\text{a})$$

$$b(\boldsymbol{\sigma}(t),\boldsymbol{w}) + \ell(t,\boldsymbol{w}) = 0\,, \qquad \boldsymbol{w} \in \boldsymbol{X}\,. \qquad (5.4\text{b})$$

a problem also referred to as the dual problem of quasi-static plasticity. These conditions reflect the optimality conditions (2.33) in the static scenario. The equilibrium constraint can be eliminated by defining the statically admissible set

$$\boldsymbol{S}(t) \equiv \boldsymbol{S}\big(\boldsymbol{b}(t),\boldsymbol{t}_N(t)\big)\,, \qquad (5.5)$$

cf. (2.25). Then, the problem reduces to a variational inequality similar to (2.34). Particularly, we seek $\boldsymbol{\sigma}(t) \in \boldsymbol{S}(t) \cap \boldsymbol{K}$ such that

$$a(\dot{\boldsymbol{\sigma}}(t),\boldsymbol{\eta}(t) - \boldsymbol{\sigma}(t)) \geq h(t,\boldsymbol{\eta}(t) - \boldsymbol{\sigma}(t))\,, \qquad \boldsymbol{\eta} \in \boldsymbol{S}(t) \cap \boldsymbol{K}\,. \qquad (5.6)$$

Concerning existence and uniqueness of a solution, we rely on the time-continuous analogue of the safe-load condition 2.1.

Assumption 5.1. *There exists* $\widetilde{\boldsymbol{\sigma}} \in W^{1,\infty}\big((0,T), \boldsymbol{\Sigma}_{\mathrm{div}} \cap L^{\infty}(\Omega, \mathrm{Sym}(d))\big)$ *and* $\varepsilon > 0$ *such that for all* $\boldsymbol{\xi} \in \mathrm{Sym}(d)$ *with* $|\boldsymbol{\xi}| \leq \varepsilon$:

$$\widetilde{\boldsymbol{\sigma}}(t) \in \boldsymbol{S}(t) \qquad \textit{and} \qquad \widetilde{\boldsymbol{\sigma}}(x,t) + \boldsymbol{\xi} \in K \quad \textit{a.e. in } \Omega. \tag{5.7}$$

Based on this assumption, existence and uniqueness (for homogeneous boundary conditions $h = 0$) was first proven in [**Joh76**], viz. there is a stress field $\boldsymbol{\sigma}$ solving problem (5.6) and having the regularity

$$\boldsymbol{\sigma} \in W^{1,2}((0,T), \boldsymbol{P}) \cap L^{\infty}((0,T), \boldsymbol{\Sigma}_{\mathrm{div}}(\boldsymbol{t}_N(t))).$$

The regularity result for the velocity field $\dot{\boldsymbol{u}} \in L^2((0,T), L^{3/2}(\Omega, \mathbb{R}^3))$, was later improved to $\boldsymbol{u} \in AC((0,T), BD(\Omega))$ in the case of incompressible plasticity, i.e. $\boldsymbol{u}$ is an absolutely continuous function into the space of bounded deformations, cf. [**MDM06, IS93**]. The proof in [**Joh76**] relies on a time discretization by finite differences and the viscoplastic regularization as introduced in Section 3.1.

1.2. The Primal Problem. Concerning the dual problem, we have seen that it is possible to obtain a characterization as the variational inequality (5.6), or the system (5.4), respectively. Similarly, we can define a primal problem in the sense of Section 3.3 which also explains why this approach is often preferred. First, the flow rule is reformulated as $\boldsymbol{\sigma}(t) \in \partial \chi_{\boldsymbol{K}}^*(\dot{\boldsymbol{\varepsilon}}_p(t))$ and using Hooke's law (5.1b), we find

$$\mathbb{C}\big[\boldsymbol{\varepsilon}(\boldsymbol{u}(t)) - \boldsymbol{\varepsilon}_p(t)\big] \in \partial \chi_{\boldsymbol{K}}^*(\dot{\boldsymbol{\varepsilon}}_p(t)).$$

In integrated form, this is

$$-\int_\Omega \Big(\mathbb{C}\big[\boldsymbol{\varepsilon}(\boldsymbol{u}(x,t)) - \boldsymbol{\varepsilon}_p(x,t)\big]\Big) : \big(\boldsymbol{\tau}(x) - \dot{\boldsymbol{\varepsilon}}_p(x,t)\big)\, dx + \chi_{\boldsymbol{K}}^*(\boldsymbol{\tau}) - \chi_{\boldsymbol{K}}^*(\dot{\boldsymbol{\varepsilon}}_p(t)) \geq 0$$

for all $\boldsymbol{\tau}$. Testing the weak equilibrium with $\boldsymbol{w} - \dot{\boldsymbol{u}}(t)$, and adding to the above inequality, we arrive at

$$q\big((\boldsymbol{u}, \boldsymbol{\varepsilon}_p), (\boldsymbol{w}, \boldsymbol{\tau}) - (\dot{\boldsymbol{u}}(t), \dot{\boldsymbol{\varepsilon}}_p(t))\big) + \chi_{\boldsymbol{K}}^*(\boldsymbol{\tau}) - \chi_{\boldsymbol{K}}^*(\dot{\boldsymbol{\varepsilon}}_p(t)) \geq \ell(t, \boldsymbol{w} - \dot{\boldsymbol{u}}(t)). \tag{5.8}$$

Here, we used the bilinear form $q(\cdot, \cdot)$ as defined in (3.12) in the absence of the hardening modulus $\mathbb{H}$. Please note that for perfect plasticity, $q(\cdot, \cdot)$ cannot be defined on $\boldsymbol{X} \times \boldsymbol{P}$ in general but only in the weaker spaces $BD(\Omega) \times \boldsymbol{M}_{\mathrm{Sym}}(\Omega)$. Only if the energy q would be positive definite, solutions in $\boldsymbol{X} \times \boldsymbol{P}$ could exist. Nevertheless, the problem can be posed in the framework of rate-independent systems in the sense of Mielke and we refer to [**Mie05**] for a survey. This theory is based on two conditions: one is a global stability property whereas the latter is an energy balance. Concerning the problem of perfect plasticity, this has been considered in [**MDM06, MDD07**] and we mainly follow these two articles. The quasi-static evolution is described by the triple

$$\boldsymbol{z}(t) := \big(\boldsymbol{u}(t), \boldsymbol{\varepsilon}_e(t), \boldsymbol{\varepsilon}_p(t)\big) \in \mathcal{Z} := BD(\Omega) \times L^2(\Omega, \mathrm{Sym}(d)) \times \boldsymbol{M}_{\mathrm{Sym}}(\Omega),$$

satisfying $\boldsymbol{\varepsilon}(\boldsymbol{u}(t)) = \boldsymbol{\varepsilon}_e(t) + \boldsymbol{\varepsilon}_p(t)$, where $\boldsymbol{\varepsilon}$ is interpreted as a mapping $\boldsymbol{\varepsilon} : BD(\Omega) \to \boldsymbol{M}_{\mathrm{Sym}}(\Omega)$. With the help of the elastic energy $\mathcal{W}_e$ as introduced in (2.13), $\boldsymbol{z}(t)$ needs to satisfy the global stability condition

$$\mathcal{W}_e(\boldsymbol{\varepsilon}_e(t)) - \ell(t, \boldsymbol{u}(t)) \leq \mathcal{W}_e(\widetilde{\boldsymbol{\varepsilon}}_e(t)) - \ell(t, \widetilde{\boldsymbol{u}}) + \chi_{\boldsymbol{K}}^*(\widetilde{\boldsymbol{\varepsilon}}_p - \boldsymbol{\varepsilon}_p(t)), \tag{5.9a}$$

for all $(\widetilde{\boldsymbol{u}}, \widetilde{\boldsymbol{\varepsilon}}_e, \widetilde{\boldsymbol{\varepsilon}}_p) \in \mathcal{Z}$ satisfying $\boldsymbol{\varepsilon}(\widetilde{\boldsymbol{u}}) = \widetilde{\boldsymbol{\varepsilon}}_e + \widetilde{\boldsymbol{\varepsilon}}_p$, as well as the energy balance

$$\mathcal{W}_e(\boldsymbol{\varepsilon}_e(t)) - \ell(t, \boldsymbol{u}(t)) + \mathrm{D}(\boldsymbol{\varepsilon}_p, (0, t)) = \mathcal{W}_e(\boldsymbol{\varepsilon}_e(0)) - \ell(t, \boldsymbol{u}(0)) - \int_0^t \dot{\ell}(s, \boldsymbol{u}(s))\, ds\,.$$
(5.9b)

In these formulas, $\ell(t)$ is defined on $BD(\Omega)^*$ and the dissipation D in the energy balance is given as

$$\mathrm{D}(\boldsymbol{\varepsilon}_p, (0, t)) = \sup_{N \in \mathbb{N}} \Big\{ \sum_{j=1}^N \chi_{\boldsymbol{K}}^* \big(\boldsymbol{\varepsilon}_p(t_j) - \boldsymbol{\varepsilon}_p(t_{j-1}) \big) : 0 = t_0 \le t_1 \le \cdots \le t_N = t \Big\}\,.$$

Note that formally also $\chi_{\boldsymbol{K}}^*$ can only be defined in the sense of measures. Based on this formulation, it was then proven in [**MDM06**, **MDD07**] that there are absolutely continuous functions

$$(\boldsymbol{u}, \boldsymbol{\varepsilon}_e, \boldsymbol{\varepsilon}_p) \in AC\big((0, T), \mathcal{Z}\big)$$

satisfying the stability and energy balance conditions ([5.9](#)) and therefore solve the quasi-static perfect plasticity problem. Here, by $AC\big((0, T), \mathcal{Z}\big)$ we denote the absolutely continuous functions from $(0, T)$ to $\mathcal{Z}$. However, even these proofs rely on a special structure of the admissible set K: whereas in the first reference, the admissible set was limited to be a cylinder in the sense of von Mises or Tresca (corresponding to incompressible plasticity), the latter exclusively considered a bounded admissible set K. In the case of incompressible plasticity, following [**MDM06**, Theorem 6.1], the dual and the primal problem are linked in the sense that if $(\boldsymbol{u}, \boldsymbol{\varepsilon}_e, \boldsymbol{\varepsilon}_p) \in AC\big((0, T), \mathcal{Z}\big)$ is a solution of the primal problem, then $\boldsymbol{\sigma}(t) = \mathbb{C}[\boldsymbol{\varepsilon}_e(t)]$ is a solution to the dual problem and vice versa. In [**MDD07**, Section 4], similar results are also presented in the case of a bounded admissible set.

2. Extended Models

2.1. Viscoplasticity. The viscoplastic regularization of the flow rule is a key ingredient in the proof presented by Johnson in [**Joh76**] concerning the existence and uniqueness result of the dual perfect plasticity problem. In the quasi-static setting, essentially there are two possibilities for employing the viscoplastic regularization: either after a time discretization in order to regularize the incremental problems as we have done it in the previous chapters or to directly transfer the problem into an ordinary differential equation in Banach, or Hilbert space, respectively. The first approach was used by Johnson in the before mentioned paper but of course, viscoplasticity does not only serve as some sort of regularization scheme. Viscoplasticity can be seen as an independent branch of material modeling including models like the Norten-Hoff or Bodner-Partom model. Such models are adressed in [**AC04**, **AC07**] and mainly result in a formulation as an ordinary differential equation in a suitable phase space. Regarding this topic, a good reference is also the book [**IS93**]. Though we only considered the viscoplastic regularization so far, we will now allow more general viscoplastic flow rules. Note that this may include any sort of flow rule satisfying appropriate properties. These models are also capable to encorporate softening effects, e.g. the Bodner-Partom model, while retaining stable solutions in Sobolev spaces.

Once more, we drop the requirement of $\boldsymbol{\sigma}(x, t) \in K$ and the flow rule ([5.1d](#)) is now single-valued, i.e.

$$\dot{\boldsymbol{\varepsilon}}_p(x, t) = H(\boldsymbol{\sigma}(x, t)) \qquad\qquad x \in \Omega\,, t \in (0, T)\,,$$

where $H : \mathrm{Sym}(d) \to \mathrm{Sym}(d)$ is a given function (not a multi-function). The viscoplastic regularization is just one special case with $H(\boldsymbol{\sigma}) = D\chi_K^\alpha(\boldsymbol{\sigma}) = \alpha \, \mathbb{C}^{-1}\big[\boldsymbol{\sigma} - P_K(\boldsymbol{\sigma})\big]$. More generally, time differentiation in Hooke's law (5.1b) gives

$$\dot{\boldsymbol{\sigma}}(x,t) = \mathbb{C}\big[\boldsymbol{\varepsilon}(\dot{\boldsymbol{u}}(x,t)) - \dot{\boldsymbol{\varepsilon}}_p(x,t)\big] = \mathbb{C}\big[\boldsymbol{\varepsilon}(\dot{\boldsymbol{u}}(x,t)) - H(\boldsymbol{\sigma}(x,t))\big]\,,$$

and together with the equilibrium condition (5.1a), we obtain a system of differential algebraic equations for $\boldsymbol{\sigma}$ and $\boldsymbol{u}$. Under standard assumptions concerning the data and Lipschitz continuity of G, we obtain existence and uniqueness with continuous dependence on the data, cf. Theorems 1.1 and 1.2 in [IS93, Section 3.1]. Additionally, we find the following regularity results:

$$\boldsymbol{\sigma} \in C^1\big((0,T), \boldsymbol{P}\big)\,, \qquad\qquad \boldsymbol{\sigma}(t) \in \boldsymbol{\Sigma}_{\mathrm{div}}(\boldsymbol{t}_N(t))\,,$$
$$\boldsymbol{u} \in C^1\big((0,T), \boldsymbol{V}\big)\,, \qquad\qquad \boldsymbol{u}(t) \in \boldsymbol{X}(\boldsymbol{u}_D(t))\,.$$

Similar results can be found in [AC04].

2.2. Quasi-Static Hardening Plasticity. In the quasi-static scenario, hardening can be incorporated following the lines of the static case, cf. Section 3.2 or Section 3.3 for the formulation as a variational inequality. With the dual force $\boldsymbol{\zeta}$ already used earlier, the admissibility (5.1c) and the flow rule (5.1d) are replaced by

$$\boldsymbol{\sigma}(x,t) + \boldsymbol{\zeta}(x,t) \in K\,, \qquad\qquad x \in \Omega\,, t \in (0,T)\,, \qquad (5.10a)$$
$$\dot{\boldsymbol{\varepsilon}}_p(x,t) \in N_K\big(\boldsymbol{\sigma}(x,t) + \boldsymbol{\xi}(x,t)\big)\,, \qquad x \in \Omega\,, t \in (0,T)\,, \qquad (5.10b)$$

and additionally we have the relation

$$\boldsymbol{\zeta}(x,t) = -\mathbb{H}[\boldsymbol{\varepsilon}_p(x,t)]\,, \qquad\qquad x \in \Omega\,, t \in (0,T)\,, \qquad (5.10c)$$

linking the dual force $\boldsymbol{\zeta}$ with the plastic strain $\boldsymbol{\varepsilon}_p$. In the formulation as a variational inequality, the introduction of kinematic hardening simply implies the non-vanishing of the hardening modulus in formulation (5.8). It is possible to treat this case in the same energetic framework, cf. [Mie05]. In [HR95, HR99], existence and uniqueness was proven directly, and also the proofs of [AC04, AC07] apply here. First results concerning the dual problem were obtained in [Joh78]. We obtain the following regularity of solutions:

$$\boldsymbol{\sigma} \in H^1\big((0,T), \boldsymbol{P}\big)\,, \qquad\qquad \boldsymbol{\sigma}(t) \in \boldsymbol{\Sigma}_{\mathrm{div}}(\boldsymbol{t}_N(t))\,,$$
$$\boldsymbol{u} \in H^1\big((0,T), \boldsymbol{V}\big)\,, \qquad\qquad \boldsymbol{u}(t) \in \boldsymbol{X}(\boldsymbol{u}_D(t))\,,$$
$$\boldsymbol{\varepsilon}_p \in H^1\big((0,T), \boldsymbol{P}\big)\,.$$

3. Non-Associated Plasticity

Once more, the flow rule (5.1d) is replaced by

$$\dot{\boldsymbol{\varepsilon}}_p(x,t) \in G(\boldsymbol{\sigma}(x,t))\,, \qquad\qquad x \in \Omega\,, t \in (0,T)\,.$$

Within the framework of viscoplasticity, the results of the previous section also apply to non-associated flow rules as long as the resulting differential equation is Lipschitz continuous. For rate-independent plasticity, we are only aware of a result presented in [Che03] which can also be found in [Mie05, Chapter 6] using slightly different notation.

3.1. Convex Composite Flow Rule. In the presence of kinematic hardening, the result given in [**Che03**] relies on a very special kind of flow rule, called the *convex composite* flow rule, also see [**Gui00**] for subdifferential inclusions of that type. The convex composite flow rule is given as

$$\dot{\boldsymbol{\varepsilon}}_p(x,t) \in \partial(M \circ \Phi)(\boldsymbol{\sigma}(x,t)) = D\Phi(\boldsymbol{\sigma}(x,t))\partial M(\Phi(\boldsymbol{\sigma}(x,t)))\,,$$

where ∂ denotes Clarke's generalized Jacobian (see Appendix A), the transformation $\Phi \in C^{1,1}(\mathrm{Sym}(d), \mathrm{Sym}(d))$ is a global Lipschitz diffeomorphism and $M : \mathrm{Sym}(d) \to \overline{\mathbb{R}}$ is a convex function. The associated theory is recovered when $\Phi \equiv \mathbb{I}$ and $M = \chi_K$.

We restrict ourselves to stating the result in the case of plasticity with kinematic hardening to avoid the introduction of additional notation. As in [**AC04, AC07**] and Subsection 5.1.2, the point of departure is the free energy

$$\mathcal{W} = \tfrac{1}{2}(\boldsymbol{\varepsilon}(\boldsymbol{u}) - \boldsymbol{\varepsilon}_p) : \mathbb{C}[\boldsymbol{\varepsilon}(\boldsymbol{u}) - \boldsymbol{\varepsilon}_p] + \tfrac{1}{2}\boldsymbol{\varepsilon}_p : \mathbb{H}[\boldsymbol{\varepsilon}_p]\,.$$

which is assumed to positive definite. Under certain regularity conditions on the data, it was proven that there exists a unique solution satisfying (5.1a), (5.1b), the convex composite flow rule and the boundary and initial conditions (5.1e)–(5.1h). However, the admissibility $\boldsymbol{\sigma}(x,t) \in K$ is not guaranteed in this setting. The solution has the regularity

$$\boldsymbol{\sigma} \in W^{1,\infty}\big((0,T), L^2(\Omega, \mathrm{Sym}(3))\big)\,, \qquad\qquad \boldsymbol{\sigma}(t) \in \Sigma_{\mathrm{div}}(\boldsymbol{t}_N(t))\,,$$
$$\boldsymbol{u} \in W^{1,\infty}\big((0,T), H^1(\Omega, \mathbb{R}^3)\big)\,, \qquad\qquad \boldsymbol{u}(t) \in \boldsymbol{X}(\boldsymbol{u}_D(t))\,,$$
$$\boldsymbol{\varepsilon}_p \in W^{1,\infty}\big((0,T), L^2(\Omega, \mathrm{Sym}(3))\big)\,.$$

3.2. Non-Associated Drucker-Prager Plasticity. Formally, quasi-static non-associated Drucker-Prager plasticity can be reformulated by variational inequalities similar to the pair (5.4) and (5.8) in associated plasticity.

3.2.1. *A "dual" Variational Inequality.* Similarly to the derivation of (4.9) in the static scenario, for perfect plasticity we obtain the "dual" variational inequality

$$f\big(\dot{\boldsymbol{\sigma}}(t), \boldsymbol{\eta} - \boldsymbol{\sigma}(t)\big) + \tilde{b}\big(\boldsymbol{\eta} - \boldsymbol{\sigma}(t), \dot{\boldsymbol{u}}(t)\big)\,dx \ge 0\,, \qquad\qquad \boldsymbol{\eta} \in \boldsymbol{K}\,, \qquad (5.11a)$$
$$b(\boldsymbol{\sigma}(t), \boldsymbol{w}) + \ell(t, \boldsymbol{w}) = 0\,, \qquad\qquad \boldsymbol{w} \in \boldsymbol{X}\,. \qquad (5.11b)$$

Note however that $\tilde{B} \ne B$ if the non-associated flow rule is used and therefore, there is no analogue to the variational inequality (5.6).

3.2.2. *A "primal" Variational Inequality.* Concerning the "primal" variational inequality, similarly to the associated setting, we can adopt the derivation of Subsection 4.2.4 to the current setting and we obtain the variational inequality (cf. (4.15) for the static analogue)

$$\widehat{q}\big((\boldsymbol{u}, \boldsymbol{\varepsilon}_p), (\boldsymbol{w} - \dot{\boldsymbol{u}}, \boldsymbol{\tau} - \dot{\boldsymbol{\varepsilon}}_p)\big) + \chi_{\boldsymbol{K}}^*(\mathbb{T}^{-1}[\boldsymbol{\tau}]) - \chi_{\boldsymbol{K}}^*(\mathbb{T}^{-1}[\dot{\boldsymbol{\varepsilon}}_p]) \ge \ell(\boldsymbol{w} - \dot{\boldsymbol{u}})\,.$$

If kinematic hardening is sufficiently large in the sense of Lemma 4.5, we expect that this variational inequality has a unique solution. However, the proof in [**HR99**, Section 7.2] relies on the symmetry of the bilinear form $\widehat{q}$ which is not at hand in the current situation, so we cannot show existence and uniqueness of solutions here.

4. Incremental Plasticity

Already at this point we want to introduce a discretization, or to be more precise a semi-discretization w.r.t. the temporal evolution. For this, let

$$0 = t_0 < t_1 < \cdots < t_N = T$$

be a partition of the time interval $[0, T]$ and let $\Delta t_n = t_n - t_{n-1}$ be the step size in the n-th time step. At the discrete time instances t_n, any time continuous quantity $\vartheta(t_n)$ is approximated by ϑ^n. To give an example, by $\boldsymbol{\sigma}^n$, $\boldsymbol{u}^n$ and ε_p^n we denote the approximations of $\boldsymbol{\sigma}(t_n)$, $\boldsymbol{u}(t_n)$ and $\varepsilon_p(t_n)$. Generally, for the time stepping we will use the backward Euler method. The merely first order accuracy of the method is acceptable for the following reasons:

(1) especially for three-dimensional problems, the total error is typically dominated by the spatial discretization,
(2) the solution normally does not possess higher regularity in time, cf. [**Wie99**] for the comparison with a second order method,
(3) the backward Euler method is B-stable, cf. [**HW02**], which is a desirable properties for plasticity problems, cf. [**SH98**, Chapter 6].

4.1. Perfect Plasticity. Once more we proceed formally as we generally cannot expect solutions in Sobolev spaces. The only time derivative in the governing equations occurs in the flow rule $\dot{\boldsymbol{\varepsilon}}(x, t) \in G(\boldsymbol{\sigma}(x, t))$. At a particular time t_n, we infer

$$\dot{\boldsymbol{\varepsilon}}(x, t_n) \in G(\boldsymbol{\sigma}(x, t_n)),$$

and using backward differences, we arrive at $\frac{1}{\Delta t_n}\left(\varepsilon_p^n(x) - \varepsilon_p^{n-1}(x)\right) \in G(\boldsymbol{\sigma}^n(x))$, or equivalently

$$\varepsilon_p^n(x) \in \varepsilon_p^{n-1}(x) + \Delta t_n G(\boldsymbol{\sigma}^n(x)).$$

Thus, starting with $\boldsymbol{u}^0 = \boldsymbol{u}_0$ and $\boldsymbol{\sigma}^0 = \boldsymbol{\sigma}_0$, we can evaluate $\varepsilon_p^0(x) = \boldsymbol{\varepsilon}(\boldsymbol{u}^0(x)) - \mathbb{C}^{-1}[\boldsymbol{\sigma}^0(x)]$ and in each time step $n = 1, \ldots, N$, the governing equations are

$$-\operatorname{div}(\boldsymbol{\sigma}^n(x)) = \boldsymbol{b}(x, t_n), \qquad\qquad x \in \Omega, \qquad\qquad (5.12\text{a})$$

$$\boldsymbol{\sigma}^n(x) = \mathbb{C}[\boldsymbol{\varepsilon}(\boldsymbol{u}^n(x)) - \varepsilon_p^n(x)], \qquad\qquad x \in \Omega, \qquad\qquad (5.12\text{b})$$

$$\boldsymbol{\sigma}^n(x) \in K, \qquad\qquad x \in \Omega, \qquad\qquad (5.12\text{c})$$

$$\varepsilon_p^n(x) \in \varepsilon_p^{n-1}(x) + \Delta t_n G(\boldsymbol{\sigma}^n(x)), \qquad\qquad x \in \Omega, \qquad\qquad (5.12\text{d})$$

$$\boldsymbol{u}^n(x) = \boldsymbol{u}_D(x, t_n), \qquad\qquad x \in \Gamma_D, \qquad\qquad (5.12\text{e})$$

$$\boldsymbol{\sigma}^n(x)\boldsymbol{n}(x) = \boldsymbol{t}_N(x, t_n), \qquad\qquad x \in \Gamma_T. \qquad\qquad (5.12\text{f})$$

This has the structure of the static problems considered in previous chapters. The only new ingredient is the presence of the plastic strain ε_p^{n-1} and of the time step size Δt_n in the flow rule (5.12d).

4.1.1. *Associated Perfect Plasticity.* Once again, $G = N_K$ and equations (5.12) define two convex minimization problems in duality. The corresponding Lagrangian L^n at time step n is given by

$$L^n(\boldsymbol{\sigma}^n, \boldsymbol{u}^n) = \tfrac{1}{2}\langle A\boldsymbol{\sigma}^n, \boldsymbol{\sigma}^n \rangle_{\boldsymbol{P}^* \times \boldsymbol{P}} + (\varepsilon_p^{n-1}, \boldsymbol{\sigma}^n)_{\boldsymbol{P}} + \Delta t_n \chi_K(\boldsymbol{\sigma}^n)$$
$$+ \langle B^*\boldsymbol{u}^n, \boldsymbol{\sigma}^n \rangle_{\boldsymbol{P}^* \times \boldsymbol{P}} - \langle F^n, \boldsymbol{u}^n \rangle_{\boldsymbol{V}^* \times \boldsymbol{V}}, \qquad\qquad (5.13)$$

with the functional $F^n \in \boldsymbol{V}^*$ given as

$$F^n(\boldsymbol{u}) = \begin{cases} -\ell(t_n, \boldsymbol{u}) & , \boldsymbol{u} \in \boldsymbol{X}(\boldsymbol{u}_D), \\ \infty & , \text{ else}. \end{cases} \tag{5.14}$$

We also refer to (2.30) and (2.21). Restricting the Lagrangian to $\boldsymbol{X}(\boldsymbol{u}_D)$, we find

$$L^n(\boldsymbol{\sigma}^n, \boldsymbol{u}^n) = \tfrac{1}{2}a(\boldsymbol{\sigma}^n, \boldsymbol{\sigma}^n) + (\boldsymbol{\sigma}^n, \boldsymbol{\varepsilon}_p^{n-1})_{\boldsymbol{P}} + \Delta t_n \chi_{\boldsymbol{K}}(\boldsymbol{\sigma}^n) + b(\boldsymbol{\sigma}^n, \boldsymbol{u}^n) + \ell(t_n, \boldsymbol{u}^n). \tag{5.15}$$

The fact $\Delta t_n \chi_{\boldsymbol{K}}(\cdot) = \chi_{\boldsymbol{K}}(\cdot)$ once more exhibits the rate-independence: the model depends on the history of deformation represented by $\boldsymbol{\varepsilon}_p^{n-1}$, but does not depend on the physical time represented by Δt_n. We therefore omit Δt_n in the following. The dual problem for obtaining $\boldsymbol{\sigma}^n$ is:

$$\begin{aligned} &\text{Minimize} \quad \tfrac{1}{2}a(\boldsymbol{\sigma}^n, \boldsymbol{\sigma}^n) + (\boldsymbol{\sigma}^n, \boldsymbol{\varepsilon}_p^{n-1})_{\boldsymbol{P}} + \chi_{\boldsymbol{K}}(\boldsymbol{\sigma}^n) - h(t_n, \boldsymbol{\sigma}^n) \\ &\text{subject to} \quad \boldsymbol{\sigma}^n \in \boldsymbol{S}(t_n). \end{aligned} \tag{5.16}$$

while the corresponding primal problem for obtaining $\boldsymbol{u}^n$ reads:

$$\text{Minimize} \quad \mathcal{E}_{\text{pl}}^n(\boldsymbol{u}^n) \qquad \text{subject to} \quad \boldsymbol{u}^n \in \boldsymbol{X}(\boldsymbol{u}_D(t_n)), \tag{5.17}$$

with

$$\mathcal{E}_{\text{pl}}^n(\boldsymbol{u}) = \Upsilon\big(\mathbb{C}\big[\boldsymbol{\varepsilon}(\boldsymbol{u}) - \boldsymbol{\varepsilon}_p^{n-1}\big]\big) - \ell(t_n, \boldsymbol{u}),$$

and Υ defined as in (2.35). We see that each incremental problem has exactly the same structure as the static problem and obviously, we cannot expect more regularity of the incremental problem.

4.1.2. *Non-Associated Perfect Plasticity.* Using (5.12d), substitution into (5.12b) along with the admissibility constraint (5.12c) yields the inclusions

$$0 \in \mathbb{C}^{-1}[\boldsymbol{\sigma}^n(x)] - \big(\boldsymbol{\varepsilon}(\boldsymbol{u}^n(x)) - \boldsymbol{\varepsilon}_p^{n-1}(x)\big) + \Delta t_n G(\boldsymbol{\sigma}^n(x)),$$
$$\boldsymbol{\sigma}^n(x) \in K, \qquad \text{a.e. in } \Omega.$$

By means of the response function $R_{\boldsymbol{K}}$ as introduced in (4.3), this gives

$$\boldsymbol{\sigma}^n = R_{\boldsymbol{K}}\big(\mathbb{C}\big[\boldsymbol{\varepsilon}(\boldsymbol{u}^n) - \boldsymbol{\varepsilon}_p^{n-1}\big]\big).$$

Substitution into the weak formulation of the equilibrium constraint results in the problem of finding $\boldsymbol{u}^n \in \boldsymbol{X}(\boldsymbol{u}_D(t_n))$ such that

$$\int_\Omega R_K(\mathbb{C}[\boldsymbol{\varepsilon}(\boldsymbol{u}^n(x)) - \boldsymbol{\varepsilon}_p^{n-1}(x)]) : \boldsymbol{\varepsilon}(\boldsymbol{w}(x))\, dx = \ell(t_n, \boldsymbol{w}), \qquad \boldsymbol{w} \in \boldsymbol{X}. \tag{5.18}$$

4.2. Viscoplastic Regularization. Contrary to perfect plasticity, the material response in incremental viscoplasticity does depend on the time step size Δt_n.

4.2.1. *Associated Perfect Plasticity.* Replacing the subdifferential of the indicator function $\frac{1}{\Delta t_n}(\boldsymbol{\varepsilon}_p^n(x) - \boldsymbol{\varepsilon}_p^{n-1}(x)) \in \partial\chi_K(\boldsymbol{\sigma}(x))$ by its Yosida approximation, we obtain the viscoplastic flow rule

$$\boldsymbol{\varepsilon}_p^n(x) = \boldsymbol{\varepsilon}_p^{n-1}(x) + \alpha\Delta t_n \, \mathbb{C}^{-1}\big[\boldsymbol{\sigma}^n(x) - P_K(\boldsymbol{\sigma}^n(x))\big].$$

Proceeding as in Section 3.1, we obtain

$$\boldsymbol{\sigma}^n = \tfrac{1}{1+\alpha\Delta t_n}\mathbb{C}[\boldsymbol{\varepsilon}(\boldsymbol{u}^n) - \boldsymbol{\varepsilon}_p^{n-1}] + \big(1 - \tfrac{1}{1+\alpha\Delta t_n}\big)P_{\boldsymbol{K}}(\mathbb{C}[\boldsymbol{\varepsilon}(\boldsymbol{u}^n) - \boldsymbol{\varepsilon}_p^{n-1}]),$$

which is (3.3) with α replaced by $\alpha\Delta t_n$. Note that α has the dimension of an inverse viscosity in the quasi-static setting. The dependence on the time step size Δt_n shows the

rate-dependence of the model. Obviously, if Δt_n gets smaller, the material response will be closer to elasticity whereas for larger time steps, plastic behavior will dominate. Via the Lagrangian

$$L^n(\boldsymbol{\sigma}^n, \boldsymbol{u}^n) = \tfrac{1}{2}a(\boldsymbol{\sigma}^n, \boldsymbol{\sigma}^n) + (\boldsymbol{\sigma}^n, \varepsilon_p^{n-1})_{\boldsymbol{P}} + \Delta t_n \chi_{\boldsymbol{K}}^{\alpha}(\boldsymbol{\sigma}^n) + b(\boldsymbol{\sigma}^n, \boldsymbol{u}^n) + \ell(t_n, \boldsymbol{u}^n),$$

the corresponding minimization problems in duality are:

$$\text{Minimize} \quad \tfrac{1}{2}a(\boldsymbol{\sigma}, \boldsymbol{\sigma}) + \Delta t_n \chi_{\boldsymbol{K}}^{\alpha}(\boldsymbol{\sigma}) - h(\boldsymbol{\sigma}) \qquad \text{subject to} \quad \boldsymbol{\sigma} \in \boldsymbol{S}(t_n),$$
$$\text{Minimize} \quad \mathcal{E}_{\text{vp},\alpha}^n(\boldsymbol{u}^n) \qquad\qquad\qquad\qquad \text{subject to} \quad \boldsymbol{u}^n \in \boldsymbol{X}(\boldsymbol{u}_D(t_n)),$$

with the functional

$$\mathcal{E}_{\text{vp},\alpha}^n(\boldsymbol{u}) = \tfrac{1}{1+\alpha \Delta t_n}\mathcal{W}_e\big(\varepsilon(\boldsymbol{u}) - \varepsilon_p^{n-1}\big) + \big(1 - \tfrac{1}{1+\alpha \Delta t_n}\big)\Upsilon(\mathbb{C}[\varepsilon(\boldsymbol{u}) - \varepsilon_p^{n-1}]) - \ell(t_n, \boldsymbol{u}).$$

The Euler condition for the primal problem is

$$\frac{1}{1+\alpha \Delta t_n} \int_{\Omega} \mathbb{C}\big[\varepsilon(\boldsymbol{u}^n(x)) - \varepsilon_p^{n-1}(x)\big] : \varepsilon(\boldsymbol{w}(x))\, dx$$
$$+ \big(1 - \tfrac{1}{1+\alpha \Delta t_n}\big) \int_{\Omega} P_K\big(\mathbb{C}\big[\varepsilon(\boldsymbol{u}(x)) - \varepsilon_p^{n-1}(x)\big]\big) : \varepsilon(\boldsymbol{w}(x))\, dx = \ell(t_n, \boldsymbol{w})$$

for all $\boldsymbol{w} \in \boldsymbol{X}$.

Theorem 5.2. *There exists a primal-dual pair $(\boldsymbol{\sigma}^n, \boldsymbol{u}^n) \in \boldsymbol{P} \times \boldsymbol{X}(\boldsymbol{u}_D(t_n))$ solving the above minimization problems in duality.*

PROOF. Both objective functions are uniformly convex w.r.t. the topologies in $\boldsymbol{P}$ and $\boldsymbol{X}$. Moreover, since $\boldsymbol{S}(t_n)$ is a closed and affine subspace, no further constraint qualification is necessary. $\qquad\square$

4.2.2. *Non-Associated Perfect Plasticity.* As indicated in Section 4.3, for general flow rules G, we postulate the viscoplastic regularization as a convex combination of the limiting problems of elasticity and perfect plasticity. We follow this approach and define

$$\boldsymbol{\sigma}^n(x) = \frac{1}{1+\alpha \Delta t_n}\mathbb{C}[\varepsilon(\boldsymbol{u}^n(x)) - \varepsilon_p^{n-1}(x)] + \frac{\alpha \Delta t_n}{1+\alpha \Delta t_n}R_K(\mathbb{C}[\varepsilon(\boldsymbol{u}^n(x)) - \varepsilon_p^{n-1}(x)]).$$

Substitution into the weak equilibrium equation then gives the variational problem of finding $\boldsymbol{u}^n \in \boldsymbol{X}(\boldsymbol{u}_D(t_n))$ such that

$$\frac{1}{1+\alpha \Delta t_n} \int_{\Omega} \mathbb{C}\big[\varepsilon(\boldsymbol{u}^n(x)) - \varepsilon_p^{n-1}(x)\big] : \varepsilon(\boldsymbol{w}(x))\, dx$$
$$+ \frac{\alpha \Delta t_n}{1+\alpha \Delta t_n} \int_{\Omega} R_K\big(\mathbb{C}\big[\varepsilon(\boldsymbol{u}(x)) - \varepsilon_p^{n-1}(x)\big]\big) : \varepsilon(\boldsymbol{w}(x))\, dx = \ell(t_n, \boldsymbol{w}) \tag{5.19}$$

Contrary to the static case, under certain conditions, this problem is always solvable if the time step size is small enough.

Theorem 5.3. *Let the response function R_K of perfect plasticity satisfy*

$$\big(R_K(\boldsymbol{\sigma}) - R_K(\boldsymbol{\eta})\big) : \mathbb{C}^{-1}[\boldsymbol{\sigma} - \boldsymbol{\eta}] \geq -L\,(\boldsymbol{\sigma} - \boldsymbol{\eta}) : \mathbb{C}^{-1}[\boldsymbol{\sigma} - \boldsymbol{\eta}],$$

for some $L \in \mathbb{R}$. Then, the variational problem (5.19) has a unique solution if $\alpha \Delta t_n L < 1$.

PROOF. The proof is the same as that of Corollary 4.7 with α replaced by $\alpha \Delta t_n$ and relies on Theorem 4.1. $\qquad\square$

We remark that unless $L \leq 0$, this is a severe restriction of the step size Δt_n if we want to consider the approximation of perfect plasticity, i.e. $\alpha \gg 1$.

4.3. Incremental Hardening Plasticity. After time discretization, the flow rule reads

$$\boldsymbol{\varepsilon}_p^n(x) \in \boldsymbol{\varepsilon}_p^{n-1} + \Delta t_n G\big(\boldsymbol{\sigma}^n(x) + \boldsymbol{\zeta}^n(x)\big).$$

and the admissibility rewrites as $\boldsymbol{\sigma}^n(x) + \boldsymbol{\zeta}^n(x) \in K$.

4.3.1. *Associated Hardening Plasticity.* As in Section 3.2, we define two minimization problems in duality by means of a Lagrangian L^n and restricted to $(\boldsymbol{P} \times \boldsymbol{P}) \times \boldsymbol{X}(\boldsymbol{u}_D(t_n))$, the Lagrangian in time step n is given as

$$L^n((\boldsymbol{\sigma}^n, \boldsymbol{\zeta}^n), \boldsymbol{u}^n) = \tfrac{1}{2}a(\boldsymbol{\sigma}^n, \boldsymbol{\sigma}^n) + \tfrac{1}{2}d(\boldsymbol{\zeta}^n, \boldsymbol{\zeta}^n) + (\boldsymbol{\sigma}^n, \boldsymbol{\varepsilon}_p^{n-1})_{\boldsymbol{P}} + \Delta t_n \chi_{\boldsymbol{K}}(\boldsymbol{\sigma}^n + \boldsymbol{\zeta}^n)$$
$$+ b(\boldsymbol{\sigma}^n, \boldsymbol{u}^n)\, dx + \ell(t_n, \boldsymbol{u}^n).$$

Again, the time step size Δt_n can be omitted due to the rate-independence of the problem and sticking to our terminology, the corresponding dual problem is given as

$$\text{Minimize} \quad \tfrac{1}{2}a(\boldsymbol{\sigma}^n, \boldsymbol{\sigma}^n) + \tfrac{1}{2}d(\boldsymbol{\zeta}^n, \boldsymbol{\zeta}^n) + (\boldsymbol{\sigma}^n, \boldsymbol{\varepsilon}_p^{n-1})_{\boldsymbol{P}} + \chi_{\boldsymbol{K}}(\boldsymbol{\sigma}^n + \boldsymbol{\zeta}^n) - h(t_n, \boldsymbol{\sigma}^n)$$
$$\text{subject to} \quad \boldsymbol{\sigma} \in \boldsymbol{S}(t_n), \quad \boldsymbol{\zeta} \in \boldsymbol{P}.$$

Proceeding like in Subsection 3.2.2, we obtain the primal functional at time step n.

$$\mathcal{E}_{\mathrm{hd}}^n(\boldsymbol{u}^n) = \Upsilon^N(\mathbb{C}[\boldsymbol{\varepsilon}(\boldsymbol{u}^n) - \boldsymbol{\varepsilon}_p^{n-1}])$$
$$+ \tfrac{1}{2}\int_\Omega \big(\boldsymbol{\varepsilon}(\boldsymbol{u}^n(x)) - \boldsymbol{\varepsilon}_p^{n-1}(x)\big) : \mathbb{D}[\boldsymbol{\varepsilon}(\boldsymbol{u}^n(x)) - \boldsymbol{\varepsilon}_p^{n-1}(x)]\, dx - \ell(t_n, \boldsymbol{u}^n).$$

Finally, the primal problem is

$$\text{Minimize} \quad \mathcal{E}_{\mathrm{hd}}^n(\boldsymbol{u}^n) \qquad \text{subject to} \quad \boldsymbol{u}^n \in \boldsymbol{X}(\boldsymbol{u}_D(t_n)). \tag{5.20}$$

Proposition 5.4. *Provided that $\mathbb{H}$ is positive definite on the symmetric second order tensors (or positive definite on the deviatoric subspace in incompressible plasticity), then the primal incremental problem* (5.20) *has a unique solution $\boldsymbol{u}^n \in \boldsymbol{X}(\boldsymbol{u}_D(t_n))$.*

PROOF. The primal incremental problem is uniformly convex w.r.t. the topology of $H^1(\Omega, \mathbb{R}^3)$, cf. Theorem 3.6, and problem (5.20) has a unique minimizer in $\boldsymbol{X}(\boldsymbol{u}_D(t_n))$. For the plastically incompressible case, we refer to the discussion in Subsection 3.2.4. □

4.3.2. *Non-Associated Hardening Plasticity.* As in Section 4.1 and particularly (4.6), by using the response function R_{hd}, we find that the governing equations

$$0 = \mathbb{C}^{-1}[\boldsymbol{\sigma}^n(x)] - \big(\boldsymbol{\varepsilon}(\boldsymbol{u}^n(x)) - \boldsymbol{\varepsilon}_p^{n-1}(x)\big) - \mathbb{H}^{-1}[\boldsymbol{\zeta}^n(x)], \qquad \text{a.e. in } \Omega, \tag{5.21a}$$
$$0 \in \mathbb{H}^{-1}[\boldsymbol{\zeta}^n(x)] + \boldsymbol{\varepsilon}_p^{n-1} + \Delta t_n G\big(\boldsymbol{\sigma}^n(x) + \boldsymbol{\zeta}^n(x)\big), \qquad \text{a.e. in } \Omega, \tag{5.21b}$$
$$\boldsymbol{\sigma}^n(x) + \boldsymbol{\zeta}^n(x) \in K, \qquad \text{a.e. in } \Omega, \tag{5.21c}$$

are satisfied by

$$\begin{bmatrix} \boldsymbol{\sigma}^n \\ \boldsymbol{\zeta}^n \end{bmatrix} = R_{\mathrm{hd}}(\mathbb{C}[\boldsymbol{\varepsilon}(\boldsymbol{u}^n) - \boldsymbol{\varepsilon}_p^{n-1}]).$$

The first component is then substituted into the weak equilibrium equation resulting in a variational problem for the displacement.

4.4. Incremental Drucker-Prager Plasticity.

4.4.1. *Perfect Plasticity.* The results of Section 4.2 concerning the static scenario directly transfer to the incremental problem. The response function corresponds to the projection $P_{\boldsymbol{K}}^F$, i.e. $\boldsymbol{\sigma}^n = P_{\boldsymbol{K}}^F(\mathbb{C}[\boldsymbol{\varepsilon}(\boldsymbol{u}) - \boldsymbol{\varepsilon}_p^{n-1}])$, and in the n-th time step we need to determine $\boldsymbol{u}^n \in \boldsymbol{X}(\boldsymbol{u}_D(t_n))$ such that

$$\int_\Omega P_K^F\big(\mathbb{C}[\boldsymbol{\varepsilon}(\boldsymbol{u}^n(x)) - \boldsymbol{\varepsilon}_p^{n-1}(x)]\big) : \boldsymbol{\varepsilon}(\boldsymbol{w}(x)) \, dx = \ell(t_n, \boldsymbol{w}), \qquad \boldsymbol{w} \in \boldsymbol{X}.$$

4.4.2. *Hardening Plasticity.* Analogously to Theorem 4.6, we state the existence and uniqueness result for the variational inequality formulation. The governing equations and the response function are just those of (5.21) with $G = \mathbb{T}[\partial\chi_K]$ and $\mathbb{T}$ given in (1.19).

Corollary 5.5. *Let the hardening modulus be of the form $\mathbb{H} = h_d\mathbb{P}_{\text{dev}} + h_v\mathbb{P}_{\text{vol}}$ with $h_d > 0$ and $h_v > \kappa\frac{(M-1)^2}{4M}$. Then, the incremental problem of non-associated Drucker-Prager plasticity with kinematic hardening has a unique solution.*

PROOF. This is the natural extension of Theorem 4.6 to the given context. □

4.4.3. *Viscoplastic Regularization.* Contrary to perfect and hardening plasticty, the viscoplastic regularization leads to rate-dependent problems, i.e. time has a physical meaning. This gives the following result.

Corollary 5.6. *The incremental problem of viscoplastic Drucker-Prager plasticity admits a unique solution $\boldsymbol{u}^n \in \boldsymbol{X}(\boldsymbol{u}_D(t_n))$ provided that $\alpha\Delta t_n(1 - M) < M$.*

PROOF. Using Lemma 4.3, we can apply Theorem 5.3 with $L = \frac{1-M}{M}$. □

Essentially, this result states that incremental non-associated Drucker-Prager viscoplasticity is well-posed for a finite regularization parameter $\alpha \in [0, \infty)$ provided that the time step size Δt_n is small enough. This has to be expected since the time-continuous problem in viscoplasticity is well-posed, cf. the previous section. On the other hand, the time step restriction is quite restrictive, e.g. $M = 1/2$ would require irrealistic small time steps $\Delta t < \frac{1}{\alpha}$.

Part 2

Aspects of Algorithmic Plasticity

CHAPTER 6

DISCRETIZATION BY THE FINITE ELEMENT METHOD

1. The Problem Setting Reconsidered

Proceeding formally, after time discretization as introduced in Section 5.4, all static and incremental problems of the first part can be stated as

$$-\operatorname{div}(\boldsymbol{\sigma}(x)) = \boldsymbol{b}(x)\,, \qquad\qquad x \in \Omega\,, \qquad\qquad (6.1\text{a})$$

$$\boldsymbol{\sigma}(x) = R\big(\mathbb{C}[\boldsymbol{\varepsilon}(\boldsymbol{u}(x)) - \boldsymbol{\tau}(x)]\big)\,, \qquad\qquad x \in \Omega\,, \qquad\qquad (6.1\text{b})$$

$$\boldsymbol{u}(x) = \boldsymbol{u}_D(x)\,, \qquad\qquad x \in \Gamma_D\,, \qquad\qquad (6.1\text{c})$$

$$\boldsymbol{\sigma}(x)\boldsymbol{n}(x) = \boldsymbol{t}_N(x)\,, \qquad\qquad x \in \Gamma_T\,, \qquad\qquad (6.1\text{d})$$

with a suitable *response function* $R : \operatorname{Sym}(d) \to \operatorname{Sym}(d)$ (see Table 6.1 for examples), and given data $\boldsymbol{\tau} \in L^2(\Omega, \operatorname{Sym}(d))$. For static problems, we have $\boldsymbol{\tau} = 0$ and in the incremental setting we find $\boldsymbol{\tau} = \boldsymbol{\varepsilon}_p^{n-1}$. For the introduction of the finite element method below, we always assume that system (6.1) admits a solution

$$(\boldsymbol{\sigma}, \boldsymbol{u}) \in \boldsymbol{\Sigma}_{\operatorname{div}}(\boldsymbol{t}_N) \times \boldsymbol{X}(\boldsymbol{u}_D)\,.$$

Note that we proceed in a very general framework and R might be any response function. Henceforth, we only make the following assumption concerning the response function which is well-founded for our considered examples.

Assumption 6.1. *The response function $R : \operatorname{Sym}(d) \to \operatorname{Sym}(d)$ is Lipschitz continuous.*

Ass. Perfect plasticity:	$R(\boldsymbol{\eta}) = P_K(\boldsymbol{\eta})$
Ass. Viscoplasticity:	$R(\boldsymbol{\eta}) = \frac{1}{1+\alpha}\boldsymbol{\eta} + \frac{\alpha}{1+\alpha}P_K(\boldsymbol{\eta})$
Ass. Kinematic hardening:	$R(\boldsymbol{\eta}) = (\mathbb{D} \circ \mathbb{C}^{-1})[\boldsymbol{\eta}] + (\mathbb{C} \circ \mathbb{N}^{-1})[P_K^N(\boldsymbol{\eta})]$
Non-ass. Drucker-Prager:	$R(\boldsymbol{\eta}) = P_K^F(\boldsymbol{\eta})$

TABLE 6.1. Examples of response functions.

For convenience, we shortly recapitulate some notation as introduced in Section 2.1:

$$
\begin{aligned}
\boldsymbol{P} &= L^2(\Omega, \mathrm{Sym}(d))\,, \\
\boldsymbol{V} &= H^1(\Omega, \mathbb{R}^d)\,, \\
\boldsymbol{\Sigma}_{\mathrm{div}}(\boldsymbol{t}_N) &= \{\boldsymbol{\sigma} \in H(\mathrm{div}, \Omega, \mathrm{Sym}(d)) : \gamma_N(\boldsymbol{\sigma}) = \boldsymbol{t}_N\}\,, \qquad\qquad \boldsymbol{\Sigma}_{\mathrm{div}} \equiv \boldsymbol{\Sigma}_{\mathrm{div}}(0)\,, \\
\boldsymbol{X}(\boldsymbol{u}_D) &= \{\boldsymbol{u} \in \boldsymbol{V} : \gamma_T(\boldsymbol{u}) = \boldsymbol{u}_D\}\,, \qquad\qquad\qquad\qquad\quad\; \boldsymbol{X} \equiv \boldsymbol{X}(0)\,.
\end{aligned}
$$

1.1. Weak Formulations. As we have seen earlier, there are mainly two approaches to the above problem – a formulation only comprising the displacement $\boldsymbol{u}$ and a mixed formulation approximating both the displacement $\boldsymbol{u}$ and the stress $\boldsymbol{\sigma}$. For the elasticity problem, both types were presented in Section 2.2.

1.1.1. *Displacement Formulation.* We explicitly use the response function and substitute the constitutive equation (6.1b) into the equilibrium equation (6.1a). Afterwards, we multiply with a test function and integrate over Ω to obtain the problem of finding $\boldsymbol{u} \in \boldsymbol{X}(\boldsymbol{u}_D)$ such that

$$
\int_\Omega R\big(\mathbb{C}[\boldsymbol{\varepsilon}(\boldsymbol{u}(x)) - \boldsymbol{\tau}(x)]\big) : \boldsymbol{\varepsilon}(\boldsymbol{w}(x))\,dx = \ell(\boldsymbol{w})\,, \qquad \boldsymbol{w} \in \boldsymbol{X}\,, \tag{6.2}
$$

with the load functional ℓ as defined in (2.10). Defining the mapping $F : \boldsymbol{X} \to \boldsymbol{X}^*$ via

$$
\langle F(\boldsymbol{u}), \boldsymbol{w}\rangle_{\boldsymbol{X}^* \times \boldsymbol{X}} = \int_\Omega R\big(\mathbb{C}[\boldsymbol{\varepsilon}(\boldsymbol{u}(x)) - \boldsymbol{\tau}(x)]\big) : \boldsymbol{\varepsilon}(\boldsymbol{w}(x))\,dx - \ell(\boldsymbol{w})\,, \tag{6.3}
$$

problem (6.2) is equivalent to

$$
F(\boldsymbol{u}) = 0\,, \qquad \boldsymbol{u} \in \boldsymbol{X}(\boldsymbol{u}_D)\,. \tag{6.4}
$$

1.1.2. *Mixed Formulation.* The mixed formulation in $\boldsymbol{P} \times \boldsymbol{X}(\boldsymbol{u}_D)$ consists of finding $(\boldsymbol{\sigma}, \boldsymbol{u})$ such that for all $(\boldsymbol{\eta}, \boldsymbol{w}) \in \boldsymbol{P} \times \boldsymbol{X}$

$$
\begin{aligned}
\int_\Omega \boldsymbol{\eta}(x) : \mathbb{C}^{-1}[\boldsymbol{\sigma}(x)]\,dx - \int_\Omega \boldsymbol{\eta}(x) : \mathbb{C}^{-1}\big[R\big(\mathbb{C}[\boldsymbol{\varepsilon}(\boldsymbol{u}(x)) - \boldsymbol{\tau}(x)]\big)\big]\,dx &= 0\,, \\
-\int_\Omega \boldsymbol{\sigma}(x) : \boldsymbol{\varepsilon}(\boldsymbol{w}(x))\,dx &= -\ell(\boldsymbol{w})\,.
\end{aligned} \tag{6.5}
$$

Making use of Hooke's law $\boldsymbol{\sigma}(x) = \mathbb{C}[\boldsymbol{\varepsilon}(\boldsymbol{u}(x)) - \boldsymbol{\varepsilon}_p(x)]$, a similar formulation can be set up for $(\boldsymbol{u}, \boldsymbol{\varepsilon}_p) \in \boldsymbol{X}(\boldsymbol{u}_D) \times \boldsymbol{P}$, i.e.

$$
\int_\Omega \mathbb{C}\big[\boldsymbol{\varepsilon}(\boldsymbol{u}(x)) - \boldsymbol{\varepsilon}_p(x)\big] : \boldsymbol{\varepsilon}(\boldsymbol{w}(x))\,dx = \ell(\boldsymbol{w})\,, \qquad \boldsymbol{w} \in \boldsymbol{X}\,,
$$

$$
\int_\Omega \mathbb{C}\big[\boldsymbol{\varepsilon}(\boldsymbol{u}(x)) - \boldsymbol{\varepsilon}_p(x)\big] - R\big(\mathbb{C}[\boldsymbol{\varepsilon}(\boldsymbol{u}(x)) - \boldsymbol{\tau}(x)]\big) : \boldsymbol{\eta}(x)\,dx = 0\,, \qquad \boldsymbol{\eta} \in \boldsymbol{P}\,.
$$

Contrary to the elasticity problem, a mixed formulation in $H(\mathrm{div}, \Omega, \mathrm{Sym}(d)) \times L^2(\Omega, \mathbb{R}^d)$ w.r.t. the stress and the displacement cannot be given directly since Green's formula (2.8) may not be applicable in the first equation due to the (generally nonsmooth) nonlinearity R. One possible remedy is the introduction of the total strain $\boldsymbol{\epsilon}(x) = \boldsymbol{\varepsilon}(\boldsymbol{u}(x))$ as an independent variable, corresponding to the *Hu-Washizu* formulation. Then, applying Green's formula to the equilibrium equation, and likewise in the weak formulation of the constraint $\boldsymbol{\epsilon} = \boldsymbol{\varepsilon}(\boldsymbol{u})$, yields the problem of finding $(\boldsymbol{\sigma}, \boldsymbol{\epsilon}, \boldsymbol{u}) \in \boldsymbol{\Sigma}_{\mathrm{div}}(\boldsymbol{t}_N) \times \boldsymbol{P} \times L^2(\Omega, \mathbb{R}^d)$ such

that for all $(\boldsymbol{\eta}, \boldsymbol{\delta}, \boldsymbol{w}) \in \boldsymbol{\Sigma}_{\mathrm{div}} \times \boldsymbol{P} \times L^2(\Omega, \mathbb{R}^d)$

$$\int_\Omega \boldsymbol{\sigma}(x) : \boldsymbol{\delta}(x)\, dx - \int_\Omega R(\mathbb{C}[\boldsymbol{\epsilon}(x) - \boldsymbol{\tau}(x)]) : \boldsymbol{\delta}(x)\, dx = 0\,,$$

$$\int_\Omega \mathrm{div}(\boldsymbol{\sigma}(x)) \cdot \boldsymbol{w}(x)\, dx = -\int_\Omega \boldsymbol{b}(x) \cdot \boldsymbol{w}(x)\, dx\,, \qquad (6.6)$$

$$\int_\Omega \boldsymbol{\eta}(x) : \boldsymbol{\epsilon}(x)\, dx + \int_\Omega \mathrm{div}\big(\boldsymbol{\eta}(x)\big) \cdot \boldsymbol{u}(x)\, dx = h(\boldsymbol{\eta})\,,$$

with h as defined in (2.19).

1.1.3. *Least Squares Formulation.* For completeness, we also mention a formulation in the least squares sense. Since (6.1) is a first order system of partial differential equations, it is possible to set up a corresponding least squares formulation leading to a system of second order differential equations. The approach consists in minimizing the functional

$$\tfrac{1}{2}\Big(\int_\Omega \big|\, \mathrm{div}(\boldsymbol{\sigma}(x)) + \boldsymbol{b}(x)\big|^2\, dx + \int_\Omega \big|\boldsymbol{\sigma}(x) - R(\mathbb{C}[\boldsymbol{\varepsilon}(\boldsymbol{u}(x)) - \boldsymbol{\tau}(x)])\big|^2\, dx\Big)\,,$$

with a suitable treatment of the boundary conditions. This formulation has been considered in [**Sta07**, **SSS09**], but we will not follow this approach here.

2. Discrete Approximation Spaces

In order to define discrete approximation spaces, we approximate $\Omega \subset \mathbb{R}^d$ by a finite set of cells $\mathcal{C}$ and thus define $\Omega_h = \bigcup_{C \in \mathcal{C}} C$. In the following, we tacitly assume $\Omega = \Omega_h$ for simplicity.

2.1. Finite Element Spaces for the Displacement. We consider a family of spaces $\{\boldsymbol{V}_h\}_{h \in \mathcal{H}} \subset C^{0,1}(\overline{\Omega}, \mathbb{R}^d) \subset \boldsymbol{V}$ and we assume that $\bigcup_{h \in \mathcal{H}} \boldsymbol{V}_h$ is dense in $\boldsymbol{V}$, i.e. for all $\boldsymbol{u} \in \boldsymbol{V}$ there are sequences $\{h_n\}_{n \in \mathbb{N}} \subset \mathcal{H}$ and $\{\boldsymbol{u}_n\}_{n \in \mathbb{N}}$ with $\boldsymbol{u}_n \in \boldsymbol{V}_{h_n}$ such that

$$\lim_{n \to \infty} \|\boldsymbol{u} - \boldsymbol{u}_n\|_{\boldsymbol{V}} = 0\,.$$

This approximation property can be interpreted as the consistency of the spaces $\{\boldsymbol{V}_h\}_{h \in \mathcal{H}}$ with $\boldsymbol{V}$. The most prominent examples of $\boldsymbol{V}_h$ are the nodal basis Lagrange finite elements spaces and in the following, let $\boldsymbol{V}_h$ be a finite element space spanned by nodal basis functions. The restriction of $\boldsymbol{u}_h \in \boldsymbol{V}_h$ to one cell $C \in \mathcal{C}$ is assumed to be polynomial and the simplest realization is given by continuous, piecewise (multi-) linear functions (on each C). We denote this space by

$$\widehat{\boldsymbol{V}}_h = \{\boldsymbol{u}_h \in C^{0,1}(\Omega, \mathbb{R}^3) : \boldsymbol{u}_h\big|_C \text{ is (multi-) linear.}\}$$

Further important examples are (multi-)quadratic elements and Serendipity elements (reduced multi-quadratic elements on cuboids, cf. [**BS02**]). Denoting by $D \subset \Gamma_D$ all nodal points on the Dirichlet part of the boundary, in analogy with Section 2.1, we define

$$\boldsymbol{X}_h(\boldsymbol{u}_D) = \{\boldsymbol{u}_h \in \boldsymbol{V}_h : \boldsymbol{u}_h(x) = \boldsymbol{u}_D(x) \text{ for all } x \in D\}\,,$$

$$\widehat{\boldsymbol{X}_h}(\boldsymbol{u}_D) = \{\boldsymbol{u}_h \in \widehat{\boldsymbol{V}}_h : \boldsymbol{u}_h(x) = \boldsymbol{u}_D(x) \text{ for all } x \in D\}\,.$$

and likewise $\boldsymbol{X}_h \equiv \boldsymbol{X}_h(0)$ and $\widehat{\boldsymbol{X}_h} \equiv \widehat{\boldsymbol{X}_h}(0)$ in case of homogeneous Dirichlet boundary conditions.

Similarly to the continuous setting, we define the discrete elasticity operator $C_h : \boldsymbol{X}_h \to \boldsymbol{X}_h^*$ by setting

$$C_h : \boldsymbol{X}_h \to \boldsymbol{X}_h^* , \qquad\qquad \langle C_h \boldsymbol{u}_h, \boldsymbol{w}_h \rangle_{\boldsymbol{X}_h^* \times \boldsymbol{X}_h} = c(\boldsymbol{u}_h, \boldsymbol{w}_h) , \qquad\qquad (6.7)$$

with the bilinear form $c(\cdot, \cdot)$ as given in (2.3).

2.2. Stress Spaces for Mixed Approximations. We shortly address the approximation of L^2 functions, and particularly of tensor-valued functions in $\boldsymbol{P}$. The simplest possibility is to use piecewise constants functions (on each cell C). This defines

$$\widehat{\boldsymbol{P}}_h = \{ \boldsymbol{\sigma}_h \in \boldsymbol{P} : \boldsymbol{\sigma}_h\big|_C \text{ is constant on all } C \in \mathcal{C} \} \subset \boldsymbol{P} .$$

On simplical meshes, i.e. triangular meshes for $d = 2$ and tetrahedral meshes for $d = 3$, the combination $\widehat{\boldsymbol{P}}_h \times \widehat{\boldsymbol{X}}_h(\boldsymbol{u}_D)$ is stable concerning the mixed formulation (6.5). In this case, $\boldsymbol{\varepsilon}(\boldsymbol{u}_h) \in \widehat{\boldsymbol{P}}_h$ for all $\boldsymbol{u}_h \in \widehat{\boldsymbol{X}}_h$ and the inf-sup-condition follows as in the continuous case, cf. Section 2.2, i.e.

$$\sup_{\boldsymbol{\eta}_h \in \widehat{\boldsymbol{P}}_h} \frac{b(\boldsymbol{\eta}_h, \boldsymbol{w}_h)}{\|\boldsymbol{\eta}_h\|_\Sigma} = \sup_{\boldsymbol{\eta}_h \in \widehat{\boldsymbol{P}}_h} \frac{-\int_\Omega \boldsymbol{\eta}_h(x) : \boldsymbol{\varepsilon}(\boldsymbol{w}_h(x)) \, dx}{\|\boldsymbol{\eta}_h\|_\Sigma} \overset{\boldsymbol{\eta}_h = -\mathbb{C}[\boldsymbol{\varepsilon}(\boldsymbol{w}_h)]}{\geq} \|\boldsymbol{w}_h\| .$$

However, also discretizations with $\boldsymbol{\varepsilon}(\boldsymbol{u}_h) \notin \widehat{\boldsymbol{P}}_h$, like the *enhanced assumed strain (EAS)* methods, can be constructed and we refer to [SR90, BCR04].

Considering the mixed approximation (6.6), we remark that the construction of numerical approximation schemes is not straight forward in the $H(\mathrm{div})$-spaces. Even for the elasticity problem, the construction of conforming finite element spaces in $\Sigma(\boldsymbol{t}_N) \times L^2(\Omega, \mathbb{R}^d)$ with piecewise polynomial structure has only been partly realized. For $d = 2$, the first stable conforming element on triangles was given in [AW02] and in [AW03], a corresponding non-conforming variant was presented. On tetrahedral meshes, a conforming element with 162 degrees of freedom per element was introduced in [AC05]. The construction of such elements is based on the differential calculus as presented in [AFW06a, AFW06b] and summarized in [AFW06c]. However, within the context of composite elements (i.e. approximation of $\boldsymbol{\sigma}$ and $\boldsymbol{u}$ on different triangulations), stable finite elements have been derived earlier [JM79].

One particular difficulty is the symmetry of the stress tensor and in order to circumvent this difficulty, symmetry may only be imposed weakly by means of the additional constraint $\boldsymbol{\sigma} = \boldsymbol{\sigma}^T$ at the cost of augmenting the corresponding system by this equation. One member of this family is the PEERS-element [ABDJ84] for $d = 2$ and for a construction in $d = 3$, we refer to [AFW07].

3. Quadrature and Discrete Spaces

Within the finite element method, integrals are typically approximated by a quadrature rule of sufficient accuracy. Therefore, let $\Xi \subset \Omega$ be a set of quadrature points and for each $\boldsymbol{\xi} \in \Xi$, the corresponding quadrature weight is denoted by $\omega_{\boldsymbol{\xi}}$. For a continuous function $g : \Omega \to \mathbb{R}$, the quadrature rule is then given via

$$\int_\Omega g(x) \, dx \approx \sum_{\boldsymbol{\xi} \in \Xi} \omega_{\boldsymbol{\xi}} g(\boldsymbol{\xi}) .$$

With a slight abuse of notation, we treat the above approximation as an equality, i.e. we will always interpret the integral sign as the finite sum over the quadrature points if we work with spatially discrete quantities. This is convenient in a finite element context

since the error caused by quadrature is typically of higher order and therefore neglectable provided that the coefficients are smooth and the quadrature has a sufficiently high accuracy. Throughout this work, we use *Gaussian quadrature* rules due to their numerical stability and accuracy. Particularly, we have $\omega_{\boldsymbol{\xi}} > 0$ for Gaussian quadrature rules. Based on the quadrature points Ξ, we introduce the discrete spaces

$$\boldsymbol{P}_h = \{\boldsymbol{\sigma}_h : \Xi \to \mathrm{Sym}(d)\}\,,$$
$$\Lambda_h = \{\lambda_h : \Xi \to \mathbb{R}^p\}\,,$$

with $p \in \mathbb{N}$ determined by the underlying application. We remark that Σ_h and Λ_h are not finite element spaces in general. However, particular choices of the quadrature rule allow the interpretation as finite element spaces. One such example is when the quadrature rule is defined cell-wise (or element-wise, respectively), and on each $C \in \mathcal{C}$, we use the approximation $\int_C g(x)\,dx \approx |C| g(\boldsymbol{\xi}_C)$ with $\boldsymbol{\xi}_C$ being the center of mass of C and $|C|$ denoting the volume of C. This quadrature rule is exact for piecewise linear functions and we have $\boldsymbol{P}_h \cong \widehat{\boldsymbol{P}}_h$. If paired with $\widehat{\boldsymbol{X}}_h(\boldsymbol{u}_D)$, the approximation in $\widehat{\boldsymbol{P}}_h \times \widehat{\boldsymbol{X}}_h(\boldsymbol{u}_D)$ is stable (cf. the previous section).

In $\boldsymbol{P}_h$, we define the norms

$$\|\boldsymbol{\sigma}_h\|_{\boldsymbol{P}_h} = \left(\sum_{\boldsymbol{\xi} \in \Xi} \omega_{\boldsymbol{\xi}} |\boldsymbol{\sigma}_h(\boldsymbol{\xi})|^2\right)^{1/2}\,, \qquad \|\boldsymbol{\sigma}_h\|_{\Sigma_h} = \left(\sum_{\boldsymbol{\xi} \in \Xi} \omega_{\boldsymbol{\xi}} \boldsymbol{\sigma}_h(\boldsymbol{\xi}) : \mathbb{C}^{-1}[\boldsymbol{\sigma}_h(\boldsymbol{\xi})]\right)^{1/2}\,,$$

and the two norms can be interpreted as discrete L^2-norms being the counterparts of $\|\cdot\|_{\boldsymbol{P}}$ and $\|\cdot\|_{\boldsymbol{\Sigma}}$.

We also remark on the symmetric gradient operator $\boldsymbol{\varepsilon} : \boldsymbol{V} \to \boldsymbol{P}$ as defined in (2.2). Since functions in $\boldsymbol{V}_h$ are continuous, $\boldsymbol{\varepsilon}(\cdot)$ is well-defined as an operator from $\boldsymbol{V}_h \to \boldsymbol{P}_h$ and

$$\boldsymbol{\varepsilon}(\boldsymbol{u}_h)(\boldsymbol{\xi}) = \tfrac{1}{2}\big(D\boldsymbol{u}_h(\boldsymbol{\xi}) + D\boldsymbol{u}_h(\boldsymbol{\xi})^T\big)\,.$$

In view of the quadrature formula, we can also define a pair of dual operators $B_h : \boldsymbol{P}_h \to \boldsymbol{V}_h^*$ and $B_h^* : \boldsymbol{V}_h \to \boldsymbol{P}_h^*$ by setting

$$\langle B_h \boldsymbol{\eta}_h, \boldsymbol{w}_h \rangle_{\boldsymbol{V}_h^* \times \boldsymbol{V}_h} = \langle B_h^* \boldsymbol{w}_h, \boldsymbol{\eta}_h \rangle_{\boldsymbol{P}_h^* \times \boldsymbol{P}_h} = -\int_\Omega \boldsymbol{\eta}_h(x) : \boldsymbol{\varepsilon}(\boldsymbol{w}_h(x))\,dx\,, \tag{6.8}$$

and we refer to (2.15) for the definition of B and B^* in the continuous setting. Whereas B_h can be interpreted as a discrete divergence operator, B_h^* corresponds to a discrete (negative) symmetric gradient operator. However note that B_h cannot be evaluated directly, since $\boldsymbol{P}_h$ is not a finite element space permitting the evaluation of the divergence (the same holds true for the piecewise constant functions in $\widehat{\boldsymbol{P}}_h$).

Analogous to the continuous setting, we also define operators

$$\begin{aligned} A_h : \boldsymbol{P}_h \to \boldsymbol{P}_h^*\,, &\qquad \langle A_h \boldsymbol{\sigma}_h, \boldsymbol{\eta}_h \rangle_{\boldsymbol{P}_h^* \times \boldsymbol{P}_h} = \int_\Omega \mathbb{C}^{-1}[\boldsymbol{\sigma}_h(x)] : \boldsymbol{\eta}_h(x)\,dx\,, \\ R_h : \boldsymbol{P}_h \to \boldsymbol{P}_h\,, &\qquad (R_h(\boldsymbol{\sigma}_h))(\boldsymbol{\xi}) = R(\boldsymbol{\sigma}_h(\boldsymbol{\xi}))\,, \end{aligned} \tag{6.9}$$

and identifying $\boldsymbol{P}_h$ and $\boldsymbol{P}_h^*$ results in $(A_h \boldsymbol{\sigma}_h)(\boldsymbol{\xi}) = \mathbb{C}^{-1}[\boldsymbol{\sigma}_h(\boldsymbol{\xi})]$. Likewise, the inverse operator $A_h^{-1} : \boldsymbol{P}_h^* \to \boldsymbol{P}_h$ locally corresponds to the application of the elasticity tensor. Finally, R_h gathers the response functions at the quadrature points and as a consequence of Assumption 6.1, we find that R_h is Lipschitz continuous.

4. Discrete Problem Formulation

Due to the difficulties of approximating $(\boldsymbol{\sigma}, \boldsymbol{u})$ in $H(\mathrm{div}, \Omega, \mathrm{Sym}(d)) \times L^2(\Omega, \mathbb{R}^d)$, we restrict ourselves to the displacement formulation (6.2) and the mixed formulation (6.5) in $\boldsymbol{P} \times \boldsymbol{X}$. Having a specific application in mind, we will also consider individually adapted problem settings like in Chapter 9. When working in the discrete setting, we tacitly replace $\boldsymbol{\tau} \in \boldsymbol{P}$ by its discrete counterpart $\boldsymbol{\tau}_h \in \boldsymbol{P}_h$. This is reasonable since either $\boldsymbol{\tau} = 0$ or $\boldsymbol{\tau} = \varepsilon_p^{n-1}$ and in the latter case, ε_p^{n-1} is typically a discrete quantity within a computational framework.

4.1. Displacement Formulation. The discrete counterpart of (6.2) is the problem of finding $\boldsymbol{u}_h \in \boldsymbol{X}_h(\boldsymbol{u}_D)$ such that

$$\int_\Omega R\big(\mathbb{C}[\boldsymbol{\varepsilon}(\boldsymbol{u}_h(x)) - \boldsymbol{\tau}_h(x)]\big) : \boldsymbol{\varepsilon}(\boldsymbol{w}_h(x))\, dx = \ell(\boldsymbol{w}_h)\,, \qquad \boldsymbol{w}_h \in \boldsymbol{X}_h\,. \tag{6.10}$$

We once more remark that the integral represents a quadrature rule and with

$$\langle F_h(\boldsymbol{u}_h), \boldsymbol{w}_h \rangle_{\boldsymbol{X}_h^* \times \boldsymbol{X}_h} = \int_\Omega R\big(\mathbb{C}[\boldsymbol{\varepsilon}(\boldsymbol{u}_h(x)) - \boldsymbol{\tau}_h(x)]\big) : \boldsymbol{\varepsilon}(\boldsymbol{w}_h(x))\, dx - \ell(\boldsymbol{w}_h)\,, \tag{6.11}$$

the problem is equivalent to the nonlinear operator equation

$$F_h(\boldsymbol{u}_h) = 0\,, \qquad \boldsymbol{u}_h \in \boldsymbol{X}_h(\boldsymbol{u}_D)\,. \tag{6.12}$$

In terms of the operators defined in the last section, F_h can be represented as

$$F_h(\boldsymbol{u}_h) = -B_h R_h\big(A_h^{-1}(-B_h^* \boldsymbol{u}_h - \boldsymbol{\tau}_h)\big) - \ell_h\,,$$

with ℓ_h being the restriction of ℓ to $\boldsymbol{X}_h$.

4.2. Mixed Formulation. We present the mixed formulation in $\widehat{\boldsymbol{P}}_h \times \widehat{\boldsymbol{X}}_h$ being a finite element formulation, and the formulation in $\boldsymbol{P}_h \times \boldsymbol{X}_h$ which is not a finite element discretization since $\boldsymbol{P}_h$ is not a function space. Both formulations are closely related with the displacement formulation.

4.2.1. *Mixed Formulation in* $\widehat{\boldsymbol{P}}_h \times \widehat{\boldsymbol{X}}_h$. We seek $(\boldsymbol{\sigma}_h, \boldsymbol{u}_h) \in \widehat{\boldsymbol{P}}_h \times \widehat{\boldsymbol{X}}_h$ such that for all $(\boldsymbol{\eta}_h, \boldsymbol{w}_h) \in \widehat{\boldsymbol{P}}_h \times \widehat{\boldsymbol{X}}_h$

$$\int_\Omega \boldsymbol{\eta}_h(x) : \mathbb{C}^{-1}[\boldsymbol{\sigma}_h(x)]\, dx - \int_\Omega \boldsymbol{\eta}_h(x) : \mathbb{C}^{-1}\big[R\big(\mathbb{C}[\boldsymbol{\varepsilon}(\boldsymbol{u}_h(x)) - \boldsymbol{\tau}_h(x)]\big)\big]\, dx = 0\,,$$

$$\int_\Omega \boldsymbol{\sigma}_h(x) : \boldsymbol{\varepsilon}(\boldsymbol{w}_h(x))\, dx = \ell(\boldsymbol{w}_h)\,. \tag{6.13}$$

With the bilinear forms $a(\cdot, \cdot)$ and $b(\cdot, \cdot)$, this is equivalent to the conditions

$$a(\boldsymbol{\sigma}_h - R(\mathbb{C}[\boldsymbol{\varepsilon}(\boldsymbol{u}_h) - \boldsymbol{\tau}_h]), \boldsymbol{\eta}_h) = 0\,, \qquad\qquad b(\boldsymbol{\sigma}_h, \boldsymbol{w}_h) = -\ell(\boldsymbol{w}_h)\,,$$

for all $\boldsymbol{\eta}_h \in \widehat{\boldsymbol{P}}_h$ and $\boldsymbol{w}_h \in \widehat{\boldsymbol{X}}_h$. We observe that $\boldsymbol{\sigma}_h$ is just the orthogonal L^2-projection of the response $R(\mathbb{C}[\boldsymbol{\varepsilon}(\boldsymbol{u}_h) - \boldsymbol{\tau}_h])$ onto the subspace of piecewise constant functions $\widehat{\boldsymbol{P}}_h$. We denote this projection by $P^h : \boldsymbol{P} \to \widehat{\boldsymbol{P}}_h$ and $\boldsymbol{\sigma}_h = P^h \boldsymbol{\sigma}$ is defined via $a(\boldsymbol{\sigma} - \boldsymbol{\sigma}_h, \boldsymbol{\eta}_h) = 0$ for all $\boldsymbol{\eta}_h \in \widehat{\boldsymbol{P}}_h$. Using P^h, it is possible to reduce the system to

$$\int_\Omega P^h\big(R(\mathbb{C}[\boldsymbol{\varepsilon}(\boldsymbol{u}_h(x)) - \boldsymbol{\tau}_h(x)])\big) : \boldsymbol{\varepsilon}(\boldsymbol{w}_h(x))\, dx = \ell(\boldsymbol{w}_h)\,, \qquad \boldsymbol{w}_h \in \widehat{\boldsymbol{X}}_h\,.$$

Apart from the projection P^h, this coincides with (6.10). We remark that the projection P^h can be computed cell-wise via

$$\boldsymbol{\sigma}_h\big|_C(x) = \frac{1}{|C|}\int_C R(\mathbb{C}[\boldsymbol{\varepsilon}(\boldsymbol{u}_h(x)) - \boldsymbol{\tau}_h(x)])\,dx\,.$$

On simplical meshes and if $\boldsymbol{\tau}_h \in \widehat{\boldsymbol{P}}_h$, the projection P^h can essentially be omitted as $\boldsymbol{\varepsilon}(\boldsymbol{u}_h) \in \widehat{\boldsymbol{P}}_h$.

4.2.2. *Mixed Formulation in* $\boldsymbol{P}_h \times \boldsymbol{X}_h$. Find $(\boldsymbol{\sigma}_h, \boldsymbol{u}_h) \in \boldsymbol{P}_h \times \boldsymbol{X}_h$ such that for all $(\boldsymbol{\eta}_h, \boldsymbol{w}_h) \in \boldsymbol{P}_h \times \boldsymbol{X}_h$

$$\int_\Omega \boldsymbol{\eta}_h(x) : \mathbb{C}^{-1}[\boldsymbol{\sigma}_h(x)]\,dx - \int_\Omega \boldsymbol{\eta}_h(x) : \mathbb{C}^{-1}\big[R\big(\mathbb{C}[\boldsymbol{\varepsilon}(\boldsymbol{u}_h(x)) - \boldsymbol{\tau}_h(x)]\big)\big]\,dx = 0\,,$$

$$\int_\Omega \boldsymbol{\sigma}_h(x) : \boldsymbol{\varepsilon}(\boldsymbol{w}_h(x))\,dx = \ell(\boldsymbol{w}_h)\,.$$

The stress $\boldsymbol{\sigma}_h$ can be evaluated independently at each quadrature point, i.e.

$$\boldsymbol{\sigma}_h(\boldsymbol{\xi}) = R(\mathbb{C}[\boldsymbol{\varepsilon}(\boldsymbol{u}_h(\boldsymbol{\xi})) - \boldsymbol{\tau}_h(\boldsymbol{\xi})])\,, \qquad \boldsymbol{\xi} \in \boldsymbol{\Xi}\,,$$

Using the explicit representation of $\boldsymbol{\sigma}_h$, after substitution into the weak equilibrium equation, we obtain the displacement formulation (6.10).

Due to the close relation between the displacement formulation and the mixed formulations given here, we will henceforth concentrate on the displacement formulation.

5. Accuracy of the Finite Element Method

The accuracy of finite element approximations has been considered for associated plasticity models. As we have already seen, there is more than one way of stating the problem of associated plasticity. Similarly, error estimates were obtained in different settings as well as for static and quasi-static problems, whereas for the latter, also errors due to time discretization were considered.

5.1. Associated Hardening Plasticity. The problems of hardening plasticity are elaborately discussed in [HR95, HR99], to which we refer for a detailed discussion.

5.1.1. *Convergence under Full Regularity.* Considering kinematic hardening in the static scenario, the solution has the regularity

$$((\boldsymbol{\sigma}, \boldsymbol{\zeta}), \boldsymbol{\varepsilon}_p, \boldsymbol{u}) \in \boldsymbol{P}^2 \times \boldsymbol{P} \times \boldsymbol{X}(\boldsymbol{u}_D)\,.$$

In [HR95, HR99], error estimates have been derived for the quasi-static problem for both $((\boldsymbol{\sigma}, \boldsymbol{\zeta}), \boldsymbol{u})$ and $(\boldsymbol{\varepsilon}_p, \boldsymbol{u})$, corresponding to a mixed formulation of the dual problem and the variational formulation of the extended primal problem presented in Section 3.3. For the mixed formulation of the dual problem in $\widehat{\boldsymbol{P}}_h^2 \times \widehat{\boldsymbol{X}}_h(\boldsymbol{u}_D)$, optimal error estimates were obtained under full regularity, i.e.

$$\|\boldsymbol{\sigma} - \boldsymbol{\sigma}_h\|_{\boldsymbol{P}} + \|\boldsymbol{\zeta} - \boldsymbol{\zeta}_h\|_{\boldsymbol{P}} + \|\boldsymbol{u} - \boldsymbol{u}_h\|_{\boldsymbol{V}} \leq C\,h\,,$$

with C independent of h but depending on the solution $(\boldsymbol{\sigma}, \boldsymbol{\zeta}, \boldsymbol{u})$. However, in the variational inequality formulation for $(\boldsymbol{u}_h, \boldsymbol{\varepsilon}_{p,h})$ in $\widehat{\boldsymbol{P}}_h \times \widehat{\boldsymbol{X}}_h(\boldsymbol{u}_D)$, they were only able to show $\|\boldsymbol{u} - \boldsymbol{u}_h\|_{\boldsymbol{V}} + \|\boldsymbol{\varepsilon}_p - \boldsymbol{\varepsilon}_{p,h}\|_{\boldsymbol{P}} \leq C\,h^{1/2}$. This suboptimal error estimate was improved in [ACZ99] to the optimal estimate

$$\|\boldsymbol{u} - \boldsymbol{u}_h\|_{\boldsymbol{V}} + \|\boldsymbol{\varepsilon}_p - \boldsymbol{\varepsilon}_{p,h}\|_{\boldsymbol{P}} \leq C\,h\,.$$

However, these results were not the first convergence results. In [**Joh78**], convergence of the stress was proven, and in [**RX96**, Section 3], optimal convergence of the displacement was proven by duality techniques, i.e. $\|\boldsymbol{u} - \boldsymbol{u}_h\|_{\boldsymbol{V}} \leq C\,h$.

We also remark that besides the above mentioned a priori estimates, there exists a corresponding a posteriori theory. For the variational inequality formulation in $(\boldsymbol{u}, \boldsymbol{\varepsilon}_p)$, this was developed in [**ACZ99**], whereas duality-based error estimators were considered in [**RX96**].

5.1.2. *Convergence under Minimal Regularity.* Convergence with a rate always requires extra regularity of the solutions. Nevertheless, it is also possible to show convergence without this regularity. This was done in [**HR00**] and a different approach relying on Γ-convergence was presented in [**MRS08, MR09, Mie08**].

5.2. Perfect Plasticity. Contrary to hardening plasticity, perfect plasticity does not admit a solution $\boldsymbol{u} \in \boldsymbol{X}(\boldsymbol{u}_D)$ but only in the weaker space $BD(\Omega)$. Nevertheless, the stress tensor always satisfies $\boldsymbol{\sigma} \in \boldsymbol{P}$ (provided that a solution exists). Thus, one is tempted to consider convergence of the stresses only. This was done in [**Rep96**] where a convergence result for the (static) model problem of von Mises plasticity was achieved. The result is based on a regularization by hardening and a suitable coupling between the hardening parameter and the mesh size parameter h. Denoting the regularization parameter by δ, under certain (local) regularity assumptions on the solution, it is possible to show that there is a function $\delta(h)$ such that $\|\boldsymbol{\sigma}^{\delta(h)} - \boldsymbol{\sigma}\|_{\boldsymbol{P}}$ converges, where $\boldsymbol{\sigma}^{\delta(h)}$ is the solution of the regularized problem with regularization parameter $\delta(h)$ and $\boldsymbol{\sigma}$ is the solution of perfect plasticity.

CHAPTER 7

A SEMISMOOTH NEWTON APPROACH TO PLASTICITY

In this chapter, we consider a generalized Newton method for the solution of the displacement problem (6.10). We prove locally superlinear convergence results for certain discrete plasticity problems arising from discretization as introduced in the previous chapter. However, superlinear convergence in a function space setting cannot be shown in general as in this case, superlinear convergence of generalized Newton methods for nonsmooth equations typically relies on some smoothing properties of the involved mappings. While this smoothing property is fulfilled for certain optimal control problems (via the control-to-state mapping), this property cannot be expected for plasticity problems in general. We will come back to this topic several times in this chapter. As we only consider local convergence, we do not use any underlying structure of the equations like the duality framework of associated plasticity. Therefore, the results in this chapter also apply to non-associated plasticity. Structure exploiting algorithms for associated plasticity, leading to an improved global performance, are considered in the next chapter. We close the chapter by considering von Mises and (non-) associated (smoothed) Drucker-Prager plasticity for which we prove superlinear convergence in the discrete setting.

At this point we also refer to Appendix A for necessary notation concerning results from nonsmooth analysis.

1. Problem Formulation

In this chapter, we focus on the discrete displacement formulation (6.10)

$$\int_\Omega R\big(\mathbb{C}[\boldsymbol{\varepsilon}(\boldsymbol{u}_h(x)) - \boldsymbol{\tau}_h(x)]\big) : \boldsymbol{\varepsilon}(\boldsymbol{w}_h(x))\, dx = \ell(\boldsymbol{w}_h)\,, \qquad \boldsymbol{w}_h \in \boldsymbol{X}_h\,,$$

(where as usual, the integral represents a Gaussian quadrature formula) and its equivalent operator formulation $F_h(\boldsymbol{u}_h) = 0$ given in (6.12). In the following, we assume that $\boldsymbol{\tau}_h \in \boldsymbol{P}_h$ is given. We observe that the only nonlinearity is the response function R, which we only assume to be Lipschitz continuous but which is not necessarily differentiable, cf. Assumption 6.1. Being Lipschitz continuous, it follows from Rademacher's theorem [**CLSW98**, Section 3.4] that except on a set of measure zero, F_h is differentiable. Hence,

---

Algorithm 7.1 Generic generalized Newton algorithm for plasticity problems

S0)   Choose $\boldsymbol{u}_h^0 \in \boldsymbol{X}_h(\boldsymbol{u}_D)$, $\epsilon \geq 0$, and set $k := 1$.

S1)   If $\|F_h(\boldsymbol{u}_h^{k-1})\|_{\boldsymbol{X}_h^*} \leq \epsilon$, stop and set $\boldsymbol{u}_h^* = \boldsymbol{u}_h^{k-1}$.

S2)   Choose an element $G_h \in \partial F_h(\boldsymbol{u}_h^{k-1})$.

S3)   Solve $G_h \Delta \boldsymbol{u}_h^k = -F_h(\boldsymbol{u}_h^{k-1})$ for $\Delta \boldsymbol{u}_h^k \in \boldsymbol{X}_h$.

S4)   Set $\boldsymbol{u}_h^k = \boldsymbol{u}_h^{k-1} + \Delta \boldsymbol{u}_h^k$ and $k := k + 1$. Go to S1).

---

we can evaluate the generalized Jacobian of F_h (see Section A.1 and particularly equation (A.1)), and we find

$$\partial F_h(\boldsymbol{u}_h) = -B_h \partial R_h \big(A_h^{-1}(-B_h^* \boldsymbol{u}_h - \boldsymbol{\tau}_h) \big) A_h^{-1}(-B_h^*) \subset L(\boldsymbol{X}_h, \boldsymbol{X}_h^*). \tag{7.1}$$

Based on this results, Algorithm 7.1 is the adaption of the generic Algorithm A.1 to the current situation.

Looking at (7.1), we see that it suffices to choose an element $S_h \in \partial R_h(\cdot) \subset L(\boldsymbol{P}_h, \boldsymbol{P}_h)$ to determine G_h in step S2) of Algorithm 7.1. Each $S_h \in \partial R_h(\cdot)$ is block-diagonal since R_h is a local (or point-wise) operator by definition (6.9), and for $\boldsymbol{\eta} \in \boldsymbol{P}_h$ and $\boldsymbol{\xi} \in \boldsymbol{\Xi}$, we find $(\partial R_h(\boldsymbol{\eta}))(\boldsymbol{\xi}) = \partial R(\boldsymbol{\eta}(\boldsymbol{\xi}))$ with the response function $R : \operatorname{Sym}(d) \to \operatorname{Sym}(d)$. Thus, in order to compute an element of $\partial R_h(\cdot)$, it is sufficient to compute an element $\mathbb{S} \in \partial R(\cdot)$ of the generalized Jacobian of the response function.

For $k \geq 1$, we define the *consistent tangent modulus* $\mathbb{C}_{\mathrm{ct}}^k(\boldsymbol{\xi}) \in L(\operatorname{Sym}(d), \operatorname{Sym}(d))$ by

$$\mathbb{C}_{\mathrm{ct}}^k(\boldsymbol{\xi}) = \mathbb{S}(\boldsymbol{\xi}) \circ \mathbb{C}, \qquad \text{with} \qquad \mathbb{S}(\boldsymbol{\xi}) \in \partial R(\mathbb{C}[\boldsymbol{\varepsilon}(\boldsymbol{u}_h^{k-1}(\boldsymbol{\xi})) - \boldsymbol{\tau}_h(\boldsymbol{\xi})]), \tag{7.2}$$

and this defines $G_h \in L(\boldsymbol{X}_h, \boldsymbol{X}_h^*)$ in the k-th iteration via

$$\langle G_h \boldsymbol{v}_h, \boldsymbol{w}_h \rangle_{\boldsymbol{X}_h^* \times \boldsymbol{X}_h} = \int_\Omega \mathbb{C}_{\mathrm{ct}}^k(x) \big[\boldsymbol{\varepsilon}(\boldsymbol{v}_h(x)) \big] : \boldsymbol{\varepsilon}(\boldsymbol{w}_h(x)) \, dx.$$

With this choice of G_h, step S3) in the algorithm consists of finding $\Delta \boldsymbol{u}_h^k \in \boldsymbol{X}_h$ such that

$$\int_\Omega \mathbb{C}_{\mathrm{ct}}^k(x) \big[\boldsymbol{\varepsilon}(\Delta \boldsymbol{u}_h^k(x)) \big] : \boldsymbol{\varepsilon}(\boldsymbol{w}_h(x)) \, dx = -r^{k-1}(\boldsymbol{w}_h), \qquad \boldsymbol{w}_h \in \boldsymbol{X}_h, \tag{7.3}$$

with the residual $r^{k-1}(\boldsymbol{w}_h) = \langle F(\boldsymbol{u}_h^{k-1}), \boldsymbol{w}_h \rangle_{\boldsymbol{X}_h^* \times \boldsymbol{X}_h}$,

$$r^{k-1}(\boldsymbol{w}_h) = \int_\Omega R\big(\mathbb{C}[\boldsymbol{\varepsilon}(\boldsymbol{u}_h^{k-1}(x)) - \boldsymbol{\tau}_h(x)] \big) : \boldsymbol{\varepsilon}(\boldsymbol{w}_h(x)) \, dx - \ell(\boldsymbol{w}_h).$$

Finally, step S4) is the usual update.

1.1. Infinite Dimensional Setting. Looking at (7.3) and (7.2), we see that these equations have a spatially continuous analogue, i.e. for given $\boldsymbol{u}^{k-1} \in \boldsymbol{X}(\boldsymbol{u}_D)$, determine $\Delta \boldsymbol{u}^k \in \boldsymbol{X}$ such that

$$\int_\Omega \mathbb{C}_{\mathrm{ct}}^k(x) \big[\boldsymbol{\varepsilon}(\Delta \boldsymbol{u}^k(x)) \big] : \boldsymbol{\varepsilon}(\boldsymbol{w}(x)) \, dx = -r^{k-1}(\boldsymbol{w}), \qquad \boldsymbol{w} \in \boldsymbol{X},$$

with $r^{k-1} = F(\boldsymbol{u}^{k-1}) \in \boldsymbol{X}^*$ and the consistent tangent modulus

$$\mathbb{C}_{\mathrm{ct}}^k(x) = \mathbb{S}(x) \circ \mathbb{C}, \qquad \text{with} \qquad \mathbb{S}(x) \in \partial R(\mathbb{C}[\boldsymbol{\varepsilon}(\boldsymbol{u}^{k-1}(x)) - \boldsymbol{\tau}(x)]), \qquad \text{a.e. in } \Omega.$$

But as the focus of this chapter is set on showing superlinear convergence, we mostly restrict ourselves to the discrete setting and only comment on the occuring difficulties in a function space setting.

2. Local Superlinear Convergence under Semismoothness Assumptions

Throughout this section, we will consider the convergence of the generalized Newton method under the assumption that F_h is semismooth, viz. F_h is locally Lipschitz and directionally differentiable and for any $G_h \in \partial F_h(\boldsymbol{u}_h + \boldsymbol{w}_h)$:

$$\|F_h(\boldsymbol{u}_h + \boldsymbol{w}_h) - F(\boldsymbol{u}_h) - G_h \boldsymbol{w}_h\|_{\boldsymbol{X}_h^*} = o(\|\boldsymbol{w}_h\|_{\boldsymbol{X}_h}) \qquad \text{as} \quad \boldsymbol{w}_h \to 0 \,.$$

If $o(\|\boldsymbol{w}_h\|_{\boldsymbol{X}_h})$ is replaced by $O(\|\boldsymbol{w}_h\|_{\boldsymbol{X}_h}^{1+p})$, we say that F_h is semismooth of order $p \in (0, 1]$. We also refer to Proposition A.2 for different characterizations of semismoothness. Looking back at the definition of F_h in Section 6.4, it is easy to see that F_h is semismooth if and only if the response function R is semismooth. Concerning examples, we refer to the last section of the present chapter.

2.1. Local Superlinear Convergence. Assuming that the elements of the generalized Jacobian in the solution are regular, we are able to show superlinear convergence of the generalized Newton method given in Algorithm 7.1.

Theorem 7.1. *Let F_h as defined in (6.11) be semismooth (of order $p \in (0, 1]$) and let $\boldsymbol{u}_h^* \in \boldsymbol{X}_h(\boldsymbol{u}_D)$ be a zero of F_h. If each $G_h \in \partial F_h(\boldsymbol{u}_h^*)$ is regular (i.e. F_h is CD-regular in $\boldsymbol{u}_h^*$), then the generalized Newton method converges locally superlinear (with order $1 + p$) to the solution $\boldsymbol{u}_h^*$ provided that $\|\boldsymbol{u}_h^* - \boldsymbol{u}_h^0\|_{\boldsymbol{X}_h}$ is sufficiently small.*

PROOF. This is simply a restatement of Theorem A.7 applied to the current situation. Specifically, Proposition A.1 guarantees the well-posedness of the iteration in a neighborhood of the solution since the CD-regularity in the solutions guarantees the regularity of ∂F in that neighborhood. $\qquad\square$

We remark that without further assumptions, the existence of a solution $\boldsymbol{u}_h^*$ is not guaranteed, cf. the simple example in Appendix B. And even if a solution exists, it may not be unique in general.

2.2. Local Superlinear Convergence under Strong Monotonicity. Under the assumption of strong monotonicity of F_h, i.e. there exists $\beta > 0$ such that

$$\langle F_h(\boldsymbol{u}_h) - F_h(\boldsymbol{w}_h), \boldsymbol{u}_h - \boldsymbol{w}_h \rangle_{\boldsymbol{X}_h^* \times \boldsymbol{X}_h} \geq \frac{\beta}{2} \|\boldsymbol{u}_h - \boldsymbol{w}_h\|_{\boldsymbol{X}_h}^2 \,,$$

we are able to guarantee superlinear convergence under semismoothness assumptions. In order to do so, we need the following result relating strong monotonicity to the regularity of elements of the generalized Jacobian.

Proposition 7.2. *Let $F_h : \boldsymbol{X}_h \to \boldsymbol{X}_h^*$ be Lipschitz continuous. Then:*

1. *F_h is monotone if and only if for every $\boldsymbol{w}_h \in \boldsymbol{X}_h$, all sub-gradients $G_h \in \partial F_h(\boldsymbol{w}_h)$ are positive semidefinite.*
2. *F_h is strongly monotone if and only if for every $\boldsymbol{w}_h \in \boldsymbol{X}_h$, all sub-gradients $G_h \in \partial F_h(\boldsymbol{w}_h)$ are positive definite.*

PROOF. Part (1) has been shown in [LS96] and the extension of the result to strongly monotone mappings is straightforward. $\qquad\square$

We remark that the above usage of the term positive (semi-) definite does not necessarily imply symmetry of the sub-gradients G_h. The above results guarantees the superlinear convergence provided that F_h is strongly monotone.

Theorem 7.3. *Let F_h be semismooth (of order $p \in (0,1]$) and suppose that F_h is strongly monotone. Then, the solution of (6.12) is unique and the generalized Newton method converges locally superlinear (with rate $1 + p$) to the solution.*

PROOF. The unique solvability even holds for the continuous case and transfers to the discrete setting. Concerning local superlinear convergence (with rate $1 + p$), we need to verify the conditions of Theorem 7.1. By Proposition 7.2(2), we know that all $G_h \in \partial F_h(\cdot)$ are regular. This implies that the linear problem (7.3) has a unique solution and $\Delta \boldsymbol{u}_h^k$ is well-defined. The semismoothness of F_h then yields local superlinear convergence (with rate $1 + p$) as a result of Theorem 7.1. $\square$

2.3. Infinite Dimensional Setting. We close the section with some remarks concerning the spatially continuous setting, i.e. $F : \boldsymbol{X} \to \boldsymbol{X}^*$. As Rademacher's theorem is no longer applicable, the generalized Jacobian cannot be defined. Nevertheless, there have been attempts to find suitable replacements of the generalized Jacobian in an infinite dimensional setting, cf. [HPUU09, Ulb03]. Following Section (A.1), it would be sufficient to find a family of mappings $G : \boldsymbol{X} \to L(\boldsymbol{X}, \boldsymbol{X}^*)$ such that

$$\|F(\boldsymbol{u} + \boldsymbol{w}) - F(\boldsymbol{u}) - G(\boldsymbol{u} + \boldsymbol{w})\boldsymbol{w}\|_{\boldsymbol{X}^*} = o(\|\boldsymbol{w}\|_{\boldsymbol{X}}) \qquad \text{as} \quad \boldsymbol{w} \to 0,$$

for all $\boldsymbol{u}$ close to a solution. If all $G(\boldsymbol{u})$ are nonsingular in a neighborhood of a solution, then the generalized Newton method as indicated in Algorithm A.1 would result in superlinear convergence. We will come back to this point later in Section 7.4 when we consider associated von Mises plasticity.

3. Application to Plasticity Problems

We apply the above convergence results to the plasticity problems considered in the first part of the thesis. For this purpose, we simply have to check the conditions of the theorems for the various problems. The results considerably extend the known results of superlinear convergence in the literature, where it has only been shown for the special case of the von Mises flow rule (with and without hardening).

3.1. Associated Plasticity. The associated plasticity models considered so far comprised the problem of perfect plasticity, kinematic hardening plasticity and the viscoplastic regularization by means of the Moreau-Yosida regularization. The latter can be interpreted as a particular instance of kinematic hardening when considering the static or incremental setting, cf. Subsection 3.2.3. For associated problems, we can assure monotonicity of F_h as it is the derivative of a proper convex functional. Moreover, in these cases the response function is a projection onto a convex set, cf. Table 6.1 for a summary, and under appropriate assumptions on K, the (strong) semismoothness of the projection can be shown, cf. Theorem A.11 and Section A.2.4.

3.1.1. *Perfect Plasticity.* Perfect plasticity was investigated in Section 2.3 and the response function R is the projection P_K onto the admissible set $K \subset \mathrm{Sym}(d)$, see (2.38). We also found that the continuous operator F is monotone but not strongly monotone w.r.t. to the topology in $\boldsymbol{X}$. Under the safe load assumption 2.1, it could be shown that a solution to the primal solution only exists in the space $BD(\Omega)$. Nevertheless, after discretization, we can try to determine $\boldsymbol{u}_h \in \boldsymbol{X}_h(\boldsymbol{u}_D)$ satisfying

$$\int_\Omega P_K\big(\mathbb{C}[\boldsymbol{\varepsilon}(\boldsymbol{u}_h(x)) - \boldsymbol{\tau}_h(x)]\big) : \boldsymbol{\varepsilon}(\boldsymbol{w}_h(x))\,dx = \ell(\boldsymbol{w}_h)\,, \qquad \boldsymbol{w}_h \in \boldsymbol{X}_h\,. \tag{7.4}$$

The existence of a solution depends on the discrete analogue of the safe-load condition 2.1, the Slater condition. For this, we define the admissible set

$$\boldsymbol{K}_h = \{\boldsymbol{\sigma}_h \in \boldsymbol{P}_h : \boldsymbol{\sigma}_h(\boldsymbol{\xi}) \in K, \boldsymbol{\xi} \in \boldsymbol{\Xi}\}. \tag{7.5}$$

Assumption 7.4. *There exist $\widehat{\boldsymbol{\sigma}} \in \boldsymbol{P}_h$ and $\varepsilon > 0$ such that for all $\boldsymbol{\eta} \in \mathrm{Sym}(d)$ with $|\boldsymbol{\eta}| \leq \varepsilon$:*

$$B_h\widehat{\boldsymbol{\sigma}} + \ell_h = 0 \quad in \;\; \boldsymbol{X}_h^* \qquad and \qquad \widehat{\boldsymbol{\sigma}}(\boldsymbol{\xi}) + \boldsymbol{\eta} \in K \quad for\ all\ \;\boldsymbol{\xi} \in \boldsymbol{\Xi}. \tag{7.6}$$

This assumption is the Slater condition for the convex set $\{\boldsymbol{\sigma}_h \in \boldsymbol{P}_h : \boldsymbol{\sigma}_h \in \boldsymbol{K}_h, B_h\boldsymbol{\sigma}_h + \ell_h = 0\}$. By duality, we obtain the existence of a solution to the equation $F_h(\boldsymbol{u}_h) = 0$.

Theorem 7.5. *Under Assumption 7.4, equation (7.4) has a solution $\boldsymbol{u}_h^* \in \boldsymbol{X}_h(\boldsymbol{u}_D)$.*

PROOF. The proof follows by Lagrangian duality as introduced in Section 2.3 for the spatially continuous case. Therefore consider the discrete Lagrangian $L_h : \boldsymbol{P}_h \times \boldsymbol{X}_h \to \overline{\mathbb{R}}$,

$$\begin{aligned}
L_h(\boldsymbol{\sigma}_h, \boldsymbol{u}_h) &= \tfrac{1}{2}\langle A_h\boldsymbol{\sigma}_h, \boldsymbol{\sigma}_h\rangle_{\boldsymbol{P}_h^* \times \boldsymbol{P}_h} + (\boldsymbol{\sigma}_h, \boldsymbol{\tau}_h)_{\boldsymbol{P}_h} + \chi_{\boldsymbol{K}_h}(\boldsymbol{\sigma}_h) \\
&\quad + \langle B_h^*\boldsymbol{u}_h, \boldsymbol{\sigma}_h\rangle_{\boldsymbol{P}_h^* \times \boldsymbol{P}_h} + \ell_h(\boldsymbol{u}_h).
\end{aligned}$$

The resulting minimization problems in duality are:

$$\begin{aligned}
\text{Minimize} &\quad \sup_{\boldsymbol{u}_h \in \boldsymbol{X}_h(\boldsymbol{u}_D)} \{L_h(\boldsymbol{\sigma}_h, \boldsymbol{u}_h)\}, \qquad \boldsymbol{\sigma}_h \in \boldsymbol{P}_h, \\
\text{Minimize} &\quad \sup_{\boldsymbol{\sigma}_h \in \boldsymbol{P}_h} \{-L_h(\boldsymbol{\sigma}_h, \boldsymbol{u}_h)\}, \qquad \boldsymbol{u}_h \in \boldsymbol{X}_h(\boldsymbol{u}_D).
\end{aligned}$$

As long as the admissible set of the dual problem is non-empty, the dual problem for $\boldsymbol{\sigma}_h$ has a unique solution due to the uniform convexity of the objective function and the closedness of the admissible set. If the Slater condition (Assumption 7.4) is fulfilled, there is no duality gap and a Lagrange multiplier $\boldsymbol{u}_h^* \in \boldsymbol{X}_h(\boldsymbol{u}_D)$ exists, solving the primal problem. However, due to the lack of uniform convexity of the primal problem, the solution is not necessarily unique. $\square$

For a introduction to Lagrangian convexity in finite dimensions, we refer to the textbooks [BNO03, BV08]. We have the following result concerning superlinear convergence.

Theorem 7.6. *Let $K \subset \mathrm{Sym}(d)$ be convex. Assume that the projection $P_K : \mathrm{Sym}(d) \to K \subset \mathrm{Sym}(d)$ is semismooth (of order p) and that the Slater condition (Assumption 7.4) holds. Then there exists a solution $\boldsymbol{u}_h^* \in \boldsymbol{X}_h(\boldsymbol{u}_D)$ of the associated perfect plasticity problem and if all elements $G_h \in \partial F_h(\boldsymbol{u}_h^*)$ are regular, then the generalized Newton method converges locally superlinear (with order $1 + p$) to the solution.*

PROOF. The existence follows from Theorem 7.5 and under the assumed assumptions, the superlinear convergence follows from the result of Theorem 7.1 with the response function $R = P_K$. $\square$

3.1.2. *Kinematic Hardening Plasticity.* We shortly repeat some notation from Section 3.2. The hardening modulus is given by $\mathbb{H} \in L(\mathrm{Sym}(d), \mathrm{Sym}(d))$ and we assume $\mathbb{H}$ to be positive definite. For incompressible plasticity, $\mathbb{H}$ only has to be definite on the deviatoric subspace $\mathrm{Sym}_0(d)$, cf. Subsection 3.2.4, but as outlined in this subsection, it is not necessary to treat these two cases individually which is why we restrict ourselves to the fully definite setting. Based on $\mathbb{H}$, the fourth order tensors

$$\mathbb{N} = \mathbb{C} + \mathbb{H}, \qquad \mathbb{D}^{-1} = \mathbb{C}^{-1} + \mathbb{H}^{-1},$$

were defined which are also symmetric and positive definite. The response function was found to be

$$R(\boldsymbol{\eta}) = (\mathbb{D} \circ \mathbb{C}^{-1})[\boldsymbol{\eta}] + (\mathbb{C} \circ \mathbb{N}^{-1})[P_K^N(\boldsymbol{\eta})] \,,$$

with $P_K^N : \mathrm{Sym}(d) \to K \subset \mathrm{Sym}(d)$ being the orthogonal projection onto K in the metric defined by the inner product induced by $\mathbb{N}^{-1}$. The primal problem is the minimization of the hardening functional (3.8) which is uniformly convex and therefore admits a unique solution. Restricting the functional $\mathcal{E}_{\mathrm{hd}}$ to $\boldsymbol{X}_h$ (the Ritz method) leads to the corresponding discrete minimization problem with the necessary and sufficient optimality condition (cf. (3.9)):

$$\int_\Omega \Big((\mathbb{C} \circ \mathbb{N}^{-1}) \big[P_K^N \big(\mathbb{C}[\boldsymbol{\varepsilon}(\boldsymbol{u}_h(x)) - \boldsymbol{\tau}_h(x)] \big) \big] + \mathbb{D}[\boldsymbol{\varepsilon}(\boldsymbol{u}_h(x)) - \boldsymbol{\tau}_h(x)] \Big) : \boldsymbol{\varepsilon}(\boldsymbol{w}_h(x)) \, dx$$
$$= \ell_h(\boldsymbol{w}_h) \,, \qquad \boldsymbol{w}_h \in \boldsymbol{X}_h \,. \tag{7.7}$$

This is indeed equivalent to substituting $R(\mathbb{C}[\boldsymbol{\varepsilon}(\boldsymbol{u}_h(x)) - \boldsymbol{\tau}_h(x)])$ into the displacement formulation (6.10). We have the following result:

Theorem 7.7. *Let $\mathbb{H}$ be a symmetric and positive definite fourth order tensor, $K \subset \mathrm{Sym}(d)$ be convex and assume that $P_K^N : \mathrm{Sym}(d) \to K \subset \mathrm{Sym}(d)$ is semismooth (of order p). Then, there exists a unique $\boldsymbol{u}_h^* \in \boldsymbol{X}_h(\boldsymbol{u}_D)$ satisfying (7.7) and the generalized Newton method converges locally superlinear (with order $p+1$) to the solution.*

PROOF. Since a solution of the continuous problem in $\boldsymbol{X}$ exists and is unique (see Theorem 3.7), we immediately obtain existence and uniqueness of a solution of the corresponding Ritz-method. Since the corresponding functional is uniformly convex and thus F_h is strongly monotone, Theorem 7.3 guarantees the local superlinear convergence (of order $1 + p$) if P_K is semismooth (of order p). □

Once again, for incompressible plasticity, $\mathbb{H}$ only has to be positive definite on the deviatoric subspace of $\mathrm{Sym}(d)$ as a consequence of Proposition 3.10.

3.1.3. *Viscoplasticity.* As observed in Subsection 3.2.3, the viscoplastic regularization is a special instance of hardening plasticity in the static or incremental setting by setting $\mathbb{H} = \frac{1}{\alpha}\mathbb{C}$ in static plasticity and similarly, $\mathbb{H} = \frac{1}{\alpha\Delta t}\mathbb{C}$ in incremental plasticity. Therefore, we obtain the same result as for kinematic hardening, i.e. the generalized Newton method converges locally superlinear if the projection P_K is semismooth. Let $\alpha \in [0, \infty)$ be the regularization parameter. Then, the response function is given as, cf. (3.3),

$$R(\boldsymbol{\eta}) = \frac{1}{1+\widehat{\alpha}}\boldsymbol{\eta} + \frac{\widehat{\alpha}}{1+\widehat{\alpha}}P_K(\boldsymbol{\eta}) \,,$$

with $\widehat{\alpha} = \alpha$ in the static scenario and $\widehat{\alpha} = \alpha\Delta t$ in the incremental setting. According to the theorem in the last subsection, we have the following result.

Corollary 7.8. *Let $\alpha \in [0, \infty)$ be the regularization parameter of the viscoplastic regularization, $K \subset \mathrm{Sym}(d)$ be convex and assume that $P_K : \mathrm{Sym}(d) \to K \subset \mathrm{Sym}(d)$ is semismooth (of order p). Then, there exists a unique solution of $F_h(\boldsymbol{u}_h) = 0$ with the response function as given above, and the generalized Newton method converges locally superlinear (with order $p+1$) to the solution.*

PROOF. We apply Theorem 7.7 with $\mathbb{H} = \frac{1}{\widehat{\alpha}}\mathbb{C}$, and use the equivalence established in Lemma 3.8. □

3.2. Non-Associated Plasticity. We have seen that contrary to associated plasticity, we can now longer rely on monotonicity arguments in general. Whereas under suitable assumptions (like the Slater condition), we could always show existence of a solution of $F_h(\boldsymbol{u}_h) = 0$ in associated plasticity, this is longer possible for non-associated plasticity even in the discrete case. We refer to Appendix B for an elementary (counter-) example. In the static setting, we were able to show existence and uniqueness of solutions for Drucker-Prager plasticity for both hardening plasticity and viscoplasticity, provided that the regularizing terms were large enough. Under this assumption also the incremental hardening problem was well-posed.

Unless regularization is large enough, we can only rely on Theorem 7.1: if the response function is semismooth (of order p), and there exists a solution at which F_h is CD-regular, then we obtain local superlinear convergence (of order $1 + p$).

3.2.1. *Incremental Viscoplasticity.* The situation turned out to be better in incremental quasi-static viscoplasticity, since then, the regularization parameter α was allowed to take arbitrary values as long as the time step size Δt_n was small enough, see Lemma 5.3. But for large α, the restriction of Δt_n was quite strong.

In the context of incremental viscoplasticity, the response function is given as

$$R(\boldsymbol{\eta}) = \tfrac{1}{1+\alpha\Delta t}\boldsymbol{\eta} + \tfrac{\alpha\Delta t}{1+\alpha\Delta t}R_K(\boldsymbol{\eta}),$$

with R_K denoting the response function of non-associated perfect plasticity. As a result of Theorem 5.3, we have the following result.

Theorem 7.9. *Consider $\alpha \in [0, \infty)$ and let the response function R_K of perfect plasticity be semismooth (of order p). Moreover, let the corresponding operator $F_{h,\mathrm{pl}} : \boldsymbol{X}_h \to \boldsymbol{X}_h^*$ of perfect plasticity satisfy*

$$\langle F_{h,\mathrm{pl}}(\boldsymbol{u}_h) - F_{h,\mathrm{pl}}(\boldsymbol{w}_h), \boldsymbol{u}_h - \boldsymbol{w}_h \rangle_{\boldsymbol{X}_h^* \times \boldsymbol{X}_h} \geq -L\|\boldsymbol{u}_h - \boldsymbol{w}_h\|^2,$$

for some $L \in \mathbb{R}$. Then, with the above response function R, there exists a solution $\boldsymbol{u}_h^* \in \boldsymbol{X}_h(\boldsymbol{u}_D)$ of $F_h(\boldsymbol{u}_h) = 0$ if $\alpha\Delta t_n L < 1$, and in this case, the generalized Newton method converges locally superlinear.

PROOF. Obviously, R is semismooth (of order p) if R_K is semismooth (of order p). The existence of a unique solution is due to Theorem 5.3. Moreover, as in the prove of this theorem, it follows that F_h is a strongly monotone operator and we can apply Theorem 7.3. □

4. Application to Specific Material Models

After proceeding in an abstract way so far, we now consider particular choices of the response function. Semismoothness of the response function for general models can be shown with the methods presented in Appendix A. For convenience, we start with the well-understood problem of von Mises plasticity. Afterwards we consider (non-) associated Drucker-Prager plasticity. For all examples, we assume that the elasticity operator $\mathbb{C}$ has the form $\mathbb{C} = 2\mu\mathbb{P}_{\mathrm{dev}} + d\,\kappa\mathbb{P}_{\mathrm{vol}}$, cf. (1.11), with the orthogonal projectors $\mathbb{P}_{\mathrm{dev}}$ and $\mathbb{P}_{\mathrm{vol}}$ as defined in (1.4).

4.1. Von Mises Plasticity / Incompressible Plasticity. The admissible set of von Mises plasticity is defined in terms of the yield function $f(\boldsymbol{\eta}) = |\operatorname{dev}(\boldsymbol{\eta})| - K_0$, see (1.18), i.e.

$$K = \{\boldsymbol{\eta} \in \operatorname{Sym}(d) : f(\boldsymbol{\eta}) \leq 0\} = \{\boldsymbol{\eta} \in \operatorname{Sym}(d) : |\operatorname{dev}(\boldsymbol{\eta})| \leq K_0\}$$

and K is closed and convex. Since the model is incompressible, it only constrains the deviator of $\boldsymbol{\sigma}$. For von Mises plasticity, the projection $P_K : \mathrm{Sym}(d) \to K \subset \mathrm{Sym}(d)$ can be evaluated explicitly. Splitting $\mathrm{Sym}(d)$ into its deviatoric and volumetric subspace by means of the orthogonal projectors $\mathbb{P}_{\mathrm{dev}}$ and $\mathbb{P}_{\mathrm{vol}}$, we see that the projection is the identity on the volumetric subspace and on the deviatoric subspace, the projection is the Euclidian projection onto the sphere with radius K_0. A short computation yields

$$
P_K(\boldsymbol{\eta}) = \boldsymbol{\eta} - \max\{0, f(\boldsymbol{\eta})\} \frac{\mathrm{dev}(\boldsymbol{\eta})}{|\mathrm{dev}(\boldsymbol{\eta})|} = \begin{cases} \boldsymbol{\eta} & , \boldsymbol{\eta} \in K, \\ \boldsymbol{\eta} - f(\boldsymbol{\eta})\frac{\mathrm{dev}(\boldsymbol{\eta})}{|\mathrm{dev}(\boldsymbol{\eta})|} & , \boldsymbol{\eta} \notin K. \end{cases}
$$

Note that formally, the first equality is not well-defined if $|\mathrm{dev}(\boldsymbol{\eta})| = 0$. But in this case, we have $\mathrm{dev}(\boldsymbol{\eta}) = 0$ by the definiteness of the norm and thus $f(\boldsymbol{\eta}) < 0$.

Lemma 7.10. *The orthogonal projection (w.r.t. to an arbitrary inner product) onto K is a PC^1 function and strongly semismooth.*

PROOF. Let $P_K : \mathrm{Sym}(d) \to K \subset \mathrm{Sym}(d)$ be the orthogonal projection w.r.t. the given inner product. To show the semismoothness of P_K, we can apply Theorem A.11 by noting that K can also be described by the C^∞ function $\tilde{f}(\boldsymbol{\eta}) = |\mathrm{dev}(\boldsymbol{\eta})|^2 - K_0^2$ and that the (CRCQ), see Definition (A.10), is trivially fulfilled whenever K is described by a single smooth constraint. Alternatively, by using the strong semismoothness of the function $m(t) = \max\{0, t\}$, see (A.2), the strong semismoothness of P_K can be shown by the chain rule, cf. Proposition A.5. The explicit representation by means of the max-function also establishes the strong semismoothness. $\qquad\square$

The projection P_K is a PC^1 function and $P_K \in C^1(\mathrm{Sym}(d)\setminus\partial K, \mathrm{Sym}(d))$. Hence, it suffices to compute the derivative of P_K for $\boldsymbol{\eta} \in \mathrm{int}(K)$ and for $\boldsymbol{\eta} \notin K$. Since P_K is the identity for $\boldsymbol{\eta} \in K$, we only consider $\boldsymbol{\eta} \notin K$. Then, $|\mathrm{dev}(\boldsymbol{\eta})| \neq 0$ and

$$
P_K(\boldsymbol{\eta}) = \boldsymbol{\eta} - f(\boldsymbol{\eta})\frac{\mathrm{dev}(\boldsymbol{\eta})}{|\mathrm{dev}(\boldsymbol{\eta})|} = \boldsymbol{\eta} - f(\boldsymbol{\eta})Df(\boldsymbol{\eta}) = K_0\frac{\mathrm{dev}(\boldsymbol{\eta})}{|\mathrm{dev}(\boldsymbol{\eta})|} + \mathbb{P}_{\mathrm{vol}}[\boldsymbol{\eta}], \qquad \boldsymbol{\eta} \notin K.
$$

Since

$$
\frac{\partial}{\partial\boldsymbol{\eta}}\left(\frac{\mathrm{dev}(\boldsymbol{\eta})}{|\mathrm{dev}(\boldsymbol{\eta})|}\right) = \frac{1}{|\mathrm{dev}(\boldsymbol{\eta})|}\left(\mathbb{P}_{\mathrm{dev}} - \frac{\mathrm{dev}(\boldsymbol{\eta})}{|\mathrm{dev}(\boldsymbol{\eta})|} \otimes \frac{\mathrm{dev}(\boldsymbol{\eta})}{|\mathrm{dev}(\boldsymbol{\eta})|}\right),
$$

we find

$$
DP_K(\boldsymbol{\eta}) = \mathbb{P}_{\mathrm{vol}} + \frac{K_0}{|\mathrm{dev}(\boldsymbol{\eta})|}\left(\mathbb{P}_{\mathrm{dev}} - \frac{\mathrm{dev}(\boldsymbol{\eta})}{|\mathrm{dev}(\boldsymbol{\eta})|} \otimes \frac{\mathrm{dev}(\boldsymbol{\eta})}{|\mathrm{dev}(\boldsymbol{\eta})|}\right), \qquad \boldsymbol{\eta} \notin K.
$$

This results can be found, e.g. in [SH98, NCWM07, Wie07, Mül09]. If $f(\boldsymbol{\eta}) = 0$, i.e. $|\mathrm{dev}(\boldsymbol{\eta})| = K_0$, then all element of the generalized Jacobian are obtained by taking the convex combinations of $\mathbb{I}$ and $\lim_{\boldsymbol{\eta}'\to\boldsymbol{\eta}} DP_K(\boldsymbol{\eta}')$ with $\boldsymbol{\eta}' \notin K$. Thus, if $|\mathrm{dev}(\boldsymbol{\eta})| = K_0$, we find

$$
\begin{aligned}
\mathbb{S} \in \partial P_K(\boldsymbol{\eta}) \Leftrightarrow \mathbb{S} &= (1-t)\mathbb{I} + t\left(\mathbb{P}_{\mathrm{vol}} + \frac{K_0}{|\mathrm{dev}(\boldsymbol{\eta})|}\left(\mathbb{P}_{\mathrm{dev}} - \frac{\mathrm{dev}(\boldsymbol{\eta})}{|\mathrm{dev}(\boldsymbol{\eta})|} \otimes \frac{\mathrm{dev}(\boldsymbol{\eta})}{|\mathrm{dev}(\boldsymbol{\eta})|}\right)\right) \\
&= \mathbb{P}_{\mathrm{vol}} + (1-t)\mathbb{P}_{\mathrm{dev}} + t\left(\mathbb{P}_{\mathrm{dev}} - \frac{\mathrm{dev}(\boldsymbol{\eta})}{|\mathrm{dev}(\boldsymbol{\eta})|} \otimes \frac{\mathrm{dev}(\boldsymbol{\eta})}{|\mathrm{dev}(\boldsymbol{\eta})|}\right) \\
&= \mathbb{I} - t\frac{\mathrm{dev}(\boldsymbol{\eta})}{|\mathrm{dev}(\boldsymbol{\eta})|} \otimes \frac{\mathrm{dev}(\boldsymbol{\eta})}{|\mathrm{dev}(\boldsymbol{\eta})|}
\end{aligned}
$$

for $t \in [0,1]$. Altogether, this gives the following characterization of ∂P_K:

$$
\partial P_K(\boldsymbol{\eta}) = \begin{cases} \{\mathbb{I}\} & , |\operatorname{dev}(\boldsymbol{\eta})| < K_0\,, \\ \left\{\mathbb{I} - t\,\dfrac{\operatorname{dev}(\boldsymbol{\eta})}{|\operatorname{dev}(\boldsymbol{\eta})|} \otimes \dfrac{\operatorname{dev}(\boldsymbol{\eta})}{|\operatorname{dev}(\boldsymbol{\eta})|} : t \in [0,1]\right\} & , |\operatorname{dev}(\boldsymbol{\eta})| = K_0\,, \\ \left\{\mathbb{P}_{\mathrm{vol}} + \dfrac{K_0}{|\operatorname{dev}(\boldsymbol{\eta})|}\left(\mathbb{P}_{\mathrm{dev}} - \dfrac{\operatorname{dev}(\boldsymbol{\eta})}{|\operatorname{dev}(\boldsymbol{\eta})|} \otimes \dfrac{\operatorname{dev}(\boldsymbol{\eta})}{|\operatorname{dev}(\boldsymbol{\eta})|}\right)\right\} & , |\operatorname{dev}(\boldsymbol{\eta})| > K_0\,. \end{cases}
$$

4.1.1. *Quadratic Convergence in the Discrete Setting.* Due to the explicit formulas for P_K and ∂P_K, von Mises plasticity (with and without hardening) is one of the most frequently used models both in engineering applications and mathematical analysis. Due to the strong semismoothness of the max-function in finite dimensions, local quadratic convergence can be shown.

Corollary 7.11. *Consider the discrete problems of von Mises plasticity in one of the following situations.*

(1) *Kinematic hardening: let $\mathbb{H}$ be positive definite on the deviatoric subspace $\operatorname{Sym}_0(d)$.*
(2) *Viscoplastic regularization: let $\alpha \in [0, \infty)$.*
(3) *Perfect plasticity: let the Slater condition (Assumption 7.4) hold and let $\boldsymbol{u}_h^*$ be a solution of $F_h(\boldsymbol{u}_h) = 0$. Further, let F_h be CD-regular in $\boldsymbol{u}_h^*$.*

Then, the generalized Newton method converges locally quadratic.

PROOF. In view of Theorem 7.7 and Corollary 7.8, quadratic convergence is assured for hardening plasticity and the viscoplastic regularization as a result of the strong semismoothness (semismoothness of order $p = 1$) of P_K. In the perfectly plastic setting, quadratic convergence can be shown under the assumption that all elements of the generalized Jacobian are regular in the solution, provided a solution exists, cf. Theorems 7.5 and 7.6. □

4.1.2. *Convergence in Function Space.* Superlinear convergence results for this model (with and without hardening) are well-known from empirical observations as already reported in [**Bla97, ACZ99, Chr02, NCWM07, Wie07**] and analytical results were presented in [**GV09**]. In this last reference, also the superlinear convergence in function space was addressed for a model with isotropic hardening. The authors used the representation of P_K in terms of the max-function within a function space setting, also see (A.5). With the trial stress $\boldsymbol{\eta} = \mathbb{C}[\boldsymbol{\varepsilon}(\boldsymbol{u}) - \boldsymbol{\tau}]$, superlinear convergence was shown if the composition of the yield function and the trial stress is a $L^{2+\varepsilon}$-function for some $\varepsilon > 0$. In this situation, the max-function is slantly differentiable from $L^{2+\varepsilon}$ into L^2. However, as stated by the authors, there is no a priori information available whether this assumption is fulfilled.

4.1.3. *Incompressible Plasticity.* Von Mises plasticity is one particular instance of incompressible plasticity. With $\widehat{K} \subset \operatorname{Sym}_0(d)$, elements $\boldsymbol{\eta} \in K$ take the form $\boldsymbol{\eta} = \delta\mathbf{1} + \widehat{\boldsymbol{\eta}}$ with $\widehat{\boldsymbol{\eta}} \in \widehat{K}$ and $\delta \in \mathbb{R}$. Particularly, the yield function f does not depend on the first invariant $\iota_{\boldsymbol{\eta}}^1 = \operatorname{tr}(\boldsymbol{\eta})$. Therefore, the projection $P_K : \operatorname{Sym}(d) \to K$ always takes the form

$$
P_K(\boldsymbol{\eta}) = \mathbb{P}_{\mathrm{vol}}[\boldsymbol{\eta}] + \widehat{P}_{\widehat{K}}(\mathbb{P}_{\mathrm{dev}}[\boldsymbol{\eta}])\,,
$$

with $\widehat{P}_{\widehat{K}} : \operatorname{Sym}_0(d) \to \widehat{K}$ being the projection w.r.t. the restriction of the inverse elasticity tensor to $\operatorname{Sym}_0(d)$, i.e. $\mathbb{C}^{-1}\big|_{\operatorname{Sym}_0(d)} = \frac{1}{2\mu}\mathbb{P}_{\mathrm{dev}}$. Since $\mathbb{P}_{\mathrm{dev}}$ is the identity on $\operatorname{Sym}_0(d)$, the projection $\widehat{P}_{\widehat{K}}$ coincides with the Euclidian projection onto $\widehat{K}$. Smoothness properties of P_K are therefore related with the smoothness properties of $\widehat{P}_{\widehat{K}}$.

4.2. Drucker-Prager Plasticity. As mentioned before, the model of von Mises plasticity is well-understood from a numerical and analytical point of view and serves as the most widely used model problem in associated plasticity. Drucker-Prager plasticity has the potential to serve as a standard model in non-associated plasticity as it is possible to give a closed form expression of the response function $R_K = P_K^F$. K is characterized by the yield function $f(\boldsymbol{\eta}) = |\operatorname{dev}(\boldsymbol{\eta})| + \frac{m}{d}\operatorname{tr}(\boldsymbol{\eta}) - C$ with $m \geq 0$ and $C \geq 0$. We restrict ourselves to $m > 0$, since otherwise, the model of von Mises obtained. For the physical interpretation of m and C, we refer to Subsections 1.2.3 and 1.2.5. By means of the yield function, the admissible set is

$$K = \{\boldsymbol{\eta} \in \operatorname{Sym}(d) : f(\boldsymbol{\eta}) \leq 0\} = \{\boldsymbol{\eta} \in \operatorname{Sym}(d) : |\operatorname{dev}(\boldsymbol{\eta})| + \tfrac{m}{d}\operatorname{tr}(\boldsymbol{\eta}) \leq C\}\,.$$

With the splitting of $\operatorname{Sym}(d) = \operatorname{Sym}_0(d) \oplus \mathbb{R}\mathbf{1}$, we see that K has the shape of a scaled and shifted second order unit cone, cf. (A.9)

$$K = \{\boldsymbol{\eta} = \widehat{\boldsymbol{\eta}} + \delta\mathbf{1} \in \operatorname{Sym}(d), (\widehat{\boldsymbol{\eta}}, \delta) \in \operatorname{Sym}_0(d) \times \mathbb{R} : |\widehat{\boldsymbol{\eta}}| \leq -m\,\delta + C\}$$

Lemma 7.12. *The orthogonal projection (w.r.t. to an arbitrary inner product) onto K is strongly semismooth.*

PROOF. This results follows from Proposition A.14. $\qquad\square$

As for von Mises plasticity, the projection onto K can be given in closed form. We evaluate the projection w.r.t. the inner product induced by $\mathbb{F}^{-1}$ with $\mathbb{F} = \mathbb{C} \circ \mathbb{T} = 2\mu\mathbb{P}_{\operatorname{dev}} + d\kappa M \mathbb{P}_{\operatorname{vol}}$ and therefore $\mathbb{F}^{-1} = \frac{1}{2\mu}\mathbb{P}_{\operatorname{dev}} + \frac{1}{d\,\kappa M}\mathbb{P}_{\operatorname{vol}}$ with $M \in (0,1]$ and remark that $M = 1$ corresponds to associated plasticity.

Lemma 7.13. *Consider $K = \{\boldsymbol{\eta} \in \operatorname{Sym}(d) : |\operatorname{dev}(\boldsymbol{\eta})| + \frac{m}{d}\operatorname{tr}(\boldsymbol{\sigma}) \leq C\}$. The orthogonal projection P_K^F w.r.t. the inner product defined by $\mathbb{F}^{-1}$ is given as*

$$P_K^F(\boldsymbol{\eta}) = \begin{cases} \boldsymbol{\eta} & , f(\boldsymbol{\eta}) \leq 0\,, \\ \frac{C}{m}\mathbf{1} & , c(\boldsymbol{\eta}) \leq 0\,, \\ \boldsymbol{\eta} - \frac{f(\boldsymbol{\eta})}{2\mu + m\,n\,\kappa}\left(2\mu\frac{\operatorname{dev}(\boldsymbol{\eta})}{|\operatorname{dev}(\boldsymbol{\eta})|} + n\,\kappa\,\mathbf{1}\right) & , else\,, \end{cases} \qquad (7.8)$$

with $n = mM$ and $c(\boldsymbol{\eta}) = m\,n\,\kappa|\operatorname{dev}(\boldsymbol{\eta})| - 2\mu\left(\frac{m}{d}\operatorname{tr}(\boldsymbol{\eta}) - C\right)$.

PROOF. For the proof, we shift the cone via the transformation $\boldsymbol{\eta} \mapsto \boldsymbol{\eta} - \frac{C}{m}\mathbf{1}$ such that the apex coincides with the origin. Thus, we consider the cone defined by $K = \{\boldsymbol{\eta} \in \operatorname{Sym}(d) : |\operatorname{dev}(\boldsymbol{\eta})| + \frac{m}{d}\operatorname{tr}(\boldsymbol{\eta}) \leq 0\}$ which allows us to set $C = 0$ in (7.8) and in the yield function. Since the Slater condition is fulfilled, the projection $\boldsymbol{\sigma} = P_K^F(\boldsymbol{\eta})$ satisfies the KKT-system

$$0 \in \mathbb{F}^{-1}[\boldsymbol{\sigma} - \boldsymbol{\eta}] + \lambda\partial f(\boldsymbol{\sigma})\,,$$
$$0 = \lambda f(\boldsymbol{\sigma})\,, \qquad \lambda \geq 0\,, \qquad f(\boldsymbol{\sigma}) \leq 0\,.$$

The first line is indeed an inclusion because the apex is a singular point on ∂K due to the non-differentiability of f. However, we can use the cone structure of K and define the polar cone (or dual cone) with respect to $\mathbb{F}^{-1}$ as

$$K^{\circ,\mathbb{F}^{-1}} = \{\boldsymbol{\eta} \in \operatorname{Sym}(d) : \boldsymbol{\tau} : \mathbb{F}^{-1}[\boldsymbol{\eta}] \leq 0 \text{ for all } \boldsymbol{\tau} \in K\}\,.$$

A short computations gives the equivalence: $\boldsymbol{\eta} \in K^{\circ,\mathbb{F}^{-1}} \Leftrightarrow c(\boldsymbol{\eta}) \leq 0$. It is well-known [HUL93a, Section 3.2] that $P_K^F(\boldsymbol{\eta}) = 0$ if and only if $\boldsymbol{\eta} \in K^{\circ,\mathbb{F}^{-1}}$ and moreover, $K \cap K^{\circ,\mathbb{F}^{-1}} = \{0\}$. Hence it remains to consider the case $\boldsymbol{\eta} \notin K \cup K^{\circ,\mathbb{F}^{-1}}$. Since the apex is the only

singular point of K, it follows that in this case the projection lies on the regular part of ∂K and the projection is therefore characterized by

$$0 = \mathbb{F}^{-1}[\boldsymbol{\sigma} - \boldsymbol{\eta}] + \lambda Df(\boldsymbol{\sigma}) , \qquad \text{and} \qquad f(\boldsymbol{\sigma}) = 0 .$$

Noting that $Df(\boldsymbol{\sigma}) = \frac{\operatorname{dev}(\boldsymbol{\sigma})}{|\operatorname{dev}(\boldsymbol{\sigma})|} + \frac{m}{d}\mathbf{1}$, after applying $\mathbb{P}_{\mathrm{dev}}$ to the first equation $\boldsymbol{\sigma} = \boldsymbol{\eta} - \lambda\mathbb{F}[Df(\boldsymbol{\sigma})]$, we obtain

$$\operatorname{dev}(\boldsymbol{\sigma}) = \operatorname{dev}(\boldsymbol{\eta}) - 2\mu\,\lambda\frac{\operatorname{dev}(\boldsymbol{\sigma})}{|\operatorname{dev}(\boldsymbol{\sigma})|} \quad \Longrightarrow \quad \operatorname{dev}(\boldsymbol{\sigma}) = \frac{|\operatorname{dev}(\boldsymbol{\sigma})|}{|\operatorname{dev}(\boldsymbol{\sigma})|+2\mu\,\lambda}\operatorname{dev}(\boldsymbol{\eta}) .$$

Taking the norm gives $|\operatorname{dev}(\boldsymbol{\sigma})| = |\operatorname{dev}(\boldsymbol{\eta})| - 2\mu\,\lambda$ from which we can conclude $\frac{\operatorname{dev}(\boldsymbol{\sigma})}{|\operatorname{dev}(\boldsymbol{\sigma})|} = \frac{\operatorname{dev}(\boldsymbol{\eta})}{|\operatorname{dev}(\boldsymbol{\eta})|}$. Similarly, we apply the trace operator and obtain $\operatorname{tr}(\boldsymbol{\sigma}) = \operatorname{tr}(\boldsymbol{\eta}) - d\,n\,\kappa\,\lambda$. Substitution into $f(\boldsymbol{\sigma}) = 0$ gives (note that $C = 0$ by the transformation)

$$0 = f(\boldsymbol{\sigma}) = |\operatorname{dev}(\boldsymbol{\sigma})| + \frac{m}{d}\operatorname{tr}(\boldsymbol{\sigma}) = |\operatorname{dev}(\boldsymbol{\eta})| + \frac{m}{d}\operatorname{tr}(\boldsymbol{\eta}) - \lambda\big(2\mu + m\,n\,\kappa\big) .$$

This explicitly gives λ in terms of $\boldsymbol{\eta}$ and we have $\lambda = \frac{f(\boldsymbol{\eta})}{2\mu+m\,n\,\kappa}$. Finally, we obtain

$$\boldsymbol{\sigma} = \boldsymbol{\eta} - \lambda\mathbb{F}[Df(\boldsymbol{\sigma})] = \boldsymbol{\eta} - \frac{f(\boldsymbol{\eta})}{2\mu+m\,n\,\kappa}\mathbb{F}\Big[\frac{\operatorname{dev}(\boldsymbol{\eta})}{|\operatorname{dev}(\boldsymbol{\eta})|} + \frac{m}{d}\mathbf{1}\Big]$$

$$= \boldsymbol{\eta} - \frac{f(\boldsymbol{\eta})}{2\mu+m\,n\,\kappa}\big(2\mu\frac{\operatorname{dev}(\boldsymbol{\eta})}{|\operatorname{dev}(\boldsymbol{\eta})|} + n\,\kappa\mathbf{1}\big) .$$

Putting all pieces together and using the back-transformation $\boldsymbol{\eta} \mapsto \boldsymbol{\eta} + \frac{C}{m}\mathbf{1}$ finally yields the desired representation of P_K^F. $\qquad\square$

In the limit case $m = n = 0$, the projection resembles von Mises plasticity.

Our next task is to give a full characterization of the generalized Jacobian of P_K^F, and we also refer to [**HYF05**]. In order to do so, we need to determine the derivative if $\boldsymbol{\eta} \notin K \cup K^{\circ,\mathbb{F}^{-1}}$. We denote this tensor by $\mathbb{S}_{\mathrm{reg}}$, i.e.

$$\mathbb{S}_{\mathrm{reg}}(\boldsymbol{\eta}) = DP_K^F(\boldsymbol{\eta}) = \mathbb{I} - \frac{1}{2\mu+m\,n\,\kappa}\Big(\mathbb{F}[Df(\boldsymbol{\eta})] \otimes Df(\boldsymbol{\eta}) + f(\boldsymbol{\eta})\mathbb{F} \circ D^2 f(\boldsymbol{\eta})\Big)$$

$$= \mathbb{I} - \frac{1}{2\mu+m\,n\,\kappa}\Bigg(\frac{2\mu\,m}{d}\mathbf{1} \otimes \frac{\operatorname{dev}(\boldsymbol{\eta})}{|\operatorname{dev}(\boldsymbol{\eta})|} + n\,\kappa\frac{\operatorname{dev}(\boldsymbol{\eta})}{|\operatorname{dev}(\boldsymbol{\eta})|} \otimes \mathbf{1} + \frac{m\,n\,\kappa}{d}\mathbf{1} \otimes \mathbf{1}$$

$$+ 2\mu\mathbb{P}_{\mathrm{dev}} + 2\mu\frac{\frac{m}{d}\operatorname{tr}(\boldsymbol{\eta})-C}{|\operatorname{dev}(\boldsymbol{\eta})|}\Big(\mathbb{P}_{\mathrm{dev}} - \frac{\operatorname{dev}(\boldsymbol{\eta})}{|\operatorname{dev}(\boldsymbol{\eta})|} \otimes \frac{\operatorname{dev}(\boldsymbol{\eta})}{|\operatorname{dev}(\boldsymbol{\eta})|}\Big)\Bigg) .$$

Lemma 7.14. *The generalized Jacobian of P_K^F is*

$$\partial P_K^F(\boldsymbol{\eta}) = \begin{cases} \{\mathbb{I}\} & , f(\boldsymbol{\eta}) < 0 , \\ \{0\} & , c(\boldsymbol{\eta}) < 0 , \\ \{\mathbb{S}_{\mathrm{reg}}(\boldsymbol{\eta})\} & , \boldsymbol{\eta} \notin K \cup K^{\circ,\mathbb{F}^{-1}} , \\ \{t\,\mathbb{S}_{\mathrm{reg}}(\boldsymbol{\eta}) : t \in [0,1]\} & , c(\boldsymbol{\eta}) = 0 , \boldsymbol{\eta} \neq \frac{C}{m}\mathbf{1} , \\ \{t\,\mathbb{I} + (1-t)\mathbb{S}_{\mathrm{reg}}(\boldsymbol{\eta}) : t \in [0,1]\} & , f(\boldsymbol{\eta}) = 0 , \boldsymbol{\eta} \neq \frac{C}{m}\mathbf{1} , \\ \{s\,\mathbb{I} + t\,\mathbb{S}_{\mathrm{reg}}(\boldsymbol{\eta}) : s,t \geq 0 \text{ and } s+t \leq 1\} & , \boldsymbol{\eta} = \frac{C}{m}\mathbf{1} . \end{cases}$$

PROOF. We simply note that P_K^F is differentiable if $\boldsymbol{\eta} \notin \partial K \cup \partial K^{\circ,\mathbb{F}^{-1}}$. This gives the first three lines. It remains to consider the cases where P_K^F is not differentiable.

- $c(\boldsymbol{\eta}) = 0$ and $\boldsymbol{\eta} \neq \frac{C}{m}\mathbf{1}$: then $\partial^B P_K^F(\boldsymbol{\eta}) = \{0, \mathbb{S}_{\mathrm{reg}}(\boldsymbol{\eta})\}$.
- $f(\boldsymbol{\eta}) = 0$ and $\boldsymbol{\eta} \neq \frac{C}{m}\mathbf{1}$: then $\partial^B P_K^F(\boldsymbol{\eta}) = \{\mathbb{I}, \mathbb{S}_{\mathrm{reg}}(\boldsymbol{\eta})\}$.

- $\boldsymbol{\eta} = \frac{C}{m}\mathbf{1}$: then $\partial^B P_K^F(\frac{C}{m}\mathbf{1}) = \{0, \mathbb{I}, \mathbb{S}_{\text{reg}}(\boldsymbol{\eta})\}$.

Taking the convex combinations of the elements of the B-subdifferential then gives the assertion. $\qquad\square$

We remark that the consistent tangent is not symmetric. To understand this, consider the consistent tangent at $\boldsymbol{\eta} \notin K \cup K^{\circ,\mathbb{F}^{-1}}$. Then, the projection lies on the regular part of ∂K and

$$\mathbb{C}_{\text{ct}} = \mathbb{S}_{\text{reg}}(\boldsymbol{\eta}) \circ \mathbb{C} = \mathbb{C} - \frac{1}{2\mu + m\,n\,\kappa}\Big(\mathbb{F}[Df(\boldsymbol{\eta})] \otimes \mathbb{C}[Df(\boldsymbol{\eta})] + f(\boldsymbol{\eta})\mathbb{F} \circ D^2 f(\boldsymbol{\eta}) \circ \mathbb{C}\Big).$$

If $\mathbb{F} \neq \mathbb{C}$, then $\mathbb{C}_{\text{ct}}$ is not symmetric as the rank-one update $\mathbb{F}[Df(\boldsymbol{\eta})] \otimes \mathbb{C}[Df(\boldsymbol{\eta})]$ is not symmetric. Thus $\mathbb{C}_{\text{ct}}$ is only symmetric if $\mathbb{T} = \mathbb{I}$, i.e. if we consider associated plasticity.

4.2.1. *Quadratic Convergence.* Again, we can apply the results of the previous section.

Corollary 7.15. *Consider the discrete problems of non-associated Drucker-Prager plasticity in one of the following situations.*

(1) *Static and quasi-static hardening plasticity with sufficient hardening: let $\mathbb{H} = h_d\mathbb{P}_{\text{dev}} + h_v\mathbb{P}_{\text{vol}}$ with $h_d > 0$ and $h_v > \kappa\frac{(M-1)^2}{4M}$ be positive definite.*
(2) *Static viscoplasticity with sufficient regularization: let $\alpha\frac{1-M}{M} < 1$.*
(3) *Incremental viscoplasticity: let $\alpha\Delta t_n\frac{1-M}{M} < 1$.*
(4) *Assume that there exists a solution $\boldsymbol{u}_h^*$ of $F_h(\boldsymbol{u}_h) = 0$ and suppose that F_h is CD-regular in $\boldsymbol{u}_h^*$.*

Then, the generalized Newton method converges locally quadratic.

PROOF. In all cases, the response function is strongly semismooth by Lemma 7.12. Concerning hardening plasticity, Lemma 4.5 gives the strong monotonicity of F_h and Theorem 7.3 guarantees the quadratic convergence. For static viscoplasticity and incremental viscoplasticity, strong monotonicity under the given assumption is due to Lemma 4.4 and Corollary 5.6. Concerning (4), we can only quote Theorem 7.1. $\qquad\square$

4.3. Smoothed Drucker-Prager Plasticity. The examples considered so far are very specific as the simple structure of the admissible set allowed to compute the response function explicitly. In smoothed Drucker-Prager plasticity, this is no longer possible but nevertheless, we are able to compute an element of the generalized Jacobian. For a smoothing parameter $\theta > 0$, the yield function is defined by (also see Section 1.2.5)

$$f_\theta(\boldsymbol{\eta}) = \sqrt{|\operatorname{dev}(\boldsymbol{\eta})|^2 + \theta^2} + \frac{m}{d}\operatorname{tr}(\boldsymbol{\eta}) - C,$$

and thus, $f_\theta \in C^\infty(\operatorname{Sym}(d), \mathbb{R})$. With the abbreviation $L(\boldsymbol{\eta}) = \sqrt{|\operatorname{dev}(\boldsymbol{\eta})|^2 + \theta^2}$, we can compute the first and second derivative.

$$Df_\theta(\boldsymbol{\eta}) = \frac{\operatorname{dev}(\boldsymbol{\eta})}{\sqrt{|\operatorname{dev}(\boldsymbol{\eta})|^2 + \theta^2}} + \frac{m}{d}\mathbf{1} = \frac{1}{L(\boldsymbol{\eta})}\operatorname{dev}(\boldsymbol{\eta}) + \frac{m}{d}\mathbf{1},$$

$$D^2 f_\theta(\boldsymbol{\eta}) = \frac{1}{\sqrt{|\operatorname{dev}(\boldsymbol{\eta})|^2 + \theta^2}}\Big(\mathbb{P}_{\text{dev}} - \frac{\operatorname{dev}(\boldsymbol{\eta}) \otimes \operatorname{dev}(\boldsymbol{\eta})}{|\operatorname{dev}(\boldsymbol{\eta})|^2 + \theta^2}\Big) = \frac{1}{L(\boldsymbol{\eta})}\Big(\mathbb{P}_{\text{dev}} - \frac{\operatorname{dev}(\boldsymbol{\eta})}{L(\boldsymbol{\eta})} \otimes \frac{\operatorname{dev}(\boldsymbol{\eta})}{L(\boldsymbol{\eta})}\Big).$$

In the following, we fix $\boldsymbol{\eta} \in \operatorname{Sym}(d)$ and by $\boldsymbol{\sigma} = P_{K,\theta}^F(\boldsymbol{\eta})$, we denote the projection. The corresponding Lagrange multiplier is again denoted by $\lambda \geq 0$. Following the lines of

Section A.2.3, evaluating the derivative of the projection requires the inverse of $\mathbb{F}^{-1} + \lambda D^2 f_\theta(\boldsymbol{\sigma})$. Remembering that $\mathbb{F}^{-1} = \frac{1}{2\mu}\mathbb{P}_{\text{dev}} + \frac{1}{d\kappa M}\mathbb{P}_{\text{vol}}$, we have

$$\mathbb{F}^{-1} + \lambda D^2 f_\theta(\boldsymbol{\sigma}) = \left(\frac{1}{2\mu} + \frac{\lambda}{L(\boldsymbol{\sigma})}\right)\mathbb{P}_{\text{dev}} + \frac{1}{d\kappa M}\mathbb{P}_{\text{vol}} - \lambda \operatorname{dev}(\boldsymbol{\sigma}) \otimes \frac{\operatorname{dev}(\boldsymbol{\sigma})}{L(\boldsymbol{\sigma})^3}$$

Introducing $\mathbb{A} = \frac{L(\boldsymbol{\sigma})+2\mu\lambda}{2\mu L(\boldsymbol{\sigma})}\mathbb{P}_{\text{dev}} + \frac{1}{d\kappa M}\mathbb{P}_{\text{vol}}$ (which is invertible as $\lambda \geq 0$), $\boldsymbol{\beta} = \lambda \operatorname{dev}(\boldsymbol{\sigma})$ and $\boldsymbol{\delta} = \frac{\operatorname{dev}(\boldsymbol{\sigma})}{L(\boldsymbol{\sigma})^3}$ we find $\mathbb{F}^{-1} + \lambda D^2 f_\theta(\boldsymbol{\sigma}) = \mathbb{A} + \boldsymbol{\beta} \otimes \boldsymbol{\delta}$. Then, the Sherman-Morrison formula yields

$$\left(\mathbb{F}^{-1} + \lambda D^2 f_\theta(\boldsymbol{\sigma})\right)^{-1} = \mathbb{A}^{-1} + \frac{\mathbb{A}^{-1}[\boldsymbol{\beta}] \otimes \mathbb{A}^{-1}[\boldsymbol{\delta}]}{1 - \boldsymbol{\beta} : \mathbb{A}^{-1}[\boldsymbol{\delta}]}\,.$$

The inverse $\mathbb{A}^{-1}$ can be computed explicitly and we have $\mathbb{A}^{-1} = \frac{2\mu L(\boldsymbol{\sigma})}{L(\boldsymbol{\sigma})+2\mu\lambda}\mathbb{P}_{\text{dev}} + d\kappa M\mathbb{P}_{\text{vol}}$. We use the abbreviation

$$\mathbb{G} \equiv \mathbb{G}(\boldsymbol{\sigma}, \lambda) = \mathbb{F}^{-1} + \lambda D^2 f_\theta(\boldsymbol{\sigma})\,,$$

and an element of the generalized Jacobian of $P^F_{K,\theta}$ can be constructed by considering the corresponding B-sub-differentials, see Appendix A. We find

$$\partial R(\boldsymbol{\eta}) \ni \mathbb{S} = \begin{cases} \mathbb{I} & ,\ \boldsymbol{\eta} \in K\,, \\ \left(\mathbb{I} - \dfrac{\mathbb{G}^{-1}[Df_\theta(\boldsymbol{\sigma})] \otimes Df_\theta(\boldsymbol{\sigma})}{Df_\theta(\boldsymbol{\sigma}):\mathbb{G}^{-1}[Df_\theta(\boldsymbol{\sigma})]}\right)\mathbb{G}^{-1} \circ \mathbb{F}^{-1} & ,\ \boldsymbol{\eta} \notin K\,. \end{cases}$$

4.3.1. *Using the Plastic Potential.* We present an alternative derivation following Section A.3, relying on the plastic potential

$$g_\theta(\boldsymbol{\eta}) = \sqrt{|\operatorname{dev}(\boldsymbol{\eta})|^2 + \theta^2} + \tfrac{n}{d}\operatorname{tr}(\boldsymbol{\eta}) - C\,,$$
$$Dg_\theta(\boldsymbol{\sigma}) = \frac{\operatorname{dev}(\boldsymbol{\eta})}{\sqrt{|\operatorname{dev}(\boldsymbol{\eta})|^2+\theta^2}} + \tfrac{n}{d}\mathbf{1} = \frac{1}{L(\boldsymbol{\eta})}\operatorname{dev}(\boldsymbol{\eta}) + \tfrac{n}{d}\mathbf{1}\,,$$
$$D^2 g_\theta(\boldsymbol{\eta}) = D^2 f_\theta(\boldsymbol{\eta})\,.$$

with $0 < n \leq m$. We find $\mathbb{T}[Df_\theta(\boldsymbol{\eta})] = Dg_\theta(\boldsymbol{\eta})$ for all $\boldsymbol{\eta} \in \operatorname{Sym}(d)$ and an element of the generalized Jacobian can also be determined by the approach of Section A.3 (with $A = \mathbb{C}^{-1}$, $f = f_\theta$ and $g = g_\theta$). Again denoting the response by $\boldsymbol{\sigma} = R(\boldsymbol{\eta}) = P^F_{K,\theta}(\boldsymbol{\eta})$, with $\widehat{\mathbb{G}} = \mathbb{C}^{-1} + \lambda(\boldsymbol{\sigma})D^2 g_\theta(\boldsymbol{\sigma})$, we find

$$\partial R(\boldsymbol{\eta}) \ni \widehat{\mathbb{S}} = \begin{cases} \mathbb{I} & ,\ \boldsymbol{\eta} \in K\,, \\ \left(\mathbb{I} - \dfrac{\widehat{\mathbb{G}}^{-1}[Dg_\theta(\boldsymbol{\sigma})] \otimes Df_\theta(\boldsymbol{\sigma})}{Df_\theta(\boldsymbol{\sigma}):\widehat{\mathbb{G}}^{-1}[Dg_\theta(\boldsymbol{\sigma})]}\right)\widehat{\mathbb{G}}^{-1} \circ \mathbb{C}^{-1} & ,\ \boldsymbol{\eta} \notin K\,. \end{cases}$$

An easy calculation shows that indeed we have $\mathbb{S} = \widehat{\mathbb{S}}$. Finally,

$$\mathbb{C}_{\text{ct}} = \widehat{\mathbb{S}} \circ \mathbb{C} = \begin{cases} \mathbb{C} & ,\ \boldsymbol{\eta} \in K\,, \\ \widehat{\mathbb{G}}^{-1} - \dfrac{\widehat{\mathbb{G}}^{-1}[Dg_\theta(\boldsymbol{\sigma})] \otimes \widehat{\mathbb{G}}^{-1}[Df_\theta(\boldsymbol{\sigma})]}{Df_\theta(\boldsymbol{\sigma}):\widehat{\mathbb{G}}^{-1}[Dg_\theta(\boldsymbol{\sigma})]} & ,\ \boldsymbol{\eta} \notin K\,, \end{cases}$$

is the consistent algorithmic tangent moduli in the sense of [SH98, Section 3.6] for a general non-associated setting and we also refer to [OM89]. We see that once we are able to compute the response $\boldsymbol{\sigma} = R(\boldsymbol{\eta}) = P^F_{K,\theta}(\boldsymbol{\eta})$, the computation of an element of the generalized Jacobian easily follows from the above formula if one is able to compute the second derivative of the plastic potential.

4.3.2. *Evaluating the Response Function.* Since the response function $R : \operatorname{Sym}(d) \to \operatorname{Sym}(d)$ cannot be evaluated in closed form for the smoothed Drucker-Prager model, evaluating $R(\boldsymbol{\eta})$ for a given $\boldsymbol{\eta} \in \operatorname{Sym}(d)$ requires the solution of the system

$$0 = \mathbb{C}^{-1}[\boldsymbol{\sigma} - \boldsymbol{\eta}] + \lambda Dg_\theta(\boldsymbol{\sigma}) \,,$$
$$0 = \lambda f_\theta(\boldsymbol{\sigma}) \,, \qquad \lambda \geq 0 \,, \qquad f_\theta(\boldsymbol{\sigma}) \leq 0 \,.$$

If $f(\boldsymbol{\eta}) \leq 0$, then $(\boldsymbol{\sigma}, \lambda) = (\boldsymbol{\eta}, 0)$ solves the above system. If $f(\boldsymbol{\eta}) > 0$, then the solution is characterized by

$$0 = \mathbb{C}^{-1}[\boldsymbol{\sigma} - \boldsymbol{\eta}] + \lambda Dg_\theta(\boldsymbol{\sigma}) \,,$$
$$0 = f_\theta(\boldsymbol{\sigma}) \,,$$

and $\lambda > 0$. For the above system, it is possible to set up a Newton method under the additional constraint $\lambda \geq 0$. Alternatively, the complementarity condition can be replaced by a NCP function, see Section A.3. We also refer to Chapter 9 concerning the active set method which is based on a reformulatation by means of a NCP function.

4.3.3. *Superlinear Convergence.* Since $f_\theta \in C^2(\operatorname{Sym}(d), \mathbb{R})$, the projection $P_{K,\theta}^F$ is semismooth, cf. Theorem A.11. Then, under the same assumptions as in Corollary 7.15, we obtain the superlinear convergence of the generalized Newton method.

Corollary 7.16. *Corollary 7.15 also holds for smoothed Drucker-Prager plasticity if quadratic convergence is replaced by superlinear convergence.*

PROOF. Semismoothness of the response function can be shown by Theorem A.11 since P_K^F is a projection in the metric defined by $\mathbb{F}^{-1}$ and K is described by the smooth function f_θ. Another possibility is to use Theorem A.15. In this case, semismoothness relies on the implicit function theorem for semismooth functions, cf. Proposition A.4. Since we are only able to show that the response function is semismooth and not strongly semismooth, we can only guarantee superlinear convergence but not quadratic convergence.   □

We remark that this result can easily be extended to more general (non-associated) models including nonlinear hardening. The key tool is the implicit function theorem for semismooth functions which we used in the proof of Theorem A.15. This approach is far more general as it does not presuppose that the response function is a projection.

CHAPTER 8

RETURN ALGORITHMS AND GLOBALIZATION TECHNIQUES

While the last chapter was dedicated to showing superlinear convergence of the generalized Newton method in the discrete setting, we will now state the algorithm in a way which is amenable to implementation. The algorithm is suited for any (incremental) plasticity model which allows the computation of the response function (as well as a corresponding generalized derivative). The algorithm itself is just the generalized Newton method of the previous chapter applied to the displacement problem $F_h(\boldsymbol{u}_h) = 0$. It is widely used in the engineering community (though not necessarily by the name of Newton's method) and is the standard algorithm for plasticity problems [**SH98**, **Sim98**]. However, convergence results are limited to very specific material models, cf. [**Bla97**, **GV09**], and the previous chapter can be seen as an attempt to generalize conditions under which the algorithm converges locally superlinear (or even quadratic). In the context of perfect plasticity, the method is also known as the *closest point projection* or *radial return* algorithm. We generally refer to the considered algorithms as *return algorithms* as already indicated in the title of the chapter.

After temporal and spatial discretization, we need to solve a series of systems of the kind $F_h(\boldsymbol{u}_h) = 0$ as introduced in the last chapter, in which we investigated the local convergence properties of the generalized Newton method and already gave a blueprint algorithm. Interestingly, globalization techniques have not been considered systematically for plasticity problems. Globalization is indeed a difficult task in non-associated plasticity due to the lack of a "natural" merit function. But concerning associated plasticity, powerful globalization concepts are available from optimization theory. However, algorithmically, optimization techniques have only been partially exploited so far, e.g. [**KLSW06**, **Wie07**]. After introducing the local variant of Newton's method for the displacement problem, we turn to globalization techniques. Whereas Section 8.2 is devoted to generally non-associated problems, Section 8.3 exclusively considers associated plasticity and we show a global convergence result in function space. On a discrete level, the problems naturally embed into the class of SC^1 minimization problems if the response function is semismooth.

1. The Semismooth Newton Algorithm

1.1. Incremental Plasticity Setting. We consider the evolution of the body Ω during the time interval $[0, T]$ which is partitioned via

$$0 = t_0 < t_1 < \cdots < t_N = T \,.$$

At time t_0, we assume to have initial conditions $\boldsymbol{u}_h(t_0) = \boldsymbol{u}_h^0 \in \boldsymbol{X}_h$ and either $\boldsymbol{\sigma}_h(t_0) = \boldsymbol{\sigma}_h^0 \in \boldsymbol{P}_h$ or $\boldsymbol{\varepsilon}_{p,h}(t_0) = \boldsymbol{\varepsilon}_{p,h}^0 \in \boldsymbol{P}_h$ in order to determine the state of the body at time t_0. In the following, we assume that $\boldsymbol{\varepsilon}_{p,h}^0$ is at our disposal. Again, for simplicity we assume $\Omega = \Omega_h$ after triangulation. Time discrete quantities will again be denoted by a superscript as in Section 5.4 and the related index is denoted by n. In each time step, a nonlinear system of equations has to be solved, i.e. determine $(\boldsymbol{\sigma}_h^n, \boldsymbol{u}_h^n) \in \boldsymbol{P}_h \times \boldsymbol{X}_h(\boldsymbol{u}_D(t_n))$ such that

$$\int_\Omega \boldsymbol{\sigma}_h^n(x) : \boldsymbol{\varepsilon}(\boldsymbol{w}_h(x)) \, dx = \ell(t_n, \boldsymbol{w}_h) \,, \qquad\qquad \boldsymbol{w}_h \in \boldsymbol{X}_h \,,$$
$$\boldsymbol{\sigma}_h^n(\boldsymbol{\xi}) = R\big(\mathbb{C}\big[\boldsymbol{\varepsilon}(\boldsymbol{u}_h^n(\boldsymbol{\xi})) - \boldsymbol{\varepsilon}_{p,h}^{n-1}(\boldsymbol{\xi})\big]\big) \,, \qquad\qquad \boldsymbol{\xi} \in \boldsymbol{\Xi} \,.$$

Again, the expression for $\boldsymbol{\sigma}_h^n$ is substituted into the equilibrium equation (note that the integral represents a quadrature rule once again) resulting in a nonlinear problem for the displacement. The index of the nonlinear iteration will be the second superscript, denoted by k. With $F_h^n : \boldsymbol{X}_h \to \boldsymbol{X}_h^*$, we denote the corresponding nonlinear system in the n-th time step for determining $\boldsymbol{u}_h^n \in \boldsymbol{X}_h(\boldsymbol{u}_D(t_n))$. For the implementation of the generalized Newton method of the previous chapter for incremental plasticity problems, we refer to Algorithm 8.1 and shortly discuss the algorithm. Steps S1) and S8) are related to the incremental structure whereas S2)–S7) are the realization of the generalized Newton method. Steps S2) and S3) are simply the evaluation of F_h^n whereas S4) checks for convergence. Finally, in S5)–S7), the solution of the linear system and the update is described.

1.2. Local Treatment of the Nonlinearity. The key feature of the algorithm is the local treatment of the nonlinearity R. This allows to solve the highly nonlinear part of the problem independently at each quadrature point $\boldsymbol{\xi} \in \boldsymbol{\Xi}$ and therefore decouples into $|\boldsymbol{\Xi}|$ subproblems. Essentially, the algorithm only involves three key routines.

(1) Given $\boldsymbol{\eta} \in \mathrm{Sym}(d)$, compute the stress $\boldsymbol{\sigma} = R(\boldsymbol{\eta}) \in \mathrm{Sym}(d)$ via the response function.
(2) Given $\boldsymbol{\eta} \in \mathrm{Sym}(d)$ and the stress response $\boldsymbol{\sigma} = R(\boldsymbol{\eta})$, compute an element $\mathbb{S} \in \partial R(\boldsymbol{\eta})$. Therefore note that $\mathbb{S}$ typically depends on $\boldsymbol{\sigma} = R(\boldsymbol{\eta})$, cf. the example of smoothed Drucker-Prager plasticity in the previous chapter.
(3) Solve the "elasticity-like" subproblems in S6).

Often, (1) and (2) are treated simultaneously as typically $\mathbb{S}$ is used for the computation of the response within a local Newton-type iteration. But while (1) and (2) can be evaluated locally at each quadrature point, problem (3), i.e.

$$\int_\Omega \mathbb{C}_{\mathrm{ct}}^{n,k-1}(x)\big[\boldsymbol{\varepsilon}\big(\Delta\boldsymbol{u}_h^{n,k}(x)\big)\big] : \boldsymbol{\varepsilon}(\boldsymbol{w}_h(x)) \, dx = -r^{n,k-1}(\boldsymbol{w}_h) \,, \qquad \boldsymbol{w}_h \in \boldsymbol{X}_h \,,$$

introduces the global coupling. This problem corresponds to the linearized constitutive law given by the consistent tangent modulus $\mathbb{C}_{\mathrm{ct}}$.

Algorithm 8.1 Return algorithm for incremental plasticity

S0) Given $\boldsymbol{\varepsilon}_{p,h}^0 \in \boldsymbol{P}_h$ and $\boldsymbol{u}_h^0 \in \boldsymbol{X}_h(\boldsymbol{u}_D(t_0))$, choose $\epsilon > 0$ and set $n := 1$.

S1) While $t_{n-1} < T$, choose $\Delta t_n > 0$ such that $\Delta t_n \leq (T - t_{n-1})$ and set $t_n = t_{n-1} + \Delta t_n$.
Choose initial guess $\boldsymbol{u}_h^{n,0} \in \boldsymbol{X}_h(\boldsymbol{u}_D(t_n))$ (e.g. $\boldsymbol{u}_h^{n,0} = \boldsymbol{u}_h^{n-1}$ + Dirichlet boundary conditions). Set $k := 1$.

S2) At each quadrature point $\boldsymbol{\xi} \in \boldsymbol{\Xi}$, compute
$$\boldsymbol{\eta}_h^{n,k-1}(\boldsymbol{\xi}) = \mathbb{C}\big[\boldsymbol{\varepsilon}(\boldsymbol{u}_h^{n,k-1}(\boldsymbol{\xi})) - \boldsymbol{\varepsilon}_{p,h}^{n-1}(\boldsymbol{\xi})\big]\,, \qquad \text{(trial stress)}\,,$$
$$\boldsymbol{\sigma}_h^{n,k-1}(\boldsymbol{\xi}) = R(\boldsymbol{\eta}_h^{n,k-1}(\boldsymbol{\xi}))\,, \qquad \text{(stress response)}\,.$$

S3) Compute the residual
$$r^{n,k-1}(\boldsymbol{w}_h) = \int_\Omega \boldsymbol{\sigma}_h^{n,k-1}(x) : \boldsymbol{\varepsilon}(\boldsymbol{w}_h(x))\,dx - \ell(t_n, \boldsymbol{w}_h)\,, \qquad \boldsymbol{w}_h \in \boldsymbol{X}_h\,.$$

S4) If $\|r^{n,k-1}\|_{\boldsymbol{X}_h^*} < \epsilon$, set $\boldsymbol{u}_h^n = \boldsymbol{u}_h^{n,k-1}$ and $\boldsymbol{\sigma}_h^n = \boldsymbol{\sigma}_h^{n,k-1}$. Go to S8).

S5) At each quadrature point $\boldsymbol{\xi} \in \boldsymbol{\Xi}$, determine $\mathbb{S}^{n,k-1}(\boldsymbol{\xi}) \in \partial R\big(\boldsymbol{\eta}_h^{n,k-1}(\boldsymbol{\xi})\big)$ and the consistent algorithmic tangent modulus $\mathbb{C}_{\mathrm{ct}}^{n,k-1}(\boldsymbol{\xi}) = \mathbb{S}^{n,k-1}(\boldsymbol{\xi}) \circ \mathbb{C}$.

S6) Determine $\Delta \boldsymbol{u}_h^{n,k} \in \boldsymbol{X}_h$ such that
$$\int_\Omega \mathbb{C}_{\mathrm{ct}}^{n,k-1}(x)\big[\boldsymbol{\varepsilon}\big(\Delta\boldsymbol{u}_h^{n,k}(x)\big)\big] : \boldsymbol{\varepsilon}(\boldsymbol{w}_h(x))\,dx = -r^{n,k-1}(\boldsymbol{w}_h)\,, \qquad \boldsymbol{w}_h \in \boldsymbol{X}_h\,.$$

S7) Set $\boldsymbol{u}_h^{n,k} = \boldsymbol{u}_h^{n,k-1} + \Delta\boldsymbol{u}_h^{n,k}$. Set $k := k + 1$ and go to S2).

S8) Compute $\boldsymbol{\varepsilon}_{p,h}^n(\boldsymbol{\xi}) = \boldsymbol{\varepsilon}(\boldsymbol{u}_h^n(\boldsymbol{\xi})) - \mathbb{C}^{-1}[\boldsymbol{\sigma}_h^n(\boldsymbol{\xi})]$ for all $\boldsymbol{\xi} \in \boldsymbol{\Xi}$.
Set $n := n + 1$ and go to S1).

1.3. Stopping Criteria - Evaluating the Dual Norm $\|\cdot\|_{\boldsymbol{X}_h^*}$. We shortly remark on the stopping criteria in step S4) in which we need to evaluate the norm in the dual space $\boldsymbol{X}_h^*$. For further usage, we will first define the (spatially continuous) dual norm of the energy norm. This is the operator norm

$$\|\ell\|_* = \sup_{\|\boldsymbol{u}\| \leq 1} \langle \ell, \boldsymbol{u} \rangle_{\boldsymbol{X}^* \times \boldsymbol{X}} = \sqrt{\langle \ell, C^{-1}\ell \rangle_{\boldsymbol{X}^* \times \boldsymbol{X}}} = \|C^{-1}\ell\|\,, \tag{8.1}$$

with C being the elasticity operator, see (2.3). That the supremum is indeed attained at

$$\boldsymbol{u} = \frac{C^{-1}\ell}{\sqrt{\langle \ell, C^{-1}\ell \rangle_{\boldsymbol{X}^* \times \boldsymbol{X}}}}\,,$$

easily follows from the Karush-Kuhn-Tucker conditions, cf. [ABM06, Section 9.6] or [KZ05, Chapter 6]. Evaluating $\|\cdot\|_*$ therefore comprises the solution of a linear elasticity problem and from a numerical point of view, this is a laborious task. Though, working in this norm will make analysis easier from time to time. Theoretically, it is also possible to define the discrete energy norm

$$\|\boldsymbol{u}_h\|_h = \int_{\Omega_h} \boldsymbol{\varepsilon}(\boldsymbol{u}_h(x)) : \mathbb{C}[\boldsymbol{\varepsilon}(\boldsymbol{u}_h(x))]\,dx\,,$$

and if $\Omega = \Omega_h$ and the quadrature rule is sufficiently accurate, we find $\|\boldsymbol{u}_h\| = \|\boldsymbol{u}_h\|_h$ for $\boldsymbol{u}_h \in \boldsymbol{X}_h$. But for the corresponding discrete dual norm

$$\|\ell_h\|_{h,*} = \|C_h^{-1}\ell_h\|_h \,.$$

we always find $\|\ell_h\|_{h,*} \neq \|\ell_h\|_*$ as $\|\cdot\|_*$ involves the inversion of the spatially continuous operator C which is not feasible numerically. But due to efficiency reasons, also the evaluation of $\|\cdot\|_{h,*}$ is generally not appropriate. Instead, we use the finite dimensionality $\dim(\boldsymbol{X}_h) = N$ of the finite element space. After fixing a basis $\{\psi^1, \dots, \psi^N\}$ of $\boldsymbol{X}_h$, we can write $\boldsymbol{u}_h = \sum_{i=1}^{N} \underline{\boldsymbol{u}}_i \psi^i$ and this gives rise to the definition of the operator $E_h : \mathbb{R}^N \to \boldsymbol{X}_h$, $\boldsymbol{u}_h = E_h \underline{\boldsymbol{u}}$, as well as its dual $E_h^* : \boldsymbol{X}_h^* \to \mathbb{R}^N$. Then, a computatable norm on $\boldsymbol{X}_h$ is given by $\|\ell_h\|_{\boldsymbol{X}_h^*} = |E_h^* \ell_h|$, with $|\cdot|$ denoting the Euclidian norm in $\mathbb{R}^N$. Unless stated otherwise, we will always use this norm on $\boldsymbol{X}_h^*$ within a computational framework.

2. Globalization Techniques

We present some simple strategies aiming to improve the global behaviour of the above algorithm. We remark that these strategies do not depend on any additional structure. We consider both the continuous and discrete equations $F(\boldsymbol{u}) = 0$ and $F_h(\boldsymbol{u}_h) = 0$ with $F : \boldsymbol{X} \to \boldsymbol{X}^*$ and $F_h : \boldsymbol{X}_h \to \boldsymbol{X}_h^*$, respectively.

2.1. Globalization by Merit Functions. Typically, the global convergence properties of Newton-type algorithms are improved by the introduction of a suitable merit function which is minimized during the iteration and the minimizer of the merit function is a solution of $F(\boldsymbol{u}) = 0$. If F is the derivative of a potential in the context of a minimization problem, the potential itself can serve as a merit function and this case will be treated in the next section. If a potential does not exist, a different merit function has to be imposed. In finite dimension, i.e. $F : \mathbb{R}^N \to \mathbb{R}^N$, the most widely used merit function is $\theta(\boldsymbol{u}) = \frac{1}{2} F(\boldsymbol{u})^T F(\boldsymbol{u})$ and sometimes also $\theta(\boldsymbol{u}) = |F(\boldsymbol{u})|$ is used with a suitable norm $|\cdot|$ in $\mathbb{R}^N$, cf. [PF03a, IK08]. However, when F is related to a differential operator, the definition of a merit function is more involved since it should reflect the continuous nature of the problem and particularly, it should be independent of the discretization.

2.1.1. *A Simple Line Search for the Discrete Equation.* We begin with a line search not fulfilling the above conditions as it heavily relies on the discrete structure obtained by discretization. On the other hand, its implementation is straight forward. Using the merit function $\theta(\boldsymbol{u}_h) = |E_h^* F_h(\boldsymbol{u}_h)|$ with $|\cdot|$ being the Euclidian norm, the above algorithm can easily be extended by a simple backtracking line search. In this case, step S7) in Algorithm 8.1 is replaced by the line search given in Algorithm 8.2. It is important to note that generally, there is no guarantee that the condition in S7d) is ever met, i.e. that the line search terminates after finitely many steps.

2.1.2. *A Line Search based on the Dual Energy Norm.* We now consider the merit function $\theta(\boldsymbol{u}_h) = \frac{1}{2} \|F_h(\boldsymbol{u}_h)\|_{h,*}^2$. This merit function still depends on the mesh size h, but now, it is possible to set up a continuous counterpart. θ has the same semismoothness properties as F_h but unfortunately, it is not (Fréchet) differentiable in general. In the following, we assume that the response function R is semismooth and consequently, the same holds for F_h and θ (as well as the directional differentiability). Let $\boldsymbol{v}_h \in \boldsymbol{X}_h$ be the solution of the elasticity problem $C_h \boldsymbol{v}_h = F_h(\boldsymbol{u}_h)$. Then, the directional derivative of θ at $\boldsymbol{u}_h$ into the

---

Algorithm 8.2 Simple backtracking line search.

S7) S7a) Choose $\beta \in (0,1)$ and set $m = 0$.

 S7b) Compute $\rho_m = \beta^m$ and set $\boldsymbol{u}_h^{n,k,m} = \boldsymbol{u}_h^{n,k-1} + \rho_m \Delta \boldsymbol{u}_h^{n,k}$.

 S7c) At each quadrature point $\boldsymbol{\xi} \in \Xi$, compute
$$\boldsymbol{\eta}_h^{n,k,m}(\boldsymbol{\xi}) = \mathbb{C}\big[\boldsymbol{\varepsilon}(\boldsymbol{u}_h^{n,k,m}(\boldsymbol{\xi})) - \boldsymbol{\varepsilon}_{p,h}^{n-1}(\boldsymbol{\xi})\big]\,,$$
$$\boldsymbol{\sigma}_h^{n,k,m}(\boldsymbol{\xi}) = R(\boldsymbol{\eta}_h^{n,k,m}(\boldsymbol{\xi}))\,,$$
$$r^{n,k,m}(\boldsymbol{w}_h) = \int_\Omega \boldsymbol{\sigma}_h^{n,k,m}(x) : \boldsymbol{\varepsilon}(\boldsymbol{w}_h(x))\,dx - \ell(t_n, \boldsymbol{w}_h)\,, \qquad \boldsymbol{w}_h \in \boldsymbol{X}_h\,.$$

 S7d) If $|E_h^* r^{n,k,m}| < |E_h^* r^{n,k-1}|$, set $\boldsymbol{u}_h^{n,k} = \boldsymbol{u}_h^{n,k,m}$, $k := k+1$ and go to S2).

 S7e) Set $m := m+1$ and go to S7b).

---

direction $\boldsymbol{w}_h$ is characterized by
$$D\theta(\boldsymbol{u}_h; \boldsymbol{w}_h) = \int_\Omega DR\big(\mathbb{C}[\boldsymbol{\varepsilon}(\boldsymbol{u}_h(x)) - \boldsymbol{\tau}_h(x)]; \mathbb{C}[\boldsymbol{\varepsilon}(\boldsymbol{w}_h(x))]\big) : \boldsymbol{\varepsilon}(\boldsymbol{v}_h(x))\,dx\,.$$

Hence, evaluating θ and its directional derivative at $\boldsymbol{u}_h$ requires the solution of a linear elasticity problem with right-hand-side $F_h(\boldsymbol{u}_h)$. Loosely following [IK08, Algorithm G, page 222] and [PF03a, Section 8.3], we modify the generalized Newton method according to Algorithm 8.3. We remark that step S7d) is not specified and a non-trivial task. In this step, a suitable descent direction for the merit function must be computed. It remains an open question how this can be handled efficiently in the current setting as the merit function is not differentiable. Moreover, the existence of a step size ρ_m satisfying the Armijo-condition in S7e) can only be proved under suitable assumptions. The reason for mentioning this rather vague algorithm is the stability in function space. However,

---

Algorithm 8.3 Modified line search with merit function $\theta(\boldsymbol{u}_h) = \frac{1}{2}\|F_h(\boldsymbol{u}_h)\|_{h,*}^2$.

S7) S7a) Choose $\beta, \gamma, \sigma \in (0,1)$.

 S7b) Set $\boldsymbol{u}_h^{n,k,0} = \boldsymbol{u}_h^{n,k-1} + \Delta \boldsymbol{u}_h^{n,k}$. At each quadrature point $\boldsymbol{\xi} \in \Xi$, compute
$$\boldsymbol{\eta}_h^{n,k,0}(\boldsymbol{\xi}) = \mathbb{C}\big[\boldsymbol{\varepsilon}(\boldsymbol{u}_h^{n,k,0}(\boldsymbol{\xi})) - \boldsymbol{\varepsilon}_{p,h}^{n-1}(\boldsymbol{\xi})\big]\,,$$
$$\boldsymbol{\sigma}_h^{n,k,0}(\boldsymbol{\xi}) = R(\boldsymbol{\eta}_h^{n,k,0}(\boldsymbol{\xi}))\,,$$
$$r^{n,k,0}(\boldsymbol{w}_h) = \int_\Omega \boldsymbol{\sigma}_h^{n,k,0}(x) : \boldsymbol{\varepsilon}(\boldsymbol{w}_h(x))\,dx - \ell(t_n, \boldsymbol{w}_h)\,, \qquad \boldsymbol{w}_h \in \boldsymbol{X}_h\,.$$

 S7c) If $\|r^{n,k,0}\|_{h,*} < \gamma \|r^{n,k-1}\|_{h,*}$, set $\boldsymbol{u}_h^{n,k} = \boldsymbol{u}_h^{n,k,0}$, $k := k+1$ and go to S2).

 S7d) Compute a suitable descent direction $\boldsymbol{d}_h^{n,k}$ of θ at $\boldsymbol{u}_h^{n,k-1}$ satisfying $D\theta(\boldsymbol{u}_h^{n,k-1}; \boldsymbol{d}_h^{n,k}) < 0$. Set $m := 0$.

 S7e) Compute $\rho_m = \beta^m$ and
$$\vartheta_m = \theta\big(\boldsymbol{u}_h^{n,k-1} + \rho_m \boldsymbol{d}_h^{n,k}\big) - \theta(\boldsymbol{u}_h^{n,k-1}) - \sigma \rho_m D\theta(\boldsymbol{u}_h^{n,k-1}; \boldsymbol{d}_h^{n,k})\,.$$

 S7f) If $\vartheta_m \le 0$, set $\boldsymbol{u}_h^{n,k} = \boldsymbol{u}_h^{n,k-1} + \rho_m \boldsymbol{d}_h^{n,k}$, $k := k+1$ and go to S2).

 S7g) Set $m := m+1$ and go to S7e).

---

in infinite dimensions, the smoothness properties of F and therefore also of θ remain unclear. Besides, evaluating θ (and likewise $D\theta(\cdot;\cdot)$) consists in solving an elasticity problem amounting in large computational costs. Nevertheless, from a theoretical point of view, the local superlinear behaviour can be preserved in the discrete case [**PHR91**].

2.2. Global Convergence under Strong Monotonicity. We consider the strongly monotone setting in the spatially continuous case. Particularly, we consider the problem of finding $\boldsymbol{u} \in \boldsymbol{X}(\boldsymbol{u}_D)$ such that $F(\boldsymbol{u}) = 0$ in $\boldsymbol{X}^*$, cf. (6.3) and (6.4), under the assumption that F is strongly monotone, i.e. there exists $\beta > 0$ such that

$$\langle F(\boldsymbol{u}) - F(\boldsymbol{w}), \boldsymbol{u} - \boldsymbol{w} \rangle_{\boldsymbol{X}^* \times \boldsymbol{X}} \geq \tfrac{\beta}{2} \|\boldsymbol{u} - \boldsymbol{w}\|^2 . \tag{8.2}$$

Under this assumption, we already proved the superlinear convergence of the generalized Newton method for the discrete problem provided that the response function R is semismooth, see Theorem 7.3. We now show global convergence of a fixed point iteration in function space, provided that F satisfies a Lipschitz condition.

Theorem 8.1. *Assume that $F : \boldsymbol{X} \to \boldsymbol{X}^*$ is strongly monotone, i.e.* (8.2) *holds, and that F is Lipschitz continuous with modulus $L \geq 0$, i.e.*

$$\|F(\boldsymbol{u}) - F(\boldsymbol{w})\|_* \leq L \|\boldsymbol{u} - \boldsymbol{w}\| .$$

Then, starting from $\boldsymbol{u}^0 \in \boldsymbol{X}(\boldsymbol{u}_D)$, the fixed point iteration

$$\boldsymbol{u}^k = \boldsymbol{u}^{k-1} + \rho \, \Delta \boldsymbol{u}^k \qquad \text{with} \qquad \Delta \boldsymbol{u}^k = -C^{-1} F(\boldsymbol{u}^{k-1}) \in \boldsymbol{X} , \tag{8.3}$$

converges to the unique solution $\boldsymbol{u}^* \in \boldsymbol{X}(\boldsymbol{u}_D)$ if $\rho \in \left(0, \frac{\beta}{L^2}\right)$.

PROOF. The proof is a standard application of the contraction mapping theorem. We define the mapping $\varphi : \boldsymbol{X} \to \boldsymbol{X}$ as $\varphi(\boldsymbol{u}) = \boldsymbol{u} - \rho C^{-1} F(\boldsymbol{u})$ and we will show that φ is a contraction. We obtain

$$\|\varphi(\boldsymbol{u}) - \varphi(\boldsymbol{w})\|^2 = \langle C\big(\varphi(\boldsymbol{u}) - \varphi(\boldsymbol{w})\big), \varphi(\boldsymbol{u}) - \varphi(\boldsymbol{w}) \rangle_{\boldsymbol{X}^* \times \boldsymbol{X}}$$
$$= \|\boldsymbol{u} - \boldsymbol{w}\|^2 - 2\rho \langle F(\boldsymbol{u}) - F(\boldsymbol{w}), \boldsymbol{u} - \boldsymbol{w} \rangle_{\boldsymbol{X}^* \times \boldsymbol{X}} + \rho^2 \|F(\boldsymbol{u}) - F(\boldsymbol{w})\|_*^2$$
$$\leq \big(1 - \rho\,\beta + \rho^2 L^2\big) \|\boldsymbol{u} - \boldsymbol{w}\|^2$$

and for $\rho \in \left(0, \frac{\beta}{L^2}\right)$, this is a contraction. $\qquad\square$

As a by-product, we also showed the existence of a solution under the given conditions and thereby completed the proof of Theorem 4.1. The same result applies to the discrete counterpart $F_h(\boldsymbol{u}_h) = 0$. The above fixed point iteration consists of solving a linear elasticity problem in each step. For associated plasticity, this iteration can be considered as a gradient algorithm with fixed step size and we will come back to this point in the next section.

Remark 8.2. *The above result applies to associated hardening plasticity and the viscoplastic regularization. Considering the example of non-associated (smoothed) Drucker-Prager plasticity, once more the hardening and the viscoplastic regularization cannot be arbitrarily small or requires a sufficiently small time step size in the incremental setting.*

We only mention that the Lipschitz constant L is moderate and for associated perfect plasticity and the corresponding viscoplastic regularization, the constant is $L = 1$. Therefore note that the response function is given by $R(\boldsymbol{\eta}) = \lambda\,\boldsymbol{\eta} + (1-\lambda)P_K(\boldsymbol{\eta})$ with $\lambda \in [0,1]$. Then, with $\boldsymbol{y} = C^{-1} F(\boldsymbol{u})$ and $\boldsymbol{z} = C^{-1} F(\boldsymbol{w})$ and setting $\boldsymbol{\tau} = 0$ for simplicity, we have

$$\|F(\boldsymbol{u}) - F(\boldsymbol{w})\|_*^2 = \langle F(\boldsymbol{u}) - F(\boldsymbol{w}), \boldsymbol{y} - \boldsymbol{z} \rangle_{\boldsymbol{X}^* \times \boldsymbol{X}}$$

$$= \int_\Omega \Big(R(\mathbb{C}[\boldsymbol{\varepsilon}(\boldsymbol{u}(x))]) - R(\mathbb{C}[\boldsymbol{\varepsilon}(\boldsymbol{w}(x))]) \Big) : \big(\boldsymbol{\varepsilon}(\boldsymbol{y}(x)) - \boldsymbol{\varepsilon}(\boldsymbol{z}(x)) \big)\, dx$$

$$= \lambda \int_\Omega \Big(\mathbb{C}[\boldsymbol{\varepsilon}(\boldsymbol{u}(x))] - \mathbb{C}[\boldsymbol{\varepsilon}(\boldsymbol{w}(x))] \Big) : \big(\boldsymbol{\varepsilon}(\boldsymbol{y}(x)) - \boldsymbol{\varepsilon}(\boldsymbol{z}(x)) \big)\, dx$$

$$+ (1 - \lambda) \int_\Omega \Big(P_K(\mathbb{C}[\boldsymbol{\varepsilon}(\boldsymbol{u}(x))]) - P_K(\mathbb{C}[\boldsymbol{\varepsilon}(\boldsymbol{w}(x))]) \Big) : \big(\boldsymbol{\varepsilon}(\boldsymbol{y}(x)) - \boldsymbol{\varepsilon}(\boldsymbol{z}(x)) \big)\, dx$$

$$\leq \lambda\, \|\mathbb{C}[\boldsymbol{\varepsilon}(\boldsymbol{u}) - \boldsymbol{\varepsilon}(\boldsymbol{w})]\|_{\boldsymbol{\Sigma}} \|\mathbb{C}[\boldsymbol{\varepsilon}(\boldsymbol{y}) - \boldsymbol{\varepsilon}(\boldsymbol{z})]\|_{\boldsymbol{\Sigma}}$$

$$+ (1-\lambda)\|P_{\boldsymbol{K}}(\mathbb{C}[\boldsymbol{\varepsilon}(\boldsymbol{u})]) - P_{\boldsymbol{K}}(\mathbb{C}[\boldsymbol{\varepsilon}(\boldsymbol{w})])\|_{\boldsymbol{\Sigma}} \|\mathbb{C}[\boldsymbol{\varepsilon}(\boldsymbol{y}) - \boldsymbol{\varepsilon}(\boldsymbol{z})]\|_{\boldsymbol{\Sigma}}$$

$$\leq \lambda\, \|\boldsymbol{u} - \boldsymbol{w}\|\, \|\boldsymbol{y} - \boldsymbol{z}\| + (1-\lambda)\|\mathbb{C}[\boldsymbol{\varepsilon}(\boldsymbol{u})] - \mathbb{C}[\boldsymbol{\varepsilon}(\boldsymbol{w})]\|_{\boldsymbol{\Sigma}} \|\boldsymbol{y} - \boldsymbol{z}\|$$

$$= \|\boldsymbol{u} - \boldsymbol{w}\|\, \|\boldsymbol{y} - \boldsymbol{z}\| = \|\boldsymbol{u} - \boldsymbol{w}\|\, \|F(\boldsymbol{u}) - F(\boldsymbol{w})\|_* \,.$$

For associated hardening plasticity, L depends on $\mathbb{H}$ but if $\mathbb{H} = H_0 \mathbb{C}$ with $H_0 > 0$ we have $L = 1$ as well, and we also refer to the Subsections 3.2.3 and 3.2.4.

2.3. Globalization by Continuation - a Homotopy Approach. In this section, we will consider the variational problem of finding $\boldsymbol{u} \in \boldsymbol{X}(\boldsymbol{u}_D)$ such that

$$(1 - \lambda) \int_\Omega \mathbb{C}[\boldsymbol{\varepsilon}(\boldsymbol{u}(x))] : \boldsymbol{\varepsilon}(\boldsymbol{w}(x))\, dx + \lambda \int_\Omega R(\mathbb{C}[\boldsymbol{\varepsilon}(\boldsymbol{u}(x))]) : \boldsymbol{\varepsilon}(\boldsymbol{w}(x))\, dx = \ell(\boldsymbol{w})\,,$$

for all $\boldsymbol{w} \in \boldsymbol{X}$, which occurs naturally by means of the viscoplastic regularization, cf. (3.5), (4.17). However, we will interpret this setting as a homotopy for solving $F(\boldsymbol{u}) = 0$, i.e.

$$0 = \langle F(\boldsymbol{u}), \boldsymbol{w} \rangle_{\boldsymbol{X}^* \times \boldsymbol{X}} = \int_\Omega R(\mathbb{C}[\boldsymbol{\varepsilon}(\boldsymbol{u}(x))]) : \boldsymbol{\varepsilon}(\boldsymbol{w}(x))\, dx - \ell(\boldsymbol{w})\,, \qquad \boldsymbol{w} \in \boldsymbol{X}\,.$$

Therefore, we define $H : [0,1] \times \boldsymbol{X} \to \boldsymbol{X}^*$ as

$$H(\lambda, \boldsymbol{u}) = (1 - \lambda)C\boldsymbol{u} + \lambda F(\boldsymbol{u})\,. \tag{8.4}$$

For $\lambda = 0$, we obtain the elasticity problem which is always well posed and for $\lambda = 1$, we obtain the underlying plasticity problem. Such homotopy or continuation methods have a long history and a classical reference is [OR70]. In the following, we will assume that for fixed $\lambda \in [0,1]$, there always exists $\boldsymbol{u}(\lambda) \in \boldsymbol{X}(\boldsymbol{u}_D)$ such that $H(\lambda, \boldsymbol{u}(\lambda)) = 0$.

After discretization, we are confronted with finding zeros of $H_h : [0,1] \times \boldsymbol{X}_h \to \boldsymbol{X}_h^*$, $H_h(\lambda, \boldsymbol{u}_h) = (1-\lambda)C_h\boldsymbol{u}_h + \lambda F_h(\boldsymbol{u})$ for given $\lambda \in [0,1]$. Assuming that F_h is semismooth (of order $p \in (0,1]$), it follows that H_h is semismooth as well. Since the generalized Newton method as introduced in the previous chapter only converges locally and therefore requires a good initial guess, a straight forward approach is Algorithm 8.4. If F (or F_h) is monotone, then the subproblems are uniquely solvable for $\lambda \in [0,1)$. If F is even strongly

---

Algorithm 8.4 Continuation method for $F_h(\boldsymbol{u}_h) = 0$.

S0) Set $\lambda_0 = 0$ and solve the elasticity problem $H(\lambda_0, \boldsymbol{u}_h^0) = 0$ for $\boldsymbol{u}_h^0 \in \boldsymbol{X}_h(\boldsymbol{u}_D)$. Set $k := 1$.

S1) If $\lambda_{k-1} = 1$, set $\boldsymbol{u}_h^* = \boldsymbol{u}_h^{k-1}$ and stop.

S2) Choose $\Delta\lambda_k > 0$ such that $\lambda_k := \lambda_{k-1} + \Delta\lambda_k \leq 1$.

S3) Solve the equation $H_h(\lambda_k, \boldsymbol{u}_h^k) = 0$ for $\boldsymbol{u}_h^k \in \boldsymbol{X}_h(\boldsymbol{u}_D)$ with the generalized Newton method and initial guess $\boldsymbol{u}_h^{k,0} = \boldsymbol{u}_h^{k-1}$.

S4) Set $k := k + 1$ and go to S1).

---

monotone, then the subproblems have a unique solution for all $\lambda \in [0, 1]$. If however, F only satisfies

$$\langle F(\boldsymbol{u}) - F(\boldsymbol{w}), \boldsymbol{u} - \boldsymbol{w} \rangle_{\boldsymbol{X}^* \times \boldsymbol{X}} \geq -L \|\boldsymbol{u} - \boldsymbol{w}\|^2 \,,$$

with $L \geq 0$, as is common in non-associated plasticity, we can only guarantee that the homotopy is well-defined if $\lambda \in [0, \frac{1}{1+L})$.

We remark that solving the subproblems $H_h(\lambda_k, \cdot) = 0$ exactly is generally not necessary unless $\lambda_k = 1$. Moreover, in step S2), $\Delta \lambda_k$ has to be chosen appropriately to guarantee that $\boldsymbol{u}_h^{k-1}$ is a good initial guess for the k-th subproblem. On the other hand, $\Delta \lambda_k$ should be large enough to make sufficient progress. Thus, a suitable update strategy must be at hand.

3. Global Convergence for Associated Plasticity

As associated plasticity can be formulated in the framework of convex minimization problems, it is natural to exploit this additional structure. Therefore, we extend the generalized Newton method for the equation $F_h(\boldsymbol{u}_h) = 0$ to the generalized Newton method for unconstrained minimization problems. But before we do so, we consider gradient-related methods for which we are able to show global convergence in function space.

For convenience of the reader, we shortly recapitulate the corresponding functionals of perfect plasticity, hardening plasticity and the viscoplastic regularization, and we refer to Sections 2.3, 3.1 and 3.2.

$$\mathcal{E}_{\text{pl}}(\boldsymbol{u}) = \Upsilon\big(\mathbb{C}[\boldsymbol{\varepsilon}(\boldsymbol{u}) - \boldsymbol{\tau}]\big) - \ell(\boldsymbol{u}) \,,$$

$$\mathcal{E}_{\text{hd}}(\boldsymbol{u}) = \Upsilon^N(\mathbb{C}[\boldsymbol{\varepsilon}(\boldsymbol{u}) - \boldsymbol{\tau}]) + \tfrac{1}{2}\big(\mathbb{D}[\boldsymbol{\varepsilon}(\boldsymbol{u}) - \boldsymbol{\tau}], \boldsymbol{\varepsilon}(\boldsymbol{u}) - \boldsymbol{\tau}\big)_{\boldsymbol{P}} - \ell(\boldsymbol{u}) \,,$$

$$\mathcal{E}_{\text{vp},\alpha}(\boldsymbol{u}) = \tfrac{\alpha}{1+\alpha}\, \Upsilon(\mathbb{C}[\boldsymbol{\varepsilon}(\boldsymbol{u}) - \boldsymbol{\tau}]) + (1 - \tfrac{\alpha}{1+\alpha})\mathcal{W}_e(\boldsymbol{\varepsilon}(\boldsymbol{u}) - \boldsymbol{\tau}) - \ell(\boldsymbol{u}) \,.$$

The potentials Υ and Υ^N are given by $\Upsilon(\boldsymbol{\sigma}) = \tfrac{1}{2}\|\boldsymbol{\sigma}\|_{\boldsymbol{\Sigma}}^2 - \tfrac{1}{2}\|\boldsymbol{\sigma} - P_K(\boldsymbol{\sigma})\|_{\boldsymbol{\Sigma}}^2$, also see (2.35), and $\Upsilon^N(\boldsymbol{\sigma}) = \tfrac{1}{2}\|\boldsymbol{\sigma}\|_N^2 - \tfrac{1}{2}\|\boldsymbol{\sigma} - P_K^N(\boldsymbol{\sigma})\|_N^2$, respectively. Each of the above functionals is convex and Fréchet differentiable, and $\mathcal{E}_{\text{hd}}$ and $\mathcal{E}_{\text{vp},\alpha}$ are even uniformly convex. Henceforth, by $\mathcal{E} : \boldsymbol{X} \to \mathbb{R}$, we will denote any of the above functionals and we consider the primal problem:

$$\text{Minimize} \quad \mathcal{E}(\boldsymbol{u}) \qquad \text{subject to} \quad \boldsymbol{u} \in \boldsymbol{X}(\boldsymbol{u}_D) \,.$$

Since $\mathcal{E}$ is convex, the necessary and sufficient optimality condition for a minimum (if it exists) is $D\mathcal{E}(\boldsymbol{u}) = 0$. As usual, we will also write $F = D\mathcal{E}$.

3.1. A Gradient-Type Algorithm and Global Convergence.
We study general gradient-related methods in $\boldsymbol{X}$ and we assume that a solution $\boldsymbol{u}^* \in \boldsymbol{X}(\boldsymbol{u}_D)$ exists. In the following, let $\{S_k\}_k \subset L(\boldsymbol{X}, \boldsymbol{X}^*)$ be a family of symmetric, uniformly elliptic and bounded operators, i.e. there are constants $0 < s_0 \leq s_1$ such that for all $k \in \mathbb{N}$ and $\boldsymbol{v}, \boldsymbol{w} \in \boldsymbol{X}$, the following holds:

$$s_0 \|\boldsymbol{w}\|^2 \leq \langle S_k \boldsymbol{w}, \boldsymbol{w} \rangle_{\boldsymbol{X}^* \times \boldsymbol{X}}, \qquad \text{and} \qquad \langle S_k \boldsymbol{v}, \boldsymbol{w} \rangle_{\boldsymbol{X}^* \times \boldsymbol{X}} \leq s_1 \|\boldsymbol{v}\| \, \|\boldsymbol{w}\|. \tag{8.5}$$

In the k-th iteration, the operator S_k is used to determine the new search direction $\Delta \boldsymbol{u}^k \in \boldsymbol{X}$. Based on these operators, we will examine the convergence properties of Algorithm 8.5. If $S_k \equiv C$, the algorithm is closely related with the fixed point iteration of the previous section. But since $F = D\mathcal{E}$ is the derivative of a potential, we can use a line search to determine the step size ρ in every iteration instead of keeping the step size fixed. For the analysis, we use the dual energy norm $\|\cdot\|_*$ as a stopping criteria, cf. (8.1). However, in

Algorithm 8.5 A gradient algorithm for associated plasticity.

S0)   Choose $\beta, \sigma \in (0, 1)$, a tolerance $\epsilon > 0$ and an initial guess $\boldsymbol{u}^0 \in \boldsymbol{X}(\boldsymbol{u}_D)$. Set $k := 1$.

S1)   If $\|D\mathcal{E}(\boldsymbol{u}^{k-1})\|_* < \epsilon$, set $\boldsymbol{u}^* = \boldsymbol{u}^{k-1}$ and stop.

S2)   Solve the problem $S_k \Delta \boldsymbol{u}^k = -D\mathcal{E}(\boldsymbol{u}^{k-1})$ for $\Delta \boldsymbol{u}^k \in \boldsymbol{X}$. Set $m := 0$.

S3)   S3a) Compute $\rho_m = \beta^m$ and
$$\vartheta_m = \mathcal{E}(\boldsymbol{u}^{k-1} + \rho_m \Delta \boldsymbol{u}^k) - \mathcal{E}(\boldsymbol{u}^{k-1}) - \sigma \rho_m \langle D\mathcal{E}(\boldsymbol{u}^{k-1}), \Delta \boldsymbol{u}^k \rangle_{\boldsymbol{X}^* \times \boldsymbol{X}}.$$

S3b) If $\vartheta_m \leq 0$, set $\rho_k = \rho_m$ and $\boldsymbol{u}^k = \boldsymbol{u}^{k-1} + \rho_k \Delta \boldsymbol{u}^k$. Set $k := k + 1$ and go to S1).

S3c) Set $m := m + 1$ and go to S3a).

contrast to the previous Section, we can now derive conditions which guarantee global convergence. As usual, for the global convergence of a gradient-related algorithm, two conditions need to be verified:

(1) admissibility of the step sizes,
(2) admissibility of the search directions.

   3.1.1. *Admissibility of the Step Size.* Step S3) of Algorithm 8.5 involves the *Armijo* line search. We will show that the Armijo line search terminates under quite natural conditions.

Lemma 8.3. *Assume that the Frechét derivative of $\mathcal{E}$ is Lipschitz continuous with modulus $L \geq 0$ w.r.t. the energy norm, i.e.*
$$\langle D\mathcal{E}(\boldsymbol{v}) - D\mathcal{E}(\boldsymbol{w}), \boldsymbol{v} - \boldsymbol{w} \rangle_{\boldsymbol{X}^* \times \boldsymbol{X}} \leq L \|\boldsymbol{v} - \boldsymbol{w}\|^2,$$
and that the operators $\{S_k\}_k$, $k \geq 1$, satisfy (8.5). Then, the Armijo line search in Algorithm 8.5 terminates whenever $\rho_m \leq \frac{2s_0(1-\sigma)}{L}$.

   PROOF. We consider one step and set $\boldsymbol{u} \equiv \boldsymbol{u}^{k-1}$ and $\Delta \boldsymbol{u} = \Delta \boldsymbol{u}^k$. With the scalar function $\varphi(\tau) = \mathcal{E}(\boldsymbol{u} + \tau \rho \Delta \boldsymbol{u})$, we find $\varphi(0) = \mathcal{E}(\boldsymbol{u})$, $\varphi(1) = \mathcal{E}(\boldsymbol{u} + \rho \Delta \boldsymbol{u})$ and
$$\varphi'(\tau) = \rho \langle D\mathcal{E}(\boldsymbol{u} + \tau \rho \Delta \boldsymbol{u}), \Delta \boldsymbol{u} \rangle_{\boldsymbol{X}^* \times \boldsymbol{X}}.$$
Since $\varphi(1) = \varphi(0) + \int_0^1 \varphi'(\tau)\, d\tau$, we infer

$$\mathcal{E}(\boldsymbol{u} + \rho \Delta \boldsymbol{u}) = \mathcal{E}(\boldsymbol{u}) + \rho \int_0^1 \langle D\mathcal{E}(\boldsymbol{u} + \tau \rho \Delta \boldsymbol{u}), \Delta \boldsymbol{u} \rangle_{\boldsymbol{X}^* \times \boldsymbol{X}}\, d\tau$$

$$= \mathcal{E}(\boldsymbol{u}) + \rho \langle D\mathcal{E}(\boldsymbol{u}), \Delta \boldsymbol{u} \rangle_{\boldsymbol{X}^* \times \boldsymbol{X}} + \int_0^1 \langle D\mathcal{E}(\boldsymbol{u} + \tau \rho \Delta \boldsymbol{u}) - D\mathcal{E}(\boldsymbol{u}), \rho \Delta \boldsymbol{u} \rangle_{\boldsymbol{X}^* \times \boldsymbol{X}}\, d\tau$$

$$\leq \mathcal{E}(\boldsymbol{u}) + \rho \langle D\mathcal{E}(\boldsymbol{u}), \Delta \boldsymbol{u} \rangle_{\boldsymbol{X}^* \times \boldsymbol{X}} + \int_0^1 \frac{L}{\tau} \|\tau \rho \Delta \boldsymbol{u}\|^2\, d\tau$$

$$\leq \mathcal{E}(\boldsymbol{u}) + \rho \langle D\mathcal{E}(\boldsymbol{u}), \Delta \boldsymbol{u} \rangle_{\boldsymbol{X}^* \times \boldsymbol{X}} + \frac{L\rho^2}{2} \|\Delta \boldsymbol{u}\|^2$$

$$\leq \mathcal{E}(\boldsymbol{u}) + \rho \langle D\mathcal{E}(\boldsymbol{u}), \Delta \boldsymbol{u} \rangle_{\boldsymbol{X}^* \times \boldsymbol{X}} + \frac{L\rho^2}{2s_0} \langle S_k \Delta \boldsymbol{u}, \Delta \boldsymbol{u} \rangle_{\boldsymbol{X}^* \times \boldsymbol{X}}.$$

From S2), we obtain $\langle S_k \Delta \boldsymbol{u}, \Delta \boldsymbol{u} \rangle_{\boldsymbol{X}^* \times \boldsymbol{X}} = -\langle D\mathcal{E}(\boldsymbol{u}), \Delta \boldsymbol{u} \rangle_{\boldsymbol{X}^* \times \boldsymbol{X}}$, and thus
$$\mathcal{E}(\boldsymbol{u} + \rho \Delta \boldsymbol{u}) \leq \mathcal{E}(\boldsymbol{u}) + \rho \left(1 - \frac{L\rho}{2s_0}\right) \langle D\mathcal{E}(\boldsymbol{u}), \Delta \boldsymbol{u} \rangle_{\boldsymbol{X}^* \times \boldsymbol{X}}.$$

Hence, if $\sigma \leq 1 - \frac{L\rho}{2s_0}$, then the Armijo condition is fulfilled and in terms of the step size ρ this is equivalent to $\rho \leq \frac{2s_0(1-\sigma)}{L}$. $\square$

We remark that typically $\sigma \in (0, \frac{1}{2})$ as only in this case, the step size $\rho = 1$ is admissible for the (quadratic) linear elasticity problem which is given by $\mathcal{E}(\boldsymbol{u}) = \frac{1}{2}\langle C\boldsymbol{u}, \boldsymbol{u}\rangle_{\boldsymbol{X}^* \times \boldsymbol{X}} - \ell(\boldsymbol{u})$, and naturally has Lipschitz modulus $L = 1$.

   3.1.2. *A Global Convergence Result.* Following [**HPUU09**, Theorem 2.2], we have the following global convergence result.

Theorem 8.4. *Let the assumptions of Lemma 8.3 be satisfied and let $\{\boldsymbol{u}^k\}_k \subset \boldsymbol{X}(\boldsymbol{u}_D)$ be generated by Algorithm 8.5. Further, assume that $\{\mathcal{E}(\boldsymbol{u}^k)\}_k \subset \mathbb{R}$ is bounded from below. Then*

$$\lim_{k\to\infty} D\mathcal{E}(\boldsymbol{u}^k) = 0\,,$$

and every accumulation point of $\{\boldsymbol{u}^k\}_k$ is a stationary point and therefore a minimizer of $\mathcal{E}$.

   PROOF. While Lemma 8.3 shows admissibility of the step sizes, it remains to check admissibility of the search directions. This means that the obtained directions are indeed suitable descent directions. This can be assured by showing the *angle condition*, i.e. the search directions $\{\Delta\boldsymbol{u}^k\}_k \subset \boldsymbol{X}$ satisfy

$$\langle D\mathcal{E}(\boldsymbol{u}^{k-1}), \Delta\boldsymbol{u}^k\rangle_{\boldsymbol{X}^*\times\boldsymbol{X}} \leq -\eta \,\|D\mathcal{E}(\boldsymbol{u}^{k-1})\|_* \,\|\Delta\boldsymbol{u}^k\|\,, \qquad k \in \mathbb{N}\,, \tag{8.6}$$

for a fixed $\eta > 0$. In order to show that the angle condition is satisfied during the algorithm, we again consider one iteration and write $S \equiv S_k$, $\Delta\boldsymbol{u} \equiv \Delta\boldsymbol{u}^k$ and $\boldsymbol{u} \equiv \boldsymbol{u}^{k-1}$. Since S is symmetric and positive definite, S defines norms on $\boldsymbol{X}$ and $\boldsymbol{X}^*$ via

$$\|\boldsymbol{w}\|_S = \sqrt{\langle S\boldsymbol{w}, \boldsymbol{w}\rangle_{\boldsymbol{X}^*\times\boldsymbol{X}}}\,, \qquad \|\ell\|_{S,*} = \sqrt{\langle \ell, S^{-1}\ell\rangle_{\boldsymbol{X}^*\times\boldsymbol{X}}} = \|S^{-1}\ell\|_S\,,$$

cf. (8.1). With (8.5), we then obtain

$$\|\ell\|_{S,*} = \sup_{\boldsymbol{w}\neq 0} \frac{\langle \ell, \boldsymbol{w}\rangle_{\boldsymbol{X}^*\times\boldsymbol{X}}}{\|\boldsymbol{w}\|_S} \leq \sup_{\boldsymbol{w}\neq 0} \frac{1}{\sqrt{s_0}} \frac{\langle \ell, \boldsymbol{w}\rangle_{\boldsymbol{X}^*\times\boldsymbol{X}}}{\|\boldsymbol{w}\|} = \frac{1}{\sqrt{s_0}}\|\ell\|_*\,,$$

and likewise $\|\ell\|_* \leq \sqrt{s_1}\|\ell\|_{S,*}$. Then,

$$\frac{1}{\sqrt{s_1}}\|D\mathcal{E}(\boldsymbol{u})\|_* \leq \|D\mathcal{E}(\boldsymbol{u})\|_{S,*} = \|S^{-1}D\mathcal{E}(\boldsymbol{u})\|_S = \|S^{-1}S\Delta\boldsymbol{u}\|_S = \|\Delta\boldsymbol{u}\|_S\,.$$

and thus $-\|\Delta\boldsymbol{u}\|_S \leq -\frac{1}{\sqrt{s_1}}\|D\mathcal{E}(\boldsymbol{u})\|_*$. From (8.5), we also find $-\|\Delta\boldsymbol{u}\|_S \leq -\sqrt{s_0}\|\Delta\boldsymbol{u}\|$ and hence,

$$\langle D\mathcal{E}(\boldsymbol{u}), \Delta\boldsymbol{u}\rangle_{\boldsymbol{X}^*\times\boldsymbol{X}} = -\langle S\Delta\boldsymbol{u}, \Delta\boldsymbol{u}\rangle_{\boldsymbol{X}^*\times\boldsymbol{X}} = -\|\Delta\boldsymbol{u}\|_S^2 \leq -\sqrt{\frac{s_0}{s_1}}\|D\mathcal{E}(\boldsymbol{u})\|_*\|\Delta\boldsymbol{u}\|\,.$$

This shows the angle condition (8.6) with $\eta = \sqrt{\frac{s_0}{s_1}} > 0$. Since η does not depend on k, all search directions are admissible during the iteration. As we assumed that $\{\mathcal{E}(\boldsymbol{u}^k)\}_k$ is bounded from below the assertion follows as in [**HPUU09**, Theorem 2.2]. $\square$

If $\mathcal{E}$ is uniformly convex, then the Algorithm 8.5 converges to the unique minimizer of $\mathcal{E}$.

3.1.3. *The Search Directions.* A special type of gradient algorithm which is very closely related to the fixed point iteration of the previous section is obtained if we always take elasticity as a preconditioner, i.e. $S_k \equiv C$. In this situation, we have the following result.

Corollary 8.5. *If $S_k \equiv C$, for perfect plasticity, kinematic hardening plasticity with $\mathbb{H} = H_0 \mathbb{C}$ and the viscoplastic regularization, the step size $\rho = 1$ in Algorithm 8.5 is always admissible if $\sigma \in (0, \frac{1}{2})$.*

PROOF. In these cases, the Lipschitz constant is $L = 1$ as we have shown in the previous section and obviously, we have $s_0 = 1$ in (8.5). Taking $\sigma \in (0, \frac{1}{2})$, it easily follows from Lemma 8.3 that the step size $\rho = 1$ is always admissible. □

However, it is well known that the above gradient method with $S_k \equiv C$ is inefficient. Usually, a method with fast local convergence properties like the (generalized) Newton method is used to compute the search direction. Afterwards, the angle condition is checked for this search direction. In the context of associated plasticity, reconsidering Subsection 7.1.1, suitable directions can be computed with the operators S_k defined via

$$\langle S_k \Delta \boldsymbol{u}^k, \boldsymbol{w} \rangle_{\boldsymbol{X}^* \times \boldsymbol{X}} = \int_\Omega \mathbb{C}_{\mathrm{ct}}^k(x) \big[\boldsymbol{\varepsilon}(\Delta \boldsymbol{u}^k(x)) \big] : \boldsymbol{\varepsilon}(\boldsymbol{w}(x)) \, dx \,, \qquad \boldsymbol{w} \in \boldsymbol{X} \,.$$

For uniformly convex problems like the viscoplastic regularization and kinematic hardening, the operators $\{S_k\}_k$ then satisfy (8.5). For perfect plasticity on the other hand, the obtained search direction may not satisfy the angle condition as $s_0 = 0$ in this case.

3.2. A Globally and Locally Superlinear Convergent Discrete Algorithm. After discretization, we consider the corresponding Ritz problem.

$$\text{Minimize} \quad \mathcal{E}_h(\boldsymbol{u}_h) \qquad \text{subject to} \quad \boldsymbol{u}_h \in \boldsymbol{X}_h(\boldsymbol{u}_D) \,, \tag{8.7}$$

with $\mathcal{E}_h : \boldsymbol{X}_h \to \mathbb{R}$ being the restriction of $\mathcal{E}$ to $\boldsymbol{X}_h$. Throughout this subsection, we assume $\mathcal{E}_h \in SC^1$, i.e. $\mathcal{E}_h$ is Fréchet differentiable and the derivative F_h is Lipschitz continuous and semismooth. These assumptions are meaningful as we have seen by the examples of the previous chapter. Each element $G_h \in \partial F_h(\cdot)$ is symmetric and positive semidefinite due to the convexity of $\mathcal{E}_h$. For convex SC^1 minimization problems, Algorithm 8.6 was proposed in [**PQ95**]. Whenever $\delta_k > 0$, the direction finding problem is well posed as G_h^k is positive semidefinite and C_h is positive definite. Thus, $\Delta \boldsymbol{u}_h^k$ is a descent direction. Concerning the Algorithm 8.6, due to [**PQ95**], we have the following results.

Proposition 8.6. *If the sequence $\{\delta_k\}_k$ is uniformly bounded and if there is a constant $c > 0$ such that $\langle (G_h^k + \delta_k C_h)\boldsymbol{w}_h, \boldsymbol{w}_h \rangle_{\boldsymbol{X}_h^* \times \boldsymbol{X}_h} \geq c\|\boldsymbol{w}_h\|_{\boldsymbol{X}_h}^2$ for all $\boldsymbol{w}_h \in \boldsymbol{X}_h$ and k sufficiently large, then every accumulation point of the sequence $\{\boldsymbol{u}_h^k\}_k$ produced by Algorithm 8.6 is a solution of (8.7) if such a solution exists.*

Essentially, this proposition states the same result as Theorem 8.4. However, if $F_h = D\mathcal{E}_h$ is semismooth, we are able to obtain superlinear convergence.

Theorem 8.7. *Let $\sigma \in (0, \frac{1}{2})$ and let $\delta_k \to 0$ as $k \to \infty$. If the sequence $\{\boldsymbol{u}_h^k\}_k \subset \boldsymbol{X}_h(\boldsymbol{u}_D)$ produced by the Algorithm 8.6 has a limit $\boldsymbol{u}_h^* \in \boldsymbol{X}_h(\boldsymbol{u}_D)$ and F_h is BD-regular at $\boldsymbol{u}_h^*$, i.e. all elements of the B-subdifferential at $\boldsymbol{u}_h^*$ are regular (see Section A.1), then:*

(1) *$\boldsymbol{u}_h^*$ is the unique solution of (8.7),*
(2) *there exists $k_0 \in \mathbb{N}$ such that $\rho_k = 1$ for all $k \geq k_0$,*
(3) *the entire sequence $\{\boldsymbol{u}_h^k\}_k$ converges superlinearly to the solution.*

Algorithm 8.6 Line search algorithm for SC^1 minimization problems.

S0)   Choose $\beta, \sigma \in (0,1)$, a tolerance $\epsilon > 0$ and an initial guess $\boldsymbol{u}_h^0 \in \boldsymbol{X}_h(\boldsymbol{u}_D)$. Set $k := 1$.

S1)   If $|E_h^* F_h(\boldsymbol{u}_h^{k-1})| < \epsilon$, set $\boldsymbol{u}_h^* = \boldsymbol{u}_h^{k-1}$ and stop.

S2)   Choose $G_h^k \in \partial F_h(\boldsymbol{u}_h^{k-1})$ and $\delta_k \geq 0$. Set $m := 0$ and solve the problem

$$\left(G_h^k + \delta_k C_h\right)\Delta \boldsymbol{u}_h^k = -F_h(\boldsymbol{u}_h^{k-1}).$$

S3)   S3a) Compute $\rho_m = \beta^m$ and

$$\vartheta_m = \mathcal{E}_h(\boldsymbol{u}_h^{k-1} + \rho_m \Delta \boldsymbol{u}_h^k) - \mathcal{E}_h(\boldsymbol{u}_h^{k-1}) - \sigma \rho_m \langle F_h(\boldsymbol{u}_h^{k-1}), \Delta \boldsymbol{u}_h^k \rangle_{\boldsymbol{X}_h^* \times \boldsymbol{X}_h}.$$

   S3b) If $\vartheta_m \leq 0$, set $\rho_k = \rho_m$ and $\boldsymbol{u}_h^k = \boldsymbol{u}_h^{k-1} + \rho_k \Delta \boldsymbol{u}_h^k$. Set $k := k + 1$ and go to S1).

   S3c) Set $m := m + 1$ and go to S3a).

The acceptance of the unit step size $\rho_k = 1$ sufficiently close to the solution was already observed in [**Fac95**]. Thus, there is no Maratos-type effect in SC^1 minimization.

In the context of the definite problems of kinematic hardening and the viscoplastic regularization we infer the following result.

Corollary 8.8. *Let $\mathcal{E}_h = \mathcal{E}_{\mathrm{hd},h}$ or $\mathcal{E}_h = \mathcal{E}_{\mathrm{vp},h}$ and set $\delta_k \equiv 0$. Then, the algorithm globally converges to the unique solution. Moreover, if F_h is semismooth of order $p \in (0,1]$, then the convergence is locally superlinear of order $1 + p$.*

PROOF. In the considered cases, G_h^k is uniformly positive definite as F_h is strongly monotone, cf. Proposition 7.2. Proposition 8.6 therefore shows that the sequence $\{\boldsymbol{u}_h^k\}_k$ converges to the unique solution and this also guarantees BD-regularity at the solution. By Theorem 8.7, there is a $k_0 \in \mathbb{N}$ such that the full step size $\rho_k = 1$ is accepted whenever $k \geq k_0$. Once $k \geq k_0$, the algorithm coincides with Algorithm 7.1, and from Theorem 7.3, the superlinear convergence with rate $1 + p$ follows. $\square$

Remark 8.9.   (1) *In some situations, it will be more appropriate to solve the system*

$$\left((1 - \delta_k)G_h^k + \delta_k C_h\right)\Delta \boldsymbol{u}_h^k = -F_h(\boldsymbol{u}_h^{k-1})$$

with $\delta_k \in [0,1]$ in step S2) of Algorithm 8.6. The reason is the acceptance of the unit step size $\rho = 1$.

(2) *Concerning perfect plasticity, once more we need to impose the existence of a solution and the BD-regularity of F_h at the solution. Additionally, we cannot take $\delta_k = 0$ from a theoretical point of view, since $G_h \in \partial F_h(\cdot)$ may not be definite.*

3.3. The Algorithm. We again adopt the incremental setting and present the modification of Algorithm 8.1, taking into account the minimization structure by employing the properties of the globally convergent Algorithm 8.6. Particularly, besides choosing the line search parameters $\beta, \sigma \in (0,1)$, we need to adjust steps S6) and S7). This is done in Algorithm 8.7. We once more remark that for strongly monotone problems, $\delta_{n,k} \equiv 0$ is possible. In the case of perfect plasticity, $\delta_{n,k} > 0$ is necessary from an a theoretical standpoint. Algorithm 8.8 describes the modification of Algorithm 8.7 according to Remark 8.9(1) which has potentially better scaling properties concerning the line search.

Algorithm 8.7 Line search algorithm for associated plasticity.

S6) Choose $\delta_{n,k} \geq 0$, set $m := 0$, and determine $\Delta \boldsymbol{u}_h^{n,k} \in \boldsymbol{X}_h$ such that for all $\boldsymbol{w}_h \in \boldsymbol{X}_h$

$$\int_\Omega \left(\mathbb{C}_{\text{ct}}^{n,k-1}(x) + \delta_{n,k}\mathbb{C} \right) \left[\boldsymbol{\varepsilon}\left(\Delta \boldsymbol{u}_h^{n,k}(x) \right) \right] : \boldsymbol{\varepsilon}(\boldsymbol{w}_h(x)) \, dx = -r^{n,k-1}(\boldsymbol{w}_h) \, .$$

S7) S7a) Compute $\rho_m = \beta^m$ and

$$\vartheta_m = \mathcal{E}_h(\boldsymbol{u}_h^{n,k-1} + \rho_m \Delta \boldsymbol{u}_h^{n,k}) - \mathcal{E}_h(\boldsymbol{u}_h^{n,k-1}) - \sigma \rho_m \langle F_h(\boldsymbol{u}_h^{n,k-1}), \Delta \boldsymbol{u}_h^{n,k} \rangle_{\boldsymbol{X}_h^* \times \boldsymbol{X}_h} \, .$$

S7b) If $\vartheta_m \leq 0$, set $\rho_{n,k} = \rho_m$ and $\boldsymbol{u}_h^{n,k} = \boldsymbol{u}_h^{n,k-1} + \rho_{n,k} \Delta \boldsymbol{u}_h^{n,k}$. Set $k := k + 1$ and go to S1).

S7c) Set $m := m + 1$ and go to S7a).

Algorithm 8.8 Modified variant of Algorithm 8.7.

S6) Choose $\beta_{n,k} > 0$, set $\gamma_{n,k} = \frac{\beta_{n,k}}{1 + \beta_{n,k}}$, $m := 0$, and find $\Delta \boldsymbol{u}_h^{n,k} \in \boldsymbol{X}_h$ s.t. for all $\boldsymbol{w}_h \in \boldsymbol{X}_h$

$$\int_\Omega \left(\gamma_{n,k} \, \mathbb{C}_{\text{ct}}^{n,k-1}(x) + (1 - \gamma_{n,k}) \, \mathbb{C} \right) \left[\boldsymbol{\varepsilon}\left(\Delta \boldsymbol{u}_h^{n,k}(x) \right) \right] : \boldsymbol{\varepsilon}(\boldsymbol{w}_h(x)) \, dx = -r^{n,k-1}(\boldsymbol{w}_h) \, .$$

3.3.1. *Evaluating the Objective Function.* We close the section by explaining how the potential $\mathcal{E}_h$ can be evaluated efficiently. In fact, the evaluation only relies on the response function and the Lagrangian and easily generalizes to more complicated flow rules, e.g. nonlinear isotropic hardening. Taking into consideration the example of kinematic hardening and looking back to Section 3.2 and Section 5.4, we find

$$\mathcal{E}_h(\boldsymbol{u}_h) = \mathcal{E}_{\text{hd},h}(\boldsymbol{u}_h) = \sup_{(\boldsymbol{\sigma}_h, \boldsymbol{\zeta}_h) \in \boldsymbol{P}_h \times \boldsymbol{P}_h} \left\{ -L_h((\boldsymbol{\sigma}_h, \boldsymbol{\zeta}_h), \boldsymbol{u}_h) \right\} \tag{8.8}$$

with the Lagrangian $L_h : \boldsymbol{P}_h \times \boldsymbol{P}_h \times \boldsymbol{X}_h \to \mathbb{R}$

$$L_h((\boldsymbol{\sigma}_h, \boldsymbol{\zeta}_h), \boldsymbol{u}_h) = \tfrac{1}{2}a(\boldsymbol{\sigma}_h, \boldsymbol{\sigma}_h) + \tfrac{1}{2}d(\boldsymbol{\zeta}_h, \boldsymbol{\zeta}_h) + (\boldsymbol{\sigma}_h, \boldsymbol{\tau}_h)_{\boldsymbol{P}} + \chi_{\boldsymbol{K}}(\boldsymbol{\sigma}_h + \boldsymbol{\zeta}_h)$$
$$+ b(\boldsymbol{\sigma}_h, \boldsymbol{u}_h) \, dx + \ell_h(\boldsymbol{u}_h) \, .$$

In the incremental setting we have $\boldsymbol{\tau}_h = \boldsymbol{\varepsilon}_{p,h}^{n-1}$ and $\ell_h(\cdot) = \ell_h(t_n, \cdot)$. The response function $R_{\text{hd}} : \boldsymbol{P}_h \to \boldsymbol{P}_h \times \boldsymbol{P}_h$ as defined in (3.10) was the solution operator of the optimization problem (8.8) and therefore

$$\mathcal{E}_h(\boldsymbol{u}_h) = -L_h\left(R_{\text{hd}}(\mathbb{C}[\boldsymbol{\varepsilon}(\boldsymbol{u}_h) - \boldsymbol{\tau}_h]), \boldsymbol{u}_h \right) \, .$$

Hence, having the Lagrangian and the response function at hand, it is straight forward to evaluate $\mathcal{E}_h$. Moreover, within the algorithm, it is possible to evaluate the residual and the potential simultaneously causing almost no additional work load.

CHAPTER 9

AN ACTIVE SET METHOD FOR PERFECT PLASTICITY

Considering the response function $R : \mathrm{Sym}(d) \to \mathrm{Sym}(d)$ in perfect plasticity, we have already seen that R is defined implicitly. Specifically, for general non-associated plasticity, the response function is (a component of) the solution operator of a set of equations/inclusions and inequalities. For associated plasticity, these are just the optimality conditions of the minimization problem corresponding to the projection operator. Typically, $p \in \mathbb{N}$ (convex) yield functions $f_i : \mathrm{Sym}(d) \to \mathbb{R}$, determine the admissible set $K = \{\boldsymbol{\sigma} \in \mathrm{Sym}(d) : f_i(\boldsymbol{\sigma}) \le 0\}$, whereas the (generalized) derivatives of the corresponding (convex) plastic potentials $g_i : \mathrm{Sym}(d) \to \mathbb{R}$, establish the direction of plastic flow. In detail, for given $\boldsymbol{\eta} \in \mathrm{Sym}(d)$, the response $\boldsymbol{\sigma} = R(\boldsymbol{\eta})$ and $0 \le \lambda \in \mathbb{R}^p$ are defined as the solution of

$$0 \in \mathbb{C}^{-1}[\boldsymbol{\sigma} - \boldsymbol{\eta}] + \partial g(\boldsymbol{\sigma})^T \lambda \,,$$
$$0 = \lambda_i f_i(\boldsymbol{\sigma}) \,, \qquad \lambda \ge 0 \,, \qquad f(\boldsymbol{\sigma}) \le 0 \,.$$

The numerical methods presented so far relied on the explicit evaluation of the response function which was substituted into the weak equilibrium equation afterwards. In this chapter, we follow a different approach by treating the above relations and the equilibrium equation simultaneously. Concerning associated plasticity, a similar method can be obtained by means of the Augmented Lagrangian as presented in the next chapter and we refer to Section 10.5.

For simplicity, we assume that g is continuously differentiable, i.e. $g \in C^1(\mathrm{Sym}(d), \mathbb{R}^p)$, but a similar approach is possible if g is merely assumed to be a convex function. With $\Lambda_h = \{\lambda_h : \boldsymbol{\Xi} \to \mathbb{R}^p\}$, we can reformulate the problem of perfect plasticity as follows: find $(\boldsymbol{\sigma}_h, \boldsymbol{u}_h, \lambda_h) \in \boldsymbol{P}_h \times \boldsymbol{X}_h(\boldsymbol{u}_D) \times \Lambda_h$ such that

$$\mathbb{C}^{-1}[\boldsymbol{\sigma}_h(\boldsymbol{\xi})] - \big(\boldsymbol{\varepsilon}(\boldsymbol{u}_h(\boldsymbol{\xi})) - \boldsymbol{\tau}_h(\boldsymbol{\xi})\big) + Dg(\boldsymbol{\sigma}_h(\boldsymbol{\xi}))^T \lambda_h(\boldsymbol{\xi}) = 0 \,, \qquad \boldsymbol{\xi} \in \boldsymbol{\Xi} \,,$$
$$\lambda_h(\boldsymbol{\xi})^T f(\boldsymbol{\sigma}_h(\boldsymbol{\xi})) = 0 \,, \qquad \lambda_h(\boldsymbol{\xi}) \ge 0 \,, \qquad f(\boldsymbol{\sigma}_h(\boldsymbol{\xi})) \le 0 \,, \qquad \boldsymbol{\xi} \in \boldsymbol{\Xi} \,, \tag{9.1}$$
$$\int_\Omega \boldsymbol{\sigma}_h(x) : \boldsymbol{\varepsilon}(\boldsymbol{w}_h(x)) \, dx = \ell(\boldsymbol{w}_h) \,, \qquad \boldsymbol{w}_h \in \boldsymbol{X}_h \,.$$

This system is describing the same problem as the displacement problem of Chapter 7 but this time, we want to tackle this system directly. In order to do so, we transfer the complementarity condition into a nonsmooth equation via an *NCP function*. For arbitrary $\gamma > 0$, we use $\phi_\gamma : \mathbb{R} \times \mathbb{R} \to \mathbb{R}$,

$$\phi_\gamma(a, b) = \min\{b, \gamma\, a\} = b - \max\{0, b - \gamma\, a\}\,,$$

as defined in (A.11). Since $\phi_\gamma(a, b) = 0$ is equivalent to $a, b \geq 0$ and $ab = 0$, we can transform the complementarity condition in (9.1) to $\phi_\gamma\big(\lambda_h(\boldsymbol{\xi}), -f(\boldsymbol{\sigma}_h(\boldsymbol{\xi}))\big) = 0$ or

$$\lambda_h(\boldsymbol{\xi}) - \max\{0, \lambda_h(\boldsymbol{\xi}) + \gamma\, f(\boldsymbol{\sigma}_h(\boldsymbol{\xi}))\} = 0\,, \qquad \boldsymbol{\xi} \in \boldsymbol{\Xi}\,,$$

with the $\max$-operator applied row-wise in $\mathbb{R}^p$. In the following, it will be convenient to use the nonlinear mapping

$$f_h : \boldsymbol{P}_h \to \Lambda_h^*\,, \qquad\qquad \langle f_h(\boldsymbol{\sigma}_h), \mu_h \rangle_{\Lambda_h^* \times \Lambda_h} = \int_\Omega f(\boldsymbol{\sigma}_h(x))^T \mu_h(x)\, dx\,,$$

and as always, the integral is representing a quadrature rule. Likewise, $g_h : \boldsymbol{P}_h \to \Lambda_h^*$ is defined. Moreover, we introduce the mapping $M : \boldsymbol{P}_h \times \Lambda_h \to \Lambda_h^*$,

$$\langle M(\boldsymbol{\sigma}_h, \lambda_h), \mu_h \rangle_{\Lambda_h^* \times \Lambda_h} = \int_\Omega \Big(\max\big\{0, \lambda_h(x) + \gamma f(\boldsymbol{\sigma}_h(x))\big\} - \lambda_h(x) \Big)^T \mu_h(x)\, dx\,.$$
$$(9.2)$$

With the help of these operators, we define

$$\Phi : \boldsymbol{P}_h \times \boldsymbol{X}_h \times \Lambda_h \to \boldsymbol{P}_h^* \times \boldsymbol{X}_h^* \times \Lambda_h^*\,,$$

$$\Phi(\boldsymbol{\sigma}_h, \boldsymbol{u}_h, \lambda_h) = \begin{bmatrix} \Phi_1(\boldsymbol{\sigma}_h, \boldsymbol{u}_h, \lambda_h) \\ \Phi_2(\boldsymbol{\sigma}_h, \boldsymbol{u}_h, \lambda_h) \\ \Phi_3(\boldsymbol{\sigma}_h, \boldsymbol{u}_h, \lambda_h) \end{bmatrix} = \begin{bmatrix} A_h \boldsymbol{\sigma}_h + B_h^* \boldsymbol{u}_h + \boldsymbol{\tau}_h + D g_h(\boldsymbol{\sigma}_h)^* \lambda_h \\ B_h \boldsymbol{\sigma}_h + \ell_h \\ M(\boldsymbol{\sigma}_h, \lambda_h) \end{bmatrix} \quad (9.3)$$

on the basis of the operators A_h, B_h as defined in Section 6.3. Consequently

$$0 = \Phi(\boldsymbol{\sigma}_h, \boldsymbol{u}_h, \lambda_h) \qquad \Longleftrightarrow \qquad (\boldsymbol{\sigma}_h, \lambda_h, \boldsymbol{u}_h) \text{ satisfies } (9.1)\,.$$

Remark 9.1. (1) *If g is not differentiable, Φ would be a multi-function as Dg_h would have to be replaced by the subdifferential ∂g_h. Then, we seek an element satisfying $0 \in \Phi(\boldsymbol{\sigma}_h, \boldsymbol{u}_h, \lambda_h)$.*

(2) *In a function space setting, the complementarity condition must hold a.e. in Ω. But as λ may not be in L^2 but merely be a measure, the mapping (9.2) is not well defined as a comparison of λ and $f(\boldsymbol{\sigma})$ is not possible.*

(3) *The parameter γ may also depend on the spatial point and on the mesh size parameter h. This issue will also be adressed in Section 9.3.*

For the ease of notation, we introduce the product space

$$\mathcal{Y}_h = \boldsymbol{P}_h \times \boldsymbol{X}_h \times \Lambda_h\,,$$

and thus, $\Phi : \mathcal{Y}_h \to \mathcal{Y}_h^*$. Whenever possible, we will use

$$\boldsymbol{y}_h = (\boldsymbol{\sigma}_h, \boldsymbol{u}_h, \lambda_h) \in \mathcal{Y}_h\,,$$

to denote elements in $\mathcal{Y}_h$.

At this point, we also remark that there are numerous NCP functions, e.g. the *Fischer-Burmeister function* $\phi_{\mathrm{FB}}(a, b) = \sqrt{a^2 + b^2} - (a + b)$. This function is slightly more complicated to handle due to the square root, but enjoys some nice properties. We refer to [**PF03a**, Section 9.1.1] for more details.

We also remark that the reformulation of the complementarity condition as a nonsmooth equation is not new in the field of plasticity. For the case of von Mises plasticity with isotropic hardening, a similar approach has been presented in [HW09].

1. The Generalized Jacobian

Since the aim of this chapter is to establish a generalized Newton method for $\Phi(\boldsymbol{y}_h) = 0$, we have a closer look at the generalized Jacobian of Φ. For the sake of clarity, we make the following simplifications.

Assumption 9.2. *The yield function and the plastic potential satisfy the following conditions:*

(1) *$p = 1$: i.e. there is only one yield function $f : \mathrm{Sym}(d) \to \mathbb{R}$ and one corresponding plastic potential $g : \mathrm{Sym}(d) \to \mathbb{R}$.*
(2) *$f \in C^{1,1}(\mathrm{Sym}(d), \mathbb{R})$ and $g \in C^{2,1}(\mathrm{Sym}(d), \mathbb{R})$, i.e. f has a (locally) Lipschitz continuous derivative and g has a (locally) Lipschitz continuous second derivative.*

The restriction to $p = 1$ is for the ease of notation as the same approach is possible for $p > 1$. The smoothness requirements can also be relaxed in the sense that concerning superlinear convergence, it is sufficient to assume f to be convex and $g \in SC^1(\mathrm{Sym}(d), \mathbb{R})$, i.e. g is continuously differentiable with a semismooth derivative. We will come back to this point later.

Despite the smoothness assumptions on f and g, the mapping Φ is not differentiable due to the occurence of the max-function. Before we can set up a generalized Newton method (which will be the task of the next section), we have an eye on the generalized Jacobian $\partial\Phi$ (or the corresponding B-subdifferential). For that purpose, we introduce the sets

$$\mathcal{A}_h(\boldsymbol{y}_h) = \{\boldsymbol{\xi} \in \Xi : \lambda_h(\boldsymbol{\xi}) + \gamma\, f(\boldsymbol{\sigma}_h(\boldsymbol{\xi})) > 0\}\,,$$
$$\mathcal{J}_h(\boldsymbol{y}_h) = \{\boldsymbol{\xi} \in \Xi : \lambda_h(\boldsymbol{\xi}) + \gamma\, f(\boldsymbol{\sigma}_h(\boldsymbol{\xi})) < 0\}\,,$$
$$\mathcal{B}_h(\boldsymbol{y}_h) = \{\boldsymbol{\xi} \in \Xi : \lambda_h(\boldsymbol{\xi}) + \gamma\, f(\boldsymbol{\sigma}_h(\boldsymbol{\xi})) = 0\}\,,$$

and we call $\mathcal{A}_h$ the *active set*. Obviously, we have $\Xi = \mathcal{A}_h(\boldsymbol{y}_h) \cup \mathcal{J}_h(\boldsymbol{y}_h) \cup \mathcal{B}_h(\boldsymbol{y}_h)$ and we also define the *inactive set* $\mathcal{I}_h(\boldsymbol{y}_h) = \mathcal{J}_h(\boldsymbol{y}_h) \cup \mathcal{B}_h(\boldsymbol{y}_h) = \Xi \setminus \mathcal{A}_h(\boldsymbol{y}_h)$.

Since the only non-smoothness is encountered in $\Phi_3 : \mathcal{Y}_h \to \Lambda_h^*$, we compute the generalized Jacobian of Φ_3. Identifying Λ_h and Λ_h^*, we find that

$$\big(\Phi_3(\boldsymbol{y}_h)\big)(\boldsymbol{\xi}) = \max\{0, \lambda_h(\boldsymbol{\xi}) + \gamma\, f(\boldsymbol{\sigma}_h(\boldsymbol{\xi}))\} - \lambda_h(\boldsymbol{\xi})\,.$$

As, apart from the origin, the max-operator is continuously differentiable, we find

(1) $\boldsymbol{\xi} \in \mathcal{A}_h(\boldsymbol{y}_h)$: then $\Phi_3(\boldsymbol{y}_h)(\boldsymbol{\xi}) = \gamma\, f(\boldsymbol{\sigma}_h(\boldsymbol{\xi}))$ and thus

$$D\Phi_3(\boldsymbol{y}_h)(\boldsymbol{\xi}) = \begin{bmatrix} \gamma\, Df(\boldsymbol{\sigma}_h(\boldsymbol{\xi})) & 0 & 0 \end{bmatrix}$$

(2) $\boldsymbol{\xi} \in \mathcal{J}_h(\boldsymbol{y}_h)$: then $\Phi_3(\boldsymbol{y}_h)(\boldsymbol{\xi}) = -\lambda_h(\boldsymbol{\xi})$ and thus

$$D\Phi_3(\boldsymbol{y}_h)(\boldsymbol{\xi}) = \begin{bmatrix} 0 & 0 & -1 \end{bmatrix}$$

(3) $\boldsymbol{\xi} \in \mathcal{B}_h(\boldsymbol{y}_h)$: with the above preparations we find the generalized Jacobian to be

$$\partial\Phi_3(\boldsymbol{y}_h)(\boldsymbol{\xi}) = \big\{\, \begin{bmatrix} (1-t)\,\gamma\, Df(\boldsymbol{\sigma}_h(\boldsymbol{\xi}) & -t \end{bmatrix} : t \in [0,1]\big\}$$

Together, this gives

$$\partial\Phi_3(\boldsymbol{y}_h)(\boldsymbol{\xi}) = \begin{cases} \left\{\begin{bmatrix} \gamma\,Df(\boldsymbol{\sigma}_h(\boldsymbol{\xi})) & 0 & 0 \end{bmatrix}\right\} & , \boldsymbol{\xi} \in \mathcal{A}_h(\boldsymbol{y}_h)\,, \\ \left\{\begin{bmatrix} (1-t)\gamma Df(\boldsymbol{\sigma}_h(\boldsymbol{\xi})) & 0 & -t \end{bmatrix} : t \in [0,1]\right\} & , \boldsymbol{\xi} \in \mathcal{B}_h(\boldsymbol{y}_h)\,, \\ \left\{\begin{bmatrix} 0 & 0 & -1 \end{bmatrix}\right\} & , \boldsymbol{\xi} \in \mathcal{J}_h(\boldsymbol{y}_h)\,. \end{cases}$$

Since Φ_1 and Φ_2 are continuously differentiable as a result of the smoothness assumptions on f and g, we have

$$\partial\Phi_1(\boldsymbol{y}_h) = \left\{ \begin{bmatrix} A_h + (D^2 g_h(\boldsymbol{\sigma}_h))^*\lambda_h & B_h^* & Dg_h(\boldsymbol{\eta}_h)^* \end{bmatrix} \right\}\,,$$
$$\partial\Phi_2(\boldsymbol{y}_h) = \left\{ \begin{bmatrix} B_h & 0 & 0 \end{bmatrix} \right\}\,,$$

with the block-diagonal tensor $\left((D^2 g_h(\boldsymbol{\sigma}_h))^*\lambda_h\right)(\boldsymbol{\xi}) = \lambda_h(\boldsymbol{\xi})D^2 g(\boldsymbol{\sigma}_h(\boldsymbol{\xi}))$.

Combining the above results gives a full characterization of the generalized Jacobian $\partial\Phi(\boldsymbol{y}_h)$. For the definition of a generalized Newton method, it remains to pick an element of $\partial\Phi(\cdot)$ and in the following, we always take $t = 1$ if $\boldsymbol{\xi} \in \mathcal{B}(\boldsymbol{y}_h)$ and we obtain

$$\partial\Phi_3(\boldsymbol{y}_h) \ni \begin{cases} \begin{bmatrix} \gamma\,Df(\boldsymbol{\sigma}_h(\boldsymbol{\xi})) & 0 & 0 \end{bmatrix} & , \boldsymbol{\xi} \in \mathcal{A}_h(\boldsymbol{y}_h)\,, \\ \begin{bmatrix} 0 & 0 & -1 \end{bmatrix} & , \boldsymbol{\xi} \in \mathcal{I}_h(\boldsymbol{y}_h)\,. \end{cases}$$

With this choice, we can finally define $D : \mathcal{Y}_h \to L(\mathcal{Y}_h, \mathcal{Y}_h^*)$ via

$$D(\boldsymbol{y}_h) = \begin{bmatrix} A_h + (D^2 g_h(\boldsymbol{\sigma}_h))^*\lambda_h & B_h^* & Dg_h(\boldsymbol{\sigma}_h)^* \\ B_h & 0 & 0 \\ \left(\gamma\,Df_h(\boldsymbol{\sigma}_h)\right)_{\mathcal{A}_h(\boldsymbol{y}_h)} & 0 & -\mathrm{id}_{\mathcal{I}_h(\boldsymbol{y}_h)} \end{bmatrix} \in \partial\Phi(\boldsymbol{y}_h)\,,$$

with $\mathrm{id}_{\mathcal{I}_h(\boldsymbol{y}_h)}$ understood as the embedding from Λ_h to Λ_h^*.

2. Solving the Linear Subproblems

With the preparations of the last section, the generalized Newton method simply is

$$\boldsymbol{y}_h^k = \boldsymbol{y}_h^{k-1} - (D^k)^{-1}\Phi(\boldsymbol{y}_h^{k-1})\,, \qquad D^k = D(\boldsymbol{y}_h^{k-1})\,. \tag{9.4}$$

So formally, in each step, a linear system with the operator D^k has to be solved. This system can either be tackled directly, or by a Schur complement reduction, it can be reduced to an "elasticity-like" subproblem. To obtain further insight into the algorithm, we present this reduction for which we use the shorthand notation $\Phi^{k-1} \equiv \Phi(\boldsymbol{y}_h^{k-1})$. In the k-th iteration, the linear system is given as

$$\begin{bmatrix} A_h + (D^2 g_h(\boldsymbol{\sigma}_h))^*\lambda_h & B_h^* & Dg_h(\boldsymbol{\sigma}_h)^* \\ B_h & 0 & 0 \\ \left(\gamma\,Df_h(\boldsymbol{\sigma}_h^{k-1})\right)_{\mathcal{A}_h^{k-1}} & 0 & -\mathrm{id}_{\mathcal{I}_h^{k-1}} \end{bmatrix} \begin{bmatrix} \Delta\boldsymbol{\sigma}_h^k \\ \Delta\boldsymbol{u}_h^k \\ \Delta\lambda_h^k \end{bmatrix} = \begin{bmatrix} -\Phi_1^{k-1} \\ -\Phi_2^{k-1} \\ -\Phi_3^{k-1} \end{bmatrix}\,, \tag{9.5}$$

with the active / inactive sets

$$\mathcal{A}_h^{k-1} \equiv \mathcal{A}_h(\boldsymbol{y}_h^{k-1}) \qquad \text{and} \qquad \mathcal{I}_h^{k-1} \equiv \mathcal{I}_h(\boldsymbol{y}_h^{k-1})\,.$$

The first equation of (9.5) is equivalent to

$$\left(\mathbb{C}^{-1} + \lambda_h(\boldsymbol{\xi})D^2 g(\boldsymbol{\sigma}_h(\boldsymbol{\xi}))\right)[\Delta\boldsymbol{\sigma}_h^k(\boldsymbol{\xi})] - \boldsymbol{\varepsilon}(\Delta\boldsymbol{u}_h^k(\boldsymbol{\xi})) + \Delta\lambda_h(\boldsymbol{\xi})Dg(\boldsymbol{\sigma}_h(\boldsymbol{\xi})) = -\Phi_1^{k-1}(\boldsymbol{\xi})\,,$$

for all $\boldsymbol{\xi} \in \Xi$ and following the notation of the last chapters, we introduce

$$\mathbb{G}_{k-1}(\boldsymbol{\xi}) = \mathbb{C}^{-1} + \lambda_h^{k-1}(\boldsymbol{\xi}) D^2 g(\boldsymbol{\sigma}_h^{k-1}(\boldsymbol{\xi})) \,.$$

Based on this tensor, we find the above equation to be equivalent to

$$\mathbb{G}_{k-1}(\boldsymbol{\xi})[\Delta\boldsymbol{\sigma}_h^k(\boldsymbol{\xi})] - \boldsymbol{\varepsilon}(\Delta\boldsymbol{u}_h^k(\boldsymbol{\xi})) + \Delta\lambda_h^k(\boldsymbol{\xi})Dg(\boldsymbol{\sigma}_h^{k-1}(\boldsymbol{\xi})) = -\Phi_1^{k-1}(\boldsymbol{\xi}) \,, \tag{9.6}$$

Similarly, the third equation of (9.5) can be rewritten as

$$\gamma\, Df(\boldsymbol{\sigma}_h^{k-1}(\boldsymbol{\xi})) : \Delta\boldsymbol{\sigma}_h^k(\boldsymbol{\xi}) = -\Phi_3^{k-1}(\boldsymbol{\xi}) \,, \qquad\qquad \boldsymbol{\xi} \in \mathcal{A}_h^{k-1} \,,$$
$$-\Delta\lambda_h^k(\boldsymbol{\xi}) = -\Phi_3^{k-1}(\boldsymbol{\xi}) \,, \qquad\qquad \boldsymbol{\xi} \in \mathcal{I}_h^{k-1} \,,$$

and as $-\Phi_3^{k-1}(\boldsymbol{\xi}) = \lambda_h(\boldsymbol{\xi}) - \max\{0, \lambda_h(\boldsymbol{\xi}) + \gamma\, f(\boldsymbol{\sigma}_h(\boldsymbol{\xi}))\}$, we obtain

$$Df(\boldsymbol{\sigma}_h^{k-1}(\boldsymbol{\xi})) : \Delta\boldsymbol{\sigma}_h^k(\boldsymbol{\xi}) = -f(\boldsymbol{\sigma}_h^{k-1}(\boldsymbol{\xi})) \,, \qquad\qquad \boldsymbol{\xi} \in \mathcal{A}_h^{k-1} \,, \tag{9.7a}$$
$$-\Delta\lambda_h^k(\boldsymbol{\xi}) = \lambda_h^{k-1}(\boldsymbol{\xi}) \,, \qquad\qquad \boldsymbol{\xi} \in \mathcal{I}_h^{k-1} \,. \tag{9.7b}$$

We see that on the active set $\mathcal{A}_h^{k-1}$, we perform a Newton step for the equation $f(\boldsymbol{\sigma}_h(\boldsymbol{\xi})) = 0$, whereas on the inactive set $\mathcal{I}_h^{k-1}$ the multiplier $\lambda_h^k(\boldsymbol{\xi}) = \lambda_h^{k-1}(\boldsymbol{\xi}) + \Delta\lambda_h^k(\boldsymbol{\xi}) = 0$ vanishes in the k-th step. This observation justifies the notion active set method. Moreover, we observe that the parameter γ only affects the active / inactive set prediction but not the solution of the linear system. Particularly, this allows to conclude that γ has no regularizing effect.

If we interpret the strain increment $\boldsymbol{\varepsilon} = \boldsymbol{\varepsilon}(\Delta\boldsymbol{u}_h^k(\boldsymbol{\xi}))$ as a given quantity, the relations (9.6) and (9.7) give rise to a linear system for the unknowns $\Delta\boldsymbol{\sigma}_h^k(\boldsymbol{\xi})$ and $\Delta\lambda_h^k(\boldsymbol{\xi})$ in terms of the strain increment at each quadrature point $\boldsymbol{\xi} \in \Xi$. The (affine-linear) solution operator of this linear system w.r.t. $\Delta\boldsymbol{\sigma}_h^k$ gives rise to the definition of a *linearized algorithmic tangent*

$$\mathbb{C}_{\mathrm{lat}}^{k-1}(\boldsymbol{\xi}) \in L(\mathrm{Sym}(d), \mathrm{Sym}(d)) \,, \tag{9.8}$$

being defined as $\mathbb{C}_{\mathrm{lat}}^{k-1}(\boldsymbol{\xi}) = \frac{\partial}{\partial\boldsymbol{\varepsilon}}\Delta\boldsymbol{\sigma}_h^k(\boldsymbol{\xi})$.

2.1. Evaluation of $\mathbb{C}_{\mathrm{lat}}^{k-1}(\boldsymbol{\xi})$. Using the active / inactive set, we distinguish pointwise between $\boldsymbol{\xi} \in \mathcal{A}_h^{k-1}$ and $\boldsymbol{\xi} \in \mathcal{I}_h^{k-1}$.

2.1.1. *On the Inactive Set $\mathcal{I}_h^{k-1}$.* In this case the evaluation is simple as we already found $\Delta\lambda_h^k(\boldsymbol{\xi}) = -\lambda_h^{k-1}(\boldsymbol{\xi})$ and hence we have

$$\Delta\boldsymbol{\sigma}_h^k(\boldsymbol{\xi}) = \mathbb{G}_{k-1}^{-1}(\boldsymbol{\xi})\Big[\boldsymbol{\varepsilon}(\Delta\boldsymbol{u}_h^k(\boldsymbol{\xi})) - \Delta\lambda_h^k(\boldsymbol{\xi})Dg(\boldsymbol{\sigma}_h^{k-1}(\boldsymbol{\xi})) - \Phi_1^{k-1}(\boldsymbol{\xi})\Big]$$
$$= \mathbb{G}_{k-1}^{-1}(\boldsymbol{\xi})\Big[\boldsymbol{\varepsilon}(\Delta\boldsymbol{u}_h^k(\boldsymbol{\xi})) + \lambda_h^{k-1}(\boldsymbol{\xi})Dg(\boldsymbol{\sigma}_h^{k-1}(\boldsymbol{\xi})) - \Phi_1^{k-1}(\boldsymbol{\xi})\Big] \,.$$

2.1.2. *On the Active Set $\mathcal{A}_h^{k-1}$.* In this situation, the linear response function is defined by the relations

$$\mathbb{G}_{k-1}(\boldsymbol{\xi})[\Delta\boldsymbol{\sigma}_h^k(\boldsymbol{\xi})] - \boldsymbol{\varepsilon}(\Delta\boldsymbol{u}_h^k(\boldsymbol{\xi})) + \Delta\lambda_h^k(\boldsymbol{\xi})Dg(\boldsymbol{\sigma}_h^{k-1}(\boldsymbol{\xi})) = -\Phi_1^{k-1}(\boldsymbol{\xi}) \,,$$
$$Df(\boldsymbol{\sigma}_h^{k-1}(\boldsymbol{\xi})) : \Delta\boldsymbol{\sigma}_h^k(\boldsymbol{\xi}) = -f(\boldsymbol{\sigma}_h^{k-1}(\boldsymbol{\xi})) \,.$$

Since the aim is to express $\Delta\boldsymbol{\sigma}_h^k(\boldsymbol{\xi})$ in terms of $\Delta\boldsymbol{u}_h^k(\boldsymbol{\xi})$ and the data of iteration $k-1$, we use a linear Schur complement reduction. This gives $\Delta\lambda_h^k(\boldsymbol{\xi})$ in terms of $\Delta\boldsymbol{u}_h^k(\boldsymbol{\xi})$ and in detail we obtain

$$\Delta\lambda_h^k(\boldsymbol{\xi}) = \frac{f(\boldsymbol{\sigma}_h^{k-1}(\boldsymbol{\xi})) + Df(\boldsymbol{\sigma}_h^{k-1}(\boldsymbol{\xi})) : \mathbb{G}_{k-1}^{-1}(\boldsymbol{\xi})\left[\boldsymbol{\varepsilon}(\Delta\boldsymbol{u}_h^k(\boldsymbol{\xi})) - \Phi_1^{k-1}(\boldsymbol{\xi})\right]}{Df(\boldsymbol{\sigma}_h^{k-1}(\boldsymbol{\xi})) : \mathbb{G}_{k-1}^{-1}(\boldsymbol{\xi})\left[Dg(\boldsymbol{\sigma}_h^{k-1}(\boldsymbol{\xi}))\right]} \tag{9.9}$$

provided that the Schur complement $Df(\boldsymbol{\sigma}_h^{k-1}(\boldsymbol{\xi})) : \mathbb{G}_{k-1}^{-1}(\boldsymbol{\xi})\left[Dg(\boldsymbol{\sigma}_h^{k-1}(\boldsymbol{\xi}))\right]$ is non-zero which we assume here (this is always true for associated plasticity and also holds for smoothed non-associated Drucker-Prager plasticity). This expression can now be substituted into the expression for $\Delta\boldsymbol{\sigma}_h^k(\boldsymbol{\xi})$ to obtain

$$\Delta\boldsymbol{\sigma}_h^k(\boldsymbol{\xi}) = \left(\mathbb{G}_{k-1}^{-1}(\boldsymbol{\xi}) - \frac{\mathbb{G}_{k-1}^{-1}(\boldsymbol{\xi})[Dg(\boldsymbol{\sigma}_h^{k-1}(\boldsymbol{\xi}))]\otimes\mathbb{G}_{k-1}^{-1}(\boldsymbol{\xi})[Df(\boldsymbol{\sigma}_h^{k-1}(\boldsymbol{\xi}))]}{Df(\boldsymbol{\sigma}_h^{k-1}(\boldsymbol{\xi})):\mathbb{G}_{k-1}^{-1}(\boldsymbol{\xi})\left[Dg(\boldsymbol{\sigma}_h^{k-1}(\boldsymbol{\xi}))\right]}\right)$$
$$\left[\boldsymbol{\varepsilon}(\Delta\boldsymbol{u}_h^k(\boldsymbol{\xi})) - \Phi_1^{k-1}(\boldsymbol{\xi})\right] - f(\boldsymbol{\sigma}_h^{k-1}(\boldsymbol{\xi}))\frac{\mathbb{G}_{k-1}^{-1}(\boldsymbol{\xi})[Dg(\boldsymbol{\sigma}_h^{k-1}(\boldsymbol{\xi}))]}{Df(\boldsymbol{\sigma}_h^{k-1}(\boldsymbol{\xi})):\mathbb{G}_{k-1}^{-1}(\boldsymbol{\xi})[Dg(\boldsymbol{\sigma}_h^{k-1}(\boldsymbol{\xi}))]}.$$

2.1.3. *The Linear Algorithmic Response Function.* Combining the above results, we define

$$\mathbb{C}_{\text{lat}}^{k-1}(\boldsymbol{\xi}) = \begin{cases} \mathbb{G}_{k-1}^{-1}(\boldsymbol{\xi}) & , \boldsymbol{\xi} \in \mathcal{I}_h^{k-1}, \\ \mathbb{G}_{k-1}^{-1}(\boldsymbol{\xi}) - \dfrac{\mathbb{G}_{k-1}^{-1}(\boldsymbol{\xi})[Dg(\boldsymbol{\sigma}_h^{k-1}(\boldsymbol{\xi}))]\otimes\mathbb{G}_{k-1}^{-1}(\boldsymbol{\xi})[Df(\boldsymbol{\sigma}_h^{k-1}(\boldsymbol{\xi}))]}{Df(\boldsymbol{\sigma}_h^{k-1}(\boldsymbol{\xi})):\mathbb{G}_{k-1}^{-1}(\boldsymbol{\xi})\left[Dg(\boldsymbol{\sigma}_h^{k-1}(\boldsymbol{\xi}))\right]} & , \boldsymbol{\xi} \in \mathcal{A}_h^{k-1}, \end{cases}$$
$$(9.10)$$

and

$$\widehat{\boldsymbol{\sigma}}_h^{k-1}(\boldsymbol{\xi}) = -\mathbb{C}_{\text{lat}}^{k-1}(\boldsymbol{\xi})\left[\Phi_1^{k-1}(\boldsymbol{\xi})\right]$$
$$+ \begin{cases} \lambda_h^{k-1}(\boldsymbol{\xi})\mathbb{G}_{k-1}^{-1}(\boldsymbol{\xi})[Dg(\boldsymbol{\sigma}_h^{k-1}(\boldsymbol{\xi}))] & , \boldsymbol{\xi} \in \mathcal{I}_h^{k-1}, \\ -f(\boldsymbol{\sigma}_h^{k-1}(\boldsymbol{\xi}))\dfrac{\mathbb{G}_{k-1}^{-1}(\boldsymbol{\xi})[Dg(\boldsymbol{\sigma}_h^{k-1}(\boldsymbol{\xi}))]}{Df(\boldsymbol{\sigma}_h^{k-1}(\boldsymbol{\xi})):\mathbb{G}_{k-1}^{-1}(\boldsymbol{\xi})\left[Dg(\boldsymbol{\sigma}_h^{k-1}(\boldsymbol{\xi}))\right]} & , \boldsymbol{\xi} \in \mathcal{A}_h^{k-1}. \end{cases} \quad (9.11)$$

This eventually gives the linear algorithmic stress response as

$$\Delta\boldsymbol{\sigma}_h^k(\boldsymbol{\xi}) = \mathbb{C}_{\text{lat}}^{k-1}(\boldsymbol{\xi})\left[\boldsymbol{\varepsilon}(\Delta\boldsymbol{u}_h^k(\boldsymbol{\xi}))\right] + \widehat{\boldsymbol{\sigma}}_h^{k-1}(\boldsymbol{\xi}), \tag{9.12}$$

and the corresponding linearized algorithmic tangent $\mathbb{C}_{\text{lat}}^{k-1}(\boldsymbol{\xi})$.

2.2. The Linear System and the Update. Having derived an expression for the stress increment in terms of the strain increment it remains to substitute (9.12) into the equilibrium equation $B_h\Delta\boldsymbol{\sigma}_h^k = -\Phi_2^{k-1}$ of (9.5). This equation can be represented as

$$\int_\Omega \mathbb{C}_{\text{lat}}^{k-1}(x)\left[\boldsymbol{\varepsilon}(\Delta\boldsymbol{u}_h^k(x))\right] : \boldsymbol{\varepsilon}(\boldsymbol{w}_h(x))\,dx$$
$$= -\int_\Omega \left(\boldsymbol{\sigma}_h^{k-1}(x) + \widehat{\boldsymbol{\sigma}}_h^{k-1}(x)\right) : \boldsymbol{\varepsilon}(\boldsymbol{w}_h(x))\,dx + \ell(\boldsymbol{w}_h), \qquad \boldsymbol{w}_h \in \boldsymbol{X}_h, \tag{9.13}$$

and once this linear system is solved for $\Delta\boldsymbol{u}_h^k \in \boldsymbol{X}_h$, we obtain $\Delta\boldsymbol{\sigma}_h^k \in \boldsymbol{P}_h$ pointwise by (9.12). Finally, on the active set, the multiplier update for $\Delta\lambda_h^k \in \Lambda_h$ is performed via (9.9). Formally, we define the update mapping

$$U : \boldsymbol{P}_h \to \boldsymbol{P}_h \times \Lambda_h, \qquad\qquad U(\boldsymbol{\eta}_h) = \left(U_1(\boldsymbol{\eta}_h), U_2(\boldsymbol{\eta}_h)\right), \tag{9.14}$$

based on the above relations such that

$$\begin{bmatrix} \Delta\boldsymbol{\sigma}_h^k \\ \Delta\lambda_h^k \end{bmatrix} = \begin{bmatrix} U_1(\boldsymbol{\varepsilon}(\Delta\boldsymbol{u}_h^k)) \\ U_2(\boldsymbol{\varepsilon}(\Delta\boldsymbol{u}_h^k)) \end{bmatrix} = U(\boldsymbol{\varepsilon}(\Delta\boldsymbol{u}_h^k)).$$

3. The Algorithm and its Convergence

Similarly to Section 8.1, we state the algorithm for incremental plasticity, but this time we restrict ourselves to perfect plasticity. The occuring subproblems in the n-th time step are solved by the active set / generalized Newton method as developed in this chapter. This is Algorithm 9.1 where we use to following notation: depending on the n-th time step, we introduce the product space

$$\mathcal{Y}_h(t_n) = \boldsymbol{P}_h \times \boldsymbol{X}_h(\boldsymbol{u}_D(t_n)) \times \Lambda_h \,,$$

for the correct handling of the Dirichlet boundary conditions. By $\Phi^n : \mathcal{Y}_h \to \mathcal{Y}_h^*$, we denote the mapping Φ as given in (9.3) with $\boldsymbol{\tau}_h = \boldsymbol{\varepsilon}_{p,h}^{n-1}$ and $\ell_h(\cdot) = \ell_h(t_n, \cdot)$, i.e.

$$\Phi^n(\boldsymbol{y}_h^n) = \begin{bmatrix} A_h \boldsymbol{\sigma}_h^n + B_h^* \boldsymbol{u}_h^n + \boldsymbol{\varepsilon}_{p,h}^{n-1} + D g_h(\boldsymbol{\sigma}_h^n)^* \lambda_h^n \\ B_h \boldsymbol{\sigma}_h^n + \ell_h(t_n) \\ M(\boldsymbol{\sigma}_h^n, \lambda_h^n) \end{bmatrix} \,.$$

Hence, we aim for finding a zero $\boldsymbol{y}_h^n \in \mathcal{Y}_h(t_n)$ of Φ^n. Essentially, steps S4)–S7) are the solution process of the Schur complement reduction and simply correspond to the solution of $D^k \Delta \boldsymbol{y}_h^{n,k} = -\Phi^{n,k-1}$. We also remark that the linear Schur complement reduction leading to the the linear system in S6) does not need to be provided explicitly but can be performed by the computer.

Algorithm 9.1 Active set method for incremental perfect plasticity.

S0) Given $\boldsymbol{\varepsilon}_{p,h}^0 \in \boldsymbol{P}_h$, choose $\epsilon > 0$ and set $n := 1$.

S1) While $t_{n-1} < T$, choose $\Delta t_n > 0$ such that $\Delta t_n \leq (T - t_{n-1})$ and set $t_n = t_{n-1} + \Delta t_n$.
     Choose initial guess $\boldsymbol{y}_h^{n,0} = (\boldsymbol{\sigma}_h^{n,0}, \boldsymbol{u}_h^{n,0}, \lambda_h^{n,0}) \in \mathcal{Y}_h(t_n)$. Set $k := 1$.

S2) Compute $\Phi^{n,k-1} = \Phi^n(\boldsymbol{y}_h^{n,k-1})$.

S3) If $\|\Phi^{n,k-1}\|_{\mathcal{Y}_h^*} < \epsilon$, set $\boldsymbol{y}_h^n = \boldsymbol{y}_h^{n,k-1}$. Go to S9).

S4) Determine the active / inactive sets
     $$\mathcal{A}_h^{n,k-1} = \mathcal{A}_h(\boldsymbol{\sigma}_h^{n,k-1}, \lambda_h^{n,k-1}) \,, \qquad \text{and} \qquad \mathcal{I}_h^{n,k-1} = \boldsymbol{\Xi} \setminus \mathcal{A}_h^{n,k-1} \,.$$

S5) Use the active/inactive set to determine $\mathbb{C}_{\text{lat}}^{n,k-1}(\boldsymbol{\xi})$ and $\widehat{\boldsymbol{\sigma}}_h^{n,k-1}(\boldsymbol{\xi})$ according to (9.10) and (9.11). Compute the residual $r^{n,k-1} \in \boldsymbol{X}_h^*$ via
     $$r^{n,k-1}(\boldsymbol{w}_h) = \int_\Omega \left(\boldsymbol{\sigma}_h^{n,k-1}(x) + \widehat{\boldsymbol{\sigma}}_h^{n,k-1}(x) \right) : \boldsymbol{\varepsilon}(\boldsymbol{w}_h(x)) \, dx - \ell(t_n, \boldsymbol{w}_h) \,.$$

S6) Determine $\Delta \boldsymbol{u}_h^{n,k} \in \boldsymbol{X}_h$ such that
     $$\int_\Omega \mathbb{C}_{\text{lat}}^{n,k-1}(x) \left[\boldsymbol{\varepsilon}\left(\Delta \boldsymbol{u}_h^{n,k}(x)\right) \right] : \boldsymbol{\varepsilon}(\boldsymbol{w}_h(x)) \, dx = -r^{n,k-1}(\boldsymbol{w}_h) \,, \qquad \boldsymbol{w}_h \in \boldsymbol{X}_h \,.$$

S7) Use the active/inactive set and the update mapping (9.14) and compute $\left(\Delta \boldsymbol{\sigma}_h^{n,k}, \Delta \lambda_h^{n,k}\right) = U(\boldsymbol{\varepsilon}(\Delta \boldsymbol{u}_h^{n,k}))$.

S8) Set $\Delta \boldsymbol{y}_h^{n,k} = (\Delta \boldsymbol{\sigma}_h^{n,k}, \Delta \boldsymbol{u}_h^{n,k}, \Delta \lambda_h^{n,k})$ and $\boldsymbol{y}_h^{n,k} = \boldsymbol{y}_h^{n,k-1} + \Delta \boldsymbol{y}_h^{n,k}$. Set $k := k+1$ and go to S2).

S9) Compute $\boldsymbol{\varepsilon}_{p,h}^n(\boldsymbol{\xi}) = \boldsymbol{\varepsilon}(\boldsymbol{u}_h^n(\boldsymbol{\xi})) - \mathbb{C}^{-1}[\boldsymbol{\sigma}_h^n(\boldsymbol{\xi})]$ for all $\boldsymbol{\xi} \in \boldsymbol{\Xi}$.
     Set $n := n+1$ and go to S1).

3.1. The Influence of γ. Up to now, we did not comment on the choice of the parameter $\gamma > 0$ in the definition of the NCP function. We will briefly indicate that an appropriate choice of γ is not obvious after all.

3.1.1. *Spatial Dependence.* As it can be seen from the derivation in the previous section, the parameter γ plays no role in the solution process of the linear system once the active / inactive set has been determined.

However, it has a huge effect on the prediction of the active / inactive set and thereby affects the overall performance of the method. Therefore note that during the iteration, it is possible that $\lambda_h^k(\boldsymbol{\xi}) \not\geq 0$. If such a situation occurs, it can be advantageous if either γ is chosen to be very small or very large. To illustrate this, we consider one quadrature point and write $\lambda^k \equiv \lambda_h^k(\boldsymbol{\xi})$ and $\boldsymbol{\sigma}^k \equiv \boldsymbol{\sigma}_h^k(\boldsymbol{\xi})$. Assume $\lambda^k < 0$ and $f(\boldsymbol{\sigma}^k) > 0$, but that the solution $(\boldsymbol{\sigma}^*, \lambda^*)$ in this point satisfies $f(\boldsymbol{\sigma}^*) < 0$ and $\lambda^* = 0$. This is also illustrated in the adjacent graphic.
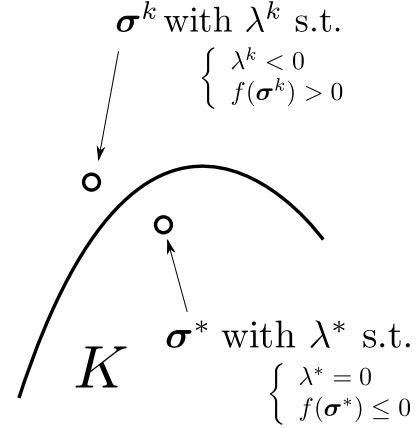
Now, the question raises, whether the next prediction identifies the active / inactive set correctly. The prediction is made whether $\lambda^k + \gamma f(\boldsymbol{\sigma}^k) > 0$ or not. Obviously, there exists $\hat{\gamma} > 0$ such that $\lambda^k + \hat{\gamma} f(\boldsymbol{\sigma}^k) = 0$, and consequently, the quadrature point is only correctly identified to be inactive if $\gamma \leq \hat{\gamma}$. Otherwise, it is incorrectly identified. Thus, in order make it possible to inactivate mistakenly actived points quickly, a low value of gamma is desirable. However, also the opposite situation can occur if the solution in this quadrature is active, i.e. $\lambda^* > 0$ and $f(\boldsymbol{\sigma}^*) = 0$. Then, the prediction is only correct if $\gamma > \hat{\gamma}$. A similar situation occurs if the current iterate satisfies $\lambda^k > 0$ but $f(\boldsymbol{\sigma}^k) < 0$. Thus, without a priori knowledge of the active / inactive set, it is not possible to choose γ in such a way that the active / inactive set is correctly predicted in the next step.

One possibility would be to always tend to inactivation, i.e. once $\lambda^k f(\boldsymbol{\sigma}^k) < 0$, the point is predicted to be inactive. This choice makes the algorithm independent of γ, but on the other hand, the algorithm can no longer be interpreted as a generalized Newton method. Thinking in terms of γ as a function $\gamma : \Omega \to \mathbb{R}$, this also suggests that γ needs not to be continuous on the boundary between the active and inactive set. This somehow reflects the continuous nature of the problem where λ may only be a measure and hence, λ and $f(\boldsymbol{\sigma})$ may not be comparable at all.

3.1.2. *Mesh-dependence.* Above, we illustrated that the algorithm may behave very sensitive with respect to γ, as particularly in the neighbourhood of the boundary between the active and inactive set (or between the plastic and elastic parts of Ω), a fixed value of γ does not seem to be appropriate. In a finite element framework, the boundary between the active and the inactive set can be attributed to be of the size $O(h)$ with h being the mesh size. Hence, it is to be expected that the algorithm is also sensitive w.r.t. the mesh size. This will be demonstrated by a numerical experiment in Section 11.1.

At this point, we once more remark that the choice of γ only has an influence on the global behaviour of the method. Locally the method converges quadratically for all $\gamma > 0$ as we will demonstrate below. However, this is a local properties and requires that the active set is already identified correctly.

3.2. Convergence of the Active Set Method. Under Assumption 9.2 and standard assumptions on the solution, the convergence of the active set / generalized Newton method is a straight forward consequence of Theorem A.7 applied to the function Φ (or Φ^n in the incremental setting).

Theorem 9.3. *Let Assumption 9.2 hold. Suppose that $\boldsymbol{y}_h^*$ satisfies $\Phi(\boldsymbol{y}_h^*) = 0$ and that Φ is CD-regular in $\boldsymbol{y}_h^*$, i.e. all elements of the generalized Jacobian $\partial\Phi(\boldsymbol{y}_h^*)$ are regular. Then, the active set / generalized Newton method (9.4) converges locally quadratic to the solution if the initial guess $\boldsymbol{y}_h^0$ is sufficiently close to the solution.*

PROOF. As Df and D^2g are Lipschitz continuous, we find that f and Dg are strongly semismooth. Since moreover, the $\max$-operator is strongly semismooth, the mapping Φ is strongly semismooth as a result of the chain rule for semismooth functions (Proposition A.5). Thus, under the assumed conditions, by Proposition A.1, sufficiently close to the solution, the occuring linear systems are uniquely solvable and the convergence is locally quadratic as a result of Theorem A.7 $\qquad\square$

Superlinear convergence can be shown under the weaker smoothness assumptions mentioned before. Particularly, $g \in SC^1$ and f convex already guarantee the semismoothness of Φ. However, this also implies that Φ_1 is not differentiable and the computation of an element of $\partial\Phi$ is more involved. Concerning associated plasticity, more precise results are available via the interpretation as a minimization problem.

4. Associated Plasticity

If the plastic potential is equal to the yield function, viz. $g \equiv f$, as found in associated plasticity, then (9.1) are the optimality (or Karush-Kuhn-Tucker) conditions of the convex minimization problem

$$
\begin{aligned}
\text{Minimize} \quad & \tfrac{1}{2}\int_\Omega \boldsymbol{\sigma}_h(x) : \mathbb{C}^{-1}[\boldsymbol{\sigma}_h(x)]\,dx + \int_\Omega \boldsymbol{\sigma}_h(x) : \boldsymbol{\tau}_h(x)\,dx \\
\text{subject to} \quad & B_h\boldsymbol{\sigma}_h + \ell_h = 0\,, \qquad f_h(\boldsymbol{\sigma}_h) \leq 0\,,
\end{aligned}
\tag{9.15}
$$

and again, $f_h(\boldsymbol{\sigma}_h) \leq 0$ is equivalent to $f(\boldsymbol{\sigma}_h(\boldsymbol{\xi})) \leq 0$ for all $\boldsymbol{\xi} \in \Xi$. This minimization problem is the discrete analogue of the dual problem of perfect plasticity (2.31) by making the admissibility constraint $\boldsymbol{\sigma}_h(\boldsymbol{\xi}) \in K = \{\boldsymbol{\eta} \in \mathrm{Sym}(d) : f(\boldsymbol{\eta}) \leq 0\}$ explicit. Thus, with $\boldsymbol{y}_h^* = (\boldsymbol{\sigma}_h^*, \boldsymbol{u}_h^*, \lambda_h^*)$ we have

$$
\Phi(\boldsymbol{y}_h^*) = 0 \quad \Longleftrightarrow \quad \boldsymbol{\sigma}_h^* \text{ solves (9.15) with Lagrange multipliers } (\boldsymbol{u}_h^*, \lambda_h^*)\,.
$$

The corresponding Lagrangian is

$$
\begin{aligned}
L_h(\boldsymbol{\sigma}_h, \boldsymbol{u}_h, \lambda_h) = {} & \tfrac{1}{2}\int_\Omega \boldsymbol{\sigma}_h(x) : \mathbb{C}^{-1}[\boldsymbol{\sigma}_h(x)]\,dx + \int_\Omega \boldsymbol{\sigma}_h(x) : \boldsymbol{\tau}_h(x)\,dx \\
& - \int_\Omega \boldsymbol{\sigma}_h(x) : \boldsymbol{\varepsilon}(\boldsymbol{u}_h(x))\,dx + \ell_h(\boldsymbol{u}_h) + \int_\Omega \lambda_h(x)^T f(\boldsymbol{\sigma}_h(x))\,dx\,.
\end{aligned}
$$

4.1. Convergence of the Active Set / Generalized Newton Method. In the context of minimization problems and variational inequalities, a lot of work has already been done concerning the properties of Φ and particularly, we refer to [QJ97] where semismoothness properties of Φ were addressed for the specific choice of $\gamma = 1$ in the definition of the NCP function ϕ_γ. In this section, we make the following assumptions concering the data which are more general than the conditions given in Assumption 9.2:

Assumption 9.4. *Let the data of the minimization problem* (9.15) *satisfy:*

(1) $f \in SC^1(\text{Sym}(d), \mathbb{R}^p)$: *this means that we allow more than one yield function and only require that f is continuously differentiable with a semismooth derivative Df :* $\text{Sym}(d) \to L(\text{Sym}(d), \mathbb{R}^p)$.

(2) *The admissible set $\{\boldsymbol{\sigma}_h \in \boldsymbol{P}_h : B_h \boldsymbol{\sigma}_h + \ell_h = 0, f_h(\boldsymbol{\sigma}_h) \leq 0\}$ of the minimization problem* (9.15) *is not empty.*

For given $\boldsymbol{y}_h \in \mathcal{Y}_h$, we define the set of *active indices* (which essentially is a set of double indices) by

$$I(\boldsymbol{y}_h) = \{(\boldsymbol{\xi}, j) \in \boldsymbol{\Xi} \times \{1, \ldots, p\} : f_j(\boldsymbol{\sigma}_h(\boldsymbol{\xi})) = 0\}.$$

Lemma 9.5. *Let $\boldsymbol{y}_h^* = (\boldsymbol{\sigma}_h^*, \boldsymbol{u}_h^*, \lambda_h^*)$ be a KKT point of* (9.15)*, i.e. $\boldsymbol{y}_h^*$ satisfies* (9.1)*. Moreover, let the (LICQ) at $\boldsymbol{y}_h^*$ hold, i.e. the matrix $\begin{bmatrix} B_h \\ (Df_h(\boldsymbol{\sigma}_h^*))_{I(\boldsymbol{y}_h^*)} \end{bmatrix}$ has full rank. Then Φ is CD-regular at $\boldsymbol{y}_h^*$, i.e. all elements of $\partial\Phi(\boldsymbol{y}_h^*)$ are regular.*

PROOF. This follows from [**QJ97**, Theorem 4.2] where this result is proven in a general nonconvex setting relying on the strong second-order sufficiency condition and the (LICQ) which together they called Robinson condition following [**Rob80, Rob82**]. The strong second-order condition is not necessary in the given context since the objective function is uniformly convex. □

The convexity of the objective function and the (LICQ) also yield the uniqueness of the multipliers $\boldsymbol{u}_h$ and λ_h.

Based on the above regularity result, we obtain the following convergence result in the spirit of [**QJ97**, Theorem 4.3].

Theorem 9.6. *Let $\boldsymbol{y}_h^*$ be a solution of $\Phi(\boldsymbol{y}_h) = 0$ and let $\boldsymbol{y}_h^*$ satisfy the conditions of Lemma 9.5. Then the active set / generalized Newton method converges locally superlinear. If moreover, $f \in C^2(\text{Sym}(d), \mathbb{R}^p)$ and $D^2 f$ is locally Lipschitz continuous, then the convergence is locally quadratic.*

PROOF. The generalized Newton method is well-defined due to the CD-regularity guaranteed by Lemma 9.5, and by Proposition A.1, there is a neighbourhood of $\boldsymbol{y}_h^*$ in which Φ is CD-regular. Φ is semismooth if f is a SC^1-function and under the additional smoothness requirements on f, we find that Φ is strongly semismooth. This gives the asserted quadratic convergence. □

4.2. Relation to the SQP Method. The SQP method for the minimization problem (9.15) consists in the successive solving of quadratic minimization problems with linearized constraints. Particularly, for a given iterate $\boldsymbol{y}_h^{k-1} = (\boldsymbol{\sigma}_h^{k-1}, \boldsymbol{u}_h^{k-1}, \lambda_h^{k-1})$, the next iterate is obtained by solving a quadratic subproblem

$$\text{Minimize} \quad \frac{1}{2} \int_\Omega \boldsymbol{\varsigma}_h^k(x) : \mathbb{M}_{k-1}(x)\big[\boldsymbol{\varsigma}_h^k(x)\big]\, dx + \int_\Omega \boldsymbol{\varsigma}_h^k(x) : \big(\mathbb{C}^{-1}[\boldsymbol{\sigma}_h^{k-1}(x)] + \boldsymbol{\tau}_h(x)\big)\, dx$$

$$\text{subject to} \quad B_h(\boldsymbol{\sigma}_h^{k-1} + \boldsymbol{\varsigma}_h^k) + \ell_h = 0, \quad f_h(\boldsymbol{\sigma}_h^{k-1}) + Df_h(\boldsymbol{\sigma}_h^{k-1})\boldsymbol{\varsigma}_h^k \leq 0,$$

with symmetric positive definite second order tensors $\mathbb{M}_{k-1}(x)$. This subproblem is uniformly convex and admits a unique solution as long as the linearized admissible set is not empty. In a convex setting, this is always fulfilled if the admissible set of (9.15) is not empty. The solution of the subproblem corresponds to the projection onto the linearized

admissible set in the metric defined by $\mathbb{M}_{k-1}$. If $\mathbb{M}_{k-1}$ is taken to be the derivative of the Lagrangian w.r.t. $\boldsymbol{\sigma}_h$, we obtain $\mathbb{M}_{k-1}(x) = \mathbb{G}_{k-1}(x)$ with $\mathbb{G}$ as defined in Section 9.1. This is a symmetric and positive definite tensor due to the convexity of problem (9.15). Having solved the quadratic subproblem, we update $\boldsymbol{\sigma}_h^k = \boldsymbol{\sigma}_h^{k-1} + \boldsymbol{\varsigma}_h^k$, and $(\boldsymbol{u}_h^k, \lambda_h^k)$ are defined as the Lagrange multipliers of the quadratic subproblem. The convergence of the SQP method can be shown under the same assumptions as those of Theorem 9.6 and we refer to [**Bon89**] or [**BGLS06**, Theorem 15.4] for a general non-convex result. Moreover, under strict complementarity of the solution, i.e. $\lambda_h^*(\boldsymbol{\xi}) - f(\boldsymbol{\sigma}_h^*(\boldsymbol{\xi})) > 0$ for all $\boldsymbol{\xi} \in \Xi$, and starting sufficiently close to the solution in the sense that the active set of the solution $\mathcal{A}_h(\boldsymbol{\sigma}_h^*, \lambda_h^*)$ coincides with the active set of the initial iterate $\mathcal{A}_h(\boldsymbol{\sigma}_h^0, \lambda_h^0)$, the iterates of the SQP method and of the active set / generalized Newton method as presented in this chapter are identical. Concerning the application of the SQP method to plasticity problems, we refer to [**Wie07**] and [**NSW09**].

4.3. Relation to Augmented Lagrangian Methods. Though, Augmented Lagrangian methods are the topic of the next chapter, we shortly comment on its relation with the active set method. If only the inequality constraints of (9.15) are treated by the Augmented Lagrangian method with parameter $\gamma > 0$, we obtain

$$L_{h,\gamma}(\boldsymbol{\sigma}_h, \boldsymbol{u}_h, \lambda_h) = \frac{1}{2} \int_\Omega \boldsymbol{\sigma}_h(x) : \mathbb{C}^{-1}[\boldsymbol{\sigma}_h(x)]\, dx + \int_\Omega \boldsymbol{\sigma}_h(x) : \boldsymbol{\tau}_h(x)\, dx + \ell(\boldsymbol{u}_h)$$

$$- \int_\Omega \boldsymbol{\sigma}_h(x) : \boldsymbol{\varepsilon}(\boldsymbol{u}_h(x))\, dx + \frac{1}{2\gamma} \int_\Omega \big| \max\{0, \lambda_h(x) + \gamma\, f(\boldsymbol{\sigma}_h(x))\}\big|^2 - |\lambda_h(x)|^2\, dx\,,$$

cf. [**Ber82**]. If $f \in SC^1(\mathrm{Sym}(d), \mathbb{R}^p)$, then $L_{h,\gamma} \in SC^1(\boldsymbol{P}_h \times \boldsymbol{X}_h \times \Lambda_h, \mathbb{R})$, see [**QS93**], and a saddle point of $L_{h,\gamma}$ is characterized by

$$0 = \mathbb{C}^{-1}[\boldsymbol{\sigma}_h(\boldsymbol{\xi})] - \big(\boldsymbol{\varepsilon}(\boldsymbol{u}_h(\boldsymbol{\xi})) - \boldsymbol{\tau}_h(\boldsymbol{\xi})\big) + \max\big\{0, \lambda_h(\boldsymbol{\xi}) + \gamma f(\boldsymbol{\sigma}_h(\boldsymbol{\xi}))\big\}\, Df(\boldsymbol{\sigma}_h(\boldsymbol{\xi}))\,,$$

$$0 = \int_\Omega \boldsymbol{\sigma}_h(x) : \boldsymbol{\varepsilon}(\boldsymbol{w}_h(x))\, dx - \ell(\boldsymbol{w}_h)\,, \qquad \boldsymbol{w}_h \in \boldsymbol{X}_h\,,$$

$$0 = \frac{1}{\gamma}\Big(\max\big\{0, \lambda_h(\boldsymbol{\xi}) + \gamma f(\boldsymbol{\sigma}_h(\boldsymbol{\xi}))\big\} - \lambda_h(\boldsymbol{\xi})\Big)\,.$$

These conditions are very similar to the condition $\Phi(\boldsymbol{y}_h) = 0$, with exception of the first equation and the rescaling of the last equation by $1/\gamma$. Indeed, for simpler problems like the obstacle problem, finding a saddle point of $L_{h,\gamma}$ by a generalized Newton method coincides with the active set method which is obtained by the reformulation of the optimality conditions by means of the NCP-function ϕ_γ. However, this identity does not hold for plasticity. The reason is the nonlinearity of the admissibility constraint in plasticity, whereas for obstacle problems, the inequality constraint is linear. In Section 10.5, we will demonstrate how an active set method can be derived from an Augmented Lagrangian approach. But this derivation has no obvious analogue in non-associated plasticity like the one presented in this chapter.

CHAPTER 10

AUGMENTED LAGRANGIAN METHODS FOR ASSOCIATED PLASTICITY

Viscoplasticity as presented in Section 3.1 gives a straight forward interpretation as a penalty method for the approximation of perfect plasticity on basis of Theorem 3.5, stating that the viscoplastic solution $\boldsymbol{\sigma}_\alpha$ converges to the solution $\overline{\boldsymbol{\sigma}}$ of perfect plasticity when $\alpha \to \infty$. The homotopy approach we gave in a more general setting in Section 8.2.3 can be interpreted as the implementation of such a penalty method for associated perfect plasticity by means of the viscoplastic regularization. In this chapter, we will embed this penalty approach into a wider class of approximation schemes - namely the Augmented Lagrangian method in the sense of [**IK00**], also see [**IK08**, Chapter 4], which reduces to the viscoplastic regularization for a specific choice of the parameters. In finite dimensions, the Augmented Lagrangian method including inequality constraints was proposed in [**Roc73**] and an extensive treatment can be found in [**Ber82**]. We will set up the Augmented Lagrangian method in a duality framework in function space based on a *generalized Moreau-Yosida approximation*. We restrict ourselves to perfect plasticity but the method can be extended to hardening plasticity as well. After introducing the generalized Moreau-Yosida approximation, we show approximation results for perfect plasticity, before we introduce the Augmented Lagrangian methods (first and second order) for perfect plasticity. For convenience, we restate the problem of perfect plasticity (2.31) (or problem (5.16) in an incremental setting).

$$\text{Minimize} \quad \tfrac{1}{2}a(\boldsymbol{\sigma},\boldsymbol{\sigma}) + \langle \boldsymbol{\tau},\boldsymbol{\sigma}\rangle_{P^*\times P} + \chi_K(\boldsymbol{\sigma}) - h(\boldsymbol{\sigma})$$
$$\text{subject to} \quad \boldsymbol{\sigma} \in S\,,$$

with $\langle \boldsymbol{\tau},\boldsymbol{\sigma}\rangle_{P^*\times P} = \int_\Omega \boldsymbol{\sigma}(x) : \boldsymbol{\tau}(x)\,dx$ and by $S \equiv S(\boldsymbol{b},\boldsymbol{t}_N)$, we denote the statically admissible set as defined in (2.25) which is a closed affine subspace of P. In this chapter, we distinguish the stress space $P = P^{**}$ and its dual P^* (the strain space). The operator $A : P \to P^*$, defined by $\langle A\boldsymbol{\sigma},\boldsymbol{\eta}\rangle_{P^*\times P} = \int_\Omega \boldsymbol{\sigma}(x) : \mathbb{C}^{-1}[\boldsymbol{\eta}(x)]\,dx$ and its inverse $\langle A^{-1}\boldsymbol{\varepsilon},\boldsymbol{\delta}\rangle_{P\times P^*} = \int_\Omega \boldsymbol{\varepsilon}(x) : \mathbb{C}[\boldsymbol{\delta}(x)]\,dx$ serve as the associated Riesz operators between P and P^*.

1. The Generalized Moreau-Yosida Approximation

1.1. The Generalized Moreau-Yosida Approximation. Whereas the viscoplastic regularization essentially was the Moreau-Yosida approximation χ_K^α of the indicator function χ_K, i.e.

$$\chi_K^\alpha(\boldsymbol{\sigma}) = \inf_{\boldsymbol{\eta} \in \boldsymbol{P}} \{\tfrac{\alpha}{2}\|\boldsymbol{\sigma} - \boldsymbol{\eta}\|_\Sigma^2 + \chi_K(\boldsymbol{\eta})\} = \tfrac{\alpha}{2}\|\boldsymbol{\sigma} - P_K(\boldsymbol{\sigma})\|_\Sigma^2\,,$$

we now introduce the generalized Moreau-Yosida approximation $\pi_K^\alpha : \boldsymbol{P} \times \boldsymbol{P}^* \to \mathbb{R}$ of χ_K which additionally depends on a given $\boldsymbol{\delta} \in \boldsymbol{P}^*$.

$$
\begin{aligned}
\pi_K^\alpha(\boldsymbol{\sigma}, \boldsymbol{\delta}) &= \inf_{\boldsymbol{\theta} \in \boldsymbol{P}} \{\chi_K(\boldsymbol{\sigma} - \boldsymbol{\theta}) + \langle \boldsymbol{\delta}, \boldsymbol{\theta}\rangle_{\boldsymbol{P}^* \times \boldsymbol{P}} + \tfrac{\alpha}{2}\|\boldsymbol{\theta}\|_\Sigma^2\} \\
&= \inf_{\boldsymbol{\eta} \in \boldsymbol{P}} \{\tfrac{\alpha}{2}\|\boldsymbol{\sigma} - \boldsymbol{\eta}\|_\Sigma^2 + \chi_K(\boldsymbol{\eta}) + \langle \boldsymbol{\delta}, \boldsymbol{\sigma} - \boldsymbol{\eta}\rangle_{\boldsymbol{P}^* \times \boldsymbol{P}}\}\,,
\end{aligned}
\tag{10.1}
$$

In the Augmented Lagrangian methods developed below, $\boldsymbol{\delta}$ will not be fixed but will be updated during the iteration. Then $\boldsymbol{\delta}$ will have an interpretation of the plastic strain (increment). For $\boldsymbol{\delta} = 0$, the standard Moreau-Yosida approximation is recovered. Already at this point, the notion Augmented Lagrangian can be justified as the quadratic penalty term is related to the equality constraint $\boldsymbol{\theta} = 0$. Using $\|\cdot\|_\Sigma^2 = \langle A\cdot, \cdot\rangle_{\boldsymbol{P}^* \times \boldsymbol{P}}$ (see Section 2.1), this can be rewritten as

$$\pi_K^\alpha(\boldsymbol{\sigma}, \boldsymbol{\delta}) = \inf_{\boldsymbol{\eta} \in \boldsymbol{P}} \left\{\tfrac{\alpha}{2}\|\boldsymbol{\eta} - (\boldsymbol{\sigma} + \tfrac{1}{\alpha}A^{-1}\boldsymbol{\delta})\|_\Sigma^2 + \chi_K(\boldsymbol{\eta})\right\} - \tfrac{1}{2\alpha}\|A^{-1}\boldsymbol{\delta}\|_\Sigma^2\,,$$

and we summarize some properties of π_K^α.

Lemma 10.1. *Consider the generalized Moreau-Yosida approximation* (10.1).

(1) *For all $\boldsymbol{\sigma} \in \boldsymbol{P}$ and $\boldsymbol{\delta} \in \boldsymbol{P}^*$, the infimum is attained at a unique point $\boldsymbol{\eta}_\alpha \equiv \boldsymbol{\eta}_\alpha(\boldsymbol{\sigma}, \boldsymbol{\delta}) = P_K(\boldsymbol{\sigma} + \tfrac{1}{\alpha}A^{-1}\boldsymbol{\delta})$.*

(2) *π_K^α is convex and Fréchet differentiable with Lipschitz continuous derivatives*

$$\langle D_{\boldsymbol{\sigma}}\pi_K^\alpha(\boldsymbol{\sigma}, \boldsymbol{\delta}), \boldsymbol{\eta}\rangle_{\boldsymbol{P}^* \times \boldsymbol{P}} = \alpha\, a\Big(\boldsymbol{\sigma} + \tfrac{1}{\alpha}A^{-1}\boldsymbol{\delta} - P_K(\boldsymbol{\sigma} + \tfrac{1}{\alpha}A^{-1}\boldsymbol{\delta}), \boldsymbol{\eta}\Big)\,,$$

$$\langle D_{\boldsymbol{\delta}}\pi_K^\alpha(\boldsymbol{\sigma}, \boldsymbol{\delta}), \boldsymbol{\varepsilon}\rangle_{\boldsymbol{P} \times \boldsymbol{P}^*} = a\Big(\boldsymbol{\sigma} - P_K(\boldsymbol{\sigma} + \tfrac{1}{\alpha}A^{-1}\boldsymbol{\delta}), A^{-1}\boldsymbol{\varepsilon}\Big)\,.$$

(3) *For all $\boldsymbol{\delta} \in \boldsymbol{P}^*$, we have*

$$\lim_{\alpha \to \infty} \pi_K^\alpha(\boldsymbol{\sigma}, \boldsymbol{\delta}) = \chi_K(\boldsymbol{\sigma})\,.$$

PROOF. We mainly follow [IK00]. As

$$\pi_K^\alpha(\boldsymbol{\sigma}, \boldsymbol{\delta}) = \inf_{\boldsymbol{\eta} \in \boldsymbol{P}} \left\{\tfrac{\alpha}{2}\|\boldsymbol{\eta} - (\boldsymbol{\sigma} + \tfrac{1}{\alpha}A^{-1}\boldsymbol{\delta})\|_\Sigma^2 + \chi_K(\boldsymbol{\eta})\right\} - \tfrac{1}{2\alpha}\|A^{-1}\boldsymbol{\delta}\|_\Sigma^2$$

we directly obtain (1) by employing the orthogonal projection P_K w.r.t. the inner product $a(\cdot, \cdot)$. Substituting $\boldsymbol{\eta}_\alpha = P_K(\boldsymbol{\sigma} + \tfrac{1}{\alpha}A^{-1}\boldsymbol{\delta})$ into π_K^α then gives

$$\pi_K^\alpha(\boldsymbol{\sigma}, \boldsymbol{\delta}) = \tfrac{\alpha}{2}\big\|(\boldsymbol{\sigma} + \tfrac{1}{\alpha}A^{-1}\boldsymbol{\delta}) - P_K(\boldsymbol{\sigma} + \tfrac{1}{\alpha}A^{-1}\boldsymbol{\delta})\big\|_\Sigma^2 - \tfrac{1}{2\alpha}\|A^{-1}\boldsymbol{\delta}\|_\Sigma^2\,. \tag{10.2}$$

and as in Proposition 3.1, we obtain

$$
\begin{aligned}
&\langle D_{\boldsymbol{\sigma}}\pi_K^\alpha(\boldsymbol{\sigma}, \boldsymbol{\delta}), \boldsymbol{\eta}\rangle_{\boldsymbol{P}^* \times \boldsymbol{P}} \\
&= \int_\Omega \alpha\mathbb{C}^{-1}\Big[\boldsymbol{\sigma}(x) + \tfrac{1}{\alpha}\mathbb{C}[\boldsymbol{\delta}(x)] - P_K\big(\boldsymbol{\sigma}(x) + \tfrac{1}{\alpha}\mathbb{C}[\boldsymbol{\delta}(x)]\big)\Big] : \boldsymbol{\eta}(x)\, dx\,,
\end{aligned}
$$

which is the asserted representation of the derivative w.r.t. $\boldsymbol{\sigma}$. The derivative w.r.t. $\boldsymbol{\delta}$ follows accordingly by the chain rule. (10.2) also gives (3) by letting $\alpha \to \infty$. $\qquad\square$

Remark 10.2.   (1) *Setting $\boldsymbol{\delta} = 0$ just gives the standard Moreau-Yosida approximation.*

     (2) *The derivative can also be expressed by means of the standard Moreau-Yosida approximation $\chi_K^\alpha(\boldsymbol{\sigma}) = \frac{\alpha}{2}\|\boldsymbol{\sigma} - P_K(\boldsymbol{\sigma})\|_\Sigma^2$ as defined in Section 3.1. Indeed, we have*

$$D_{\boldsymbol{\sigma}}\pi_K^\alpha(\boldsymbol{\sigma}, \boldsymbol{\delta}) = D\chi_K^\alpha\big(\boldsymbol{\sigma} + \tfrac{1}{\alpha}A^{-1}\boldsymbol{\delta}\big). \tag{10.3}$$

     (3) *By (10.2), we find*

$$0 \le \pi_K^\alpha(\boldsymbol{\sigma}, \boldsymbol{\delta}) + \tfrac{1}{2\alpha}\|A^{-1}\boldsymbol{\delta}\|_\Sigma^2. \tag{10.4}$$

     (4) *In finite dimension, the formula for the derivative follows from the theorem of Danskin, cf. [Dan67].*

1.2. The Dual Representation of π_K^α. As shown in [IK00], the generalized Moreau-Yosida approximation also has a dual representation which can be derived in a duality framework similar to Section 2.2.3. It turns out that

$$\pi_K^\alpha(\boldsymbol{\sigma}, \boldsymbol{\delta}) = \sup_{\boldsymbol{\epsilon} \in P^*} \big\{ (\boldsymbol{\sigma}, \boldsymbol{\epsilon})_P - \chi_K^*(\boldsymbol{\epsilon}) - \tfrac{1}{2\alpha}\|A^{-1}(\boldsymbol{\epsilon} - \boldsymbol{\delta})\|_\Sigma^2 \big\}$$

where χ_K^* is the support function of K, i.e. the Fenchel-conjugate function of χ_K. Since the expression in braces is uniformly concave w.r.t. ε, the supremum is attained at a unique point

$$\boldsymbol{\epsilon}_\alpha \equiv \boldsymbol{\epsilon}_\alpha(\boldsymbol{\sigma}, \boldsymbol{\delta}) = D_{\boldsymbol{\sigma}}\pi_K^\alpha(\boldsymbol{\sigma}, \boldsymbol{\delta}). \tag{10.5}$$

This formula suggests that $\boldsymbol{\epsilon}_\alpha$ is an approximation to the plastic strain (or the plastic strain increment) and indeed, for $\alpha \to \infty$, the right hand side of the dual representation of π_K^α converges to the Fenchel-conjugate function of χ_K^* which is $\big(\chi_K^*\big)^* = \chi_K$. Therefore, $D_{\boldsymbol{\sigma}}\pi_K^\alpha(\boldsymbol{\sigma}, \boldsymbol{\delta})$ is an approximation to the subdifferential $\partial\chi_K(\boldsymbol{\sigma})$ of the indicator function.

2. Approximation of Perfect Plasticity

In this section, we show how perfect plasticity can be approximated with the help of the generalized Moreau-Yosida approximation by letting $\alpha \to \infty$. This result is well-known for the standard Moreau-Yosida approximation and we extend these results to the generalized approximation.

2.1. Problem Setting and Optimality Conditions. With the functional

$$J : \boldsymbol{P} \to \mathbb{R}, \qquad\qquad J(\boldsymbol{\sigma}) = \tfrac{1}{2}a(\boldsymbol{\sigma}, \boldsymbol{\sigma}) + (\boldsymbol{\sigma}, \boldsymbol{\tau})_P - h(\boldsymbol{\sigma}) \tag{10.6}$$

the problem of associated perfect plasticity reduces to

$$\text{Minimize} \quad J(\boldsymbol{\sigma}) + \chi_K(\boldsymbol{\sigma}) \quad \text{subject to} \quad \boldsymbol{\sigma} \in \boldsymbol{S}. \tag{10.7}$$

The functional J is quadratic and uniformly convex and this also shows that J is bounded from below and is weakly lower semicontinuous. Regarding the given problem setting, the corresponding optimality system is

$$\langle DJ(\boldsymbol{\sigma}), \boldsymbol{\eta} - \boldsymbol{\sigma}\rangle_{P^* \times P} + \chi_K(\boldsymbol{\eta}) - \chi_K(\boldsymbol{\sigma}) \ge 0 \quad \text{for all } \boldsymbol{\eta} \in \boldsymbol{S},$$

also see (2.34). Now, we introduce the regularized minimization problem by means of the generalized Moreau-Yosida approximation.

$$\text{Minimize} \quad J(\boldsymbol{\sigma}) + \pi_K^\alpha(\boldsymbol{\sigma}, \boldsymbol{\delta}) \quad \text{subject to} \quad \boldsymbol{\sigma} \in \boldsymbol{S}, \tag{10.8}$$

for $\alpha > 0$ and $\boldsymbol{\delta} \in \boldsymbol{P}^*$. From the remark in the preceeding section we know that the regularized objective function is uniformly convex and bounded from below for given $\boldsymbol{\delta}$. Therefore, the regularized problem admits a unique solution $\boldsymbol{\sigma}_\alpha$ satisfying the necessary and sufficient optimality condition

$$\langle DJ(\boldsymbol{\sigma}_\alpha), \boldsymbol{\eta} - \boldsymbol{\sigma}_\alpha \rangle_{\boldsymbol{P}^* \times \boldsymbol{P}} + \langle D_{\boldsymbol{\sigma}} \pi_K^\alpha(\boldsymbol{\sigma}_\alpha, \boldsymbol{\delta}), \boldsymbol{\eta} - \boldsymbol{\sigma}_\alpha \rangle_{\boldsymbol{P}^* \times \boldsymbol{P}} \geq 0 \qquad \text{for all } \boldsymbol{\eta} \in \boldsymbol{S}.$$

By (10.5), we write $D_{\boldsymbol{\sigma}} \pi_K^\alpha(\boldsymbol{\sigma}_\alpha, \boldsymbol{\delta}) = \boldsymbol{\epsilon}_\alpha$ and hence optimality can as well be expressed as

$$\langle DJ(\boldsymbol{\sigma}_\alpha), \boldsymbol{\eta} - \boldsymbol{\sigma}_\alpha \rangle_{\boldsymbol{P}^* \times \boldsymbol{P}} + \langle \boldsymbol{\epsilon}_\alpha, \boldsymbol{\eta} - \boldsymbol{\sigma}_\alpha \rangle_{\boldsymbol{P}^* \times \boldsymbol{P}} \geq 0 \qquad \text{for all } \boldsymbol{\eta} \in \boldsymbol{S}.$$

2.2. Approximation of Perfect Plasticity. We show that by means of the generalized Moreau-Yosida approximation, the stress field of the perfectly plastic limit can be approximated in a stable manner. This convergence results also covers the approximation results of Section 3.1. Particularly, we will proof Theorem 3.5. We begin with some preliminary results and notation.

Definition 10.3. *Throughout this section, we use the following notation.*

(1) *By $\boldsymbol{\sigma}_\alpha$, we denote the solution of the regularized problem (10.8).*
(2) *By $\widehat{\boldsymbol{\sigma}}$, we denote the element in the safe load condition (Assumption 2.1) which we assume to be satisfied henceforth.*
(3) *We only consider $J(\boldsymbol{\sigma}) = \frac{1}{2} a(\boldsymbol{\sigma}, \boldsymbol{\sigma}) + (\boldsymbol{\tau}, \boldsymbol{\sigma})_P$, i.e. we set $h = 0$ (homogeneous Dirichlet boundary conditions on Γ_D).*

Lemma 10.4. *For the solution $\boldsymbol{\sigma}_\alpha$ of the regularized problem (10.8), the following holds.*

$$\pi_K^\alpha(\widehat{\boldsymbol{\sigma}}, \boldsymbol{\delta}) - \pi_K^\alpha(\boldsymbol{\sigma}_\alpha, \boldsymbol{\delta}) \geq \alpha\, a\Big(\boldsymbol{\sigma}_\alpha + \tfrac{1}{\alpha} A^{-1}\boldsymbol{\delta} - P_K(\boldsymbol{\sigma}_\alpha + \tfrac{1}{\alpha} A^{-1}\boldsymbol{\delta}), \widehat{\boldsymbol{\sigma}} - \boldsymbol{\sigma}_\alpha\Big), \quad (10.9a)$$

$$a(\boldsymbol{\sigma}_\alpha, \boldsymbol{\sigma}_\alpha - \widehat{\boldsymbol{\sigma}}) + (\boldsymbol{\tau}, \boldsymbol{\sigma}_\alpha - \widehat{\boldsymbol{\sigma}})_P$$
$$+ \alpha\, a\Big(\boldsymbol{\sigma}_\alpha + \tfrac{1}{\alpha} A^{-1}\boldsymbol{\delta} - P_K(\boldsymbol{\sigma}_\alpha + \tfrac{1}{\alpha} A^{-1}\boldsymbol{\delta}), \boldsymbol{\sigma}_\alpha - \widehat{\boldsymbol{\sigma}}\Big) = 0, \quad (10.9b)$$

$$\big\|\boldsymbol{\eta} + \tfrac{1}{\alpha} A^{-1}\boldsymbol{\delta} - P_K(\boldsymbol{\eta} + \tfrac{1}{\alpha} A^{-1}\boldsymbol{\delta})\big\|_{\boldsymbol{\Sigma}} \leq \tfrac{1}{\alpha}\|A^{-1}\boldsymbol{\delta}\|_{\boldsymbol{\Sigma}}, \quad \text{for all } \boldsymbol{\eta} \in \boldsymbol{K}, \quad (10.9c)$$

$$\big\|\boldsymbol{\sigma}_\alpha - P_K(\boldsymbol{\sigma}_\alpha)\big\|_{\boldsymbol{\Sigma}} \leq \big\|\boldsymbol{\sigma}_\alpha + \tfrac{1}{\alpha} A^{-1}\boldsymbol{\delta} - P_K(\boldsymbol{\sigma}_\alpha + \tfrac{1}{\alpha} A^{-1}\boldsymbol{\delta})\big\|_{\boldsymbol{\Sigma}} + \tfrac{2}{\alpha}\|A^{-1}\boldsymbol{\delta}\|_{\boldsymbol{\Sigma}} \quad (10.9d)$$

PROOF. Since $\pi_K^\alpha(\cdot, \boldsymbol{\delta})$ is convex and differentiable, (10.9a) follows from the characterization of differentiable convex functions by means of their derivatives and the characterization of the derivative $D_{\boldsymbol{\sigma}} \pi_K^\alpha$ given in Lemma 10.1.

Concerning (10.9b), note that $2\boldsymbol{\sigma}_\alpha - \widehat{\boldsymbol{\sigma}} \in \boldsymbol{S}$ and $2\widehat{\boldsymbol{\sigma}} - \boldsymbol{\sigma}_\alpha \in \boldsymbol{S}$. Testing the optimality condition with these test functions and using Lemma 10.1(2) again, we obtain the assertion.

Looking at (10.9c), we remark that if $\boldsymbol{\eta} + \tfrac{1}{\alpha} A^{-1}\boldsymbol{\delta} \notin \boldsymbol{K}$, then

$$\big\|\boldsymbol{\eta} + \tfrac{1}{\alpha} A^{-1}\boldsymbol{\delta} - P_K(\boldsymbol{\eta} + \tfrac{1}{\alpha} A^{-1}\boldsymbol{\delta})\big\|_{\boldsymbol{\Sigma}} = \text{dist}_{\|\cdot\|_{\boldsymbol{\Sigma}}}(\boldsymbol{\eta} + \tfrac{1}{\alpha} A^{-1}\boldsymbol{\delta}, \boldsymbol{K})$$
$$\leq \|\boldsymbol{\eta} + \tfrac{1}{\alpha} A^{-1}\boldsymbol{\delta} - \boldsymbol{\eta}\|_{\boldsymbol{\Sigma}} = \tfrac{1}{\alpha}\|A^{-1}\boldsymbol{\delta}\|_{\boldsymbol{\Sigma}}$$

as the projection P_K minimizes the distance to $\boldsymbol{K}$ in the given norm.

Finally, (10.9d) follows from

$$\|\boldsymbol{\sigma}_\alpha - P_{\boldsymbol{K}}(\boldsymbol{\sigma}_\alpha)\|_{\boldsymbol{\Sigma}}$$
$$= \left\|\boldsymbol{\sigma}_\alpha + \tfrac{1}{\alpha}A^{-1}\boldsymbol{\delta} - P_{\boldsymbol{K}}\big(\boldsymbol{\sigma}_\alpha + \tfrac{1}{\alpha}A^{-1}\boldsymbol{\delta}\big) - \tfrac{1}{\alpha}A^{-1}\boldsymbol{\delta} + P_{\boldsymbol{K}}\big(\boldsymbol{\sigma}_\alpha + \tfrac{1}{\alpha}A^{-1}\boldsymbol{\delta}\big) - P_{\boldsymbol{K}}(\boldsymbol{\sigma}_\alpha)\right\|_{\boldsymbol{\Sigma}}$$
$$\le \left\|\boldsymbol{\sigma}_\alpha + \tfrac{1}{\alpha}A^{-1}\boldsymbol{\delta} - P_{\boldsymbol{K}}\big(\boldsymbol{\sigma}_\alpha + \tfrac{1}{\alpha}A^{-1}\boldsymbol{\delta}\big)\right\|_{\boldsymbol{\Sigma}} + \left\|\tfrac{1}{\alpha}A^{-1}\boldsymbol{\delta}\right\|_{\boldsymbol{\Sigma}}$$
$$\quad + \left\|P_{\boldsymbol{K}}\big(\boldsymbol{\sigma}_\alpha + \tfrac{1}{\alpha}A^{-1}\boldsymbol{\delta}\big) - P_{\boldsymbol{K}}(\boldsymbol{\sigma}_\alpha)\right\|_{\boldsymbol{\Sigma}}$$
$$\le \left\|\boldsymbol{\sigma}_\alpha + \tfrac{1}{\alpha}A^{-1}\boldsymbol{\delta} - P_{\boldsymbol{K}}\big(\boldsymbol{\sigma}_\alpha + \tfrac{1}{\alpha}A^{-1}\boldsymbol{\delta}\big)\right\|_{\boldsymbol{\Sigma}} + \tfrac{2}{\alpha}\|A^{-1}\boldsymbol{\delta}\|_{\boldsymbol{\Sigma}}$$

and in the last estimate we used the non-expansiveness of the projection in the norm $\|\cdot\|_{\boldsymbol{\Sigma}}$. $\qquad\square$

The following lemma gives a priori estimates for the stress field $\boldsymbol{\sigma}_\alpha$.

Lemma 10.5. *Let the safe-load condition (Assumption 2.1) hold. Then, for fixed $\boldsymbol{\delta} \in \boldsymbol{P}^*$ and $\alpha \ge 1$, there exists a constant $C > 0$ such that*

$$\|\boldsymbol{\sigma}_\alpha\|_{\boldsymbol{\Sigma}} \le C\,, \qquad\qquad and \qquad\qquad \pi_{\boldsymbol{K}}^\alpha(\boldsymbol{\sigma}_\alpha, \boldsymbol{\delta}) \le C\,.$$

PROOF. By (10.9a) and (10.9b), we find

$$a(\boldsymbol{\sigma}_\alpha, \boldsymbol{\sigma}_\alpha - \widehat{\boldsymbol{\sigma}}) + (\boldsymbol{\tau}, \boldsymbol{\sigma}_\alpha - \widehat{\boldsymbol{\sigma}})_{\boldsymbol{P}}$$
$$= \alpha\, a\Big(\boldsymbol{\sigma}_\alpha + \tfrac{1}{\alpha}A^{-1}\boldsymbol{\delta} - P_{\boldsymbol{K}}\big(\boldsymbol{\sigma}_\alpha + \tfrac{1}{\alpha}A^{-1}\boldsymbol{\delta}\big), \widehat{\boldsymbol{\sigma}} - \boldsymbol{\sigma}_\alpha\Big)$$
$$\le \pi_{\boldsymbol{K}}^\alpha(\widehat{\boldsymbol{\sigma}}, \boldsymbol{\delta}) - \pi_{\boldsymbol{K}}^\alpha(\boldsymbol{\sigma}_\alpha, \boldsymbol{\delta})$$
$$= \tfrac{\alpha}{2}\left\|\widehat{\boldsymbol{\sigma}} + \tfrac{1}{\alpha}A^{-1}\boldsymbol{\delta} - P_{\boldsymbol{K}}\big(\widehat{\boldsymbol{\sigma}} + \tfrac{1}{\alpha}A^{-1}\boldsymbol{\delta}\big)\right\|_{\boldsymbol{\Sigma}}^2 - \tfrac{1}{2\alpha}\|A^{-1}\boldsymbol{\delta}\|_{\boldsymbol{\Sigma}}^2$$
$$\quad - \left(\tfrac{\alpha}{2}\left\|\boldsymbol{\sigma}_\alpha + \tfrac{1}{\alpha}A^{-1}\boldsymbol{\delta} - P_{\boldsymbol{K}}\big(\boldsymbol{\sigma}_\alpha + \tfrac{1}{\alpha}A^{-1}\boldsymbol{\delta}\big)\right\|_{\boldsymbol{\Sigma}}^2 - \tfrac{1}{2\alpha}\|A^{-1}\boldsymbol{\delta}\|_{\boldsymbol{\Sigma}}^2\right)$$
$$\le \tfrac{\alpha}{2}\left\|\widehat{\boldsymbol{\sigma}} + \tfrac{1}{\alpha}A^{-1}\boldsymbol{\delta} - P_{\boldsymbol{K}}\big(\widehat{\boldsymbol{\sigma}} + \tfrac{1}{\alpha}A^{-1}\boldsymbol{\delta}\big)\right\|_{\boldsymbol{\Sigma}}^2 \le \tfrac{1}{2\alpha}\|A^{-1}\boldsymbol{\delta}\|_{\boldsymbol{\Sigma}}^2$$

where the last estimate follows from (10.9c). Since $\boldsymbol{\delta} \in \boldsymbol{P}^*$ is fixed, for $\alpha \ge 1$, we therefore obtain

$$a(\boldsymbol{\sigma}_\alpha, \boldsymbol{\sigma}_\alpha) \le a(\boldsymbol{\sigma}_\alpha, \widehat{\boldsymbol{\sigma}}) - (\boldsymbol{\tau}, \boldsymbol{\sigma}_\alpha)_{\boldsymbol{P}} + (\boldsymbol{\tau}, \widehat{\boldsymbol{\sigma}})_{\boldsymbol{P}} + \tfrac{1}{2}\|A^{-1}\boldsymbol{\delta}\|_{\boldsymbol{\Sigma}}^2$$

Using the Cauchy-Schwarz and Young's inequality then gives the bound for $\boldsymbol{\sigma}_\alpha$. We now turn to the bound for $\pi_{\boldsymbol{K}}^\alpha(\boldsymbol{\sigma}_\alpha, \boldsymbol{\delta})$.

$$\pi_{\boldsymbol{K}}^\alpha(\boldsymbol{\sigma}_\alpha, \boldsymbol{\delta}) \overset{(10.9a)}{\le} \pi_{\boldsymbol{K}}^\alpha(\widehat{\boldsymbol{\sigma}}, \boldsymbol{\delta}) - \alpha\, a\Big(\boldsymbol{\sigma}_\alpha + \tfrac{1}{\alpha}A^{-1}\boldsymbol{\delta} - P_{\boldsymbol{K}}\big(\boldsymbol{\sigma}_\alpha + \tfrac{1}{\alpha}A^{-1}\boldsymbol{\delta}\big), \widehat{\boldsymbol{\sigma}} - \boldsymbol{\sigma}_\alpha\Big)$$
$$\overset{(10.9b)}{=} \tfrac{\alpha}{2}\left\|\widehat{\boldsymbol{\sigma}} + \tfrac{1}{\alpha}A^{-1}\boldsymbol{\delta} - P_{\boldsymbol{K}}\big(\widehat{\boldsymbol{\sigma}} + \tfrac{1}{\alpha}A^{-1}\boldsymbol{\delta}\big)\right\|_{\boldsymbol{\Sigma}}^2 - \tfrac{1}{2\alpha}\|A^{-1}\boldsymbol{\delta}\|_{\boldsymbol{\Sigma}}^2$$
$$\quad - a(\boldsymbol{\sigma}_\alpha, \boldsymbol{\sigma}_\alpha - \widehat{\boldsymbol{\sigma}}) - (\boldsymbol{\tau}, \boldsymbol{\sigma}_\alpha - \widehat{\boldsymbol{\sigma}})_{\boldsymbol{P}}$$
$$\overset{(10.9c)}{\le} \tfrac{1}{2\alpha}\|A^{-1}\boldsymbol{\delta}\|_{\boldsymbol{\Sigma}}^2 - \tfrac{1}{2\alpha}\|A^{-1}\boldsymbol{\delta}\|_{\boldsymbol{\Sigma}}^2 - a(\boldsymbol{\sigma}_\alpha, \boldsymbol{\sigma}_\alpha - \widehat{\boldsymbol{\sigma}}) - (\boldsymbol{\tau}, \boldsymbol{\sigma}_\alpha - \widehat{\boldsymbol{\sigma}})_{\boldsymbol{P}}\,.$$

The boundedness of $\pi_{\boldsymbol{K}}^\alpha(\boldsymbol{\sigma}_\alpha, \boldsymbol{\delta})$ then follows from the estimate for $\boldsymbol{\sigma}_\alpha$. $\qquad\square$

Theorem 10.6. *If the safe load condition is satisfied, then the solution $\boldsymbol{\sigma}_\alpha$ of the regularized problem (10.8) converges strongly to the solution of the perfect plasticity problem (10.7) as $\alpha \to \infty$.*

PROOF. Since $\boldsymbol{\sigma}_\alpha$ is bounded, there is a weakly convergent subsequence (again denoted by $\boldsymbol{\sigma}_\alpha$) converging to some $\overline{\boldsymbol{\sigma}} \in \boldsymbol{P}$. Since $\boldsymbol{S}$ is a closed subspace and $\boldsymbol{\sigma}_\alpha \in \boldsymbol{S}$, we also find $\overline{\boldsymbol{\sigma}} \in \boldsymbol{S}$, i.e. $\overline{\boldsymbol{\sigma}}$ is in equilibrium.

We will now show $\overline{\boldsymbol{\sigma}} \in \boldsymbol{K}$. In order to do this, first notice that

$$\|\boldsymbol{\sigma}_\alpha - P_{\boldsymbol{K}}(\boldsymbol{\sigma}_\alpha)\|_{\boldsymbol{\Sigma}}^2 \overset{(10.9d)}{\leq} 2\big\|\boldsymbol{\sigma}_\alpha + \tfrac{1}{\alpha}A^{-1}\boldsymbol{\delta} - P_{\boldsymbol{K}}\big(\boldsymbol{\sigma}_\alpha + \tfrac{1}{\alpha}A^{-1}\boldsymbol{\delta}\big)\big\|_{\boldsymbol{\Sigma}}^2 + \tfrac{8}{\alpha^2}\|A^{-1}\boldsymbol{\delta}\|_{\boldsymbol{\Sigma}}^2$$

$$= \tfrac{4}{\alpha}\Big(\pi_{\boldsymbol{K}}^\alpha(\boldsymbol{\sigma}_\alpha, \boldsymbol{\delta}) + \tfrac{1}{2\alpha}\|A^{-1}\boldsymbol{\delta}\|_{\boldsymbol{\Sigma}}^2\Big) + \tfrac{8}{\alpha^2}\|A^{-1}\boldsymbol{\delta}\|_{\boldsymbol{\Sigma}}^2 \leq \tfrac{C}{\alpha},$$

for some $C > 0$ and $\alpha \geq 1$ due to the boundedness of $\pi_{\boldsymbol{K}}^\alpha(\boldsymbol{\sigma}_\alpha, \boldsymbol{\delta})$ as proven in Lemma 10.5. The functional $\boldsymbol{\eta} \mapsto \|\boldsymbol{\eta} - P_{\boldsymbol{K}}(\boldsymbol{\eta})\|_{\boldsymbol{\Sigma}}^2$ is convex and differentiable and therefore weakly lower semicontinuous in $\boldsymbol{P}$. Thus,

$$\|\overline{\boldsymbol{\sigma}} - P_{\boldsymbol{K}}(\overline{\boldsymbol{\sigma}})\|_{\boldsymbol{\Sigma}}^2 \leq \liminf_{\alpha \to \infty} \|\boldsymbol{\sigma}_\alpha - P_{\boldsymbol{K}}(\boldsymbol{\sigma}_\alpha)\|_{\boldsymbol{\Sigma}}^2 \leq \limsup_{\alpha \to \infty} \|\boldsymbol{\sigma}_\alpha - P_{\boldsymbol{K}}(\boldsymbol{\sigma}_\alpha)\|_{\boldsymbol{\Sigma}}^2 = 0$$

by the above estimate.

It remains to prove that $\overline{\boldsymbol{\sigma}}$ is optimal for the perfect plasticity problem (10.7). We have

$$J(\boldsymbol{\sigma}_\alpha) = \tfrac{1}{2}a(\boldsymbol{\sigma}_\alpha, \boldsymbol{\sigma}_\alpha) + (\boldsymbol{\sigma}_\alpha, \boldsymbol{\tau})_{\boldsymbol{P}}$$

$$\overset{(10.4)}{\leq} \tfrac{1}{2}a(\boldsymbol{\sigma}_\alpha, \boldsymbol{\sigma}_\alpha) + (\boldsymbol{\sigma}_\alpha, \boldsymbol{\tau})_{\boldsymbol{P}} + \pi_{\boldsymbol{K}}^\alpha(\boldsymbol{\sigma}_\alpha, \boldsymbol{\delta}) + \tfrac{1}{2\alpha}\|A^{-1}\boldsymbol{\delta}\|_{\boldsymbol{\Sigma}}^2$$

$$\leq \tfrac{1}{2}a(\boldsymbol{\eta}, \boldsymbol{\eta}) + (\boldsymbol{\eta}, \boldsymbol{\tau})_{\boldsymbol{P}} + \pi_{\boldsymbol{K}}^\alpha(\boldsymbol{\eta}, \boldsymbol{\delta}) + \tfrac{1}{2\alpha}\|A^{-1}\boldsymbol{\delta}\|_{\boldsymbol{\Sigma}}^2$$

for all $\boldsymbol{\eta} \in \boldsymbol{S}$ due to the optimality of $\boldsymbol{\sigma}_\alpha$ for the regularized problem. Particularly, this also holds for all $\boldsymbol{\eta} \in \boldsymbol{S} \cap \boldsymbol{K}$ and by (10.9c) we find

$$\pi_{\boldsymbol{K}}^\alpha(\boldsymbol{\eta}, \boldsymbol{\delta}) \leq 0 \qquad \text{for all } \boldsymbol{\eta} \in \boldsymbol{K} \cap \boldsymbol{S},$$

and consequently

$$J(\boldsymbol{\sigma}_\alpha) \leq J(\boldsymbol{\eta}) + \tfrac{1}{2\alpha}\|A^{-1}\boldsymbol{\delta}\|_{\boldsymbol{\Sigma}}^2 \qquad \text{for all } \boldsymbol{\eta} \in \boldsymbol{S} \cap \boldsymbol{K}.$$

Since J is uniformly convex and weakly lower semicontinuous, we eventually get

$$J(\overline{\boldsymbol{\sigma}}) \leq \liminf_{\alpha \to \infty} J(\boldsymbol{\sigma}_\alpha) \leq \limsup_{\alpha \to \infty} J(\boldsymbol{\sigma}_\alpha) \leq J(\boldsymbol{\eta}) \qquad \text{for all } \boldsymbol{\eta} \in \boldsymbol{S} \cap \boldsymbol{K},$$

and this shows the optimality of $\overline{\boldsymbol{\sigma}}$. The uniform convexity of J also shows uniqueness of the solution, and setting $\boldsymbol{\eta} = \overline{\boldsymbol{\sigma}} \in \boldsymbol{S} \cap \boldsymbol{K}$ in the above inequality also shows that the whole sequence converges. As $J(\cdot)$ is just the squared and shifted norm function, also strong convergence follows. $\square$

2.3. An Estimate for ϵ_α and u_α.

2.3.1. *The Plastic Strain.* For every $\alpha > 0$, the quantity ϵ_α as introduced in (10.5) is an approximation to the plastic strain (static plasticity) or the plastic strain increment (incremental plasticity). In perfect plasticity, the plastic strain in not contained in L^2 generally but only in the weaker space $\boldsymbol{M}_{\mathrm{Sym}}(\Omega)$, see Section 5.1. This is reflected in the following α-dependent estimate.

Corollary 10.7. *Let ϵ_α be as in (10.5). Then, for all $\alpha \geq 1$, there exists $C > 0$ independent of α, such that*

$$\tfrac{1}{\sqrt{\alpha}}\|A^{-1}\epsilon_\alpha\|_{\boldsymbol{\Sigma}} \leq C. \tag{10.10}$$

PROOF. The proof easily follows from the characterization of the derivative given in Lemma 10.1. Since

$$\epsilon_\alpha = D_{\boldsymbol{\sigma}}\pi_{\boldsymbol{K}}^\alpha(\boldsymbol{\sigma}_\alpha, \boldsymbol{\delta}) = \alpha\, A\Big(\boldsymbol{\sigma}_\alpha + \tfrac{1}{\alpha}A^{-1}\boldsymbol{\delta} - P_{\boldsymbol{K}}\big(\boldsymbol{\sigma}_\alpha + \tfrac{1}{\alpha}A^{-1}\boldsymbol{\delta}\big)\Big),$$

we find

$$
\begin{aligned}
\|A^{-1}\boldsymbol{\epsilon}_\alpha\|_{\boldsymbol{\Sigma}}^2 &= \alpha^2\big\|\boldsymbol{\sigma}_\alpha + \tfrac{1}{\alpha}A^{-1}\boldsymbol{\delta} - P_{\boldsymbol{K}}\big(\boldsymbol{\sigma}_\alpha + \tfrac{1}{\alpha}A^{-1}\boldsymbol{\delta}\big)\big\|_{\boldsymbol{\Sigma}}^2 \\
&= 2\alpha\big(\pi_{\boldsymbol{K}}^\alpha(\boldsymbol{\sigma}_\alpha,\boldsymbol{\delta}) + \tfrac{1}{2\alpha}\|A^{-1}\boldsymbol{\delta}\|_{\boldsymbol{\Sigma}}^2\big) \le \alpha\,C\,,
\end{aligned}
$$

with $C > 0$ for all $\alpha \ge 1$ as a result of Lemma 10.5. Taking the square root gives the assertion. □

2.3.2. *The Displacement Field.* So far, the displacement field was hidden in the definition of the statically admissible set $\boldsymbol{S}$. Due to the linear structure of $\boldsymbol{S}$, the optimality conditions of the regularized problem can be rephrased as

$$
\langle DJ(\boldsymbol{\sigma}_\alpha) + \boldsymbol{\epsilon}_\alpha + B^*\boldsymbol{u}_\alpha, \boldsymbol{\eta}\rangle_{\boldsymbol{P}^*\times\boldsymbol{P}} = 0\,, \qquad \boldsymbol{\eta} \in \boldsymbol{P}\,, \tag{10.11}
$$

and $b(\boldsymbol{\sigma}_\alpha, \boldsymbol{w}) = -\ell(\boldsymbol{w})$ for all $\boldsymbol{w} \in \boldsymbol{X}$.

Corollary 10.8. *For the displacement field $\boldsymbol{u}_\alpha \in \boldsymbol{X}(\boldsymbol{u}_D)$ and $\alpha \ge 1$, the α-dependent estimate*

$$
\frac{1}{\sqrt{\alpha}}\|\boldsymbol{u}_\alpha\| \le C \tag{10.12}
$$

holds with $C > 0$ being independent of α.

PROOF. The optimality condition (10.11) is equivalent to

$$
\boldsymbol{\sigma}_\alpha + A^{-1}\big(\boldsymbol{\tau} + \boldsymbol{\epsilon}_\alpha + B^*\boldsymbol{u}_\alpha\big) = 0\,.
$$

Applying the $\|\cdot\|_{\boldsymbol{\Sigma}}$ norm and since $\|\cdot\| = \|A^{-1}B^*\cdot\|_{\boldsymbol{\Sigma}}$, we find

$$
\|\boldsymbol{u}_\alpha\| \le \|\boldsymbol{\sigma}_\alpha + A^{-1}\boldsymbol{\tau}\|_{\boldsymbol{\Sigma}} + \|A^{-1}\boldsymbol{\epsilon}_\alpha\|_{\boldsymbol{\Sigma}} \le (1 + \sqrt{\alpha})\,C
$$

with a constant $C > 0$ independent of α. Considering $\alpha \ge 1$ completes the proof. □

2.3.3. *A priori Estimates.* Altogether, we obtain the following a priori estimate valid for $\alpha \ge 1$.

$$
\|\boldsymbol{\sigma}_\alpha\|_{\boldsymbol{\Sigma}} + \frac{1}{\sqrt{\alpha}}\big(\|\boldsymbol{u}_\alpha\| + \|A^{-1}\boldsymbol{\epsilon}_\alpha\|_{\boldsymbol{\Sigma}}\big) \le C\,.
$$

By using the optimality condition (10.11), we also see that the elastic strain $-B^*\boldsymbol{u}_\alpha - \boldsymbol{\epsilon}_\alpha$ can be approximated stably as

$$
\|A^{-1}(-B^*\boldsymbol{u}_\alpha - \boldsymbol{\epsilon}_\alpha)\|_{\boldsymbol{\Sigma}} = \|\boldsymbol{\sigma}_\alpha + A^{-1}\boldsymbol{\tau}\|_{\boldsymbol{\Sigma}}\,.
$$

This seems reasonable if we look back to Section 5.1.

3. Solving the Regularized Subproblems

We consider the regularized problem (10.8) and derive the corresponding primal minimization problem and its optimality condition. As for the viscoplastic regularization given in Section 3.1, the corresponding primal functional will turn out to be uniformly convex with modulus $\frac{1}{1+\alpha}$.

3.1. The Primal Regularized Problem. Making the constraint $\boldsymbol{\sigma}_\alpha \in \boldsymbol{S}$ explicit, for fixed $\boldsymbol{\delta} \in \boldsymbol{P}^*$, the optimality conditions of the regularized problem (also see (10.11)) are given by

$$a(\boldsymbol{\sigma}_\alpha, \boldsymbol{\eta}) + (\boldsymbol{\eta}, \boldsymbol{\tau})_{\boldsymbol{P}} + b(\boldsymbol{\eta}, \boldsymbol{u}_\alpha)$$
$$+ \alpha\, a\big(\boldsymbol{\sigma}_\alpha + \tfrac{1}{\alpha}A^{-1}\boldsymbol{\delta} - P_K(\boldsymbol{\sigma}_\alpha + \tfrac{1}{\alpha}A^{-1}\boldsymbol{\delta}), \boldsymbol{\eta}\big) = 0\,, \qquad \boldsymbol{\eta} \in \boldsymbol{P}\,,$$
$$b(\boldsymbol{\sigma}_\alpha, \boldsymbol{w}) = -\ell(\boldsymbol{w})\,, \qquad \boldsymbol{w} \in \boldsymbol{X}\,.$$

Lemma 10.9. *The stress response is given by*

$$\boldsymbol{\sigma}_\alpha = \tfrac{1}{1+\alpha}A^{-1}\big(-B^*\boldsymbol{u}_\alpha - \boldsymbol{\tau} - \boldsymbol{\delta}\big) + \tfrac{\alpha}{1+\alpha}P_K\Big(A^{-1}\big(-B^*\boldsymbol{u}_\alpha - \boldsymbol{\tau} + \tfrac{1}{\alpha}\boldsymbol{\delta}\big)\Big)\,,$$

and pointwise a.e., this is

$$\boldsymbol{\sigma}_\alpha(x) = \tfrac{1}{1+\alpha}\mathbb{C}\big[\boldsymbol{\varepsilon}(\boldsymbol{u}_\alpha(x)) - \boldsymbol{\tau}(x) - \boldsymbol{\delta}(x)\big]$$
$$+ \tfrac{\alpha}{1+\alpha}P_K\big(\mathbb{C}\big[\boldsymbol{\varepsilon}(\boldsymbol{u}_\alpha(x)) - \boldsymbol{\tau}(x) + \tfrac{1}{\alpha}\boldsymbol{\delta}(x)\big]\big)\,.$$

PROOF. We omit the argument x and pointwise a.e., the first equation of the optimality conditions is equivalent to

$$\boldsymbol{\sigma}_\alpha - \mathbb{C}[\boldsymbol{\varepsilon}(\boldsymbol{u}_\alpha) - \boldsymbol{\tau}] + \alpha\Big(\boldsymbol{\sigma}_\alpha + \tfrac{1}{\alpha}\mathbb{C}[\boldsymbol{\delta}] - P_K\big(\boldsymbol{\sigma}_\alpha + \tfrac{1}{\alpha}\mathbb{C}[\boldsymbol{\delta}]\big)\Big) = 0\,.$$

Rearranging and adding $\tfrac{1}{\alpha}\mathbb{C}[\boldsymbol{\delta}]$ on both sides gives

$$\boldsymbol{\sigma}_\alpha + \tfrac{1}{\alpha}\mathbb{C}[\boldsymbol{\delta}] = \mathbb{C}\big[\boldsymbol{\varepsilon}(\boldsymbol{u}_\alpha) - \boldsymbol{\tau} + \tfrac{1}{\alpha}\boldsymbol{\delta}\big] - \alpha\Big(\boldsymbol{\sigma}_\alpha + \tfrac{1}{\alpha}\mathbb{C}[\boldsymbol{\delta}] - P_K\big(\boldsymbol{\sigma}_\alpha + \tfrac{1}{\alpha}\mathbb{C}[\boldsymbol{\delta}]\big)\Big) = 0\,.$$

With $\boldsymbol{\theta} = \boldsymbol{\sigma}_\alpha + \tfrac{1}{\alpha}\mathbb{C}[\boldsymbol{\delta}]$, this can be rewritten as $\boldsymbol{\theta} = \mathbb{C}\big[\boldsymbol{\varepsilon}(\boldsymbol{u}_\alpha) - \boldsymbol{\tau} + \tfrac{1}{\alpha}\boldsymbol{\delta}\big] - \alpha\big(\boldsymbol{\theta} - P_K(\boldsymbol{\theta})\big)$ and by Lemma 3.2, we find

$$P_K\big(\boldsymbol{\sigma}_\alpha + \tfrac{1}{\alpha}\mathbb{C}[\boldsymbol{\delta}]\big) = P_K(\boldsymbol{\theta}) = P_K\big(\mathbb{C}\big[\boldsymbol{\varepsilon}(\boldsymbol{u}_\alpha) - \boldsymbol{\tau} + \tfrac{1}{\alpha}\boldsymbol{\delta}\big]\big)$$

Substitution of this expression yields

$$(1+\alpha)\big(\boldsymbol{\sigma}_\alpha + \tfrac{1}{\alpha}\mathbb{C}[\boldsymbol{\delta}]\big) = \mathbb{C}\big[\boldsymbol{\varepsilon}(\boldsymbol{u}_\alpha) - \boldsymbol{\tau} + \tfrac{1}{\alpha}\boldsymbol{\delta}\big] + \alpha\, P_K\big(\mathbb{C}\big[\boldsymbol{\varepsilon}(\boldsymbol{u}_\alpha) - \boldsymbol{\tau} + \tfrac{1}{\alpha}\boldsymbol{\delta}\big]\big)$$

and dividing by $(1 + \alpha)$ and subtracting $\tfrac{1}{\alpha}\mathbb{C}[\boldsymbol{\delta}]$ implies the claimed representation of the stress response. $\qquad\square$

For $\boldsymbol{\delta} = 0$, the stress response of the viscoplastic regularization (3.2) is recovered.

Using Lemma 10.9 in the optimality conditions, it follows that $\boldsymbol{u}_\alpha \in \boldsymbol{X}(\boldsymbol{u}_D)$ is optimal w.r.t. the primal problem if $F_\alpha(\boldsymbol{u}_\alpha) = 0$ with $F_\alpha : \boldsymbol{X} \to \boldsymbol{X}^*$ defined as

$$\langle F_\alpha(\boldsymbol{u}_\alpha), \boldsymbol{w}\rangle_{\boldsymbol{X}^* \times \boldsymbol{X}} = \tfrac{1}{1+\alpha}\int_\Omega \mathbb{C}\big[\boldsymbol{\varepsilon}(\boldsymbol{u}_\alpha(x)) - \boldsymbol{\tau}(x) - \boldsymbol{\delta}(x)\big] : \boldsymbol{\varepsilon}(\boldsymbol{w}(x))\, dx$$

$$+ \tfrac{\alpha}{1+\alpha}\int_\Omega P_K\big(\mathbb{C}\big[\boldsymbol{\varepsilon}(\boldsymbol{u}_\alpha(x)) - \boldsymbol{\tau}(x) + \tfrac{1}{\alpha}\boldsymbol{\delta}(x)\big]\big) : \boldsymbol{\varepsilon}(\boldsymbol{w}(x))\, dx - \ell(\boldsymbol{w})\,. \tag{10.13}$$

Reconsidering Theorem 3.3, we observe that F_α is strongly monotone with modulus $\tfrac{1}{1+\alpha}$, i.e.

$$\langle F_\alpha(\boldsymbol{u}) - F_\alpha(\boldsymbol{w}), \boldsymbol{u} - \boldsymbol{w}\rangle_{\boldsymbol{X}^* \times \boldsymbol{X}} \geq \tfrac{1}{1+\alpha}\|\boldsymbol{u} - \boldsymbol{w}\|^2\,,$$

and F is the derivative of the uniformly convex primal functional

$$\mathcal{E}_\alpha(\boldsymbol{u}) = \tfrac{1}{1+\alpha}\tfrac{1}{2}\big\|A^{-1}\big(B^*\boldsymbol{u} + \boldsymbol{\tau} + \boldsymbol{\delta}\big)\big\|_\Sigma^2 + \tfrac{\alpha}{1+\alpha}\Upsilon\big(-A^{-1}(B^*\boldsymbol{u} + \boldsymbol{\tau} - \tfrac{1}{\alpha}\boldsymbol{\delta})\big) - \ell(\boldsymbol{u}_\alpha)\,,$$

with Υ being the potential of the projection (2.35).

Algorithm 10.1 A penalty method for the approximation of perfect plasticity.

S0) Given $\boldsymbol{\tau} \in \boldsymbol{P}^*$, choose $\boldsymbol{\delta} \in \boldsymbol{P}^*$, $\alpha_1 > 0$ and $\boldsymbol{u}_{\alpha_0} \in \boldsymbol{X}(\boldsymbol{u}_D)$. Set $k := 1$.

S1) Solve the regularized primal problem $F_{\alpha_k}(\boldsymbol{u}_{\alpha_k}) = 0$ with F_α given in (10.13) with one of the methods of the previous chapters and initial guess $\boldsymbol{u}_{\alpha_{k-1}}$.

S2) Use $\boldsymbol{u}_{\alpha_k}$ to compute $\boldsymbol{\sigma}_{\alpha_k}$ according to Lemma 10.9.

S3) Set $k := k + 1$ and choose $\alpha_k > \alpha_{k-1}$. Go to S1).

3.2. A Simple Penalty Method. We present a simple penalty method for the approximation of the stress field of perfect plasticity relying on the approximation result of the previous section, i.e. we approximate the minimizer $\overline{\boldsymbol{\sigma}}$ of problem (10.7) by a sequence $\{\boldsymbol{\sigma}_{\alpha_k}\} \subset \boldsymbol{S}$, each $\boldsymbol{\sigma}_{\alpha_k}$ being the solution of the regularized problem (10.8) with parameter α_k.

We remark that the algorithm is not amenable to implementation in the presented form and only serves as a basis for theoretical considerations. The idea of the penalty method is to compute a good initial guess for the next iteration in which a higher value of the penalty parameter is used. We remark that formally, the speed of convergence of the penalty method is directly related to the growth properties of the sequence of penalty parameters $\{\alpha_k\}_k$.

The approach via a penalty method is in the spirit of the exterior path following algorithms presented in [**HK06b**, **HK06a**], and especially [**HK06a**] considers low multiplier regularity in the context of optimal control problems. In those works, multiplier updates are avoided if no stable a priori bounds are available for the multipliers. This reflects the situation of perfect plasticity where only the parameter dependent estimates of the previous section are at hand concerning the displacement field and the plastic strain. Thus, this approach requires the limit $\alpha \to \infty$.

Path following methods are not new in the field of elastoplasticity, cf. [**KLSW06**], where an interior path following algorithm (interior point method) was proposed.

4. The Augmented Lagrangian Method

In the previous section, we gave an approximation result for the stress field in perfect plasticity. However, this requires $\alpha \to \infty$ and the regularized problems (10.8) become progressively harder to solve as α increases. Nevertheless, Algorithm 10.1 does not rely on more regularity than guaranteed by the problem.

In this section, we will introduce a linearly convergent method for fixed $\alpha > 0$ under additional regularity assumptions on the solution of the perfect plasticity problem, namely that the plastic strain is contained in L^2 rather than merely in the measure space $M_{\mathrm{Sym}}(\Omega)$. However, this extra regularity cannot be assured as we have shown in the parameter depended estimates of Section 10.2. On the other hand, hardening plasticity does indeed guarantee the required regularity, so that the method should be stable for that problem. Though, for the outline of the algorithm, perfect plasticity is better suited since the model is simpler than hardening plasticity.

The key issue for convergence while holding α fixed will be to change $\boldsymbol{\delta}$ in every iteration and we will replace $\boldsymbol{\delta}$ by $\boldsymbol{\epsilon}_{\alpha_{k-1}}$ in each step of the algorithm. But before we state the algorithm, we study some of its characteristics.

4.1. Optimality Systems. The following result summarizes [**IK08**, Theorem 4.43, Theorem 4.46] and can also be found in [**IK00**].

Proposition 10.10. *Let $\boldsymbol{\sigma}_\alpha$ be the minimizer of the regularized problem (10.8) and let $\boldsymbol{\epsilon}_\alpha$ be defined via (10.5).*

(1) *Suppose that $\boldsymbol{\sigma}_\alpha$ converges strongly to $\overline{\boldsymbol{\sigma}}$ in $\boldsymbol{P}$ as $\alpha \to \infty$ and that $\{\boldsymbol{\epsilon}_\alpha\}$ has a weak cluster point in $\boldsymbol{P}^*$. Then, for each cluster point $\overline{\boldsymbol{\epsilon}} \in \boldsymbol{P}^*$*

$$\overline{\boldsymbol{\epsilon}} \in \partial \chi_{\boldsymbol{K}}(\overline{\boldsymbol{\sigma}}) \qquad and \tag{10.14a}$$

$$\langle DJ(\overline{\boldsymbol{\sigma}}), \boldsymbol{\eta} - \overline{\boldsymbol{\sigma}} \rangle_{\boldsymbol{P}^* \times \boldsymbol{P}} + \langle \overline{\boldsymbol{\epsilon}}, \boldsymbol{\eta} - \overline{\boldsymbol{\sigma}} \rangle_{\boldsymbol{P}^* \times \boldsymbol{P}} \geq 0 \qquad for\ all\ \boldsymbol{\eta} \in \boldsymbol{S}. \tag{10.14b}$$

(2) *Let $\boldsymbol{\delta} \in \boldsymbol{P}^*$ be fixed. Then, the sequence $\boldsymbol{\epsilon}_\alpha = D_{\boldsymbol{\sigma}} \pi_{\boldsymbol{K}}^\alpha(\boldsymbol{\sigma}_\alpha, \boldsymbol{\delta})$ is uniformly bounded for all $\alpha \geq 1$ if there exists $\overline{\boldsymbol{\epsilon}} \in \partial \chi_{\boldsymbol{K}}(\overline{\boldsymbol{\sigma}})$ such that (10.14) holds and in this case, $\boldsymbol{\epsilon}_\alpha$ converges weakly to $\overline{\boldsymbol{\epsilon}}$.*

We already found that $\boldsymbol{\sigma}_\alpha$ converges strongly to $\overline{\boldsymbol{\sigma}}$ and then the first part of this theorem shows that if $\{\boldsymbol{\epsilon}_\alpha\}$ as defined in (10.5) has a weak cluster point $\overline{\boldsymbol{\epsilon}}$, then $\overline{\boldsymbol{\sigma}}$ solves the perfect plasticity problem and the plastic strain (increment) $\overline{\boldsymbol{\epsilon}}$ is indeed contained in L^2. Reconsidering the a priori estimates, this also shows that the displacement field is in $\boldsymbol{X}(\boldsymbol{u}_D)$. However, the existence of a weak cluster point cannot be guaranteed, cf. the numerical example in Section 11.1. The second statement shows that if the plastic strain (increment) has the extra regularity $\overline{\boldsymbol{\epsilon}} \in \boldsymbol{P}^*$, then the whole sequence $\{\boldsymbol{\epsilon}_\alpha\}$ is bounded and converges weakly to the solution.

This result shows that we have to impose regularity assumptions if we want to consider algorithms incorporating the plastic strain (increment) $\boldsymbol{\epsilon}$ in every iteration.

Assumption 10.11. *Henceforth, let the solution of the perfect plasticity problem have the extra regularity*

$$(\overline{\boldsymbol{\sigma}}, \overline{\boldsymbol{\epsilon}}) \in \boldsymbol{P} \times \boldsymbol{P}^*.$$

In particular, $(\overline{\boldsymbol{\sigma}}, \overline{\boldsymbol{\epsilon}})$ satisfies (10.14).

At this point, we finally introduce the Augmented Lagrangian

$$L_\alpha(\boldsymbol{\sigma}, \boldsymbol{\epsilon}) = J(\boldsymbol{\sigma}) + \pi_{\boldsymbol{K}}^\alpha(\boldsymbol{\sigma}, \boldsymbol{\epsilon}). \tag{10.15}$$

and the following proposition is patterned after [**IK08**, Theorem 4.45].

Proposition 10.12. *Assume that $(\overline{\boldsymbol{\sigma}}, \overline{\boldsymbol{\epsilon}}) \in \boldsymbol{P} \times \boldsymbol{P}^*$ satisfies (10.14) and let $\alpha > 0$. Then, $\overline{\boldsymbol{\epsilon}} \in \partial \chi_{\boldsymbol{K}}(\overline{\boldsymbol{\sigma}})$ can be expressed as*

$$\overline{\boldsymbol{\epsilon}} = D_{\boldsymbol{\sigma}} \pi_{\boldsymbol{K}}^\alpha(\overline{\boldsymbol{\sigma}}, \overline{\boldsymbol{\epsilon}}), \tag{10.16}$$

with $\overline{\boldsymbol{\sigma}}$ being the unique solution of:

$$Minimize \quad J(\boldsymbol{\sigma}) + \pi_{\boldsymbol{K}}^\alpha(\boldsymbol{\sigma}, \overline{\boldsymbol{\epsilon}}) = L_\alpha(\boldsymbol{\sigma}, \overline{\boldsymbol{\epsilon}}) \qquad subject\ to \quad \boldsymbol{\sigma} \in \boldsymbol{S}.$$

Based on this proposition, it is also possible to restate the optimality system (10.14) as

$$\langle DJ(\overline{\boldsymbol{\sigma}}), \boldsymbol{\eta} - \overline{\boldsymbol{\sigma}} \rangle_{\boldsymbol{P}^* \times \boldsymbol{P}} + \langle \overline{\boldsymbol{\epsilon}}, \boldsymbol{\eta} - \overline{\boldsymbol{\sigma}} \rangle_{\boldsymbol{P}^* \times \boldsymbol{P}} \geq 0 \qquad for\ all\ \boldsymbol{\eta} \in \boldsymbol{S}, \tag{10.17a}$$

$$\overline{\boldsymbol{\epsilon}} - D_{\boldsymbol{\sigma}} \pi_{\boldsymbol{K}}^\alpha(\overline{\boldsymbol{\sigma}}, \overline{\boldsymbol{\epsilon}}) = 0. \tag{10.17b}$$

However, the first condition cannot be evaluated directly which is why we use (10.11) to replace the first condition by

$$\langle DJ(\overline{\boldsymbol{\sigma}}) + \overline{\boldsymbol{\epsilon}} + B^* \overline{\boldsymbol{u}}, \boldsymbol{\eta} \rangle_{\boldsymbol{P}^* \times \boldsymbol{P}} = 0, \qquad \boldsymbol{\eta} \in \boldsymbol{P}, \tag{10.18a}$$

$$\langle B \overline{\boldsymbol{\sigma}}, \boldsymbol{w} \rangle_{\boldsymbol{X}^* \times \boldsymbol{X}} + \ell(\boldsymbol{w}) = 0, \qquad \boldsymbol{w} \in \boldsymbol{X}, \tag{10.18b}$$

taking into account the displacement field. It is then easy to see that the conditions (10.17b) and (10.18) are equivalent to the requirement that $(\overline{\boldsymbol{\sigma}}, \overline{\boldsymbol{u}}, \overline{\boldsymbol{\epsilon}}) \in \boldsymbol{P} \times \boldsymbol{X}(\boldsymbol{u}_D) \times \boldsymbol{P}^*$ is a saddle point of the full Augmented Lagrangian

$$\overline{L}_\alpha(\boldsymbol{\sigma}, \boldsymbol{u}, \boldsymbol{\epsilon}) = J(\boldsymbol{\sigma}) + \pi_K^\alpha(\boldsymbol{\sigma}, \boldsymbol{\epsilon}) + b(\boldsymbol{\sigma}, \boldsymbol{u}) + \ell(\boldsymbol{u}). \tag{10.19}$$

4.2. The Algorithm and its Convergence. We now present the first order Augmented Lagrangian method. After stating the algorithm we will show convergence provided Assumption 10.11 holds.

4.2.1. *The Augmented Lagrangian Method.* The blueprint algorithm of the Augmented Lagrangian method is Algorithm 10.2. The regularized problem in step S1) can once more be solved via its primal representation (10.13) with the methods of the previous chapters, and particularly, the methods of Section 8.3 can be applied. The multiplier update in S2) is motivated by (10.16) and corresponds to a fixed point iteration for the optimality condition (10.17b). Step S3) and S4) consist of the evaluation of the stopping criteria. In step S3) it is not necessary to check (10.18b) again, since it is not depending on the multiplier update in S2) and as a consequence, it is already fulfilled due to S1). In practical applications however, the minimization problem in S1) may not necessarily be solved exactly and checking of the equilibrium equation may be necessary in S3).

4.2.2. *Convergence of the Algorithm.* Before we state the convergence of the Augmented Lagrangian method, we give an alternative interpretation of the multiplier update in S2). For this purpose, we define the value function

$$V_\alpha : \boldsymbol{P}^* \to \mathbb{R}, \qquad\qquad V_\alpha(\boldsymbol{\epsilon}) = \inf_{\boldsymbol{\sigma} \in \boldsymbol{S}} L(\boldsymbol{\sigma}, \boldsymbol{\epsilon}), \tag{10.20}$$

and for given $\boldsymbol{\epsilon} \in \boldsymbol{P}^*$, the solution of the regularized problem (10.8) depending on $\boldsymbol{\epsilon}$ will be denoted by $\boldsymbol{\sigma}_\alpha(\boldsymbol{\epsilon}) \in \boldsymbol{P}$. Then, the condition $\overline{\boldsymbol{\epsilon}} \in \partial \chi_K(\overline{\boldsymbol{\sigma}})$, with $\overline{\boldsymbol{\sigma}}$ being the solution of the perfect plasticity problem, can be rewritten as

$$\overline{\boldsymbol{\epsilon}} = D_{\boldsymbol{\sigma}} \pi_K^\alpha (\boldsymbol{\sigma}_\alpha(\overline{\boldsymbol{\epsilon}}), \overline{\boldsymbol{\epsilon}}).$$

We already mentioned that the multiplier update in step S2) of the above algorithm can be interpreted as a fixed point iteration. We give an additional interpretation as a gradient method for the problem of maximizing the value function V_α. Therefore note that V_α is uniformly concave since $\boldsymbol{\epsilon} \mapsto J(\boldsymbol{\sigma}) + \pi_K^\alpha(\boldsymbol{\sigma}, \boldsymbol{\epsilon})$ is uniformly concave for all $\boldsymbol{\sigma} \in \boldsymbol{S}$ and

---

Algorithm 10.2 The Augmented Lagrangian method for the approximation of perfect plasticity.

S0) Given $\boldsymbol{\tau} \in \boldsymbol{P}^*$, choose $\alpha > 0$, $\boldsymbol{\epsilon}_\alpha^0 \in \boldsymbol{P}^*$ and $\epsilon > 0$. Set $k := 1$.

S1) Determine $(\boldsymbol{\sigma}_\alpha^k, \boldsymbol{u}_\alpha^k) \in \boldsymbol{P} \times \boldsymbol{X}(\boldsymbol{u}_D)$ by solving (10.8) via its primal representation (10.13).

S2) Update $\boldsymbol{\epsilon}_\alpha^k = D_{\boldsymbol{\sigma}} \pi_K^\alpha(\boldsymbol{\sigma}_\alpha^k, \boldsymbol{\epsilon}_\alpha^{k-1})$.

S3) Compute the residuals

$$r_{\boldsymbol{\sigma}}^k(\boldsymbol{\eta}) = \langle DJ(\boldsymbol{\sigma}_\alpha^k) + \boldsymbol{\epsilon}_\alpha^k + B^* \boldsymbol{u}_\alpha^k, \boldsymbol{\eta} \rangle_{\boldsymbol{P}^* \times \boldsymbol{P}}, \qquad \boldsymbol{\eta} \in \boldsymbol{P},$$
$$r_{\boldsymbol{\epsilon}}^k(\boldsymbol{\eta}) = \langle \boldsymbol{\epsilon}_\alpha^k - D_{\boldsymbol{\sigma}} \pi_K^\alpha(\boldsymbol{\sigma}_\alpha^k, \boldsymbol{\epsilon}_\alpha^k), \boldsymbol{\eta} \rangle_{\boldsymbol{P}^* \times \boldsymbol{P}}, \qquad \boldsymbol{\eta} \in \boldsymbol{P}.$$

S4) If $\|A^{-1} r_{\boldsymbol{\sigma}}^k\|_{\boldsymbol{\Sigma}} + \|A^{-1} r_{\boldsymbol{\epsilon}}^k\|_{\boldsymbol{\Sigma}} < \epsilon$, stop. Otherwise, set $k := k + 1$ and go to S1).

taking the infimum over all $\boldsymbol{\sigma} \in \boldsymbol{S}$ then results in a uniformly concave function. Moreover, following [**IK08**, Lemma 4.47], we know the following about the value function V_α.

Proposition 10.13. *The value function* (10.20) *is Lipschitz continuous with the Lipschitz constant being independent of α and the value function is Fréchet differentiable with derivative*

$$DV_\alpha(\boldsymbol{\epsilon}) = \boldsymbol{\sigma}_\alpha(\boldsymbol{\epsilon}) - P_{\boldsymbol{K}}\big(\boldsymbol{\sigma}_\alpha(\boldsymbol{\epsilon}) + \tfrac{1}{\alpha}A^{-1}\boldsymbol{\epsilon}\big)\,,$$

with $\boldsymbol{\sigma}_\alpha(\boldsymbol{\epsilon})$ being the solution of the regularized problem (10.8) *depending on $\boldsymbol{\epsilon}$.*

In view of this result, we reconsider the update formula in S2).

$$\begin{aligned}
\boldsymbol{\epsilon}_\alpha^k &= D_{\boldsymbol{\sigma}}\pi_{\boldsymbol{K}}^\alpha(\boldsymbol{\sigma}_\alpha^k, \boldsymbol{\epsilon}_\alpha^{k-1}) = \alpha A\Big(\boldsymbol{\sigma}_\alpha^k + \tfrac{1}{\alpha}A^{-1}\boldsymbol{\epsilon}_\alpha^{k-1} - P_{\boldsymbol{K}}\big(\boldsymbol{\sigma}_\alpha^k + \tfrac{1}{\alpha}A^{-1}\boldsymbol{\epsilon}_\alpha^{k-1}\big)\Big) \\
&= \boldsymbol{\epsilon}_\alpha^{k-1} + \alpha A\Big(\boldsymbol{\sigma}_\alpha^k - P_{\boldsymbol{K}}\big(\boldsymbol{\sigma}_\alpha^k + \tfrac{1}{\alpha}A^{-1}\boldsymbol{\epsilon}_\alpha^{k-1}\big)\Big) \\
&= \boldsymbol{\epsilon}_\alpha^{k-1} + \alpha A\, DV_\alpha(\boldsymbol{\epsilon}_\alpha^{k-1})\,.
\end{aligned}$$

Here $A : \boldsymbol{P} \to \boldsymbol{P}^*$ once more serves as the Riesz operator between the stress space $\boldsymbol{P}$ and the strain space $\boldsymbol{P}^*$. The update in this form is also consistent with the update formulas given in [**Ber82**, Chapter 3] for the finite dimensional case. The interpretation of the update as a gradient algorithm for the value function V_α, just as the interpretation as a fixed point iteration for the optimality condition suggests that the method is linearly convergent. This is indeed shown by the next theorem, which is patterned after [**IK00**].

Theorem 10.14. *Let $\alpha > 0$ be fixed and assume that $\overline{\boldsymbol{\epsilon}} \in \boldsymbol{P}^*$ exists such that $\overline{\boldsymbol{\epsilon}} \in \partial\chi_{\boldsymbol{K}}(\overline{\boldsymbol{\sigma}})$ and $(\overline{\boldsymbol{\sigma}}, \overline{\boldsymbol{\epsilon}}) \in \boldsymbol{P} \times \boldsymbol{P}^*$ fulfill the optimality condition* (10.14) *(or equivalently* (10.17)*). Then, the sequence $(\boldsymbol{\sigma}_\alpha^k, \boldsymbol{\epsilon}_\alpha^k)$ is bounded in $\boldsymbol{P} \times \boldsymbol{P}^*$ and satisfies*

$$\|\boldsymbol{\sigma}_\alpha^k - \overline{\boldsymbol{\sigma}}\|_{\boldsymbol{\Sigma}}^2 + \tfrac{1}{2\alpha}\|A^{-1}(\boldsymbol{\epsilon}_\alpha^k - \overline{\boldsymbol{\epsilon}})\|_{\boldsymbol{\Sigma}}^2 \le \tfrac{1}{2\alpha}\|A^{-1}(\boldsymbol{\epsilon}_\alpha^{k-1} - \overline{\boldsymbol{\epsilon}})\|_{\boldsymbol{\Sigma}}^2\,,$$

and

$$\sum_{k=1}^\infty \|\boldsymbol{\sigma}_\alpha^k - \overline{\boldsymbol{\sigma}}\|_{\boldsymbol{\Sigma}}^2 \le \tfrac{1}{2\alpha}\|A^{-1}(\boldsymbol{\epsilon}_\alpha^0 - \overline{\boldsymbol{\epsilon}})\|_{\boldsymbol{\Sigma}}^2\,.$$

PROOF. Using (10.3) as given in Remark 10.2, we find

$$\begin{aligned}
\boldsymbol{\epsilon}_\alpha^k &= D_{\boldsymbol{\sigma}}\pi_{\boldsymbol{K}}^\alpha\big(\boldsymbol{\sigma}_\alpha^k, \boldsymbol{\epsilon}_\alpha^{k-1}\big) = D\chi_{\boldsymbol{K}}^\alpha\big(\boldsymbol{\sigma}_\alpha^k + \tfrac{1}{\alpha}A^{-1}\boldsymbol{\epsilon}_\alpha^{k-1}\big)\,, \\
\overline{\boldsymbol{\epsilon}} &= D_{\boldsymbol{\sigma}}\pi_{\boldsymbol{K}}^\alpha\big(\overline{\boldsymbol{\sigma}}, \overline{\boldsymbol{\epsilon}}\big) = D\chi_{\boldsymbol{K}}^\alpha\big(\overline{\boldsymbol{\sigma}} + \tfrac{1}{\alpha}A^{-1}\overline{\boldsymbol{\epsilon}}\big)\,,
\end{aligned}$$

with the standard Moreau-Yosida approximation $\chi_{\boldsymbol{K}}^\alpha$ as defined in Section 3.1. By Lemma 3.1, we find that

$$\begin{aligned}
&\langle \boldsymbol{\epsilon}_\alpha^k - \overline{\boldsymbol{\epsilon}}, \boldsymbol{\sigma}_\alpha^k + \tfrac{1}{\alpha}A^{-1}\boldsymbol{\epsilon}_\alpha^{k-1} - (\overline{\boldsymbol{\sigma}} + \tfrac{1}{\alpha}A^{-1}\overline{\boldsymbol{\epsilon}})\rangle_{\boldsymbol{P}^* \times \boldsymbol{P}} \\
&= \Big\langle D\chi_{\boldsymbol{K}}^\alpha\big(\boldsymbol{\sigma}_\alpha^k + \tfrac{1}{\alpha}A^{-1}\boldsymbol{\epsilon}_\alpha^{k-1}\big) - D\chi_{\boldsymbol{K}}^\alpha\big(\overline{\boldsymbol{\sigma}} + \tfrac{1}{\alpha}A^{-1}\overline{\boldsymbol{\epsilon}}\big), \\
&\qquad \boldsymbol{\sigma}_\alpha^k + \tfrac{1}{\alpha}A^{-1}\boldsymbol{\epsilon}_\alpha^{k-1} - \big(\overline{\boldsymbol{\sigma}} + \tfrac{1}{\alpha}A^{-1}\overline{\boldsymbol{\epsilon}}\big)\Big\rangle_{\boldsymbol{P}^* \times \boldsymbol{P}} \\
&\ge \big\|A^{-1}\big(D\chi_{\boldsymbol{K}}^\alpha\big(\boldsymbol{\sigma}_\alpha^k + \tfrac{1}{\alpha}A^{-1}\boldsymbol{\epsilon}_\alpha^{k-1}\big) - D\chi_{\boldsymbol{K}}^\alpha\big(\overline{\boldsymbol{\sigma}} + \tfrac{1}{\alpha}A^{-1}\overline{\boldsymbol{\epsilon}}\big)\big)\big\|_{\boldsymbol{\Sigma}}^2 = \tfrac{1}{\alpha}\|A^{-1}(\boldsymbol{\epsilon}_\alpha^k - \overline{\boldsymbol{\epsilon}})\|_{\boldsymbol{\Sigma}}^2\,.
\end{aligned}$$

Thus,

$$\begin{aligned}
\langle \boldsymbol{\epsilon}_\alpha^k - \overline{\boldsymbol{\epsilon}}, \boldsymbol{\sigma}_\alpha^k - \overline{\boldsymbol{\sigma}}\rangle_{P^* \times P} &= \langle \boldsymbol{\epsilon}_\alpha^k - \overline{\boldsymbol{\epsilon}}, \boldsymbol{\sigma}_\alpha^k + \tfrac{1}{\alpha}A^{-1}\boldsymbol{\epsilon}_\alpha^{k-1} - (\overline{\boldsymbol{\sigma}} + \tfrac{1}{\alpha}A^{-1}\overline{\boldsymbol{\epsilon}})\rangle_{P^* \times P} \\
&\quad - \tfrac{1}{\alpha}\langle \boldsymbol{\epsilon}_\alpha^k - \overline{\boldsymbol{\epsilon}}, A^{-1}(\boldsymbol{\epsilon}_\alpha^{k-1} - \overline{\boldsymbol{\epsilon}})\rangle_{P^* \times P} \\
&\geq \tfrac{1}{\alpha}\|A^{-1}(\boldsymbol{\epsilon}_\alpha^k - \overline{\boldsymbol{\epsilon}})\|_{\Sigma}^2 - \tfrac{1}{2\alpha}\Big(\|A^{-1}(\boldsymbol{\epsilon}_\alpha^k - \overline{\boldsymbol{\epsilon}})\|_{\Sigma}^2 + \|A^{-1}(\boldsymbol{\epsilon}_\alpha^{k-1} - \overline{\boldsymbol{\epsilon}})\|_{\Sigma}^2\Big) \\
&= \tfrac{1}{2\alpha}\|A^{-1}(\boldsymbol{\epsilon}_\alpha^k - \overline{\boldsymbol{\epsilon}})\|_{\Sigma}^2 - \tfrac{1}{2\alpha}\|A^{-1}(\boldsymbol{\epsilon}_\alpha^{k-1} - \overline{\boldsymbol{\epsilon}})\|_{\Sigma}^2 \,.
\end{aligned}$$

Next, we reconsider the optimality conditions

$$\begin{aligned}
\langle DJ(\boldsymbol{\sigma}_\alpha^k) + \boldsymbol{\epsilon}_\alpha^k, \boldsymbol{\eta} - \boldsymbol{\sigma}_\alpha^k\rangle_{P^* \times P} &\geq 0\,, \qquad \boldsymbol{\eta} \in S\,, \\
\langle DJ(\overline{\boldsymbol{\sigma}}) + \overline{\boldsymbol{\epsilon}}, \boldsymbol{\eta} - \overline{\boldsymbol{\sigma}}\rangle_{P^* \times P} &\geq 0\,, \qquad \boldsymbol{\eta} \in S\,,
\end{aligned}$$

for the regularized problem (10.8) and the perfect plasticity problem (10.8). Since both $\boldsymbol{\sigma}_\alpha^k, \overline{\boldsymbol{\sigma}} \in S$, testing with $\overline{\boldsymbol{\sigma}}$ and $\boldsymbol{\sigma}_\alpha^k$, respectively, and subsequent addition leads to

$$\langle DJ(\boldsymbol{\sigma}_\alpha^k) - DJ(\overline{\boldsymbol{\sigma}}), \boldsymbol{\sigma}_\alpha^k - \overline{\boldsymbol{\sigma}}\rangle_{P^* \times P} + \langle \boldsymbol{\epsilon}_\alpha^k - \overline{\boldsymbol{\epsilon}}, \boldsymbol{\sigma}_\alpha^k - \overline{\boldsymbol{\sigma}}\rangle_{P^* \times P} \leq 0\,.$$

Because $DJ(\boldsymbol{\sigma}_\alpha^k) - DJ(\overline{\boldsymbol{\sigma}}) = A(\boldsymbol{\sigma}_\alpha^k - \overline{\boldsymbol{\sigma}})$, the above estimate for the second term gives

$$\|\boldsymbol{\sigma}_\alpha^k - \overline{\boldsymbol{\sigma}}\|_{\Sigma}^2 + \tfrac{1}{2\alpha}\|A^{-1}(\boldsymbol{\epsilon}_\alpha^k - \overline{\boldsymbol{\epsilon}})\|_{\Sigma}^2 - \tfrac{1}{2\alpha}\|A^{-1}(\boldsymbol{\epsilon}_\alpha^{k-1} - \overline{\boldsymbol{\epsilon}})\|_{\Sigma}^2 \leq 0\,.$$

This gives the first assertion and summing up w.r.t. k, we obtain the second bound, which also shows the linear convergence of the method. □

This theorem shows linear convergence provided that the plastic strain possesses extra regularity. The above estimate also shows that convergence is faster if α is large. This suggests to combine the results of the previous and the current section, i.e. to perform the multiplier update and increase the penalty parameter if convergence is not fast enough. This extension can easily be incorporated and is presented in Algorithm 10.3. Moreover, we only require inexact solving of the subproblem.

Algorithm 10.3 The Augmented Lagrangian with penalty update and inexact solving.

S0) Given $\boldsymbol{\tau} \in P^*$, choose $\alpha_0 > 0$, $\boldsymbol{\epsilon}_\alpha^0 \in P^*$ and $\epsilon > 0$. Set $k := 1$.

S1) Determine $(\boldsymbol{\sigma}^k, \boldsymbol{u}^k) \in P \times X(\boldsymbol{u}_D)$ by approximately solving (10.8) with penalty parameter α_{k-1} via its primal representation (10.13).

S2) Update $\boldsymbol{\epsilon}^k = D_{\boldsymbol{\sigma}}\pi_K^{\alpha_{k-1}}(\boldsymbol{\sigma}^k, \boldsymbol{\epsilon}^{k-1})$.

S3) Compute the residuals

$$\begin{aligned}
r_{\boldsymbol{\sigma}}^k(\boldsymbol{\eta}) &= \langle DJ(\boldsymbol{\sigma}^k) + \boldsymbol{\epsilon}^k + B^*\boldsymbol{u}^k, \boldsymbol{\eta}\rangle_{P^* \times P}\,, \qquad \boldsymbol{\eta} \in P\,, \\
r_{\boldsymbol{\epsilon}}^k(\boldsymbol{\eta}) &= \langle \boldsymbol{\epsilon}^k - D_{\boldsymbol{\sigma}}\pi_K^{\alpha_{k-1}}(\boldsymbol{\sigma}^k, \boldsymbol{\epsilon}^k), \boldsymbol{\eta}\rangle_{P^* \times P}\,, \qquad \boldsymbol{\eta} \in P\,, \\
r_{\boldsymbol{u}}^k(\boldsymbol{w}) &= \langle B\boldsymbol{\sigma}^k + \ell, \boldsymbol{w}\rangle_{X^* \times X}\,, \qquad \boldsymbol{w} \in X\,.
\end{aligned}$$

S4) If $\|A^{-1}r_{\boldsymbol{\sigma}}^k\|_{\Sigma} + \|A^{-1}r_{\boldsymbol{\epsilon}}^k\|_{\Sigma} + \|\!|r_{\boldsymbol{u}}^k|\!\|_* < \epsilon$, stop.

S5) Determine $\alpha_k \geq \alpha_{k-1}$, set $k := k+1$ and go to S1).

---

5. Second Order Iterations

The multiplier update as presented in the previous section naturally leads to a linearly convergent algorithm. In this section, we will derive a potentially faster algorithm by directly considering a saddle point of the full Augmented Lagrangian $\overline{L}_\alpha$ as defined in (10.19). Based on this formulation, it will be possible to reobtain the radial return algorithm for perfect plasticity as presented in Chapters 7 and 8. However, also a different formulation is possible which is related to an active set method as presented in Chapter 9.

5.1. The Radial Return Algorithm. For perfect plasticity, the response function was just the projection onto the admissible set, i.e. $\boldsymbol{\sigma}(x) = P_K(\boldsymbol{\eta}(x))$ with the trial stress $\boldsymbol{\eta}(x) = \mathbb{C}\big[\boldsymbol{\varepsilon}(\boldsymbol{u}(x)) - \boldsymbol{\tau}(x)\big]$. We show that this relation can also be characterized by means of a saddle point of the full Augmented Lagrangian $\overline{L}_\alpha$.

Theorem 10.15. *Let* $(\overline{\boldsymbol{\sigma}}, \overline{\boldsymbol{u}}, \overline{\boldsymbol{\epsilon}}) \in \boldsymbol{P} \times \boldsymbol{X}(\boldsymbol{u}_D) \times \boldsymbol{P}^*$ *be a saddle point of the Augmented Lagrangian* $\overline{L}_\alpha(\boldsymbol{\sigma}, \boldsymbol{u}, \boldsymbol{\epsilon})$, *i.e.*

$$\overline{L}_\alpha(\overline{\boldsymbol{\sigma}}, \boldsymbol{u}, \boldsymbol{\epsilon}) \leq \overline{L}_\alpha(\overline{\boldsymbol{\sigma}}, \overline{\boldsymbol{u}}, \overline{\boldsymbol{\epsilon}}) \leq \overline{L}_\alpha(\boldsymbol{\sigma}, \overline{\boldsymbol{u}}, \overline{\boldsymbol{\epsilon}})\,, \tag{10.21}$$

for all $(\boldsymbol{\sigma}, \boldsymbol{u}, \boldsymbol{\epsilon}) \in \boldsymbol{P} \times \boldsymbol{X}(\boldsymbol{u}_D) \times \boldsymbol{P}^*$. *Then* $\overline{\boldsymbol{\sigma}}(x) = P_K\big(\mathbb{C}\big[\boldsymbol{\varepsilon}(\overline{\boldsymbol{u}}(x)) - \boldsymbol{\tau}(x)\big]\big)$ *holds a.e.*

PROOF. The conditions for a saddle point of $\overline{L}_\alpha$ can be recast as $D\overline{L}_\alpha(\overline{\boldsymbol{\sigma}}, \overline{\boldsymbol{u}}, \overline{\boldsymbol{\epsilon}}) = 0$. This is equivalent to

$$0 = A\big(\overline{\boldsymbol{\sigma}} + A^{-1}\boldsymbol{\tau}\big) + D_{\boldsymbol{\sigma}}\pi_K^\alpha(\overline{\boldsymbol{\sigma}}, \overline{\boldsymbol{\epsilon}}) + B^*\overline{\boldsymbol{u}}\,, \qquad\qquad \text{in } \boldsymbol{P}^*\,, \tag{10.22a}$$

$$0 = B\overline{\boldsymbol{\sigma}} + \ell\,, \qquad\qquad \text{in } \boldsymbol{X}^*\,, \tag{10.22b}$$

$$0 = D_{\boldsymbol{\epsilon}}\pi_K^\alpha(\overline{\boldsymbol{\sigma}}, \overline{\boldsymbol{\epsilon}})\,, \qquad\qquad \text{in } \boldsymbol{P}\,. \tag{10.22c}$$

which itself is equivalent to (10.17b) and (10.18) as we already found earlier. Using Lemma 10.1, we can rewrite the first and the last condition as

$$0 = A\overline{\boldsymbol{\sigma}} - A\big(-A^{-1}(B^*\overline{\boldsymbol{u}} + \boldsymbol{\tau})\big) + \alpha A\big(\overline{\boldsymbol{\sigma}} + \tfrac{1}{\alpha}A^{-1}\overline{\boldsymbol{\epsilon}} - P_K\big(\overline{\boldsymbol{\sigma}} + \tfrac{1}{\alpha}A^{-1}\overline{\boldsymbol{\epsilon}}\big)\big)\,, \quad \text{in } \boldsymbol{P}^*\,,$$

$$0 = \overline{\boldsymbol{\sigma}} - P_K\big(\overline{\boldsymbol{\sigma}} + \tfrac{1}{\alpha}A^{-1}\overline{\boldsymbol{\epsilon}}\big)\,, \qquad\qquad \text{in } \boldsymbol{P}\,.$$

The second equality already shows $\overline{\boldsymbol{\sigma}} \in \boldsymbol{K}$. Introducing $\boldsymbol{\eta} = -A^{-1}\big(B^*\overline{\boldsymbol{u}} + \boldsymbol{\tau}\big)$ which locally is the trial stress $\boldsymbol{\eta}(x) = \mathbb{C}\big[\boldsymbol{\varepsilon}(\boldsymbol{u}(x)) - \boldsymbol{\tau}(x)\big]$ and $\boldsymbol{\theta} = \overline{\boldsymbol{\sigma}} + \tfrac{1}{\alpha}A^{-1}\overline{\boldsymbol{\epsilon}}$, this is

$$0 = A(\overline{\boldsymbol{\sigma}} - \boldsymbol{\eta}) + \alpha A\big(\boldsymbol{\theta} - P_K(\boldsymbol{\theta})\big) = 0\,, \qquad \text{and} \qquad \overline{\boldsymbol{\sigma}} = P_K(\boldsymbol{\theta})\,.$$

Combining both equations results in

$$P_K(\boldsymbol{\theta}) - \boldsymbol{\eta} + \alpha\big(\boldsymbol{\theta} - P_K(\boldsymbol{\theta})\big) = 0\,,$$

and this gives $\boldsymbol{\eta} - P_K(\boldsymbol{\theta}) = \alpha\big(\boldsymbol{\theta} - P_K(\boldsymbol{\theta})\big)$. As $\alpha > 0$, we find that $P_K(\boldsymbol{\theta}) = P_K(\boldsymbol{\eta})$ since

$$a\big(\boldsymbol{\eta} - P_K(\boldsymbol{\theta}), \boldsymbol{\varsigma} - P_K(\boldsymbol{\theta})\big) = \alpha\, a\big(\boldsymbol{\theta} - P_K(\boldsymbol{\theta}), \boldsymbol{\varsigma} - P_K(\boldsymbol{\theta})\big) \leq 0\,, \qquad \text{for all } \boldsymbol{\varsigma} \in \boldsymbol{K}\,.$$

This follows from the characterization of the projection P_K, cf. (2.7) and also Lemma 3.2. Consequently, $\overline{\boldsymbol{\sigma}} = P_K(\boldsymbol{\eta})$ and this shows the theorem. □

Substituting $\overline{\boldsymbol{\sigma}} = P_K(\boldsymbol{\eta})$ into the equilibrium equation then results in the problem

$$\int_\Omega P_K\big(\mathbb{C}\big[\boldsymbol{\varepsilon}(\overline{\boldsymbol{u}}(x)) - \boldsymbol{\tau}(x)\big]\big) : \boldsymbol{\varepsilon}(\boldsymbol{w}(x))\,dx = \ell(\boldsymbol{w})\,, \qquad \boldsymbol{w} \in \boldsymbol{X}\,,$$

and this is just the optimality condition of the primal problem in perfect plasticity, see Section 2.3. This gives a new interpretation of the radial return as a nonlinear Schur complement reduction of the system $D\overline{L}_\alpha(\overline{\sigma}, \overline{u}, \overline{\epsilon}) = 0$. We also note that α does no longer occur in the present formulation and contrary to the first order iteration, the subproblems do not possess additional regularity. In a finite dimensional context, similar nonlinear Schur complement reductions have been considered in [GK09].

5.2. An Active Set Method. We recovered the radial return algorithm by a nonlinear Schur complement reduction of the saddle point conditions (10.22). But just as in the previous chapter, it is possible to consider the full system. Using the product space

$$\mathcal{Y} = \boldsymbol{P} \times \boldsymbol{X} \times \boldsymbol{P}^*\,,$$

and writing $\boldsymbol{y} = (\boldsymbol{\sigma}, \boldsymbol{u}, \boldsymbol{\epsilon})$, we define $\Psi : \mathcal{Y} \to \mathcal{Y}^*$ via $\Psi = D\overline{L}_\alpha$, i.e.

$$\Psi(\boldsymbol{y}) = \begin{bmatrix} A\boldsymbol{\sigma} - A(-A^{-1}(B^*\boldsymbol{u} + \boldsymbol{\tau})) + \alpha A(\boldsymbol{\sigma} + \frac{1}{\alpha}A^{-1}\boldsymbol{\epsilon} - P_{\boldsymbol{K}}(\boldsymbol{\sigma} + \frac{1}{\alpha}A^{-1}\boldsymbol{\epsilon})) \\ B\boldsymbol{\sigma} + \ell \\ \boldsymbol{\sigma} - P_{\boldsymbol{K}}(\boldsymbol{\sigma} + \frac{1}{\alpha}A^{-1}\boldsymbol{\epsilon}) \end{bmatrix},$$

and this results in the problem of finding $(\overline{\sigma}, \overline{u}, \overline{\epsilon})$ such that $\Psi(\overline{\sigma}, \overline{u}, \overline{\epsilon}) = 0$ characterizing a saddle point of the full Augmented Lagrangian. For this system a generalized Newton method can be applied as follows: suppose that $Q : \boldsymbol{P} \to L(\boldsymbol{P}, \boldsymbol{P})$ is an approximation to the derivative of $P_{\boldsymbol{K}}$. Then, defining $D : \mathcal{Y} \to L(\mathcal{Y}, \mathcal{Y}^*)$,

$$D(\boldsymbol{y}) = \begin{bmatrix} A + \alpha A(\mathrm{id} - Q(\boldsymbol{\sigma} + \frac{1}{\alpha}A^{-1}\boldsymbol{\epsilon})) & B^* & \mathrm{id} - Q(\boldsymbol{\sigma} + \frac{1}{\alpha}A^{-1}\boldsymbol{\epsilon}) \\ B & 0 & 0 \\ \mathrm{id} - Q(\boldsymbol{\sigma} + \frac{1}{\alpha}A^{-1}\boldsymbol{\epsilon}) & 0 & -\frac{1}{\alpha}Q(\boldsymbol{\sigma} + \frac{1}{\alpha}A^{-1}\boldsymbol{\epsilon})A^{-1} \end{bmatrix}$$

results in the generalized Newton method

$$\boldsymbol{y}^k = \boldsymbol{y}^{k-1} - D(\boldsymbol{y}^{k-1})^{-1}\Psi(\boldsymbol{y}^{k-1})\,.$$

In a function space setting, we cannot show the superlinear convergence of the above iteration since $P_{\boldsymbol{K}}$ is not slantly differentiable in general, also see Appendix A.1. A further difficulty is that there is no obvious choice for Q in an infinite dimensional setting. However, going to the discrete setting and assuming that P_K is semismooth, $Q(\cdot) \in \partial P_K(\cdot)$ guarantees the superlinear convergence of the method in the discrete setting. Adopting the ideas of the previous chapter, an active / inactive set can be described by

$$\mathcal{A}(\boldsymbol{\sigma}, \boldsymbol{\epsilon}) = \{x \in \Omega : \boldsymbol{\sigma}(x) + \frac{1}{\alpha}\mathbb{C}[\boldsymbol{\epsilon}(x)] \in K\}\,, \qquad \mathcal{I}(\boldsymbol{\sigma}, \boldsymbol{\epsilon}) = \Omega \setminus \mathcal{A}(\boldsymbol{\sigma}, \boldsymbol{\epsilon})\,.$$

On the inactive set, we then take $Q = \mathrm{id}$ and it remains to give a meaning to Q on the active set.

Part 3

Verification and Performance of Numerical Methods

A Brief Introduction

It is now the time to report on the numerical performance of the presented algorithms. For this purpose, the algorithms were implemented in the parallel finite element software suite M++ [**Wie04**, **Wie10**] supporting parallel multigrid. M++ can be seen as a sequel to the parallel finite element suite UG [**BBJ$^+$97**, **BBJ$^+$98**, **BJL$^+$99**, **BJL$^+$00**, **BJL$^+$01**] using object-oriented programming techniques.

Since we focus on the verification and performance of the nonlinear algorithms, we do not go too much into details concerning other important aspects of computational plasticity, e.g. spatial discretization, linear solvers and the time stepping but only give a brief overview at this point.

- Spatial discretization: throughout, we use (multi-) linear finite elements concerning the spatial discretization of the displacement field, whereas stresses and strains are approximated at quadrature points, cf. Chapter 6. Though it is known that higher order elements yield better approximations, cf. [**Mül09**], higher order element discretizations exhibit no qualitative difference w.r.t. the performance of the nonlinear algorithms on which we focus here.

- Linear solvers: since non-associated plasticity naturally leads to non-symmetric linear systems of equations, we use preconditioned GMRES and (stabilized) BiCG methods, cf. [**Saa03**, **vdV03**]. From time to time, we also use a direct parallel solver [**Mau**]. For the iterative solvers, we use a geometric multigrid method for preconditioning and as the occuring linear systems may be badly conditioned (or even singular), we employ multiple pre- and post-smoothing. Typically, we use a Gauß-Seidel method on each processor and the (parallel) smoother is then defined additively (with damping) via the contributions of the individual processors. For the coarse grid problem, we use a direct parallel solver. This solver is not optimal in the sense of parallel efficiency since it requires massive parallel communication but on the other side gives additional robustness if the linear system is badly conditioned as observed in [**Mül09**].

- Time stepping: as indicated in Section 5.4, we use the backward Euler method throughout. In most applications, we consider a fixed time step size. However, in some situations we resort to a simple adaptive time stepping scheme which relies on the numerical performance of the nonlinear solver at the previous time step.

CHAPTER 11

ASSOCIATED PLASTICITY

In this chapter, we exclusively consider associated von Mises plasticity for which in particular the algorithms for minimization problems apply, i.e. the gradient type algorithms of Section 8.3 and the Augmented Lagrangian methods of Chapter 10. We start with a stability study of von Mises perfect plasticity and then compare the different algorithms for a benchmark setting in perfect plasticity. The results will show that for associated plasticity, the standard radial return algorithm (which is the generalized Newton method of Chapter 7) can be improved considerably if the minimization structure of the problem is exploited. Afterwards, we consider a computationally challenging three-dimensional example.

1. Approximation of Perfect Plasticity – a Numerical Study

1.1. Problem Setting. We consider a benchmark example of a two-dimensional plate with a circular hole in a plane strain framework [**SR03**]. This means that the problem is embedded into 3d by forcing a zero displacement in the x_3-direction, i.e. $\boldsymbol{u}_3 \equiv 0$, and we require that all strain tensors $\boldsymbol{\varepsilon} \in \mathrm{Sym}(3)$ satisfy $\boldsymbol{\varepsilon}_{3i} = \boldsymbol{\varepsilon}_{i3} = 0$ for $i = 1, 2, 3$. However, the stress component $\boldsymbol{\sigma}_{33}$ is generally non-zero. We use the model of von Mises plasticity with isotropic elasticity, i.e. the yield function is $f(\boldsymbol{\eta}) = |\operatorname{dev}(\boldsymbol{\eta})| - K_0$, and the elasticity tensor is $\mathbb{C} = 2\mu\mathbb{P}_{\mathrm{dev}} + 3\kappa\mathbb{P}_{\mathrm{vol}}$. The used material constants are presented in Table 11.1.

The domain is $\Omega = (0, 10)^2 \setminus B_1(10, 0)$, where $B_1(10, 0)$ denotes the ball of radius 1 around the point $(10, 0)$. Thus, Ω models a quarter of a circular plate, and we impose symmetry conditions on the lower part and on the right, i.e. $\boldsymbol{u}_2(x) \equiv 0$ if $x_2 = 0$ and $\boldsymbol{u}_1(x) \equiv 0$ if $x_1 = 10$. On the upper boundary, we apply a traction force

$$\ell(t, \boldsymbol{v}) = 100\,t \int_0^{10} \boldsymbol{v}(x_1, 10)\,dx_1\,,$$

Shear modulus:	μ	67 670	MPa
Bulk modulus:	κ	176 500	MPa
Yield Stress:	K_0	400	MPa

TABLE 11.1. Parameters for the 2d study of von Mises plasticity.

Level	3	4	5	6	7	8
Degrees of Freedom	33 282	132 098	526 338	2 101 250	8 396 802	33 570 818
Cells	16 384	65 536	262 144	1 048 576	4 194 304	16 777 216
Quadrature Points	65 536	262 144	1 048 576	4 194 304	16 777 216	67 108 864

TABLE 11.2. Computational details for the 2d example of a circular plate with hole.

which linearly increases with t. This is also illustrated in Figure 11.1 where also the coarse mesh is shown consisting of 256 quadrilaterals.

Since we consider a perfectly plastic model and the traction force increases linearly in time, there are a times $t^* \geq \tilde{t} > 0$ such that $S(t) \cap K \neq \emptyset$ for all $t \leq t^*$ (i.e. a solution of the dual problem exists). Moreover, on $[0, \tilde{t})$, the safe load condition is assumed to be fulfilled, cf. Assumptions 2.1 and 5.1. As the problem is also rate-independent and the load depends linearly on t, time can be identified with the load. The load at t^* is the so called *limit load*. If $t > t^*$, there is no statically admissible stress field contained in K and the dual problem fails to have a solution. For the given material parameters, the (numerically determined) limit load approximately fulfills $t^* \in (5.05, 5.1]$.

1.2. Stability Study. The following study is motivated by the a priori estimates of Section 10.2 and henceforth, we adopt the notation of that chapter. We only consider a static scenario (or only one time step in an incremental setting), with the load evaluated at $\hat{t} = 5.05$ which is very close to the limit load t^*. Since, the problem is perfectly plastic, we cannot expect uniform bounds for all quantities. Additionally, we consider the approximation by means of the Moreau-Yosida regularization for various penalty parameters α. This corresponds to the generalized Moreau-Yosida approximation with $\delta = 0$. By a subscript α, we denote solutions of the regularized problem with penalty parameter α whereas the perfectly plastic approximations are overlined. For the numerical study, we consider several quantities (as indicated in Table 11.3) on different levels of

(a) Loading and boundary conditions   (b) Coarse grid
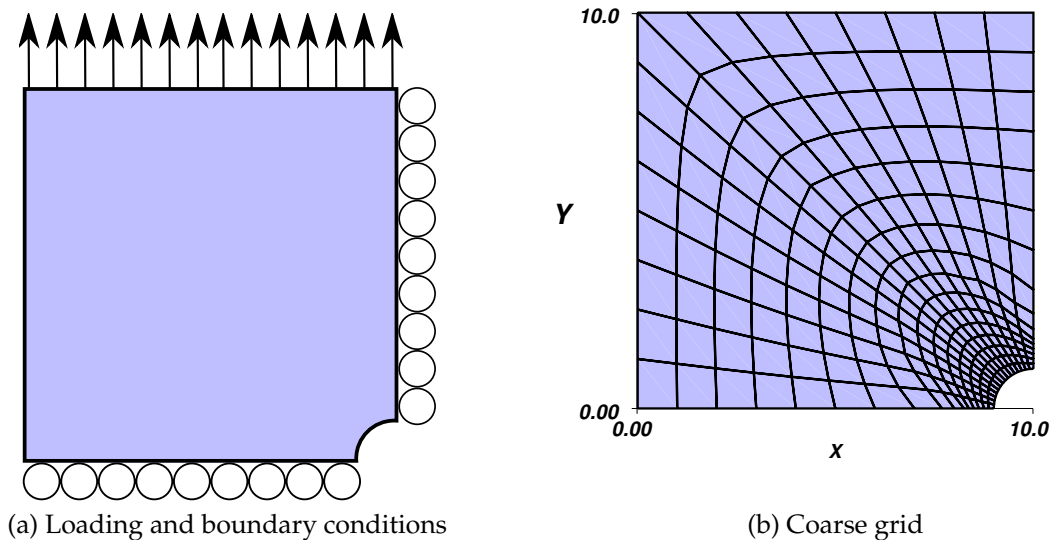
FIGURE 11.1. Problem setting for the circular plate with hole.

Quantity	Bounded
$\|A^{-1}\overline{\epsilon}\|_{\Sigma}$	no
$\|\overline{u}\|$	no
$\|\overline{u}\|_{L^2(\Omega,\mathbb{R}^2)}$	yes
$\|\overline{\sigma}\|_{\Sigma}$	yes

(a) Perfect plasticity

Quantity	Bounded
$\|A^{-1}\epsilon_{\alpha}\|_{\Sigma}$	yes (depending on α)
$\|u_{\alpha}\|$	yes (depending on α)
$\|u_{\alpha}\|_{L^2(\Omega,\mathbb{R}^2)}$	yes (independent of α)
$\|\sigma_{\alpha}\|_{\Sigma}$	yes (independent of α)

(b) Viscoplasticity

TABLE 11.3. Expected behavior in perfect plasticity / viscoplasticity.

mesh-refinement (h-refinement). For successive mesh refinement, we expect the plastic strain and the displacement gradient not to converge in L^2 in the absense of regularization, cf. Corollaries 10.7 and 10.8. However, since the stress field can be approximated stably (Theorem 10.6) and since $BD(\Omega)$ embeds continuously into $L^2(\Omega,\mathbb{R}^2)$ for $d = 2$ (see Section 2.1), we expect these quantities to be bounded. The obtained results are shown in Table 11.4. The second number in each cell gives the difference to the corresponding value on the coarser mesh. Considering the last columns ($\alpha = \infty$) corresponding to perfect plasticity, our expectations seem to be fulfilled as the plastic strain and the energy norm of the displacement do not converge. Quite interestingly, there seems to be convergence up to mesh refinement level 6, but afterwards divergence is encountered.

Contrary, for the lowest regularization parameter ($\alpha = 1e2$), all quantities seem to converge as $h \to 0$, which is expected from a theoretical point of view. Uniform boundedness should also hold for all other finite regularization parameters. However, as the bounds for the plastic strain and the energy norm of the displacement depend on α, we see the discrepancy between analysis and numerical reality: though the computations are performed with millions degrees of freedom, the mesh size is still too large to observe results predicted by the theory. Particularly, a difference between perfect plasticity and viscoplasticity with $\alpha \geq 1e6$ can hardly be observed.

Concerning the convergence w.r.t. the regularization parameter, we see that the perfectly plastic model serves as an upper bound for all quantities. What can also be read off the table is the uniform boundedness of the stresses in L^2 for all regularization parameters α and all mesh sizes (similarly for the displacement in L^2).

Level	$\alpha = 1e2$	$\alpha = 1e4$	$\alpha = 1e6$	$\alpha = 1e8$	$\alpha = \infty$
3	5.5903	12.29	12.64	12.64	12.64
4	5.6157 (0.0254)	12.79 (0.50)	13.22 (0.58)	13.22 (0.58)	13.22 (0.58)
5	5.6230 (0.0073)	12.94 (0.15)	13.41 (0.19)	13.42 (0.20)	13.42 (0.20)
6	5.6252 (0.0022)	12.99 (0.05)	13.48 (0.07)	13.48 (0.06)	13.48 (0.06)
7	5.6259 (0.0007)	13.04 (0.05)	13.57 (0.09)	13.58 (0.10)	13.58 (0.10)
8	5.6262 (0.0003)	13.12 (0.08)	13.81 (0.24)	13.82 (0.24)	13.82 (0.24)

(a) Plastic strain: $\|A_h^{-1}\boldsymbol{\epsilon}_h\|_{\boldsymbol{\Sigma}}$

Level	$\alpha = 1e2$	$\alpha = 1e4$	$\alpha = 1e6$	$\alpha = 1e8$	$\alpha = \infty$
3	14.0758	19.14	19.43	19.43	19.43
4	14.0932 (0.0174)	19.55 (0.41)	19.90 (0.47)	19.91 (0.48)	19.91 (0.48)
5	14.0980 (0.0048)	19.67 (0.12)	20.06 (0.16)	20.06 (0.15)	20.06 (0.15)
6	14.0994 (0.0014)	19.71 (0.05)	20.11 (0.05)	20.11 (0.05)	20.11 (0.05)
7	14.0999 (0.0005)	19.75 (0.05)	20.18 (0.07)	20.18 (0.07)	20.18 (0.07)
8	14.1000 (0.0001)	19.80 (0.05)	20.34 (0.16)	20.35 (0.17)	20.35 (0.17)

(b) Displacement: Energy norm $\||\boldsymbol{u}_h\||$.

Level	$\alpha = 1e2$	$\alpha = 1e4$	$\alpha = 1e6$	$\alpha = 1e8$	$\alpha = \infty$
3	0.20882	0.26006	0.26251	0.26254	0.26254
4	0.20904 (0.00022)	0.26327 (0.00321)	0.26615 (0.00364)	0.26618 (0.00364)	0.26619 (0.00365)
5	0.20910 (0.00006)	0.26422 (0.00095)	0.26727 (0.00112)	0.26730 (0.00122)	0.26730 (0.00121)
6	0.20912 (0.00002)	0.26448 (0.00026)	0.26758 (0.00031)	0.26761 (0.00031)	0.26761 (0.00031)
7	0.20912 (0.00000)	0.26457 (0.00009)	0.26769 (0.00011)	0.26772 (0.00011)	0.26773 (0.00012)
8	0.20912 (0.00000)	0.26461 (0.00004)	0.26779 (0.00010)	0.26782 (0.00010)	0.26782 (0.00009)

(c) Displacement: L^2 norm $\|\boldsymbol{u}_h\|_{L^2(\Omega,\mathbb{R}^2)}$.

Level	$\alpha = 1e2$	$\alpha = 1e4$	$\alpha = 1e6$	$\alpha = 1e8$	$\alpha = \infty$
3	11.4328	11.4764	11.4779	11.4779	11.4779
4	11.4329 (0.0001)	11.4773 (0.0009)	11.4790 (0.0011)	11.4790 (0.0011)	11.4790 (0.0011)
5	11.4329 (0.0000)	11.4776 (0.0003)	11.4793 (0.0003)	11.4793 (0.0003)	11.4793 (0.0003)
6	11.4330 (0.0001)	11.4777 (0.0001)	11.4794 (0.0001)	11.4794 (0.0001)	11.4794 (0.0001)
7	11.4330 (0.0000)	11.4777 (0.0000)	11.4794 (0.0000)	11.4795 (0.0001)	11.4795 (0.0001)
8	11.4330 (0.0000)	11.4778 (0.0001)	11.4795 (0.0001)	11.4795 (0.0000)	11.4795 (0.0000)

(d) Stress: $\|\boldsymbol{\sigma}_h\|_{\boldsymbol{\Sigma}}$.

TABLE 11.4. Norms of the different quantities.

2. Verification of Numerical Methods

As demonstrated above, we cannot expect uniform bounds for the underlying problem and therefore, mesh-independent convergence of numerical methods cannot be expected in general. Nevertheless, some of the methods we presented before seem to converge almost mesh-independent as we will demonstrate. For this, we compare several methods, namely the standard radial return algorithm with a simple backtracking line search (RR) which essentially is Newton's method applied to the first order optimality condition, the radial return algorithm with an energy-based line search (RRmin) which is Newton's method for unconstrained minimization, the first order Augmented Lagrangian method (ALM) and the active set method (AS). Details concerning the different methods are listed in Table 11.5. We will also consider a gradient method (Grad) which is related to (RRmin).

2.1. Problem Statement and Numerical Performance of the Methods. Contrary to the previous section, this time the load is applied incrementally and we divide the time interval $[0, 5.05]$ uniformly into 10 subintervals with $\Delta t \equiv \Delta t_n = 0.505$ and time instances $t_n = n\Delta t$, $n = 0, \dots, 10$. The last three time steps are considered in the Table 11.6. For (RR), (RRmin) and (AS), the number of iterations (which coincides with the number of linear systems to be solved) is listed, whereas for (ALM), the number of (ALM) steps as well as the number of linear systems (LS) is shown.

We can observe that the standard algorithm (RR) is only competitive in time step 8 in which the plastic volume fraction is about 0.8%. In time step 9, (RR) shows strong mesh-dependence whereas it did not converge within the maximum number of iterations in time step 10 for higher levels of mesh refinement. The other three methods essentially behave mesh-independent in time step 8 and 9, and also in time step 10, these method seem to be almost stable. Due to the lack of a globalization strategy, the active set method (AS) did not converge on Level 7. This is also related to the linear solver and we will come back to this issue. In the next subsections, we will have a closer look at the individual methods.

2.2. (RR), (RRmin) and Gradient-Type Methods. As indicated above, (RR) is a generalized Newton method applied to an equation (the first order optimality condition), whereas (RRmin) is a generalized Newton method for the solution of the (unconstrained)

Method	Type	Algorithm
Radial Return (RR)	Primal	Algorithm 8.1 with the simple backtracking line search (Algorithm 8.2). This does not reflect the minimization structure.
Radial Return Min. (RRmin)	Primal	Algorithm 8.1 with the modification of Algorithm 8.7 and $\delta^{n,k} \equiv 0$, i.e. the same search direction as in (RR) is used. The line search is based on the primal energy.
Augmented Lagrange (ALM)	(Primal-) Dual	The first order Augmented Lagrangian method with multiplier update and adaptive selection of the penalty parameters, Algorithm 10.3.
Active Set (AS)	Primal-Dual	Algorithm 9.1 without a line search, i.e. we always take the full Newton stepsize. The parameter γ (see the discussion in Section 9.3) is chosen to be 1e-5.

TABLE 11.5. Overview of the methods.

Level	(RR)	(RRmin)	(ALM)	(AS)
3	6 steps	6 steps	4 steps (7 LS)	6 steps
4	8 steps	7 steps	4 steps (9 LS)	7 steps
5	9 steps	7 steps	4 steps (9 LS)	7 steps
6	11 steps	8 steps	5 steps (10 LS)	8 steps
7	13 steps	7 steps	5 steps (10 LS)	–

(a) Time step 8 from $t = 3.535 \ldots 4.04$. Plastic volume fraction $\approx 0.8\%$.

Level	(RR)	(RRmin)	(ALM)	(AS)
3	9 steps	8 steps	5 steps (9 LS)	8 steps
4	13 steps	9 steps	5 steps (10 LS)	9 steps
5	22 steps	10 steps	5 steps (10 LS)	10 steps
6	38 steps	10 steps	5 steps (11 LS)	10 steps
7	70 steps	9 steps	6 steps (11 LS)	–

(b) Time step 9 from $t = 4.04 \ldots 4.545$. Plastic volume fraction $\approx 3.5\%$.

Level	(RR)	(RRmin)	(ALM)	(AS)
3	37 steps	10 steps	6 steps (12 LS)	10 steps
4	70 steps	10 steps	7 steps (13 LS)	10 steps
5	> 100 steps	11 steps	8 steps (15 LS)	11 steps
6	> 100 steps	11 steps	8 steps (16 LS)	11 steps
7	> 100 steps	16 steps	9 steps (16 LS)	–

(c) Time step 10 from $t = 4.545 \ldots 5.05$. Plastic volume fraction $\approx 35\%$.

TABLE 11.6. Iteration count for the different methods.

primal minimization problem and therefore accounts for the additional minimization structure. Locally, the convergence properties of both algorithms are the same as we have shown in Section 8.3. However, away from the solution, the situation is different, since globalization relies on different strategies: (RR) only considers the residual at the current iteration and uses line searching to reduce the residual. Contrary, line searching in (RRmin) is based on the primal energy (5.17) (or (2.36) in the static setting)

$$\mathcal{E}_{\mathrm{pl}}(\boldsymbol{u}) = \Upsilon(\mathbb{C}[\boldsymbol{\varepsilon}(\boldsymbol{u}) - \boldsymbol{\varepsilon}_p^{n-1}]) - \ell(\boldsymbol{u}) \,.$$

Accordingly, (RRmin) has more information during the iteration and we expect better global convergence properties. This is indeed the case, cf. Table 11.6.

We observe that after time step 8, merely about 0.8% of Ω is plastified but already at this point, (RR) begins to show mesh-dependent behavior. However, in this time step, (RRmin) behaves mesh-independent. The explanation for the bad behavior of (RR) is the use of the simple backtracking line search (Algorithm 8.2) which is based on the derivative $F = D\mathcal{E}_{\mathrm{pl}}$ of the primal energy rather than on the energy itself as in (RRmin). In Figure 11.2, the evolutions of the residual and the energy during the iteration are presented and for convenience, the initial energy is shifted to 0. We observe that in the first iterations of (RRmin), the residual is not necessarily reduced (it is even increased), but
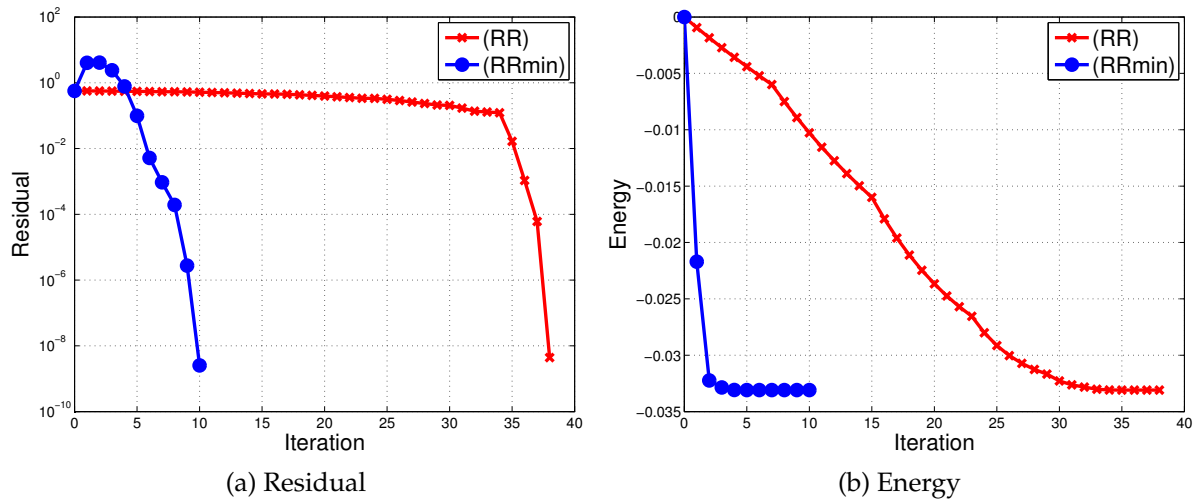
FIGURE 11.2. Residual and energy decay during the iteration on Level 6, time step 9.

we substantially decrease the primal energy. This contrasts (RR) where we reduce the residual in each step by the line search, but hardly decrease the energy. Both methods accept the full Newton step size in the final iterations and therefore converge quadratically (or at least superlinearly) as can be seen from Subfigure (a). In both cases, the initial residual is reduced by a factor of 1e-8. Concerning (RRmin), the number of iterations remains more or less constant. The only exception is encountered in time step 10 going from Level 6 to 7.

At this point however, we also have to mention that for different problems (and particularly in 3d), a pure energy-based line search was not always successful as the residuals in the first iterations increased too much which also caused higher iteration numbers. Thus, from our numerical experience, it is necessary to take into account both the residual and the energy.

2.2.1. *A Gradient Method.* Actually, (RRmin) is a special implementation of the general gradient method (Algorithm 8.7). We now present some for the modified variant (Algorithm 8.8) which does not use the pure Newton direction, but the search direction is obtained by (locally) using a convex combination of $\mathbb{C}_{ct}$ and $\mathbb{C}$. If the portion of $\mathbb{C}$ does not vanish, it is assured that the obtained direction is a descent direction. For further reference, this algorithm will be denoted by (Grad). In detail, for different values of β, we use $\frac{\beta}{1+\beta}\mathbb{C}_{ct} + \frac{1}{1+\beta}\mathbb{C}$ (see Algorithm 8.8) to determine the search direction Δu. The larger β, the closer the search direction is to the Newton direction and we expect faster local convergence for increasing β. Formally, (RRmin) corresponds to $\beta = \infty$. The results are shown in Figure 11.3. As expected, we obtain linear convergence for fixed values of β, but we also see that for $\beta = 1000$, this convergence is quite fast. Moreover, in the first iterations, none of the parameter seems to be superior. Only for fast local convergence, a higher value of β is necessary. Physically, the used tangent corresponds to the viscoplastic regularization with $\alpha = \frac{\beta}{\Delta t}$ or to kinematic hardening with modulus $\mathbb{H} = \frac{1}{1+\beta}\mathbb{C}$.

2.3. (ALM) Method. Whereas (RR) and (RRmin) are purely primal methods, the Augmented Lagrangian method structurally is a dual method. For the computation, we used Algorithm 10.3, and in each (ALM) step, a regularized subproblem of the type
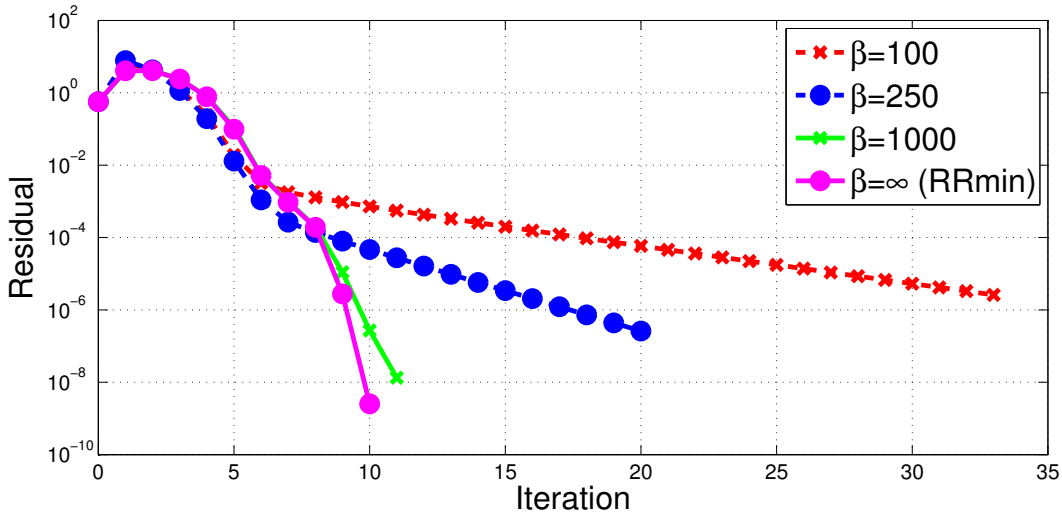
FIGURE 11.3. Residuals of the gradient algorithm (Grad) for different values of β on level 6, time step 9.

(10.8) with penalty parameter α_{k-1} has to be solved. The subproblems are solved via the corresponding regularized primal problems (10.13) with the globally and locally super-linear convergent Algorithm 8.7 (with $\delta_{n,k} \equiv 0$) and for efficiency, we use inexact solving. The penalty parameters α_k are limited by $\overline{\alpha} = 1\mathrm{e}5$ which is well confirmed by the results of the previous subsection. As a first guess, we typically choose $\alpha \approx 1000$. Even though the limitation of the penalty parameter implies only linear convergence as a consequence of Theorem 10.14, $\overline{\alpha}$ is sufficiently large to observe fast convergence in the final iterations. This can be seen in the last column of Table 11.7, or in Figure 11.4, respectively.

By Theorem 10.14, once the penalty parameter is fixed, the best we can expect is linear convergence. This can indeed be observed here since the penalty parameter is kept fixed from the beginning of the fourth iteration. Though, α is large enough to yield very fast linear convergence. In each of the final iterations, the total error is (approximately) reduced by a factor of 1e-2. Moreover, in the final iterations, the subproblems are solved in only one or two iterations (column LS in Table 11.7). In conclusion, the last 5 linear system solves are responsible for the largest part of the error reduction. Even more favorable, the remaining linear systems are only needed to be solved with a lower penalty

(ALM) step	LS	Penalty	Equilibrium	Flow rule	Complement.	Total
0	–	–	2.230e+01	1.193e-00	3.043e-08	2.350e+01
1	5	1 000	5.225e-00	8.413e-00	1.138e+03	1.152e+03
2	1	8 154	5.231e-00	2.298e-00	3.814e+01	4.566e+01
3	5	66 501	1.027e-02	8.969e-01	1.825e-00	2.732e-00
4	1	100 000	2.339e-03	1.031e-02	1.395e-02	2.661e-02
5	1	100 000	1.526e-04	1.934e-04	2.617e-04	6.077e-04
6	2	100 000	8.893e-10	7.287e-06	9.863e-06	1.715e-05
7	1	100 000	8.792e-10	2.581e-07	3.493e-07	6.083e-07
8	0	100 000	8.833e-10	2.837e-10	2.539e-10	1.421e-09

TABLE 11.7. Convergence history of (ALM) on Level 6, time step 10.
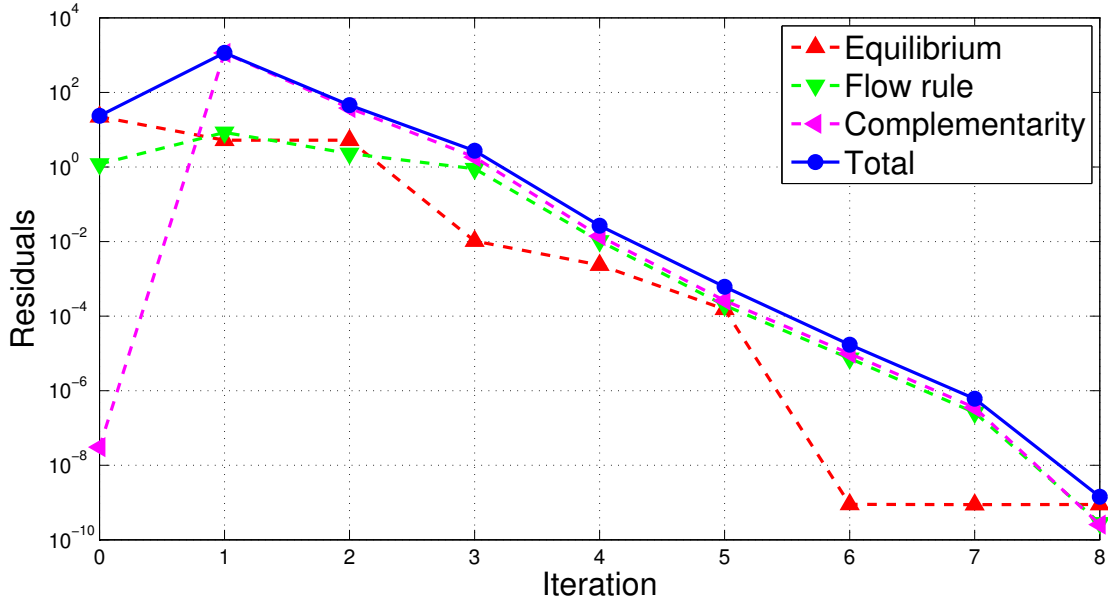
FIGURE 11.4. Convergence of (ALM) on Level 6, time step 10.

parameter as merely the final linear systems use the penalty parameter $\overline{\alpha} = 1e5$. The obtained convergence rates parallel the fast linear convergence of (Grad) presented above, provided that the parameter β is chosen sufficiently large.

We briefly remark on the penalty update for which we recall some notation from Section 10.4.

$$r_{\boldsymbol{\sigma}}^k(\boldsymbol{\eta}) = \langle DJ(\boldsymbol{\sigma}^k) + \boldsymbol{\epsilon}^k + B^*\boldsymbol{u}^k, \boldsymbol{\eta}\rangle_{\boldsymbol{P}^* \times \boldsymbol{P}}\,, \qquad \boldsymbol{\eta} \in \boldsymbol{P}\,,$$
$$r_{\boldsymbol{\epsilon}}^k(\boldsymbol{\eta}) = \langle \boldsymbol{\epsilon}^k - D_{\boldsymbol{\sigma}}\pi_{\boldsymbol{K}}^{\alpha_{k-1}}(\boldsymbol{\sigma}^k, \boldsymbol{\epsilon}^k), \boldsymbol{\eta}\rangle_{\boldsymbol{P}^* \times \boldsymbol{P}}\,, \qquad \boldsymbol{\eta} \in \boldsymbol{P}\,,$$
$$r_{\boldsymbol{u}}^k(\boldsymbol{w}) = \langle B\boldsymbol{\sigma}^k + \ell, \boldsymbol{w}\rangle_{\boldsymbol{X}^* \times \boldsymbol{X}}\,, \qquad \boldsymbol{w} \in \boldsymbol{X}\,.$$

The penalty parameter is updated in one of the following situations:

(1) $\max\{\|A^{-1}r_{\boldsymbol{\epsilon}}^k\|_{\boldsymbol{\Sigma}}, \|A^{-1}r_{\boldsymbol{\sigma}}^k\|_{\boldsymbol{\Sigma}}\} \gg \|r_{\boldsymbol{u}}^k\|_{\boldsymbol{X}^*}$: since the equilibrium equation is independent of α, this indicates that the current penalty parameter is too small. Moreover, in this situation, exact solving is not necessary. This explains why in the second step only one iteration is performed.

(2) $\|A^{-1}r_{\boldsymbol{\epsilon}}^k\|_{\boldsymbol{\Sigma}} > \|A^{-1}r_{\boldsymbol{\sigma}}^k\|_{\boldsymbol{\Sigma}}$: in this case, the current iterate lacks complementarity and this also suggests to increase α. This explains the fast increase of the penalty parameter after the second iteration.

In the last iteration, the linear system was not needed to be solved anymore, since the residual $r_{\boldsymbol{u}}$ already was below the prescribed tolerance. Thus, in the last step only a multiplier update was performed corresponding to a gradient step for the value function (10.20). The iteration was terminated after the overall error was reduced by factor 1e-8.

2.4. (AS) Method. The computations with the active set method were performed with $\gamma = 1e-5$. This choice of γ will be justified below. As mentioned earlier, we use no globalization strategy, i.e. line searching is not applied. Moreover, the computation on Level 7 was not accessible, since the linear systems could not be solved by the standard multigrid preconditioner. A possible explanation for the failure of standard multigrid

techniques is that the active / inactive set prediction cannot be resolved on the coarse mesh. This problem was already observed for similar problems, cf. [**KKT03**, **KY94**]. In view of this, we employ a parallel direct solver which is limited to Level 6.

In Table 11.8, we give a convergence history and we shortly explain the computed quantities. The column "Prediction" shows the number of actively predicted points and we see a monotonic increase in the total number. This is not necessarily the case as is demonstrated below. The column "Flow rule" corresponds to $\|A_h^{-1}\Phi_1(\boldsymbol{y}_h^k)\|_{\boldsymbol{\Sigma}_h}$ whereas the column "Equilibrium" shows $\|\Phi_2(\boldsymbol{y}_h^k)\|_{\boldsymbol{X}_h^*} = |E_h^*\Phi_2(\boldsymbol{y}_h^k)|$ (cf. Section 8.1 for norms on $\boldsymbol{X}_h$). The column "Feasibility" is the quantity

$$\int_{\Omega} \max\{0, f(\boldsymbol{\sigma}_h(x))\}^2 \, dx \,, \tag{11.1}$$

and is related to the admissibility of $\boldsymbol{\sigma}_h$. This is a reasonable quantity to observe in the context of associated plasticity and has the additional advantage to be independent of γ which would not be the case if we consider the norm of Φ_3. However, for non-associated plasticity, it might not suffice to consider that quantity. The sum of the three quantities is the overall error, which is reduced by a factor 1e-8 during the iteration. From the table and the corresponding Figure 11.5, quadratic convergence can be observed in the final iteration. Since (AS) is a primal-dual method and the equilibium equation is linear, the stress field is always statically admissible during the iteration (within the prescribed tolerance). This can also be observed in Table 11.8 and Figure 11.5.

Iteration	Prediction	Equilibrium	Flow rule	Feasibility	Total
0	206836	3.153e+01	1.193e-00	1.689e-11	3.272e+01
1	416181	2.064e-10	8.316e-02	1.255e+02	1.256e+02
2	455154	1.947e-09	2.419e-01	7.648e+01	7.672e+01
3	479262	1.307e-08	1.180e-01	4.988e+01	5.000e+01
4	489007	1.079e-09	4.679e-02	2.810e+01	2.815e+01
5	493854	2.089e-10	1.187e-02	1.242e+01	1.243e+01
6	495763	4.616e-11	1.741e-03	3.147e-00	3.149e-00
7	496286	1.395e-11	9.500e-05	2.975e-01	2.976e-01
8	496377	1.025e-12	1.824e-06	1.349e-02	1.349e-02
9	496392	9.082e-13	2.906e-08	1.903e-03	1.903e-03
10	496397	9.029e-13	7.218e-10	1.191e-04	1.191e-04
11	496397	9.046e-13	3.380e-12	1.183e-10	1.226e-10

TABLE 11.8. Convergence history of (AS) on Level 5, time step 10.

2.4.1. *The Influence of γ.* As we already remarked in Section 9.3, the active set method is expected to be sensitive to the choice of γ and also on the mesh size. Thus, we examine the behavior of (AS) for different values of γ as well as for varying mesh size h. The iteration count is listed in Table 11.9.

As it can be seen from the table, lower values of γ seem to be favourable for the given problem. The reason is already described in Section 9.3: lower values of γ make it easier to inactive mistakenly actived points. Moreover, the prediction strategy is less aggressive. This can be seen in Figure 11.6 where the number of predicted points during the iteration is plotted for $\gamma = 1$ and $\gamma = $1e-4. Since initially, the number of predicted points
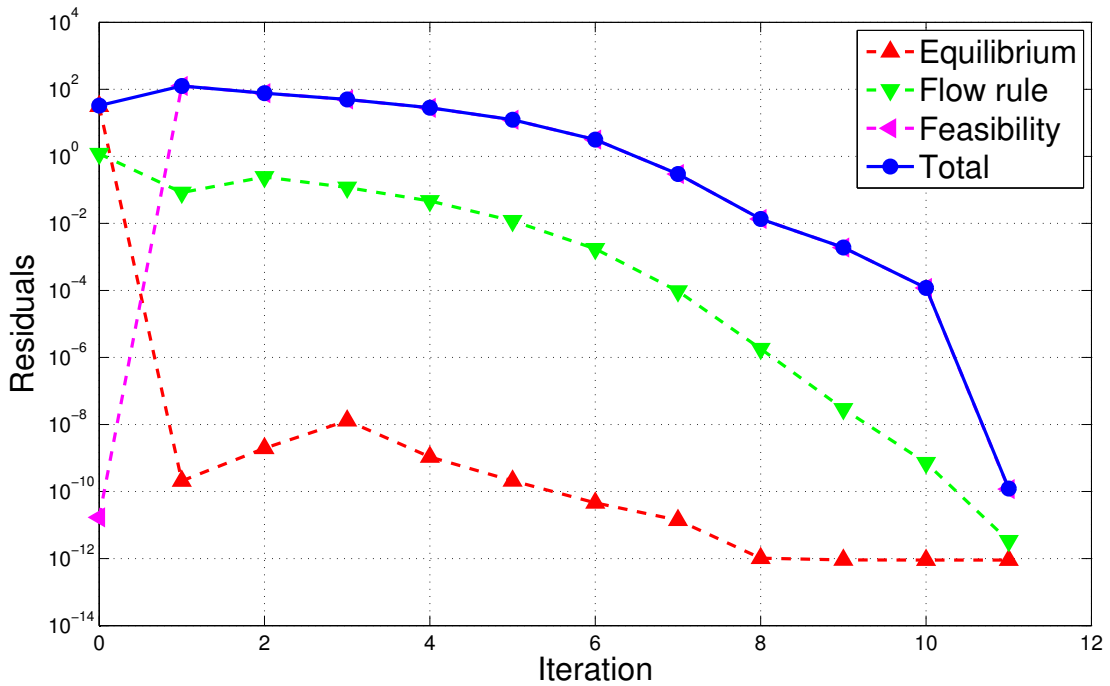
FIGURE 11.5. Convergence of (AS) on Level 5, time step 10.

is the same (the number of the previous time step), the active set predictions for the first iteration are identical and overestimate the true active set. But afterwards, the curves are fairly different. Whereas for $\gamma = 1e-4$, the next two iterates decrease the number of predicted points significantly, the predicted number of points is even further increased for $\gamma = 1$. Starting from iteration 3, $\gamma = 1e-4$ gives a monotonic increase in the predicted number of active points while for $\gamma = 1$, the prediction seems to oscillate before a monotonic decrease starts. We conclude that if inactivation is necessary, a smaller value of γ gives superior convergence properties and this can also explain why the algorithm did not converge for too large values of γ on the higher levels.

Reconsidering Table 11.9, we observe that mesh-dependence seems to be related to the choice of γ. For $\gamma = 1$, the iteration count increases with ongoing mesh refinement. Also, for $\gamma = 1e-2$ mesh-dependent behavior seems to take place at least in the final time

| | Level 2 | | | Level 3 | | | Level 4 | | | Level 5 | | | Level 6 | | |
γ	1	1e-2	1e-4	1	1e-2	1e-4	1	1e-2	1e-4	1	1e-2	1e-4	1	1e-2	1e-4
TS 5	6	5	5	7	6	5	9	7	5	14	7	6	13	8	7
TS 6	5	5	5	10	6	5	10	7	6	15	8	6	13	8	7
TS 7	6	5	5	8	7	5	15	7	6	8	9	7	15	9	7
TS 8	8	7	6	10	7	6	10	7	7	10	9	7	12	9	8
TS 9	13	8	7	16	9	8	21	10	8	24	11	9	28	12	10
TS 10	16	10	9	18	13	10	–	16	10	–	19	11	–	–	11

TABLE 11.9. Iteration count of (AS) for different values of γ at the time steps 5 to 10. "–" denotes not converged within 80 iterations.
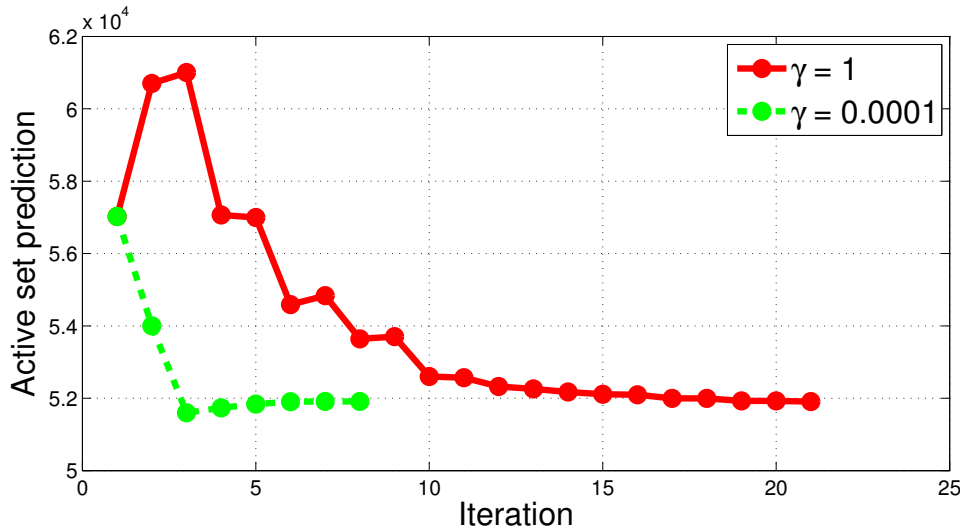
FIGURE 11.6. Predicted active quadrature points by (AS) on Level 4, time step 9 for different values of γ.

steps. For $\gamma = 1e\text{-}4$, the method seems to behave almost mesh-independent, but just as for the other values of γ, we expect the onset of mesh-dependent behavior if we would be able to further refine the mesh. Thus, there seems to be a relation between γ and h. However, without additional (analytical) insight into the problem, the nature of this relation remains unclear.

2.5. Comparison of the Methods. Mainly, the algorithms can be distinguished into primal (RR,RRmin,Grad), dual (ALM) and primal-dual (AS) algorithms. On a continuous level, the primal problem is not well-posed in standard Sobolev spaces, see Section 2.3, and consequently, it is not to be expected that primal (and even primal-dual) algorithms perform well. Nevertheless, exploiting the minimization structure of the primal problem und using a (primal) energy-based line search, the algorithms (RRmin) and (Grad) exhibit satisfying stability properties. A further advantage of primal methods results from the fact that the primal problem is an unconstrained minimization problem since constraints are explicitly fulfilled by the response function (a projection in perfect plasticity).

As mentioned above, also primal-dual methods like the active set method (AS) are not generally expected to behave mesh-independent, and for the given problem, this could only be achieved for specific choices of γ. Wrong choices of γ even lead to divergence of the iteration. An advantage of the method is that in each iteration, only one linear system has to be solved. This contrasts the primal methods, where in each quadrature point, a constrained minimization problem has to be solved (the projection). Moreover, the Schur complement reduction which we explicitly derived in Section 9.2 can be handled by the computer, i.e. it is only necessary to set up the linear system (9.5) and let the computer do the rest. However, globalization techniques are more difficult to implement. One reason is the dependence on γ, which introduces a scaling between the components Φ_3 and Φ_1, Φ_2 which is not fully understood so far. It is also the reason why we tested for feasibility (11.1) in the above numerical study.

Methods based on the Augmented Lagrangian seem to be superior from a theoretical point of view, even though the implementation as used in this chapter might not be

stable either, cf. Section 10.4 (and particularly Assumption 10.11), where we assumed that the solution is contained in standard Sobolev spaces. Nevertheless, Algorithm 10.1 stably approximates the stress field in perfect plasticity even if no extra-regularity of the solution is available. From a numerical point of view, the situation is a bit different as it can be seen from the stability study at the beginning of the chapter. Up to refinement level 8, a difference between perfect plasticity and viscoplasticity with parameter $\alpha = $ 1e6 can hardly be obtained. Thus, numerically, it is reasonable to include the multiplier update. A drawback of the method is that the subproblems are still nonlinear, even if they are well-posed analytically. Hence, in order to be competitive, inexact solving and an update strategy for the multiplier are necessary. This demands for some insight into the problem.

Looking at the iteration count and the computational complexity (which is related to the solution of linear systems), the methods (RRmin), (ALM) yield similar results. (AS) is also competitive as long as a robust solver for the linear systems is at hand and γ is reasonably chosen.

3. A Test Configuration

3.1. Problem Setting. We now turn to a three-dimensional example. Again, we use the model of von Mises plasticity with the parameters given in Table 11.1. We consider a tensile / compression test for the workpiece illustrated in Figure 11.7. In Subfigure (b), the full workpiece is illustrated and Subfigure (a) shows the computational domain including symmetry boundary conditions. (c) finally shows the projection of Ω onto the x_i–x_k planes and also the point $P = (3, 22, 2)$ is shown at which we will consider load-displacement curves. Due to the symmetry conditions, we only consider an eighth of the full workpiece but remark that despite the symmetries, the problem is three-dimensional.

With the functions

$$L(t) = 3.505 \sin(\tfrac{\pi}{2}\, t) \qquad \text{and} \qquad S(\boldsymbol{w}) = \int_0^7 \int_0^4 100 \boldsymbol{w}_2(x_1, 22, x_3)\, dx_3\, dx_1\,,$$

the applied load is given as $\ell(t, \boldsymbol{v}) = L(t)S(\boldsymbol{v})$. As it can be seen from Figure 11.8, the limit load is expected to be slightly above $3.505S(\boldsymbol{v})$. We consider the time interval $[0, 4]$ corresponding to a complete load cycle. Up to $t = 1$, the configuration corresponds to a tensile test. Due to the smaller cross-section at the face with symmetry boundary conditions w.r.t. x_2, we expect to see necking, i.e. a reduction of the cross-section. Generally, we will refer to that part of Ω as the "lower part". Once the tensile phase is completed, between $t = 1$ and $t = 2$, elastic unloading takes place before the compression phase starts at $t = 2$. The maximal compressive force is applied at $t = 3$ and afterwards, elastic unloading takes place again. As before, the computations are performed on different levels of mesh-refinement, also see Table 11.10. Since we use the Augmented Lagrangian

Level	0	1	2	3	4	5
Degrees of Freedom	2 520	16 305	116 271	875 931	6 795 315	53 523 555
Cells	536	4 288	34 304	274 432	2 195 456	17 563 648
Quadrature Points	4 288	34 304	274 432	2 195 456	17 563 648	140 509 184
Internal variables	51 456	411 648	3 293 184	26 345 472	210 763 776	1 686 110 208

TABLE 11.10. Computational details for the 3d test configuration

(a) 3d view of the coarse mesh with symmetry boundary conditions and load.

(b) 3d view of the workpiece.

(c) Projections of the geometry onto the x_1–x_2, x_1–x_3 and x_2–x_3 plane.
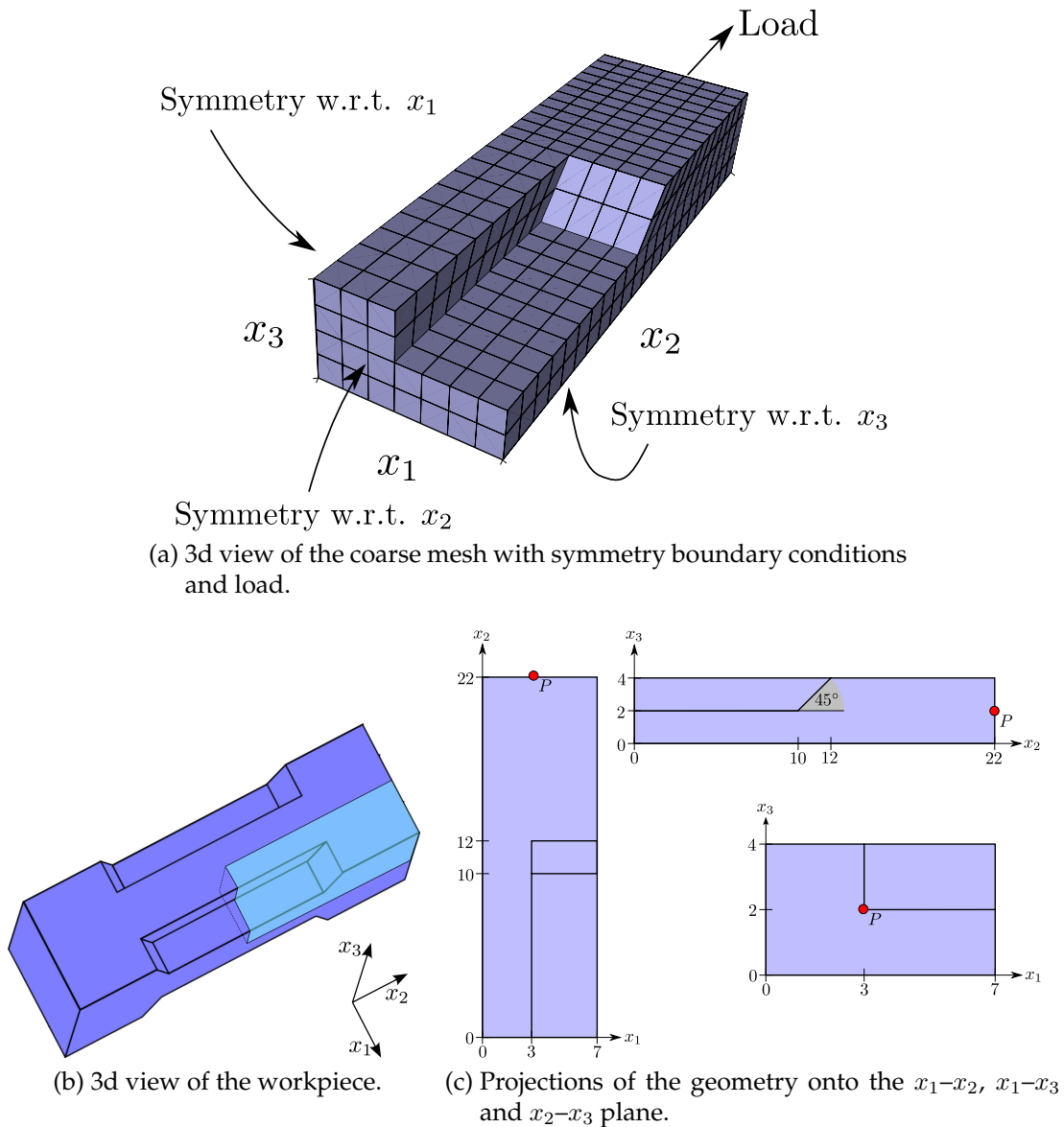
FIGURE 11.7. Problem setting for the 3d workpiece.

method (ALM), besides the plastic strain ε_p^{n-1} of the previous time step, it is also necessary to store the plastic strain increment ϵ at each quadrature point. Accordingly, in each quadrature point we store 12 ($\dim(\mathrm{Sym}(3)) = 6$) internal variables. For the present case of incompressible plasticity, it is possible to reduce this number to 10 ($\dim(\mathrm{Sym}_0(3)) = 5$). The time interval $[0,4]$ was non-uniformly partitioned into 80 subintervals corresponding to 80 load steps. At the peak loads at $t = 1$ and $t = 3$, the time step size is significantly smaller. The full cycle on the time interval $[0,4]$ is only performed up to mesh refinement level 4, while on level 5, we only considered the tensile phase $t \in [0,1]$ (also see the next subsection).

Figure 11.8 shows the obtained hysteresis curves at the point $P = (3, 22, 2)$ which is situated on the face of the boundary where the force is exerted. The hysteresis curve is w.r.t. to the x_2-displacement $\boldsymbol{u}_2(P, t)$. As expected from the perfectly plastic model, once the yield strength is reached, it is seemingly possible to further deform the body without a further load increase. The yield strength is correctly identified on all meshes, but the

predicted displacements are fairly different. This can be seen in Subfigures (b) and (c) which provide a zoom into the hysteresis curve at the maximal tensile and compression force. The graphics suggests that the load-displacement curves converge linearly with the mesh size h. This is also illustrated in the Figure 11.10 in which also mesh refinement level 5 is included.
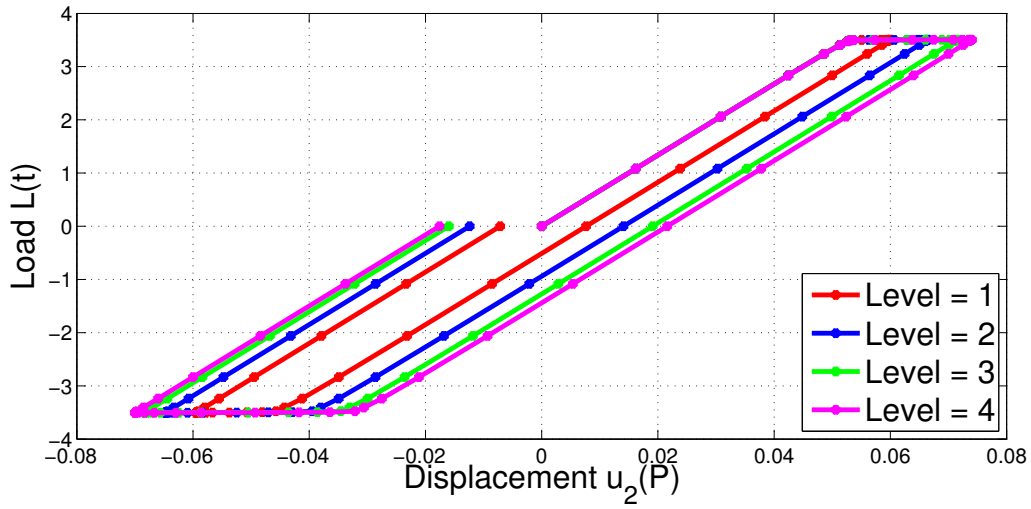
(a) Hysteresis curve at $P = (3, 22, 2)$ for different levels of mesh refinement
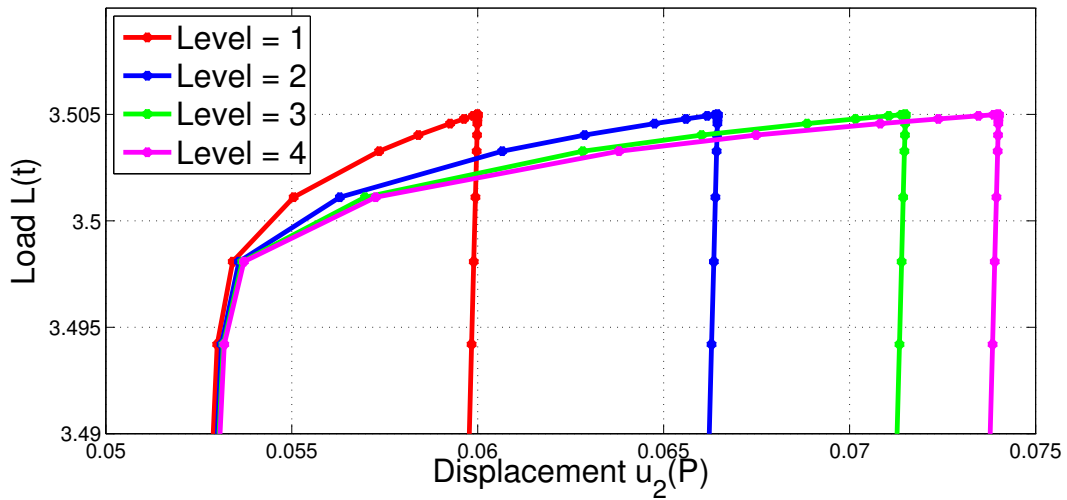
(b) Zoom in hysteresis curve at $P = (3, 22, 2)$.
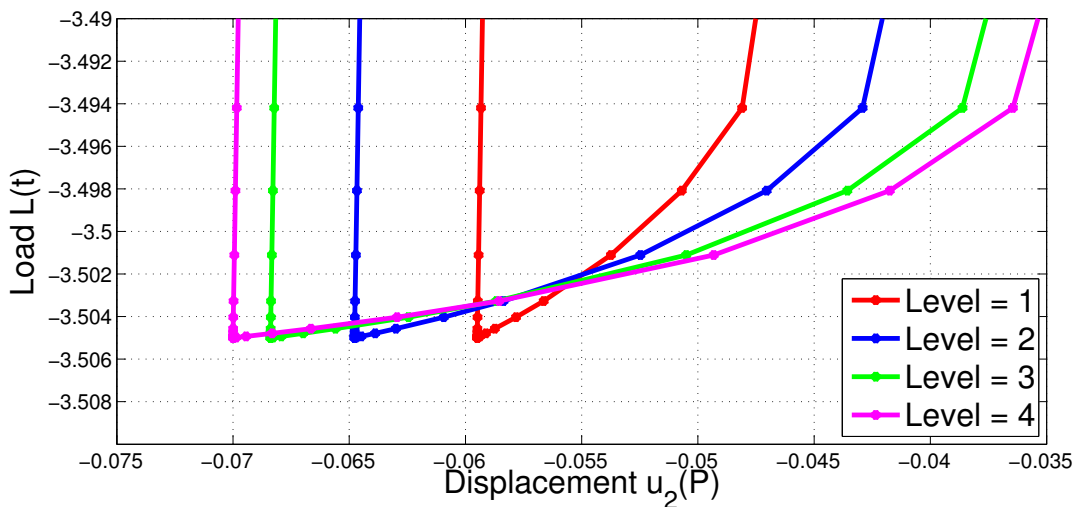
(c) Zoom in hysteresis curve at $P = (3, 22, 2)$.

FIGURE 11.8. Hysteresis curve at $P = (3, 22, 2)$ for different levels of mesh refinement.

3.2. The Augmented Lagrangian Method (ALM). Due to the promising results of the previous section, we use the Augmented Lagrangian method (ALM) with the same parameters as presented before as presented in the previous section.

3.2.1. *Stability and Convergence.* Concerning the stability of (ALM) w.r.t. the mesh size, we consider the time interval $[0, 1]$ which corresponds to the tensile phase of the loading process. Computations are performed up to mesh refinement level 5 corresponding to approximately 50 million degrees of freedom for the displacement field, cf. Table 11.10. The time interval is non-uniformly partitioned into 20 subintervals and figure 11.9 shows how many linear systems were needed to be solved at the individual time steps. As indicated above, around $t = 1$ corresponding to the maximal tensile force, the time step size is considerably smaller if compared to the first time steps. This explains why the number of linear systems even decreases in the final time steps. Small time steps Δt_n are indeed necessary to give a suitable initial guess for the nonlinear iteration. Nevertheless, even very small time steps require robust methods in the vicinity of the limit load if the mesh size is small. Surprisingly, the method shows the worst convergence behavior on refinement level 4, whereas on level 5, the number of linear systems and the convergence is comparable to level 3. A closer look reveals that on level 4, more line searches are necessary for the regularized subproblems.

To give an example concerning the convergence behavior of the Augmented Lagrangian method, we consider time step 15 in more detail. Table 11.11 shows the total error during the iteration in this time step. Therefore note that contrary to Figure 11.9, in this table we do not consider the number of linear systems but the number of total (ALM) steps. Similar to the two-dimensional example, we obtain very fast linear convergence in the last (ALM) steps in which the penalty parameter is fixed. In the final iterations, the equilibrium equation is typically fulfilled within the prescribed tolerance and only multiplier updates are performed. This also explains why on level 5, there are 7 (ALM) steps, but only 5 linear systems that need to be solved.

As indicated in the previous section, it appears that the load-displacement curves at the point $P = (3, 22, 2)$ converges linearly with the mesh size h. This can indeed be observed
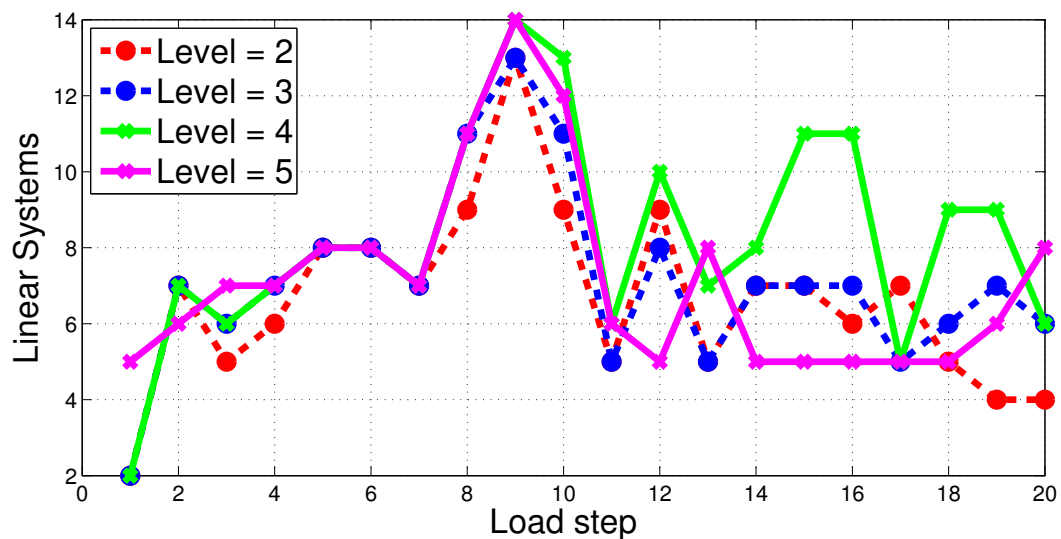
FIGURE 11.9. Number of linear systems for (ALM) in the tensile phase $t \in [0, 1]$ for different levels of mesh refinement.

(ALM) step	Level 2	Level 3	Level 4	Level 5
0	2.089e-02	1.828e-02	1.686e-02	1.601e-02
1	3.858e-00	4.557e-00	4.788e-00	4.872e-00
2	1.970e-01	3.445e-01	2.115e-01	9.035e-01
3	2.058e-02	3.895e-02	3.393e-02	3.231e-02
4	8.661e-03	1.682e-02	1.095e-02	3.425e-04
5	1.266e-05	3.171e-05	8.232e-03	1.096e-06
6	4.687e-08	1.285e-06	1.225e-02	2.291e-08
7	2.063e-09	2.172e-09	1.223e-02	1.976e-09
8			3.283e-05	
9			4.340e-07	
10			2.171e-09	

TABLE 11.11. (ALM) convergence in time step 15.

by looking at Figure 11.10 which provides a magnified view on the load-displacement curves.

3.2.2. *Parallel Performance.* We briefly consider the parallel performance and efficiency. All computations were performed at the parallel cluster InstitutsCluster [**KIT10**] at the Steinbuch Center for Computing (SCC) of the Karlsruhe Institute of Technology (KIT). Computational details are shown in Table 11.12. Having a closer look at the table, the parallel scale-up (concerning the total runtime) is not optimal when the problem size is scaled with the resources (asymptotically the problem size increases by a factor of 8 with each additional mesh refinement level). The main reason for this is the direct parallel solver for the coarse grid problem in the multigrid method which requires a lot of communication. Nevertheless, we used this coarse grid solver for stability reasons. As observed in [**Mül09**, Chapter 4.4], a better parallel scaling can be obtained by using an iterative linear solver for the coarse grid problem at the expense of robustness near the limit load. But as our primary interest is the performance of the nonlinear solution algorithm, we decided for the more robust variant. Additionally, despite non-increasing total numbers of linear systems (Figure 11.9) from level 4 to 5, the occuring linear subproblems are harder to solve for higher levels of mesh refinement. This is to be expected for the perfectly plastic model. To give an example: in time step 9, 14 linear systems have to be solved on mesh refinement levels 4 and 5. But whereas on level 4, only 92 multigrid

Level	#Processors	Total memory	Linear Systems	Total Runtime
5	512	$\leq 1\,024\,\text{GB}$	143	6 h 48 m
5	256	$\leq 1\,024\,\text{GB}$	143	7 h 37 m
4	128	$\leq 128\,\text{GB}$	165	2 h 21 m
4	64	$\leq 128\,\text{GB}$	165	4 h 10 m
4	32	$\leq 128\,\text{GB}$	165	4 h 58 m
3	16	$\leq 16\,\text{GB}$	143	1 h 35 m
3	8	$\leq 16\,\text{GB}$	143	3 h 14 m
3	4	$\leq 16\,\text{GB}$	143	3 h 47 m

TABLE 11.12. Comparison of the total runtime for different numbers of processors on different levels of mesh refinement.
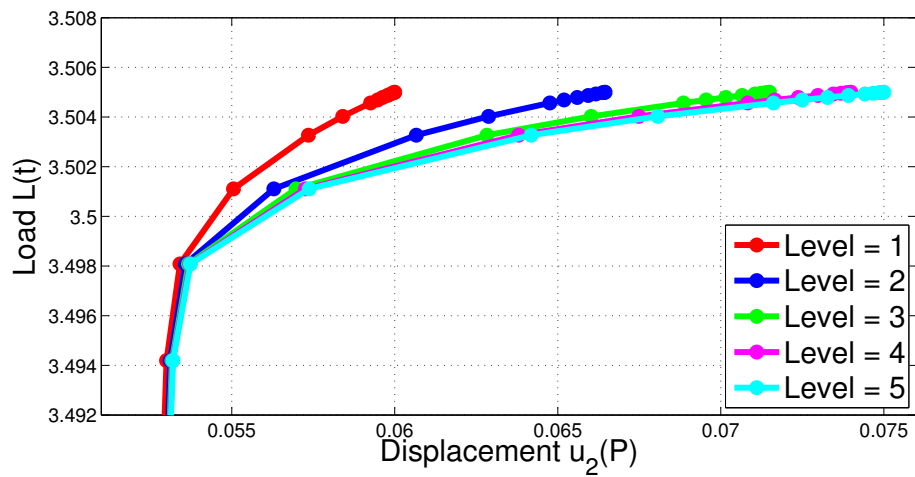
(a) Load-displacement curve at P.
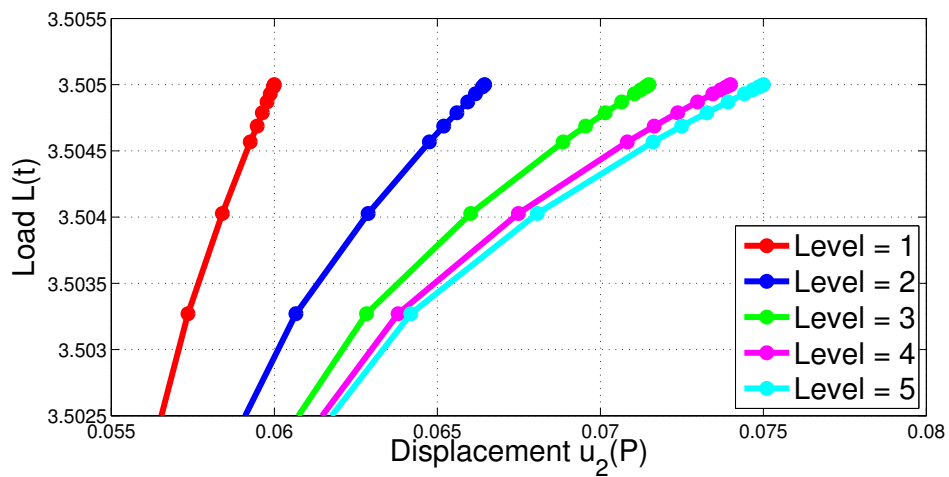
(b) Zoom in load-displacement curve at P.

FIGURE 11.10. Load-displacement curves at $P = (3, 22, 2)$ for different levels of mesh refinement. We observe linear convergence.

cycles were necessary for the solution of the linear systems, this number increases to 106 multigrid cycles on level 5. This gives an additional contribution to the total runtime.

3.2.3. *Graphical Illustration.* We close the section with some illustrations. Figure 11.11 shows the obtained displacements at the end of the tensile phase. The displacement is scaled 50 times and clearly shows the expected necking behavior within the lower part of Ω. Besides the vector norm, also the individual displacement components are shown. The equivalent stress $|\operatorname{dev}(\boldsymbol{\sigma})|$ is shown in Figure 11.12 for different loads. Whenever $|\operatorname{dev}(\boldsymbol{\sigma})| = K_0 = 400\,\text{MPa}$, plastic behavior is to be expected. As it can be seen, plastic deformation starts at the reentrant corner and the reentrant edges, where a singularity has to be expected even in the case of elasticity. However, if the load is further increased the whole lower part plastifies. This can also be seen in Figure 11.13 which shows the development of the accumulated plastic strain $\int_0^{t_n} |\dot{\boldsymbol{\varepsilon}}_p(t)|\,dt \approx \sum_{l=1}^{n} |\boldsymbol{\varepsilon}_p^l - \boldsymbol{\varepsilon}_p^{l-1}|$ during the tensile phase. Starting at the edges, more and more plastic deformation sets on in the area with smaller cross-section. Please note that in that zone, plastic deformation sets on just after about 99.7% of the maximum load is applied, cf. Figure 11.13(c–f) where no plastic deformation is found in that part of Ω. But afterwards, very small changes in the applied load cause a rapid development of plastic strains in that region. Contrary, on the bulk upper part, no plastic deformation is encountered.

(a) Vector norm $|\boldsymbol{u}(x,1)|$

(b) x_1-displacement $\boldsymbol{u}_1(x,1)$

(c) x_2-displacement $\boldsymbol{u}_2(x,1)$

(d) x_3-displacement $\boldsymbol{u}_3(x,1)$
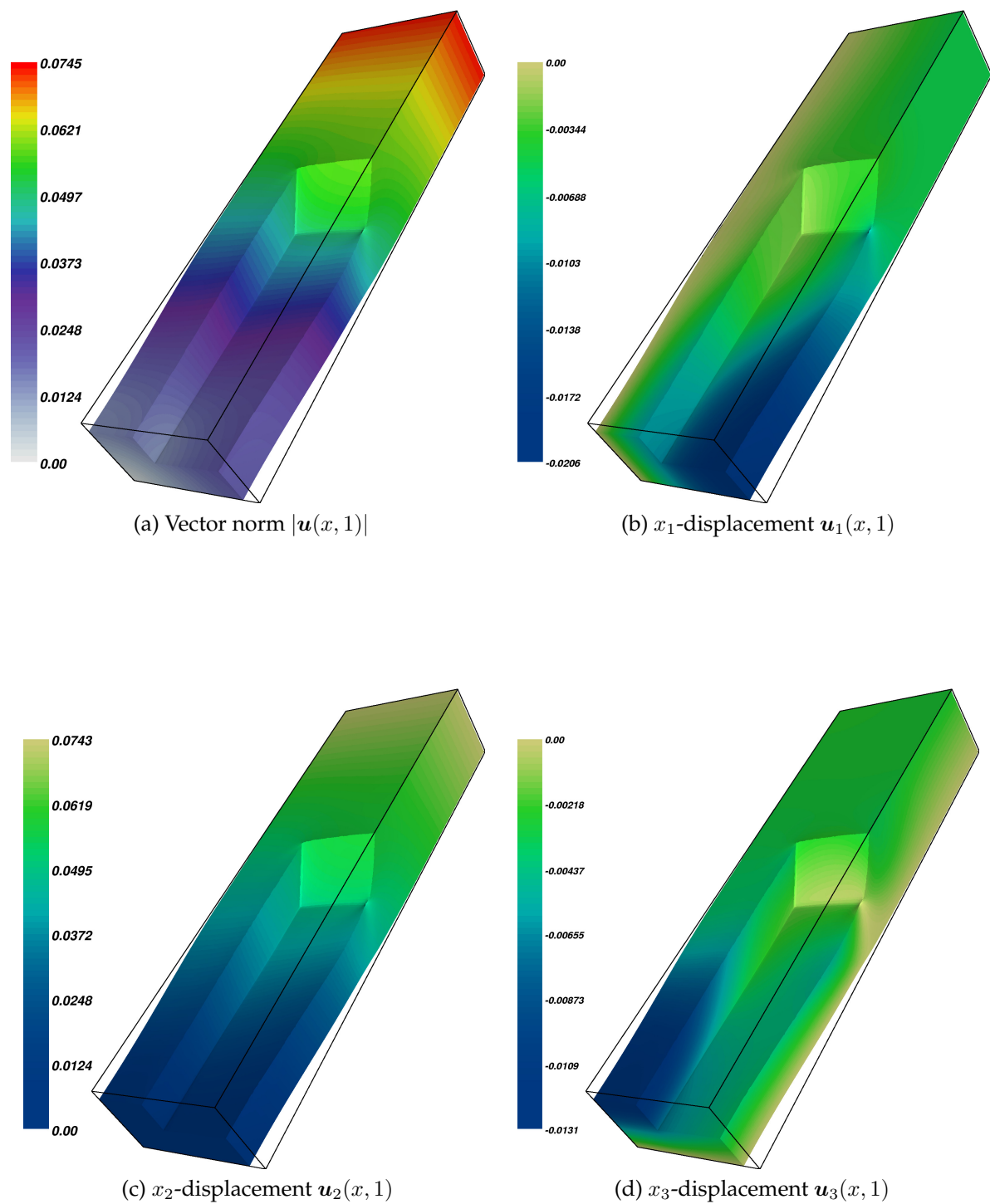
FIGURE 11.11. Displacement $\boldsymbol{u}(x,1)$ at the end of the tensile loading phase. The displacement is scaled 50 times and one can easily recognize necking behavior, i.e. a reduction of the cross-sectional area.

(a) 80.9% of the maximum load

(b) 97.25% of the maximum load
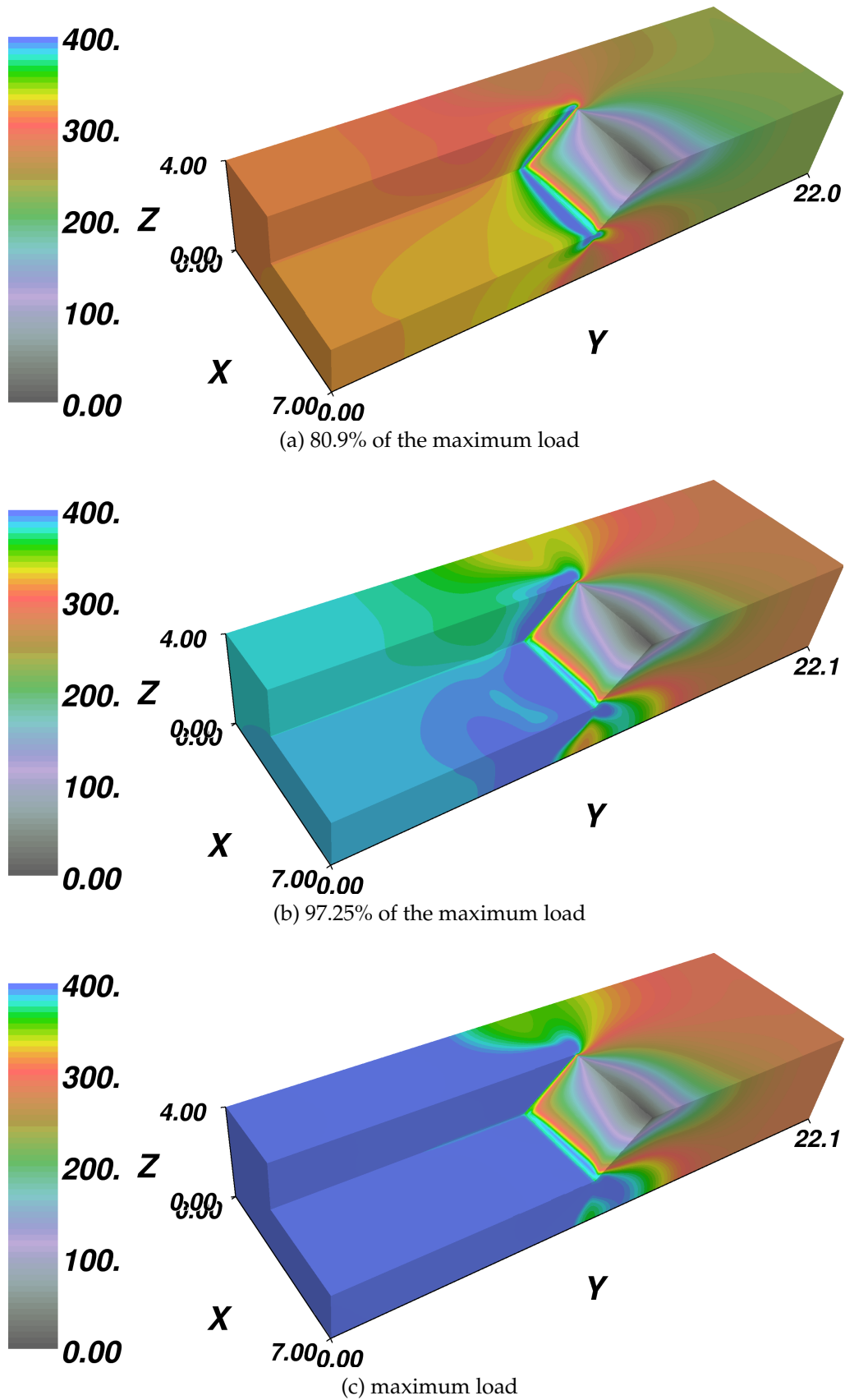
(c) maximum load

FIGURE 11.12. Equivalent stress $|\operatorname{dev}(\boldsymbol{\sigma}(x,t))|$ for different applied loads. Plastic deformation occurs whenever $|\operatorname{dev}(\boldsymbol{\sigma}(x),t)| = 400\,\mathrm{MPa}$, i.e. in the blue shaded areas.
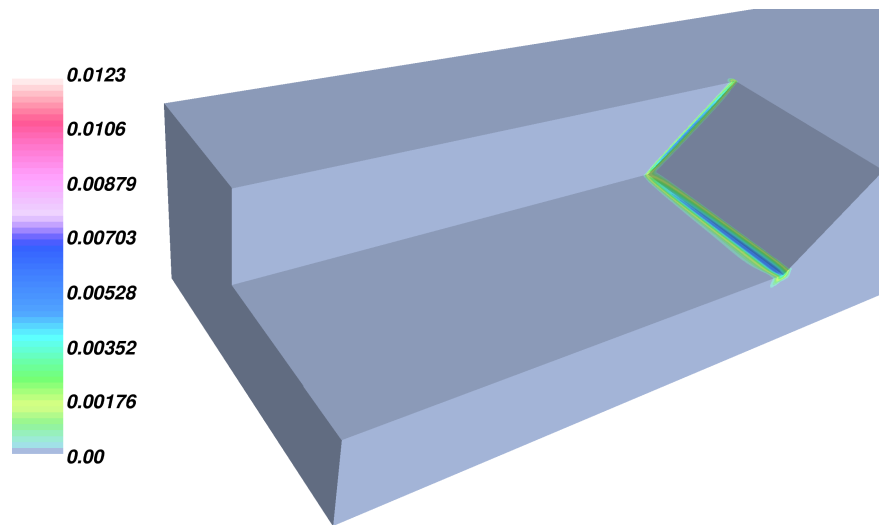
(a) 80.9% of the maximum load
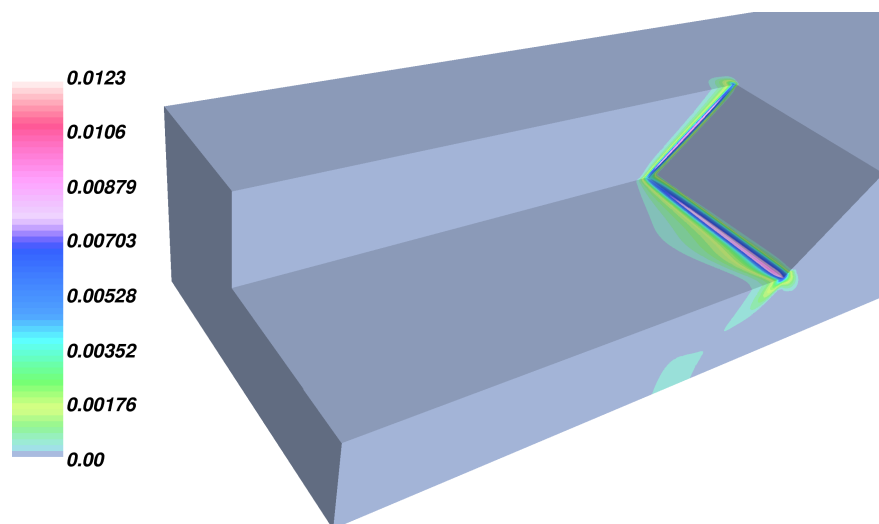
(b) 97.25% of the maximum load
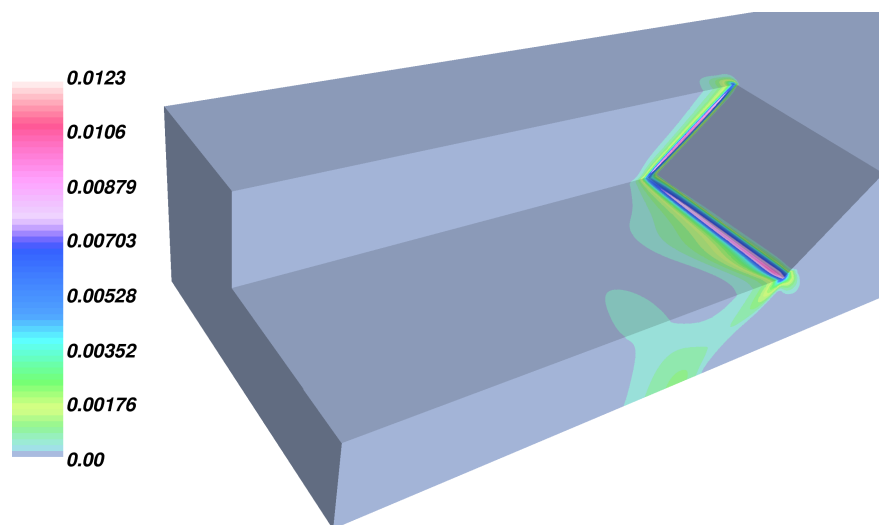
(c) 99.69% of the maximum load

FIGURE 11.13. Accumulated plastic strain $\int_0^{t_n} |\dot{\varepsilon}_p(x, t)| \, dt$.
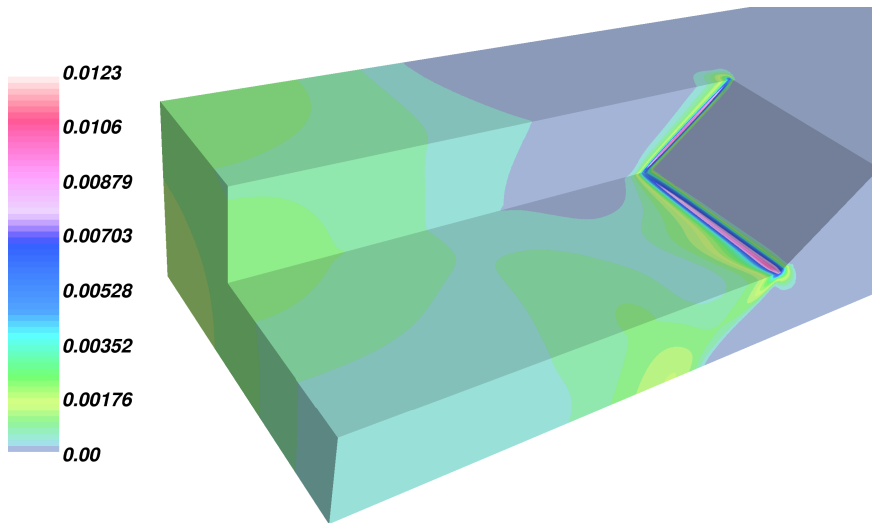
(d) 99.89% of the maximum load
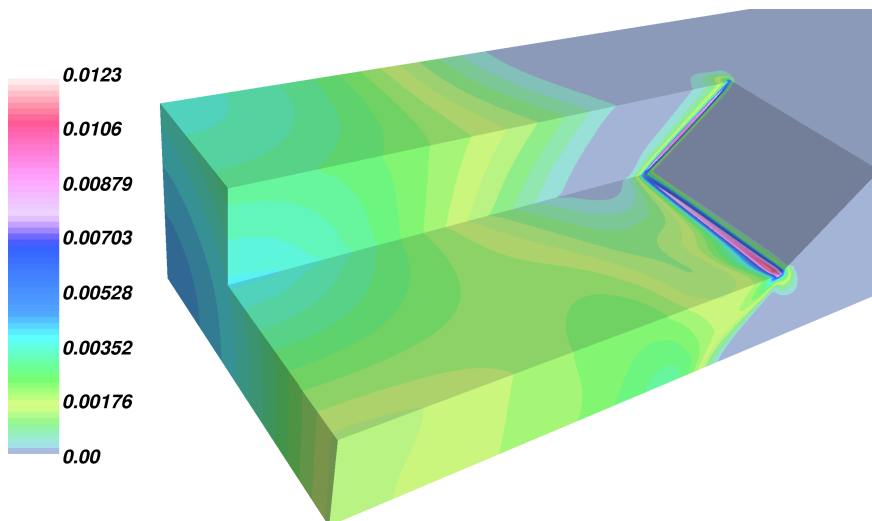
(e) 99.97% of the maximum load
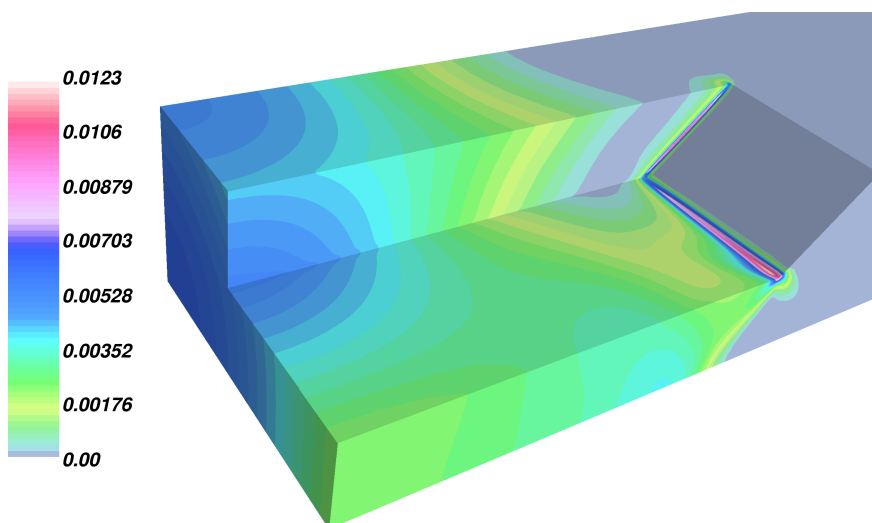
(f) Maximum load

FIGURE 11.13. Accumulated plastic strain $\int_0^{t_n} |\dot{\boldsymbol{\varepsilon}}_p(x, t)|\, dt$.

CHAPTER 12

NON-ASSOCIATED DRUCKER-PRAGER PLASTICITY

We begin with a numerical study in a two-dimensional setting. Particularly, we want to examine the interplay between non-associativity in perfect Drucker-Prager plasticity and mesh refinement on the other side. Since existence and uniqueness of solutions cannot be guaranteed, we expect to observe this ill-posedness in some way or the other. Additionally, we study the convergence properties of the return mapping algorithm and the active set method, before we turn to a three-dimensional slope failure problem.

1. A Study of Non-Associated Drucker-Prager Plasticity

1.1. Problem Setting. We consider one half of a strip footing, described by $\Omega = (0, 10)^2$ which has symmetry boundary conditions on the left and on the right w.r.t. the x_1-direction and which is fixed on the lower boundary. On the upper boundary, a compressive force is exerted as indicated in Figure 12.1 on half of the surface. We also consider the two control points $P = (0, 10)$ and $Q = (5, 5)$ at which we will consider load-displacement curves. The initial mesh consists of four quadrilateral cells as indicated in the graphic.

Level	5	6	7	8
Degrees of Freedom	8 450	33 282	132 098	526 338
Cells	4 096	16 384	65 536	262 144
Quadrature Points	16 384	65 536	262 144	1 048 576

TABLE 12.1. Computational details for the 2d example of the strip footing.

Looking back at Section 1.2.5, the yield function of Drucker-Prager plasticity is given by

$$f(\boldsymbol{\sigma}) = |\operatorname{dev}(\boldsymbol{\sigma})| + k_0(\tan\phi \frac{\operatorname{tr}(\boldsymbol{\sigma})}{3} - c),$$

169

(a) Full footing

(b) Computational domain
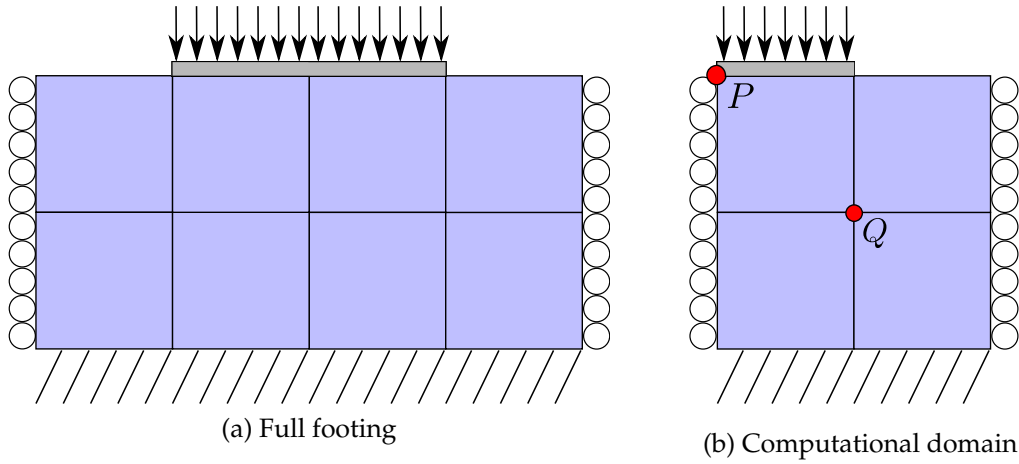
FIGURE 12.1. Geometry of the strip footing with points $P = (0, 10)$ and $Q = (5, 5)$.

with the angle of friction ϕ and the cohesion c. Non-associativity was introduced by means of the angle of dilatancy $\psi \leq \phi$ which is incorporated into the plastic potential

$$g(\boldsymbol{\sigma}) = |\operatorname{dev}(\boldsymbol{\sigma})| + k_0 (\tan\psi \frac{\operatorname{tr}(\boldsymbol{\sigma})}{3} - c) \,.$$

The used material parameters are presented in Table 12.2 and the ratio between the angle of friction and the angle of dilatancy determines the degree of non-associativity. In the next subsection, we will demonstrate that the choice of ψ has a significant impact on the material response.

Shear modulus:	μ	5.5	MPa
Bulk modulus:	κ	12.07	MPa
Cohesion:	c	0.01	MPa
Friction angle:	ϕ	30°	
Dilatancy angle:	ψ	$1 - 30°$	
Scaling factor:	k_0	0.7	

TABLE 12.2. Parameters for the 2d study of Drucker-Prager plasticity.

1.2. Load-Displacement Curves and the Effect of Non-Associativity. We begin with a study of the effect of non-associativity in perfect Drucker-Prager plasticity. Therefore, we study the load-displacement curves at the points P and Q for varying degree of non-associativity, i.e. for different choices of the angle of dilatancy ψ. The load-displacement curves are shown in Figure 12.2, and all curves were obtained on mesh refinement level 7 with variable time stepping. In P, the solution has symmetry boundary conditions w.r.t. x_1, thus we only consider the x_2-displacement $\boldsymbol{u}_2(P, t)$. This is depicted in Subfigure (a) and we see that the limit load decreases in non-associated materials. On the other hand, for fixed load, the non-associated material seems to exhibit larger displacements. We turn to the point Q, and Subfigure (b) shows the x_1-displacement $\boldsymbol{u}_1(Q, t)$. The obtained curve is similar to the first one. However, looking at the x_2-displacement $\boldsymbol{u}_2(Q, t)$ in (c), the situation changes significantly. Whereas for the associated material ($\psi = 30°$), we obtain a positive x_2-displacement once plastic deformation sets on, for the non-associated material we observe the opposite. This can also be seen in (d) where the path $Q(t)$ of

(a) Displacement $\boldsymbol{u}_2(P,t)$

(b) Displacement $\boldsymbol{u}_1(Q,t)$

(c) Displacement $\boldsymbol{u}_2(Q,t)$

(d) Path of the material point Q in the x_1–x_2 plane
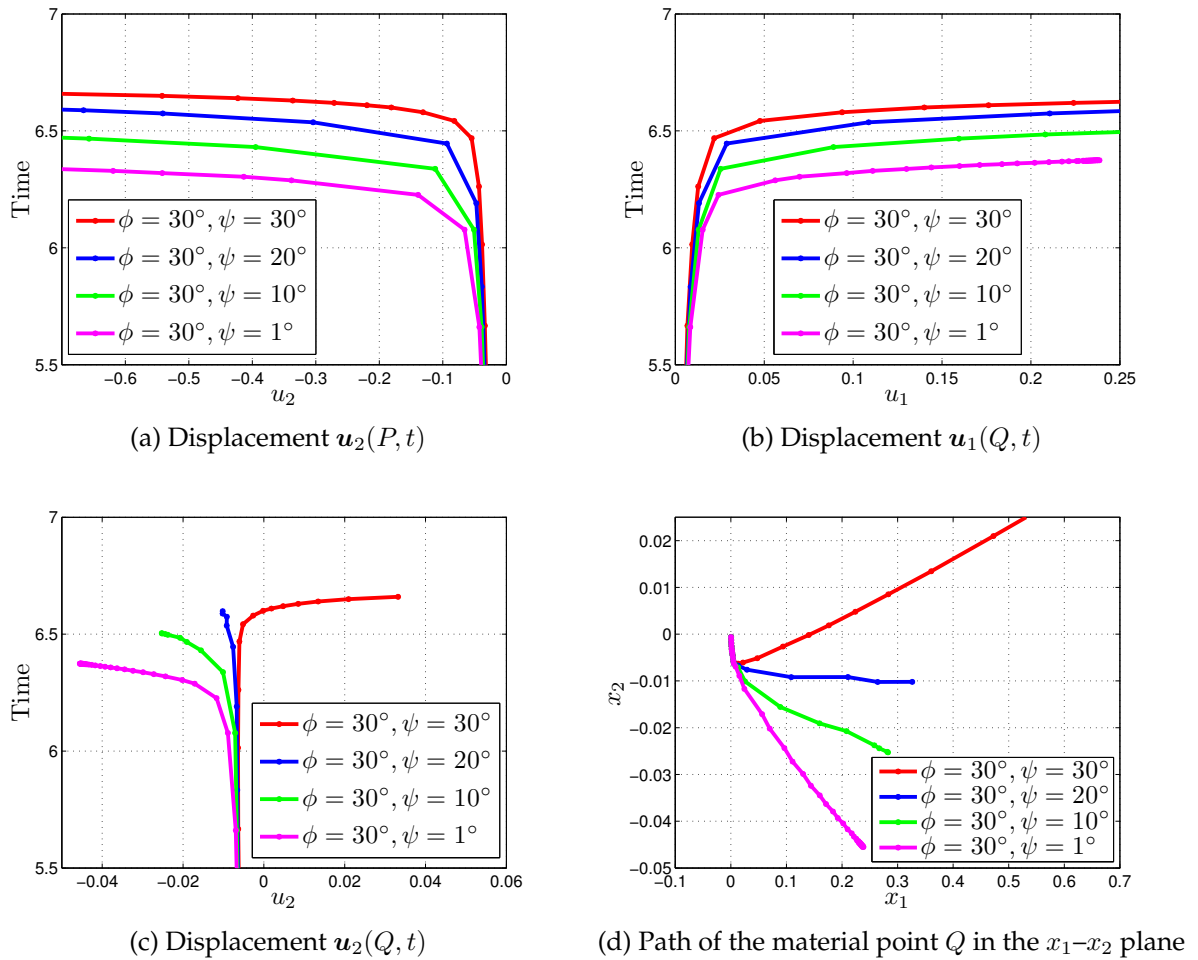
FIGURE 12.2. Load-Displacement curves at $P = (0,10)$ and $Q = (5,5)$.

the material point (or particle) Q is shown. Essentially, (d) is the combination of the displacements obtained in (b) and (c). For the associated material, the point moves upward, whereas for the non-associated material, it moves downward to the lower right bottom of the footing. This behavior can be explained as follows: since the associated material allows volumetric plastic strains, the pressure load produces large volumetric plastic strains below the load and the volume increases considerably. Since the load is directed into the negative x_2-axis, away from the region where the load is applied, the volume increase due to plastic deformation results in an upward movement of the material. For the non-associated material, the plastic volume increase is much smaller and the whole footing settles down.

A difference between associated and non-associated plasticity can also be recognized qualitatively when considering Figure 12.3. The subfigures show the vector-norm of $\boldsymbol{u}$ close to the limit load for $\psi = 30°$ and $\psi = 1°$. Whereas for the non-associated material ($\psi = 1°$), a sharp slip line is observable as it is also demonstrated in the magnified view (d), the associated material distributes the deformation into the whole domain Ω and the maximum displacement is observed on the free boundary and points upward. This is a result of the large volume change caused by plastic deformation which is not present in non-associated plasticity. In the magnified views around the point $(5,10)$, the vectors point into the direction of the displacement. Evidently, the associated material moves

upward, whereas the non-associated material hardly exhibits a vertical displacement. This can also explain the load-displacement curve 12.2(c), and 12.2(d), respectively.

(a) $\phi = \psi = 30°$ (associated).

(b) $\phi = 30°$ and $\psi = 1°$ (non-associated).

(c) $\phi = \psi = 30°$ (associated).

(d) $\phi = 30°$ and $\psi = 1°$ (non-associated).
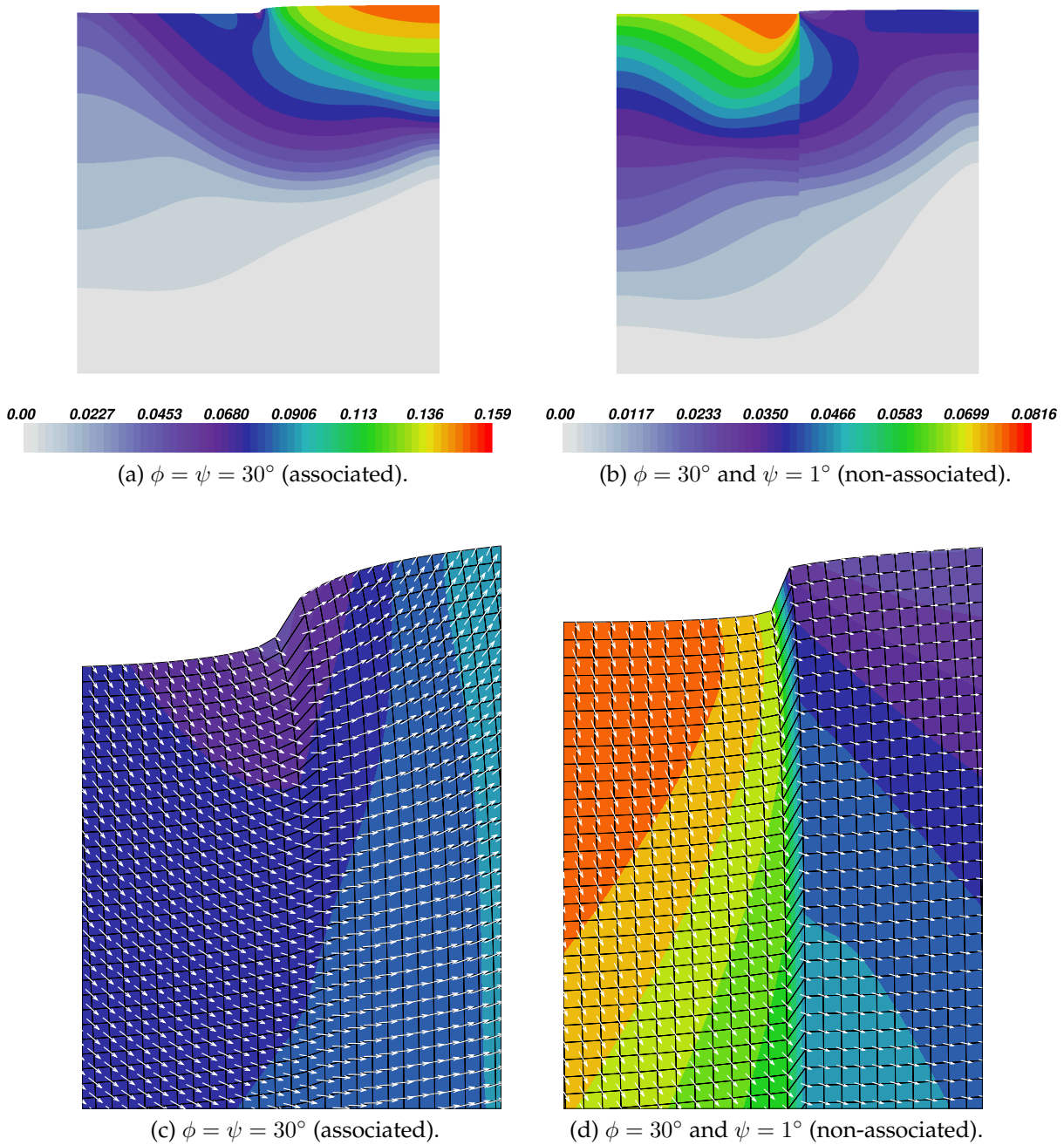
FIGURE 12.3. Qualitative difference between associated and non-associated plasticity. (a) and (b) show the vector norm $|u|$ on Ω. (c) and (d) magnify the region around $x = (5, 10)$.

1.3. Mesh Convergence. As outlined in the beginning of the section, non-associated perfect plasticity is generally ill-posed in the sense that existence and uniqueness of solutions is not guaranteed, also see Appendix B. Thus, if we progressively refine the mesh we expect to observe this behavior somehow. In Figure 12.4 we consider the load-displacement curves at P for associated and non-associated plasticity for different levels of mesh refinement. In associated plasticity, Subfigure (a) suggests that the load-displacement curve converges linearly if the mesh is refined. The same was already observed in the previous chapter for associated von Mises plasticity. Moreover, it appears that the load-displacement curve is well defined. Subfigure (b) considers non-associated plasticity with $\psi = 1°$. Apparently, there is some limit load in the sense that the computation could not proceed beyond that time instance. However, on refinement level 8, it seems that the material fails just after the elastic limit is reached and (c) provides a magnified view into the load-displacement curve on level 8. We observe that contrary to associated plasticity, the curve is non-monotone and the zig-zagging behavior seems to be an indicator for the ill-posedness of the model since the point P is just below the monotonically increasing load, and in a quasi-static setting (no dynamical forces), an increase of the vertical displacement $\boldsymbol{u}_2$ should not be possible. A closer look shows that this behavior, though not as obvious, also occurs for $\psi = 10°$ and $\psi = 20°$.

(a) $\phi = \psi = 30°$ (associated).

(b) $\phi = 30°$ and $\psi = 1°$ (non-associated).

(c) $\phi = 30°$ and $\psi = 1°$ (non-associated). Magnified view on level 8.
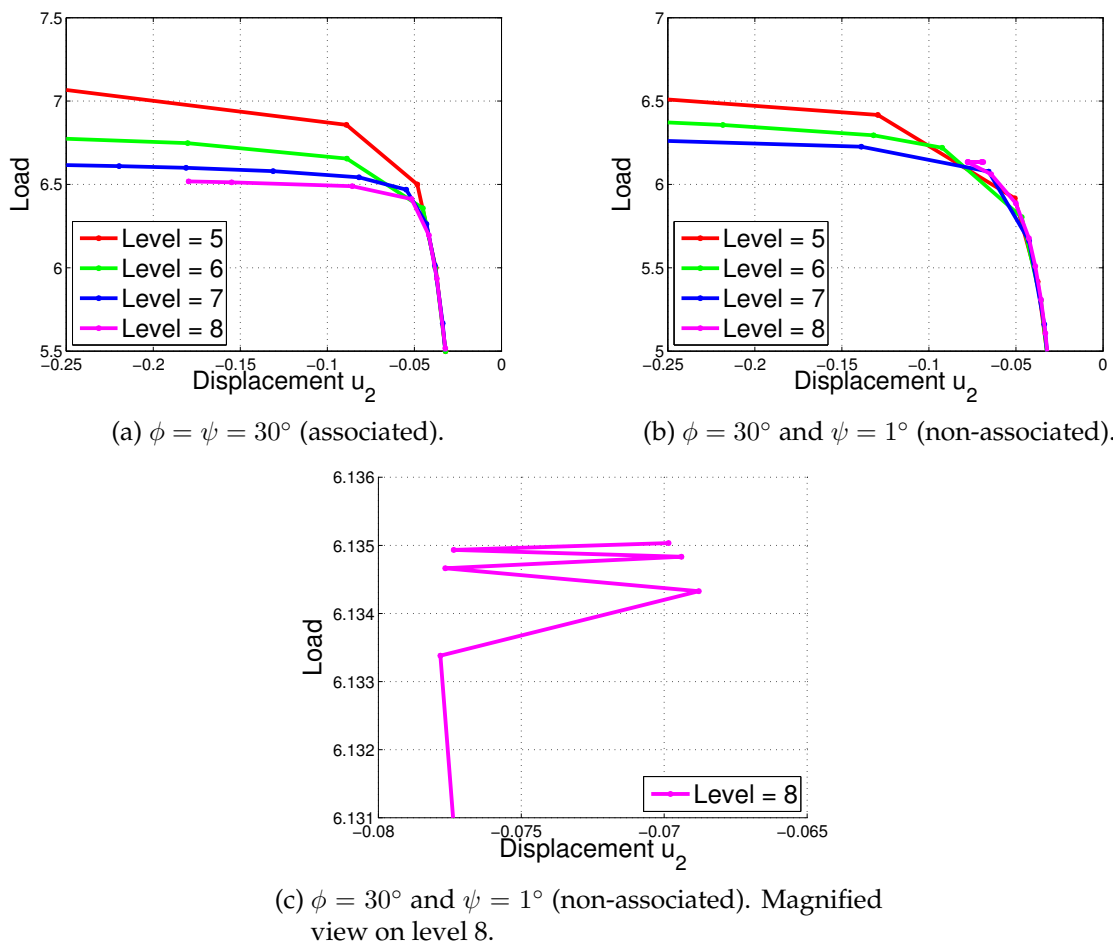
FIGURE 12.4. Load-displacement curves at P for different levels of mesh refinement.

1.4. Superlinear Convergence of (Smoothed) Drucker-Prager Plasticity. After having set the focus on the material model, we now have an eye on the convergence properties of the algorithms. Since the model is non-associated, we cannot use minimization algorithms due to the lack of a suitable merit function. Therefore, we focus on the generalized Newton method (RR) as introduced in Chapter 7 and also consider the active set method (AS) of Chapter 9. We expect at least superlinear convergence as a result of Sections 7.4 and 9.3. In order to observe the convergence behavior, we fix the angle of dilatancy at $\psi = 15°$ and the angle of friction at $\phi = 30°$. Besides the Drucker-Prager model, we also consider the smoothed Drucker-Prager material model for which we choose the smoothing parameter $\theta = 0.0001$. The active set method (AS) is only applied to the smoothed Drucker-Prager model, since the yield function / plastic potential in Drucker-Prager plasticity is not even differentiable. The parameter γ in the active set method was chosen to be $\gamma = 0.0001$. Concerning the dependence of (AS) on γ, we obtained similar results as in the previous chapter, i.e. smaller values of γ seem to be favorable.

For the convergence study, the time interval $[0, 6]$ is uniformly partitioned into 60 time steps corresponding to a fixed time step size $\Delta t \equiv \Delta t_n = 0.1$. In Table 12.4, we present the convergence behavior at different time steps. By (RR), we again denote Algorithm 8.1 with the simple backtracking line search (Algorithm 8.2) and similarly, (AS) again denotes Algorithm 9.1 without a globalization technique. The lack of a globalization technique for the active set method is also the reason why we consider relatively small time steps Δt. Nevertheless, in some time steps, the active set method did not converge since the initial guess was not good enough. In these cases, the time step size was successively halved until the method converged. This occured in the time steps from $4.5 \ldots 4.6$, $4.6 \ldots 4.7$ and $4.9 \ldots 5.0$. Afterwards, the method converged with the full step size up to $t = 6.0$.

For the smoothed Drucker-Prager model, the response function $R : \mathrm{Sym}(d) \to \mathrm{Sym}(d)$ cannot be evaluated in closed form, cf. Section 7.4, and in each quadrature point, a nonlinear system of equations has to be solved. However, this has almost no effect on the total runtime since the evaluation of the response function is local and the largest part of the total runtime in spent for the solution of the linear systems. Using a direct parallel solver on 64 processors, concerning the total runtime for the 60 time steps, there is practically no difference between Drucker-Prager plasticity (where the response can be evaluated explicitly) and smoothed Drucker-Prager plasticity (where the response must be evaluated numerically), see Table 12.3. A comparison with the active set method is only meaningful as long as (AS) converged with the full time step size $\Delta t = 0.1$. As long as this was the case, (AS) was the fastest method.

Total Runtime for ...	(RR) DP	(RR) sDP	(AS) sDP
$t = 0 \ldots 4$ (40 time steps)	3 m 00 s	3 m 00 s	2 m 50 s
$t = 5 \ldots 6$ (10 time steps)	1 m 26 s	1 m 27 s	1 m 07 s
$t = 0 \ldots 6$ (60 time steps)	5 m 43 s	5 m 39 s	9 m 26 s***

TABLE 12.3. Runtime comparison on 64 processors on level 7. ***The total runtime for (AS) up to $t = 6.0$ is not meaningful since (AS) did not always converge for the given time step size.

Iteration	(RR) DP	(RR) sDP	(AS) sDP
0	4.429e-05	4.433e-05	1.891e-03
1	2.878e-05	4.428e-05	6.258e-06
2	1.024e-05	2.868e-06	1.267e-05
3	3.898e-07	9.588e-08	3.280e-07
4	1.139e-08	1.849e-09	2.176e-09
5	1.893e-14	2.495e-15	4.194e-12

(a) Time step 20

Iteration	(RR) DP	(RR) sDP	(AS) sDP
0	8.205e-05	8.214e-05	2.128e-03
1	8.312e-06	8.268e-06	7.856e-06
2	4.469e-07	4.355e-07	1.209e-06
3	1.534e-08	2.199e-08	9.137e-09
4	4.636e-14	7.875e-14	2.813e-11

(b) Time step 40

Iteration	(RR) DP	(RR) sDP	(AS) sDP
0	2.840e-04	2.840e-04	2.687e-03
1	1.464e-04	1.494e-04	4.882e-05
2	5.026e-06	5.135e-06	2.960e-05
3	1.032e-06	1.095e-06	4.167e-07
4	3.432e-07	3.373e-07	5.580e-09
5	1.597e-07	1.520e-07	4.576e-09
6	6.924e-08	5.974e-08	1.339e-09
7	2.206e-08	1.132e-08	2.556e-10
8	1.554e-11	4.724e-13	5.780e-11

(c) Time step 60

TABLE 12.4. Convergence of the generalized Newton method (RR) and the active set method (AS) for the strip footing problem at different time steps. The computation was performed on mesh refinement level 7 with the non-associated model $\phi = 30°$ and $\psi = 15°$. Besides applying (RR) to the Drucker-Prager model (DP), we also consider (RR) and (AS) applied to the smoothed Drucker-Prager model (sDP) with smoothing parameter $\theta = 0.0001$, cf. Subsection 1.2.5. For (RR) DP and (AS) sDP, we expect quadratic convergence by Corollary 7.15 and Theorem 9.3, while we were only able to show superlinear convergence concerning (RR) sDP. Superlinear convergence can indeed be observed in all cases, but a difference between quadratic and superlinear convergence can hardly be observed in this application. Actually, the best convergence properties are even observed for (RR) sDP in this example.

2. A Slope Failure Problem

In this section, we consider a 3d slope failure problem. The slope geometry and boundary conditions are shown in Figure 12.5. Again, we use the Drucker-Prager material model model, but this time, we use the viscoplastic regularization with parameter $\alpha = 2000$. We remark that for the considered time step size $\Delta t_n \sim 0.1$, the regularization parameter α is far too large to fulfill the conditions of Corollary 5.6, i.e. we generally cannot expect the existence of a unique solution. Though time has a physical meaning in viscoplasticity, the material response only depends on the product $\alpha \Delta t$ and therefore the considered time horizon $[0, 3.5]$ is somewhat artificial. Using the correspondence between viscoplasticity and kinematic hardening plasticity, the material response is similar to kinematic hardening plasticity with hardening modulus $\mathbb{H} = H_0 \mathbb{C}$ and $H_0 = \frac{1}{1+\alpha\Delta t} \sim 0.005$. For the computation, we use (RR), i.e. Algorithm 8.1 with the simple backtracking line search 8.2. Similarly to the previous section concerning (AS), in some time steps, the generalized Newton method (RR) did not converge for the given time step size and in this situations the time step size was halved until the generalized Newton method converged. We remark that in this case, the material response is less stiff due to the reduction of the relative relaxation $\alpha \Delta t_n$.

The material parameters can be found in Table 12.5. Within Ω, a body force is prescribed (gravity) and on a part of the upper boundary (the blue shaded area in Figure 12.5), also a traction force applies. The loading regime is as follows: up to time $\widehat{t} = 1$, the gravity force is applied incrementally and afterwards kept constant whereas no traction force is applied up to $\widehat{t}$. Beyond $\widehat{t}$, the traction force is increased linearly with time. As a result of the geometry, during the gravity loading phase, the deformation is homogeneous w.r.t. the x_1-direction. But after $t = \widehat{t}$, the deformation is fully three dimensional since the traction force triggers a 3d shear band. With the functions $L_g(t) = \min\{t, \widehat{t}\}$ and $L_t(t) = \max\{0, t - \widehat{t}\}$, the load functional takes the form

$$\ell(t, \boldsymbol{w}) = -L_g(t) \int_\Omega \gamma \boldsymbol{w}_3(x)\, dx - L_t(t) \int_0^3 \int_9^{12} \frac{1}{400} \boldsymbol{w}_3(x_1, x_2, 6)\, dx_2\, dx_1\,.$$

The loading process is also illustrated in Subfigure 12.5(b). The slope geometry is such that plastic behavior already sets on in the gravity loading phase, i.e. the self-weight of the slope triggers plastic deformation and as indicated above, this deformation is homogeneous w.r.t. the x_1-direction due to the geometry of Ω.

Shear modulus:	μ	5.5	MPa
Bulk modulus:	κ	12.07	MPa
Cohesion:	c	0.008	MPa
Friction angle:	ϕ	25°	
Dilatancy angle:	ψ	$5 - 25°$	
Scaling factor:	k_0	0.7	
Specific weight:	γ	0.033	MPa/m
Viscoplasticity:	α	2000	1/s
Time step size:	Δt	~ 0.1	s

TABLE 12.5. Parameters for the slope failure problem.

Table 12.6 presents the computational details. In each quadrature point, the history variable ε_p^{n-1} needs to be stored for the computation. Again, we also consider load-displacement curves at two different points. The points $P = (0, 4, 4)$ and $Q = (4, 12, 3)$ are also marked in Figure 12.5.

Level	0	1	2	3	4	5
Degrees of Freedom	4392	14943	108 603	826 995	6 452 451	50 973 123
Cells	512	4 096	32 768	262 144	2097152	16 777 216
Quadrature Points	4 096	32 768	262 144	2097152	16 777 216	134 217 728
Internal variables	24 576	196 608	1 572 864	12 582 912	100 663 296	805 306 368

TABLE 12.6. Computational details for the slope failure problem.

(a) 3d view of the coarse mesh.

(b) Loading regime.

(c) Projections of the geometry onto the x_1–x_2, x_1–x_3 and x_2–x_3 plane.
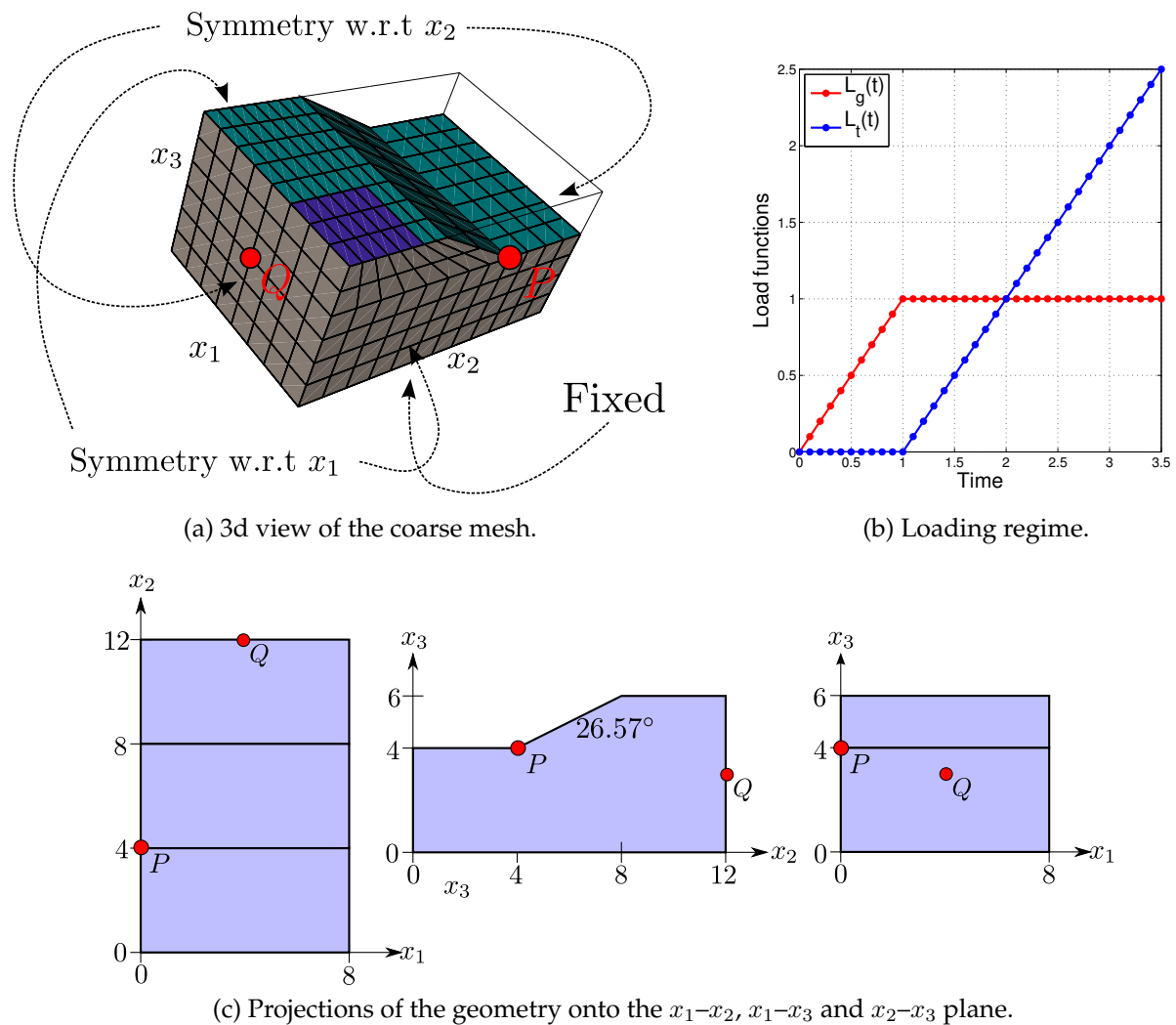
FIGURE 12.5. Geometry of the slope and the loading regime.

2.1. Load-Displacement Curves. On mesh refinement level 4 and for different angles of dilatancy ψ, we consider load-displacement curves at the points $P = (0, 4, 4)$ and $Q = (4, 12, 3)$ as well as the paths of the corresponding material points during the time interval $[0, 3.5]$. Subfigures 12.6(a,b) show the load-displacement curves w.r.t. the x_2- and x_3-component at P (note that $\boldsymbol{u}_1(P, t) = 0$ due to symmetry conditions). Qualitatively, the obtained curves are very similar for the different dilatancy angles. Nevertheless, having a closer look at the obtained displacements, there are significant differences, e.g. the final $\boldsymbol{u}_3(P, t)$ displacement in Subfigure (b). Subfigures (c,d) correspond to the paths of the material points. In the non-associated material, the total displacements in P are smaller for a given load when compared to the associated material. This can be explained by the larger volumetric plastic strains in the associated model.

It is interesting to observe that on mesh refinement level 4 and for $\psi = 5°$, the generalized Newton method always converged with the step size $\Delta t \equiv \Delta t_n = 0.1$, wheres for $\psi = 15°$ and $\psi = 25°$, it was necessary to halve the step size in some of the final time steps. This can also be recognized by having a closer look at the load-displacement curves. We just remark that for $\psi = 25°$ (corresponding to associated plasticity), more robust methods could have been used, cf. the previous Chapter.

(a) Displacement $\boldsymbol{u}_2(P)$.

(b) Displacement $\boldsymbol{u}_3(P)$.

(c) Path of the material point P (x_2-x_3 plane).

(d) Path of the material point Q (x_1-x_3 plane).
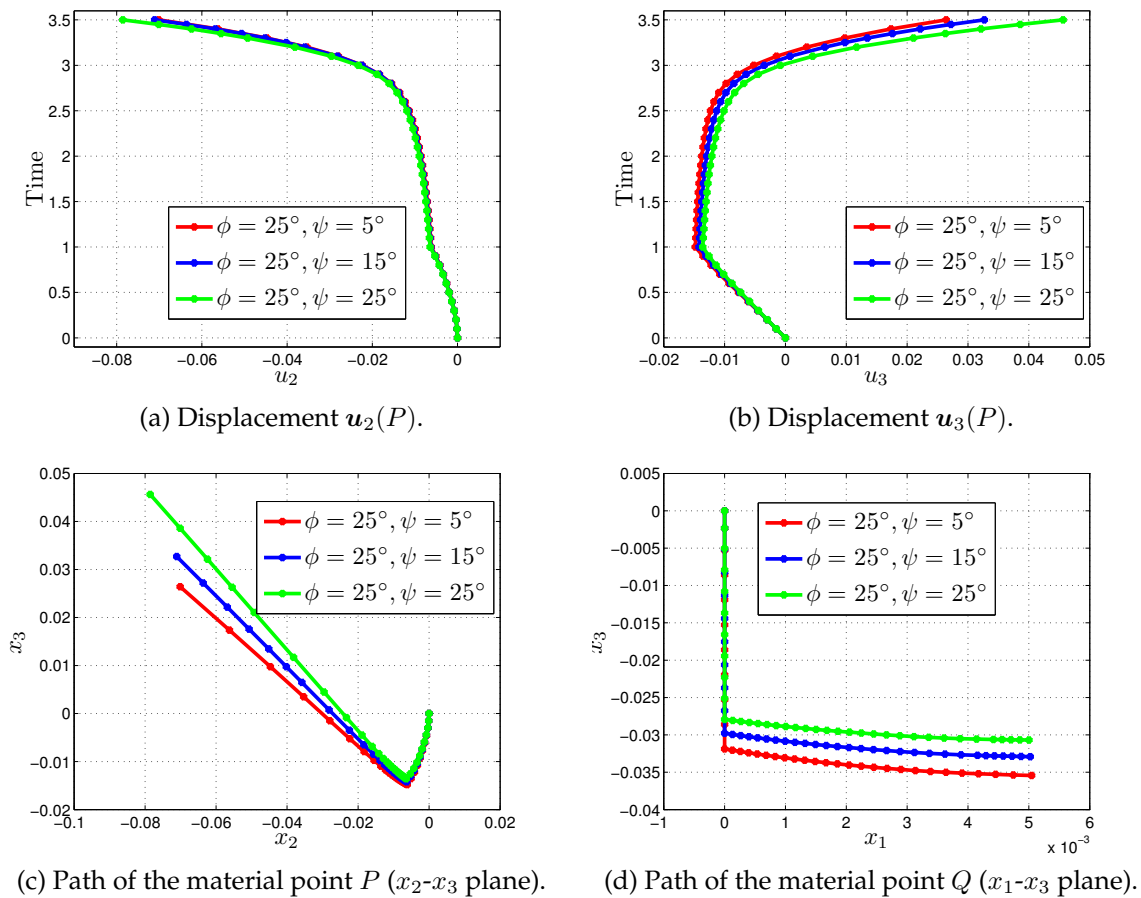
FIGURE 12.6. Load-displacement curves at $P = (0, 4, 4)$ and paths of the material points P and $Q = (4, 12, 3)$. The angle of friction is fixed at $\phi = 25°$ and we consider $\psi = 25°$ (associated) and $\psi = 15°$, $\psi = 5°$ (non-associated).

2.2. Mesh Convergence. Similar to the previous sections, we also consider the dependence on the mesh size h. For this, we examine associated Drucker-Prager plasticity ($\psi = 25°$) and the non-associated material ($\psi = 5°$). On mesh refinement level 5 and for $t \geq 3$, the generalized Newton method did not always converge for the time step size $\Delta t_n = 0.1$ and hence a comparison of the load-displacement curves is only reasonable up to time $t = 3$. From a theoretical point of view, for fixed α, the associated model admits uniform bounds (which however depend on α), cf. Subsection 10.2. In the following graphics, the results of associated plasticity are always illustrated with dashed lines, whereas the non-associated model is indicated by solid lines. We examine several quantities concerning their convergence as $h \to 0$. Particularly, these are $\|\boldsymbol{\sigma}\|_{\boldsymbol{\Sigma}}$, $\|\boldsymbol{u}\|$ and the load-displacement curves at P. The results can be found in Figures 12.7–12.10. In the first figure, the convergence of the stresses are observed. The curves of the associated model and the non-associated look very similar and a difference can only be observed in the magnified view. The norm $\|\boldsymbol{\sigma}\|_{\boldsymbol{\Sigma}}$ seems to converge linearly for both the associated
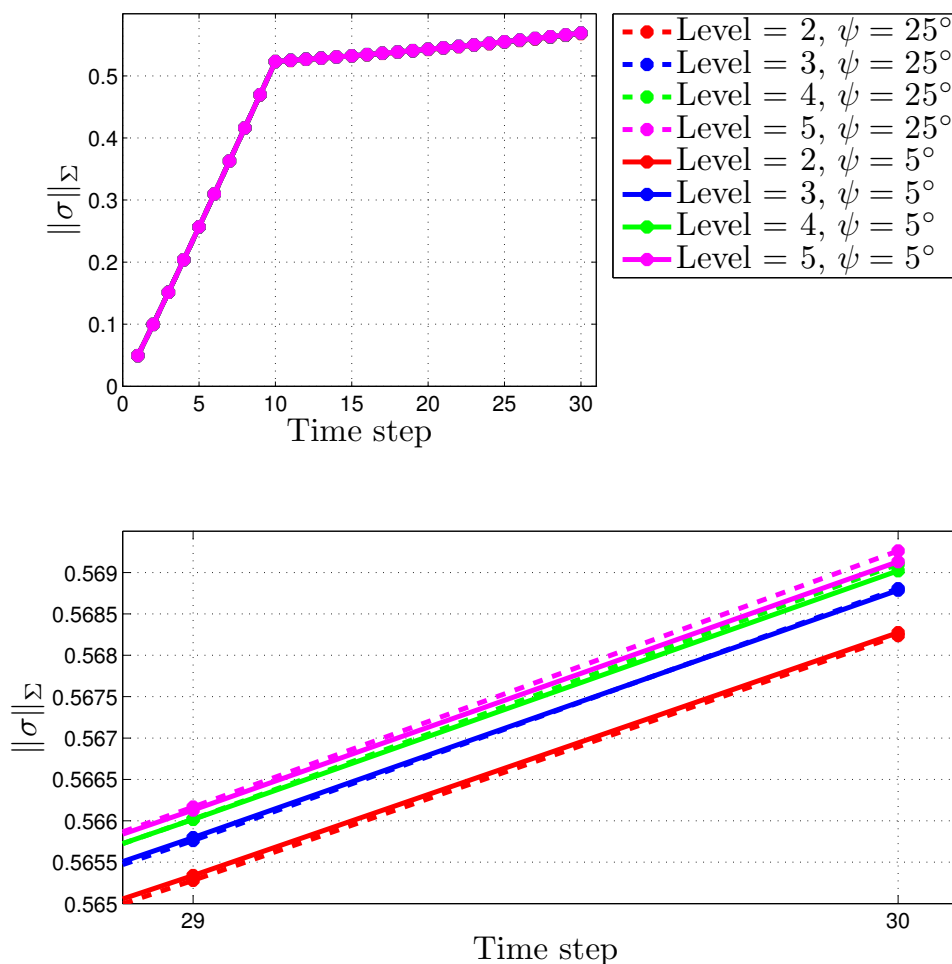
FIGURE 12.7. Convergence of $\|\boldsymbol{\sigma}\|_{\boldsymbol{\Sigma}}$ for $\phi = \psi = 25°$ (associated, dashed lines) and $\phi = 25°$, $\psi = 5°$ (non-associated, solid lines) for different levels of mesh refinement. The graphic suggests linear convergence for both models.

and the non-associated model. Conversely, convergence of the displacements in the energy norm remains unclear even for the associated model as can be seen in Figure 12.8. As this quantity is generally unbounded in the perfectly plastic setting, one explanation is that the mesh size still is too coarse to observe convergence for the given value of α. Concerning the non-associated model, the situation is even worse.

Looking at the load-displacement curves at P, the situation is similar. Surprisingly, the non-associated model seems to exhibit better convergence properties as it can be read off from Figures 12.9 and 12.10. However, looking at the second magnified view in Figure 12.9, we see that for the non-associated model, the curves on levels 2 and 5, and the curves on levels 3 and 4, are nearly identical at the end of the gravity loading phase. While the curves for the different levels of mesh refinement are always separated in the associated setting, this no longer holds true in the non-associated setting.
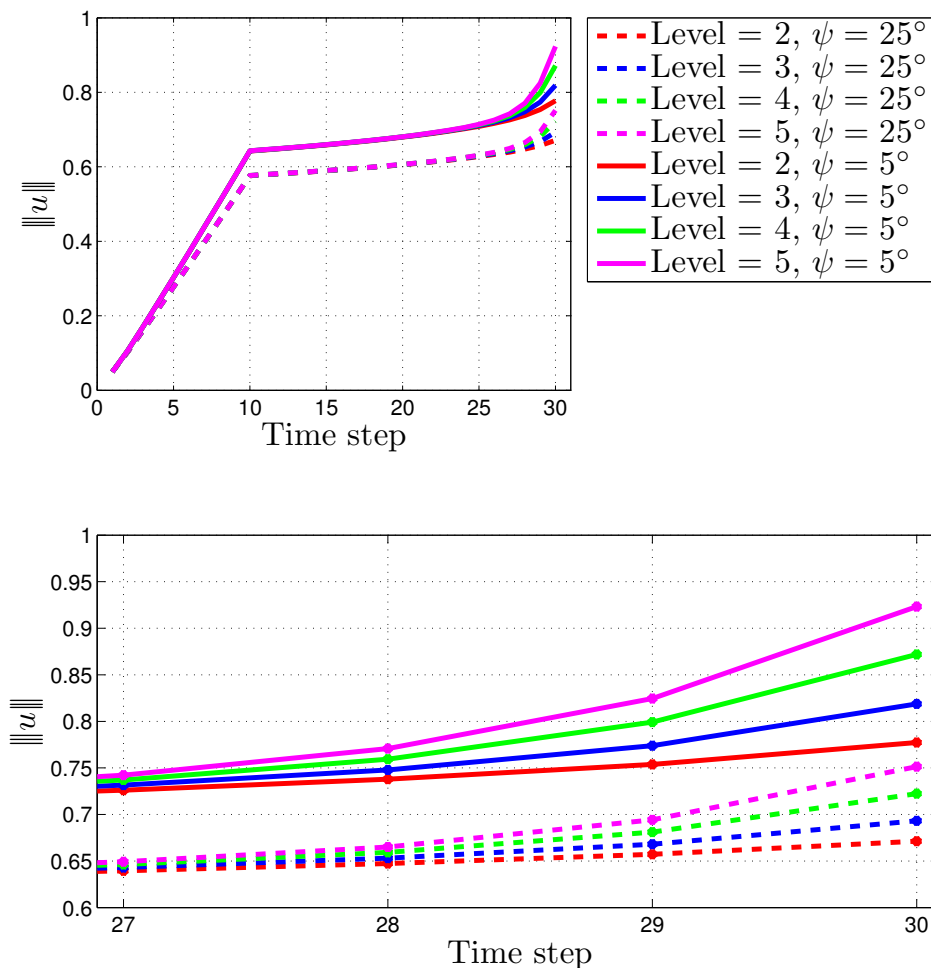
FIGURE 12.8. Convergence of $\|u\|$ for $\phi = \psi = 25°$ (associated, dashed lines) and $\phi = 25°$, $\psi = 5°$ (non-associated, solid lines) for different levels of mesh refinement. Convergence remains an open question for both models.
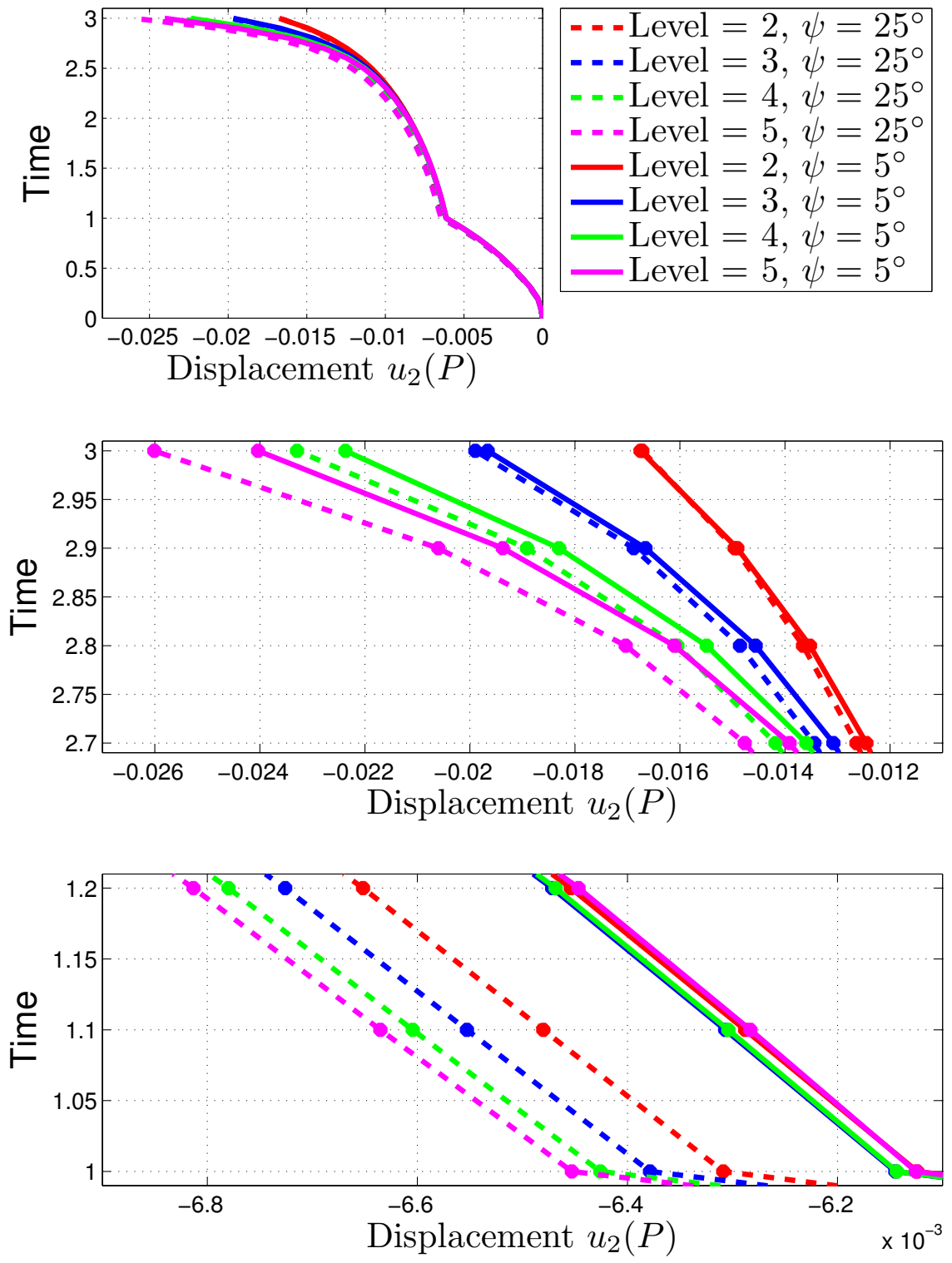
FIGURE 12.9. Load-displacement curve at P: x_2-displacement $\boldsymbol{u}_2(P, t)$.
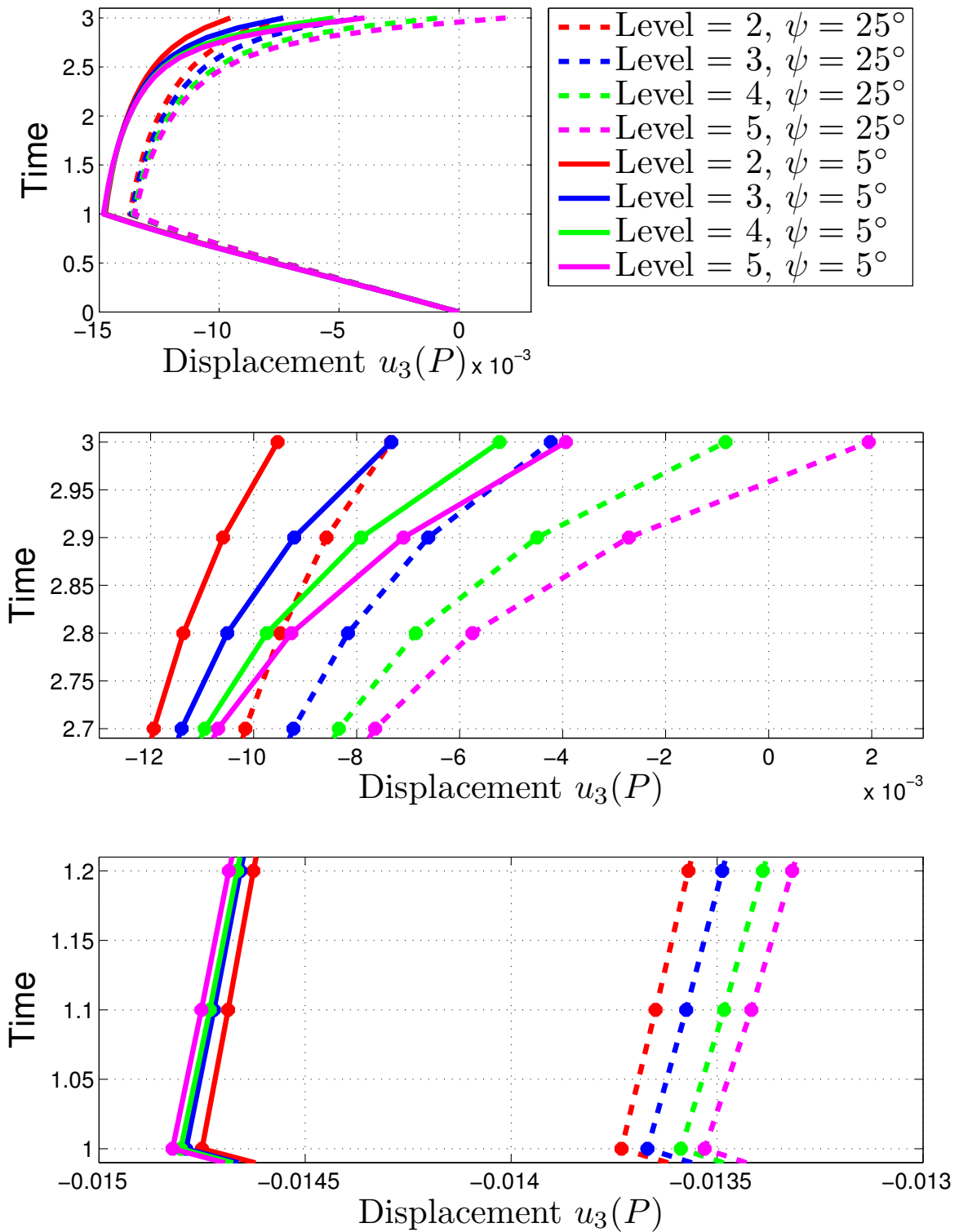
FIGURE 12.10. Load-displacement curve at P: x_3-displacement $\boldsymbol{u}_3(P, t)$.

2.3. Illustration. In the end, we want to give some graphical illustrations. Due to the large data sets, all graphics were produced on the basis of the computations on mesh refinement level 4 (to give an examples: for one time step, the data set of the displacement field has the size $\sim 320\,\text{MB}$). In Figure 12.11, the accumulated plastic strain $\int_0^T |\dot{\boldsymbol{\varepsilon}}_p(x,t)|\,dt \approx \sum_{n=1}^N |\boldsymbol{\varepsilon}_p^n(x) - \boldsymbol{\varepsilon}_p^{n-1}(x)|$ is shown for the associated model ($\psi = 25°$) and the non-associated model ($\psi = 15°$ and $\psi = 5°$). In all graphics, the same color scale is used and we observe that for decreasing angle of dilatancy ψ, the shear band localizes. The development of the shear band for $\psi = 5°$ is also shown in Figure 12.12. At the end of the gravity loading phase at $t = 1$, the deformation is homogeneous w.r.t. the x_1-direction and plastic strains occur at the toe of the slope and within the base. After $t = 1$, the load is applied on a part of the upper boundary. This triggers a three-dimensional deformation. For increasing load, large plastic strains are found beneath the load and moreover, a slip surface is created indicating a "toe failure", cf. Subfigures (d,e).

Figure 12.13 shows the final displacement (scaled by a factor of three) at time $T = 3.5$. Again, the same color scale is used for the associated and non-associated model and for smaller values of ψ, we obtain larger deformations below the load. At the toe of the slope however, the associated model tends to show larger displacements as it can easily be seen from the load-displacement curves of the previous Subsection, cf. Figures 12.9 and 12.10. Once more, this seems to be a consequence of the large volumetric plastic strains of the associated model. Finally, Figure 12.14 shows a magnified view of the x_2-displacement $\boldsymbol{u}_2(x,T)$ in the failure zone. In this graphic, also the mesh on refinement level 4 is indicated.
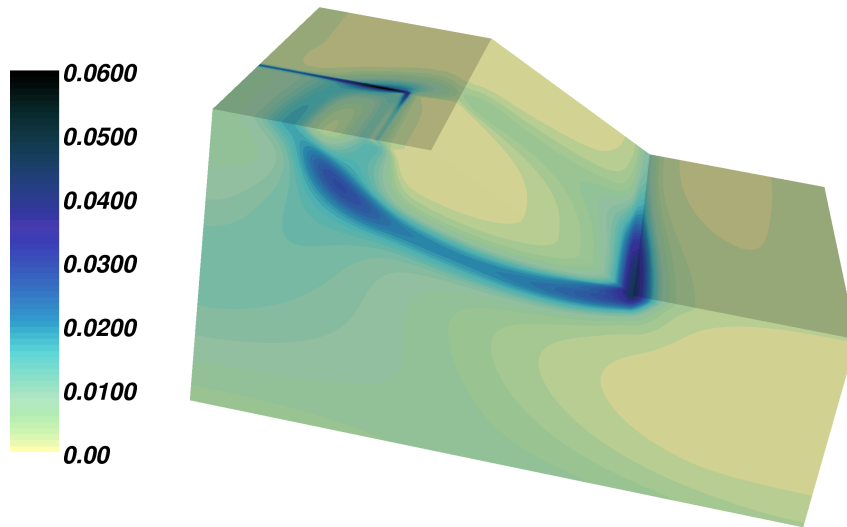
(a) $\phi = 25°$ and $\psi = 5°$ (non-associated).
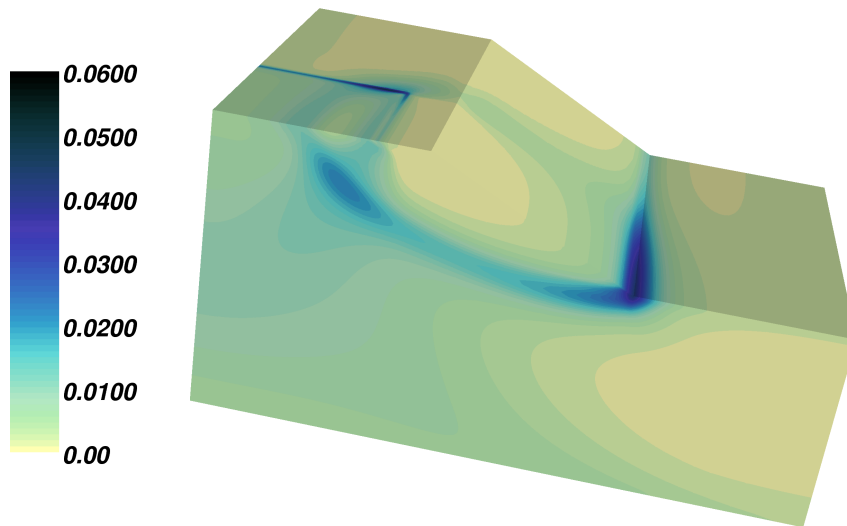
(b) $\phi = 25°$ and $\psi = 15°$ (non-associated).
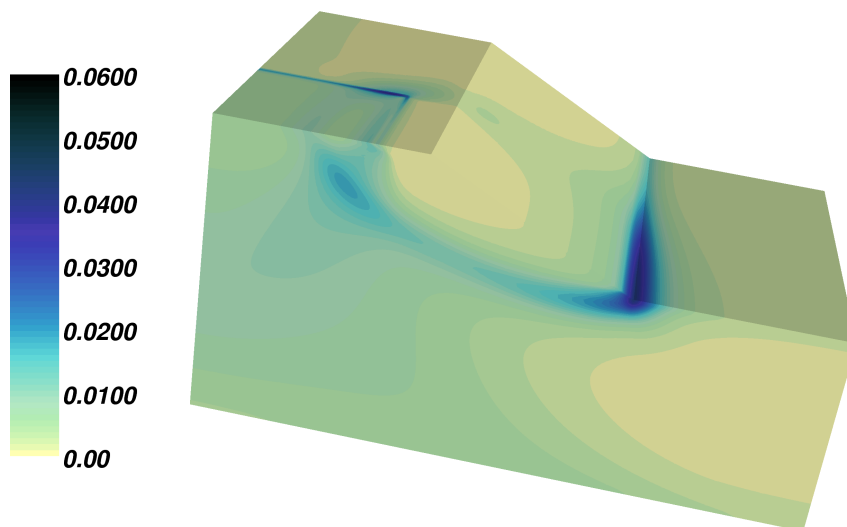
(c) $\phi = \psi = 25°$ (associated).

FIGURE 12.11. Accumulated plastic strain $\int_0^t |\dot{\varepsilon}_p(x,s)|\,ds$ at time $t = 2.9$ for different angles of dilatancy.
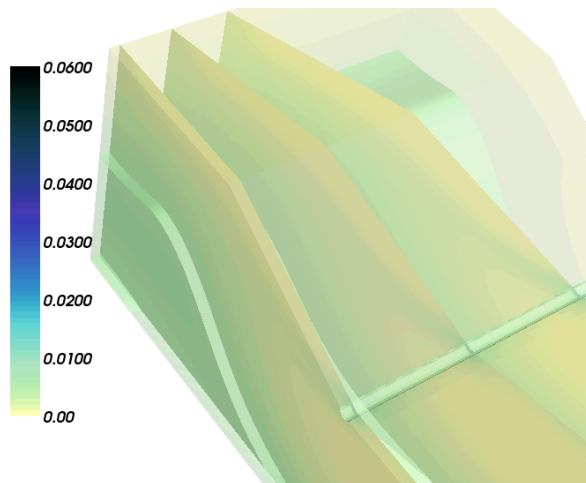
(a) $t = 1.0$, Isosurface at 0.005.
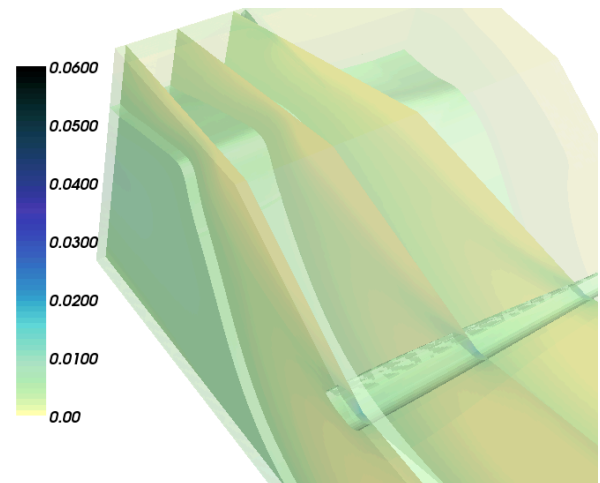
(b) $t = 2.0$, Isosurface at 0.005.
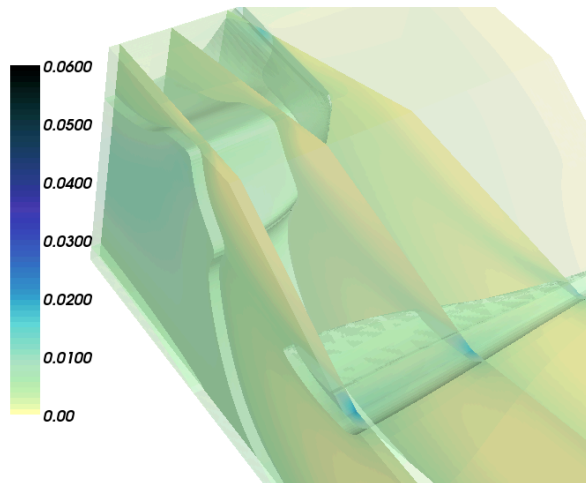
(c) $t = 2.5$, Isosurface at 0.007.
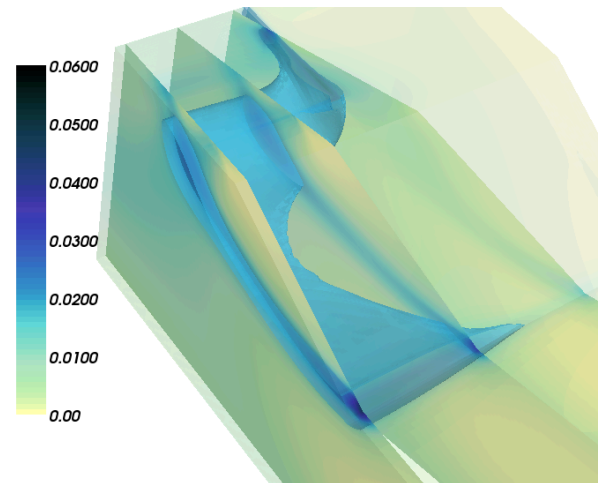
(d) $t = 2.9$, Isosurface at 0.02.
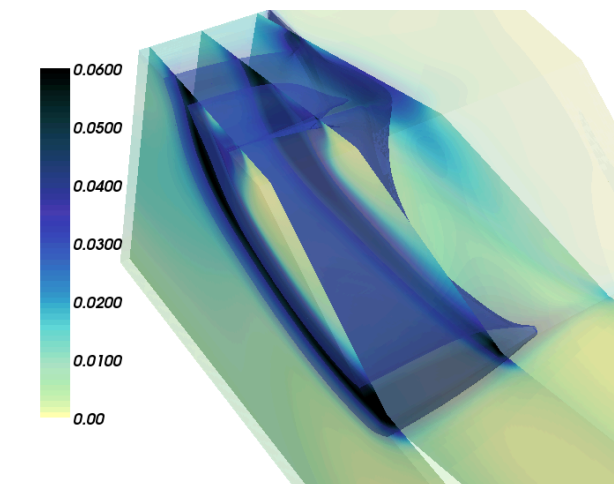
(e) $t = 3.2$, Isosurface at 0.04.
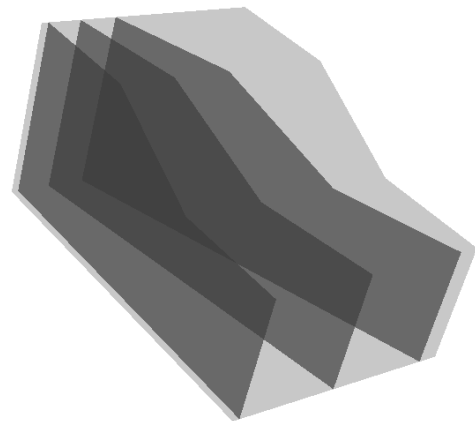
(f) Cutplanes.

FIGURE 12.12. Shear band development: $\phi = 25°$ and $\psi = 5°$ (non-associated).
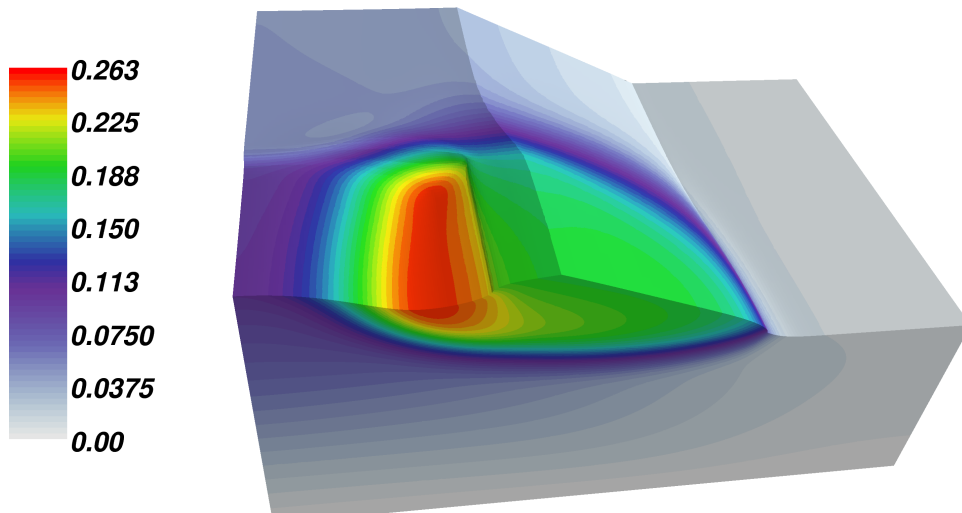
(a) $\phi = 25°$ and $\psi = 5°$ (non-associated).
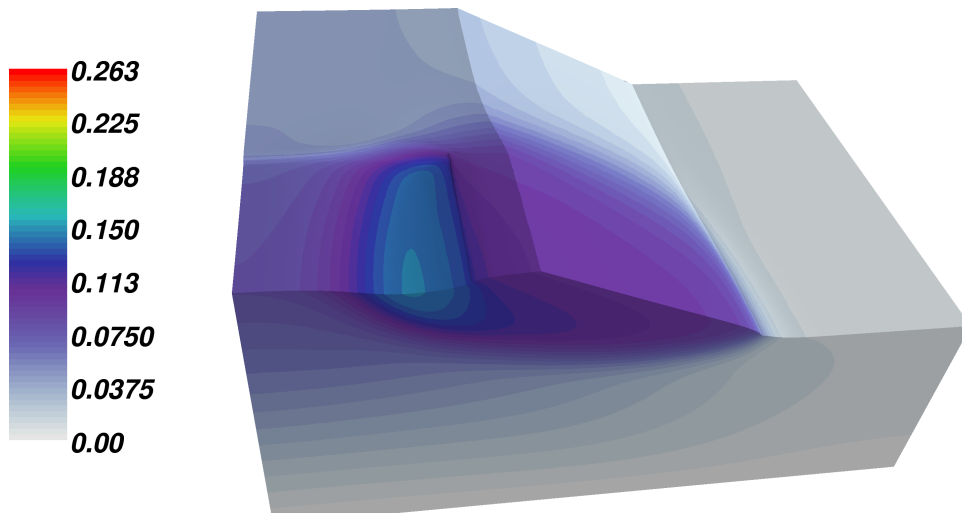
(b) $\phi = 25°$ and $\psi = 15°$ (non-associated).
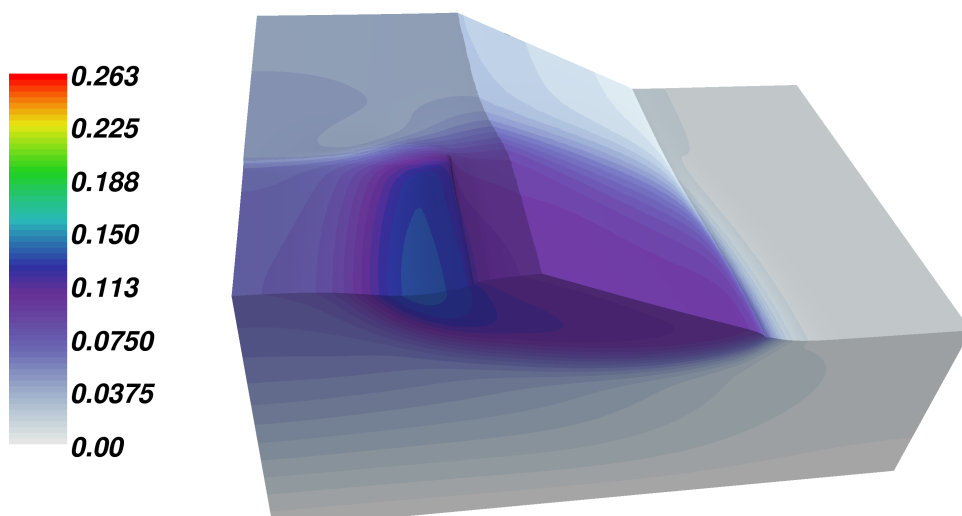
(c) $\phi = \psi = 25°$ (associated).

FIGURE 12.13. Displacement at final time $t = 3.5$ for different angles of dilatancy. The figures show the vector norm $|\boldsymbol{u}(x, 3.5)|$ and the displacement is scaled (only) three times.
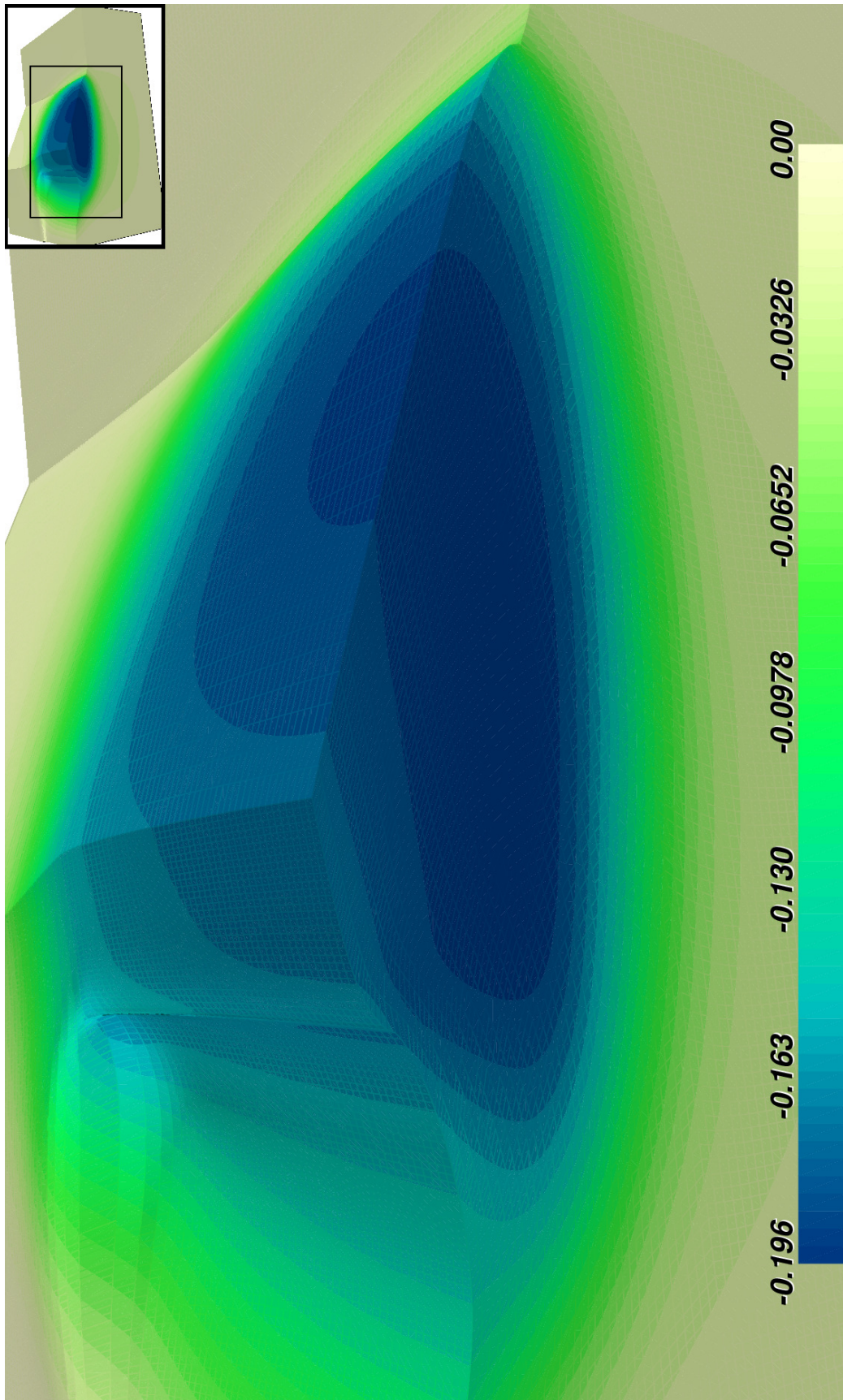
FIGURE 12.14. Magnified view of the u_2 displacement at time $t = 3.5$. The computation was performed on mesh refinement level 4 and the mesh is indicated in the graphic. Again, the displacement is scaled by a factor of three.

Part 4

Appendix

APPENDIX A

NONSMOOTH ANALYSIS AND THE PROJECTION OPERATOR

In this chapter, we provide a summary of results concerning nonsmooth analysis including generalized derivatives, implicit function theorems, semismoothness of functions and generalized Newton methods. We also consider properties of projection operators in finite dimensional spaces. Specifically, we will show the (strong) semismoothness of the projection operator for particular sets K. We do this in a more abstract framework and for convenience, this framework will be set in $\mathbb{R}^N$. We consider the projection operator $P : \mathbb{R}^N \to K \subset \mathbb{R}^N$ w.r.t. the inner product $a(x, y) = x^T A y$ and corresponding norm $|x|_A = \sqrt{a(x, x)}$ onto a closed convex set $K \subset \mathbb{R}^N$. Here, the matrix $A \in \mathbb{R}^{N,N}$ is symmetric and positive definite. It is well known that the projection $P(x)$ is characterized by the variational inequality

$$a\big(x - P(x), z - P(x)\big) \leq 0 \qquad z \in K\,,$$

and that for a given $x \in \mathbb{R}^N$, the projection is the unique solution of the minimization problem

$$\text{Minimize} \quad |y - x|_A \qquad \text{subject to} \quad y \in K\,.$$

In the associated norm, P is non-expansive, i.e. Lipschitz continuous with modulus 1,

$$|P(x) - P(y)|_A \leq |x - y|_A \qquad x, y \in \mathbb{R}^N\,.$$

As we have seen before, this characterization also holds in the infinite dimensional case. Analytically, the case $A = I$ is dominant. However, this is no limitation from an analytical point of view, since the projection can also be characterized as the solution of an equivalent Euclidian problem:

$$\text{Minimize} \quad |z - w| \qquad \text{subject to} \quad A^{-1/2} z \in K\,.$$

with the correspondence $w = A^{1/2} y$ and $z = A^{1/2} x$. Hence, everything that is valid for the Euclidean projection also holds true for the projection w.r.t. the norm $|\cdot|_A$.

1. Nonsmooth Analysis and Generalized Newton Methods

We shortly recapitulate some basic concepts of nonsmooth analysis, and in particular we consider different differentiability concepts for generally non-differentiable functions. The goal is to enlarge the class of functions for which a (generalized) variant of Newton's method converges superlinearly. After introducing some concepts particularly designed for finite dimensional spaces, we shortly consider the infinite dimensional case. Good references for this topic are [IK08, Section 8] and [PF03a, Section 7].

1.1. Basic Concepts of Nonsmooth Analysis – the Finite Dimensional Case. Let $F : \mathbb{R}^N \to \mathbb{R}^M$ be a function. If F is differentiable at $x \in \mathbb{R}^N$, then $DF(x) \in \mathbb{R}^{M,N}$ denotes the usual Jacobian. The *directional derivative* of F at x into direction $h \in \mathbb{R}^N$ is denoted by

$$DF(x; h) := \lim_{t \downarrow 0} \tfrac{1}{t} \big(F(x + th) - F(x) \big),$$

and if F is differentiable at x, we have $DF(x; h) = DF(x)h$. Moreover, the function F is *B(ouligand)-differentiable* at x if it is directionally differentiable at x and the directional derivative satisfies

$$\tfrac{1}{|h|} \big(F(x + h) - F(x) - DF(x; h) \big) = o(|h|) \qquad \text{as} \quad h \to 0, h \neq 0.$$

In the following we restrict ourselves to (locally) Lipschitz continuous functions and it is well-known that in this case, B-differentiability and directional differentiability are equivalent. Moreover, by Rademacher's theorem [CLSW98, Section 3.4], F is differentiable almost everywhere and by $\Theta_F \subset \mathbb{R}^N$, we denote the points where F is differentiable. The set

$$\partial^B F(x) := \{B \in \mathbb{R}^{M,N} : B = \lim_{y \to x, \, y \in \Theta_F} DF(y)\}$$

is the *B-subdifferential* of F at x and if F is differentiable at x, then $\partial^B F(x) = \{DF(x)\}$. Based on the B-subdifferential, Clarke's generalized Jacobian, cf. [Cla83], is given as the convex hull of the B-subdifferential,

$$\partial F(x) = \operatorname{conv}\{\partial^B F(x)\}. \tag{A.1}$$

It can be shown that $\partial F(x)$ is nonempty, compact and convex and obviously $\partial F(x) = \{DF(x)\}$ if F is differentiable at x. We remark that we use the same symbol for the generalized Jacobian and the convex subdifferential. This is justified because for a scalar convex function, the convex subdifferential and the generalized Jacobian coincide, see [KK02, Section 1.2].

The *C-subdifferential* $\partial^C F(x)$ is defined as

$$\partial^C F(x) = \big(\partial F_1(x)^T \times \cdots \times \partial F_M(x)^T \big)^T,$$

and obviously $\partial^B F(x) \subset \partial F(x) \subset \partial^C F(x)$. The function F is called

- BD-regular (Bouligand-regular) at x, if all elements of $\partial^B F(x)$ are regular, i.e.: if $B \in \partial^B F(x)$, then B is regular,
- CD-regular (Clarke-regular) at x, if all elements of $\partial F(x)$ are regular, i.e.: if $C \in \partial F(x)$, then C is regular.

Note that CD-regularity is a stronger requirement as for $m(x) = |x|$ (the absolute value function), we find $\partial^B m(0) = \{-1, 1\}$ but $\partial m(0) = [-1, 1]$ and hence $0 \in \partial m(0)$ but $0 \notin \partial^B m(0)$, so m is BD-regular but not CD-regular. The following result follows from [PF03a, Theorem 7.5.3].

Proposition A.1. *Suppose that $F : \mathbb{R}^N \to \mathbb{R}^M$ is CD-regular at x^*. Then, there exists $\delta > 0$ such that F is CD-regular at all $x \in B(x^*, \delta) = \{y \in \mathbb{R}^N : |x^* - y| < \delta\}$.*

The same result obviously holds for BD-regularity as $\partial^B F(\cdot) \subset \partial F(\cdot)$.

For the rapid convergence of Newton's method for nonsmooth equations, semismooth-ness plays a central role. For vector-valued functions, this concept was introduced in [**QS93**] extending the scalar case given in [**Mif77**]. F is *semismooth* at x if it is locally Lipschitz continuous at x and if

$$\lim_{\substack{V \in \partial F(x + th'), \\ t \downarrow 0, \ h' \to h}} V h'$$

exists for all $h \in \mathbb{R}^N$. There are several equivalent formulations of semismoothness even allowing the transfer to the infinite dimensional case. We begin with some characteriza-tions of semismoothness, cf. [**QS93**, **SS02**]:

Proposition A.2. *For $F : \mathbb{R}^N \to \mathbb{R}^M$, the following statements are equivalent:*

(1) *F is semismooth at x.*
(2) *F is locally Lipschitz at x, $DF(x; \cdot)$ exists and for any $G \in \partial F(x + h)$:*

$$|Gh - DF(x; h)| = o(|h|) \qquad as \quad h \to 0 \,.$$

(3) *F is locally Lipschitz at x, $DF(x; \cdot)$ exists and for any $G \in \partial F(x + h)$:*

$$|F(x + h) - F(x) - Gh| = o(|h|) \qquad as \quad h \to 0 \,.$$

(4) *F is locally Lipschitz at x, $DF(x; \cdot)$ exists and for all $x + h \in \Theta_F$:*

$$|DF(x + h)h - DF(x; h)| = o(|h|) \qquad as \quad h \to 0 \,.$$

(5) *F is locally Lipschitz at x, and for all $x + h \in \Theta_F$:*

$$|F(x + h) - F(x) - DF(x + h)h| = o(|h|) \qquad as \quad h \to 0 \,.$$

When $o(|h|)$ is replaced by $O(|h|^{1+p})$, $p \in (0, 1]$, we say that F is semismooth of order p, and in the case $p = 1$ we say that F is strongly semismooth.

Depending on the given context, one of these different formulations may be most conve-nient. We consider the following examples of semismooth functions.

- A simple example for a strongly semismooth function is the max-function and we also give the generalized Jacobian.

$$m : \mathbb{R} \to \mathbb{R}\,, \qquad m(t) = \max\{0, t\}\,, \qquad \partial m(t) = \begin{cases} 1 & , \ t > 0 \,, \\ [0, 1] & , \ t = 0 \,, \\ 0 & , \ t < 0 \,. \end{cases} \qquad \text{(A.2)}$$

- *Piecewise C^1 functions* (or PC^1 functions): a function $F : \mathbb{R}^N \to \mathbb{R}^M$ is PC^1 if it is locally Lipschitz and if there is a finite selection (pieces) of smooth functions $F^i \in C^1(\mathbb{R}^N, \mathbb{R}^M)$ such that for all $x \in \mathbb{R}^N$ the set $I(x) = \{i : F(x) = F^i(x)\}$ is not empty. Properties of PC^1 functions were considered in [**KS94**]. The generalized Jacobian at x of such a function is given as

  $$\partial F(x) = \text{conv}\{DF^s(x) : x \in \overline{\text{int}(I^{-1}(s))}\}\,,$$

  and we also refer to [**KK02**]. We call a function f locally PC^1 at x if there is a neighbourhood $\mathcal{U}(x)$ such that f is PC^1 in $\mathcal{U}(x)$. Furthermore, if f is locally PC^1

at all $x \in \mathbb{R}^N$, we call the function locally PC^1 on $\mathbb{R}^N$. Locally PC^1 functions are semismooth, also see [**PF03a**, Proposition 7.4.6].

- Tame functions: this is a broader, but less accessible set of semismooth functions introduced in [**BDL09**].
- SC^1 *functions*: a function $f : \mathbb{R}^N \to \mathbb{R}$ is a SC^1 function if $f \in C^{1,1}(\mathbb{R}^N, \mathbb{R})$ and if $F(\cdot) = Df(\cdot)^T$ is semismooth, i.e. f is a differentiable function with Lipschitz continuous and semismooth derivative $F(x) = Df(x)^T$. For SC^1 function, the following second order approximation result holds:

$$\lim_{\substack{V \in \partial F(x+h) \\ |h| \to 0}} \frac{1}{|h|^2} \Big(f(x+h) - f(x) - F(x)^T h - \tfrac{1}{2} h^T V h \Big) = 0 \tag{A.3}$$

Following [**vHK08**, Lemma 2.2], semismoothness can also be defined in terms of the ∂^B and ∂^C-subdifferential:

Proposition A.3. *Let $F : \mathbb{R}^N \to \mathbb{R}^M$ be locally Lipschitz and directionally differentiable and let $x \in \mathbb{R}^N$ be an arbitrary point. Then the following statements are equivalent:*

(1) *F is semismooth at x, i.e. for all $G \in \partial F(x+h)$: $|Gh - DF(x;h)| = o(|h|)$ as $h \to 0$.*
(2) *For all $G \in \partial^B F(x+h)$: $|Gh - DF(x;h)| = o(|h|)$ as $h \to 0$.*
(3) *For all $G \in \partial^C F(x+h)$: $|Gh - DF(x;h)| = o(|h|)$ as $h \to 0$.*
(4) *F_i is semismooth for all components $i = 1, \ldots, M$, i.e. for all $H_i \in \partial F_i(x+h)$: $|H_i h - DF_i(x;h)| = o(|h|)$ as $h \to 0$.*

Based on this equivalent formulations, in [**vHK08**], the following implicit function theorem for semismooth equations was proven on the basis of an inverse function theorem given in [**PSS03**]. Concerning this theorem, we need the following notation. Let $Y : \mathbb{R}^N \times \mathbb{R}^M \to \mathbb{R}^N$ be locally Lipschitz. Then $\Pi_x \partial Y(x, y)$ denotes the set of all matrices $M \in \mathbb{R}^{N,N}$ such that there exists a matrix $N \in \mathbb{R}^{N,M}$ such that $\begin{bmatrix} M & N \end{bmatrix} \in \mathbb{R}^{N,N+M}$ belongs to $\partial Y(x, y)$. Similarly, $\Pi_y Y(x, y)$ is defined. Then, the following holds:

Proposition A.4. *Let $Y : \mathbb{R}^N \times \mathbb{R}^M \to \mathbb{R}^N$ be locally Lipschitz and semismooth in a neighbourhood of a point $(x^*, y^*) \in \mathbb{R}^N \times \mathbb{R}^M$ satisfying $Y(x^*, y^*) = 0$ and let all matrices in $\Pi_x \partial Y(x^*, y^*)$ be nonsingular. Then, there exists an open neighbourhood $\mathcal{U}(y^*)$ of y^* and a function $S : \mathcal{U}(y^*) \to \mathbb{R}^N$ which is locally Lipschitz and semismooth such that $S(y^*) = x^*$ and $Y(S(y), y) = 0$ for all $y \in \mathcal{U}(y^*)$.*

A similar theorem was given in [**Sun01**]. However, not within the framework of semismoothness, but he showed that if Y has a "superlinear approximation property", then the implicitly defined function inherits this property. An implicit function theorem for Lipschitz functions was already shown in [**Cla83**].

We close this subsection by stating a chain rule for (strongly) semismooth functions. The following result can be found in [**PF03a**, Proposition 7.4.4].

Proposition A.5. *Let $F : \mathbb{R}^N \to \mathbb{R}^M$ be (strongly) semismooth in a neighbourhood of $\hat{x} \in \mathbb{R}^N$ and let $G : \mathbb{R}^M \to \mathbb{R}^P$ be (strongly) semismooth in a neighbourhood of $F(\hat{x})$. Then $H : \mathbb{R}^N \to \mathbb{R}^P$, $H = G \circ F$ is (strongly) semismooth in a neighbourhood of $\hat{x}$.*

We remark that this proposition was only proven for $G : \mathbb{R}^M \to \mathbb{R}$, being a scalar function. However, by proposition A.3(4), this also holds for vector-valued functions.

1.2. The Infinite Dimensional Case. Since Rademacher's theorem does not hold in infinite dimensional spaces, the concept of semismoothness in terms of the generalized Jacobian as introduced above is not applicable. However, looking at the different equivalent formulations of semismoothness, it is formulation (3) in Proposition A.2 which is essential for showing superlinear convergence of a generalized Newton method. By dropping the requirement $G \in \partial F(x + h)$ as the generalized Jacobian cannot be defined in function space, several concepts have been introduced. In [**CQN00**], the notion of a slant derivative was introduced. This concept was slightly extended in [**HIK03**], and we repeat this definition at this point. Let X and Z be Banach spaces. The mapping $F : D \subset X \to Z$ is called *slantly differentiable* on an open subset $U \subset D$ if there exists a family of mappings $G : U \to L(X, Z)$ such that

$$\|F(x + h) - F(x) - G(x + h)h\|_Z = o(\|h\|_X) \qquad \text{as} \quad h \to 0\,, \tag{A.4}$$

for every $x \in U$. In subsequent work, the same authors also used the notions of Newton differentiability or generalized differentiability.

In [**KK02**, Chapter 6], functions $G : U \to L(X, Y)$ that satisfy (A.4) are called Newton functions and the set of such functions is denoted as a Newton map. Going back to the finite dimensional case and using the notion of a Newton map, $F : \mathbb{R}^N \to \mathbb{R}^M$ is semismooth at x if $\partial F(\cdot)$ is a Newton map.

As an example, let us consider the pointwise $\max$ function. For $\Omega \subset \mathbb{R}^d$ open and bounded, define

$$M : L^q(\Omega, \mathbb{R}) \to L^p(\Omega, \mathbb{R})\,, \qquad (Mu)(x) = \begin{cases} u(x) & , \ u(x) \geq 0\,, \\ 0 & , \ \text{else} \end{cases} \quad \text{a.e. in } \Omega\,. \tag{A.5}$$

M is well-defined whenever $1 \leq p \leq q \leq \infty$, and for some arbitrary but fixed $\delta \in \mathbb{R}$, we define

$$G : L^q(\Omega, \mathbb{R}) \to L(L^q(\Omega, \mathbb{R}), L^p(\Omega, \mathbb{R})) \qquad (G(u))(x) = \begin{cases} 1 & , \ u(x) > 0\,, \\ \delta & , \ u(x) = 0\,, \\ 0 & , \ u(x) < 0\,. \end{cases}$$

Following [**HIK03**], we find that G cannot serve as a Newton-map (or slant derivative) if $p = q$, but if $p < q$, G is a slant derivative of M.

A different concept of semismoothness in function space was developed in [**Ulb03**]. There, the focus was set on the definition of a generalized differential in function space suitable to prove superlinear convergence of Newton's method (with an additional smoothing step if necessary).

1.3. Generalized Newton Methods. Adopting the framework of the last subsection, we now consider the problem of finding $x^* \in X$ such that $F(x^*) = 0$ and we assume that $F : D \to Z$ is slantly differentiable in a neighbourhood $U \subset X$ of x, with the generalized derivative $G : U \to L(X, Z)$. Consider the generalized Newton method as given in Algorithm A.1. We have the following results, see [**HIK03**, **CQN00**]:

Theorem A.6. *Let x^* be a solution of $F(x) = 0$ and suppose that F is generalized differentiable in a neighbourhood U of x^* and that $G(x)$ is nonsingular for all $x \in U$ with $\|G(x)^{-1}\|$ uniformly bounded on U. Then, the Newton-iteration*

$$x^k = x^{k-1} - G(x^{k-1})^{-1}F(x^{k-1})$$

is well-defined and converges superlinearly to x^* provided that $\|x^0 - x^*\|$ is small enough.

Algorithm A.1 Generic Newton algorithm.

S0)   Choose $x^0 \in U$ and set $k := 1$.

S1)   Check for convergence by a suitable stopping rule.

S2)   Determine a generalized derivative $G(x^{k-1})$ of F at x^{k-1}.

S3)   Solve $G(x^{k-1})d^k = -F(x^{k-1})$ for d^k and set $x^k = x^{k-1} + d^k$.

S4)   Set $k := k + 1$ and go to S1).

In finite dimenions, provided that $\partial F(\cdot)$ is a Newton map, a suitable choice for $G(x^{k-1})$ is an arbitrary element of the generalized Jacobian $\partial F(x^{k-1})$, thereby yielding superlinear convergence provided that F is semismooth at x^* and $G(x)$ is regular around x^*. This is summarized in the following theorem taken from [**QS93**, Theorem 3.2]:

Theorem A.7. *Let x^* be a solution of $F(x) = 0$ with $F : \mathbb{R}^N \to \mathbb{R}^N$ being locally Lipschitz continuous and semismooth (of order p) at x^*. Moreover, assume that all $G \in \partial F(x^*)$ are nonsingular (i.e. F is CD-regular at x^*). Then, the Newton-iteration*

$$x^k = x^{k-1} - (G^k)^{-1} F(x^{k-1}), \qquad G^k \in \partial F(x^{k-1}),$$

is well-defined and converges superlinearly (with rate $1 + p$) to x^* provided that $|x^0 - x^*|$ is small enough.

For semismooth Lipschitz functions, there also exists a Newton-Kantorovich type theorem, cf. [**QS93**, Theorem 3.3], which we do not state here.

2. Semismoothness of the Projection Operator

2.1. The Projection Operator. Since the projection operator $P : \mathbb{R}^N \to K \subset \mathbb{R}^N$ is Lipschitz continuous, by Rademacher's theorem it follows that P is differentiable almost everywhere. However, it is not clear a priori in which points P is differentiable. Obviously, on the boundary of K, the derivative cannot exist classically. However, when $x \in K$, the directional derivative can be given explicitly in terms of the projection onto the tangent cone at x, cf. [**Zar71**, **Har77**, **HUL93a**]. In the given references, this was proven for the Euclidean projection, but the proof also applies in our context and we shortly prove this result. For this result, we introduce the tangent cone $\mathcal{T}_K(y)$ of K at $y \in K$ as the set

$$\mathcal{T}_K(y) = \{h \in \mathbb{R}^N : \exists\{y^k\} \subset K, y^k \to y \text{ and } t_k \downarrow 0 \text{ s.t. } h = \lim_{k \to \infty} \frac{1}{t_k}(y^k - y)\}$$

If K is convex, we have $\mathcal{T}_K(y) = \lim \mathrm{ext}_{t \downarrow 0} \frac{1}{t}(K - y)$, where the *limes exterior* is the set of all cluster points of all selections, cf. [**HUL93a**, Appendix A.5]. If $y \in \mathrm{int}(K)$, then obviously $\mathcal{T}_K(y) = \mathbb{R}^N$, so the interesting case is $y \in \partial K$.

Lemma A.8. *For $y \in K$, the directional derivative in direction $h \in \mathbb{R}^N$ of the projection P is given by the projection onto the tangent cone at y in the metric defined by A, i.e.*

$$DP(y; h) = \lim_{t \downarrow 0} \frac{1}{t}\Big(P(y + th) - P(y)\Big) = P_{\mathcal{T}_K(y)}(h).$$

PROOF. We first show that the difference quotient $\frac{1}{t}(P(y+th) - y)$ is the projection of h onto the cone $\frac{1}{t}(K - y)$ w.r.t. the metric $|\cdot|_A$. For arbitrary $z \in \frac{1}{t}(K - y)$, i.e. $z = \frac{1}{t}(w - y)$

for some $w \in K$, we have

$$
\begin{aligned}
a\big(h &- \tfrac{1}{t}(P(y + th) - y), z - \tfrac{1}{t}(P(y + th) - y)\big) \\
&= a\big(h - \tfrac{1}{t}(P(y + th) - y), \tfrac{1}{t}(w - y - (P(y + th) - y))\big) \\
&= \frac{1}{t^2} a\big(y + th - P(y + th), w - P(y + th)\big) \le 0 \,,
\end{aligned}
$$

where the last inequality follows from the characterization of the projection. Hence the difference quotient $\frac{1}{t}(P(y + th) - y)$ is the projection of h onto the cone $\frac{1}{t}(K - y)$. The assertion follows by letting $t \to 0$. $\square$

It remains the question of differentiability when $y \notin K$. This question cannot be answered in general, since it depends on the smoothness of the boundary of K. Particularly, in [Kru69] and [Sha94] it was shown that the projection cannot be differentiable in general when $y \notin K$. Positive results concerning differentiability were obtained in [Hol73], where it is shown that $P \in C^1$ in $\mathbb{R}^N \setminus K$, if ∂K is C^2. Under additional regularity conditions, the converse was proven in [FP82], also cf. [Nol95]. However, it turns out that a C^2 regular boundary ∂K is far too restrictive.

2.2. A General Result. In this subsection, K is described by $p \in \mathbb{N}$ smooth and convex functions $f_i \in C^2(\mathbb{R}^N, \mathbb{R})$ and we also write $f : \mathbb{R}^N \to \mathbb{R}^p$. Then, $K \subset \mathbb{R}^N$ is characterized by

$$
K = \{x \in \mathbb{R}^N : f(x) \le 0\} = \{x \in \mathbb{R}^N : f_i(x) \le 0 \text{ for } i = 1, \ldots, p\} \,. \tag{A.6}
$$

K could contain affine equality constraints as well but we do not discuss this here, cf. [PR96]. For $x \in K$, we denote the set of active indices by

$$
I(x) = \{i \in \{1, \ldots, p\} : f_i(x) = 0\} \,.
$$

In the situation without equality constraints, the *Mangasarian-Fromovitz constraint qualification* (MFCQ) requires that there is a $h \in \mathbb{R}^N$ such that $Df_i(x)h < 0$ for all $i \in I(x)$ and it is well-known that the (MFCQ) is implied by the Slater condition, i.e. there exists a $\widehat{x} \in K$ with $f(\widehat{x}) < 0$. Therefore, let $i \in I(x)$ and then

$$
0 > f_i(\widehat{x}) = f_i(\widehat{x}) - f_i(x) \ge Df_i(x)(\widehat{x} - x)
$$

due to the convexity of f_i. Thus, setting $h = \widehat{x} - x$ gives the result. Under (MFCQ), there exists a Lagrange multiplier $\lambda \in \mathbb{R}^p$, $\lambda \ge 0$ such that the projection $x = P(y)$ is characterized by the Karush-Kuhn-Tucker (KKT) conditions

$$
\begin{aligned}
&A(x - y) + Df(x)^T \lambda = 0 \,, \\
&\lambda \ge 0 \,, \qquad f(x) \le 0 \qquad \text{and} \qquad \lambda_i f_i(x) = 0 \text{ for } i = 1, \ldots, p \,.
\end{aligned} \tag{A.7}
$$

We will now establish differentiability properties of P at $y \notin K$. In order to do so, we need to introduce the *critical cone* of the projection w.r.t. the metric induced by A. For $x = P(y)$, we define

$$
\mathcal{C}_K(y) = \mathcal{T}_K(x) \cap (x - y)^{\perp_A} = \mathcal{T}_K(P(y)) \cap (P(y) - y)^{\perp_A} \,,
$$

cf. [PF03b, Section 4] and $\perp_A$ denotes the orthogonality w.r.t. the inner product induced by A. If $y \in K$ (i.e. $y = P(y) = x$), we have $\mathcal{C}_K(y) = \mathcal{T}_K(y)$. To give an illustration, Figure A.1 shows possible shapes of the critical cone if $y \notin K$ in $\mathbb{R}^2$. From A.1(c), one can readily observe that $\mathcal{C}_K(x)$ is a cone in general.
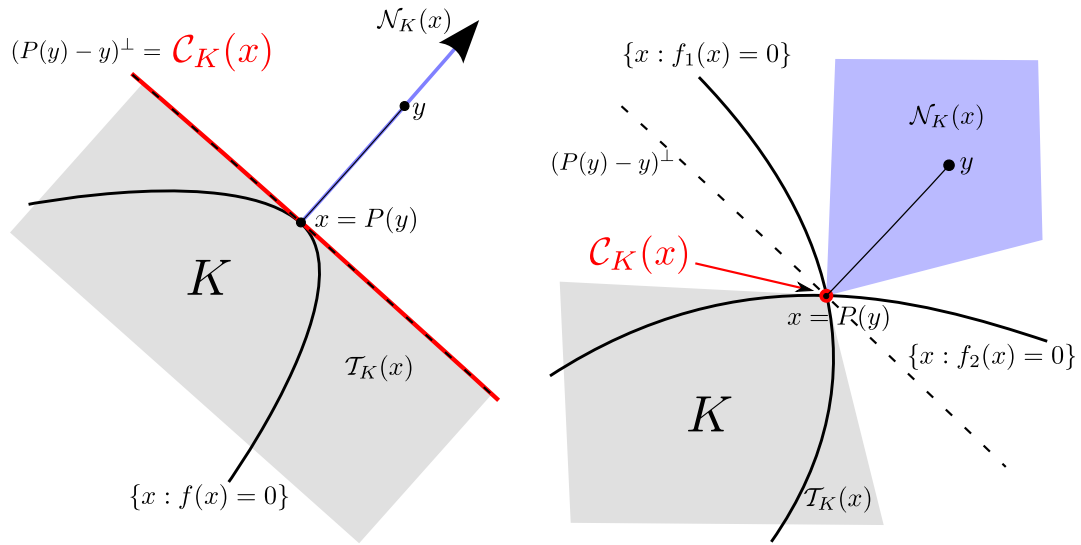
(a) Single active constraint: The critical cone coincides with the subspace $(y - x)^\perp$.

(b) Two active constraints and $y - x \subset \operatorname{int} \mathcal{N}_k(x)$: the critical cone reduces to $\mathcal{C}_K(x) = \{0\}$.
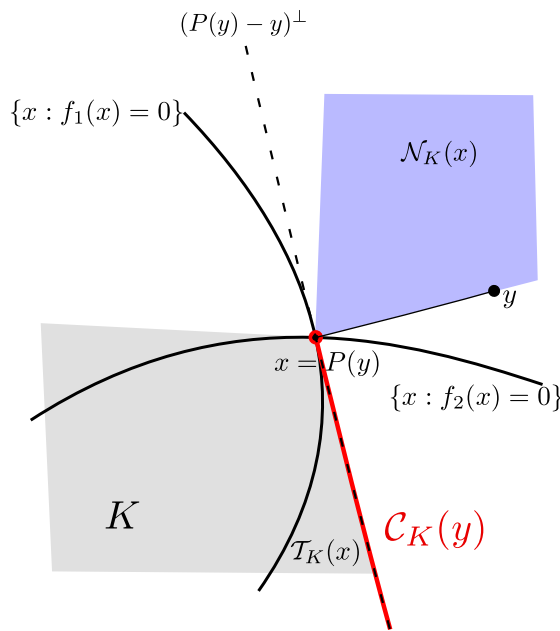
(c) Two active constraints and $y - x \subset \partial \mathcal{N}_K(x)$: the critical cone is a ray starting at 0 and is parallel to $y - x$, i.e. $\mathcal{C}_K(y)$ is a cone.

FIGURE A.1. Possible shapes of the critical cone in 2d for one and two active constraints w.r.t. the Euclidian metric. The tangent cone $\mathcal{T}_K(x)$ is shaded in grey, the normal cone $\mathcal{N}_K(x)$ in light blue and the critical $\mathcal{C}_K(x)$ in red. The dashed line is the subspace $(P(y) - y)^\perp$. For illustration, the cones and subspaces are shifted to $x = P(y)$.

Moreover, we define

$$G(y, \lambda) = A + \sum_{i=1}^{p} \lambda_i D^2 f_i(P(y)) \,.$$

Due to [**PR96**, Theorem 2], we have the following result:

Proposition A.9. *Suppose that (MFCQ) holds at* $x = P(y) \in K$ *with* K *as given in* (A.6)*. Then* P *is Bouligand-differentiable (in particular directionally differentiable) at* y *and for each* $h \in \mathbb{R}^N$*, there exists* $\lambda \in \mathbb{R}^p$*,* $\lambda \geq 0$ *such that*

$$DP(y; h) = P_{\mathcal{C}_K(y)}^{G(y,\lambda)}(G(y, \lambda)^{-1} Ah) \,, \tag{A.8}$$

with the projection $P_{\mathcal{C}_K(y)}^{G(y,\lambda)}$ *onto the critical cone* $\mathcal{C}_K(y)$ *in the metric induced by* $G(y, \lambda)$*.*

Note that in [**PR96**] and [**PF03b**], a slightly different notation for the projection onto the critical cone was used and their derivation was for A being the identity. Again, this gives a characterization of the directional derivative of P at an arbitrary point with the derivative being a projection onto a polyhedron.

In order to prove the semismoothness of the projection mapping, we need to introduce a different constraint qualification than the (MFCQ).

Definition A.10. *Let* K *be of the form* (A.6)*. At* $x \in K$*, the* constant rank constraint qualification *(CRCQ) holds if there is a neighbourhood* U *of* x *such that for every subset* $J \subset I(x)$ *and all* $z \in U$*, the set* $\{Df_i(z) : i \in J\}$ *has the same rank (which depends on* J*).*

Obviously, the (CRCQ) at $x \in K$ is implied by the (LICQ), i.e. the derivatives $\{Df_i(x) : i \in I(x)\}$ are linearly independent at x. However, the (CRCQ) neither implies nor is implied by the (MFCQ).

The following theorem is a conclusion of the results given in [**PR96**, **QS93**].

Theorem A.11. *Let* K *have the form* (A.6) *with* $f \in C^2(\mathbb{R}^N, \mathbb{R}^p)$ *and let* $y \in \mathbb{R}^N$ *be arbitrary. If the (CRCQ) holds at* $P(y)$*, then the projection* P *is semismooth at* $y \in \mathbb{R}^N$ *and the directional derivative is given as, cf.* (A.8)*:*

$$DP(y; h) = P_{\mathcal{C}_K(y)}^{G(y,\lambda)}(G(y, \lambda)^{-1} Ah) \,.$$

PROOF. The proof relies on several theorems in the above mentioned articles and can also be found in [**PF03b**, **PF03a**]. Following [**PF03b**, Theorem 4.5.2], we remark that under the (CRCQ), the projection is locally PC^1 for all $y \in \mathbb{R}^N$. Then, the semismoothness follows by [**PF03a**, Proposition 7.4.6]. Further, in [**PR96**, Theorems 7 and 8] it is shown that under (CRCQ), the directional derivative at y is given as

$$DP(y; h) = P_{\mathcal{C}_K(y)}^{G(y,\lambda)}(G(y, \lambda)^{-1} Ah)$$

for all $y \in \mathbb{R}^N$, therefore extending Proposition A.9. $\qquad \square$

2.3. Evaluating the Derivative in a Simple Case. The above subsection gives a characterization of the directional derivative of the projection by means of the projection onto the critical cone in a different metric, see (A.8). If K is defined by only one convex function, i.e. $K = \{x \in \mathbb{R}^N : f(x) \leq 0\}$ with a convex function $f \in C^2(\mathbb{R}^N, \mathbb{R})$, this result can be simplified and the derivative can be given in closed form if the projection $x = P(y)$ is known. Therefore note that if $y \notin K$, the critical cone is given as

$$\mathcal{C}_K(y) = \mathcal{T}_K(P(y)) \cap (P(y) - y)^{\perp_A} = \{h \in \mathbb{R}^N : Df(P(y))h = 0\} \,,$$

and is a linear subspace. We consider several cases:

(1) $y \in \text{int } K$: obviously $DP(y; h) = h$.
(2) $y \in \partial K$: By Lemma A.8, we find $DP(y; h) = P_{\mathcal{T}_K(y)}(h)$ and if K is described by a single constraint, $\mathcal{T}_K(y)$ is a halfspace, i.e. $\mathcal{T}_K(y) = \{h \in \mathbb{R}^N : Df(y)h \leq 0\}$. Hence,

$$P_{\mathcal{T}_K(x)}(h) = h - \max\{0, Df(x)h\} \frac{A^{-1}Df(x)^T}{Df(x)A^{-1}Df(x)^T}$$

$$= \begin{cases} h & , Df(y)h \leq 0, \\ \left(I - \frac{A^{-1}Df(x)^T Df(x)}{Df(x)A^{-1}Df(x)^T}\right)h & , Df(y)h > 0. \end{cases}$$

(3) If $y \notin K$, let $\lambda \geq 0$ be the Lagrange multiplier of the projection. The directional derivative is then given by $DP(y; h) = P_{\mathcal{C}_K(y)}^{G(y,\lambda)}(G(y,\lambda)^{-1}Ah)$ and as we have seen above $\mathcal{C}_K(y) = \{h \in \mathbb{R}^N : Df(x)h = 0\}$. Thus, the derivative is characterized as the solution d of the minimization problem

Minimize $\frac{1}{2}(d - G(y,\lambda)^{-1}Ah)^T G(y,\lambda)(d - G(y,\lambda)^{-1}Ah)$

subject to $d \in \mathcal{C}_K(y) = \{d \in \mathbb{R}^N : Df(x)d = 0\}$.

This is equivalent to finding a minimum of $\frac{1}{2}(d^T G(y,\lambda)d - d^T Ah)$ on $\mathcal{C}_K(y)$. This is a projection onto a linear space and can be given explicitly as

$$DP(y; h) = \left(I - \frac{G(y,\lambda)^{-1}Df(x)^T Df(x)}{Df(x)G(y,\lambda)^{-1}Df(x)^T}\right)G(y,\lambda)^{-1}Ah.$$

We will obtain the same result in different setting from the implicit function theorem below.

2.4. The projection operator in special cases.

2.4.1. *Semismoothness of the Projection onto a Polyhedron.* In this section, we consider the case when K is a polyhedron, i.e. an intersection of half-spaces. For this, let $B \in \mathbb{R}^{M,N}$ and $b \in \mathbb{R}^M$ be given such that the set K has a representation

$$K = \{x \in \mathbb{R}^N : Bx \leq b\}$$

The following result can be found in [Sch94].

Proposition A.12. *The projection $P : \mathbb{R}^N \to K$ onto the polyhedron K is piecewise affine and hence PC^1, i.e. there are affine functions $P^i : \mathbb{R}^N \to \mathbb{R}^N$ such that the active set $I(x) = \{i : P(x) = P^i(x)\}$ is not empty for all $x \in \mathbb{R}^N$.*

Particularly, each piece P^i is a projection onto an affine subspace $K_i \subset \mathbb{R}^N$ and we have $K = \cap_{i \in \mathbb{N}} K_i$. Each K_i can be identified with a face of the polyhedron K. Moreover, we have:

Corollary A.13. *The projection $P : \mathbb{R}^N \to K$ onto the polyhedron K is strongly semismooth.*

PROOF. This follows from [PF03a, Proposition 7.4.7] showing that each piecewise affine mapping is strongly semismooth.   □

2.4.2. *Semismoothness of the Projection onto the Second Order Cone.* In this section $K \subset \mathbb{R}^N$ is assumed to have a representation

$$K = \{x \in \mathbb{R}^N : x = (\widehat{x}, x_0) \in \mathbb{R}^{N-1} \times \mathbb{R} : |\widehat{x}| \le x_0\} \tag{A.9}$$

The set K is also called *Lorentz cone, ice cream cone* or *second order unit cone* being a special realization of the general second order cone

$$\{x \in \mathbb{R}^N : |Bx - b| \le c^T x + d\}$$

with $B \in \mathbb{R}^{M,N}$, $b \in \mathbb{R}^M$, $c \in \mathbb{R}^N$ and $d \in \mathbb{R}$. For an introduction to second order cone programming (SOCP) which is the main field of application concerning second order cones, we refer to [**BLLV98**, **AG03**]. The Lorentz cone also appears in second order cone complementarity problems (SOCCP), i.e. the problem of finding $(x, y, z) \in \mathbb{R}^N \times \mathbb{R}^N \times \mathbb{R}^M$ such that

$$x \in \mathcal{K}, \quad y \in \mathcal{K}, \quad x^T y = 0, \quad F(x, y, z) = 0$$

with a continuously differentiable mapping $F : \mathbb{R}^N \times \mathbb{R}^N \times \mathbb{R}^M \to \mathbb{R}^N \times \mathbb{R}^M$ and $\mathcal{K} \subset \mathbb{R}^N$ is the Cartesian product of Lorentz cones of suitable dimension. The (SOCCP) contains the (SOCP) as a special case as well as the nonlinear complementarity problems. This is the reason why the projection onto this class of convex sets is well-studied in the literature. We have the following result:

Proposition A.14. *The projection $P : \mathbb{R}^N \to K$ onto the second order unit cone K is strongly semismooth.*

This result has been proven by several authors by slightly different methods. Particularly, we mention [**CSS03**, **HYF05**, **GM06**, **CCT04**] and remark that in [**HYF05**], a complete characterization of Clarke's generalized Jacobian is given.

Similarly to the smooth case, the directional derivative $DP(x; h)$ can be interpreted as a skewed projection of h onto the tangent cone of K at x, see [**PSS03**, Proposition 13].

3. Semismoothness of Generalized Equations

After having considered the semismoothness of the projection operator which is implicitly defined by the KKT system (A.7), we now turn to the properties of functions implicitly defined by systems of equations similar to the KKT conditions. Specifically, we consider semismoothness properties of the functions $(x(y), \lambda(y))$ which is implicitly defined by the relations

$$\begin{aligned} A(x - y) + \lambda Dg(x)^T &= 0, \\ f(x) \le 0, \qquad \lambda \ge 0, \qquad \text{and} \qquad \lambda f(x) &= 0, \end{aligned} \tag{A.10}$$

where $f, g \in C^2(\mathbb{R}^N, \mathbb{R})$ are assumed to be convex. According to the definition of the response function, we will use the notation $R(y) = x = x(y)$.

With the help of the *NCP function* $\phi : \mathbb{R} \times \mathbb{R} \to \mathbb{R}$, defined as

$$\phi(a, b) = b - \max\{0, b - \gamma a\} \tag{A.11}$$

with $\gamma > 0$ arbitrary, we can rewrite the complementarity condition as

$$\phi(\lambda, -f(x)) = 0 \qquad \Longleftrightarrow \qquad f(x) \le 0, \ \lambda \ge 0, \text{ and } \lambda f(x) = 0.$$

We define $Y : (\mathbb{R}^N \times \mathbb{R}) \times \mathbb{R}^N \to (\mathbb{R}^N \times \mathbb{R})$ as

$$Y\big((x,\lambda),y\big) = \begin{bmatrix} A(x-y) + \lambda Dg(x)^T \\ \lambda - \max\{0, \lambda + \gamma f(x)\} \end{bmatrix}$$

and if $\big((x^*,\lambda^*),y^*\big)$ satisfy (A.10), then $Y\big((x^*,\lambda^*),y^*\big) = 0$. We have the following result:

Theorem A.15. *If $Df(x)\big(A + \lambda D^2 g(x)\big)^{-1} Dg(x)^T > 0$ for all $x \in \mathbb{R}^N$ and $\lambda \geq 0$, then there exists a semismooth Lipschitz function $S : \mathbb{R}^N \to (\mathbb{R}^N \times \mathbb{R})$, $S(y) = (R(y), \lambda(y))$ such that $\big((R(y), \lambda(y)), y\big)$ satisfies (A.10). Furthermore, the function $R : \mathbb{R}^N \to K \subset \mathbb{R}^N$ is semismooth and Lipschitz continuous.*

PROOF. The proof relies on the implicit function theorem for semismooth function (Proposition A.4). We define $m : \mathbb{R} \to \mathbb{R}$ as $m(t) = \max\{0, t\}$ and m is strongly semismooth with $\partial m(0) = [0, 1]$. Consequently, Y is semismooth as $f, g \in C^2(\mathbb{R}^N, \mathbb{R})$ and the composition of two semismooth functions is again semismooth, see Theorem A.5. In order to use the implicit function theorem we need show the regularity of the elements of $\Pi_{(x,\lambda)} \partial Y\big((x,\lambda),y\big)$. We have

$$\partial Y\big((x,\lambda),y\big) = \begin{cases} \left\{ \begin{bmatrix} A + \lambda D^2 g(x) & Dg(x)^T & -A \\ 0 & 1 & 0 \end{bmatrix} \right\} & , \lambda + \gamma f(x) < 0 \\[3ex] \left\{ \begin{bmatrix} A + \lambda D^2 g(x) & Dg(x)^T & -A \\ -\gamma Df(x) & 0 & 0 \end{bmatrix} \right\} & , \lambda + \gamma f(x) > 0 \\[3ex] \left\{ \begin{bmatrix} A + \lambda D^2 g(x) & Dg(x)^T & -A \\ -t\gamma Df(x) & 1-t & 0 \end{bmatrix} : t \in [0,1] \right\} & , \lambda + \gamma f(x) = 0 . \end{cases}$$

If $\lambda + \gamma f(x) < 0$, $\Pi_{(x,\lambda)} \partial Y\big((x,\lambda),y\big)$ is single-valued and if $\lambda \geq 0$, the only element is invertible since $A + \lambda D^2 g(x)$ is positiv definite by the convexity of g. Thus, it remains to check that

$$\begin{bmatrix} A + \lambda D^2 g(x) & Dg(x)^T \\ -t\gamma Df(x) & 1-t \end{bmatrix}$$

is regular for all $t \in (0, 1]$. A matrix of the type $\begin{bmatrix} K & B_1^T \\ B_2 & -C \end{bmatrix}$ with regular K is non-singular if and only if the Schur complement $C + B_2 K^{-1} B_1^T$ is regular [**BGL05**, Section 3.3]. In the present situation this is equivalent to

$$-1 + t - \gamma \, t \, Df(x)\big(A + \lambda D^2 g(x)\big)^{-1} Dg(x)^T \neq 0 .$$

This is fulfilled if

$$1 - \gamma Df(x)\big(A + \lambda D^2 g(x)\big)^{-1} Dg(x)^T \neq \frac{1}{t} .$$

Since $\frac{1}{t} \geq 1$, this condition is satisfied if

$$1 - \gamma Df(x)\big(A + \lambda D^2 g(x)\big)^{-1} Dg(x)^T < 1$$

or equivalently if $Df(x)\big(A + \lambda D^2 g(x)\big)^{-1} Dg(x)^T > 0$. This holds by assumption and we conclude that all elements of $\Pi_{(x,\lambda)} \partial Y\big((x,\lambda),y\big)$ are regular. Now, let $\big((x^*,\lambda^*),y^*\big)$ satisfy $Y\big((x^*,\lambda^*),y^*\big) = 0$. By Proposition A.4, there exists a neighbourhood $\mathcal{U}(y^*)$ and a semismooth Lipschitz function $S : \mathcal{U}(y^*) \to (\mathbb{R}^N \times \mathbb{R})$ such that $Y(S(y), y) = 0$ for all $y \in \mathcal{U}(y^*)$. Finally, Proposition A.3 shows that the individual components $R(y)$ and $\lambda(y)$ of $S(y)$ are semismooth. $\qquad\square$

3.1. Elements of the Generalized Jacobian. If $y \in K$, i.e. $f(y) \leq 0$, then $R(y) = y$ and the identity is contained in the generalized Jacobian. If $f(y) > 0$, then $\lambda > 0$ must hold and by complementarity also $f(x) = 0$. Thus locally around y, the response function is determined by the equalities $A(x - y) + \lambda Dg(x)^T = 0$ and $f(x) = 0$. Thus locally Y is given as (setting $\gamma = 1$)

$$Y\big((x, \lambda), y\big) = \begin{bmatrix} A(x - y) + \lambda Dg(x)^T \\ f(x) \end{bmatrix},$$

and for $y \notin K$, we seek (x, λ) such that $Y((x, \lambda), y) = 0$. In this setting the implicit function theorem for continuously differentiable functions applies, and under the assumptions of the theorem, the derivative $D_{(x,\lambda)}Y((x, \lambda), y)$ is regular (this corresponds to $\lambda + \gamma f(x) > 0$ in the representation of the generalized Jacobian of Y in the proof of the theorem). Thus the derivative of $S(y)$ is

$$D_y S(y) = -D_{(x,\lambda)}Y(S(y), y)D_y Y(S(y), y)$$

$$= -\begin{bmatrix} A + \lambda(y)D^2 g(R(y)) & Dg(R(y))^T \\ Df(R(y)) & 0 \end{bmatrix}^{-1} \begin{bmatrix} -A \\ 0 \end{bmatrix}.$$

Writing $x = R(y)$ and $\lambda = \lambda(y)$, we set $G = A + \lambda D^2 g(x) = A + \lambda(y)D^2 g(R(y))$ and by a Schur decomposition we obtain

$$\begin{bmatrix} G & Dg(x)^T \\ -Df(x) & 0 \end{bmatrix}^{-1} = \begin{bmatrix} G^{-1} - \frac{G^{-1}Dg(x)^T Df(x)G^{-1}}{Df(x)G^{-1}Dg(x)^T} & \frac{G^{-1}Dg(x)}{Df(x)G^{-1}Dg(x)^T} \\ \frac{G^{-1}Df(x)}{Df(x)G^{-1}Dg(x)^T} & -\frac{1}{Df(x)G^{-1}Dg(x)^T} \cdot \end{bmatrix}$$

Thus, we have

$$D_y R(y) = \left(G^{-1} - \frac{G^{-1}Dg(x)^T Df(x)G^{-1}}{Df(x)G^{-1}Dg(x)^T}\right)A = \left(I - \frac{G^{-1}Dg(x)^T Df(x)}{Df(x)G^{-1}Dg(x)^T}\right)G^{-1}A$$

We remark that if $g = f$, the present situation is identical to Section A.2.3 and particularly, the assumptions of the theorem are always satisfied, thereby showing the semismoothness of the projection operator when K is defined by only one smooth function $f \in C^2(\mathbb{R}^N, \mathbb{R})$. We also remark that the characterization of the derivative in the case $y \notin K$ coincide. Whereas we used the characterization of the derivative as a projection onto the critical cone above, the same characterization is obtained by using the implicit function theorem. Since $R : \text{Sym}(d) \to K$ is differentiable except on the boundary of K, we also find that R is a PC^1 function and the generalized derivative can be constructed as the convex hull of the corresponding B-subdifferentials.

APPENDIX B

A SCALAR COUNTEREXAMPLE

Problem Setting. In Chapter 4, we stressed that non-associated plasticity may in general be ill-posed. In order to illustrate this, we introduce an example in $\mathbb{R}^2$ having a structure which is very similar to the Drucker-Prager plasticity problem. We compare associated and non-associated plasticity and show that the former always has a solution under the Slater condition, the finite-dimensional equivalent of the safe-load condition 2.1. Contrary, the non-associated model, depending on the loading scenario, may fail to have a solution, or it may be non-unique.

Henceforth, we assume $\mathbb{C} = \mathbb{C}^{-1} = \mathbb{I}$, so the Euclidian metric coincides with the metric induced by the inverse elasticity tensor. This will be important in the non-associated setting later on, cf. Chapter 4. The associated problem is given by

$$
\begin{aligned}
&\boldsymbol{\sigma} + B^*\boldsymbol{u} + \lambda Df(\boldsymbol{\sigma}) = 0\,, \\
&B\boldsymbol{\sigma} = -\ell\,, \\
&f(\boldsymbol{\sigma}) \leq 0\,, \qquad \lambda \geq 0\,, \qquad \lambda f(\boldsymbol{\sigma}) = 0\,,
\end{aligned}
\tag{B.1}
$$

and in the non-associated setting, the first equation is modified:

$$
\begin{aligned}
&\mathbb{T}^{-1}\big[\boldsymbol{\sigma} + B^*\boldsymbol{u}\big] + \lambda Df(\boldsymbol{\sigma}) = 0\,, \\
&B\boldsymbol{\sigma} = -\ell\,, \\
&f(\boldsymbol{\sigma}) \leq 0\,, \qquad \lambda \geq 0\,, \qquad \lambda f(\boldsymbol{\sigma}) = 0\,.
\end{aligned}
\tag{B.2}
$$

We introduce a simple model by assuming $\boldsymbol{u} \in \mathbb{R}$ and $\boldsymbol{\sigma} \in \mathbb{R}^2$. Moreover, $B \in \mathbb{R}^{1,2}$ and the dual operator $B^* \in \mathbb{R}^{2,1}$ is given by its transpose, i.e. $B^* = B^T$. With $M \in (0, 1]$, we set

$$
\mathbb{T} = \begin{bmatrix} M & 0 \\ 0 & 1 \end{bmatrix}\,, \qquad B = -\begin{bmatrix} 1 & \delta \end{bmatrix}\,, \qquad \text{and} \qquad f(\boldsymbol{\sigma}) = \boldsymbol{\sigma}_1 + \boldsymbol{\sigma}_2\,.
$$

Setting $M = 1$ recovers the associated problem. For $\ell \in \mathbb{R}$, we define

$$
\boldsymbol{K} = \{\boldsymbol{\sigma} \in \mathbb{R}^2 : f(\boldsymbol{\sigma}) \leq 0\}\,, \qquad \text{and} \qquad \boldsymbol{S} = \{\boldsymbol{\sigma} \in \mathbb{R}^2 : B\boldsymbol{\sigma} = -\ell\}\,,
$$

and as a consequence, we find

$$
\boldsymbol{K} \cap \boldsymbol{S} = \emptyset \qquad \Longleftrightarrow \qquad \ell > 0 \text{ and } \delta = 1\,.
\tag{B.3}
$$

Thus, the Slater condition, i.e. there exists $\widehat{\boldsymbol{\sigma}} \in \boldsymbol{K} \cap \boldsymbol{S}$ such that $f(\widehat{\boldsymbol{\sigma}}) < 0$, is satisfied whenever $\delta \neq 1$ and if $\delta = 1$, then it is satisfied if $\ell < 0$. For the ease of notation, we define $\mathbf{1} = \begin{bmatrix} 1 & 1 \end{bmatrix}^T$, and consequently $f(\boldsymbol{\sigma}) = \mathbf{1}^T \boldsymbol{\sigma}$.

Associated Plasticity. The associated problem (B.1) is the optimality system of

$$\text{Minimize} \quad \tfrac{1}{2}|\boldsymbol{\sigma}|^2 \quad \text{subject to} \quad \boldsymbol{\sigma} \in \boldsymbol{K} \cap \boldsymbol{S}.$$

The projection of an arbitrary element $\boldsymbol{\sigma} \in \mathbb{R}^2$ onto $\boldsymbol{K}$ w.r.t. the Euclidian metric is given by

$$P(\boldsymbol{\sigma}) = \begin{cases} \boldsymbol{\sigma} & , f(\boldsymbol{\sigma}) \leq 0, \\ \boldsymbol{\sigma} - \tfrac{1}{2}f(\boldsymbol{\sigma})Df(\boldsymbol{\sigma}) & , f(\boldsymbol{\sigma}) > 0, \end{cases} = \begin{cases} \boldsymbol{\sigma} & , f(\boldsymbol{\sigma}) \leq 0, \\ \boldsymbol{\sigma} - \tfrac{1}{2}f(\boldsymbol{\sigma})\mathbf{1} & , f(\boldsymbol{\sigma}) > 0, \end{cases}$$

and with $\Upsilon(\boldsymbol{\sigma}) = \tfrac{1}{2}|\boldsymbol{\sigma}|^2 - \tfrac{1}{2}|\boldsymbol{\sigma} - P(\boldsymbol{\sigma})|^2$, see (2.35) and (2.36), we consider the primal functional

$$\mathcal{E}(\boldsymbol{u}) = \Upsilon(-B^*\boldsymbol{u}) - \ell\,\boldsymbol{u} = \tfrac{1}{2}\Big(\big|-B^*\boldsymbol{u}\big|^2 - \big|-B^*\boldsymbol{u} - P(-B^*\boldsymbol{u})\big|^2\Big) - \ell\,\boldsymbol{u}$$

$$= \tfrac{1}{2}\Big((1+\delta^2)\boldsymbol{u}^2 - \tfrac{(1+\delta)^2}{2}\max\{\boldsymbol{u},0\}^2\Big) - \ell\,\boldsymbol{u}.$$

Thus, the primal problem consists of minimizing $\mathcal{E}(\boldsymbol{u})$ over $\mathbb{R}$. Again, $\mathcal{E}$ is convex and the first order optimality condition is $F(\boldsymbol{u}) = 0$ with $F(\boldsymbol{u}) := -BP(-B^*\boldsymbol{u}) - \ell$. Then

$$F(\boldsymbol{u}) = \begin{bmatrix} 1 & \delta \end{bmatrix} \begin{bmatrix} \boldsymbol{u} - \tfrac{1+\delta}{2}\max\{\boldsymbol{u},0\} \\ \delta\boldsymbol{u} - \tfrac{1+\delta}{2}\max\{\boldsymbol{u},0\} \end{bmatrix} - \ell = (1+\delta^2)\boldsymbol{u} - \tfrac{1+2\delta+\delta^2}{2}\max\{\boldsymbol{u},0\} - \ell$$

$$= (1+\delta^2)\boldsymbol{u} - \tfrac{(1+\delta)^2}{2}\max\{\boldsymbol{u},0\} - \ell = \begin{cases} (1+\delta^2)\,\boldsymbol{u} - \ell & , \boldsymbol{u} \leq 0, \\ \tfrac{1}{2}(\delta-1)^2\,\boldsymbol{u} - \ell & , \boldsymbol{u} > 0. \end{cases}$$

We shortly comment on the coercivity of $\mathcal{E}$. Obviously, we have $\mathcal{E}(\boldsymbol{u}) \to \infty$ quadratically if $\boldsymbol{u} \to -\infty$. Hence, it remains to consider $\boldsymbol{u} > 0$. Then

$$\mathcal{E}(\boldsymbol{u}) = \tfrac{1}{4}(\delta-1)^2\,\boldsymbol{u}^2 - \ell\,\boldsymbol{u}.$$

Obviously, whenever $\delta \neq 1$, we have quadratic growth. However, if $\delta = 1$, coercivity is only assured if $\ell < 0$. Thus, the conditions for coercivity are fulfilled whenever the Slater condition is satisfied. We also discuss this relation in view of monotonicity properties of the derivative $F(\boldsymbol{u}) = D\mathcal{E}(\boldsymbol{u})$. Since $\mathcal{E}$ is a convex function, F is montonically increasing as the derivative of a convex function. It is easy to see that $F(\boldsymbol{u}) = 0$ always has a unique solution if the Slater condition is fulfilled. But if $\delta = 1$ and $\ell = 0$, i.e. the Slater condition is not fulfilled but $\boldsymbol{K} \cap \boldsymbol{S} \neq \emptyset$, uniqueness of a solution is lost since all $\boldsymbol{u} \geq 0$ are solutions. If $\boldsymbol{K} \cap \boldsymbol{S} \neq \emptyset$, then $F(\boldsymbol{u})$ has no solutions.

Non-Associated Plasticity. We define $R : \mathbb{R}^2 \to \boldsymbol{K} \subset \mathbb{R}^2$ as the orthogonal projection w.r.t. the inner product induced by $\mathbb{T}^{-1} = \begin{bmatrix} \tfrac{1}{M} & 0 \\ 0 & 1 \end{bmatrix}$. We then have

$$R(\boldsymbol{\sigma}) = \begin{cases} \boldsymbol{\sigma} & , \boldsymbol{\sigma} \in K, \\ \boldsymbol{\sigma} - \tfrac{1}{1+M}f(\boldsymbol{\sigma})\mathbb{T}[Df(\boldsymbol{\sigma})] & , \boldsymbol{\sigma} \notin K, \end{cases} = \begin{cases} \boldsymbol{\sigma} & , \boldsymbol{\sigma} \in K, \\ \boldsymbol{\sigma} - \tfrac{1}{1+M}f(\boldsymbol{\sigma})\mathbb{T}[\mathbf{1}] & , \boldsymbol{\sigma} \notin K. \end{cases}$$

We pick our standard element of the generalized Jacobian, i.e.

$$\partial R(\boldsymbol{\sigma}) \ni \mathbb{S} := \begin{cases} \mathbb{I} & , \boldsymbol{\sigma} \in K, \\ \mathbb{I} - \tfrac{1}{1+M}Df(\boldsymbol{\sigma}) \otimes \mathbb{T}[\mathbf{1}] & , \boldsymbol{\sigma} \notin K, \end{cases}$$

and we also have the representation

$$\mathbb{S} = \begin{cases} \mathbb{I} & , \boldsymbol{\sigma} \in K\,, \\ \mathbb{E} & , \boldsymbol{\sigma} \notin K\,, \end{cases} \qquad \text{with} \qquad \mathbb{E} = \frac{1}{1+M} \begin{bmatrix} 1 & -M \\ -1 & M \end{bmatrix}.$$

If $M \neq 1$, the generalized derivative of R is not symmetric with respect to the Euclidean inner product (which coincides with the metric of $\mathbb{C}^{-1} = \mathbb{I}$) since $\mathbb{E} \neq \mathbb{E}^T$. However, it is symmetric with respect to the inner product $\langle \boldsymbol{\sigma}, \boldsymbol{\eta} \rangle_{\mathbb{T}^{-1}} = \boldsymbol{\sigma}^T \mathbb{T}^{-1}[\boldsymbol{\eta}]$. Therefore note that $\mathbb{E}^T \mathbb{T}^{-1} = \mathbb{T}^{-1} \mathbb{E}$ and thus

$$\langle \mathbb{E}[\boldsymbol{\sigma}], \boldsymbol{\eta} \rangle_{\mathbb{T}^{-1}} = (\mathbb{E}[\boldsymbol{\sigma}])^T \mathbb{T}^{-1}[\boldsymbol{\eta}] = \boldsymbol{\sigma}^T (\mathbb{E}^T \mathbb{T}^{-1})[\boldsymbol{\eta}] = \boldsymbol{\sigma}^T \mathbb{T}^{-1} \big[\mathbb{E}[\boldsymbol{\eta}]\big] = \langle \boldsymbol{\sigma}, \mathbb{E}[\boldsymbol{\eta}] \rangle_{\mathbb{T}^{-1}}.$$

Moreover, it is easily seen that $\mathbb{E}$ has a zero eigenvalue and is positive semi-definite. We now evaluate $F(\boldsymbol{u}) = -BR(-B^*\boldsymbol{u}) - \ell$ and find

$$\begin{aligned} F(\boldsymbol{u}) &= \begin{bmatrix} 1 & \delta \end{bmatrix} \begin{bmatrix} \boldsymbol{u} - \frac{(1+\delta)M}{1+M}\max\{\boldsymbol{u},0\} \\ \delta\boldsymbol{u} - \frac{(1+\delta)}{1+M}\max\{\boldsymbol{u},0\} \end{bmatrix} - \ell \\ &= (1+\delta^2)\boldsymbol{u} - \frac{1}{1+M}\big((1+\delta)M + \delta(1+\delta)\big)\max\{\boldsymbol{u},0\} - \ell \\ &= \begin{cases} (1+\delta^2)\boldsymbol{u} - \ell & , \boldsymbol{u} \leq 0\,, \\ \frac{1}{1+M}\big(M\delta^2 - (1+M)\delta + 1\big)\boldsymbol{u} - \ell & , \boldsymbol{u} > 0\,, \end{cases} \\ &= \begin{cases} (1+\delta^2)\boldsymbol{u} - \ell & , \boldsymbol{u} \leq 0\,, \\ \frac{1}{1+M}(\delta-1)(\delta-\frac{1}{M})\boldsymbol{u} - \ell & , \boldsymbol{u} > 0\,. \end{cases} \end{aligned}$$

Contrary to the associated case, $F(\boldsymbol{u})$ is no longer monotone even if the safe load condition is fulfilled. To see this, take $\delta \in (1, \frac{1}{M})$ which assures the validity of the safe-load condition, cf. (B.3). In this situation, we easily see that F is strictly monotonically increasing for $\boldsymbol{u} \in (-\infty, 0]$ and strictly monotonically decreasing in $(0, \infty)$. Depending on ℓ, there is either no solution ($\ell > 0$), one solution ($\ell = 0$) or two solutions ($\ell < 0$):

(1) $\ell > 0$: then, $F(0) = -\ell < 0$, thus there cannot exists a solution to $F(\boldsymbol{u}) = 0$.
(2) $\ell = 0$: then, $F(0) = 0$, and we have exactly one solution at $\boldsymbol{u}^* = 0$.
(3) $\ell < 0$: then, $F(0) = -\ell > 0$. Thus there are two solutions: one on the positive half-line and one on the negative. Particularly, we find

$$\boldsymbol{u}_1^* = \frac{\ell}{1+\delta^2} < 0\,, \qquad \text{and} \qquad \boldsymbol{u}_2^* = \frac{(1+M)\ell}{(\delta-1)(\delta-\frac{1}{M})} > 0\,.$$

At first sight one might wonder why monotonicity of F is lost despite the fact that the generalized derivative of the projection R is at least positive semidefinite. The answer is the non-symmetry with respect to the inverse elasticity tensor $\mathbb{C}^{-1} = \mathbb{I}$. If it would be symmetric w.r.t. this metric, then Sylvester's law of inertia would assure the positive semidefiniteness. However, as $\mathbb{E}$ is not symmetric w.r.t. the Euclidian inner product, nothing can be said about $B\mathbb{E}B^*$ (remember $B^* = B^T$). Particularly, the sign of $B\mathbb{E}B^*$ strongly depends on the shape of B. However note that for $\delta \notin (1, \frac{1}{M})$, the above example always has a unique solution.

In summary: Even if $\boldsymbol{K} \cap \boldsymbol{S}$ is not empty and the Slater condition is satisfied, the non-associated problem may not have a solution and even if a solution exists it can be non-unique.

An Illustration. Figure B.1 shows the energy $\mathcal{E}$ of the associated model and the function F for the associated (dashed lines) and the non-associated model (solid lines). For the latter, we use $M = 1/4$ and the critical interval is $\delta \in (1, 1/M) = (1, 4)$. Moreover, we vary δ and the load ℓ. In detail, we consider combinations of $\delta \in \{1/2, 1, 2\}$ and $\ell \in \{-1, 0, 1\}$. Table B.1 summarizes whether solutions exist or not. Since the Slater condition is always fulfilled as long $\delta \neq 1$ and $\ell < 0$, a unique solution exists in these cases for the associated model. If $\delta = 1$ and $\ell = 0$, the Slater condition is not satisfied but the admissible set is not empty and the primal problem has infinitely many solutions. For $\delta = 1$ and $\ell > 0$, the admissible set is empty and no solutions exist. In the non-associated setting, if $\delta = 1/2$, F is always strictly increasing and a unique solution exists. For $\delta = 1$, F coincides with the associated F. However, for $\delta = 2$, depending on the load ℓ, the number of solutions changes whereas the associated model always admits a unique solution.

	$\delta = 1/2$	$\delta = 1$	$\delta = 2$
$\ell = -1$	unique solution	unique solution	unique solution
$\ell = 0$	unique solution	infinitely many solutions (Slater condition is not satisfied)	unique solution
$\ell = 1$	unique solution	no solution (admissible set is empty)	unique solution

(a) Associated setting

	$\delta = 1/2$	$\delta = 1$	$\delta = 2$
$\ell = -1$	unique solution	unique solution	two solutions
$\ell = 0$	unique solution	infinitely many solutions (Slater condition is not satisfied)	unique solution
$\ell = 1$	unique solution	no solution (admissible set is empty)	no solution (admissible set is not empty)

(b) Non-associated setting

TABLE B.1. Existence of solutions in the associated and non-associated setting.
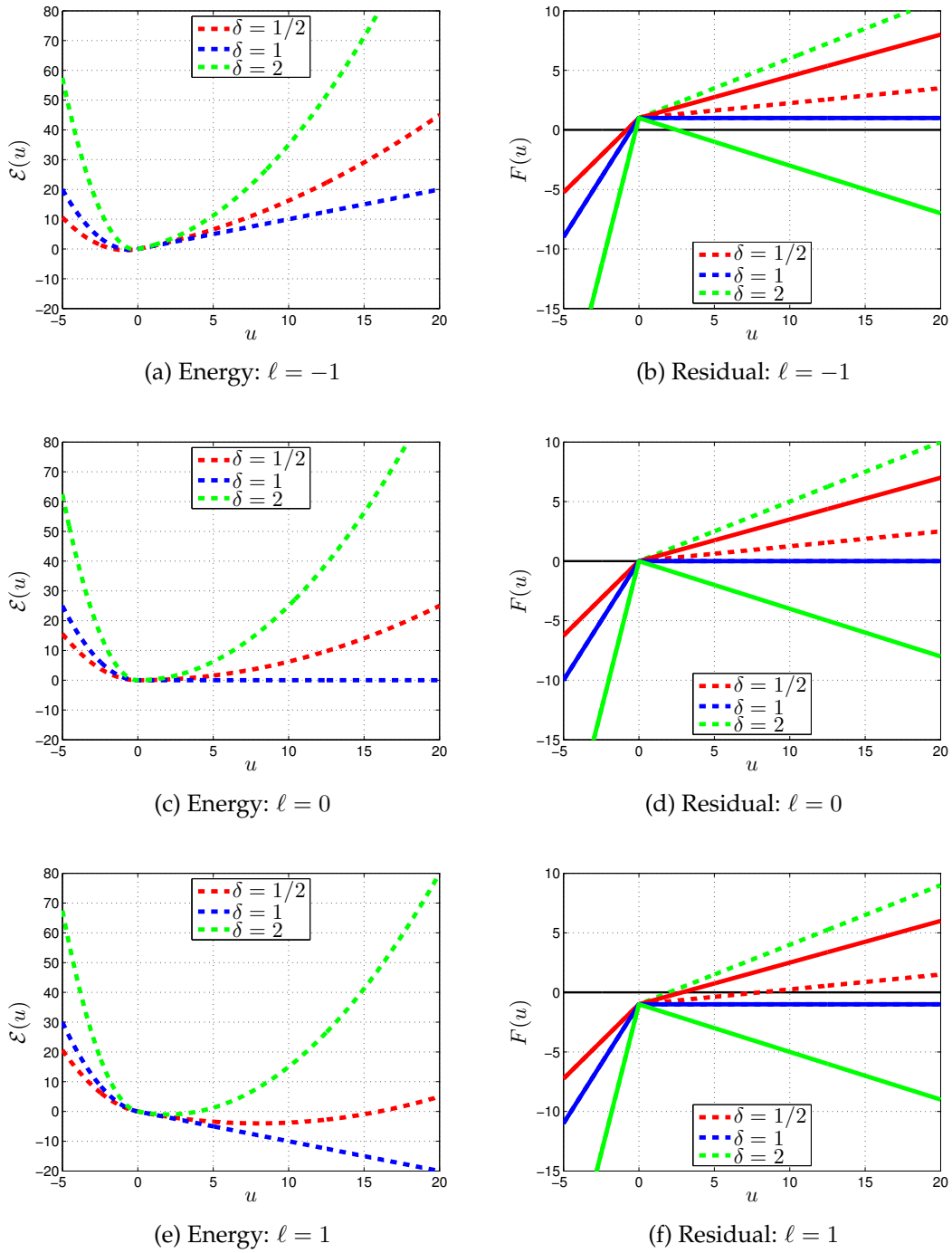
FIGURE B.1. Energy and residual of the associated model (dashed lines) and residual of the non-associated model with $M = 1/4$ (solid lines) for different loads ℓ and different values of δ.

BIBLIOGRAPHY

[ABDJ84] Douglas N. Arnold, Franco Brezzi, and Jim Douglas Jr. PEERS: A new mixed finite element for plane elasticity. *Japan J. Appl. Math.*, 1(2):347–367, 1984.

[ABM06] Hedy Attouch, Giuseppe Buttazzo, and Gérard Michaille. *Variational analysis in Sobolev and BV spaces : applications to PDEs and optimization*. MPS-SIAM series on optimization. Society for Industrial and Applied Mathematics, Philadelphia, 2006.

[AC04] Hans-Dieter Alber and Krzystof Chełmiński. Quasistatic problems in viscoplasticity theory I: Models with linear hardening. In *Gohberg, Israel (ed.) et al., Operator theoretical methods and applications to mathematical physics. The Erhard Meister memorial volume. Oper. Theory, Adv. Appl. 147, 105-129 (2004).* Birkhäuser, 2004.

[AC05] Scot Adams and Bernardo Cockburn. A mixed finite element method for elasticity in three dimensions. *J. Sci. Comput.*, 25(3):515–521, 2005.

[AC07] Hans-Dieter Alber and Krzysztof Chełmiński. Quasistatic problems in viscoplasticity theory. II: Models with nonlinear hardening. *Math. Models Methods Appl. Sci.*, 17(2):189–213, 2007.

[ACZ99] J. Alberty, C. Carstensen, and D. Zarrabi. Adaptive numerical analysis in primal elastoplasticity with hardening. *IMA Journal of Numerical Analysis*, 171:175–204, 1999.

[Ada75] R. A. Adams. *Sobolev Spaces*. Academic Press, New York, 1975.

[AF90] Jean-Pierre Aubin and Hélène Frankowska. *Set-valued analysis*. Systems and control. Birkhäuser, Boston, Mass., 1990.

[AFW06a] Douglas N. Arnold, Richard S. Falk, and Ragnar Winther. Differential complexes and stability of finite element methods. I: The de Rham complex. Arnold, Douglas N. (ed.) et al., Compatible spatial discretizations. The IMA Volumes in Mathematics and its Applications 142, 23-46., 2006.

[AFW06b] Douglas N. Arnold, Richard S. Falk, and Ragnar Winther. Differential complexes and stability of finite element methods. II: The elasticity complex. Arnold, Douglas N. (ed.) et al., Compatible spatial discretizations. The IMA Volumes in Mathematics and its Applications 142, 47-67., 2006.

[AFW06c] Douglas N. Arnold, Richard S. Falk, and Ragnar Winther. Finite element exterior calculus, homological techniques, and applications. *Acta Numerica*, 15:1–155, 2006.

[AFW07] Douglas N. Arnold, Richard S. Falk, and Ragnar Winther. Mixed finite element methods for linear elasticity with weakly imposed symmetry. *Math. Comput.*, 76(260):1699–1723, 2007.

[AG03] Farid Alizadeh and Donald Goldfarb. Second-order cone programming. *Math. Program.*, 95(1):3–51, 2003.

[AH05] Kendall E. Atkinson and Weimin Han. *Theoretical numerical analysis : a functional analysis framework*. Texts in applied mathematics ; 39. Springer, New York, NY, 2. ed. edition, 2005.

[Alb98] H.-D. Alber. *Materials with Memory*, volume 1682 of *Lecture Notes in Mathematics*. Springer-Verlag Berlin, 1998.

[Alt06] Hans Wilhelm Alt. *Lineare Funktionalanalysis: Eine anwendungsorientierte Einführung*. Springer, Berlin, 2006.

[AW02]   Douglas N. Arnold and Ragnar Winther. Mixed finite elements for elasticity. *Numer. Math.*, 92(3):401–419, 2002.

[AW03]   Douglas N. Arnold and Ragnar Winther. Nonconforming mixed elements for elasticity. *Math. Models Methods Appl. Sci.*, 13(3):295–307, 2003.

[BBJ+97]   P. Bastian, K. Birken, K. Johannsen, S. Lang, N. Neuß, H. Rentz-Reichert, and C. Wieners. UG – a flexible software toolbox for solving partial differential equations. *Comp. Vis. Sci.*, 1:27–40, 1997.

[BBJ+98]   P. Bastian, K. Birken, K. Johannsen, S. Lang, V. Reichenberger, H. Rentz-Reichert, C. Wieners, and G. Wittum. A parallel software-platform for solving problems of partial differential equations using unstructured grids and adaptive multigrid methods. In E. Krause and W. Jäger, editors, *High Performance Computing in Science and Engineering '98*, pages 326–339, Berlin, 1998. SPRINGER.

[BCDS01]   L. Bousshine, A. Chaaba, and G. De Saxcé. Softening in stress-strain curve for Drucker-Prager non-associated plasticity. *International Journal of Plasticity*, 17(1):21–46, 2001.

[BCR04]   D. Braess, C. Carstensen, and B. D. Reddy. Uniform convergence and a posteriori error estimators for the enhanced strain finite element method. *Numer. Math.*, 96(3):461–479, 2004.

[BdC05]   A. Bermúdez de Castro. *Continuum thermomechanics*. Progress in mathematical physics ; 43. Birkhäuser, Basel, 2005.

[BDL09]   J. Bolte, A. Daniilidis, and A. Lewis. Tame functions are semismooth. *Math. Prog.*, 2009.

[Ber82]   D. P. Bertsekas. *Constrained optimization and Lagrange multiplier methods*. Computer science and applied mathematics. Acad. Pr., New York, 1982.

[BF91]   F. Brezzi and M. Fortin. *Mixed and Hybrid Finite Element Methods*. Springer-Verlag Berlin, 1991.

[BF02]   A. Bensoussan and J. Frehse. *Regularity results for nonlinear elliptic systems and applications*, volume 151 of *Applied Mathematical Sciences*. Springer-Verlag Berlin, 2002.

[BGL05]   M. Benzi, G. H. Golub, and J. Liesen. Numerical solution of saddle point problems. *Acta Numerica*, 14(-1):1–137, 2005.

[BGLS06]   J. F. Bonnans, J. C. Gilbert, C. Lemarechal, and C. A. Sagastizabal. *Numerical Optimization*. Springer-Verlag Berlin, 2006.

[BJL+99]   P. Bastian, K. Johannsen, S. Lang, S. Nägele, V. Reichenberger, C. Wieners, G. Wittum, and C. Wrobel. Advances in high-performance computing: Multigrid methods for partial differential equations and its applications. In E. Krause and W. Jäger, editors, *High Performance Computing in Science and Engineering '99*, pages 506–519, Berlin, 1999. Springer-Verlag Berlin.

[BJL+00]   P. Bastian, K. Johannsen, S. Lang, V. Reichenberger, C. Wieners, G. Wittum, and C. Wrobel. Parallel solutions of partial differential equations with adaptive multigrid methods on unstructured grids. In E. Krause and W. Jäger, editors, *High Performance Computing in Science and Engineering '00*, pages 496–508, Berlin, 2000. Springer-Verlag Berlin.

[BJL+01]   P. Bastian, K. Johannsen, S. Lang, V. Reichenberger, C. Wieners, and G. Wittum. High-accuracy simulation of density driven flow in porous media. In E. Krause and W. Jäger, editors, *High Performance Computing in Science and Engineering '01*, pages 500–511, Berlin, 2001. Springer-Verlag Berlin.

[Bla97]   R. Blaheta. Convergence of Netwon-type methods in incremental return mapping analysis of elasto-plastic problems. *Comput. Meth. Appl. Mech. Engrg.*, 147:167–185, 1997.

[BLLV98]   S. Boyd, M. S. Lobo, H. Lebret, and L. Vanderberghe. Applications of second-order-cone programming. *Linear Algebra and its applications*, 284:193–228, 1998.

[BNO03]   D. P. Bertsekas, A. Nedic, and A. E. Ozdaglar. *Convex analysis and optimization*. Athena scientific optimization and computation series ; 1. Athena Scientific, Belmont, Mass., 2003.

[Bon89]   J.F. Bonnans. Local study of Newton type algorithms for constrained problems. Optimization, Proc. 5th French-German Conf., Varetz/Fr 1988, Lect. Notes Math. 1405, 13-24 (1989)., 1989.

[Bra07]   D. Braess. *Finite Elemente : Theorie, schnelle Löser und Anwendungen in der Elastizitätstheorie*. Springer, Berlin, 4. edition, 2007.

[Bre74]   F. Brezzi. On the existence, uniqueness and approximation of saddle-point problems arising from Lagrangian multipliers. *Rev. Française Automat. Informat. Recherche Opérationnelle Sér. Rouge*, 8(R-2):129–151, 1974.

[BS02]   S. C. Brenner and L. R. Scott. *The mathematical theory of finite element methods*, volume 15 of *Texts in applied mathematics*. Springer, New York, 2. edition, 2002.

[BV08]   S. P. Boyd and L. Vandenberghe. *Convex optimization*. Cambridge Univ. Press, Cambridge, 6th edition, 2008.

[CC04]   P. G. Ciarlet and P. Jr. Ciarlet. Another approach to linearized elasticity and Korn's inequality. *Comptes Rendus Mathematique*, 339(4):307 – 312, 2004.

[CCT04]   J.-S. Chen, X. Chen, and P. Tseng. Analysis of nonsmooth vector-valued functions associated with second-order cones. *Math. Prog.*, 101(1B):95–117, 2004.

[Che03]   K. Chelmiński. On quasistatic inelastic models of gradient type with convex composite constitutive equations. *Cent. Eur. J. Math.*, 1(4):670–689, 2003.

[Chr02]   P. W. Christensen. A nonsmooth Newton method for elastoplastic problems. *Comput. Meth. Appl. Mech. Engrg.*, 191:1189–2119, 2002.

[Cla83]   F. H. Clarke. *Optimization and Nonsmooth Analysis*. Wiley, 1983.

[CLSW98]   F.H. Clarke, Y.S. Ledyaev, R.J. Stern, and P.R. Wolenski. *Nonsmooth analysis and control theory*. Springer, New York, 1998.

[Cou04]   O. Coussy. *Poromechanics*. Wiley, Chichester, 2. edition, 2004.

[CQN00]   X. Chen, L. Qi, and Z. Nashed. Smoothing methods and semismooth methods for nondifferentiable operator equations. *SIAM J. Numer. Anal*, 38:todo, 2000.

[CSS03]   X. D. Chen, D. Sun, and J. Sun. Complementarity functions and numerical experiments on some smoothing Newton methods for second-order-cone complementarity problems. *Comput. Optim. Appl.*, 25(1-3):39–56, 2003.

[Dac89]   B. Dacorogna. *Direct methods in the calculus of variations*, volume 78 of *Applied mathematical sciences*. Springer, Berlin, 1989.

[Dan67]   J. M. Danskin. *The theory of Max-Min and its application to weapons allocation problems*. Ökonometrie und Unternehmensforschung 5. Springer, Berlin, 1967.

[dB00]   R. de Boer. *Theory of Porous Media*. Springer-Verlag Berlin, Berlin, 2000.

[DL76]   G. Duvaut and J. L. Lions. *Inequalities in Mechanics and Physics*, volume 219 of *Grundlehren der mathematischen Wissenschaften*. Springer-Verlag Berlin, 1976.

[DS02]   R. O. Davis and A. P. S. Selvadurai. *Plasticity and geomechanics*. Cambridge Univ. Press, 2002.

[Ehl02]   W. Ehlers. Foundations of multiphasic and porous materials. In W. Ehlers and J. Bluhm, editors, *Porous Media: Theory, Experiments and Numerical Applications*, pages 75–87, Berlin, 2002. Springer-Verlag Berlin.

[ER04]   François Ebobisse and B.Daya Reddy. Some mathematical problems in perfect plasticity. *Comput. Methods Appl. Mech. Eng.*, 193(48-51):5071–5094, 2004.

[Ern04]   Jean-Luc Ern, Alexandre ; Guermond. *Theory and practice of finite elements*. Applied mathematical sciences ; 159. Springer, New York, 2004.

[ET76]   I. Ekeland and R. Temam. *Convex analysis and variational problems*. North-Holland, 1976.

[Eva08]   L. C. Evans. *Partial differential equations*, volume 19 of *Graduate studies in mathematics*. American Mathematical Society, Providence, RI, 2008.

[Fac95]   Francisco Facchinei. Minimization of SC^1 functions and the Maratos effect. *Oper. Res. Lett.*, 17(3):131–137, 1995.

[FP82]   S. Fitzpatrick and R.R. Phelps. Differentiability of the metric projection in Hilbert space. *Trans. Am. Math. Soc.*, 270:483–501, 1982.

[FS00]   M. Fuchs and G. Seregin. *Variational Methods for Problems from Plasticity Theory and for Generalized Newtonian Fluids*. Lecture Notes in Mathematics. Springer-Verlag Berlin, 2000.

[Giu03]   E. Giusti. *Direct methods in the calculus of variations*. World Scientific, New Jersey, 2003.

[GK09]   C. Gräser and R. Kornhuber. Nonsmooth Newton methods for set-valued saddle point problems. *SIAM J. Numer. Anal.*, 47(2):1251–1273, 2009.

[Glo84]   R. Glowinski. *Numerical Methods for nonlinear Variational Problems*. Springer-Verlag Berlin, 1984.

[GM06]   M. Goh and F. Meng. On the semismoothness of projection mappings and maximum eigenvalue functions. *J. of Global Optimization*, 35(4):653–673, 2006.

[GR86]   V. Girault and P.-A. Raviart. *Finite element methods for Navier-Stokes equations*. Springer-Verlag Berlin, 1986.

[Gui00]   S. Guillaume. Subdifferential evolution inclusion in nonconvex analysis. *Positivity*, 4(4):357–395, 2000.

[Gur81]   M. Gurtin. *An introduction to Continuum Mechanics*. Academic Press, New York, 1981.

[GV09]   P. G. Gruber and J. Valdman. Solution of one-time-step problems in elastoplasticity by a slant newton method. *SIAM J. on Sci. Comp.*, 31(2):1558–1580, 2009.

[Har77]   A. Haraux. How to differentiate the projection on a convex set in Hilbert space. Some applications to variational inequalities. *J. Math. Soc. Japan*, 29:615–631, 1977.

[HFdS03]   M. Hjiaj, J. Fortin, and G. de Saxcé. A complete stress update algorithm for the non-associated Drucker-Prager model including treatment of the apex. *Int. J. Engrg. Scie.*, 41:1109–1143, 2003.

[HIK03]   M. Hintermüller, K. Ito, and K. Kunisch. The primal-dual active set strategy as a semi-smooth Newton method. *SIAM J. Optimization*, 13:865–888, 2003.

[HK06a]   M. Hintermüller and K. Kunisch. Feasible and noninterior path-following in constrained minimization with low multiplier regularity. *SIAM J. Control Optim.*, 45(4):1198–1221, 2006.

[HK06b]   Michael Hintermüller and Karl Kunisch. Path-following methods for a class of constrained minimization problems in function space. *SIAM J. Optim.*, 17(1):159–187, 2006.

[Hol73]   R. B. Holmes. Smoothness of certain metric projections on Hilbert space. *Trans. Am. Math. Soc*, 184:87–100, 1973.

[HPUU09]   M. Hinze, R. Pinnau, M. Ulbrich, and S. Ulbrich. *Optimization with PDE Constraints*, volume 23 of *Mathematical Modelling: Theory and Applications*. Springer, Dordrecht, 2009. In: Springer-Online.

[HR95]   W. Han and B. D. Reddy. Computational plasticity: The variational basis and numerical analysis. *Computational Mechanics Advances*, 2:283–400, 1995.

[HR99]   W. Han and B. D. Reddy. *Plasticity: Mathematical Theory and Numerical Analysis*. Springer-Verlag Berlin, 1999.

[HR00]   W. Han and B. D. Reddy. Convergence of approximations to the primal problem of plasticity under conditions of minimal regularity. *Numerische Mathematik*, 87:283–315, 2000.

[HUL93a]   J.-B. Hiriart-Urruty and C. Lemaréchal. *Convex analysis and minimization algorithms I - Fundamentals*. Springer-Verlag Berlin, 1993.

[HUL93b]   J.-B. Hiriart-Urruty and C. Lemaréchal. *Convex analysis and minimization algorithms II - Advanced theory and bundle methods*. Springer-Verlag Berlin, 1993.

[HW02]   E. Hairer and G. Wanner. *Solving ordinary differential equations*, volume 2: Stiff and differential algebraic problems of *Springer series in computational mathematics ; 14*. Springer, Berlin, 2. rev. ed., 2. corr. print. edition, 2002.

[HW09]   C. Hager and B. Wohlmuth. Nonlinear complementarity functions for plasticity problems with frictional contact. *Computer Methods in Applied Mechanics and Engineering*, 198(41-44):3411 – 3427, 2009.

[HYF05]   S. Hayashi, N. Yamashita, and M. Fukushima. A combined smoothing and regularization method for monotone second-order cone complementarity problems. *SIAM J. Optim.*, 15(2):593–615, 2005.

[IK00]   Kazufumi Ito and Karl Kunisch. Augmented Lagrangian methods for nonsmooth, convex optimization in Hilbert spaces. *Nonlinear Analysis*, 41(5-6):591 – 616, 2000.

[IK08]   Kazufumi Ito and Karl Kunisch. *Lagrange multiplier approach to variational problems and applications*. Advances in design and control ; 15. Society for Industrial and Applied Mathematics, Philadelphia, PA, 2008. Includes bibliographical references and index.

[IS93]   I. R. Ionescu and M. Sofonea. *Functional and Numerical Methods in Viscoplasticity*. Oxford University Press, 1993.

[IT79]   A. D. Ioffe and V. M. Tihomirov. *Theory of extremal problems*. Studies in mathematics and its applications ; 6. North-Holland, Amsterdam, 1979.

[JM79]   C. Johnson and B. Mercier. Some equilibrium finite element methods for two-dimensional problems in continuum mechanics. Energy methods in finite element analysis, Vol. dedic. to the Mem. of B. Fraeijs de Veubeke, 213-224 (1979)., 1979.

[Joh76]   C. Johnson. Existency theorems for plasticity problems. *J. Math. Pures Appl.*, 55:431–444, 1976.

[Joh78]   C. Johnson. On plasticity with hardening. *J. Appl. Math. Anal.*, 62:325–336, 1978.

[KIT10]   KIT Steinbuch Center for Computing (SCC). *InstitutsCluster User Guide*, 2010.

[KK02]   R. Klatte and B. Kummer. *Nonsmooth Equations in Optimization*, volume 60 of *Nonconvex Optimization and Its Applications*. Kluwer, 2002.

[KKT03]   T. Kärkkäinen, K. Kunisch, and P. Tarvainen. Augmented Lagrangian active set methods for obstacle problems. *J. Optimization Theory Appl.*, 119(3):499–533, 2003.

[KLSW06]   K. Krabbenhoft, A.V. Lyamin, S.W. Sloan, and P. Wriggers. An interior-point algorithm for elastoplasticity. *Int. J. Numer. Methods Eng.*, 69(3):592–626, 2006.

[Kru69]   J.B. Kruskal. Two convex counterexamples: A discontinuous envelope function and a nondifferentiable nearest-point mapping. *Proc. Am. Math. Soc.*, 23:697–703, 1969.

[KS94]   Ludwig Kuntz and Stefan Scholtes. Structural analysis of nonsmooth mappings, inverse functions, and metric projections. *J. Math. Anal. Appl.*, 188(2):346–386, 1994.

[KY94]   Ralf Kornhuber and Harry Yserentant. Multilevel methods for elliptic problems on domains not resolved by the coarse grid. Keyes, David E. (ed.) et al., Domain decomposition methods in scientific and engineering computing. Proceedings of the 7th international conference on domain decomposition, October 27-30, 1993, Pennsylvania State University, PA, USA. Providence, RI: American Mathematical Society. Contemp. Math. 180, 49-60 (1994)., 1994.

[KZ05]   Andrew Kurdila and Michael Zabarankin. *Convex functional analysis*. Systems and control: Foundations and applications. Birkhäuser, Basel, 2005. Includes bibliographical references and index.

[Lem00]   Jean-Louis Lemaitre, Jean ; Chaboche. *Mechanics of solid materials*. Cambridge Univ. Press, Cambridge [u.a.], 2000.

[LS96]   Dinh The Luc and S. Schaible. Generalized monotone nonsmooth maps. *J. Convex Anal.*, 3(2):195–205, 1996.

[Lub06]   Jacob Lubliner. *Plasticity theory*. Dover Publications, 2006.

[Mas93]   G. Dal Maso. *An introduction to gamma-convergence*. Progress in nonlinear differential equations and their applications ; 8. Birkhäuser, Boston, 1993.

[Mau]   D. Maurer. PhD thesis in preparation (Karlsruhe Institute of Technology).

[MDD07]   G. Dal Maso, A. Demyanov, and A. DeSimone. Quasistatic evolution problems for pressure-sensitive plastic materials. *Milan J. Math.*, 75:117–134, 2007.

[MDM06]   G. Dal Maso, A. DeSimone, and M.G. Mora. Quasistatic evolution problems for linearly elastic-perfectly plastic materials. *Arch. Rational Mech. Anal.*, 180:237–291, 2006.

[MH94]   Jerrold E. Marsden and Thomas J. R. Hughes. *Mathematical foundations of elasticity*. Dover Publications, 1994.

[Mie05]   A. Mielke. Evolution of rate-independent systems. In C. Dafermos and E. Feireisl, editors, *Handbook of Differential Equations: Evolutionary Differential Equations*. North-Holland, 2005.

[Mie08]   Alexander Mielke. Numerical approximation techniques for rate-independent inelasticity. In B. Reddy, editor, *IUTAM Symposium on Theoretical, Computational and Modelling Aspects of Inelastic Media : proceedings of the IUTAM Symposium held at Cape Town, South Africa, January 14 - 18, 2008*, IUTAM Bookseries ; 11, pages 53–64. Springer, 2008.

[Mif77]   R. Mifflin. Semismooth and semiconvex functions in constrained optimization. *SIAM J. Control and Optimization*, 15:959–972, 1977.

[ML99]   C. Miehe and M. Lambrecht. Two non-associated isotropic elastoplastic hardening models for frictional materials. *Acta Mechanica*, 135:73–90, 1999.

[MR09]   Alexander Mielke and Tomáš Roubíček. Numerical approaches to rate-independent processes and applications in inelasticity. *ESAIM, Math. Model. Numer. Anal.*, 43(3):399–428, 2009.

[MRS08]   Alexander Mielke, Tomáš Roubíček, and Ulisse Stefanelli. Γ-limits and relaxations for rate-independent evolutionary problems. *Calc. Var. Partial Differ. Equ.*, 31(3):387–416, 2008.

[Mül09]   Wolfgang Müller. *Numerische Analyse und parallele Simulation von nichtlinearen Cosserat-Modellen*. PhD thesis, Karlsruher Institut für Technologie (KIT), 2009.

[NCWM07]   P. Neff, K. Chelminski, and C. Wieners W. Müller. A numerical solution method for an inifinitesimal elasto-plastic cosserat model. *Mathematical Models and Methods in Applied Sciences (M3AS)*, 17:1211–1240, 2007.

[Nol95]   Dominikus Noll. Directional differentiability of the metric projection in Hilbert space. *Pac. J. Math.*, 170(2):567–592, 1995.

[NSW09]   Patrizio Neff, Antje Sydow, and Christian Wieners. Numerical approximation of incremental infinitesimal gradient plasticity. *Int. J. Numer. Methods Eng.*, 77(3):414–436, 2009.

[OM89]   Michael Ortiz and John B. Martin. Symmetry-preserving return mapping algorithms and incrementally extremal paths: A unification of concepts. *Int. J. Numer. Methods Eng.*, 28(8):1839–1853, 1989.

[OR70]   James M. Ortega and Werner C. Rheinboldt. *Iterative solution of nonlinear equations in several variables*. Computer science and applied mathematics. Acad. Press, New York [u.a.], 1970.

[PF03a]   Jong-Shi Pang and Francisco Facchinei. *Finite dimensional variational inequalities and complementarity problems*, volume 2:. Springer, New York, 2003.

[PF03b]   Jong-Shi Pang and Francisco Facchinei. *Finite dimensional variational inequalities and complementarity problems*, volume 1:. Springer, New York, 2003.

[PHR91]   Jong-Shi Pang, Shih-Ping Han, and Narayan Rangaraj. Minimization of locally Lipschitzian functions. *SIAM J. Optim.*, 1(1):57–82, 1991.

[PQ95]   Jong-Shi Pang and Liqun Qi. A globally convergent newton method for convex sc^1 minimization problems. *J. Optim. Theory. Appl.*, 85(3):633–648, 1995.

[PR96]   Jong-Shi Pang and Daniel Ralph. Piecewise smoothness, local invertibility, and parametric analysis of normal maps. *Math. Oper. Res.*, 21(2):401–426, 1996.

[PR01]   J-P. Penot and R. Ratsimahalo. On the yosida approximation of operators. *Proceedings Section A: Mathematics - Royal Society of Edinburgh*, 131:945–966(22), 17 August 2001.

[PSS03]   Jong-Shi Pang, Defeng Sun, and Jie Sun. Semismooth homeomorphisms and strong stability of semidefinite and lorentz complementarity problems. *Math. Oper. Res.*, 28(1):39–63, 2003.

[PZ99]   D.M. Potts and L. Zdravković. *Finite element analysis in geotechnical engineering: theory*. Thomas Telford Ltd., 1999.

[QJ97]   Liqun Qi and Houyuan Jiang. Semismooth Karush-Kuhn-Tucker equations and convergence analysis of Newton and quasi-Newton methods for solving these equations. *Math. Oper. Res.*, 22(2):301–325, 1997.

[QS93]   Liqun Qi and Jie Sun. A nonsmooth version of newton's method. *Math. Program.*, 58(3):353–367, 1993.

[Rep96]   S. I. Repin. Errors of finite element methods for perfect plasticity. *Math. Models Meth. Appl. Sci.*, 5:587–604, 1996.

[Rob80]   Stephen M. Robinson. Strongly regular generalized equations. *Mathematics of Operations Research*, 5(1):43–62, 1980.

[Rob82]   Stephen M. Robinson. Generalized equations and their solutions. Part II: Applications to nonlinear programming. *Math. Program. Study*, 19:200–221, 1982.

[Roc73]   R.T. Rockafellar. The multiplier method of Hestenes and Powell applied to convex programming. *J. Optimization Theory Appl.*, 12:555–562, 1973.

[Rou05]   Tomáš Roubíček. *Nonlinear partial differential equations with applications*. Birkhäuser. Basel , 2005.

[Růž04]   Michael Růžička. *Nichtlineare Funktionalanalysis: Eine Einführung*. Springer, Berlin, 2004.

[RW98]   Ralph Tyrrell Rockafellar and Roger J.-B. Wets. *Variational analysis*. Springer, 1998.

[RX96]   S. I. Repin and L. S. Xanthis. A posteriori estimation for elasto-plastic problems based on duality theory. *Comput. Meth. Appl. Mech. Engrg.*, 138:317–339, 1996.

[Saa03]   Youcef Saad. *Iterative methods for sparse linear systems*. SIAM, Society for Industrial and Applied Mathematics, Philadelphia, PA, 2. edition, 2003.

[Sch94]   S. Scholtes. Introduction to piecewise differentiable equations, habilitation thesis. Technical report, Institut für Statistik und Mathematische Witschaftstheorie, University of Karlsruhe, Preprint No. 54, 1994.

[SH98]   J. C. Simo and T. J. R. Hughes. *Computational Inelasticity*. Springer-Verlag Berlin, 1998.

[Sha94]   A. Shapiro. Directionally nondifferentiable metric projection. *J. Optimization Theory Appl.*, 81(1):203–204, 1994.

[Sho97]   R.E. Showalter. *Monotone operators in Banach space and nonlinear partial differential equations*. American Mathematical Society, 1997.

[Sim98]   J.C. Simo. Numerical analysis and simulation of plasticity. Ciarlet, P. G. (ed.) et al., Handbook of numerical analysis. Vol. 6: Numerical methods for solids (Part 3). Numerical methods for fluids (Part 1). Amsterdam: Elsevier. 183-499 (1998)., 1998.

[SKG88]   J.C. Simo, J.G. Kennedy, and S. Govindjee. Non-smooth multisurface plasticity and viscoplasticity. loading/unloading conditions and numerical algorithms. *Int. J. Numer. Meth. Eng.*, 26:2161–2185, 1988.

[SR90]   J.C. Simo and M.S. Rifai. A class of mixed assumed strain methods and the method of incompatible modes. *Int. J. Numer. Methods Eng.*, 29(8):1595–1638, 1990.

[SR03]   Erwin Stein and Ekkehard Ramm, editors. *Error controlled adaptive finite elements in solid mechanics*. Wiley, Chichester, 2003.

[SS02]   Defeng Sun and Jie Sun. Semismooth matrix-valued functions. *Math. Oper. Res.*, 27(1):150–169, 2002.

[SSS09]   A. Schwarz, J. Schröder, and G. Starke. Least-squares mixed finite elements for small strain elasto-viscoplasticity. *Int. J. Numer. Methods Eng.*, 77(10):1351–1370, 2009.

[Sta07]   Gerhard Starke. An adaptive least-squares mixed finite element method for elasto-plasticity. *SIAM J. Numer. Anal.*, 45(1):371–388, 2007.

[Sun01]   Defeng Sun. A further result on an implicit function theorem for locally lipschitz functions. *Operation Research Letters*, 28(4):193–198, 2001.

[Suq78a]   Pierre-Marie Suquet. Existence et régularité des solutions des équations de la plasticité. *C. R. Acad. Sci. Paris Sér. A-B*, 286(24):A1201–A1204, 1978.

[Suq78b]   Pierre-Marie Suquet. Sur un nouveau cadre fonctionnel pour les équations de la plasticité. *C. R. Acad. Sci. Paris Sér. A-B*, 286(23):A1129–A1132, 1978.

[Suq79]   Pierre M. Suquet. Un espace fonctionnel pour les équations de la plasticite. *Ann. Fac. Sci. Toulouse, V. Ser., Math.*, 1:77–87, 1979.

[Tem85]   R. Temam. *Mathematical Problems in Plasticity*. Bordas, Paris, 1985.

[TS80]   R. Temam and G. Strang. Functions of bounded deformation. *Arch. Rational Mech. Anal.*, 75:7–21, 1980.

[Ulb03]   Michael Ulbrich. Semismooth Newton methods for operator equations in function spaces. *SIAM J. Optim.*, 13(3):805–841, 2003.

[vdV03]   H. van der Vorst. *Iterative Krylov methods for large linear systems*, volume 13 of *Cambridge monographs on applied and computational mathematics*. Cambridge University Press, Cambridge, 2003.

[vHK08]   Anna von Heusinger and Christian Kanzow. Sc1 optimization reformulations of the generalized nash equilibrium problem. *Optimization Methods Software*, 23(6):953–973, 2008.

[VP96]   K. C. Valanis and J. F. Peters. Ill-posedness of the initial and boundary value problems in non-associative plasticity. *Acta Mechanica*, 114:1–25, 1996.

[Wie99]   C. Wieners. Multigrid methods for Prandtl-Reuß plasticity. *Numer. Lin. Alg. Appl.*, 6:457–478, 1999.

[Wie04]   C. Wieners. Distributed point objects. A new concept for parallel finite elements. In R. Kornhuber, R. Hoppe, J. Périaux, O. Pironneau, O. Widlund, and J. Xu, editors, *Domain Decomposition Methods in Science and Engineering*, volume 40 of *Lecture Notes in Computational Science and Engineering*, pages 175–183. Springer-Verlag Berlin, 2004.

[Wie07]   C. Wieners. Nonlinear solution methods for infinitesimal perfect plasticity. *Z. Angew. Math. Mech. (ZAMM)*, 87(8-9):643–660, 2007.

[Wie08]   Christian Wieners. Sqp methods for incremental plasticity with kinematic hardening. In B. Reddy, editor, *IUTAM Symposium on Theoretical, Computational and Modelling Aspects of Inelastic Media : proceedings of the IUTAM Symposium held at Cape Town, South Africa, January 14 - 18, 2008*, IUTAM Bookseries ; 11, pages 143–153. Springer, 2008.

[Wie10]   C. Wieners. A geometric data structure for parallel finite elements and the application to multigrid methods with block smoothing. *Comp. Vis. Sci.*, 13(4):161–175, 2010.

[Zar71]   E.H. Zarantonello. Projections on convex set in Hilbert space and spectral theory. In E.H. Zarantonello, editor, *Contributions to nonlinear functional analysis*, Publications of the Mathematics Research Center ; 27, New York, 1971. Acad.Pr.

[Zei90]   E. Zeidler. *Nonlinear Functional Analysis and its Applications I-IV*. Springer-Verlag Berlin, 1986-1990.